

NASA-CP-2260-VOL-3
19830020235

NASA Conference Publication 2260

The Multispectral Imaging Science Working Group: Final Report

Volume III Appendices

*Proceedings of working groups sponsored
by NASA Headquarters Earth and Planetary Exploration Division,
Office of Space Science and Applications
September 1, 1982*

NASA

The Multispectral Imaging Science Working Group: Final Report

Volume III Appendices

Scott C. Cox, Editor

Proceedings of working groups sponsored
by NASA Headquarters Earth and Planetary Exploration Division,
Office of Space Science and Applications and
held in Pasadena, California, San Antonio, Texas and
Silver Spring, Maryland, 1982



National Aeronautics
and Space Administration

Scientific and Technical
Information Branch

All measurement values are expressed in the International System of Units (SI) in accordance with NASA Policy Directive 2220.4, paragraph 4.

LIST OF APPENDICES

APPENDIX I: Presentation Material for Multispectral Imaging Science Working Group (June 17, 1982)

- 1. Botanical Sciences Team. C. J. Tucker
- 14. Geology Team M. Settle
- 22. Geographic Science Team. N. Bryant
- 48. Hydrology Team R. Ragan
- 55. Information Science Team F. Billingsley
- 75. Image Science Team K. Ando

APPENDIX II: Working Papers for Geographic Science Team

- 2. Mapping Urban Land Cover From Space. L. Gaydos
- 10. Projected Technological Requirements for Remote Sensing of Terrain Variables. C. Hutchinson

APPENDIX III: Working Papers for Hydrology Science Team

- 2. An Overview on Application of Future Remote Sensing Systems to Irrigation L. Miller
- 8. Evapotranspiration and Remote Sensing. T. Schmugge &
R. Gurney
- 23. Cost Effectiveness of Conventional Versus Landsat Land Use Data for Hydrologic Modeling T. S. George &
R. S. Taylor
- 28. High Resolution Impacts on Private Consulting

31. Summary of Hydrologic Modeling Interests
in Remote Sensing. A. Feldman
33. USDA-ARS Hydrology Lab T. J. Jackson
38. The Role of Multispectral Scanner as
Data Sources for EPA Hydrology Models. R. Slack &
D. Hill
42. High Resolution Analysis C. J. Robinove
47. Drainage Basins/Soil Moisture Uses
for Visible Infrared Data
52. Thermal Infrared Research, Where Are
We Now?. J. L. Hatfield &
R. D. Jackson

APPENDIX IV: Working Papers for Geology Science Team

2. Lithologic Units Through Analysis of Visible,
Near-Infrared, and Mid-Infrared
Measurements L. C. Rowan
8. Radiometric Considerations in Remote
Sensing Systems. F. G. Goetz
12. On Optimum Design of Remote Sensing and
Data Analysis Systems. J. E. Conel &
H. R. Long
14. Potential of Multisensor Data and Strategies
for Data Acquisition and Analysis. D. Evans &
R. Blom
18. Geologic Utility of Improved Orbital
Measurements A. R. Gillespie
20. Middle Infrared Remote Sensing
For Geology. A. B. Kahle
30. Airborne Infrared Mineral Mapping
Survey of Marysvale, Utah. W. Collins &
S. H. Chang
65. Effects of Spatial Resolution. M. Abrams
69. Effect of Aluminum Substitution on the
Reflectance Spectra of Hematite. R. V. Morris,
H. V. Lauer &
W. W. Mendell

73. Visible and Near-IR Spectral Reflectance
of Geologically Important Materials. R. B. Singer
82. Spatial and Spectral Resolution Necessary
for Remotely Sensed Vegetation Studies.B. N. Rock
87. Analysis of Lithology - Vegetation
Mixes in Multispectral Images. J. B. Adams,
M. Smith &
J. D. Adams
91. Geologic Utility of Improved Orbital Measurement
Capabilities in Reference to Non-Renewable
Resources. H. Stewart &
S. Marsh
96. Considerations Concerning Future
Satellite Experiments. G. L. Raines
100. A Next-Generation Mapping
Spectrometer R. B. Singer
105. Detection of Small Thermal Features
by Means of Two-Band Radiometry. H. H. Kieffer
- APPENDIX V: Working Papers for Image Science and Information
Science Working Groups
2. Registration Workshop Report H. K. Ramapriyan
31. Non-NASA Sensors M. S. Maxwell
40. MAPSAT Compared to Other Earth-
Sensing Concepts A.P. Colvocoresses
48. An Automated Mapping Satellite
System (MAPSAT). A.P. Colvocoresses
66. Design Tradeoffs for a Multispectral
Linear Array (MLA) Instrument. A. M. Mika
75. High Density Schottky Barrier IRCCD Sensors
for SWIR Applications at Intermediate
Temperature. H. Elabd &
T. S. Villani
86. Multispectral Linear Array (MLA) Science
and Technology Program W. L. Barnes
115. The Imaging Spectrometer Approach. J. B. Wellman
137. Imaging Spectrometer Technologies for
Advanced Earth Remote Sensing. J. B. Wellman,
et al.

- 145. I.R. Area Array Status J. Rode
- 171. Absolute Radiometric Calibration of
Advanced Earth Remote Sensing. P. N. Slater
- 177. JPL Airborne Instrument Activities,
An Overview. G. Vane
- 187. Airborne Multispectral Linear Array
Instruments at Goddard Space Flight
Center J. R. Irons,
J. C. Smith &
W. L. Barnes
- 195. NASA-NSTL Earth Resources Laboratory
Sensor Development J. Flanagan
- 204. Image Data Compression; Application
to Imaging Spectrometers R. F. Rice &
J. J. Lee
- 228. On-Board Image Compression T. J. Lynch
- 245. USGS Remote Image Processing
System (RIPS). E. Masouka
- 253. Image Processing via VLSI;
A Concept Paper. R. Nathan
- 286. Mixture Pixels P. Swain

APPENDIX I

PRESENTATION MATERIAL
FOR
MULTISPECTRAL IMAGING SCIENCE WORKING GROUP

JUNE 17, 1982

BOTANICAL SCIENCES TEAM
PRESENTED BY: C.J. TUCKER

BOTANICAL SCIENCES TEAM

MULTISPECTRAL IMAGING SCIENCE WORKING GROUP

APRIL 14-15, 1982 AT ORI

2
COCHAIRMAN: C. J. TUCKER (NASA) AND C. L. WIEGAND (USDA)

MEMBERS: G. BADWHAR (JSC), B. CIBULA (NSTL), E. CRIST (ERIM), C. DAURGHY (LARS),
R. FRASER (GSFC), D. KIMES (GSFC), D. PITTS (JSC), B. ROCK (JPL),
C. SCHNETZLER (GSFC), S. UNGAR (GISS/GSFC)

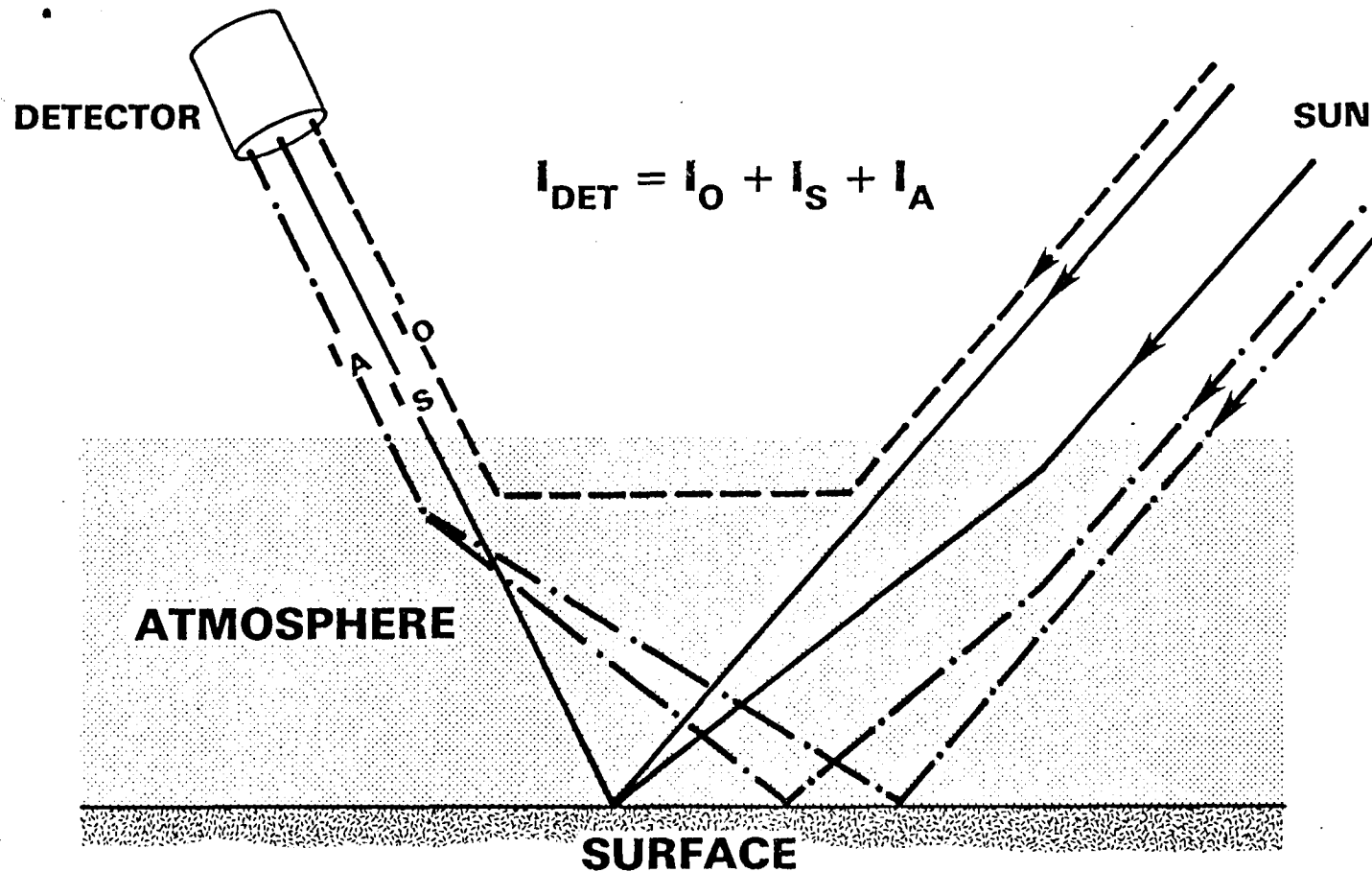
SIGNIFICANT IMPROVEMENTS IN THE ORBITAL ABILITY TO REMOTELY SENSE
VEGETATED TARGETS WILL RESULT FROM

- UNDERSTANDING OF ATMOSPHERIC EFFECTS
- APPROPRIATE SPATIAL RESOLUTION
- NARROW SPECTRAL BANDWIDTHS
- ADDITIONAL SPECTRAL BANDS
- TEMPORAL FREQUENCY OF 2-3 DAYS

EFFECTS OF THE ATMOSPHERE UPON RADIATIVE TRANSFER

- RESTRICT MOST BANDS TO ATMOSPHERIC WINDOWS
- VERTICAL AND HORIZONTAL DISTRIBUTION OF AEROSOLS, DUST, CONDENSATION NUCLEI, ICE CRYSTALS, WATER VAPOR, CLOUD DROPLETS, TRACE GASES, ETC. NEEDED
- RELATIONSHIP BETWEEN AVAILABLE METEOROLOGICAL DATA AND ATMOSPHERIC OPTICAL PARAMETERS NEEDS TO BE ESTABLISHED
- ADJACENCY EFFECTS UNDERSTANDING NEEDED
- CONCURRENT DETAILED SURFACE MEASUREMENTS, ATMOSPHERIC MEASUREMENTS, AIRCRAFT MEASUREMENTS, AND SATELLITE MEASUREMENTS NEEDED.
- POSSIBILITIES OF ATMOSPHERIC "SOUNDER" BANDS SHOULD BE INVESTIGATED

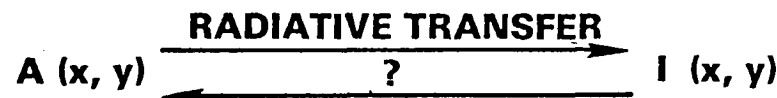
REMOTE SENSING OVER A NON-UNIFORM SURFACE



$$I_{DET} = I_O + I_S + I_A \quad \text{FOR AVERAGE CONDITIONS}$$

$$100\% = 48\% + 38\% + 14\% \quad \lambda = 0.55 \mu m, A = 0.1$$

- I_O —ATMOSPHERIC RADIANCE SCATTERED FROM THE SOLAR BEAM INTO THE DETECTOR
- I_S —THE "SIGNAL"—RADIANCE FROM THE TARGET ATTENUATED BY THE ATMOSPHERE
- I_A —THE DIFFUSE LIGHT SCATTERED FROM BRIGHT AREAS TO THE DARK AREAS (ADJACENCY EFFECT)



APPROPRIATE SPATIAL RESOLUTION FOR TASK AT HAND

- 10-30 M FOR HIGH SPATIAL FREQUENCY COVER TYPES FOR SMALL AGRICULTURAL PLOTS
- 500-5000 M FOR LARGE-SCALE EARTH FEATURES CONSISTANT WITH CLIMATE PHENOMENA
- TARGET SIZE DISTRIBUTIONS NEEDED
- ADJACENCY EFFECTS, "TEXTURAL" INFORMATION, ETC. WITH FINER SPATIAL RESOLUTIONS

MAJOR PLANT COMMUNITIES: AREA, NPP, AND C STORAGE*

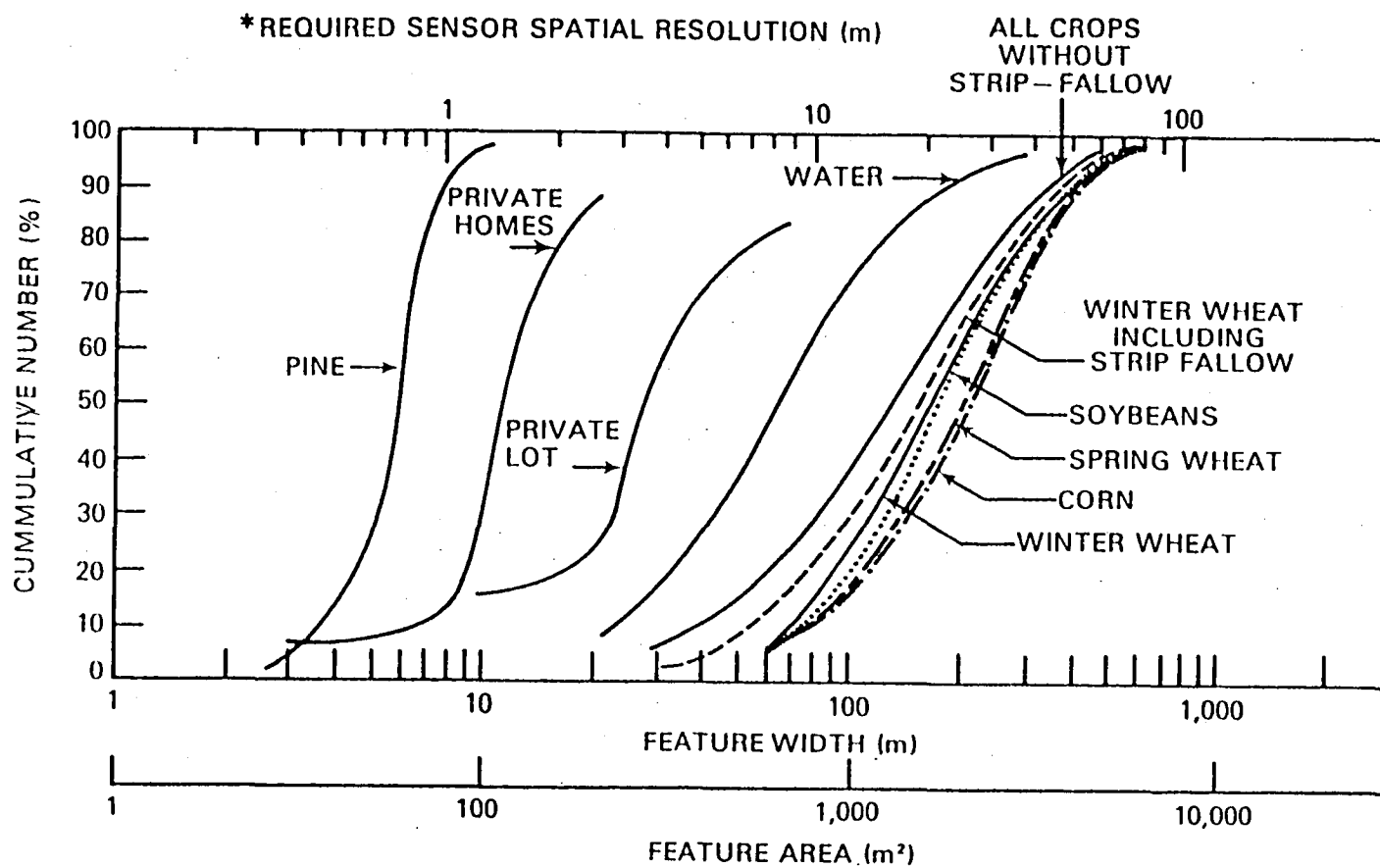
VEGETATION TYPE	AREA 10 ⁶ km ²	PERCENT OF LAND AREA	NPP 10 ¹⁵ g C yr ⁻¹	PERCENT OF NPP	PLANT MASS 10 ¹⁵ g C	PERCENT OF MASS
TROPICAL RAIN FOREST	17.0	11.4	16.8	31.8	344.0	41.6
TROPICAL SEASONAL FOREST	7.5	5.0	5.4	10.2	117.0	14.2
TEMPERATE EVERGREEN FOREST	5.0	3.4	2.9	5.5	79.0	9.6
TEMPERATE DICIDUOUS FOREST	7.0	4.7	3.8	7.2	95.0	11.5
BOREAL FOREST	12.0	8.1	4.3	8.1	108.0	13.1
WOODLAND AND SHRUBLAND	8.5	5.7	2.7	5.1	22.0	2.7
SAVANNA	15.0	10.1	6.1	11.6	27.0	3.3
TEMPERATE GRASSLAND	9.0	6.0	2.4	4.5	6.3	0.8
TUNDRA AND ALPINE MEADOW	8.0	5.4	0.5	0.9	2.3	0.3
DESERT SCRUB	18.0	12.1	0.7	1.3	5.9	0.7
ROCK, ICE, AND SAND	24.0	16.1	0.03	0.1	0.2	0.02
CULTIVATED LAND	14.0	9.4	4.1	7.8	6.3	0.8
SWAMP AND MARSH	2.0	1.3	2.7	5.1	13.5	1.6
LAKE AND STREAM	2.0	1.3	0.4	0.8	0.02	0.002
TOTAL CONTINENTAL	149.0	100.0	52.8	100.0	826.5	100.0

77%

*FROM: WHITTAKER AND LIKENS 1973.

SPATIAL INFORMATION CONTENT FOR RENEWABLE RESOURCES

SIZE DISTRIBUTION OF TYPICAL GROUND COVERS



(REFERENCE: AgRISTARS, L.MILLER,
J. BARKER AND R. WHITMAN , 1980)

* ASSUMES 8x8 PIXEL AREA CONTAINED
WITHIN SMALLEST FEATURE DESIRED
FOR ADEQUATE AREA MEASUREMENT

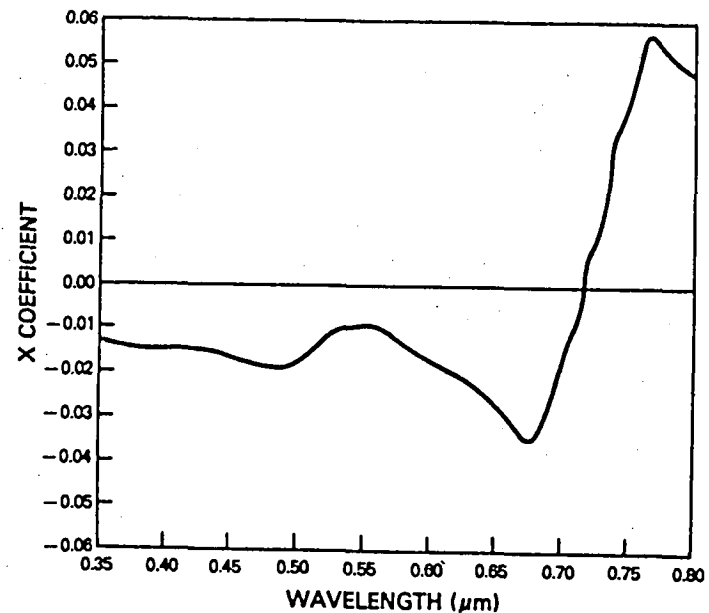
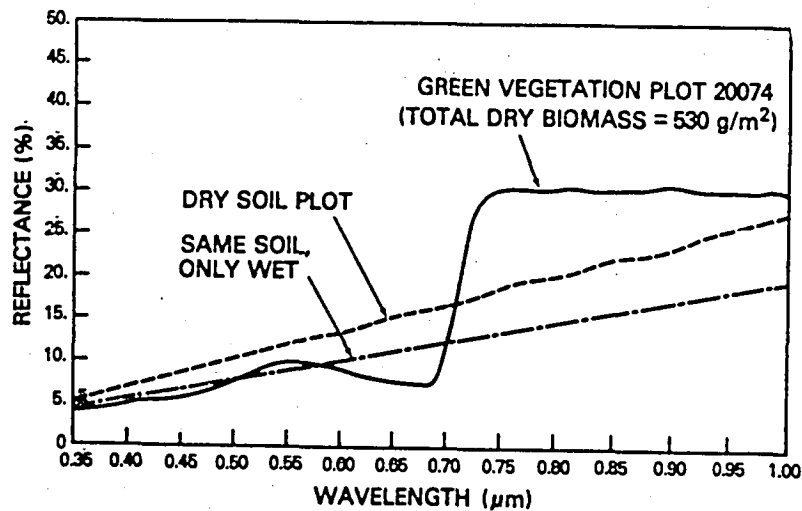
JLB/SCC



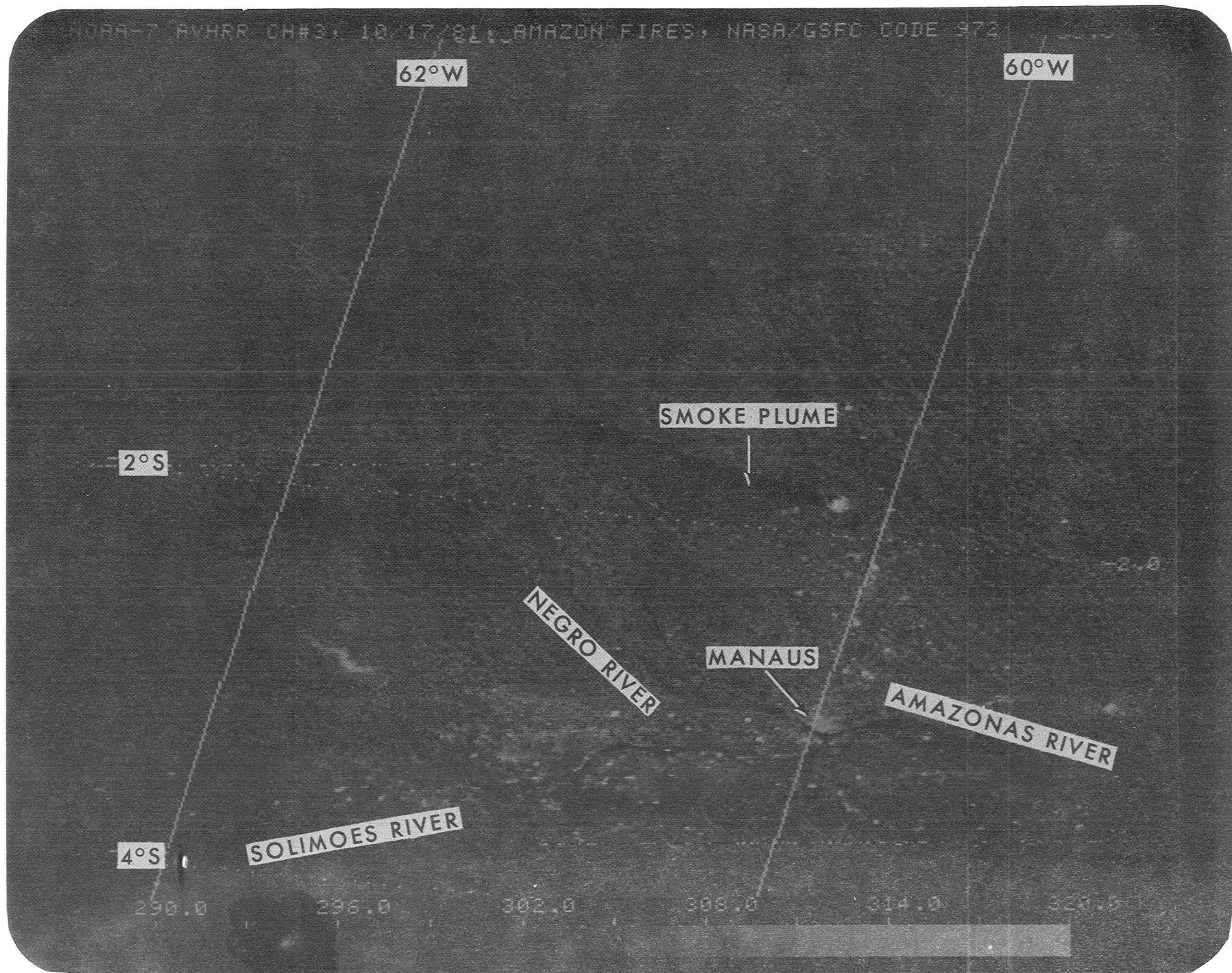
SPECTRAL RESOLUTION IMPROVEMENTS

- NARROW BANDWIDTHS TO MAXIMIZE SPECTRAL CONTRASTS AND MINIMIZE ATMOSPHERIC EFFECTS
- BANDS CENTERED AT ~ 0.44 , 0.55 , 0.66 , 0.85 , 1.65 , AND $2.2 \mu\text{M}$ FOR MONITORING GREEN LEAF VEGETATION
- $3.5\text{--}3.9 \mu\text{M}$ BAND FOR FIRE DETECTION AND $10.5\text{--}12.5 \mu\text{M}$ THERMAL BAND FOR CLOUD DETECTION
- ADDITIONAL RESEARCH NEEDED
 - HIGH RESOLUTION SPECTRAL DATA
 - DIRECTIONAL REFLECTANCE DISTRIBUTION
 - POLARIZATION
 - $0.75\text{--}0.78 \mu\text{M}$, $1.0\text{--}1.3 \mu\text{M}$, AND OTHER SPECTRAL REGIONS OF CONTROVERSY (I.E., NO CONSENSUS)
 - ATMOSPHERIC "SOUNDER" BANDS

WHY USE THE RED AND PHOTOGRAPHIC IR PORTIONS OF THE SPECTRUM?

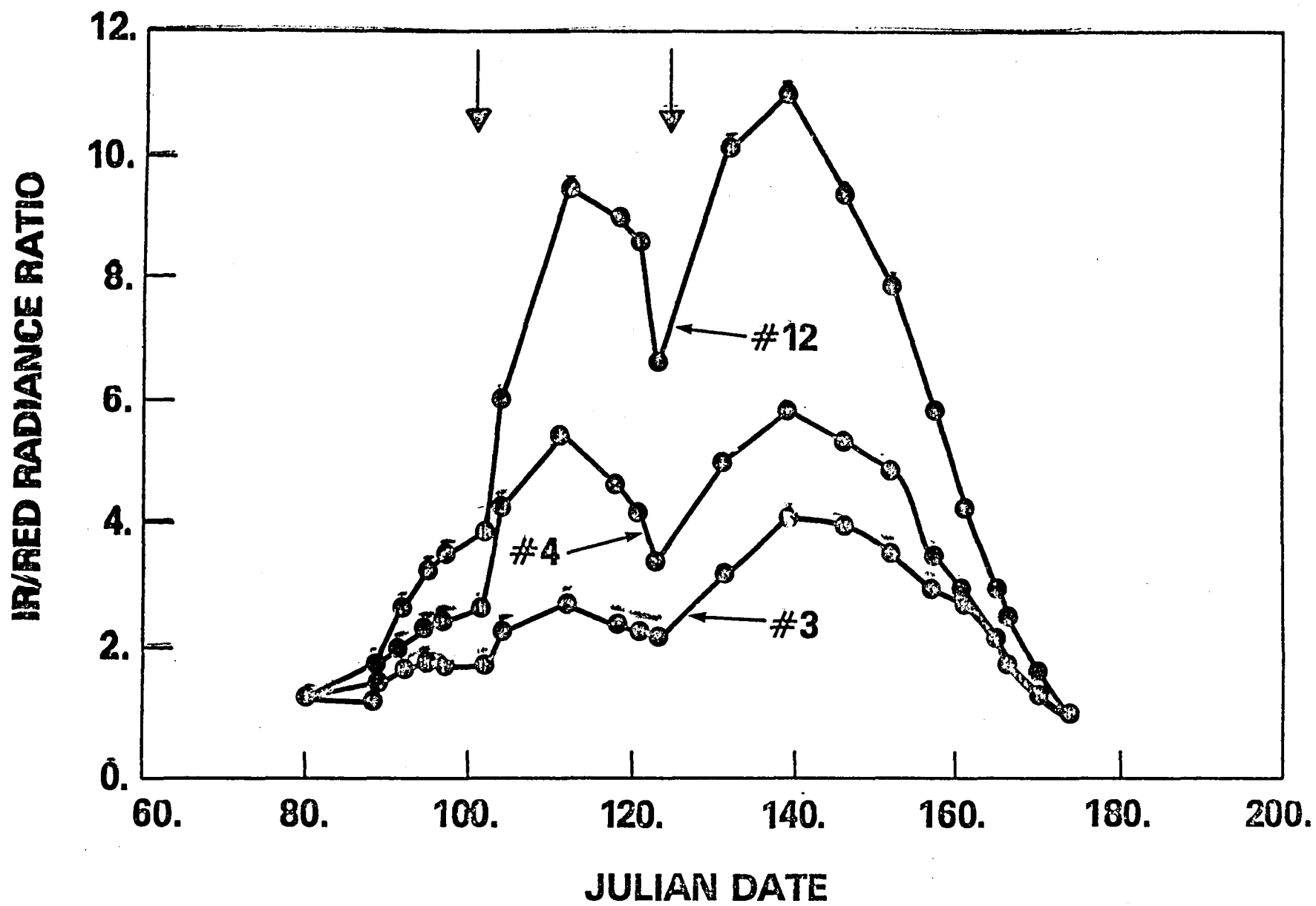


BECAUSE THE SOIL-VEGETATION CONTRAST IS AT A MAXIMUM FOR THESE REGIONS.



RADIOMETRIC AND TEMPORAL RESOLUTION REQUIREMENTS

- GOAL IS TO MAINTAIN RADIANCE/REFLECTANCE DIFFERENCES THROUGH RADIATIVE TRANSFER FOR RANGE OF VIEWING CONDITIONS
- DETERMINED BY ATMOSPHERIC EFFECT(S) UPON ORBITAL MEASUREMENT ACCURACY
- TEMPORAL FREQUENCY OF 4-6 DAYS NEEDED AT SELECTED TIMES
 - SENESCENCE
 - FLOWERING, HARVEST, ETC.
 - STRESS ONSET/RECOVERY
 - "ACTS OF GOD"
- ASSUMING CLOUD COVER PROBABILITY OF 50% LOWERS TEMPORAL FREQUENCY TO 2-3 DAYS AT SELECTED TIMES



GEOLOGY TEAM
PRESENTED BY: MARK SETTLE

MULTISPECTRAL IMAGING SCIENCE WORKING GROUP
GEOLOGY TEAM

LONG TERM RESEARCH RECOMMENDATIONS

- o LABORATORY RESEARCH
 - NEW METHODS OF FIELD SAMPLING
 - THEORETICAL MODELS OF MICROSCALE SPECTRAL MIXING
- o UTILITY OF IMPROVED SPATIAL RESOLUTION
 - MULTISTAGE FIELD EXPERIMENTATION EMPLOYING PORTABLE SPECTROMETERS, AIRBORNE SCANNERS, AND ORBITAL IMAGING INSTRUMENTS (MACROSCALE MIXING)
- o UTILITY OF IMPROVED SPECTRAL RESOLUTION
 - DEFINE SPECTRAL THRESHOLD FOR THE IDENTIFICATION OF SPECIFIC MINERAL SPECIES THROUGH HIGH RESOLUTION SURVEYS OF SELECTED TEST SITES
- o UTILITY OF IMPROVED RADIOMETRIC SENSITIVITY
 - CONDUCT MULTISPECTRAL SURVEYS OF SELECTED TEST SITES WITH VARIABLE SIGNAL QUANTIZATION (8-12 BIT)
- o GEOBOTANICAL REMOTE SENSING RESEARCH
 - SEPARATION OF GEOLOGICAL AND BOTANICAL SPECTRAL SIGNATURES IN INDIVIDUAL PICTURE ELEMENTS
 - EXPERIMENTAL LAB STUDIES OF GEOBOTANICAL CORRELATIONS THAT MORE FULLY SIMULATE NATURAL CONDITIONS
 - TEST SITE STUDIES DESIGNED TO TEST SPECIFIC GEOBOTANICAL HYPOTHESES

MULTISPECTRAL IMAGING SCIENCE WORKING GROUP

GEOLOGY TEAM

DESIRED MEASUREMENT CAPABILITIES OF THE NEXT GENERATION OF ORBITAL IMAGING SENSORS

	-----SPECTRAL REGION----- (WAVELENGTH, MICROMETERS)			
	<u>0.4-1.0</u>	<u>1.0-2.0</u>	<u>2.0-2.5</u>	<u>8-14</u>
SPECTRAL RESOLUTION	0.05um (selected 0.01um bands)	0.05um	0.02um	0.5um
SPATIAL RESOLUTION	30m	30m	30m	30m
RADIOMETRIC SENSITIVITY	-----1% of the incoming signal,-----			NEDT=0.2K at 300K
RADIOMETRIC CALIBRATION	-----RELATIVE-----			ABSOLUTE

MULTISPECTRAL IMAGING SCIENCE WORKING GROUP

GEOLOGY TEAM

NEAR TERM RECOMMENDATIONS CONCERNING FUTURE ORBITAL IMAGING CAPABILITIES

EXPERIMENTAL OBJECTIVES

- o EVALUATE THE COMBINED UTILITY OF NARROWBAND MULTISPECTRAL IMAGING IN BOTH THE VISIBLE AND INFRARED FOR LITHOLOGIC IDENTIFICATION OF GEOLOGIC MATERIALS
- o EVALUATE THE COMBINED UTILITY OF MULTISPECTRAL IMAGING IN THE VISIBLE AND INFRARED FOR LITHOLOGIC MAPPING ON A GLOBAL BASIS

GROUND RULES

- o RECOMMENDATIONS ARE FIRMLY BASED ON PAST RESEARCH RESULTS
- o RECOMMENDATIONS FOCUS ON DESIRED RESOLUTION AND SENSITIVITY, NOT ON SPECIFIC MEASUREMENT BANDS
- o RECOMMENDATIONS SPECIFY GENERIC MEASUREMENT CAPABILITIES DESIRED IN DIFFERENT SPECTRAL REGIONS, AND DO NOT REPRESENT A PROPOSAL FOR A MONOLITHIC SENSOR
- o TEAM DID NOT CONSIDER TECHNICAL DESIGN CHALLENGES OR ASSOCIATED DATA REDUCTION PROBLEMS

MULTISPECTRAL IMAGING SCIENCE WORKING GROUP

GEOLOGY TEAM

CURRENT LITHOLOGIC MAPPING CAPABILITIES

- o DISCRIMINATION OF IRON OXIDES BASED ON REFLECTANCE VARIATIONS IN THE VISIBLE AND NEAR INFRARED (0.5-1.0 MICROMETER WAVELENGTH REGION)
- o DISCRIMINATION OF CLAY MINERALS BASED ON REFLECTANCE VARIATIONS IN THE SHORTWAVE INFRARED (2.0-2.5 MICROMETER REGION)
- o DISCRIMINATION OF QUARTZ-BEARING ROCKS BASED ON EMISSIVITY VARIATIONS IN THE THERMAL INFRARED (8-12 MICROMETER REGION)
- o EXPERIMENTAL DETECTION OF GEOBOTANICAL STRESS BASED ON REFLECTANCE VARIATIONS IN THE VISIBLE AND REFLECTED INFRARED (0.5-2.0 MICROMETER REGION)

CURRENT LITHOLOGIC MAPPING CAPABILITIES

VISIBLE-NEAR IR (0.5-1.0 MICROMETERS)

IRON OXIDES

HEMATITE [Fe_2O_3]

GOETHITE [Fe O (OH)]

SHORTWAVE IR (2.0-2.5 MICROMETERS)

CLAY MINERALS

MONTMORILLONITE [$\text{Al}_2 \text{Si}_4 \text{O}_{10} (\text{OH})_2 \cdot n \text{H}_2\text{O}$]

KAOLINITE [$\text{Al}_4 \text{Si}_4 \text{O}_{10} (\text{OH})_8$]

ALUNITE [$\text{KAl}_3 (\text{SO}_4)_2 (\text{OH})_6$]

JAROSITE [$\text{K Fe}_3 (\text{SO}_4)_2 (\text{OH})_6$]

THERMAL IR (8-12 MICROMETERS)

SEDIMENTARY ROCKS

SILICATE VS. NON-SILICATE ROCKS

[SANDSTONES]

[CARBONATES]

[SILTSTONES]

[SHALES]

IGNEOUS ROCKS

OCCURRENCE AND RELATIVE PROPORTIONS OF
QUARTZ [SiO_2]

MULTISPECTRAL IMAGING SCIENCE WORKING GROUP

GEOLOGY TEAM

WORKSHOP OUTCOME

- o SUMMARY OF THE CURRENT STATE-OF-THE-ART
- o RECOMMENDATIONS CONCERNING NEAR-TERM EXPERIMENTAL IMAGING CAPABILITIES FROM ORBIT
- o LONGER TERM RESEARCH REQUIRED FOR THE DEVELOPMENT OF ADVANCED SENSORS DURING THE 1990'S

WORKSHOP ON THE USE OF FUTURE MULTISPECTRAL IMAGING CAPABILITIES FOR LITHOLOGIC MAPPING
CALIFORNIA INSTITUTE OF TECHNOLOGY
APRIL 20-21, 1982

MISWG GEOLOGY TEAM MEMBERS

MARK SETTLE*, NASA HEADQUARTERS

LARRY ROWAN, USGS (RESTON)

BOB SINGER, UNIVERSITY OF HAWAII

ANNE KAHLE, JPL

MIKE ABRAMS, JPL

BILL COLLINS, COLUMBIA UNIVERSITY

ALEX GOETZ, JPL

BILL KOWALIK, CHEVRON FIELD RESEARCH COMPANY

JOHN ADAMS*, UNIVERSITY OF WASHINGTON

INVITEES

HAROLD LANG, JPL

JIM CONEL, JPL

DIANE EVANS, JPL

HUGH KIEFER, USGS (FLAGSTAFF)

GARY RAINES, USGS (DENVER)

WENDELL MENDELL, NASA/JSC

ALAN GILLESPIE, JPL

HARRY STEWART, SUN EXPLORATION COMPANY

*CO-CHAIRMEN

GEOGRAPHIC SCIENCE TEAM
PRESENTED BY: NEVIN BRYANT

GEOGRAPHIC SCIENCE

CONCERN:

EARTH AS THE HOME OF MAN

PURSUIITS:

IDENTIFICATION, MAPPING, AND UNDERSTANDING THE
SPATIAL DISTRIBUTION, USE AND INTERRELATIONSHIP
OF PHENOMENA

RATIONALE FOR LAND USE/LAND COVER

- LAND USE/LAND COVER DATA REQUIRED TO ANALYZE SPATIAL PATTERNS AND THEIR DYNAMICS
 - BASIC EARTH SURFACE PHENOMENA
 - SURFACE EXPRESSION OF CRITICAL INTERFACE BETWEEN MAN AND THE EARTH PHYSICAL SYSTEM
- POTENTIAL USES:
 - BASE LINE
 - TREND ASSESSMENT
 - PREDICTIVE MODELS
- NEXT STEP:

LEVEL III CLASSIFICATION = QUANTUM STEP

 - MSS & TM SUPPORT LEVEL I & II
 - ACHIEVABLE

RATIONALE FOR GEOMORPHOLOGY

- GEOMORPHOLOGY IMPACTS MAN'S USE OF THE LAND
 - BASIC EARTH SURFACE PHENOMENA
 - STUDY OF FORM, COMPOSITION AND LONG-TERM PROCESSES (DECADES)
- POTENTIAL USES:
 - LAND CAPABILITY AND SUITABILITY
 - ENVIRONMENTAL IMPACT ASSESSMENT
 - PROCESS MODELS
- NEXT STEP:
 - INTERNALLY CONSISTENT, AREALLY EXTENSIVE DATA FOR QUANTITATIVE PROCESS ANALYSIS
 - ACHIEVABLE

RATIONALE FOR CARTOGRAPHY

- MAPS PRODUCTS 1:25,000 - 1:250,000 SCALE REQUIRED WORLDWIDE
 - 50 PERCENT OF LAND AREA IS NOT MAPPED TOPOGRAPHICALLY AT SCALES OF 1:100,000 OR LARGER
- POTENTIAL USES:
 - SURVEY AND MANAGEMENT OF RESOURCES
 - GEO-REFERENCED DATA BASES
 - DIGITAL TERRAIN DATA
- NEXT STEP:
 - GLOBAL CARTOGRAPHY SYSTEMS MEETING NATIONAL MAP ACCURACY STANDARDS AT 1:25,000
 - DIFFICULT

STATE-OF-THE-ART

- GEOGRAPHIC INFORMATION SYSTEMS UNDER DEVELOPMENT
 - REMOTE SENSING DATA
 - TERRAIN DATA
 - ANCILLARY DATA

- LAND USE/LAND COVER
 - LEVEL I AND II ACHIEVABLE WITH MSS AND TM
 - LEVEL III OBTAINED FROM HIGH RESOLUTION PHTOTGRAPHS UTILIZING LIMITED SPECTRAL REGIONS
 - DYNAMICS OF PHENOMENA LARGELY IGNORED

STATE-OF-THE-ART (CONT.)

- GEOMORPHOLOGY

- MSS AND TM USEFUL IN DELINEATING PHYSIOGRAPHIC REGIONS
- HIGH RESOLUTION AERIAL PHOTOGRAPHY PROVIDES THE QUANTITATIVE DATA FOR PROCESS ANALYSIS

- CARTOGRAPHY

- MSS CAN PROVIDE 1:250,000 HORIZONTAL PLANIMETRY
- TM UNTESTED
- FILM CAMERAS/5M RESOLUTION PROVIDES 1:50,000 HORIZONTAL PLANIMETRY (SKYLAB)

PRIORITIZED SUMMARY OF GEOGRAPHIC SCIENCE DATA GAPS

1. BASIC SPECTROMETER DATA (NOTE EXPERIMENTS)
 - SYSTEMATIC VARIATION IN SPATIAL RESOLUTION
 - NARROW WAVEBANDS; 0.3 - 12.4 MICRONS
 - VARIOUS CLIMATIC REGIMES AND ENVIRONMENTAL CONDITIONS
 - VARIOUS SEASONS
2. SPATIAL FREQUENCY INFORMATION ON COVER TYPES
3. ANALYZE INTERACTION OF SPATIAL RESOLUTION, TARGET HETEROGENEITY,
AND SPECTRAL SIGNATURES FOR COVER TYPES

PRIORITIZED SUMMARY OF GEOGRAPHIC SCIENCE DATA GAPS (CONT.)

4. DEVELOPMENT OF CLASSIFICATION APPROACHES THAT MAXIMIZE UTILITY OF HIGHER RESOLUTION DATA
5. TIME SERIES DATA ACQUISITIONS WITHIN CLIMATIC REGIMES TO ASSESS BOTH SEPARABILITY OF COVER TYPES AND LAND COVER CHANGES
6. ACCURATE REGISTRATION AND RECTIFICATION
 - G/S DATA BASE DEVELOPMENT
 - ANCILLARY DATA INTEGRATION
 - STEREO AND OFF-NADIR DATA ACQUISITIONS
7. DATA FROM VERY STABLE PLATFORMS FOR CARTOGRAPHIC APPLICATIONS

SUMMARY OF CANDIDATE EXPERIMENTS

I. LAND USE/LAND COVER

- URBAN/SUBURBAN LEVEL III LAND USE DESCRIMINATION
- URBAN VS. RURAL COVER TYPE DESCRIMINATION AND CHANGE
- SURFACE MINING OPERATIONS DESCRIMINATION & RECLAMATION MONITORING

II. GEOMORPHOLOGY

- PROCESSES INFLUENCING PERIGLACIAL LANDFORMS
- "CATOSTROPHIC" EVENTS EFFECT UPON LANDFORMS
- SEMIARID AND ARID LANDFORMS SPECTRAL AND SPATIAL CHARACTERIZATION AND ASSOCIATIONS
- DRAINAGE NETWORK AND DRAINAGE BASIN ANALYSIS

III. CARTOGRAPHY

- COMPARISON OF FILM, AREA-AND LINE-ARRAY DATA
- INTERRELATIONSHIPS BETWEEN TOPOGRAPHY, SUN ELEVATION AND AZIMUTH, AND VIEWING DIRECTION AS RELATED TO INFORMATION EXTRACTION

SUMMARY OF DATA REQUIREMENT FOR EXPERIMENT

I. LAND USE/LAND COVER

	URBAN LEVEL III	URBAN VS. RURAL III	SURFACE MINING III
FIELD SURVEYS	CRITICAL	CRITICAL	CRITICAL
SPECTRORADIOMETRY	CRITICAL	CRITICAL	CRITICAL
COLLATERAL DATA	YES	YES	YES
HIGH RES. PHOTOGRAPHY	CIR & PANCHROMATIC B&W	CIR	CIR
TEMPORAL REGISTRATION	(DYNAMICS 2 PIXELS)	(DYNAMICS 2 PIXELS)	(DYNAMICS 0.5 PIXEL)
RECTIFICATION	YES	YES	YES
BASE LINE SPATIAL RES.	5M	5M	5M
SPECTRAL REQ. **	0.4-12.4	0.4-12.4	0.4-12.4
TEMPORAL RES.	TIME SERIES	TIME SERIES	TIME SERIES
TERRAIN DATA *	N/A	N/A	YES
SPECIAL REQUIREMENTS	DIURNAL ACQUISITIONS	DIURNAL ACQUISITIONS	VARIATION IN LOOK ANGLES

* EITHER EXISTING DTM OR FLIGHT EXPERIMENT

** SPECIFIC BANDS TO BE DETERMINED

SUMMARY OF DATA REQUIREMENTS FOR EXPERIMENTS

II GEOMORPHOLOGY

	PERIGLACIAL	ARID	CATOSTROPHIC EVENTS	DRAINAGE
FIELD SURVEYS	CRITICAL	CRITICAL	CRITICAL	CRITICAL
SPECTRORADOMETRY	CRITICAL	CRITICAL	CRITICAL	CRITICAL
COLLATERAL DATA	YES	YES	YES	YES
HIGH RESOLUTION	CIR	NATURAL COLOR	NATURAL COLOR OR CIR	NATURAL OR CIR
PHOTOGRAPHY				
TEMPORAL REGISTRATION	N/A	N/A	0.5 PIXEL CAPABILITY	N/A
RECTIFICATION	YES	YES	CRITICAL	CRITICAL
BASE LINE SPATIAL RES.	5M	5M	5-30M	5M
SPECTRAL REQ.**	0.4-12.4	0.4-12.4	0.4-12.4	0.4-12.4
TEMPORAL RES.	3 FLIGHTS JUN-SEPT	EACH SEASON	EVENT DEPENDENT	EACH SEASON
TERRAIN DATA*	YES	YES	YES	YES
SPECIAL REQ.	NOON OVERFLIGHT	HIGH & LOW SUN ANGLES	EVENT DEPENDENT	NONE

* EITHER EXISTING DTM OR FLIGHT EXPERIMENT

** SPECIFIC BANDS TO BE DETERMINED

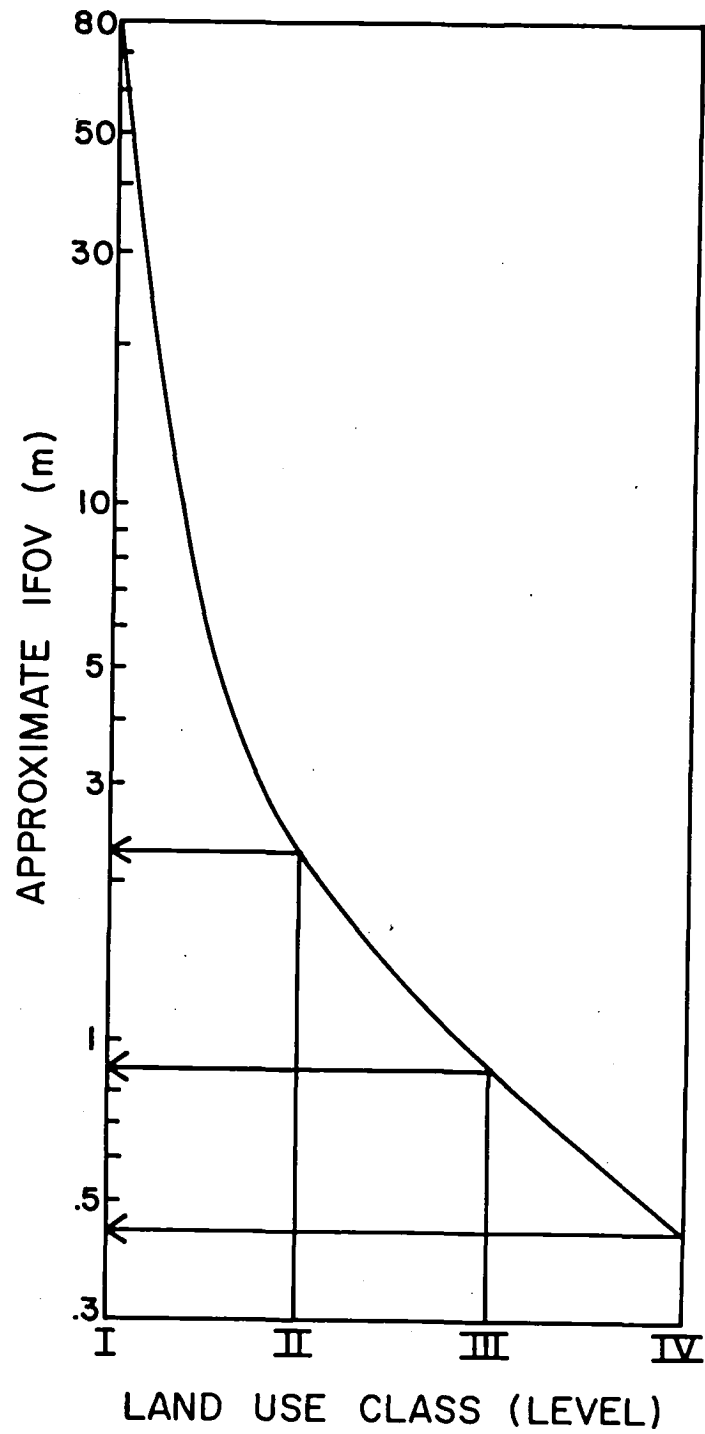
SUMMARY OF DATA REQUIREMENTS FOR EXPERIMENT

III CARTOGRAPHY

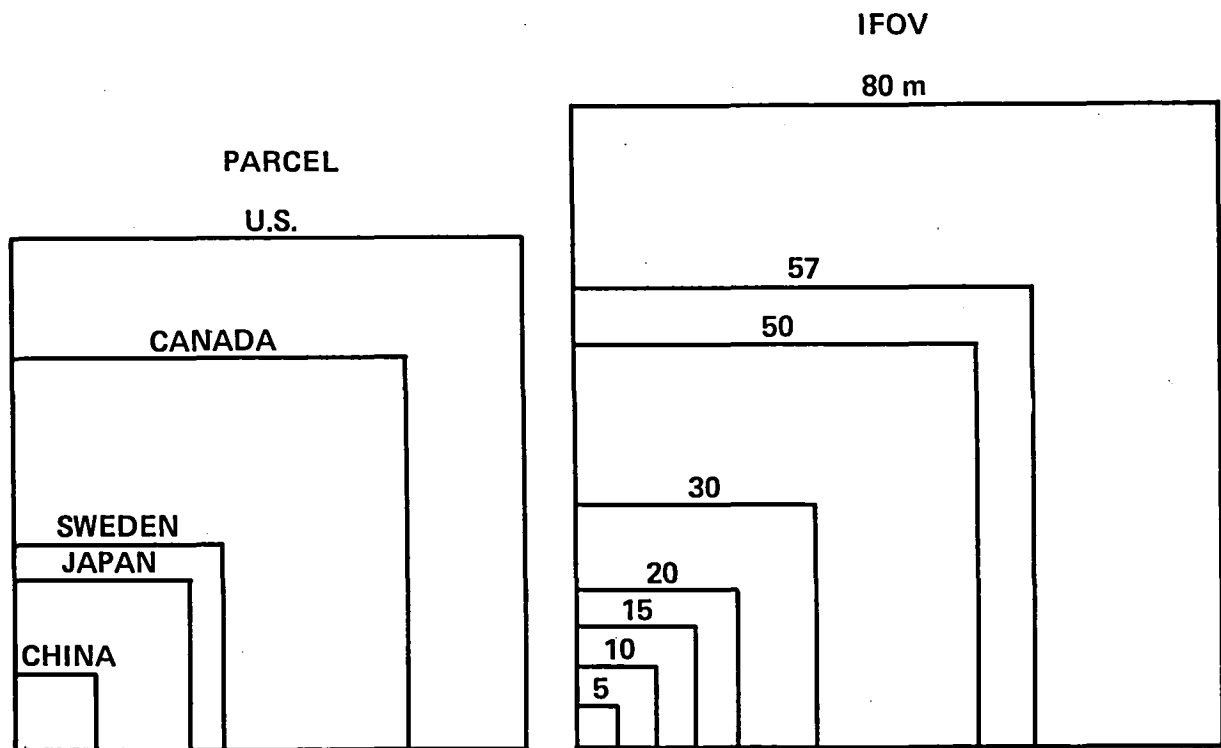
	SENSOR COMPARISON	INTERRELATIONSHIP ANALYSIS
FIELD SURVEYS	YES	N/A
SPECTRORADIOMETRY	N/A	N/A
COLLATERAL DATA	YES	YES
HIGH RES. PHOTOGRAPHY	B&W VISIBLE AND IR	B&W VISIBLE AND IR
TEMPORAL REGISTRATION	N/A	N/A
RECTIFICATION	CRITICAL	CRITICAL
BASE LINE SPATIAL RES.	2M	2M
SPECTRAL REQ.	VIS & NIR	NIR & NIR
TEMPORAL RES.	N/A	N/A
TERRAIN DATA	STEREO PAIRS	STEREO PAIRS
SPECIAL REQUIREMENTS	EXTREMELY STABLE PLATFORM	EXTREMELY STABLE PLATFORM

*Land use and land cover classification system for
use with remote sensor data*

Level I		Level II	
1 Urban or Built-up Land		11	Residential.
		12	Commercial and Services.
		13	Industrial.
		14	Transportation, Communi- cations, and Utilities.
		15	Industrial and Commercial Complexes.
		16	Mixed Urban or Built-up Land.
		17	Other Urban or Built-up Land.
2 Agricultural Land		21	Cropland and Pasture.
		22	Orchards, Groves, Vine- yards, Nurseries, and Ornamental Horticultural Areas.
		23	Confined Feeding Opera- tions.
		24	Other Agricultural Land.
3 Rangeland		31	Herbaceous Rangeland.
		32	Shrub and Brush Range- land.
		33	Mixed Rangeland.
4 Forest Land		41	Deciduous Forest Land.
		42	Evergreen Forest Land.
		43	Mixed Forest Land.
5 Water		51	Streams and Canals.
		52	Lakes.
		53	Reservoirs.
		54	Bays and Estuaries.
6 Wetland		61	Forested Wetland.
		62	Nonforested Wetland.
7 Barren Land		71	Dry Salt Flats.
		72	Beaches.
		73	Sandy Areas other than Beaches.
		74	Bare Exposed Rock.
		75	Strip Mines. Quarries, and Gravel Pits.
		76	Transitional Areas.
		77	Mixed Barren Land.
8 Tundra		81	Shrub and Brush Tundra.
		82	Herbaceous Tundra.
		83	Bare Ground Tundra.
		84	Wet Tundra.
		85	Mixed Tundra.
9 Perennial Snow or Ice		91	Perennial Snowfields.
		92	Glaciers.



SOURCE: WELCH (1978)

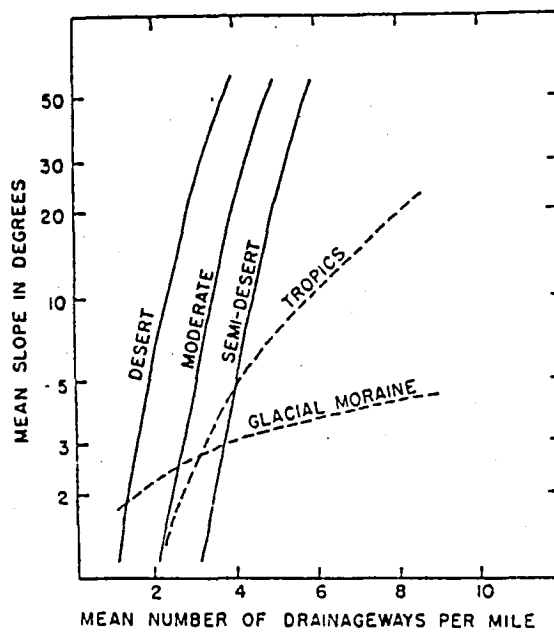


THE AVERAGE URBAN LAND PARCEL SIZES IN DIFFERENT COUNTRIES COMPARED TO IFOV's OF 5 TO 80 M. SPATIAL RESOLUTION REQUIREMENTS WILL VARY WITH GEOGRAPHIC REGION.

SOURCE: R. WELCH, UNIVERSITY OF GEORGIA

Classification of geomorphological features (after Tricart, 1965).

Order	Units of earth's surface in km ²	Characteristics of units, with examples	Equivalent climatic units	Basic mechanisms controlling the relief	Time-span of persistence
I	10 ⁷	continents, ocean basins	large zonal systems controlled by astronomical factors	differentiation of earth's crust between sial and sima	10 ⁸ years
II	10 ⁶	large structural entities (Scandinavian Shield, Tethys, Congo basin)	broad climatic types (influence of geographical factors on astronomical factors)	crustal movements, as in the formation of geosynclines. Climatic influence on dissection	10 ⁸ years
III	10 ⁴	main structural units (Paris basin, Jura, Massif Massif)	subdivisions of the broad climatic types, but with little significance for erosion	tectonic units having a link with paleogeography; erosion rates influenced by lithology	10 ⁷ years
IV	10 ²	basic tectonic units; mountain massifs, horsts, fault troughs	regional climates influenced predominantly by geographical factors, especially in mountainous areas	influenced predominantly by tectonic factors; secondarily by lithology	10 ⁷ years
limit of isostatic adjustments					
V	10	tectonic irregularities, anticlines, synclines, hills, valleys	local climate, influenced by pattern of relief; adret, ubac, altitudinal effects	predominance of lithology and static aspects of structure	10 ⁶ –10 ⁷ years
VI	10 ⁻¹	landforms; ridges, terraces, cirques, moraines, debris, etc.	mesoclimate, directly linked to the landform, e.g. nivation hollow	predominance of processes, influenced by lithology	10 ⁴ years
VII	10 ⁻⁶	microforms; solifluction lobes, polygonal soils, nebkas, badland gullies	microclimate, directly linked with the form, e.g. lapies (karren)	predominance of processes, influenced by lithology	10 ² years
VIII	10 ⁻⁸	microscopic, e.g. details of solution and polishing	micro-environment	related to processes and to rock texture	



Morphometry of major climatic regions (After Peltier, 1962).

U.S. NATIONAL MAP ACCURACY STANDARDS

- A. HORIZONTAL - 90% OF WELL-DEFINED POINTS SHALL BE PLOTTED (AT THE MAP SCALE) TO WITHIN ± 0.5 mm OF THEIR CORRECT POSITION, e.g.,

MAP SCALE = 1:100,000
 ± 0.5 mm AT MAP SCALE = ± 50 m ON GROUND

THUS, 90% OF POINTS MUST BE WITHIN ± 0.5 mm ON THE MAP AND ± 50 m ON THE GROUND.

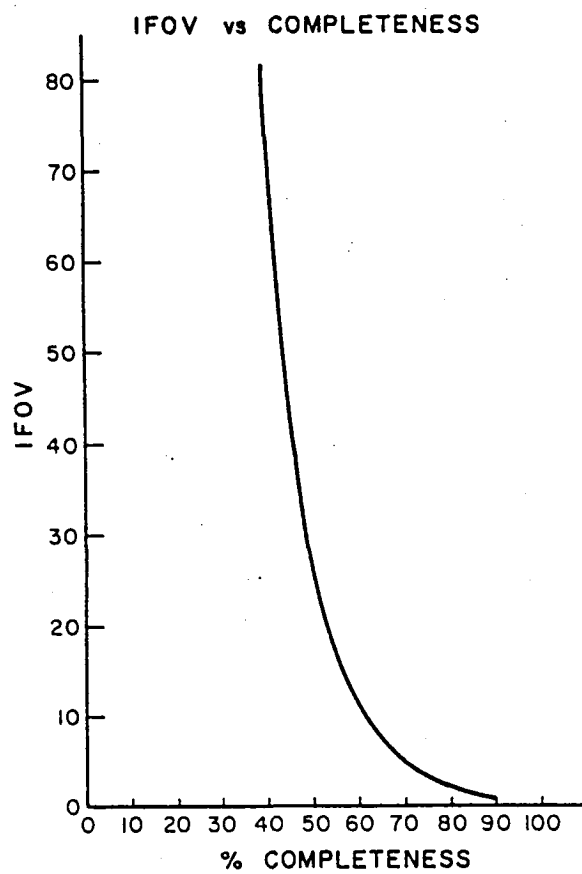
- B. VERTICAL - 90% OF THE ELEVATIONS DETERMINED FROM CONTOURS SHALL BE CORRECT TO WITHIN 1/2 THE CONTOUR INTERVAL (C.I.), e.g.,

C.I. = 100 m

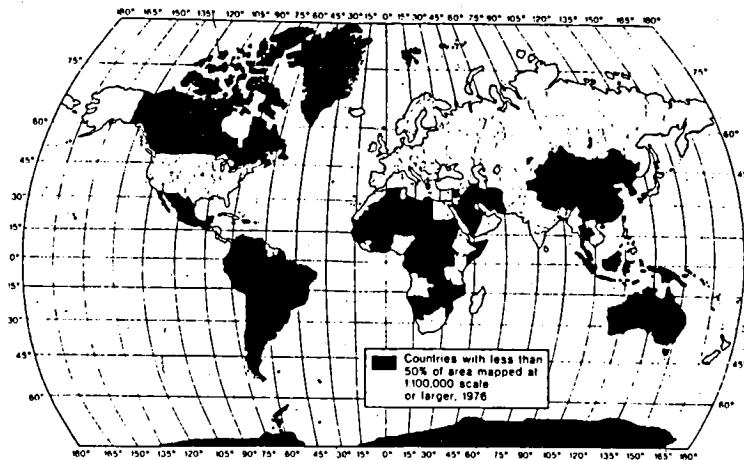
THUS, 90% OF ELEVATIONS REFERENCED TO CONTOURS SHALL BE CORRECT TO WITHIN ± 50 m.

ACCURACY OF GROUND CONTROL POINTS OBTAINED FROM MAPS MEETING NMAS

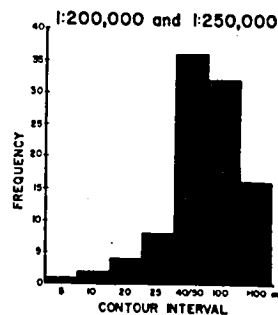
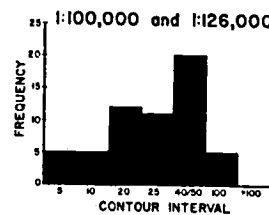
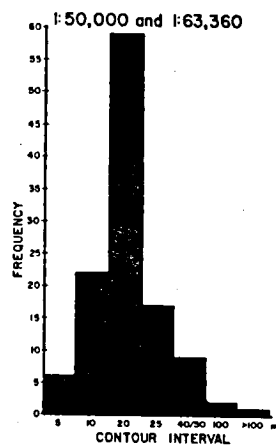
<u>SCALE OF MAP</u>	<u>HORIZONTAL RMSE</u>	<u>CONTOUR INTERVAL</u>	<u>(C.I./3.3-C.I./2)</u>
1:250,000	75 m	100 m	30-50 m
1:200,000	60	100	30-50
1:100,000	30	50	15-25
1:50,000	15	20	6-10
1:25,000	7.5	10	3-5



RW/UGA, 1982



THE SHADED AREAS REPRESENT COUNTRIES OR REGIONS WITH 50 PERCENT OR LESS OF THEIR AREA MAPPED AT 1:100,000 SCALE OR LARGER IN 1976 (UNITED NATIONS, 1976).



HISTOGRAMS OF CONTOUR INTERVALS FOR TOPOGRAPHIC MAPS AT SCALES OF 1:50,000, 1:100,000, AND 1:250,000 (UNITED NATIONS, 1976)

GEOGRAPHIC SCIENCE WORKSHOP
MULTISPECTRAL IMAGING SCIENCE WORKING GROUP

Dates: April 28-30, 1982

Location: Marriott Hotel
711 East Riverwalk
San Antonio, Texas 78205
(512) 224-4555

SCHEDULE

I. Wednesday afternoon, April 28, 1982 Salon A

Introduction

1:00-1:30pm	R. Whitman	Objectives of Working Group
	N. Bryant	Objectives of Workshop
1:30-2:15	G. Vane	Background on MLA Systems.

Justification and Requirements

2:15-3:00pm	R. Witmer	Level III Land use/Land Cover Classification Requirements.
3:00-3:45pm	R. Welch	National Map Accuracy Standards for Planimetry and Elevation Determination.
3:45-4:30pm	J. Estes	Geomorphology (Landform and Drainage Elements Detection.)

State of the Art

4:30-5:00pm	F. Sabins	Spatial and Spectral Resolution for Landform and Drainage Element Detection.
5:00-7:00pm	Dinner	
7:00-7:30pm	J. Clark	Spatial and Spectral Resolutions in an Urban Environment.
7:30-8:00pm	D. Williams	Summary of TMS Results.

8:00-8:30pm D. Quattrochi Spatial and Spectral Resolutions in Strip Mine Recognition.

II. Thursday, April 29, 1982 The Buoy Room

8:30-9:00am Organization of and Charge to Working Groups.

9:00am-12:00noon Break out into panels for initial discussions on requirements and state of the art.

12:00noon-1:00pm Lunch

1:00-2:30pm Panel writeups on requirements and state of the art.

2:30-4:30pm Viewgraph reviews on requirements and state of the art by panel chairmen with general discussion.

4:30-5:30pm Initial discussion on critical gaps in scientific knowledge and definition of candidate remote sensing experiments to further develop knowledge.

5:30-7:00pm Dinner

7:00-9:00pm Panel writeups on knowledge gaps and candidate experiments.

III. Friday, April 30, 1982 Salon A

8:30-10:00am Viewgraph reviews of knowledge gaps and candidate experiments by panel chairmen with general discussion.

10:00am-12:00noon Panels edit and expand upon general discussion for workshop documentation.

12:00noon-1:00pm Lunch

1:00-3:00pm Panel chairmen present highlights and select key summary tables, illustrations, and graphs.

3:00pm Executive Summary Draft
(N. Bryant and R. Whitman).

Panel: Cartography (R. Welch chairman)

Areas of Concern: Spatial and geometric resolution requirements for photographic/analog or digital photogrammetry from spaceborne MLA sensors. Of particular concern are the impacts of National Maps Accuracy requirements upon MLA system precision to determine planimetry/orthophoto mapping and elevation at various scales (1:250,000 to 1:24,000). An analysis of relief effects upon off-nadir viewing should also be made.

Panel Members:

Mr. Fred Billingsley
JPL

Dr. Steven Guphill
USGS

Dr. Roy Welch
Univ. of Georgia

Dr. Albert Zobrist
JPL

Panel: Land Use/Land Cover (R. Witmer chairman)

Areas of Concern: Spatial and spectral resolution requirements for photo interpretation and/or multispectral pattern recognition of cultural surface cover. Of particular interest are the recognition of man-made structures in urban and urban fringe regions. Other topics of interest include the delineation of and detection of changes in the landscape created by man's activities, such as strip mines, roads and railroads, and utility right of ways.

Panel Members:

Mr. Jerry Clark
JPL

Mr. Dale Quattrochi
NSTL

Mr. Leonard Gaydos
USGS

Mr. Darryl Williams
GSFC

Dr. Robert Holz
Univ. of Texas

Dr. Richard Witmer
USGS

Dr. John Jensen
Univ. of South Carolina

Panel: Geomorphology (J. Estes chairman)

Areas of Concern: Spatial and spectral resolution requirements for photo interpretation and/or multispectral pattern recognition of geomorphic elements. Of particular interest would be glacial and pariglacial landforms, eolian and coastal landforms, and karst topography. Manmade landform elements, such as berms, dikes, and levees should also be considered. Drainage elements of particular interest would include perennial and intermittent stream beds, flood plains, and alluvial fans. Manmade drainage elements, such as canals, diversion channels, and spreading basins should also be considered.

Panel Members:

Dr. Nevin Bryant
JPL

Dr. John Estes
Univ. California Santa Barbara

Dr. Charles Hutchinson
Univ. of Arizona

Ms. Leslie Morrissey
ARC

Charge to Panels:

Thursday Morning

1. Develop a position statement on the basic scientific rationale for the panel's areas of concern noting the potential role future missions with improved spatial and spectral resolution can play in supporting advancement of the discipline.
2. Develop a position statement on anticipated requirements, and the role for improved spatial and spectral resolution on future missions.
3. Outline the current state of the art in the application of remote sensing imagery (0.3-12.4 microns) to area of concern. Use the Wednesday discussions as a point of departure. Note the available reference material.

Thursday Afternoon

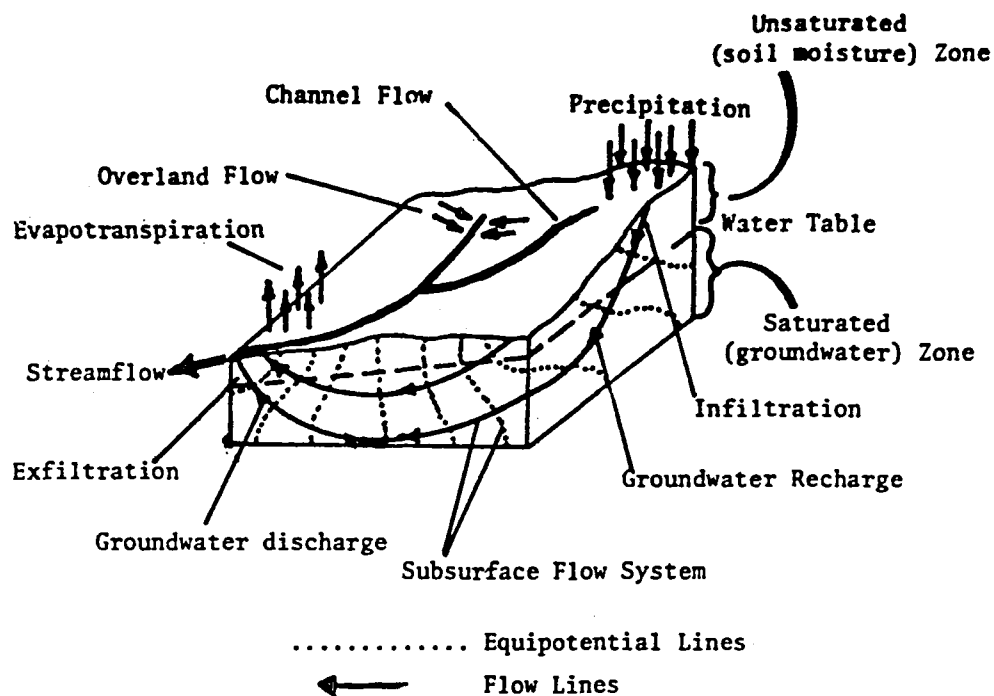
4. Identify areas where critical gaps in our knowledge of the potential contribution to be made by MLA spaceborne sensors.
5. Propose experiments that should be conducted to test and document areas of concern regarding the potential for MLA imaging systems. This should include synthetic and standardized data sets, airborne, shuttleborne, and free-flyer experiments. Note the spatial and spectral resolution requirements and repeat visit cycle requirements that should provide the most valuable information content. Note the probable nature of data use (i.e. digital modelling, photo-interpretation, multispectral classification).
6. Identify research tasks that the panel feels should be pursued to enhance near and medium range capabilities. Recommend levels of effort (man-years, dollars) and task duration. Prioritize the research tasks.

HYDROLOGY TEAM
PRESENTED BY: ROBERT RAGAN

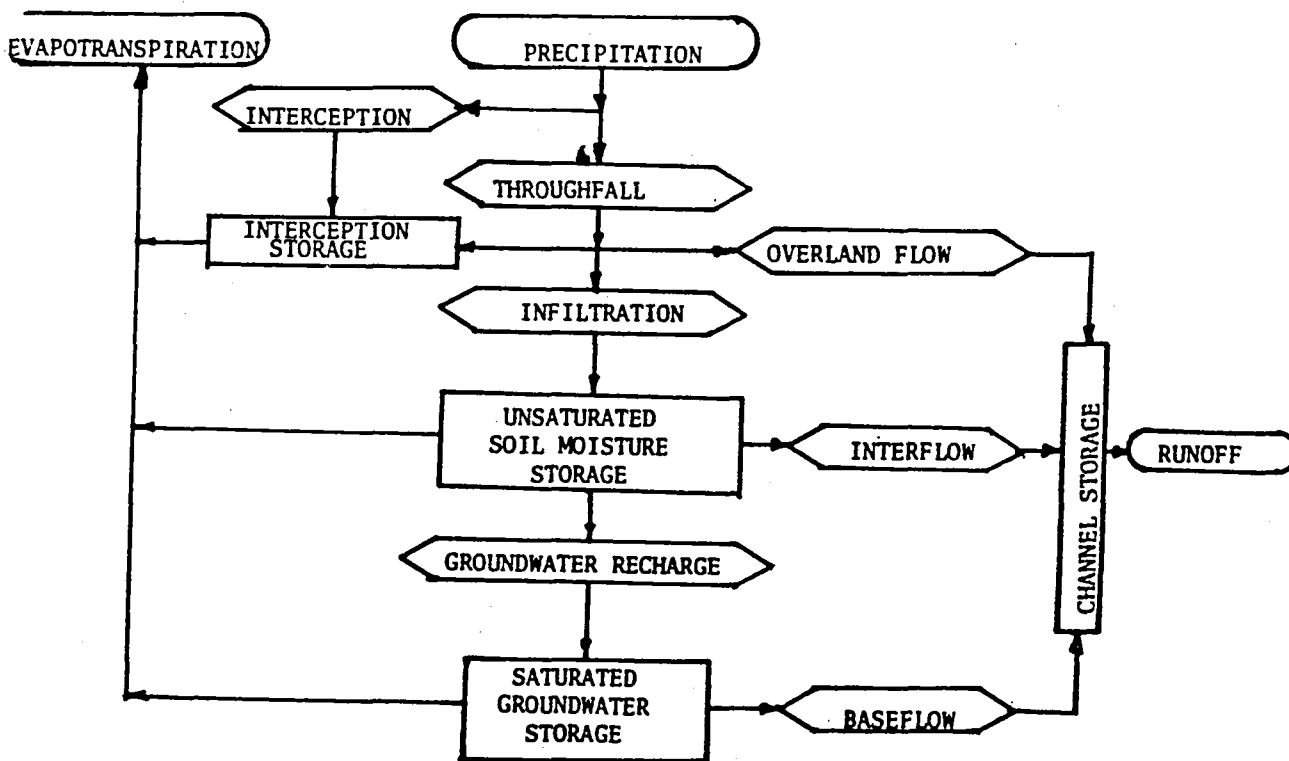
THE DEVELOPMENT AND MANAGEMENT OF HIGH QUALITY HUMAN
HABITATION ON A TERRESTRIAL SCALE IS CONTINGENT ON THE
RESOLUTION OF INCREASINGLY COMPLEX ISSUES RELATED TO THE
DEVELOPMENT AND MANAGEMENT OF A LIMITED WATER RESOURCE.

HYDROLOGY

- **HYDROLOGY IS AN EARTH SCIENCE CONCERNED WITH THE OCCURRENCE, DISTRIBUTION, MOVEMENT, AND PROPERTIES OF THE WATERS OF THE EARTH AND THEIR ENVIRONMENTAL RELATIONSHIPS.**
- **THE HYDROLOGIST MUST PROVIDE QUANTITATIVE INFORMATION ON THE TEMPORAL/SPATIAL DISTRIBUTION OF WATER FOR THE PLANNING, DESIGN AND OPERATIONS/MANAGEMENT DECISION MAKING PROCESSES USING:**
 - HISTORICAL RECORDS**
 - REAL TIME DATA**
 - STATISTICAL ANALYSIS**
 - SYSTEM SIMULATION**



HYDROLOGIC PROCESSES IN A WATERSHED



TYPICAL HYDROLOGIC MODEL STRUCTURE

● MISSION AREAS: MUNICIPAL/INDUSTRIAL WATER SUPPLY

IRRIGATION

FLOOD/DROUGHT CONTROL

QUALITY MAINTENANCE

ENERGY

RECREATION

● PROCESSES: PRECIPITATION

SNOW PACK

SOIL MOISTURE

SURFACE STORAGE

GROUNDWATER

EVAPO-TRANSPIRATION

STREAMFLOW

GENERAL PROBLEMS

- **CURRENT INFORMATION GATHERING TECHNIQUES PROVIDE VERY LIMITED DEFINITION OF THE SYSTEM**
- **SIMULATION MODELS ARE DELIBERATELY DESIGNED TO USE LIMITED DATA**
- **SPATIAL/TEMPORAL DEFINITION IS EXTREMELY LIMITED**
- **ABILITY TO DEFINE THE STATE OF INDIVIDUAL PROCESSES IS LIMITED**
- **MODELS DO NOT REFLECT STATE OF THE ART KNOWLEDGE BECAUSE OF DATA DEFINITION PROBLEMS**

MAJOR PROBLEM AREAS REQUIRING
MULTISPECTRAL IMAGING-BASED
RESEARCH TO ADVANCE SCIENCE

- A • DEFINITION OF SPATIALLY DISTRIBUTED EVAPOTRANSPIRATION RATES FOR LARGE AREAS
- E • FLOODING DYNAMICS OF WETLANDS
- A • DEFINITION OF TEMPORAL/SPATIAL DISTRIBUTION OF SOIL MOISTURE DYNAMICS IN LARGE AREAS
- B • DETERMINATION OF SNOW WATER EQUIVALENT
- G • DEFINITION OF RUNOFF AND SEDIMENT YIELD FROM UNGAGED WATERSHEDS
- A • DETERMINATION OF SPATIAL/TEMPORAL DISTRIBUTIONS OF STORM RAINFALL
- C • RELATIONSHIP BETWEEN REMOTELY MEASURED SURFACE ROUGHNESS AND HYDRAULIC ROUGHNESS OF LAND SURFACES AND STREAM NETWORKS
- C • DEFINITION OF HYDROLOGIC PROPERTIES OF SOILS AND SURFICIAL MATERIALS
- D • INTERPRETATION OF ACTIVE/PASSIVE MEASUREMENTS OF FLOURSCENCE AND POLARIZATION OF WATER AND ITS CONTAINED SUBSTANCES
- D • DETERMINATION AND MODELING OF THREE DIMENSIONAL CHARACTERISTICS OF WATER BODIES
- C • INTERPRETATION OF SPECTRAL EMISSIVITY OF LAND AND WATER SURFACES
- C • DETERMINATION OF THE RELATIONSHIP BETWEEN TEXTURE OF TERRAIN AND THE HYDROLOGIC RESPONSE OF WATERSHEDS
- D • DISCRIMINATION BETWEEN SEDIMENT AND CHLOROPHYLL IN WATER
- C • IMPROVING THE DETERMINATION OF HYDROLOGIC LAND COVER AS RELATED TO THE MODELING OF THE RUNOFF PROCESSES
- A • IMPROVING IRRIGATION MANAGEMENT STRATEGIES
- F • ROLE OF BARRIER ISLAND DYNAMICS IN COASTAL ZONE PROCESSES

A. Water Balance Problems Centering on Surface/Atmosphere Interfoces

B Unique Problem Area

C. Basin Physiography

D. Water Quality

E & F Unique Problem Areas

G. Objective of A-E is to provide scientific base to allow significant improvement in modeling

INFORMATION SCIENCE TEAM

PRESENTED BY: FRED BILLINGSLEY

INFORMATION EXTRACTION AND DATA HANDLING

OBJECTIVES

- HELP IDENTIFY BOUNDS OF PRACTICAL MISSIONS
- IDENTIFY DATA HANDLING AND ANALYSIS SCENARIOS
- IDENTIFY AND SUPPLY THE REQUIRED ENABLING TECHNOLOGY
- IDENTIFY AND SUPPLY THE DESIGN DATA BASE FOR PARAMETER SELECTION

INFORMATION EXTRACTION AND DATA HANDLING

AREAS OF CONCERN

- DATA HANDLING ASPECTS OF SYSTEM DESIGN
- ENABLING TECHNOLOGY FOR DATA HANDLING
- ENABLING TECHNOLOGY FOR ANALYSIS

INFORMATION EXTRACTION AND DATA HANDLING

INFORMATION EXTRACTION MILIEU - POTENTIAL MODES

- SUPPORT TO INDIVIDUAL P.I. RESEARCH
- ORGANIZED SUPPORT TO RESEARCH TASKS
- DESIGN OF SYSTEMATIC RESEARCH PROGRAM DATA SYSTEM
- SUPPORT TO RESEARCH DATA SYSTEM OPERATION

INFORMATION EXTRACTION AND DATA HANDLING

COMMON THEMES - ANALYSIS

- ANALYSIS OF ATMOSPHERE PROBLEMS NEEDS SOLUTION
- EFFECTS OF BETTER RESOLUTION (SPATIAL, SPECTRAL) PROMISING BUT UNPROVEN
- REGISTRATION PROBLEMS WILL BE WORSE WITH SMALLER PIXELS
- OFF-NADIR VIEWING PROMISING, BUT WILL ADD NEW PROBLEMS
- GEOGRAPHIC INFORMATION SYSTEM DEVELOPMENT NEEDED TO ALLOW ANALYSIS TASKS TO CONCENTRATE ON ANALYSIS

INFORMATION EXTRACTION AND DATA HANDLING

COMMON THEMES - DATA HANDLING

- PARAMETER SELECTION FOR RESEARCH SYSTEM NEEDS DATA BASE
- RESEARCH SCENARIOS WILL BE DIFFERENT THAN OPERATIONAL SCENARIOS
- RESEARCH PROGRAM WILL COLLECT LARGE AMOUNTS OF DATA -
DATA HANDLING MUST BE EFFICIENT
- VLSI AND OTHER NEW TECHNOLOGIES MUST BE ADAPTED TO REMOTE
SENSING RESEARCH NEEDS

INFORMATION EXTRACTION AND DATA HANDLING

SYSTEM DESIGN

STATUS

- PRESENT SYSTEM (LANDSAT) IS SURVEY-MODE WITH CENTRALIZED PROCESSING AND ARCHIVE
- DATA DELIVERY IS MANUAL (TAPE), SLOW
- MINIMAL SPECIAL PROCESSING AVAILABLE
- LITTLE DATA OTHER THAN FROM MSS AVAILABLE

CONTRIBUTING FACTORS

- SYSTEM IS EXPERIMENTAL BUT OPERATIONAL USE IS ATTEMPTED
- OPEN SKIES IMPLIES MORE DATA PROCESSING THAN OTHERWISE NEEDED
- DATA ANALYSIS HAS CONCENTRATED ON LANDSAT DATA

INFORMATION EXTRACTION AND DATA HANDLING

SYSTEM DESIGN

CRITICAL ISSUES

- INCREASING DATA RATES WILL MAKE FUTURE SYSTEM DESIGN MORE CRITICAL
- PRODUCTION EFFICIENCIES MUST BE EVALUATED EVEN IN AN EXPERIMENTAL SYSTEM
- NO DESIGN DATA BASE FOR FUTURE MISSION DESIGN
- DATA FORM CAUSES USER PROBLEMS, PARTICULARLY IN REGISTRATION

RECOMMENDATIONS FOR INVESTIGATION

- ALTERNATE SYSTEM ARCHITECTURES NEED STUDY
- PROVIDE DATA BASE FOR DESIGN OF FUTURE MISSIONS
- INCLUDE USER INFORMATION EXTRACTION MODELS IN SYSTEM DESIGN
- PROVIDE DATA IN OPTIMUM FORM

INFORMATION EXTRACTION AND DATA HANDLING

DATA HANDLING TECHNOLOGY

STATUS

- DECREASING MEMORY COSTS ALLOW MORE COMPUTER MEMORY AND THE RELATED INCREASED PROCESSING CAPABILITY
- MICROPROCESSOR CAPABILITIES INCREASING RAPIDLY
- NEW STORAGE MEDIUM (DIGITAL VIDEO DISKS) IMMINENT
- VERY LARGE SCALE INTEGRATED CIRCUIT (VLSI) TECHNOLOGY IMPROVING, BUT NO DEVELOPMENTS PARTICULARLY FOR REMOTE SENSING

CONTRIBUTING FACTORS

- SALES VOLUME FOR REMOTE SENSING NOT SUFFICIENT TO DRIVE THE TECHNOLOGY

INFORMATION EXTRACTION AND DATA HANDLING

DATA HANDLING TECHNOLOGY

CRITICAL ISSUES

- INCREASING DATA RATES WILL OVERLOAD PRESENT-TECHNOLOGY SYSTEMS
- PRESENT SYSTEM DESIGN, BASED ON MAG TAPE, HINDERS RANDOM ACCESS
- SYSTEMS FOR HANDLING GEOGRAPHIC DATA IN INFANCY

RECOMMENDATIONS FOR INVESTIGATION

- NEW TECHNOLOGIES ALLOW NEW SYSTEM CONFIGURATIONS - DESIGN STUDIES NEEDED:
 - CENTRALIZED VS. DISTRIBUTED PROCESSING
 - ON-BOARD VS. GROUND PROCESSING
 - DATA COMPRESSION
 - VIDEO DISK TECHNOLOGY
 - VLSI
- SPONSOR THE DEVELOPMENT OF COMPREHENSIVE GEOGRAPHIC INFORMATION SYSTEMS

INFORMATION EXTRACTION AND DATA HANDLING

RECTIFICATION AND REGISTRATION

STATUS

- RECTIFICATION IS REQUIRED ON EVERY IMAGE
- REGISTRATION ACCURACY GENERALLY 0.5 TO 1.5 PIXELS
- PAUCITY OF WORLDWIDE MAPS PROHIBITS GEODETIC IMAGE LOCATION
- INTERPOLATION EFFECTS STILL NOT GENERALLY UNDERSTOOD/ACCEPTED
- LARGE AREA MOSAICKING IS TEDIOUS

CONTRIBUTING FACTORS

- EPHEMERIS AND ATTITUDE KNOWLEDGE IS INSUFFICIENT FOR GEODETIC LOCATION WITHOUT GROUND CONTROL
- GROUND CONTROL OFTEN NOT AVAILABLE, EVEN WITH MAPS
- INTRAIMAGE DISTORTIONS (E.G., LANDSAT-D) PARTICULARLY TROUBLESOME
- INTERPOLATION VARIABLY AFFECTS ANALYSIS

INFORMATION EXTRACTION AND DATA HANDLING

RECTIFICATION AND REGISTRATION

CRITICAL ISSUES

- INTRAIMAGE DISTORTIONS IN SENSOR MUST BE AVOIDED
- EPHEMERIS AND ATTITUDE KNOWLEDGE NEED IMPROVING
- CONTROL POINT CORRELATION NEEDS FURTHER STUDY
- REGISTRATION OF OFF-NADIR IMAGES WILL BE DIFFICULT
- FOR THE RELATED AIRCRAFT DATA, ATTITUDE KNOWLEDGE AND REGISTRATION ARE SEVERE PROBLEMS

RECOMMENDATIONS FOR INVESTIGATION

- DETERMINE HOW BEST TO USE CONTROL POINTS
- DETERMINE HOW TO VERIFY GEOMETRIC PERFORMANCE
- DETERMINE EFFECTS OF (VARIOUS) DATA COMPRESSION TECHNIQUES ON REGISTRATION
- FURTHER STUDY THE EFFECTS OF INTERPOLATION

INFORMATION EXTRACTION AND DATA

INFORMATION EXTRACTION ANALYSIS

STATUS

- LOW-DIMENSIONALITY ANALYSIS MATURING (SPECTRAL AND SPATIAL)
- HIGH-DIMENSIONALITY ANALYSIS PRIMITIVE (SPECTRAL AND SPATIAL)
- TEMPORAL ANALYSIS IS AD HOC; AGRICULTURE PHENOLOGIC STAGE ANALYSIS IS MATURING

CONTRIBUTING FACTORS

- REGISTRATION AND DATA HANDLING PROBLEMS HAVE HINDERED ANALYSIS EFFORTS, PARTICULARLY WITH MULTIREOLUTION DATA
- SENSOR AND DATA CHARACTERIZATIONS HAVE BEEN INCOMPLETE
- GENERALIZED MODELING TECHNIQUES ARE INADEQUATE
- EQUIPMENT DIVERSITY HINDERS INTERCHANGES

INFORMATION EXTRACTION AND DATA

INFORMATION EXTRACTION - ANALYSIS

CRITICAL ISSUES

- UTILITY OF ABSOLUTE RADIOMETRICALLY CALIBRATED DATA IS UNKNOWN
- UTILITY OF GREATER RADIOMETRIC RESOLUTION IS UNKNOWN
- UTILITY OF HIGHER SPATIAL RESOLUTION EXCITING BUT UNPROVEN
- UTILITY OF MORE SPECTRAL BANDS EXCITING BUT UNPROVEN
- HIGH-DIMENSIONALITY ANALYSIS PROMISING BUT DIFFICULT

RECOMMENDATIONS FOR INVESTIGATION

- CONDUCT EXPERIMENTS WITH PARAMETERS EXCEEDING EXPECTED MISSION PARAMETERS TO DETERMINE UTILITY THRESHOLDS
- PROVIDE METHODS FOR CROSS-DISCIPLINE FERTILIZATION
- DETERMINE BETTER WAYS OF CONVERTING ANALYSIS CONCEPTS TO SOFTWARE
- INVESTIGATE AND CHARACTERIZE TOTAL SYSTEM INCLUDING ATMOSPHERE
- INVESTIGATE THE USE OF HIGHER-DIMENSION ANALYSIS SUCH AS TEXTURE

INFORMATION EXTRACTION AND DATA HANDLING

INFORMATION EXTRACTION - ENABLING TECHNOLOGY

STATUS

- GEOMETRIC OPERATIONS AND MULTISPECTRAL CLASSIFICATION (ESPECIALLY) REQUIRE EXCESSIVE AMOUNTS OF COMPUTER TIME
- LARGE SYSTEM OPERATION IS EXPENSIVE; SMALL SYSTEMS ARE LIMITED
- SEVERAL MODERATE SIZE SYSTEMS ARE AVAILABLE, BASED ON GENERAL PURPOSE COMPUTERS
- GEOGRAPHIC INFORMATION SYSTEMS ARE USED BUT ARE SPECIALIZED, INFLEXIBLE, AND DIVERSE

CONTRIBUTING FACTORS

- REMOTE SENSING REQUIREMENTS NOT EXTENSIVE ENOUGH TO CAUSE SPECIALIZED TECHNOLOGY DEVELOPMENTS
- SOFTWARE DEVELOPMENT HAS NOT BEEN SPONSORED TO THE POINT WHICH WOULD COALESCE THE VARIOUS AD HOC SYSTEMS
- LACK OF DATA COMMONALITY STANDARDS HINDERS THE USE OF GEOGRAPHIC DATA

INFORMATION EXTRACTION AND DATA HANDLING

INFORMATION EXTRACTION - ENABLING TECHNOLOGY

CRITICAL ISSUES

- GEOGRAPHICAL PROCESSING ALGORITHMS AND THE EVER-INCREASING DATA SET SIZE ARE OUTSTRIPPING GENERAL PURPOSE COMPUTER CAPABILITIES
- LACK OF SOFTWARE AND DATA INTERCHANGE STANDARDS HINDER CROSS-FERTILIZATION

RECOMMENDATIONS FOR INVESTIGATION

- INVESTIGATE THE POSSIBLE ANALYSIS SOFTWARE MODIFICATIONS TO ALLOW THE USE OF VLSI
- INVESTIGATE POTENTIAL NEW COMPUTER ARCHITECTURES SUITABLE FOR GEOGRAPHIC (SPATIAL) PROBLEMS
- PROMOTE THE DEVELOPMENT OF MODULAR HARDWARE AND SOFTWARE TO ALLOW WIDER TECHNOLOGY INTERCHANGE
- INVESTIGATE/DEVELOP NETWORKING SYSTEMS TO ALLOW NON-LOCAL PROCESSING

INFORMATION EXTRACTION AND DATA HANDLING

. POTENTIAL SUPPORT MODE - SUPPORT TO INDIVIDUAL P.I.

- ENCOURAGE PI DATA COMMONALITY
- ASSIST PI DATA INTERCHANGE
- SPONSOR CROSS-DISCIPLINE RESEARCH

E.G., ATMOSPHERE STUDIES
OBJECT SIZE DISTRIBUTIONS
INTERPOLATION
REGISTRATION
OFF-NADIR VIEWING

INFORMATION EXTRACTION AND DATA HANDLING

POTENTIAL SUPPORT MODE - ORGANIZED SUPPORT TO RESEARCH TASKS

- PROVIDE CROSS DISCIPLINE DATA SOURCES (E.G., AIRCRAFT, SHUTTLE, ... INSTRUMENTS AND FLIGHT SUPPORT)
- PROVIDE COORDINATED DATA SETS VIA GEOGRAPHIC INFORMATION SYSTEMS
- FACILITATE CROSS DISCIPLINE DATA DISTRIBUTION
- DEVELOP VLSI FOR EFFICIENT DATA HANDLING
- SPONSOR CROSS DISCIPLINE RESEARCH (AS ABOVE)

INFORMATION EXTRACTION AND DATA HANDLING

POTENTIAL SUPPORT MODE - SYSTEMATIC DATA SYSTEM DESIGN

- GATHER THE DECISION DATA BASE TO ENABLE PARAMETER TRADEOFFS
- PERFORM TRADEOFF STUDIES SUCH AS:
 - ON BOARD VS. GROUND PROCESSING
 - DATA COMPRESSION TECHNIQUES
 - OPTIMUM BIT ALLOCATION (SPATIAL VS. SPECTRAL VS. QUANTIZATION)
 - SYSTEM MODE
- SPONSOR CROSS-DISCIPLINE RESEARCH
- DEVELOP ARCHIVAL/RETRIEVAL TECHNIQUES
- DEVELOP GIS, FORMATTING AND LABELING TECHNIQUES
- DEVELOP VLSI AND NEW SYSTEM ARCHITECTURE AS REQUIRED
- DEVELOP OTHER SYSTEM-ENABLING TECHNOLOGIES SUCH AS VIDEO DISKS
- DEVELOP TECHNIQUES FOR PROVIDING MULTITYPE DATA SETS

INFORMATION EXTRACTION AND DATA HANDLING

POTENTIAL SUPPORT MODE - SUPPORT TO SYSTEM OPERATION

- PROVIDE (AN) EFFICIENT ARCHIVAL/CATALOG/RETRIEVAL SYSTEM(S)
- PROVIDE EFFICIENT GIS, LABELING AND FORMATTING GUIDELINES
- IMPLEMENT NEW SYSTEM DESIGNS, WITH VLSI AS APPLICABLE
- PROVIDE SYSTEM CHARACTERIZATION

IMAGE SCIENCE TEAM

PRESENTED BY: KEN ANDO

RECOMMENDATIONS (TENTATIVE)

- THERE IS A PRESSING NEED FOR A AIRBORNE SPECTROMETER CLASS INSTRUMENT FOR FUNDAMENTAL RESEARCH IN THE NEW DOMAIN (FOR REMOTE SENSING) OF HIGH SPECTRAL AND SPATIAL RESOLUTION. ONE OR MORE AIRCRAFT SENSOR DEVELOPMENTS SHOULD BE INITIATED AS PART OF AN OVERALL AIRCRAFT MEASUREMENT RESEARCH PROGRAM.
- DEVELOP AND FABRICATE PORTABLE FIELD INSTRUMENTS, CONDUCT SUPPORTIVE TESTS, AND PROVIDE DATA FOR RESEARCH
- CONTINUE SCIENCE STUDIES TO CONVERGE THE SENSOR DESIGN AND PROVIDE AN IMPROVED SCIENCE BASIS AND RATIONALE FOR MLA TYPE SYSTEMS.
- DEVELOP SPECIFIC MISSION SCENARIOS WITH FURTHER INPUTS FROM THE DISCIPLINE PANEL AS PART OF THE FOLLOW-ON TO THE MSWIG EFFORT.
- FOSTER AN INVOLVEMENT OF A BROADER CROSS SECTION OF THE REMOTE SENSING COMMUNITY INCLUDING UNIVERSITIES TO DEVELOP A CONSTITUENCY AND ADVOCACY GROUP FOR THIS TECHNOLOGY.
- CONTINUE ON-GOING ENGINEERING AND CRITICAL DEVELOPMENTS IN AREAS SUCH AS WIDE FIELD OPTICS, FOCAL PLANES, AND SPECTRAL FILTER TECHNIQUES.
- DEVELOP A BETTER UNDERSTANDING OF THE TRADES AND INTERACTIONS BETWEEN THE GROUND AND SPACE SEGMENT FOR STRAWMAN SCENARIOS.

GSFC MLA PROGRAM ELEMENTS

- 0 TECHNOLOGY DEVELOPMENT
 - SHORTWAVE INFRARED (SWIR) HYBRID (HGCDTE) DETECTOR ARRAYS (2 CONTRACTS - \$4.5M EACH)
 - MONOLITHIC SWIR DETECTOR ARRAYS (\$950K)
 - VISIBLE/NEAR INFRARED DETECTOR ARRAYS (\$950K)
 - DESPOSITION OF SPECTRAL FILTERS ON DETECTOR ARRAYS (\$100K)
 - PASSIVE COOLERS (\$100K)
 - SPECTRAL BEAM SPLITTERS (\$45K)
- 0 INSTRUMENT/MISSION DESIGN STUDIES
 - INSTRUMENT DEFINITION STUDIES (4 CONTRACTS, \$450K EACH)
 - END-TO-END SYSTEM STUDIES (4 CONTRACTS, \$250K EACH)
- 0 SUPPORTING SCIENCE
 - SENSOR PARAMETER ANALYSIS
 - PERFORMANCE MODELING
- 0 IN-HOUSE CAPABILITY UPGRADE
 - SENSOR CONCEPT EVALUATION
 - DETECTOR ASSESSMENT LABORATORY
 - CALIBRATION SOURCE DEVELOPMENT
 - FIELD EXPERIMENTS

LAND REMOTE SENSING SYSTEM INDEX

INSTRUMENTS FLOWN

MSS - MULTI-
SPECTRAL
SCANNER
SYSTEM
(LANDSAT
1-3)

SMIR - SHUTTLE
MULTI-
SPECTRAL
RADIOMETER
(SHUTTLE
OSTA-2)

INSTRUMENTS UNDER DEVELOPMENT

TM - THEMATIC
MAPPER
(1982)

SPOT - HRV -
SYSTEME
PROBATOIRE
D'OBSERVA-
TION DE LA
TERRE (1984)

MESSR - MULTI-
SPECTRAL
ELECTRONIC
SELF-SCAN-
ING RADIO-
METER
(1985)

VTIR - VISIBLE AND
THERMAL
INFRARED
RADIOMETER
(1985)

INSTRUMENT CONCEPTS

MLA - MULTI-
SPECTRAL
LINEAR
ARRAY
(1987-)

SIR - SHUTTLE
IMAGING
SPECTRO-
METER
(A: 1987-)
(B: 1989-)

ISFF - IMAGING
SPECTRO-
METER
FREE-
FLYER
(1990-)

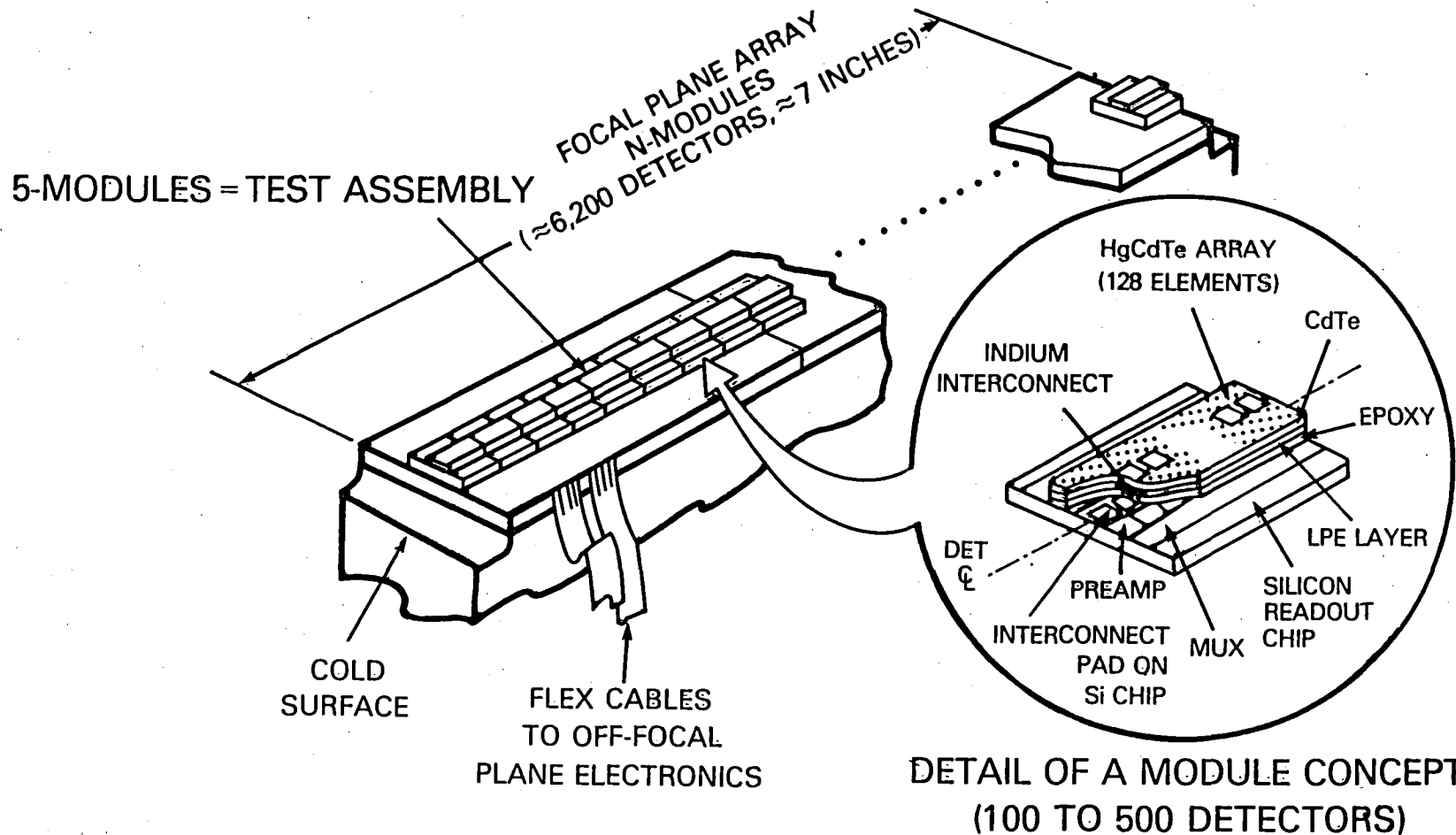
SMIR - SHUTTLE
MULTI-
SPECTRAL
INFRARED
RADIO-
METER
(II: 1985-)
(III: 1987-)

AIRCRAFT INSTRUMENTS

AIS - AIRBORNE
IMAGING
SPECTRO-
METER
(1982)

AVIRIS - ADVANCED
VISUAL AND
INFRARED
IMAGING
SPECTRO-
METER
(1985)

A CONCEPT HYBRID SWIR ARRAY



PRIMARY SWIR FPA DEVELOPMENT

OBJECTIVE:

- o DEVELOP A HgCdTe FOCAL PLANE FOR IMAGING IN THE 1-2.5 μ M SWIR BAND

APPROACH:

- o 42-MONTH TWO-PHASE DEVELOPMENT EFFORT
- o TWO CONTRACTS FOR PARALLEL 42-MONTH EFFORTS
- o ~\$5M PER CONTRACT

STATUS:

- o PROPOSALS FROM SBRC, HONEYWELL, AND ROCKWELL IN EVALUATION
- o DUAL AWARDS, CONTRACT STARTS IN EARLY 1983

INSTRUMENT REQUIREMENTS

• RADIOMETRIC

BAND	LARGEST FOV, M	MIN SNR
1	0.45-0.52	73
2	0.56-0.60	149
3	0.63-0.69	126
4	0.76-0.90	168
5	1.55-1.75	54
6	2.08-2.35	27

V
I
S
I
B
I
L
I
T
Y

• *NOMINAL ALTITUDE

10/20M OPTION

• CALIBRATION

ABSOLUTE END TO END
RELATIVE BAND TO BAND
WITHIN BAND

5%
10%
0.5%

• REGISTRATION

SEPARATION BAND 1-6
POSITION (KNOWLEDGE)
ARRAY LENGTH
BAND PARALLELISM

PIXELS, MAX

20.0
0.1
± 3.0
± 0.2

• POINTING ACCURACY

PRECISION

± 0.1
± 0.01

• POLARIZATION SENSITIVITY

7%

• MTF (NYQ)

30%

• MISSION

ORBITAL ALTITUDES

705 KM (NOMINAL)

470, 285 KM

(ALTERNATIVE)

ORBITAL INCLINATION

SUN SYNCHRONISM

EQUATOR CROSSING

9:30 TO 30 P.M.

COVERAGE

185 KM AT 705 KM, 15°

STEREO MODE

1/2 DE IN TRACK

MISSED SCENE MODE

30 CROSS TRACK

LIFE

5 YEAR (85%
PROBABILITY)

DATA LINKS

FWO (50 MBPS TO

DRS

DINE (100 MBPS DIRECT

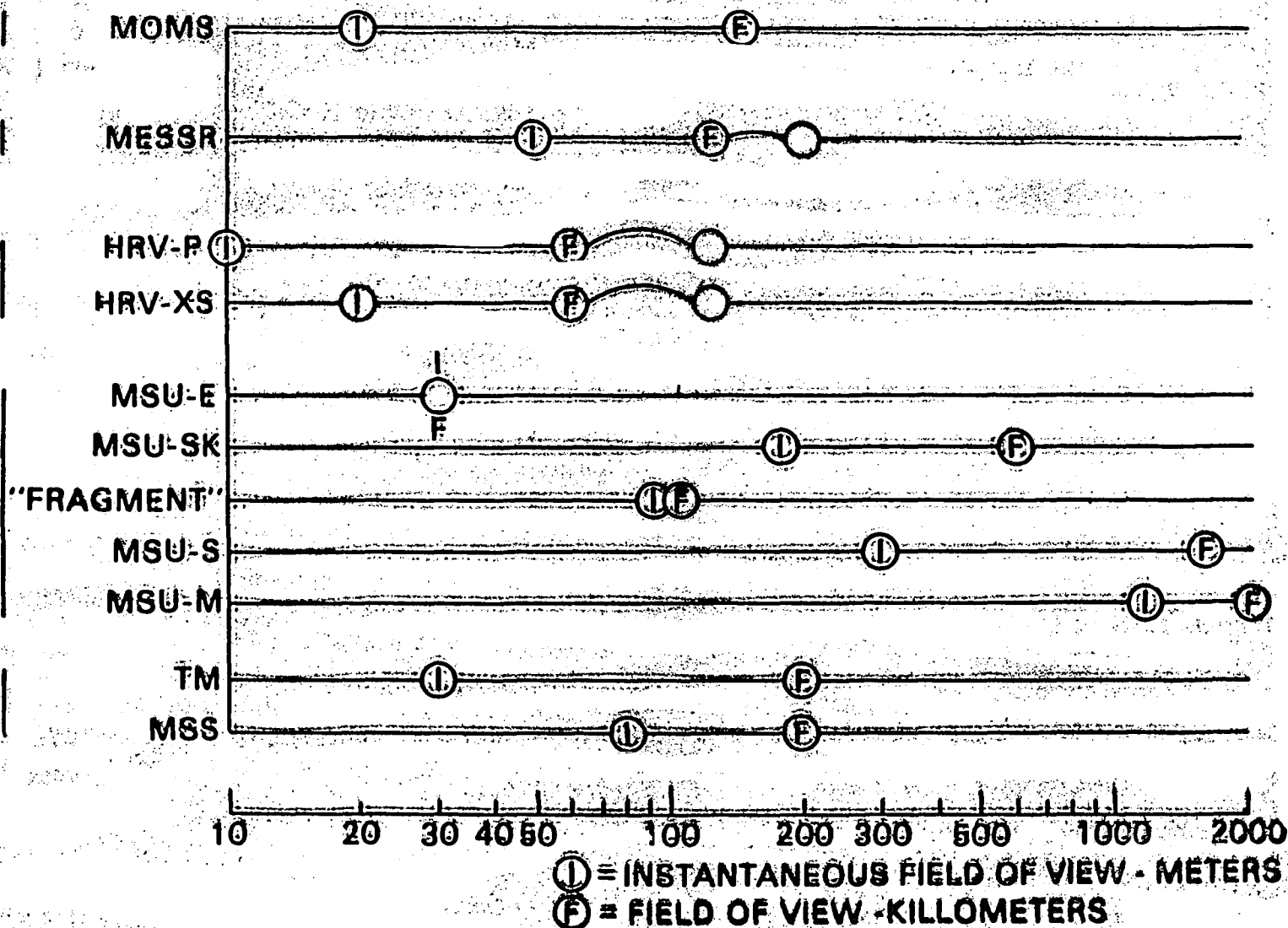
SHUTTLE LAUNCH

FOREIGN LAND OBSERVING SYSTEMS

<u>NAME/COUNTRY</u>	<u>LAUNCH DATE</u>	<u>GENERAL DESCRIPTION</u>	<u>RESOLUTION (M)</u>	<u>STATUS</u>
SPOT/FRANCE	MAY 1984 (ARIANE)	3 SPECTRAL BANDS & 1 PANCHROMATIC BAND; 60KM SWATH, SIDE-LOOKING STEREO CAPABILITY; 2 TAPE RECORDERS	20 MULTISPECTRAL 10 PANCHROMATIC	ENGINEERING MODEL IN TEST DATA COMMERCIAL- IZATION PLANNED BY CONSORTIUM \$500 TO \$1,000/DIGITAL SCENE SPOT 2 (1986), SPOT 3 (1989), AND SPOT 4 (1992) PLANNED TO ASSURE DATA CONTINUITY--SPOT 3 & 4 MAY ALSO CARRY SAR
MOMS/GERMANY	1982 (SHUTTLE) 1983 (SPACELAB)	2 SPECTRAL BANDS, 140KM SWATH OPTICALLY BUTTED RETICON ARRAYS DIRECT CONTOUR MAPS VIA STEREO VIEWING	20	IN DEVELOPMENT FOR 1982 SHUTTLE AND SPACELAB EXPERIMENT
ERS-1/JAPAN	1987	SAR, VIS/IR SENSOR, EARTH RESOURCES/ GEOLOGICAL OBSER- VATIONS	20-50M ?	MITI/NASDA DEFINITION PHASE
MOS-1/JAPAN	1989 (BELTA/N2) SECOND STAGE	OCEAN COLOR AND TEMPERATURE MONITOR WITH VISIBLE PUSHBROOM SCANNER, THERMAL INFRARED AND MICROWAVE RADIO- METERS, MARINE AND LAND OBSERVATIONS	50	IN DEVELOPMENT
AERS-1/ESA		LAND OBSERVING MLA INSTRUMENT, VISIBLE, NIR & SWIR CAPABILITY, C-BAND SAR		UNDER STUDY

"RESOLUTION" - (I FOV) AND FIELD OF VIEW OF THE SENSORS

LANDSAT METEOR S/C SPOT MOS-1 SPAS-01



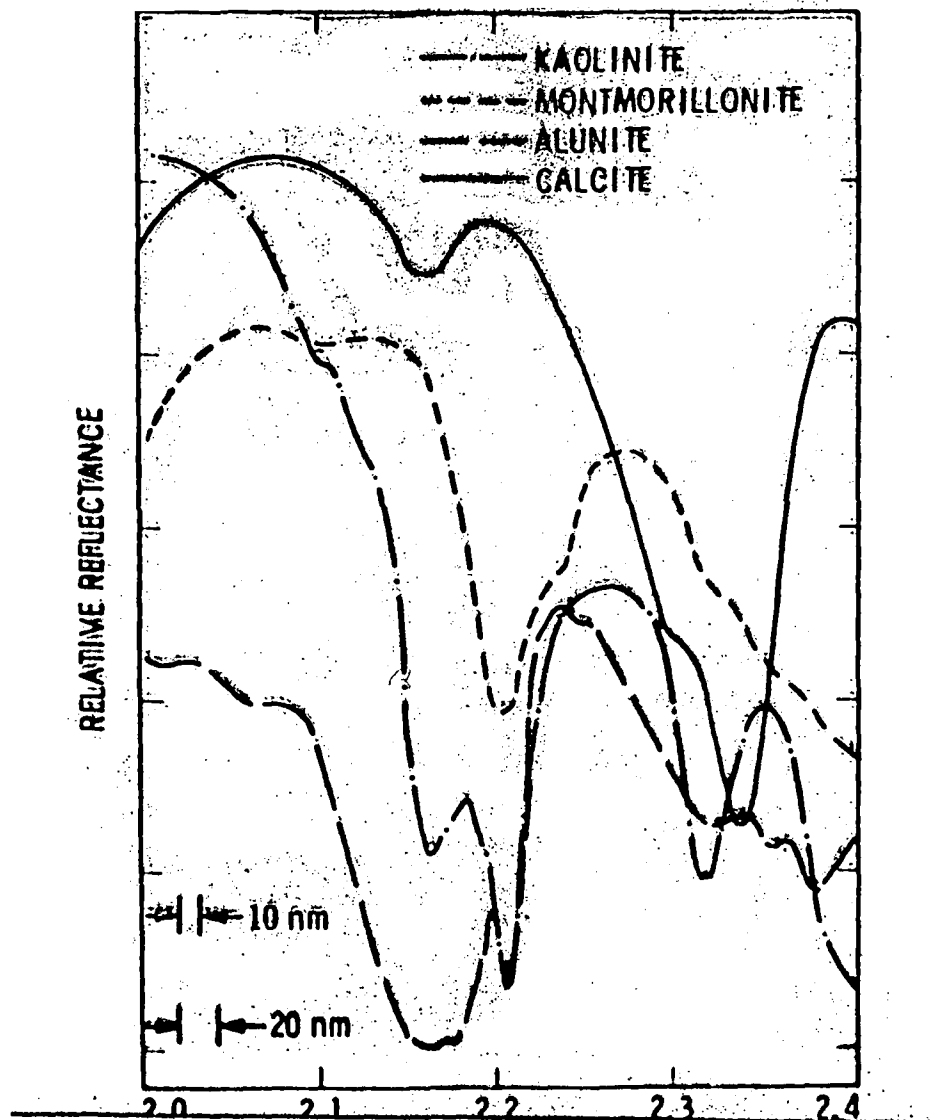
IMAGING SCIENCE WORKSHOP

OBJECTIVES

SUMMARIZE THE CURRENT STATE-OF-THE-ART OF SENSOR TECHNOLOGY, IDENTIFY CRITICAL ISSUES AND PROVIDE LONG RANGE GUIDANCE FOR THE DEVELOPMENT AND TESTING OF MULTISPECTRAL IMAGING TECHNOLOGY IN SPACE.

DEFINE NEEDED TECHNOLOGY AND INFORMATION EXTRACTION EXPERIMENTS IN THE LIGHT OF THE MEASUREMENT REQUIREMENTS AND SCIENTIFIC EXPERIMENTS DEVELOPED BY THE TERRESTRIAL SCIENCE DISCIPLINE GROUPS.

REFLECTANCE SPECTRA FOR TYPICAL HYDROTHERMAL ALTERATION MINERALS



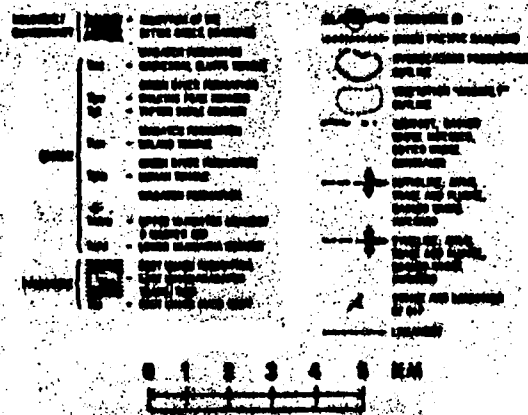
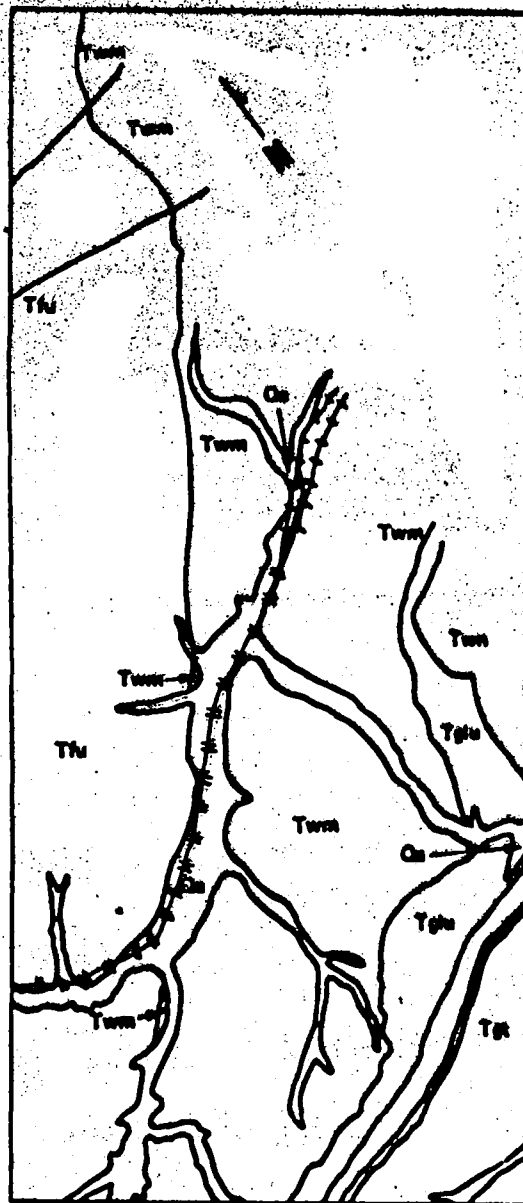


Figure 3-4. Composite geologic interpretations of Patrick Draw, Wyoming, from Landsat MSS data (left) (Roehler, 1977) and Thematic Mapper Simulator NS-001 data (right) (Long et. al., 1981). These two interpretations shown at the same scale illustrate the difference in detail detectable with 79 m and 18 m IFOVs respectively.



JPL MLA PROGRAM ELEMENTS

o TECHNOLOGY DEVELOPMENT

- MERCURY CADMIUM TELLURIDE HYBRID DETECTOR ARRAYS
- INDIUM ANTIMONIDE LINEAR AND AREA ARRAYS
- ADVANCED OPTICAL DESIGN CONCEPTS AND ANALYSIS
- COOLER DEVELOPMENT FOR SPACE SHUTTLE APPLICATIONS
- ADVANCED ONBOARD PROCESSING ANALYSIS AND SIMULATION

o SHUTTLE/SPACE PLATFORM IMAGING SPECTROMETER (SIS)

- FUNCTIONAL DESIGN OF INSTRUMENT SYSTEM
- STS INTERFACE STUDY INCLUDING POINTING SYSTEM
- EFFECTS OF ORBIT CHARACTERISTICS ON IMAGE GEOMETRY

o AIRCRAFT EXPERIMENTAL PROGRAM

- DEVELOPMENT OF RESEARCH OBJECTIVES
- INSTRUMENT DEFINITION AND COSTING

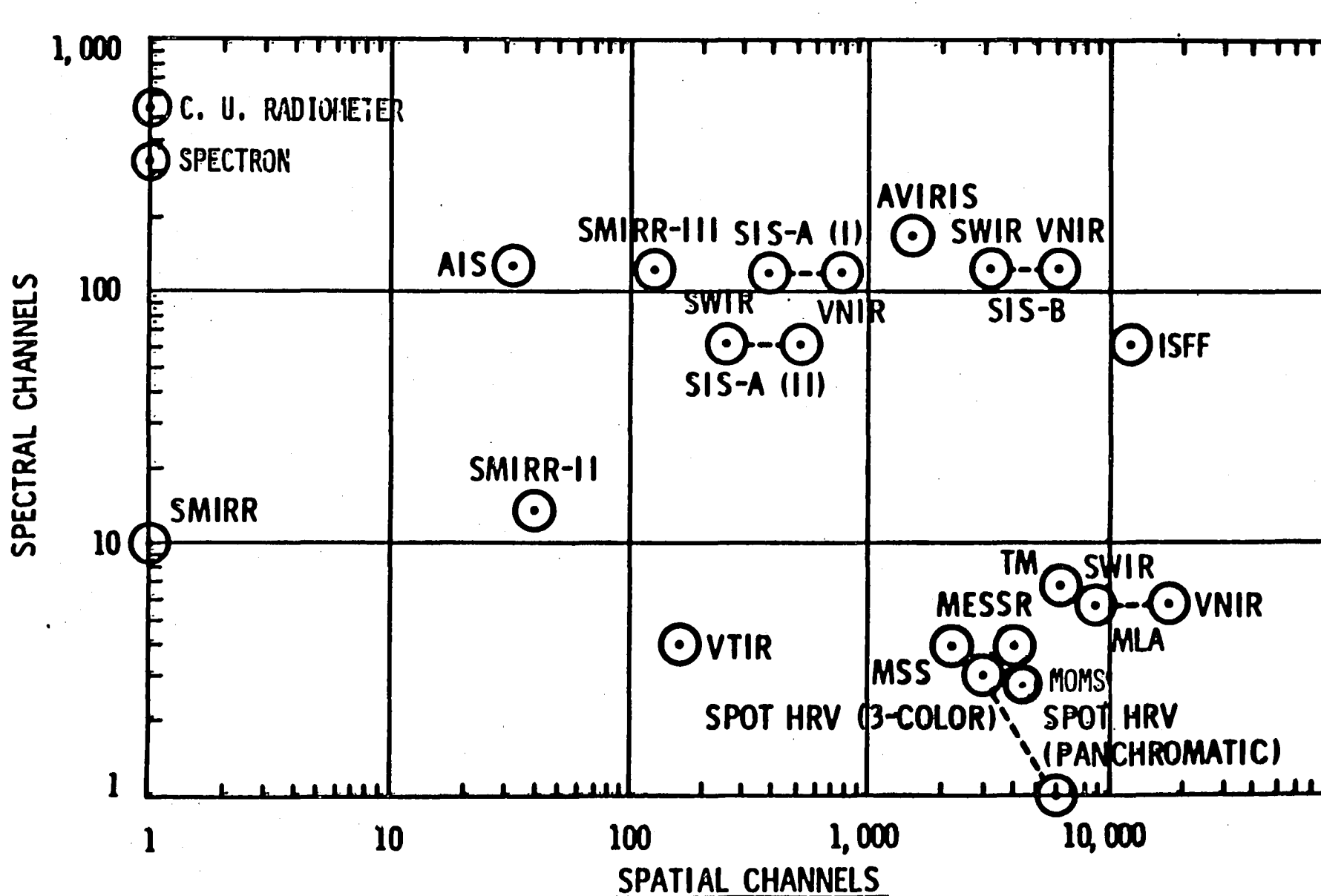
o IS APPLICATIONS DEVELOPMENT

- DISCIPLINES REQUIREMENTS FOR IS DATA
- GROUND PROCESSING TECHNIQUES AND SYSTEM STUDY

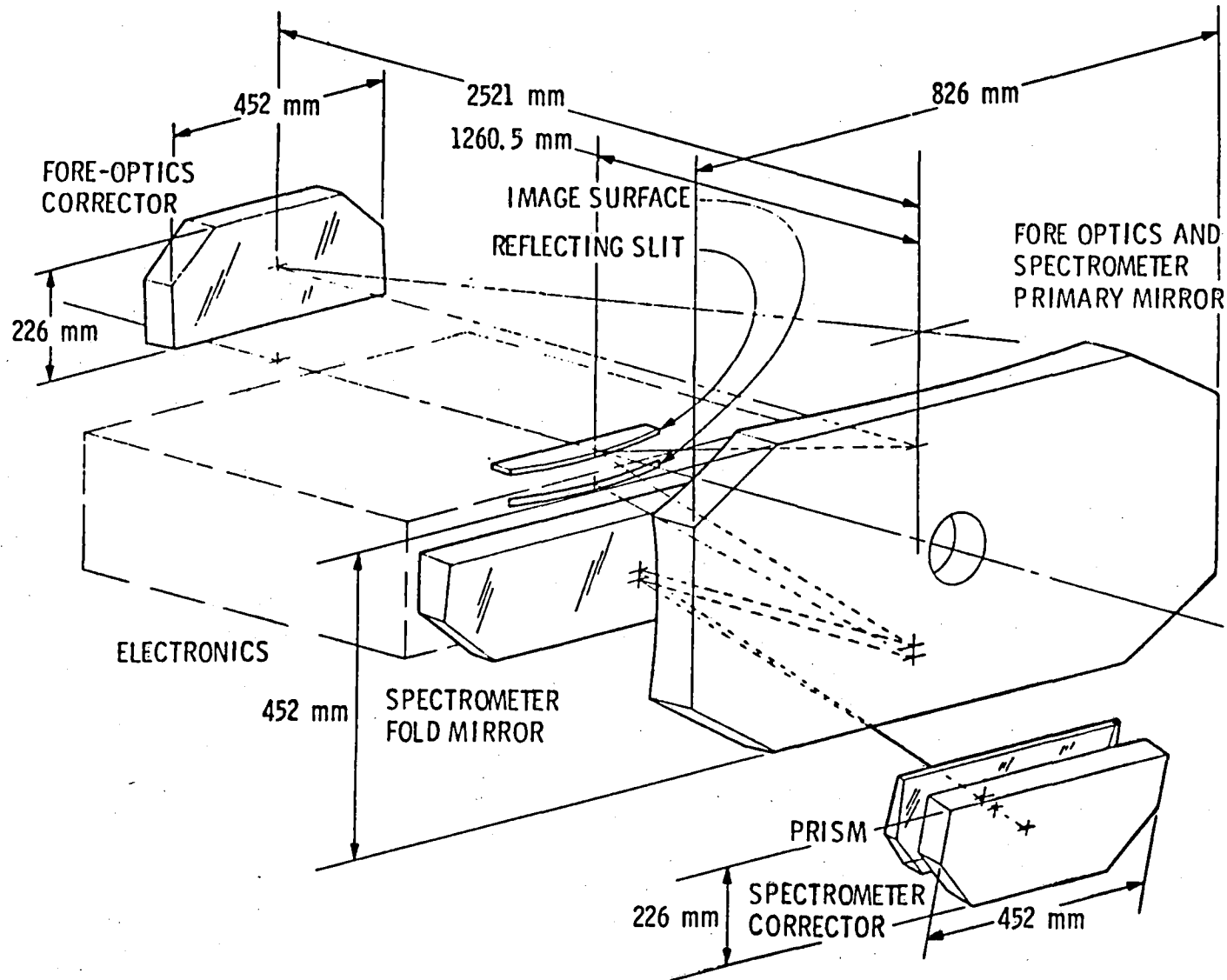
CONCLUSIONS

- A SIGNIFICANT TECHNOLOGY BASE FOR SOLID STATE PUSHBROOM SENSORS EXISTS AND IS IN THE PROCESS OF FURTHER EVOLVING THROUGH SUBSTANTIAL NASA AND COLLATERAL DOD FUNDING.
- TWO DIFFERENT BUT COMPLEMENTARY SENSOR APPROACHES AND THE ASSOCIATED TECHNOLOGIES WERE PRESENTED. SPACEBORNE AND AIRCRAFT INSTRUMENTS VARIANTS UNDER DEVELOPMENT WERE REVIEWED.
- ADAPTIVE AND FIXED ON-BOARD DATA COMPRESSION SCHEMES APPLICABLE TO AN MLA SPACEBORNE INSTRUMENT ARE AVAILABLE. DPCM, WHICH PROVIDES MODEST (~2.4:1) DATA COMPRESSION RATIOS, IS PROBABLY PREFERABLE FOR NEAR TERM HARDWARE IMPLEMENTATION. ADAPTIVE SYSTEMS WHICH PROVIDE GREATER COMPRESSION RATIOS, NEED FURTHER STUDY.
- 32X32 ELEMENT SWIR HgCdTe HYBRID DEVICES SUITABLE FOR AIRCRAFT INSTRUMENT USE ARE BECOMING AVAILABLE. BUTTABLE, 64X64 ELEMENT DEVICES FOR THE IMAGING SPECTROMETER APPLICATIONS WILL BE AVAILABLE IN ABOUT TWO YEARS.
- THE INTEGRAL FILTER MULTISPECTRAL LINEAR ARRAY APPROACH APPEARS TO BE THE MOST DIRECT AND PROMISING FOCAL PLANE APPROACH FOR AN MLA INSTRUMENT.
- THE LINEAR ARRAY SWIR HgCdTe MODULE DEVELOPMENTS SHOULD YIELD DEVICES IN ABOUT TWO YEARS. Pd-Si SCHOTTKY BARRIER LINEAR ARRAYS ARE PROMISING AS A NEAR TERM LOW COST ALTERNATIVE. COLLATERAL DOD DEVELOPMENTS WILL PROVIDE SIGNIFICANT SUPPORT IN THIS AREA.
- SELF CALIBRATING ABSOLUTE SILICON DETECTORS COULD BE THE BASIS FOR A SIGNIFICANT IMPROVEMENT IN OUR ON-BOARD INSTRUMENT CALIBRATION ACCURACY.
- IMAGING SPECTROMETER TYPE INSTRUMENT REQUIRED FOR ACQUISITION OF CALIBRATED NARROW BAND SPECTRA. A WIDE RANGE OF OPTIONS EXIST.
- A SPECTRALLY AND SPATIALLY VERSATIVE INSTRUMENT NEEDED TO ADDRESS THE DIVERSE RESEARCH REQUIREMENTS EXPRESSED BY THE DISCIPLINE PANELS. KEY TECHNOLOGICAL DRIVERS RESULTS FROM THE GEOLOGY AND CARTOGRAPHIC REQUIREMENTS.

COMPARISON OF MULTISPECTRAL SENSORS FOR REMOTE SENSING (FIELD, AIRCRAFT AND SPACE)



SHUTTLE IMAGING SPECTROMETER (SIS)



SELF CALIBRATED ABSOLUTE SILICON DETECTOR

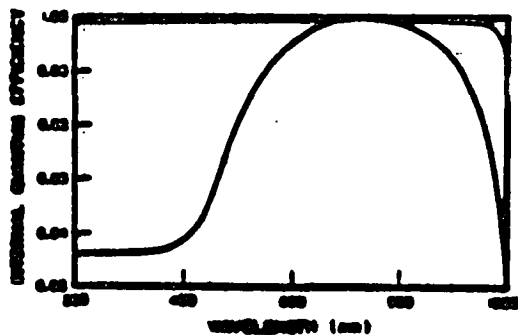


Fig. 1. Typical photodiode internal quantum efficiency without biasing (lower curve) and with biasing (upper curve), reference 9.

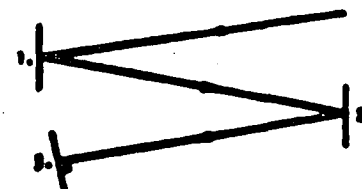


Fig. 2. A three-disc arrangement to minimize specular reflection losses.

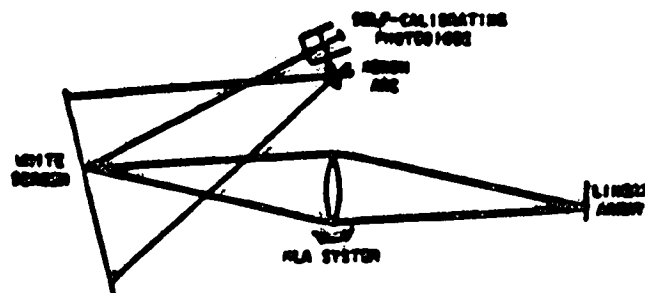


Fig. 4. The factory procedure for absolute spectroradiometric calibration.

VIS/NIR MULTISPECTRAL CCD DEVELOPMENT

OBJECTIVE:

- o DEVELOP A VIS/NIR CCD ARRAY THAT WILL SERVE AS THE BASIC UNIT FOR AN MLA FOCAL PLANE.

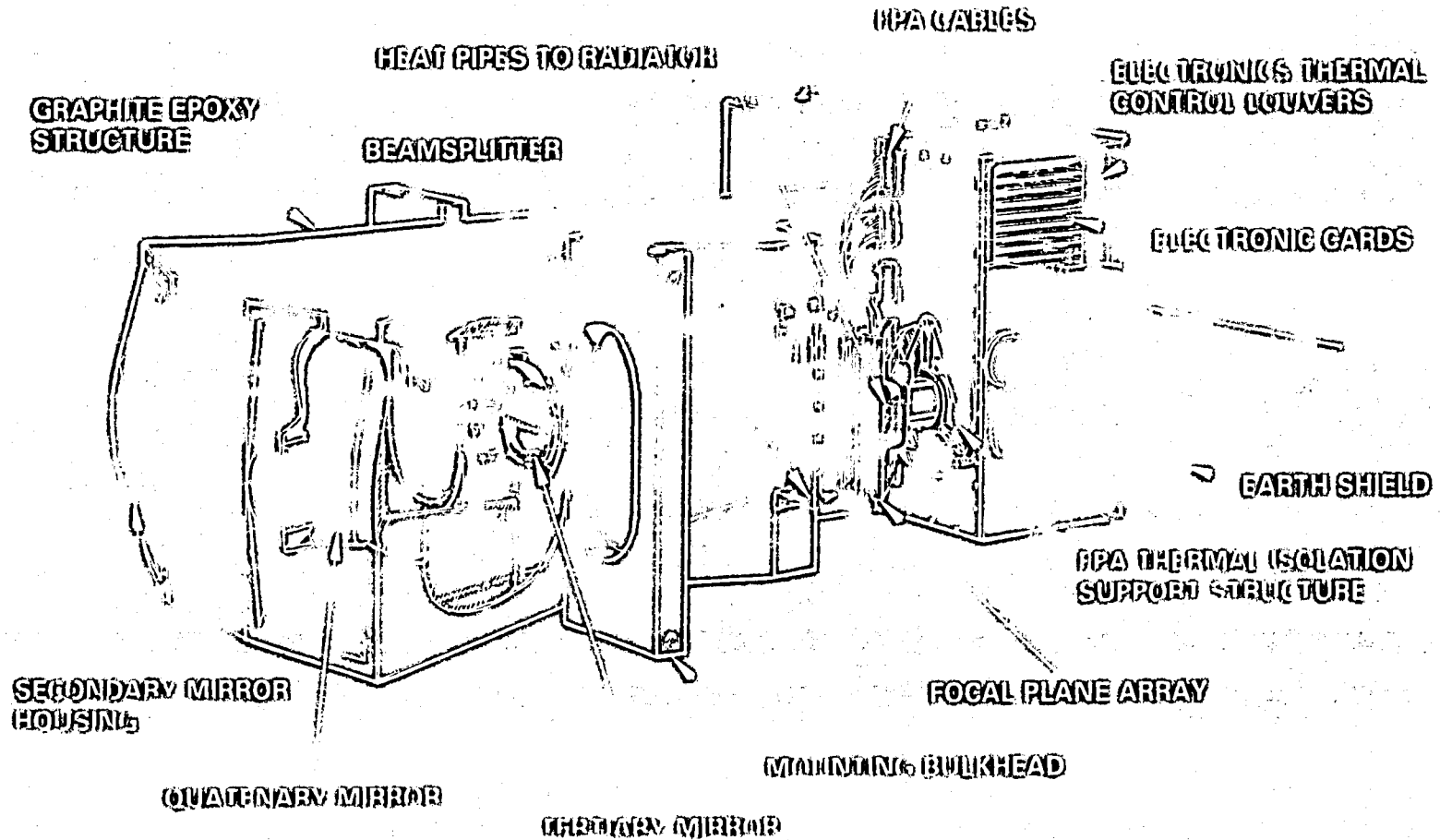
APPROACH:

- o 24-MONTH \$1.2M CONTRACT TO DEVELOP AND VALIDATE APPROACH.
- o CCD DESIGN: FOUR 1024-ELEMENT LINEAR ARRAYS WITH INTEGRAL BANDPASS FILTERS ON A MONOLITHIC STRUCTURE.
- o DESIGN, FABRICATE AND TEST FIVE MODULE FOCAL PLANE.

STATUS:

- o PROPOSALS FROM RCA, FAIRCHILD, WESTINGHOUSE AND HUGHES IN EVALUATION.
- o CONTRACTOR SELECTION AND AWARD BY AUGUST 1982.

MLA INSTRUMENT WITHOUT COVERS AND STEREO MODULE



NASA/DOE/ESA
5002

INTEGRAL SPHERE

PRIMARY MIRROR

SECONDARY MIRROR

DETECTOR ARRAYS

SCHMIDT CORRECTOR MIRROR

GRAVITATIONAL COLLIMATOR

HEAT PIPE

**PRIMARY
MIRROR**

**STEREO
MIRROR**

CHALLENGE COURAGE

HEAT PIPE

DETECTOR ARRAYS

**SCHMIDT
CORRECTOR
MIRROR**

DIFFUSION

VEL

INSTRUMENT ROLLS FOR GROSS TRACK VIEWING

TRANSFORMER

55W
175K

QUARTZ

TERTIARY

SECONDARY

PRIMARY

INITIALIVE ORDER

HEAT PIPE

BEAMSPLITTER & DETECTORS

55 W
175 K

QUARTIC

VEL

TILTS FOR CROSS TRACK VIEWING

**STEREO
MIRROR**

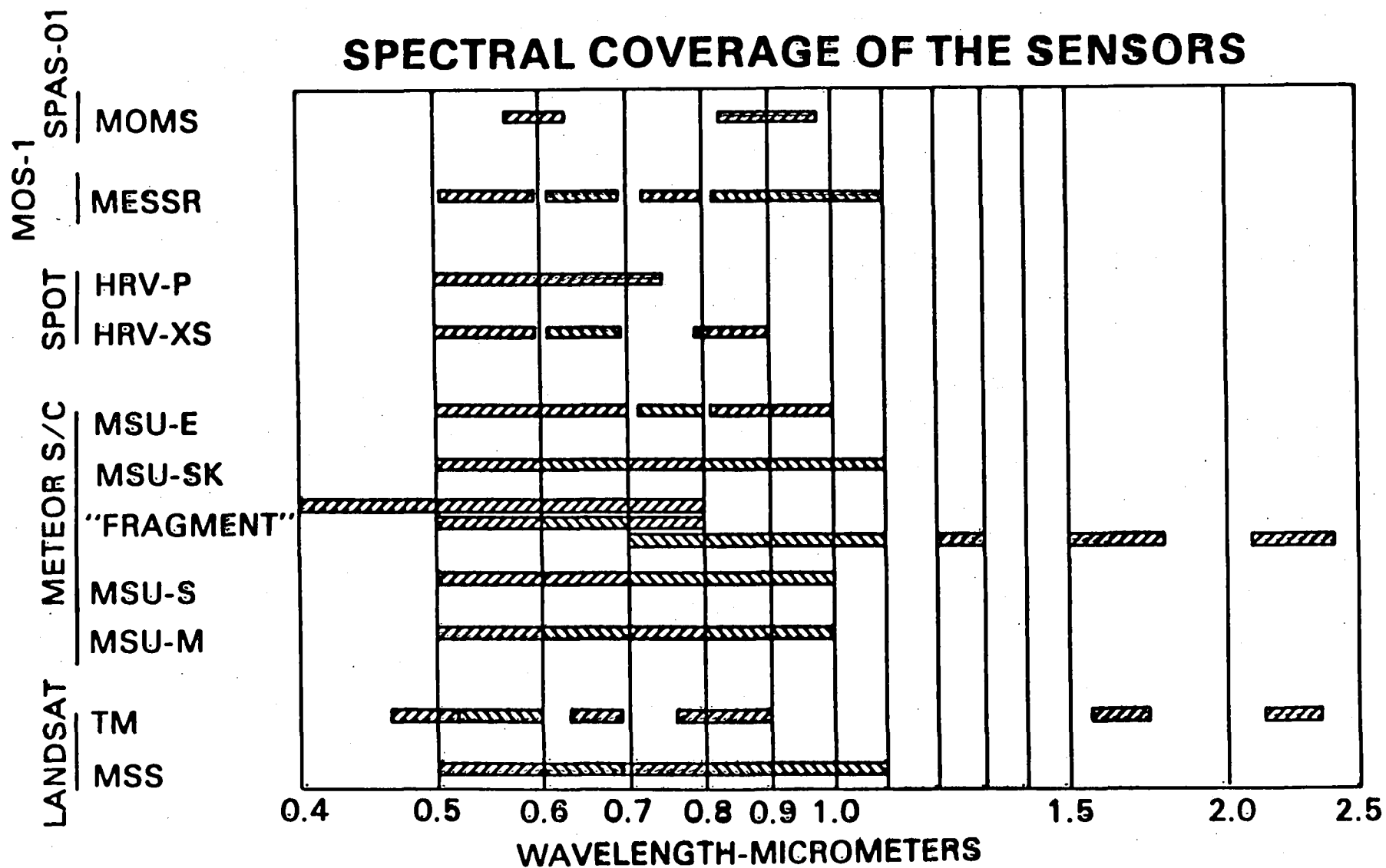
TERTIARY
SECONDARY
PRIMARY

INTEGRATING
CALCULATOR

STEREO
MIRROR

NASA JOEL82-1038(1)
5-19-82

SPECTRAL COVERAGE OF THE SENSORS



IMAGING SCIENCE WORKSHOP

AGENDA

NON-NASA SENSOR

MAPSAT

MLA SENSOR CONCEPTS

SENSOR TRADEOFF ISSUES

VISIBLE/IR SENSOR REVIEW

GSFC SUPPORTING TECHNOLOGY PROGRAMS

IMAGING SPECTROMETER

IR AREA ARRAY STATUS

CALIBRATION OVERVIEW

AIRCRAFT DATA PROGRAMS

ON-BOARD DATA PROCESSING

M. MAXWELL (GSFC)

A. COLVOCORESSES (USGS)

H. RICHARD (GSFC)

A. MIKA (SRRC)

J. LOWRANCE (PRINCETON)

W. BARNES (GSFC)

J. WELLMAN (JPL)

J. RODE (ROCKWELL)

P. SLATER (UNIV. OF ARIZONA)

G. VANE (JPL)

J. FLANAGAN (NSTL)

J. IRONS (GSFC)

R. RICE (JPL)

T. LYNCH (GSFC)

**IMAGING SCIENCE
PANEL MEMBERS**

KEN J. ANDO

PHILLIP H. SLATER

THOMAS B. MCCORD

ROBERT PELZMAN

JOHN WELLMAN

MARVIN MAXWELL

JOHN LOWRANCE

NASA HEADQUARTERS

UNIVERSITY OF ARIZONA

UNIVERSITY OF HAWAII

LOCKHEED RESEARCH LABS

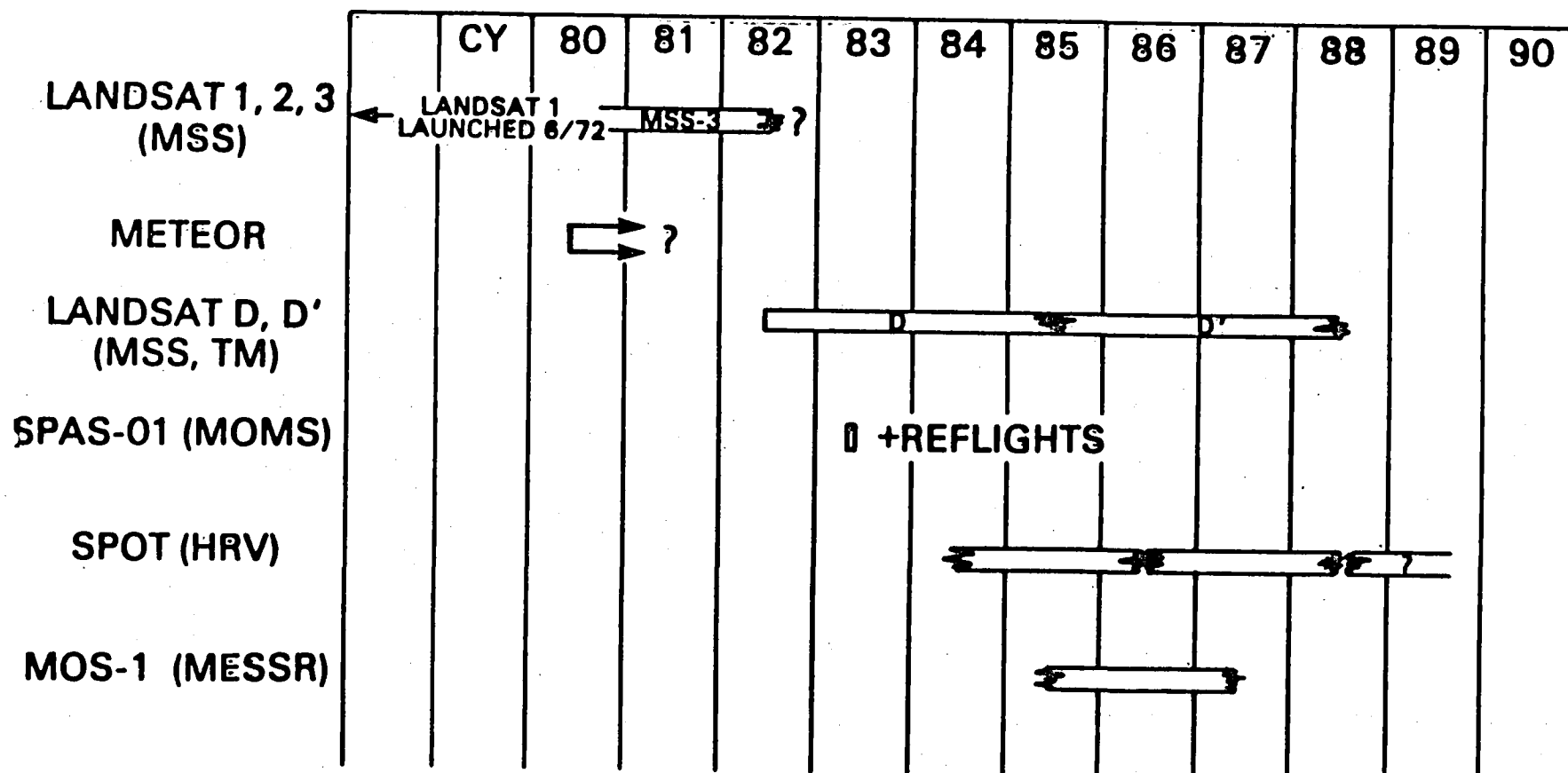
JET PROPULSION LABORATORY

GODDARD SPACE FLIGHT CENTER

PRINCETON UNIVERSITY

SCHEDULE OF PAST AND PROPOSED FLIGHTS

86



APPENDIX II

WORKING PAPERS
GEOGRAPHIC SCIENCE TEAM
MULTISPECTRAL IMAGING SCIENCE WORKING GROUP

MAPPING URBAN LAND COVER FROM SPACE SOME OBSERVATIONS FOR FUTURE PROGRESS

Leonard Gaydos
U.S. Geological Survey

Introduction

A definitive work on classifying land use and land cover from remotely sensed data is that by Anderson, Hardy, Roach, and Witmer (1976). They proposed a multilevel classification system since adopted by the U.S. Geological Survey for operational mapping of land use and land cover at Levels I and II (figure 1). The classes proposed have been compared with virtually every attempt since to classify land use and land cover with remotely sensed data.

-
- | | |
|--------------------------|---|
| 1 Urban or Built-up Land | 11 Residential |
| | 12 Commercial and Services |
| | 13 Industrial |
| | 14 Transportation, Communications,
and Utilities |
| | 15 Industrial and Commercial Complexes |
| | 16 Mixed Urban or Built-up Land |
| | 17 Other Urban or Built-up Land |

Figure 1

Most of the work on the USGS classification system predated knowledge of requirements necessary for attempting classification using digital data from Landsat. Though Landsat is referred to within the paper, the remotely sensed data used to define the mappable classes were hard-copy image products, typically aerial photographs, not digital data. Much effort and documentation has gone into demonstrating how Landsat digital data could be used to achieve USGS Level II classes. Some studies have shown how some of these efforts go beyond Level II, but little attention has been spent on explaining why certain Level II classes were not mapped adequately. It is just that type of knowledge that we need most, now that requirements for new sensing systems are being proposed. Perhaps a look at some of the successes and failures of mapping land cover from Landsat digital data and a look at the techniques used for image interpretation and their relationship to sensor parameters will give us a start in defining requirements for new sensors.

Experience With Landsat

When the first Earth resources satellite (Landsat-1) was launched 10 years ago, most investigators looked forward to interpreting the visual imagery reconstructed from data acquired by both the Return Beam Vidicon (RBV) and the more unfamiliar Multispectral Scanner (MSS). Interpreters had learned their trade using aerial photographs. The first Landsat images were interpreted in this way, and though the novelty of using data from space was exciting, the results for land cover mapping were disappointing. About all that could be discerned for urban areas were their locations indicated by areas on the images that had an "electric blue" color.

It was not until some researchers investigated the digital data that the "electric blue" areas were separated into some reasonable components. Residential areas were usually found to be separable from commercial or industrial areas. Parks, especially the distinctive golf courses used as control points, were separated quite clearly. Some transportation lines were picked up, not by distinctive classes, but as strings of "misclassified" pixels stretching across the urban fabric and extending into the countryside.

In using digital data these researchers were able to detect detail with the help of a computer that their colleagues couldn't make out in the fuzzy images they viewed and interpreted optically. They also used the computer's ability to deal with spectral data from four bands at once and separate multispectral classes from each other by statistical methods. But these advances, which have been responsible for the development of the field of digital image analysis, have tended to cut this breed of analyst off from the use of most of those elements of image interpretation developed over the years: size, shape, shadow, tone/color, texture, pattern, site, association, and resolution (Estes and others, 1975).

Most of the work in separating classes using the computer has been accomplished using tone/color. Results from defining and using texture as an interpretive element have been mixed, and thus the texture element is generally not used today except in special cases. Site has been an element used with increasing frequency, especially with the comparison of Landsat data with terrain, geologic, or soils data. It is only when the analyst takes manual control of the system and edits obvious errors in classification that he makes use of some of the remaining elements including not only site, but size, shape, pattern, and association.

So it is basically with only one interpretation element (color) and considerable assistance from the computer that digital image analysis has progressed. Interpretation in urban areas presents many difficulties; especially trying is the identification of the class Residential. Spectrally this class is exceedingly complex and close to signatures of many other

classes. In low-density areas the Residential signature becomes confused with Brush, Agriculture, or Forestland. In high-density areas, it becomes confused with Commercial or Industrial. In spite of this difficulty, many have attempted to map sub-classes of residential: older, newer, dense, sparse, wooded, etc. The basic problem remains. Because of the diversity of man's dwelling habitat, it remains beyond the Landsat MSS's best attempts to map it adequately in all cases.

Most investigators have not tried to subdivide separate Commercial and Industrial classes. Though the USGS system recognizes the problem of separating these uses when they are intermixed, as in an industrial park, it does separate them in other cases. Working in a realm where it is not possible to see the details that aid interpretation like parking lots, railroad sidings, stockpiles of raw materials, etc., the digital data interpreter collects the pavement, concrete, and rooftop signatures together and presents us with a combined class. Even that degree of generalization is sometimes confused with Water, Shadow, Lava Flows, and Rangeland unless the analyst intervenes using some site or shape data he can process himself.

The Transportation class is even more elusive. In the USGS system includes communications and utilities and consists of major highways and railroads, airports, seaports, pumping stations, and power transmission substations. Included in this class are not only the characterizing feature, like an airport runway, but all the associated facilities like terminal buildings, parking lots, intervening land, and buffer zones. Any spectral class could conceivably belong in this group. The Transportation class is interpreted from photographs using size, shape, pattern, site, and association with frequent assists from supplemental data for confirmation. About the most the digital analysts can point to are linear associations of residential pixels out in the country that define an interstate highway or the commercial-industrial pixels that cover a runway.

The Other Urban or Built-up Land class usually has the same signature as grass and barren land classes. The latter two classes are usually not changed to the Other Urban class within the urban area as the USGS system requires. Instead, most maps from analysis of digital data have rangeland and agricultural pixels peppering the urban area. Some components of this class such as zoos, waste dumps, spillways, and ski areas are usually missed altogether.

To sum up, though many have tried, none have succeeded in meeting the requirements for USGS Level II classes in urban areas using Landsat digital data. The use of digital data has produced mixed results when compared to photo-interpretation of the visual imagery, and interpretation has proceeded using relatively few of the elements of image interpretation.

Requirements For Mapping Levels II and III

Cognizant of the difficulties faced in mapping Level II classes, we shall proceed into the more speculative realm of Level III. USGS Professional Paper 964 leaves development of Level III to interested users motivated by their particular needs. Some of those users have responded with Level III classification criteria. The U.S. Geological Survey conducted a demonstration project with highly urbanized San Mateo County and produced land use and land cover maps of the county to Level III at 1:24,000 scale. The classes that were mapped at this level within the Urban and Built-up Level I class are listed in figure 2 and used as examples in the following discussion.

11 Residential	111 1 or less units/hectare
	112 2 to 8 units/hectare
	113 9 or more units/hectare
12 Commercial and Services	121 retail and wholesale
	122 commercial outdoor recreation
	123 educational
	124 hospital, rehabilitation or other public
	125 military
	126 other public
	127 research centers
13 Industrial	131 heavy industrial
	132 light industrial
14 Transportation, Communications, and Utilities	141 highway
	142 railway
	143 airport
	144 port facility
	145 power line
	146 sewage
15 Industrial and Commercial Complexes	
16 Mixed Urban or Built-up Land	
17 Other Urban or Built-up Land	171 extensive recreation
	172 cemetery
	173 parts
	174 open space/urban

Figure 2

Density of dwelling units was the criterion used for subdividing the Residential class. Some density information can be inferred from examination of the spectral ranges of residential pixels, but this has been an imperfect method owing to natural diversity of basic cover types that are integrated within the pixel. Increased resolution should add to the ability of measuring density through signature analysis, but at some point pixels will be focussed on individual basic land covers like rooftops, pavement, grass, and trees. Research should be done to determine the effect differing resolutions have on being able to map residential density using spectral information alone, using spectral and textural, and using spectral, textural, and association. Interpretation using the latter techniques should be done both digitally and visually.

It should be realized that although increased resolution should improve the ability to map residential density, it will also demand more sophisticated digital techniques. A photointerpreter does not have to be taught how to use the technique of association. He only needs an image sharp enough to recognize the basic land cover features and his experience in knowing how these features relate to one another in the landscape. Making good use of improved resolution within the digital domain so we can maintain the advantages digital data have demonstrated will be a large challenge that will be assisted by findings in the fields of cybernetics, robotics, and machine intelligence. Some attention should be directed towards applying findings from that body of experience towards making our pattern-recognition algorithms smarter.

Separation of commercial from industrial uses will be the most difficult to achieve with imagery alone. Identification is possible now only because of the ability of a photointerpreter to identify objects using size, shape, and site. Piles of raw materials, smokestacks, or railroad sidings are first noticed and then used to recognize several buildings and intervening land as a factory through association. Resolution has to be sufficient to recognize those related features, but, even with the very best resolution, digital techniques for processing those data falls short of the ability of the photointerpreter. Some simple models could be devised to recognize certain feature types, however. One might teach the computer to recognize some types of commercial by classifying all buildings directly fronting on the street (if one could separate the building from the street). Or a more complex discrimination could be attempted. The building separated from the street by pavement or concrete (probably seen spectrally as a bulge in the street) and occupied by parked cars during a weekend pass of the satellite could be assumed to be commercial as well.

Perhaps a more fruitful technique lay in utilizing supplemental data such as zoning maps in a layered classifier. This supplemental data will be more important as one dips down into Level III so we may as well use them as soon as possible. There comes a point when it becomes academic to design a Rube Goldberg

mechanism for discriminating a shopping center from an electronics research facility when everyone in town knows which is which and when they've been on maps for years. Our challenge is in efficiently utilizing all the data available in characterizing the landscape not in making more work for ourselves.

The Transportation classes generally can most readily be recognized by shape as linear features. Classification by that criterion has been hampered so far by breaks in the linear pattern, characteristic of coarse resolution. Research should be done into seeing the effect that different resolutions have on the continuity of highways, railways, and power lines of varying widths and in designing algorithms to recognize these features. Once identified, it should be possible to separate types of transportation from one another by spectral data. Association will be needed to group related buildings and land into the functional class Transportation, Communications, and Utilities described by Anderson. Here again, we should not overlook the use of existing maps and data to make our job much easier.

The Other Urban or Built-up class consists mostly of non-urban covers in an urban setting. This is mapped fairly well now though most do not bother to stratify this class from the non-urban agricultural and forest land classes. The real challenge here with increased resolution is going to be in separating grass and trees that are part of the fabric of residential neighborhoods and some commercial industrial areas from parks and vacant land. One might even imagine a case where maximum resolution is used to define classes like Residential, Commercial, Industrial, and Transportation using all the techniques available and then degrading the resolution so only open space above certain minimums gets called out separately.

Other Considerations

With discussion of Other Urban or Built-up we get close to some fundamental questions that will be confronting us as we attempt to map Levels II and III with remotely sensed data. At what point does a street become Transportation and cease to be part of the surrounding Commercial class? When is a low-density residential area considered open space? Are we mapping the landscape as it is or as we imagine it? Can we even agree on how it really is?

Different users will have different ideas about how it should be done. Planners usually see the world in parcels and as it appears on zoning maps. A park isn't a park unless it has a sign proclaiming its existence. A stream valley containing residential lots backed up to it will not exist as open space if the property line runs all the way down hill, but will be proclaimed as open space if property lines stop short of the stream channel.

Others who may use maps developed from remote sensing in urban areas will see the world quite differently. Someone inter-

ested in assessing potential energy use may want to map every building separated by function and may appreciate a thermal look at night to assess heat loss. Someone looking at solar energy potential will be interested in similar classes but will have an additional interest in topography and orientation to the sun. Urban hydrologists are going to be concerned with the amount and dispersion of basic land cover types as they differ in their permeability characteristics. Demographers are going to want to know residential density and relationship to enumerated districts. Everyone is going to want to look at change.

We have discussed the successes and failures of mapping land cover with the present Landsat multispectral scanner and have presented some ideas on how Level II and Level III class discrimination might be improved with data of higher resolution and more sophisticated interpretation methods. There has been one underlying assumption. When multispectral data collected from space have resolution sharp enough to photointerpret, that tried and true method can be used to map all classes mappable from remotely sensed data. Since the art of photointerpretation is likely to flourish with the advent of higher resolution data from space, at least until more sophisticated digital techniques are developed, more research should be done to determine quality of photointerpretation of multispectral data of various resolutions.

Throughout this discussion, resolution has been the sensor characteristic judged to be most critical for urban applications. There is general agreement with the recommendations of the Land Resources Panel of the Multispectral Resource Sampler Workshop (ORI, 1979) with the additional point that while increased resolution will always help the photointerpreter do a better job, it will not really help, and may even hinder, the digital analyst until more sophisticated elements of interpretation are developed. Much information on urban morphology needs to be collected and utilized in interpretation models that include site and association factors.

This is not to imply that other sensor characteristics are unimportant for urban applications. Almost surely data in the blue and thermal bands will be of help in discriminating hard surface materials and in separating urban from non-urban. Unfortunately, the intense work that has been done in examining spectral responses for agricultural, natural vegetation, and geologic applications has not been accomplished adequately in an urban setting. While urban targets are made up of some of the basic land covers that have been studied, some special attention should be paid to examining the characteristics of these in an urban setting.

Much less is really known about the effects of bandwidth or quantization levels for urban applications. Again, urban applications can learn from the findings of others on these effects, but some experiments using urban test sites would be most desirable in strengthening overall conclusions.

Conclusion

So it comes down to two overriding considerations, resolution and more sophisticated analysis techniques. Much progress has been made in studying the urban environment from space, but much work remains. For digital data from spacecraft sensors to have a great impact on urban studies, data of higher resolution must be acquired, and analysis techniques must be developed to utilize them in ways analogous to the art of the photointerpreter.

References

Anderson, James R., Hardy, Ernest E., Roach, John T., and Witmer, Richard E., 1976, A land use and land cover classification system for use with remote sensor data: U.S. Geological Survey Professional Paper 964, 27 p.

Estes, John E. and Simonett, David S., editors, 1975, Fundamentals of image interpretation, in Reeves, Robert G. and others, eds., Manual of remote sensing: American Society of Photogrammetry, Falls Church, Va., p. 869-882.

ORI, Inc., 1979, Multispectral resource sampler summary report of the workshop: Ft. Collins, Co., 197 p.

**Working Report: Projected Technological Requirements for
Remote Sensing of Terrain Variables**

**Prepared by
Charles F. Hutchinson, Director
Applied Remote Sensing Program
Office of Arid Lands Studies
College of Agriculture
University of Arizona
Tucson**

**for
Multispectral Imaging Science Working Group
Geographic Science Workshop
San Antonio, Texas
April 28-30, 1982**

**Sponsored by
Earth and Planetary Exploration Division
National Aeronautics and Space Administration**

April 1982

Working Report: Projected Technological Requirements for
Remote Sensing of Terrain Variables

PREFACE

To my knowledge, there are few, if any, references that comprehensively describe landform or drainage characteristics in terms of their spatial or spectral properties. To compensate for the gaps in my own experience in this area, I consulted with colleagues at the University of Arizona in the departments of Geography and Regional Development; Geosciences; Soils, Water, and Engineering; and Electrical Engineering. Except for direct contributions by Victor Baker, I received considerable encouragement and sympathy from this group but no resounding consensus on recommendations. This, I feel, says much about the difficulty of the problem.

INTRODUCTION

There have been two basic approaches to the study of landforms and drainage, and both have relied heavily on remote sensing. One, represented by the collected work of Baker and

Holz, has focused on water and the organization of drainage patterns. The primary goal of this hydrogeomorphic approach has been to achieve a basic understanding of fluvial processes with the hope of developing the ability to predict stream behavior.

The second major approach to the study of landform and drainage has been in terrain analysis. This subject deals with "land" as an assemblage of linked attributes, e.g. soil and vegetation. Terrain analysis is commonly performed to assess land capability for agricultural or engineering purposes.

This working paper reviews some of the contributions of remote sensing to both of these areas with the intention of identifying characteristics that should receive future support in system and sensor configuration planning.

HYDROGEOMORPHOLOGY

Remote sensing applications to the field of hydrogeomorphology during the past 10 years have occurred in three areas: fluvial morphological studies, peak discharge modeling, and hydrogeomorphic floodplain mapping. The data sources for these investigations range from large-scale (1:12,000) to small-scale (1:750,000) orbital photography.

Fluvial Morphological Studies

The recent availability of orbital photography and imagery has provided coverage of hydrological systems formerly inaccessible or unmapped. The Apollo-Soyuz Test Project (ASTP) has provided coverage of the central Amazon basin of South America, affording a first view of many of the smaller rivers and streams within this drainage system. The photography from this joint project allowed the identification of floodplain limits, abandoned channels, changes in land use and vegetation, and settlements, all of which are important in assessing variability and change in hydrological systems (Holz et al, 1979). Another study of drainage system characteristics used ASTP products to measure channel patterns, width, meandering, sinuosity, and relative age of channel features (Holz and Baker, 1979). A problem encountered with this data source is the difficulty in obtaining accurate measurements of sinuosity since the imagery is oblique.

Modeling Peak Discharge

Morphometry involves the measurement and quantification of morphological features of the earth's surface. An important and comparatively recent application of morphometry to the subfield of hydrogeomorphology involves the measurement of landforms related to drainage with an objective of predicting

peak discharge and, indirectly, the extent of flooding for an area.

The "upstream" approach to hydrogeomorphology, in large part, is based on the relationship of discharge to both transient and permanent controls, the latter of which include hydromorphic features of the landscape (Baker, 1976). Parametric modeling of these features has revealed the importance of two fundamental parameters -- drainage density and basin magnitude -- in the relationship.

Both of these parameters can be derived directly from photography using automated digitizing and computer processing techniques to translate them into usable form. While the orbital photography provides less information on low-order streams, it is still useful for evaluating the magnitude of the basin and for identifying higher-order stream segments (Baker, Holz and Patton, 1975).

Despite the demonstrated power of morphometric measurements in predicting discharge, the application has been given relatively little use, owing in large part to:

1. The tedious task of measuring parameters such as drainage density, bifurcation ratio, and stream order;
2. Difficulties of data acquisition and variable resolution of data sources such as maps, photographs, and imagery; and,
3. Subjective errors of judgment resulting from manual

interpretation (Baker, Holz and Hulke, 1974).

Peak discharge modeling of watersheds involves the collection and derivation of relationships between streamflow and characteristics of the drainage system such as channel density, order, drainage basin area, and relief. One study identified 995 first-order streams, gullies, and segments within a 3.4-square-mile area using conventional large-scale (1:13,000) black-and-white aerial photography (Patton and Baker, 1976). A more detailed investigation compared both medium- and large-scale black-and-white and color infrared photography (1:48,000 and 1:123,000, respectively) for drainage parameters including presence of standing water, land use change, alluvial surfaces, erosion and soil change, bedrock exposures, and first-order stream frequency (Baker, Holz and Hulke, 1974). The results of this study indicate that the scale is less critical than the use of color infrared rather than black-and-white photography. The investigators identify only one less first-order stream on the small-scale (95) than on the medium-scale color infrared photography (96), but can discern only 84 first-order channels on the medium-scale black-and-white photography.

A more intensive comparative investigation used conventional large-scale photography (1:20,000), with Skylab EREP 190A/B imagery (1:750,000 and 1:500,000, respectively), to determine drainage area, Strahler stream order, Shreve

magnitude, and number of segments by order (Baker, 1976). This investigation reveals that resolution is more critical between the orbital photographs in identifying stream parameters, since the investigators identify only 14 first order streams on the smaller-scale photography in contrast to 44 on the larger-scale photography. The latter is nearly as effective a data source as conventional topographic maps. A major problem encountered with orbital photography is the determination of relief, a critical parameter in the discharge model (Baker, Holz and Patton, 1975).

Flood Hazard Mapping

Remote sensing data also have been used for "down-stream" evaluation of flood hazard by mapping abandoned river features and vegetation indicative of terrain that is rarely flooded (Baker and Holz, 1978). The utility of geomorphic mapping of flood hazard zones lies in its potential use for statewide or regional planning activities to provide interim flood hazard information before detailed hydrological studies at a local scale. The immediate deficiencies of these techniques include improved spatial resolution of imagery, increased coverage frequency for flood-effect assessment, and evaluation of morphometric measurements and their relationship to discharge in climatic and physiographic realms outside of those already tested.

One study used small-scale (1:116,000) color infrared

photography to define a flood hazard area based on the identification of channel forms, regional flood lines, and texture of sediments (Baker, 1976). This same study also revealed the observable extent of flooding from pre- and post-event image comparison using 1:123,000 high-altitude photography and 1:750,000 Skylab photography. This method of multitemporal analysis also has been used to estimate recurrence intervals of flooding (Baker, Holz, and Patton, 1975).

Other surface features have been used to evaluate flood-prone areas on aerial photography. One study, using high altitude color infrared photography, identified vegetation that is typically found in floodplains (Baker and Holz, 1978). This method, which requires extensive field support for data verification, is valuable primarily in arid areas having comparatively sparse vegetation.

TERRAIN ANALYSIS

Terrain analysis (also variously known as land classification and integrated survey) and remote sensing have been closely linked since the concept first was applied extensively in Australia. Major publications on terrain analysis (Stewart, 1968; Mitchell, 1973; and Thie and Ironside, 1976) have dealt extensively with remote sensing techniques.

Recently, a book was published dealing specifically with remote sensing and terrain analysis (Townshend, 1981).

A number of projects covering a large part of the earth's surface have been done (for example, Perrin and Mitchell, 1970). However, techniques for mapping terrain have been and are criticized for the subjective ways in which units are sometimes recognized (Hutchinson, 1981). As a result, a recognized sub-branch of terrain analysis has focused on the development of quantitative landform parameters (Mabbut, 1968). Quantitative criteria for describing landforms, developed for use with aerial photography, range from very detailed (Parry, Heginbottom and Cowan, 1968; scale of 1:5,000) to very gross (USAWES, 1959; scales of 1:400,000 to 1:5 million). Generally, these criteria were developed for rural development planning or military applications and thus have had a limited distribution.

Quantitative assessment of terrain variables for specific applications use many of the same features identified for hydrogeomorphological studies. One application used remote sensing to assess trafficability in remote areas for off-road vehicles. The parameters used include surficial geology, percent of area permanently waterlogged, tree density, and micro-relief. Conventional aerial photography at 1:31,680 provided data for the first three parameters, while 1:6,000 scale was needed for accurate assessment of the last two parameters (Schreier and Lavkulich, 1978).

A secondary data input to this system was from Landsat 1

digital data. Bands 4 and 7 are used to contrast vegetation and water cover, improving the overall mapping of trafficability (Schreier and Lavkulich, 1979).

Land classification in the broadest sense involves delineating areas in which a recurring pattern of topography, soils, and vegetation occurs. Remote sensing is demonstrated as a data source for structural characteristics of the topographical factor by aiding to identify stream frequency and various "ecological" factors, including vegetative cover (King, 1970). Both relief:frequency (R:F) and relief:density (R:D) curves were employed in defining land systems in a subsequent study, with frequency and density characteristics obtained from 1:125,000 photo mosaics. The relief was determined stereoscopically from 1:60,000 stereopairs (King, 1972).

Land classification also has involved modeling of terrain features such as structural characteristics of diastrophic forms (fault systems and their orientation), drainage frequency, and channel patterns of width, length, variability, and sinuosity (Speight, 1977). These parameters were successfully derived from 1:40,000 aerial photography over a remote area of Papua, New Guinea. The author cites a 20-meter limit of resolution, considered to be adequate for the scale of the study of an area of 5,000 square kilometers.

Because of the limited applications, restricted distribution, and various scales employed in most of these studies, no summaries of criteria have been prepared. Although

there is increasing contact between groups involved in terrain analysis (witnessed by the international meetings held in Bratislava, Czechoslovakia, in 1979 and Veldhoven, The Netherlands, in 1981), it is unrealistic to expect a consensus on landform parameters.

RECOMMENDATIONS

The recurring theme presented here is that there is little consensus on or guidance for the measurement of landform parameters and, as a result, that it is difficult to recommend specific spatial and spectral resolutions without extensive background research that attempts 1) to synthesize work done on quantitative descriptions of landforms, and 2) to determine regional variation in selected quantitative parameters.

The Committee on Earth Sciences of the Space Science Board, National Research Council, has struggled recently with a set of similar problems in developing recommendations for acquiring of orbital imagery for use in monitoring geomorphic processes. The Committee's conclusions were as follows:

1. The program of future research must achieve a balance between existing, proven sources of data and the development of of space-measurement systems employing

techniques proven useful in the laboratory.

2. Digital topographic data must be acquired for all land surfaces as a primary means to determine the morphology of the continental crust.

3. The determination of morphology can best be achieved with a combination of this topographic data and digital imagery in the visible and near-infrared wavelengths. Digital radar imagery also can provide considerable primary information on landforms.

4. A global program of orbital observations is needed for comparing hydrological systems.

5. Orbital sensors must obtain a ground resolution of 30 meters or less, and a frequency of coverage of two days to one week to provide detail for process mapping.

6. On scientific and strategic grounds, a coordination of space, airborne, and ground investigation measurements is indispensable for a global program.

7. NASA must continue to periodically review the development of instruments and measurement techniques to insure that current applications needs are being met (National Research Council, Space Science Board, Committee on Earth Sciences, 1982).

Clearly, these recommendations are intended to guide policy and the general direction of research and program development, rather than to serve as a basis for system design. Without additional groundwork, it is unlikely that we can do much better.

General Recommendations for Further Work

Both approaches to the study of landform and drainage would benefit by improvements beyond the 30-meter resolving capability of Landsat D. Optimal resolution values for 1) detecting low-order streams, 2) monitoring erosion, and 3) identifying vegetative cover are likely to vary from region to region. To determine these values, it is recommended that:

1. An exhaustive literature search be performed in the general and restricted publications describing specific parametric terrain analyses;
2. Field studies of selected watersheds be conducted in several different climatic regions to estimate optimal resolution for different environments; and,
3. An effort of international scope be made to define those attributes of landforms and vegetation that may be evaluated by photointerpretation, and a formal descriptive technique adopted to facilitate systematic improvement in techniques of mapping or extrapolation (Speight, 1977).

References

- Baker, Victor R. 1976. "Hydrogeomorphic methods for the regional evaluation of flood hazards." *Environmental Geology* 1: (1976), pp. 261-281.
- Baker, Victor R., and Robert K. Holz. 1978. *Remote Sensing of Flood Hazards in Central Texas*. Austin, Texas: Texas Natural Resources Information System (TNRIS-003). 19 pp.
- Baker, Victor R., Robert K. Holz, and Steven D. Hulke. 1974. "A hydrogeomorphic approach to evaluating flood potential in central Texas from orbital and suborbital remote sensing imagery." *Environmental Research Institute of Michigan, Proceedings of the Ninth International Symposium on Remote Sensing of the Environment* (15-19 April, 1974). pp. 629-645.
- Baker, Victor R., Robert K. Holz, and Peter C. Patton. 1975. "Flood hazard studies in central Texas using orbital and suborbital remote sensing imagery." *Proceedings of the NASA Earth Resources Survey Symposium, Houston, Texas* (June, 1975). pp. 2253-2294.
- Holz, Robert K. and Victor R. Baker. 1979. "An examination of fluvial morphological characteristics of western Amazon streams from Apollo-Soyuz photographs." *American Water Resources Association, Satellite Hydrology* (June 1979), n.p.
- Holz, R.K., V.R. Baker, S.M. Sutton Jr., and M.M. Penteado-Orellana. 1979. "South American river morphology and hydrology." *Apollo-Soyuz Test Project, Summary Science Report (Vol. II), NASA Special Publication 412*, pp. 545-594.
- Hutchinson, Charles F. 1981. "Use of digital Landsat data for integrated survey." *Arid Lands Resource Inventories: Developing Cost-Efficient Methods* (La Paz, Mexico - Nov. 30-Dec. 6, 1980), U.S. Department of Agriculture, Forest Service, General Technical Report WO-28. pp. 240-249.
- King, R. Bruce. 1970. "A parametric approach to land system classification." *Geoderma*, 4:(1970), pp. 37-46.
- _____. 1972. "Relief-stream frequency (R-F) diagram: method of displaying physiographic regions." *Journal of Geology* 80:6(Nov. 1972), pp. 740-743.
- _____. 1975. "A comparison of information theory interdependence and product-moment correlation analyses as applied to geomorphic and soils data." *Zeitschrift fur Geomorphologie*, 19:4(Dec. 1975), pp. 393-404.

- Mabbutt, J.A. 1968. "Review of concepts of land classification," in G.A. Stewart, ed., Land Evaluation. Melbourne: Macmillan of Australia.
- Mitchell, Colin. 1973. Terrain Evaluation: The World's Landscapes. London: Longman Group Ltd. 221 pp.
- National Research Council, Space Science Board, Committee on Earth Sciences. 1982. A Strategy for Earth Science from Space in the 1980's. (Part I: Solid Earth and Oceans). Washington, D.C.: National Academy Press. 99 pp.
- Parry, J.T., J.A. Heginbottom, and W.R. Cowan. 1968. "Terrain analysis in mobility studies for military vehicles." in G.A. Stewart, ed., Land Evaluation. Melbourne: Macmillan of Australia.
- Patton, Peter C., and Victor R. Baker. 1976. "Morphometry and floods in small drainage basins subject to diverse hydrogeomorphic controls." Water Resources Research, 12:5 (October 1976), pp. 941-952.
- Perrin, R.M.S., and C.W. Mitchell. 1970. "An appraisal of physiographic units for predicting site conditions in arid areas." Military Engineering Experimental Establishment Report No. 1111 (2 vols).
- Schreier, H., and L.M. Lavkulich. 1978. "A numerical terrain classification scheme for off-road terrain trafficability assessments." Geoforum, 9:(1978), pp. 225:234.
- _____. 1979. "A numerical approach to terrain analysis for off-road trafficability." Photogrammetric Engineering and Remote Sensing, 45:4 (May 1979), pp. 635-642.
- Speight, J. Garry. 1977. "Landform pattern description from aerial photographs." Photogrammetria, 32: (1977), pp. 161-182.
- Stewart, G.A. (ed.) 1968. Land Evaluation. Melbourne: Macmillan of Australia.
- Thie, J., and G. Ironside. 1976. Ecological (Biophysical) Land Classification in Canada. Proceedings of the First Meeting, Canada Committee on Ecological (Biophysical) Land Classification (25-28 May, 1976, Ontario). 269 pp.
- Townshend, J.R.G., ed. 1981. Terrain Analysis and Remote Sensing. London: Allen Unwin. 240 pp.
- United States Army Engineer Waterways Experiment Station (USAWES). 1959. Handbook: A Technique for Preparing Desert Terrain Analogs. Technical Report No. 3-506.

APPENDIX III

WORKING PAPERS
HYDROLOGY TEAM
MULTISPECTRAL IMAGING SCIENCE WORKING GROUP

APPLICATION OF FUTURE REMOTE SENSING SYSTEMS TO IRRIGATION

LEE D. MILLER
NEBRASKA REMOTE SENSING CENTER

GENERAL AREAS OF DISCUSSION

I. PUBLIC MANAGEMENT OF AGRICULTURAL WATER SUPPLY/DEMAND

OBJECTIVE: MODEL WATER CONSUMPTION

SHORT RANGE USE OF INFORMATION:
PROPORTIONING OF AVAILABLE WATER
CROP MANAGEMENT - WHAT TO PLANT

LONG RANGE USE OF INFORMATION
CONSUMPTION PERMITS
STATE AND FEDERAL STATUTES
INTERBASIN TRANSFERS
GROUND WATER RECHARGE

REQUIRES: AREA ESTIMATES OF IRRIGATED CROPS
*currently good in dryland areas and marginal in mixed
irrigated/nonirrigated ares of same crops*
CROP TYPE

USER: FEDERAL AND STATE AGENCIES ... WATER DISTRICTS

II. IRRIGATION SCHEDULING FOR DISTRIBUTED MANAGEMENT OF YIELDS

OBJECTIVES
BACKGROUND
INFORMATION NEEDS FROM REMOTE SENSING ON A SPATIAL BASIS
INFORMATION / DATA DISTRIBUTION
ON SITE DATA PROCESSING
MODELING FOR DECISIONS
ACCEPTANCE / USE OF RESULTS

} *see attached pages*

USER: IDIVIDUAL FARMER, RANCHER, AGRICULTURAL CONSULTANT

26 APRIL 82

IRRIGATION SCHEDULING FOR DISTRIBUTED MANAGEMENT OF CROP YIELDS (BY FARMER/RANCHER)

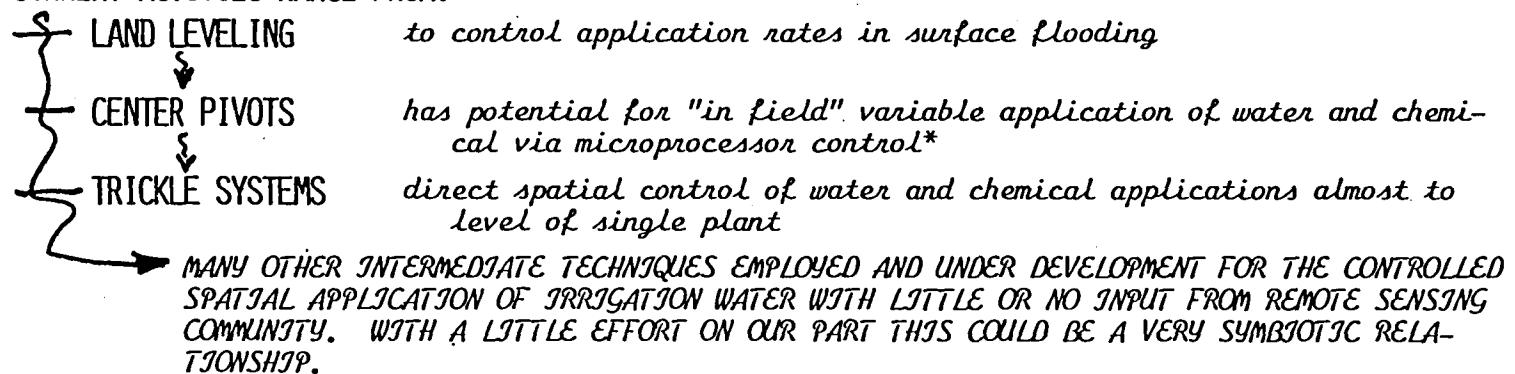
OBJECTIVES:

1. MANAGEMENT OF WATER APPLICATION FOR OPTIMAL YIELDS.
2. ENERGY MANAGEMENT FOR OPTIMAL YIELDS.
3. NUTRIENT APPLICATION FOR OPTIMAL YIELDS.

BACKGROUND STATEMENT:

INDEPENDENT OF REMOTE SENSING IRRIGATORS ARE DEVELOPING THE METHODOLOGY FOR THE SPATIAL CONTROL OF THE APPLICATION OF WATER TO INDIVIDUAL FIELDS TO ACHIEVE THE ABOVE OBJECTIVES.

CURRENT ACTIVITIES RANGE FROM:



**such a system might even have its own remote sensors on board.*

INFORMATION NEEDS FROM REMOTE SENSING ON A SPATIAL BASIS

BASED PRIMARILY ON WHAT MIGHT BE FEASIBLE WITH OPTICAL REMOTE SENSORS

1. CANOPY PHYSIOLOGY --
 - LEAF WATER CONTENT
 - GREEN BIOMASS - (*functioning versus non-functioning*)
 - BROWN BIOMASS
 - LEAF SURFACE AREA (*not equal LAI*)
 - GEOMETRY (*e.g. for wilt status*)
 - CANOPY TEMPERATURE
2. SOIL WATER STATUS --
 - SURFACE
 - SUBSURFACE (*non-optical sensors*)

ALL THE ABOVE ARE POTENTIALLY AVAILABLE FROM REMOTE SENSORS AND THE REAL QUESTIONS TO BE ADDRESSED

- INCLUDE:
1. TIMING?
 - HOW TO ACHIEVE DATA FREQUENCY REQUIRED (*e.g. off axis pointing*)
 - TIME OF DAY
 - NEED FOR INSTANTANEOUS MEASUREMENTS
 - NEED FOR INTEGRATED MEASUREMENTS (*e.g. HCMM idea*)
 - SCHEDULING COVERAGE (*widely distributed spatial demands*)
 2. SPATIAL RESOLUTION?
 - HIGH RESOLUTION AND POINTABLE INTO IRRIGATED AREAS*
 3. ACCURACY?
 - RADIOMETRIC
 - GEOMETRY AND GEOENCODING
 4. INFO/DATA DISTRIBUTION? (*see seperate sheet*)

*as a group IRRIGATED CROP LANDS are the most intensively managed agricultural lands requiring remote sensing inputs while providing maximum yield and return per acre. they are however grouped into areas of concentration toward which a sensor could be pointed.

INFORMATION / DATA DISTRIBUTION

- GOALS:
1. OVERNIGHT *near real time direct video broadcast (e.g. daytime data delayed for broadcast during low use night periods.*
 2. NO CENTRAL STORAGE *digital data encoded into video, transmitted and then decoded back to digital on site.*
 3. ON SITE CAPTURE *capture on video recorder as analog.*
 4. LOW COST *orient whole process toward consumer products: antennas, recorders, displays, processors, ...*

REQUIRES RESULTS OF FUTURE WORK WITH MODELS, ETC. TO DETERMINE HOW MUCH PROCESSING FROM "DATA" TO "INFORMATION" IS PERFORMED AT A CENTRAL SITE BEFORE DISTRIBUTION

? DISTRIBUTE INFORMATION SUCH AS SPATIAL VARIATION IN LEAF WATER CONTENT, GREEN BIOMASS, ETC.

- BECAUSE:
1. MODEL REQUIRES COMPLICATED TUNING
 2. MODEL REQUIRES COMPUTING POWER NOT AVAILABLE ON SITE

? DISTRIBUTE DATA SUCH AS "CLEAN" MULTISPECTRAL IMAGES WITH SYSTEMATIC, GEOMETRIC, AND OTHER IMAGE RELATED ADJUSTMENTS

- BECAUSE:
1. FARM MANAGEMENT MODEL REQUIRES LOCAL ON SITE INPUTS *(see section on modeling)*
 2. SOME IMAGE CORRECTIONS REQUIRE LOCAL OBSERVATIONS FROM USER *(solar incoming, atmospheric observations, etc.)*

ON SITE DATA PROCESSING

CLOSELY CONTROLLED BY DISTRIBUTION AND MODELING REQUIREMENTS

NOT CLOSELY CONTROLLED BY SPATIAL RESOLUTION AND OTHER PRIME CONSIDERATIONS OF OUR CURRENT EXPERIENCES WITH CENTRALIZED SYSTEMS

CONSIDERATIONS AND COMMENTS:

HARDWARE *not limiting now or in the future!*

1. ALL OBJECTIVES CAN BE MET TODAY FOR TODAY'S DATA/INFO/MODELS FOR TODAY'S IMAGES IF THEY WERE AVAILABLE TO FARMER/RANCHER
2. THERE IS EXTENSIVE USE OF SUITABLE MICROPROCESSORS AND OTHER RELATED DATA CAPTURE AND DISPLAY DEVICES ON THE FARM TODAY

SOFTWARE

DATA FORMATS

LOW COST HARDWARE DEVELOPMENTS IN COMMERCIAL PRODUCTS AREA OF DIRECT IMPACT

IN NEXT 3 YEARS: *should begin experimentation with use immediately*

1. *a faster processor will be available on the farm with 16bit words and 1megabyte of memory (Radio Shack, Apple IV, Sage, Fortune, ...)*
2. *200megabyte, low cost, optical read/write disk (i.e. capacity for 6 MSS images) with a size and price related to current floppy disks (Sharp Electronics)*
3. *Digital recording still cameras with film playback units (Sony Mavika)*

IN NEXT 3 TO 10 YEARS: *the actual time framework of any new land oriented R.S. system*

1. *a 32bit micromainframe on a desk*
2. *flat, large screen, high resolution, digital image displays*
3. *1000 gigabytes of low cost, read write storage on digital optical disks*

MODELING FOR DECISIONS

TO BE EXECUTED ON SITE ON THE SPECIFIC FIELD ON A SPATIAL BASIS

SHOULD RUN AT ALL LEVELS OF COMPLEXITY; I.E. SHOULD RUN WITH ONLY REMOTE SENSING INPUTS BUT ALSO WITH INCREASING LEVEL OF COMPLEXITY AND ACCURACY WITH INCREASING INPUT OF FARMER COLLECTED, ON SITE INFORMATION

CURRENT MODELS TESTED IN REMOTE SENSING CONTEXT TAKE LITTLE ACCOUNT OF EXTENSIVE INFORMATION AVAILABLE FOR INPUT OF FARMER ON SITE!

WHEN WE REORIENT OUR APPROACH TO RUN ON SITE THE FOLLOWING NEW AND VERY SIGNIFICANT INPUTS ARE AVAILABLE FOR EACH FIELD:

SPATIAL VARIATION IN FIELD OF:

SOIL TYPE AND PROPERTIES
TOPOGRAPHY
TREATMENTS/ EARLIER APPLICATIONS OF WATER
CHEMICALS
MECHANICAL

MANAGEMENT PRACTICES OF:

CROP TYPE
CHEMICAL APPLICATIONS
CROP CALENDAR/ PLANTING DATE AND METHOD
GROWTH STAGE VS. TIME

POINT MEASUREMENTS VS. TIME OF ENVIRONMENT:

ON SITE PRECIPITATION
AIR TEMPERATURE
HUMIDITY
E.T. ESTIMATES
WIND SPEED

ACCEPTANCE / USE OF RESULTS

1. CAN BE ACCOMPLISHED WITH A MINIMUM OF EFFORT - ECONOMIC INCENTIVES ALREADY EXIST
2. EQUIPMENT REQUIRED ALREADY BECOMING AVAILABLE ON SITE FOR OTHER RELATED REASONS
3. USE EXISTING EXISTING EDUCATIONAL/DISTRIBUTION CHANNELS TO FARMER/RANCHER VIA EXTENSION AGENT, AGRICULTURAL CONSULTANTS, CO-OPS, ETC.

EVAPOTRANSPIRATION and REMOTE SENSING

by

T. Schmugge and R. Gurney

NASA/GODDARD SPACE FLIGHT CENTER

Greenbelt, Maryland 20771

ABSTRACT

Evapotranspiration is the process in which water in the liquid phase is extracted from the soil and transferred to the atmosphere in the vapor phase. This transfer can occur as evaporation directly from the soil surface or transpiration from plant leaves. There are three things required for the process to occur: 1) energy (580 cal/gm) for the change of phase of the water; 2) a source of the water, i.e. adequate soil moisture in the surface layer or the in the root zone of the plant; and 3) a sink for the water, i.e. a moisture deficit in the air above the ground.

Remote sensing can contribute information to the first two of these conditions by providing estimates of solar insolation, surface albedo, surface temperature, vegetation cover, and soil moisture content. In addition there have been attempts to estimate precipitation and shelter air temperature from remotely sensed data. The problem remains to develop methods for effectively using these sources of information to make large area estimates of evapotranspiration.

INTRODUCTION

Evaporation and transpiration (evapotranspiration or ET) estimates are required for several purposes, including irrigation scheduling, water balance calculations, run-off prediction and meteorological and climatological studies. Long-term estimates of evapotranspiration may be made using water balance methods, as in lysimetry or evaporation pans, or at a larger scale in river basins. However, there is considerable uncertainty in these measurements, particularly for short time periods, and it is often difficult to generalize the measurements to large areas. Many areas do not have any hydrologic measurements and for these areas Thornthwaite (1947) suggested an empirical approach to estimate long-term evaporation from routine meteorological observations, principally monthly mean temperature. Penman (1948) derived a more physically-based expression which uses standard meteorological data to estimate potential evapotranspiration. This was for a short grass cover with an adequate water supply. This model has served as the theoretical basis for most of the currently used models. However their application is still limited to locations where standard meteorological data are available. In principle, remotely sensed measurements, offer methods for extending these models to much larger areas including those where data may be sparse. Although no method is as yet operational the utility of such measurements is sufficiently great to encourage further work.

To understand better how remote sensing may contribute it is

instructive to examine first the basic energy and moisture balance equations.

Energy and Moisture Balance

The energy balance of a soil or vegetated surface is governed by a conservation equation. In the absence of precipitation or advection, we may write

$$R_n + G + H + LE = 0 \quad (1)$$

where R_n is the net radiation flux, G the soil heat flux, and H the sensible heat flux and LE the latent heat flux in the atmospheric boundary layer. The latter is the product of the water vapor flux, E , and the latent heat of vaporization of water per unit mass, L .

The net radiation flux is the sum of the incoming and outgoing short and long wave radiation fluxes:

$$R_n = (1 - \alpha_s)R_s + e_L (R_L - \sigma T_c^4) \quad (2)$$

where R_s is the incoming short-wave radiation and R_L is incoming long-wave radiation, α_s is the short-wave soil/crop reflectivity or albedo, e_L is the long-wave emissivity, σ is the Stefan-Boltzman constant and T_c is the soil surface temperature in Kelvins.

The soil heat flux is related to the temperature gradient in the soil dT/dz and to the thermal conductivity λ

$$G = \lambda \, dT/dz \quad (3)$$

This relationship leads to a form of the diffusion equation

$$d(\lambda \, dT/dz)/dz = C_v \, dT/dt \quad (4)$$

where C_v is the volumetric heat capacity of the soil. This equation may be solve numerically to give a temperature profile in the soil, taking either T_c or G as the upper boundary condition and some known temperature at a given depth in the soil as the lower boundary condition.

The sensible and latent heat fluxes may both be estimated from the transport equations. The sensible heat flux H may be expressed as

$$H = \rho \, C_p (T_a - T_c) / r_a \quad (5)$$

where ρ is the air density, C_p is the specific heat of the air and r_a is the aerodynamic resistance. The latent heat flux may be expressed as

$$LE = \frac{\rho \, C_p}{\gamma} \frac{(e_a - e_s)}{r_a - r_s} \quad (6)$$

where γ is the psychrometric constant, e_a is the atmospheric vapor pressure in the boundary layer, e_s is the saturated vapor pressure at the temperature T_c , and r_s is the stomatal diffusion resistance to water vapor transport.

Equations (2), (3), (5) and (6) are a mathematical model of the surface energy balance in terms of the soil surface temperature and a set of meteorological measurements, which at least in principle, are measured or estimated routinely. The energy and moisture fluxes are intimately related because the latent heat flux gives the amount of water evaporated and transpired.

One formulation of potential evapotranspiration that lends itself to remote sensing inputs is that developed by Priestly and Taylor (1972). They obtained for saturated surfaces

$$LE = \alpha [s/(s + \gamma)](R_n - G) \quad (8)$$

where s is the slope of vapor pressure versus temperature curve, and α is an empirical evaporation constant which they determined to be 1.26. Barton (1979) and Davies and Allen (1973) have modified the result for unsaturated surface by treating α as a function of the surface layer soil moisture. Barton used airborne microwave radiometers to remotely sense soil moisture in his study of evaporation from bare soils and grasslands.

Remotely Sensed Measurements

Several types of remotely sensed observations may be made by measuring the electromagnetic radiation in a particular waveband either reflected or emitted from the earth's surface. The incoming solar radiation can be estimated from satellite

observations of cloud cover primarily from geosynchronous orbits. For clear sky conditions, the surface albedo may be estimated by measurements covering the entire visible and near-infrared wavelengths, while measurements at narrow spectral bands can be used to determine vegetative cover. The surface temperature can be estimated from measurements at thermal infrared wavelengths, i.e. the 10.5 to 12.5 micron waveband, of the emitted radiant flux and from some estimate of the surface emissivity (for actual surfaces ϵ is usually close to unity). The microwave emission and reflection or backscatter from soil, primarily for wavelengths between 5 and 21 cm, is dependent on the dielectric properties of the soil which are strong functions of the soil moisture content. There are uncertainties in the determination of soil moisture values from microwave measurements introduced by factors such as surface roughness and vegetative cover but it appears that microwave methods can estimate the soil moisture content in the surface 5 cm layer of the soil with 4 or 5 levels of discrimination.

Remotely sensed measurements may be made from a variety of platforms. Operational work is largely conducted using satellites, which offer repetitive coverage but suffer from reduced spatial resolution compared to aircraft. Currently only visible and infrared data are available from satellite. Aircraft platforms are primarily used for experimental studies because of the greater control possible.

Applications of Remotely Sensed Measurements

In recent years there has been much progress made in the remote sensing of a number of parameters which can contribute to the estimation of evapotranspiration. These include: surface temperature, surface soil moisture, surface albedo, vegetative cover, and incoming solar radiation. There has been little progress made in the direct remote sensing of the atmospheric parameters which affect evapotranspiration such as: surface air temperature, water vapor gradients, and surface winds. Thus approaches for evapotranspiration estimation using remotely sensed data will have to work around these missing data.

The evaporation from the soil surface is directly related to the vapor pressure difference between the surface and lower atmospheric boundary layer, and the water supply in the soil. Assuming that there is a suitable supply of water in the soil, the most important controlling factor is the difference $[e_a - e_s]$ in equation (6), which is largely determined by the corresponding temperature difference. Thus there is a strong relationship under certain conditions between the canopy and air temperature differences and the evapotranspiration rate. This comparison of canopy and air temperatures has been used to detect crop water stress for irrigated crops in the southwestern part of the United States and these relationships have been described in a series of papers from the group at the US Water Conservation Laboratory in Phoenix (Jackson et al., 1981 and references cited therein).

Estimates of the net radiation from geostationary satellite data are used by Kanemasu (1982) in a Priestly-Taylor type of equation to estimate evapotranspiration. The resulting moisture

flux is then used to drive a water balance model for predicting crop yields. They also used Landsat multispectral data to obtain vegetation indices.

A more complete but less practical approach is that adopted by Soer(1980), Rosema et al. (1978), and Carlson (1981), amongst others, in which the energy balance (equations 1 - 6) is modelled and the moisture balance is inferred from the heat flow in the soil. Equations (2), (4), (5), and (6) can be manipulated to obtain an expression for the surface energy balance in terms of the surface temperature and a set of meteorological measurements which, at least in principle, are measured or estimated routinely. The initial estimate of the soil/crop surface temperature T will almost certainly not satisfy the continuity requirement of equation (1) because of numerical simplifications and so it is necessary to use an iterative numerical optimization technique to ensure that the condition in equation (1) is satisfied. The technique may be adapted to give estimates of the surface temperature T_c at every time step at which routine meteorological observations are available. The Tergra (Soer, 1980) model uses a Businger-Dyer (Eusinger et al., 1971 and Dyer, 1967) approach to estimate the turbulent diffusion resistance r_a . This gives r_a as a function of wind velocity and the stability of the atmospheric boundary layer just above the surface. A simple empirical parameterization of the stomatal resistance r_s and an explicit finite difference soil heat flux model are used.

The Tellus model (Rosema, et al., 1978) is somewhat similar except that the model is calibrated against both a daytime and a

nighttime surface temperature. A Newton-Raphson numerical integration scheme is used to optimize two parameters: the surface relative humidity, effectively related to the resistance to water transport across the surface boundary layer, and the thermal inertia of the soil. The finite difference scheme uses an expanding grid with thinner soil layers near the surface (Rosema et al., 1978). This model has been used to create look-up tables, which were used with airborne thermal infrared surface temperature data and albedo estimates to give maps of cumulative daily evapotranspiration (Dejace et al., 1979). Other studies (Gurney 1978) have shown that the Tergra and Tellus models give results relatively close to those estimated or measured by other means. Carlson (1981) developed a similar model, with a simple soil heat flux component. Using satellite data from the Heat Capacity Mapping Mission he obtained reasonable results under non-stressed conditions from vegetated surfaces. Elkington and Hogg (1981) used an approach based on the Tergra model to estimate evapotranspiration. However they used a simple set of inputs, estimating net radiation from the Brunt equation and the other boundary conditions from routine meteorological observations taken at nearby standard weather stations. Their results are sufficiently encouraging to suggest that the simplifications which would be required for an operational approach are indeed possible.

Bernard et al. (1981) in a simulation study have examined the use soil moisture estimates from a radar to calculate evapotranspiration rates. The microwave estimates of the surface soil moisture were used as the upper boundary condition in a water

balance model. The study provides a good indication of the utility of microwave soil moisture sensing for estimating evapotranspiration.

A more physically based and realistic model has been developed by Camillo and Schmugge (1981). Both energy and moisture fluxes are modelled. The space-time dependence of temperature and moisture content are described by a set of diffusion type partial differential equations, and the model uses a predictor/corrector method to numerically integrate them, yielding both moisture and temperature profiles in the soil as functions of time. The model was used to simulate energy and moisture fluxes under field conditions using data from Phoenix, Arizona. The qualitative agreement between the observations and the model was very good, indicating that the model is a reasonably accurate representation of the physical processes involved. A further example of the use of the model is given in Gurney and Camillo (1982). This model, because it simulates the moisture profile explicitly in addition to the temperature profile, requires an initial moisture profile. At least in principle this may also be derived using remotely sensed microwave measurements. As the model is most sensitive to changes in the surface soil temperature and soil moisture, which is that part of the profile accessible to the microwave thermal infrared measurements, this is a very realistic application of remotely sensed data. If it is possible to take initial conditions from remotely sensed measurements and the boundary conditions either from routine meteorological observations or remotely sensed measurements, the

estimation of actual evapotranspiration from remotely sensed measurements becomes feasible.

There are various other measurements which have either been suggested as inputs to evapotranspiration estimates or in principle could be used as additional model inputs. Multispectral information may be used to estimate the health of vegetation and the biomass (Tucker, 1980, Holben, et al., 1980, and Kanemasu, 1982) and hence to give an indication of the evapotranspiration rate.

The major problems with all remote sensing methods of evapotranspiration are: 1) the process of transpiration is still not well understood and parameterized for structured crops such as cereals or complex vegetation, such as trees; 2) in the presence of vegetation the surface temperature T_c estimated by a thermal infrared sensor is at an unknown level within the vegetation; and 3) the most appropriate use of microwave observations of surface soil moisture in the presence of vegetation needs to be determined. For the future we expect that the most practical method will probably use a multi-spectral approach including repetitive observations at the visible, near and thermal infrared, and microwave wavelengths. This will afford the possibility of estimating solar insolation, surface vegetative cover and/or albedo, surface temperature, and surface soil moisture from remotely sensed data and incorporating them into models of the type described here.

ACKNOWLEDGEMENT

One of the authors (RJG) is a National Academy of Science/National Research Council Resident Research Associate in the Hydrological Sciences Branch at the Goddard Space Flight Center.

REFERENCES

- Barton, I.J., 1978. A case study comparison of microwave radiometer measurements over bare and vegetated surfaces. J. Geophys. Res., 83: 3513-3517
- Bernard, R., H. Vauclin, and D. Vidal-Madjar, 1981. Possible use of active microwave remote sensing data for prediction of regional evaporation by numerical simulation of soil water movement in the unsaturated zone. Water Resources Res., 17: 1603-1610.
- Businger, J.A., J.C. Wyngaard, Y. Izumi, and E.F. Bradley, 1971. Flux profile relationships in the atmospheric surface layer. J. Atmos. Sci., 28: 181-189.
- Camillo, P. and T.J. Schmugge, 1981. A computer program for the simulation of heat and moisture flow in soils. NASA Technical Memorandum TM-82121.
- Carlson, T.N., J.K. Dodd, S.G. Benjamin and J.N. Cooper, 1981. Remote estimation of surface energy balance, moisture availability and thermal inertia over urban and rural areas. J. Appl. Meteor., 20: 67-87.
- Davies, J.A. and C.D. Allen, 1973. Equilibrium, potential and actual evaporation from cropped surfaces in southern Ontario. J. Appl. Meteor., 12: 649-657.
- Dejace, J., J. Megier, M. Kohl, G. Maracci, P. Reiniger, G.

Tassone, J. Huygen, 1979. Mapping thermal inertia, soil moisture and evaporation from aircraft day and night thermal data. 13th ERIM Symposium on Remote Sensing, Manila:1015-1024.

Dyer, A.J., 1967. The turbulent transport of heat and water vapor in an unstable atmosphere. Quart. J. Roy. Meteor. Soc., 93: 501-508.

Elkington, M.D. and J. Hogg, 1981. The characteristics of soil moisture content and actual evapotranspiration from crop canopies using thermal infrared remote sensing. Proc. Remote Sensing Soc., Reading.

Gurney, R.J. and P.J. Camillo, 1982. The effects of soil and atmospheric boundary layer variables on evapotranspiration and soil moisture studies. This meeting.

Gurney, R.J., 1978. Estimation of soil moisture content and actual evapotranspiration using thermal infrared remote sensing. Proc. Remote Sensing Society: 101-109.

Holben, B.N., C.J. Tucker, and C.J. Fan, 1980. Spectral assessment of soybean leaf area and leaf biomass. Photogrammetric Engineering and Remote Sensing, 46: 651-656.

Jackson, R.D., S.B. Idso, R.J. Reginato, and P.J. Pinter, 1981. Canopy temperature as a crop water stress indicator. Water Resources Research, 17: 1133-1138.

Kanemasu, E.T., 1982. Use of satellite information to estimate

- evapotranspiration. This meeting.
- Penman, H.L., 1948. Natural evaporation from open water, bare soil and grass. Proc. Roy. Soc., London, A193: 129-145.
- Price, J.C., 1980. The potential of remotely sensed thermal infrared data to infer surface soil moisture and evaporation. Water Resources Research, 16: 787-795.
- Priestly, C.H.B. and R.J. Taylor, 1972. On the assessment of surface heat flux and evaporation using large-scale parameters. Mon. Wea. Rev., 100: 81-92.
- Rosema, A., J.H. Bijleveld, P. Reiniger, G. Tassone, R.J. Gurney, K. Blyth, 1978. Tellus, a combined surface temperature, soil moisture and evaporation mapping approach. Proc. 12th ERIM Symp. on Remote Sensing, Ann Arbor, pp10.
- Soer, G.J.R., 1980. Estimation of regional evapotranspiration and soil moisture conditions using remotely sensed crop surface temperatures. Remote Sensing of Environment, 9: 27-45.
- Thornthwaite, C.W., 1948. An approach toward a rational classification of climates. Geophysical Review, 38: 55.
- Tucker, C.J., 1980. Remote sensing of leaf water content in the near-infrared. Remote Sensing of Environment, 10: 23-32.

COST EFFECTIVENESS OF CONVENTIONAL
VERSUS LANDSAT LAND USE DATA FOR HYDROLOGIC MODELING

Water Management and Control ASVT
Final Report

PREPARED FOR

National Aeronautics and Space Administration
Goddard Space Flight Center
Greenbelt, Maryland

PREPARED BY

Thomas S. George
Robert S. Taylor

WATER RESOURCES ENGINEERS
an Operating Unit of Camp Dresser & McKee INC.
Springfield, Virginia

September 1980

II. SUMMARY AND CONCLUSIONS

STUDY SUMMARY

The purpose of this chapter is to summarize the findings of the study and to present specific conclusions and recommendations that can be drawn from this work. A detailed analysis of six case studies has been performed to investigate the cost effectiveness of using Landsat obtained land use data as opposed to conventionally obtained land use data in hydrologic modeling. Five of the six case studies are Corps of Engineers Expanded Flood Plain Information (XFPI) investigations carried out by Corps Districts throughout the United States. The other test basin is one that is used as a training site for courses in hydrology and flood plain management presented by the Hydrologic Engineering Center (HEC) of the U.S. Army Corps of Engineers in Davis, California. For each case study information was collected on the methods and costs associated with obtaining land use information by conventional means for use in the hydrologic modeling phase of the XFPI reports. In addition, information on costs and procedures was also obtained for developing the required land use information based on a methodology that relies on Landsat imagery. This study compares these costs and develops a procedure to investigate the relative effectiveness of the two alternative means to acquire land use data needed for the hydrologic modeling.

The cost of obtaining the conventional land use data is shown to range between \$3,000 - \$16,000 for the six test basins. The corresponding resultant cost associated with obtaining the land use information based on Landsat imagery are \$2,000 - \$5,000. Thus, from a pure cost standpoint the Landsat approach for gathering land use data has a cost advantage in some cases. The next aspect investigated in this study is the relative effectiveness of each approach.

Based on the criteria developed during the course of this study for evaluating the various measures, the overall results of the effectiveness analysis show that the differences between the relative effectiveness of the conventional and Landsat methods for obtaining land use for hydrologic modeling purposes for each of the six test watersheds are insignificant. Therefore, the conventional approach is not generally more effective than the Landsat approach, nor is the Landsat approach generally more effective than the conventional approach.

This effectiveness analysis is not performed under the most ideal conditions. The emphasis has been placed on the effectiveness of conventional and Landsat methods for developing land use data for hydrologic analyses. All of the conventional studies, except Castro Valley, were part of an XFPI study which developed land use information for additional purposes. The Landsat land use development was only carried out to be applied to hydrologic analyses. However, the analysis of effectiveness is carried out with these differences taken into consideration as much as possible.

From the cost comparison and the fact that each method, conventional and Landsat, is shown to be equally effective in developing land use data for hydrologic studies, the cost effectiveness of the conventional or Landsat

method is found to be a function of basin size for the test watersheds analyzed. Castro Valley, a watershed of 5 square miles is definitely cost effective using the conventional method. Trail Creek with its 12 square mile area and the fact that the conventional cost may be underestimated, is a borderline case. The remaining watersheds show that the Landsat method is cost effective.

COST EFFECTIVENESS CONCLUSION

The total cost effectiveness analysis shows that there exists a point near 10 square miles in study area size where the conventional and Landsat methods depart as to their cost effectiveness. As a general conclusion, the cost effectiveness study, although limited in its number of test watersheds and performed under other than ideal study conditions, shows that for developing land use information for use in hydrologic studies the conventional method is cost effective for watershed study areas containing less than 10 square miles and that the Landsat method is cost effective for areas containing more than 10 square miles.

SUMMARY OF FINDINGS

Several additional specific conclusions and findings can be extracted from an analysis of the work performed in this study. They are grouped into two major categories as follows:

Study Findings

- This study presents conclusions based on six case studies and its validity depends entirely on the relatively small sample, however, previous research concurs with the findings of this work;
- Conventional land use classification costs per square mile of study area decrease as area increases;
- Land use classification costs by the use of satellite imagery for basins the size of those in our study is not highly dependent on the size of the basin;
- If existing land use data are scarce the cost of obtaining new land use data are much higher for conventional techniques than by Landsat means;
- The cost for HEC to perform Landsat based land use classification were nearly identical to the contracted costs for the same work;
- For large basins and large storm events hydrologic models are relatively insensitive to land use classifications, however, for small basins and/or small storms the model results (flows) become very sensitive to the land use employed;

- Use of the Landsat classification approach requires some special skills which are not presently standardly available in all technical offices dealing with hydrologic studies;
- Landsat imagery does not presently have the resolution required to do detailed land use classification for use in flood damage surveys or have the resolution needed to represent small areas with very diversified land uses;
- For detailed flood plain studies it would appear to be a cost effective approach to use Landsat derived land use for hydrologic calculating and to supplement this land use data with more detailed information in the actual flood plain area for use in economic analyses; and
- It is not feasible to attempt to develop a cost/benefit analysis of the incorporation of Landsat derived land use information into hydrologic modeling studies with the sparseness of existing case studies and the wide variation in the data and study circumstances encountered.

Findings for Future Studies

- A complete definition and analysis of the two land use approaches is presented which should aid decision makers in selecting one method for use in their work;
- For a complete evaluation of the application of one of the methodologies a potential user should not just look at the results of this study but should look at all the individual measures of effectiveness and their relationships to the users exact needs;
- For a given project the measures of effectiveness and their relative weights could be quite different than those presented in this study and should be evaluated more nearly on a case by case basis;
- For the Landsat methodology the cost to classify any portion of a satellite scene is close to being the same as classifying the whole scene. However, ground truth and verification costs would increase. Nevertheless, it would still be advantageous to do the whole scene and save the results for other potential users;
- If the user community is required to directly bear the costs of the operation of the Landsat system, the cost of obtaining land use data from satellite imagery will increase;

- The use of grid cell data bank types of data management systems will likely increase in the future and the Landsat methodology for land use classification is highly compatible with this system;
- The improved resolution of Landsat-D will improve and expand the use of satellite data in hydrologic studies and possibly environmental and economic studies;
- Development of different classification techniques than those commonly used now along with new enhancement procedures may improve land use classification of satellite data, thus making its use in hydrologic studies even more desirable;
- Potential long term users should consider that there is no guarantee that the satellite will last its expected life or that its subsequent replacement is inevitable;
- There appears to be a great untapped potential for use by agencies, in addition to the Corps of Engineers, of Landsat derived land use information in conjunction with grid cell based data management systems, particularly those involved in planning and hydrology;
- A large potential for the use of satellite imagery seems to exist in other facets of water resources management in addition to flood plain hydrology; and
- Additional data from other case studies should be collected and added to that in this report to further solidify the findings of this work and hopefully lead to even more detailed conclusions.

Subsequent sections of this report detail the various phases involved in the cost effectiveness analysis.

High Resolution Impacts on Private Consulting

1. Introduction

The impact on the private consultant is much the same as the impact on the public sector whether federal, state or local. Basically, because an environmental engineering firm such as CDM which deals in hydrology and other water resources project is hired by the public sector to perform certain studies for two reasons: 1) the particular agency or office does not have the expertise or 2) they do not have the staff to carry out the job within the time frame necessary.

The consultant, however, is not bound by the contractor, in all cases, to do a job a specific way. He has the leeway to develop and suggest methodologies for performing specific tasks. After all he is a "consultant" and he gets paid for his professional advise and opinions.

Therefore, in order for the consultant to provide the best service to his clients, he must be aware of the new technologies, their capabilities and limitations. In fact, he must know the results of this workshop's objectives, especially the current state of knowledge.

2. Present System Uses

In the past much of the consulting work has been associated with the use of data classified into land use categories for hydrologic, environmental and economic (damages) analyses. Land use data from Landsat, and from aeri-als, existing maps, field surveys, etc. have been compared for their cost effectiveness in several studies. Other areas of image use are for locating existing features such as lakes for inventory, dump sites for hazardous waste studies, rock formations and drainage patterns for reservoir site studies and fractures for analyses of carbonate aquifer systems. Multispectral imaging can be used

for preliminary evaluation of lake quality and eutrophic state, location of high erosion potential areas (of special concern would be where sediment is introduced into a reservoir effecting its volume and water quality), discharge plume studies, determination of circulation patterns in coastal areas for temperature and quality studies, and development of roughness coefficients from land cover for wave crest analysis in coastal flood studies.

3. Implications of High Resolution Imaging

There are two types of impacts which present themselves: a) higher resolution providing greater detail of the "same old parameters" and b) totally new information which may produce new parameters and new relationships for a variety of studies including hydrologic studies.

a. Same Old Parameters - Higher resolution can aid in most all aspects of the acquisition of the "same old parameters" by providing the detail necessary to more accurately define the data base. In many cases, however, greater detail is not always necessary (but new parameters and relationships may be!).

As an example of the same parameters, consider residential land use. Presently many classification techniques or attempts have only one residential category. In the hydrologic analysis of small watersheds this may be inadequate and therefore there is a need for distinguishing among low, medium and high density residential. Higher resolution will allow the classification of other land use subcategories which would be beneficial to the study of small urban watersheds. The ability to classify many subcategories of major land uses will also allow the user to view the data based on his needs and he will not be at the mercy of limited or inappropriate categories. Higher resolution will also aid in the analysis of stream channel and adjacent areas. In the past Landsat data proved to be adequate for hydrologic studies of larger watershed but did not have the resolution for flood plain surveys for damage studies. Greater resolution may then allow satellite data to be used for hydrologic and economic studies. High resolution can provide us with a better look at the same thing. But what about looking at something new?

b. New Parameters - Private consultants are like everyone else, they do not especially want to do more of the same in greater detail. New horizons are what stimulate the private consultant and he wants to be involved in new scientific research and development. The question is, whether the new measurement capability will allow us to develop new parameters and subsequently new relationships for many types of applications. Will we still be looking at land use categories and curve numbers or will new hydrologic components and new modeling techniques grow out of the new scientific information? If new data evaluation and modeling methods are to be forthcoming, the private consultant can provide an enormous service with his background in mathematics, computer science, engineering and his knowledge of the practical needs for a safe and clean environment. New information can be applied to hydrologic studies, however another field in which the consultant is highly involved is water quality. Another question is whether the high resolution, spatial and spectral, will aid in water quality studies. As with hydrology, new parameters and new model techniques may be developed as a result of the data acquired. The private consultant will be called on to provide his services.

A. Feldman

DRAFT

SUMMARY OF HYDROLOGIC MODELING INTERESTS IN REMOTE SENSING

Background

Remote sensing of geographic information can be separated into two general types of technology: (1) point measurement on the ground and (2) spatial average measurements from aircraft or satellites. Both of these technologies require data transmission facilities to communicate the data observations at the collection point to the data analysis center.

Point measurements (e.g. rainfall, streamflow, soil type, land use, evaporation, etc.) have been the basis for virtually all hydrologic modeling data to date. The physical processes represented by the models are usually averages over some increments of time and space. Spatial averages are approximated by as many point measurements (aerial photos for some parameters) as warranted by the study budget and objectives. Satisfactory results have been obtained when the necessary data are available.

A critical parameter in all hydrologic flood models is the status of the soil moisture at the beginning of a storm. Dry soil conditions can render a major storm virtually harmless. Wet soil conditions can make even minor storms dangerously productive in flood runoff. Some models, particularly operational flood forecasting models, endeavor to estimate the current soil moisture conditions through a mathematical accounting of spatially averaged point measurements of previous precipitation, infiltration, and evapotranspiration, and the runoff from a basin. These models, termed "continuous" simulation models, compute the theoretical soil moisture conditions (usually some index thereof) for the current status of the system. They are "ready to go" when new precipitation occurs.

Other models, particularly flood analysis models, operate only for "single" flood events. They utilize soil moisture parameters but the values of those parameters must be prescribed by the user as input to the model. If soil moisture conditions are not known at the beginning of a storm, they can only be approximated as one observed the runoff (streamflow) produced by the storm.

Both "continuous" and "single event" models can have a very detailed representation of the runoff processes in a watershed. The continuous models, while theoretically superior (more complete representation of the hydrologic processes), are usually much more expensive to calibrate. The expense is in the data preparation, computer time, and analysts' time. Single event models, on the other hand, can be quite inexpensive to calibrate.

The previous discussion is limited to flood forecasting and designing flooding control measures. Hydrologic analysis for other purposes (e.g., water supply) may require an assessment of streamflow over long period of time.

Current Uses of Remote Sensing in Hydrology

Many different forms of land-based point data collection stations are in use today. The principal types of data collected are precipitation, streamflow, temperature and snow depth. The data are transmitted by land lines, microwave and/or via satellite.

Spatial-average measurements (from aircraft or satellite) of hydrologic processes are much less commonly used. Land cover for use in hydrologic modeling has been successfully determined from satellite imagery (NASA Water Control ASVT). In that ASVT, the Hydrologic Engineering Center used land cover, as determined from LANDSAT imagery, to establish SCS curve number runoff parameters in four watersheds across the U.S. Conventionally determined land use and resulting curve numbers were used to estimate flood frequency curves from design storms. When LANDSAT land cover was substituted into the methodology, there were no significant differences from the frequency curves determined using conventionally determined land use. Although hydrologic land use determination by satellite has been effectively demonstrated, it is still not routinely used in hydrologic studies.

Ground-based radar measurement of relative rainfall intensity over watersheds has been used in operational flood forecasting. Cloud-top temperatures and densities have been used to infer rainfall potential but not in operational flood forecasting sense. The extent of flooded areas has also been measured by aircraft and satellite. Aircraft have also been used to make detailed measurement of stream/river cross sections and other topographic features.

Desired Uses of Remote Sensing in Hydrology

The two most important hydrologic variables, precipitation and soil moisture, are probably the most poorly measured on a spatial-average basis. Better and more timely information on the precipitation input to and soil moisture status of a watershed would make major improvements in the current flood forecast capabilities.

Existing sensors for soil moisture (passive microwave and gamma by aircraft) need field testing for utility in hydrologic modeling. They should be tested for a variety of field conditions including terrain types and ground cover. High altitude aircraft and satellite sensor systems should be developed.

Corps Applications

There is an immediate need for such improved flood forecasting techniques at existing Corps' flood control reservoirs. Better forecasts will allow better reservoir operation and reduced flood damage. There would also be a considerable savings in the calibration effort required for the continuous flood forecasting models. That is, the current soil moisture could be obtained directly from aircraft/satellite measurements (near real time) and save the analysis effort required to compute the soil moisture condition before a storm. The foregoing is true both in the calibration and operational aspects hydrologic model usage.

DRAFT

USDA-ARS Hydrology Laboratory

T. J. Jackson

MISWG Hydrology Workshop

April 26, 1982

The USDA-ARS Hydrology Laboratory is investigating remote sensing techniques for measuring hydrologic parameters and variables. Current research deals with runoff Curve Numbers (CN), evapotranspiration (ET), and soil moisture. CN and ET research utilizes visible and infrared measurements and soil moisture investigations focus on the microwave region of the electromagnetic spectrum. Previous studies have involved visible and near infrared data in estimating the percent of impervious area.

CN research is aimed at developing and evaluating methods for using remote sensing for the USDA-SCS. The role of remote sensing in the SCS procedures is shown in Figure 1. It is essentially an alternative source of land cover information. However, sources such as Landsat also have the advantage of a computer compatible format.

Whether or not remote sensing will eventually play an operational role will depend upon its cost-effectiveness. Improved spectral and spatial measurements will influence the effectiveness side of these tradeoffs.

Curve number accuracy is limited by the number of land cover categories that can be reliably defined, which in turn depends upon the available spectral bands and the spatial resolution. In this application, the accuracy can be evaluated by the expected error in estimating the CN of the basic modeling unit, a subwatershed. Conventional methods are assumed to have a small constant error as shown in Figure 2. Investigations have shown that when using Landsat data the error depends upon the subwatershed size and decays as it increases. Figure 2 shows that if the decision criterion was error the user would not choose Landsat for areas less than S in size.

Improved spectral and spatial measurements should shift the error-subwatershed size relationship down as illustrated in Figure 2. Under these conditions, remote sensing is advantageous at a smaller subwatershed size S'.

Our research has not considered the questions of what spectral information could improve the procedure and how improved spatial resolution would affect accuracy. The reason for this is that we are focusing on making the best use of existing data sources. However, these problems are important and could be studied using laboratory and/or small scale experiments. Research on these subjects would be similar to the problems involved in crop discrimination and urban land cover studies. At this state it is not possible to say whether spectral or spatial measurement improvement is more valuable.

Aside from the question of the best spectral bands, studies are needed to evaluate the temporal features of remotely sensed data. Classification and analysis for CN depends upon the time of year. However, studies to identify optimal conditions have not been conducted. Also, the use of multi-date data has not been adequately investigated.

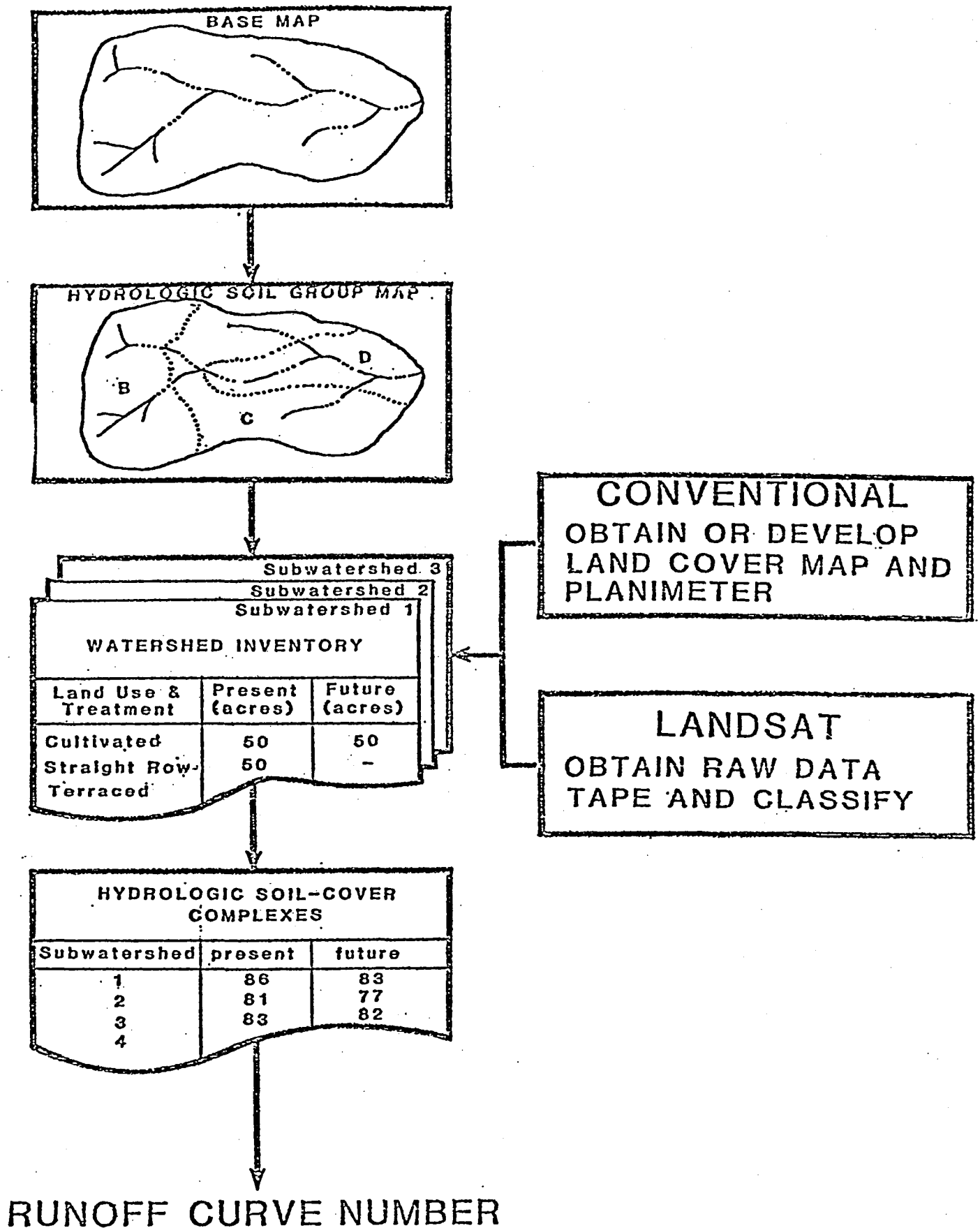


Figure 1. - Comparison of Conventional and Remote Sensing Approaches to Curve Number Estimation.

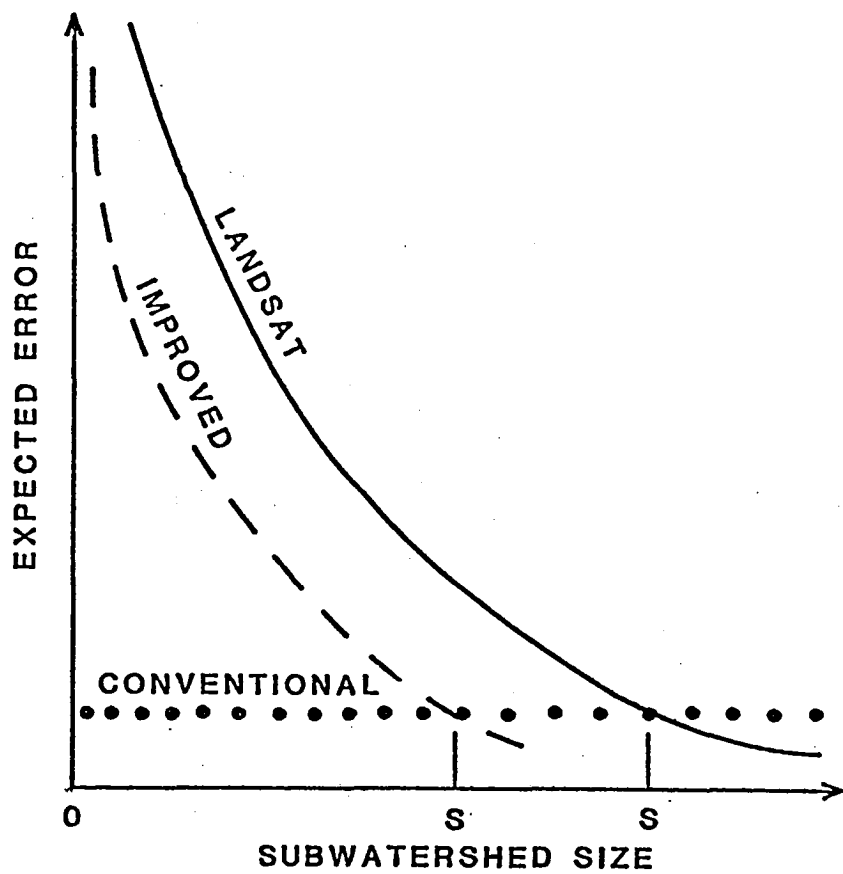


Figure 2. - General Relationship Between the Expected Error in Estimsting the CN and Subwatershed Size.

Other problems that should be considered which significantly affect the utility of remotely sensed data in quasi-operational applications, such as CN estimation, are data calibration and registration. Information extraction will always be limited by calibration. It seems that procedures could be developed to make this more quantitative. CN estimation, as illustrated in Figure 1, involves the combination of several data bases, remotely sensed land cover being one. Accuracy and reliability depend upon registering these. Reliable and easy to implement procedures for ground registration would be useful. Also, since all data bases are ultimately referenced to the USGS topographic maps, why not obtain the data at a matching 1:24,000 spatial scale?

Another topic of interest is the estimation of the percent of impervious area directly from remotely sensed data without intermediate land cover classification. Based upon available Landsat bands, procedures for doing this have been developed. One example is shown in Figure 3. Studies to determine the optimal spectral bands have not been conducted and would be useful. Relationships between the expected error and the size of the study area have been developed based upon Landsat data bases, however, the effect of spatial resolution has not been investigated.

Current research in ET estimation employs an energy and moisture budget approach for the interpretation of thermal infrared data as acquired by the NOAA operational satellites. The 1.1 kilometer spatial resolution of the Advanced Very High Resolution Radiometer prevents field by field evaluation of moisture characteristics and thus has potential utility only for regional scale ET assessment. Aircraft data should be acquired and analyzed to ascertain the significance of improved spatial resolution in the analysis of thermal infrared data.

REFERENCES

- Bondelid, T. R., Jackson, T. J., and McCuen, R. H., 1980, Comparison of Conventional and Remotely Sensed Estimates of Runoff Curve Numbers in Southeastern Pennsylvania, Proceedings of the ACSM-ASP Annual Meeting, St. Louis, Mo.
- Bondelid, T. R., Jackson, T. J., and McCuen, R. H., 1981, A Computer Based Approach to Estimating Runoff Curve Numbers Using Landsat Data, AgRISTARS Technical Report, CR-R1-04040.
- Carlson, T. N., Dodd, J. K., Benjamin, S. G., and Cooper, J. N., 1982, Satellite Estimation of Surface Energy Balance, Moisture Availability and Thermal Inertia, Journal of Applied Meteorology 20, pp. 67-87.
- Jackson, T. J., 1975, Computer Aided Techniques for Estimating the Percent of Impervious Area from Landsat Data, Proceedings of the Workshop on Environmental Applications of Multispectral Imagery, Ft. Belvoir, Va.
- Jackson, T. J., and McCuen, R. H., 1979, Accuracy of Impervious Area Values Estimated Using Remotely Sensed Data, Water Resources Bulletin, Vol. 15, No. 2, pp. 436-446.

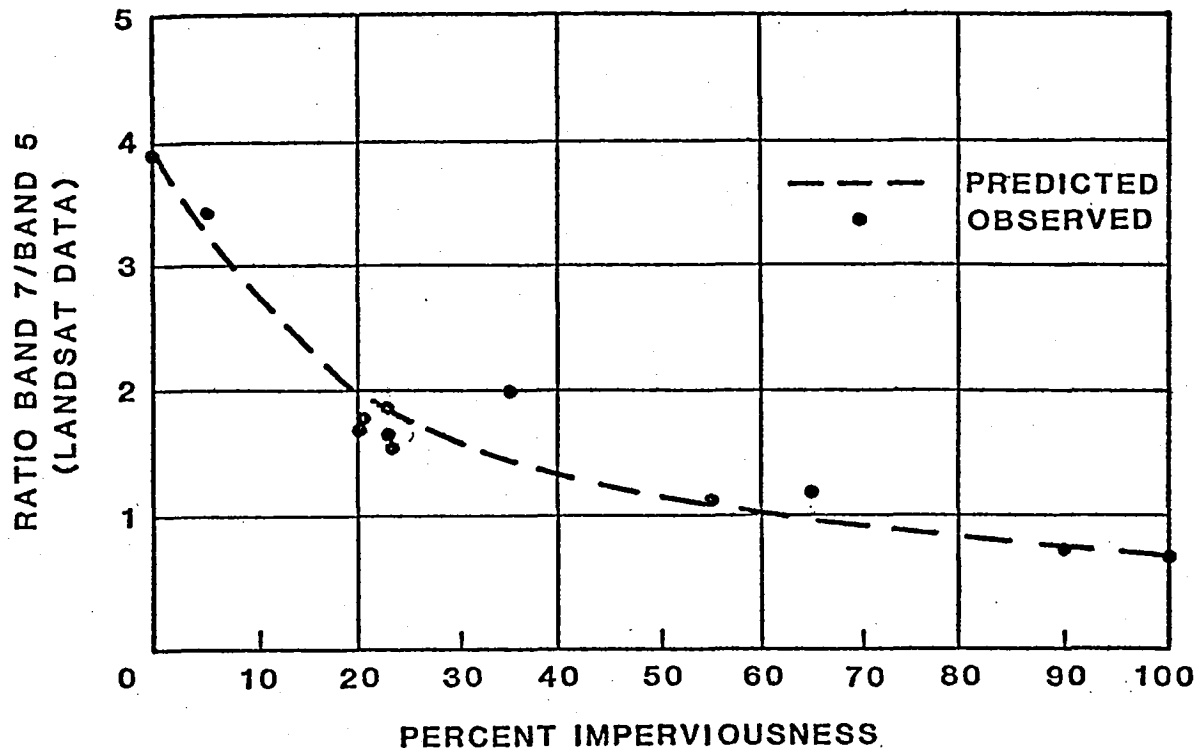


Figure 3. - Relationship Between the Percent of Impervious Area and the Ratio of Two Landsat Bands (McKeon, et al., 1979).

THE ROLE OF MULTISPECTRAL SCANNERS AS DATA SOURCES
FOR EPA HYDROLOGIC MODELS
(For Discussion at the MISWC Hydrology Workshop, April 26-28, 1982)
by
Rebecca Slack and David Hill

Models are used by scientists with the Environmental Protection Agency (EPA) as aids to understanding the complexities of natural phenomena, their interactions, and the impact of man's activities. As environmental controls become more expensive and the penalties of judgment errors become more severe, models as analytical tools must be increasingly efficient and accurate. Construction, execution, and improvement of any model requires large amounts of accurate data. Unfortunately, current modeling capabilities exceed most available data bases. For this reason, scientists are studying the potential of remote sensors to provide environmental data over large areas of the world. Environmental models, such as those used by EPA, are usually based on physical, chemical, and biological parameters. Although many parameters may be used as input, model response is largely determined by a small subset of key parameters which must be complete and quite accurate. Remote sensing must contribute to these key parameters efficiently and cost-effectively if it is to play an important role in environmental modeling.

Most modeling efforts in the EPA are carried out at the three Environmental Monitoring Systems Laboratories (EMSL) or at one of a number of smaller research laboratories across the country. All remote sensing is handled by either the Environmental Photographic Interpretation Center (EPIC) at Warrenton, Virginia, or at its parent laboratory, the EMSL at Las Vegas, Nevada. EPIC's main emphasis is photo acquisition and interpretation while multispectral scanner and satellite data interpretation as well as MSS research is at Las Vegas. EMSL-LV owns a Daedalus 1260 11-channel multispectral scanner. Thus most projects involving the acquisition of remotely sensed data for modeling have involved EMSL-LV. A few of these projects were for providing input data for a specific model, but most have resulted in the demonstration of the feasibility of obtaining parameters which could be used in modeling. Examples of such projects are as follows:

- A study by D. D. Frank and S. M. Lieu of Hydrocomp, Inc. (contracted by EPA) specifically compared data derived from Landsat with conventionally derived data as input into the model, Hydrological Simulation Program - FORTRAN (HSPF). HSPF was designed to simulate hydrologic and water quality processes in natural and man-made water systems. One set of water quality parameters was calculated from Landsat data using transformation functions that relate land use classes to pollutant loading rates and potency factors (number of pounds of pollutant per ton of sediment). Another set of parameters was derived using conventional field methods. Simulations were then run, and outputs from the two sets of data were compared. Output included hydrologic response such as overland flow, interflow, and baseflow, and water quality criteria: annual loading of sediment, biological oxygen demand, ammonia, and orthophosphates. The Landsat-derived data performed at least as well as the conventionally-derived data and had many advantages, not the least of which was an estimated cost savings of 30 to 50 percent.

- EMSL-LV derived and mapped water quality parameters at Flathead Lake, Montana, using the Daedalus 1260. Comparative water quality data were collected concurrently with the flight times. Best subset multiple linear regression analysis showed strong correspondences between the MSS values and the conventionally-derived values. Quantitative, digital maps of surface temperature, total phosphorus, nitrate nitrogen, total suspended solids, and transparency were then produced for the entire lake by parallelepiped classification of regression transformed MSS data. These maps will be used to characterize the distribution of turbidity plumes within Flathead Lake and to predict the effect of increasing urbanization in the Flathead River basin on the lake's trophic state.
- EMSL-LV is currently working together with EPA researchers in Corvallis, Oregon, to evaluate the effects of acid rain in the Adirondacks. MSS data are being studied as a possible source of parameters needed to model the buffering capability of lakes. Among water quality parameters and relationships being evaluated are runoff, pH, transparency, total suspended solids, and phytoplankton. Overflights using the Daedalus 1260 have been made and preliminary results appear promising. A report is expected to be released next spring.
- An extensive four-phase study using Landsat data was done on Lake Champlain, Vermont. Phase I addressed classification of Landsat MSS data for classification of water quality parameters including chlorophyll a. Phase II extended the classification of those parameters to other lakes in the state. Phase III used the Daedalus MSS to produce digital images describing classification of aquatic vegetation in lower Lake Champlain and adjacent land cover types. Phase IV, being undertaken by the University of Vermont, is examining the rest of the water quality in the rest of the state's lakes using a multirate approach.
- A combination of Landsat MSS data and contact-sensed data along with multivariate statistical techniques were used to successfully classify the trophic status of 145 lakes in Illinois. Five trophic indicators (chlorophyll a, inverse of Secchi depth, total phosphorus, conductivity, and total organic nitrogen) were transformed into two multivariate indices. These indices, as dependent variables, and the four Landsat bands, as independent variables, were utilized in regression models to cluster the lakes into trophic rankings.
- Appalachicola Bay is one of Florida's greatest shellfishing areas. Problems with shellfish contamination and toxicity from non-point source runoff keep reoccurring during the past several years. Water quality sampling using a standard grid pattern was very labor intensive and required extensive interpretation. Dr. Jack Hill, now with Louisiana State University, when studying the runoff and flow patterns within the Bay using Landsat data, concluded that the sampling sites could be more efficiently located. When sampling sites were relocated according to flow patterns, suspected contaminants and the effects of runoff from clearcutting were more precisely located. This type of approach, keyed into water quality models, and limited ground-truth sampling could prove very useful for environmental assessments of complex estuaries.

These projects are just some examples of how MSS data have or could meet hydrologic modeling input needs. Remote sensing is also being studied as a promising tool in related areas such as the detection of leachate from landfills, algae blooms, septic tank failures, wetlands clearing and drainage, identification of acids from bases stored in barrels using thermal sensors, and identification of organic carbons and chlorophyll a using a laser fluoressensor.

To advance the use of remote sensing, EPA should encourage the use of current technology for water quality studies by establishing or accepting standards that relate water quality parameters to remotely sensed data. Since this has not been done, the states have been reluctant to use remote sensing because they were uncertain EPA would accept the data as valid. Under the present Administration, however, the states are encouraged to develop and implement their own unique programs including water quality standards. If remote monitoring can meet the state's criteria, then that state can now decide for itself whether or not remote sensing is a sensible, economical approach.

Application of remote sensing would be helped by a greater awareness of its capabilities on the part of EPA and the state pollution control programs. They need to be educated as to its potential as a tool for water quality planning, and as a tool is how it should be presented -- not as a panacea. Remote sensing can best be used as an extension of field sampling by using regression models -- not as a replacement for field sampling.

Several remote sensing research projects could potentially serve as "spark-plugs" for stimulating greater remote sensing application in EPA, but the Agency has very limited resources for additional projects at this time. The only program receiving increased funds is hazardous waste.

Research projects that would be useful are:

- Establishing a unified data base by taking already established techniques and conducting corresponding studies in different physiographic regions of the country. A lack of standardization in present studies prevents EPA from knowing what MSS channels and what hydrologic parameters can be expected to be useful in different regions. Techniques for dealing with regional variations need to be developed.
- Identification of optimum scanners for identification of hydrologic parameters over various parts of the country. This information should be taken in consideration in planning for future satellites.
- Scanner missions could be included aboard the space shuttle. Vast amounts of hydrologic data using different sensors could be collected and then studied to determine the optimum.
- Data for time series models could be provided by continuous monitoring from satellites in synchronous orbit. Perhaps the system could be programmed to flag water quality anomalies.
- Multidate studies would greatly benefit if atmospheric calibration was improved. Atmospheric calibration is perhaps one of the greatest problems encountered in doing any type of multidate study.

- Refinement of land cover classification would enhance the use of satellite-derived information. For example, pesticide pollution is an area of major concern. Since pesticides are often very organism specific, refinement of agricultural classification (crop type, for example) has significant potential in modeling risk analyses for evaluating pesticides in a given area.
- Another possible study would be to consider the effects of accuracy gains in the estimation of basic watershed characteristics. Just how sensitive are water quality parameters to changes in watershed characteristics? For example, how does a change in land use in the basin affect the dissolved oxygen?
- How accurate must hydrologic parameters be? If the sensitivities of hydrologic parameters were known, remote sensing could be more accurately evaluated as a tool.

Multispectral scanners have provided parametric data that either have been or can be used in environmental models, but their full potential is far from being recognized. The future of MSS as a tool lies in researchers' ability to instill an awareness of its capabilities to those people who work in the realms of practical application. To do so, MSS data must be readily available, cost-effective, and have an established accuracy level.

High Resolution Analysis^{1/}

C. J. Robinove

The purpose of this statement is to explain in general the possibilities for the use of high resolution analysis in the field of hydrology and water resources. High resolution analysis is considered here to mean high spectral resolution, not high spatial resolution.

The current state of knowledge of high spectral resolution analysis in hydrology is meager. Spectroscopy for the identification and measurement of the concentration of constituents in water is highly developed for laboratory use and is capable of measuring the concentration of many substances in water at levels of micrograms and nanograms per liter. Remote measurement of the quality of water has, to date, involved only measurement of sediment concentration by reflected light, measurement of chlorophyll and phaeopigments (Nimbus CZCS), and the measurement of fluorescence with the Fraunhofer Line Discriminator (FLD). The FLD can detect fluorescing substances in water at levels of less than one part per billion of Rhodamine WT equivalents but is not diagnostic of chemical species.

I have not considered here the use or development of high spectral resolution methods in other disciplines such as geology (rock discrimination), agricultural or natural vegetation, soils, or cultural features. Identification and discrimination of such features by high resolution analysis can be done, and improved upon, and inferences on the hydrologic characteristics can then be made. High resolution spectral analysis in those fields does not give direct hydrologic information.

^{1/} This is an informal statement of problems and recommendations prepared for the Hydrology Workshop of the Multispectral Imaging Science Working Group, April 26, 1982.

Critical gaps in scientific knowledge that need to be filled before new technology can be evaluated involve the spectral response of water, substances dissolved and suspended in water, and substances floating on water. A major example is the sensing of oil on water. Mapping and monitoring of oil slicks has been done in the visible, near infrared, thermal infrared, and ultraviolet regions of the spectrum, and it is clear that the most complete mapping can be done in the ultraviolet region. Ultraviolet sensing has been done only from aircraft at altitudes of 1000 meters or less because of the attenuation of ultraviolet radiation in the atmosphere which severely limits its sensing at higher altitudes and precludes its use from satellite altitudes. Is there a way around this problem? Is there a way of measuring the ultraviolet reflection at the surface from satellite altitudes? This gap in knowledge may well be worth filling.

Witzig and Whitehurst (1980) have reviewed the use of Landsat MSS data for the trophic classification of lakes. A copy of their paper is attached. This excellent review points out that there is a serious lack of sensors that can measure the fundamental reflectance of water. It seems likely that the use of high spectral resolution sensors in a reasonable number of narrow bands may be able to sense reflectance or emission characteristics of water and its contained materials that will be correlatable with the commonly used water-quality variables. It seems unlikely that remote sensing instruments can be built that have detection sensitivities for dissolved constituents in water that are as low as those that are now achieved with laboratory instruments. Nevertheless, the ability of remote sensors in airborne or spaceborne platforms to survey large areas rapidly and synoptically may outweigh the lack of sensitivity to individual constituents.

Candidate remote sensing experiments should be conducted both empirically and on the basis of testing of hypotheses. An example of an empirical experiment would be the use of the Thematic Mapper (or the airborne TM simulator) to view water bodies in various trophic states to determine if the previously unavailable bands are useful in characterizing trophic state.

Experiments to test hypotheses might involve such hypotheses as "the backscattering of light from sediment particles in water is dependent upon the composition, size, and concentration of the particles."

Experiments should also be made in an empirical way to determine if the fluorescence characteristics of substances in water are diagnostic of the type and concentration of the substances.

The technological alternatives available to experiment with problems of sensing water quality are (1) to use existing remote sensing instrumentation in an empirical mode and (2) to develop new instruments to either test hypotheses or to conduct empirical experiments. Goldberg and Weiner (1977) in their paper "Feasibility and technology for making remote measurements of solutes in water" (copy attached) recommend construction of a Raman spectrometer which could ". . . rapidly map the concentration of many water solutes, even in water bodies that are difficult to access by ground." This suggestion should be evaluated in light of developments in the 5 years since their paper was published.

Goldberg has informed me recently that the advances in optical multichannel analyzers and in Fourier and Hadamard transform methods in spectroscopy may now make it possible to build a remote reflectance spectrometer with equivalent of several hundred narrow bands which could be used for empirical experiments in remote measurement of water quality. Attached is a paper by Marshall and Comisarow (1975), "Fourier and Hadamard transform methods in spectroscopy" which outlines the advantages of these techniques over the commonly used spectrometric (or multiband remote sensing) techniques.

The technological developments required are involved in the use of available methods and instruments developed for other purposes (such as optical multichannel detectors) for water-quality sensing. Consideration should be given to utilizing such instruments initially in the laboratory and later in the field for empirical studies of water-quality characteristics.

No specific information extraction research is proposed for the extraction of information from multispectral data. Developments in Fourier transform spectroscopy should be investigated for their applicability.

Drainage Basins/Soil Moisture Uses for Visible Infrared Data

Some form of visible infrared data is essential to the use of remote sensing for appraisal of watershed drainage areas and for the estimation of soil moisture. It is, however, difficult to conceive of significant advantages in either area of application that will result from improved spatial resolution of these data. Improved spectral resolution, on the other hand, may provide better mapping of the characteristics that we need for drainage areas and for agricultural areas where soil moisture is estimated.

Visible-infrared data in the past have been used both in a qualitative and quantitative sense to make preliminary assessment of watershed characteristics. Quantitative evaluation of drainage area, aerial extent of snow cover, topography or slopes, stream channel numbers and land use have been common tools for practicing hydrologists for years. Some of these characteristics are more readily quantified with digital data and modern processing techniques. With the exception of the extent of snow cover these watershed characteristics are all relatively stable with time.

Three major characteristics of much greater importance to watershed hydrologists are: 1. Mapping of the hydrologic character of surface soils, i.e. infiltration rate, hydraulic conductivity or storage capacity; 2. Mapping soil moisture; and 3. Mapping of water content of snow. Mapping any one of these will require the use of microwave systems, however, none of these can be adequately mapped by microwave over significant areas of the land without supplemental visible-infrared data.

An attempt has been made to modify or adjust microwave data over vegetated areas by use of classification or a biomass estimation to provide improved

estimates of soil moisture, Figure 1 from a recent study by S. Theis. A simple biomass estimator, the perpendicular vegetation index (PVI), was found more useful overall than a 100% correct classification of five vegetation types. The biomass estimation is used in this study as a surrogate measure of the water content of the vegetation--the actual parameter that is adding confusion to the microwave energy from the surface soil water mix. We show this figure to illustrate that the visible-infrared information required to make this estimation is an absolute requirement.

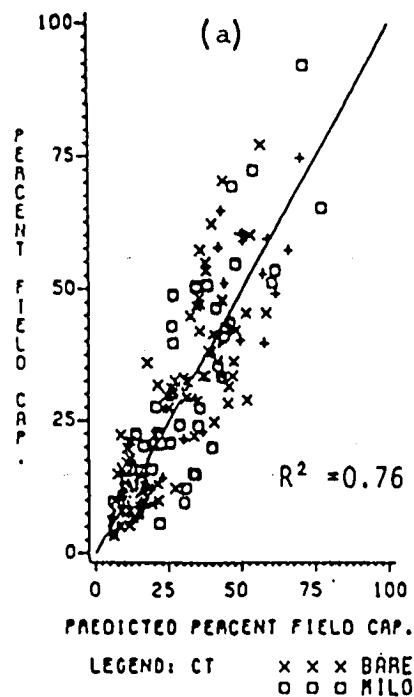
When acceptable soil moisture measurement can be made in a time series, the remote sensing classification of soils becomes a possibility. Using information from two models, one for soil moisture profile definition [Hillel] and one for passive microwave emission [Schmugge], it can be shown that time series changes in emissivity can be used to indicate the hydraulic character of soils, Figure 2. To accomplish this classification a precise and reasonably accurate estimate of soil moisture is required, therefore, we must have the visible-infrared data available if significant portions of the land surface are to be classified as to soil type.

Both the soil moisture and soil classification will most likely be limited to cells greater than 5 x 5 km in size. There is, therefore, little likelihood that improved spatial resolution would improve the results. In the Theis study, the thematic mapper simulator from JSC was used to calculate the biomass. In addition, data from the 11 channel scanner on the C-130 and data from Landsat were available for a portion of the study. There was some indication that better spectral resolution improved the estimate of biomass.

The third significant need for remote sensing of watersheds, the estimation of snow water content, requires a different array of microwave sensors and most likely will require different visible and infrared data. It is evident

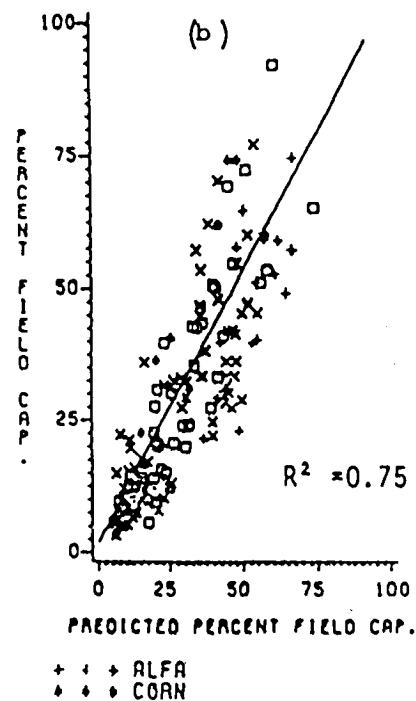
CLASSIFICATION TECHNIQUE

MEASURED VS. PREDICTED PERCENT FIELD CAP.
(NON-CORN FIELDS)



DIRECT COMBINATION

(PVI LESS THAN 4.3)



The ability of the L-band radiometer to predict percent field capacity when used a) with classification technique (no corn), and b) with direct combination technique (excluding fields with PVI greater than 4.3).

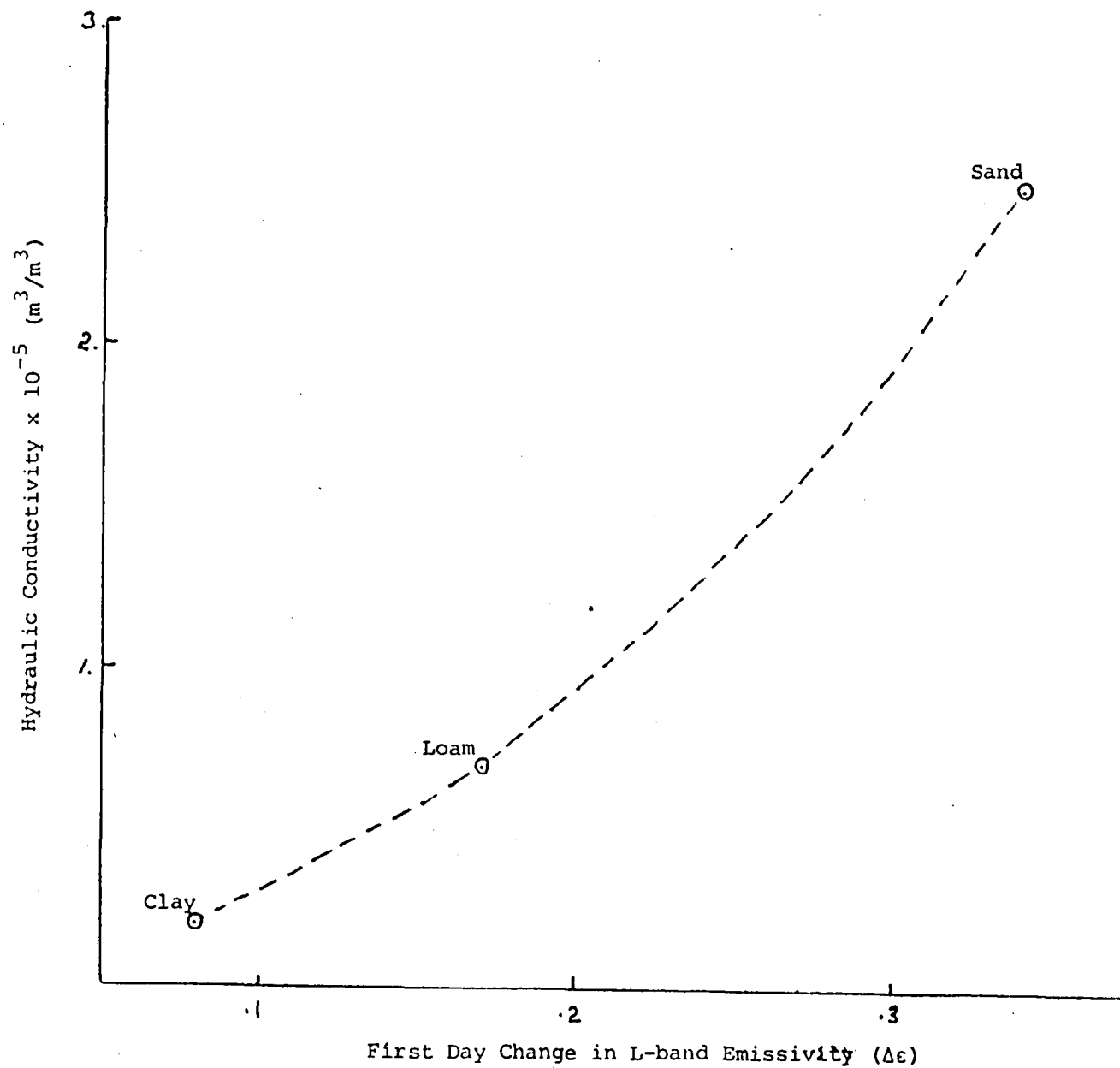


Figure 2. The relation between the change in L-band passive microwave return and hydraulic properties of the surface soils. (Data from Hillel and Van Bavel.)

that extension of the range in the near infrared provided in the thematic mapper will provide the opportunity to separate clouds and snow cover. It is not, however, evident that any significant improvement in snow area estimation will come from improved spatial resolution.

Improved spatial resolution will provide the hydrologist with improved data on very small watersheds (1 km^2 , or less). This may aid some small area research efforts of an academic nature but the results from hydrologic studies of small areas cannot necessarily be extrapolated to larger areas.

Generally, it would appear that improved spatial resolution will not be of value to the watershed hydrologist while better spectral resolution at selected frequencies may improve estimates needed in this work. It is evident from the Theis study that there are several options for selection of bands from the Thematic Mapper to provide an acceptable biomass estimate. These could be selected to also be of value to snow mapping and water quality requirements thus minimizing the total data volume needed.

THERMAL INFRARED RESEARCH

WHERE ARE WE NOW?

J. L. Hatfield
University of California - Davis

R. D. Jackson
USDA-ARS, U. S. Water Conservation Laboratory

The Past

In recent years much attention has been given to utilization of thermal infrared measurement for application to agriculture and hydrology. A portion of this interest has arisen because thermal infrared measurements are relatively easy to make with sensitive, portable infrared thermometers. The use of IR temperatures in agriculture and hydrology is based on the energy balance equation,

$$R_n = \frac{\rho C_p (T_s - T_a)}{r_a} + \frac{\rho C_p}{\gamma} \frac{[e_s(T_s) - e_a]}{r_a + r_s}$$

where R_n is the net radiation, ρ the density of air, C_p the specific heat capacity of air, T_s the surface temperature, T_a the air temperature at some height z above the surface, r_a the aerodynamic resistance calculated at the height z , γ the psychrometric constant, $e_s(T_s)$ the saturation vapor pressure at T_s , e_a the actual vapor pressure of the air, and r_s the surface resistance to water vapor flow. This and other forms of the energy balance have been utilized to estimate evapotranspiration or crop stress.

The thermally driven energy balance equation has been used to estimate ET and stress over small areas within a field as well as large areas. Bartholic et

al (1970) first showed how evapotranspiration using temperature measurements could be predicted, he later expanded this concept to use aircraft data (Bartholic et al, 1972). This approach has been modified by Brown and Rosenberg (1973) and most recently by Soer (1980). Unfortunately, there has not been an evaluation of these approaches over a complete growing season of any one crop or over any large region. Stone and Horton (1974), Blad and Rosenberg (1976) and Heilman and Kanemasu (1976) have provided limited evaluations and showed how and where potential problems may lie in the application of these methods. These methods may provide a real-time application of soil moisture through soil moisture balance models utilizing evapotranspiration.

Jackson (1982) presented a thorough review of the use of thermal infrared to detect crop stress. The research history of thermal IR techniques is fairly recent. Tanner (1963) was one of the first to suggest that infrared thermometry could be used to detect moisture stress. Since that beginning three different approaches to detect stress have been reported. Fuchs and Tanner (1966) proposed that water stress could be assessed from a comparison of canopy temperatures from the field in question to that of a well-watered area of the same crop. Wiegand and Namken (1966) proposed that canopy-air temperature ($T_s - T_a$) differences would be indicative of water stress. Aston and van Bavel (1972) later proposed that the variability of surface temperature would be indicative of moisture stress and would increase as the crop extracted water.

Recently, Clawson and Blad (1982) found that when the temperature of a field in question was 1.0°C above a well-watered plot and irrigation was applied the yields were reduced. However, there was also less water applied to these plots, thereby producing a water savings in comparison to the yield reduction.

Clawson and Blad (1982) also proposed that a variability greater than 0.7°C would indicate the need for irrigation in corn and found that this value would only be valid when the canopy cover was nearly complete. Hatfield (unpublished data) in a study of spatial variability in grain sorghum showed the variability along a 100 m transect within three different irrigation treatments. A clear relationship between the variability along the transect and the amount of water extracted from the soil profile was not evident. It was encouraging that the points along the transect were random, indicating that one could sample randomly within a field regardless of the soil moisture level. It is still necessary to define the optimum pixel size for satellite sensors.

Most research has been directed toward the utilization of measurements of T_s and T_a and expressed as $T_s - T_a$. Idso et al (1977) and Jackson et al (1977) showed that the midday measurement of T_s and T_a and the resultant difference could be summed and related to crop yield and soil water extraction. These models exhibited a linear relationship between crop yield and the stress-degree-days (SDD). Hatfield (1982a) found it was necessary to incorporate spectral measurements as a measure of potential harvestable yield in order to account for the yearly variation in growth and yield-stress relationships. Recent research has shown that other environmental variables are necessary to include in that use $T_s - T_a$ measurements to better detect crop stress. Idso et al (1981a) found that $T_s - T_a$ in a well-watered crop was linearly related to vapor pressure deficit. As the vapor pressure deficit increased the $T_s - T_a$ value decreased. They also proposed that the upper limit of canopy temperature above air temperature would be independent of vapor pressure deficit. A plant water stress index calculated from these lines was related to leaf water potential

(Idso et al, 1981) and to soil moisture extraction (Hatfield, 1982b). Before this method could become operational, the validity of the upper and lower baseline would have to be evaluated for a variety of species and cultivars.

Hatfield (1982) found there was an exponential relationship between the plant water stress index and available water extracted from the soil profile. Jackson (1981), however, cautioned that changing rooting volume and ground cover would have to be accounted for in these relationships. This aspect needs continued research before any method can be applied over a growing season.

Jackson et al (1981) suggested another approach utilizing midday measurements of T_s and T_a along with net radiation and vapor pressure deficit. From these data, a crop water stress index was calculated and is related to the ratio of actual to potential evapotranspiration. They showed this index to follow the water extraction patterns in wheat very closely. Slack et al (1981) used these same variables in a regression model to relate $(T_s - T_a)$ to water extraction in corn for Minnesota but since this model is based on regression analysis it may not be applicable to large areas or remote sensing platforms. This approach however, does include the environmental parameters of energy balance with local adjustment factors. These types of relationships need to be compared with the theoretically based evapotranspiration crop water stress index models to determine if a locally adjusted stress indices may be more useful than the more theoretically based models. This would be particularly true in the estimation of soil water status within individual fields for the purpose of irrigation scheduling.

All of the approaches discussed up to now have been based on daily readings. The lack of a satellite platform with a resolution applicable to agriculture will have to possess a temporal resolution of a few days. In an attempt to evaluate the temporal resolution of remote acquired data, Vieira and Hatfield (1982) have analyzed the temporal behavior of air temperature and surface temperature over bare soil. Bare soil was chosen for this study in order to eliminate the effect of the changing ground cover present in a growing crop. Standard geostatistical analyses were performed on data sets from 1977, 1978 and 1979 and involved the analysis of the temporal features of each parameter. In all years, the data were collected daily from January through June. It was found that both air and surface temperature became independent regionalized variates after a lag of 5 days. These analyses were made on the residuals from a 10-day smoothed average because of the lack of second-order stationarity in the original data. The importance of this finding reveals that if estimates are to be made of surface temperature from an ancillary meteorological parameter such as air temperature a resolution of 5 days or less is needed. When cross-variograms were calculated for air and surface temperature the data for the three years fit the same models. This suggests that, for bare soil, surface temperature could be estimated from air temperature for a period up to 5 days. This type of relationship needs to be evaluated for a growing season with changing ground cover to determine if similar models could be developed and they would be applicable over a range of conditions and locations. It is possible that the temporal resolution may even require more detailed sampling than the 5-day values found for the bare soil cases.

There have been several attempts to compare ground-based thermal infrared measurements with those from aircraft sensors. One study applicable to this discussion was reported by Hatfield et al (1982) in which comparisons of air and ground measurements were made over a large agricultural area in California. It was found that the comparisons were within 1°C when the field was recently irrigated and bare or was completely covered with vegetation. Bare, dry soil surfaces exhibited the largest differences between the aircraft and the ground-based measurements due to sampling problems. In a subsequent study over bare soil, it was found that surface temperature was random along both north-south and east-west transects within a field as was surface soil moisture. This suggests that random sampling could successfully be used to compare ground-based measurements to aircraft provided that samples could be taken that would be comparable to the minimum resolution on the aircraft. Bare soil studies on surface temperature along a transect following an irrigation showed that the surface warmed as it dried but did not exhibit spatial structure. This effect was noted with both an 8 and 20° fov hand-held infrared thermometers positioned in a nadir direction 1 m above the surface (Vauclin et al, 1981). Soil moisture was also random along this transect. It is difficult to extrapolate these data to satellite platforms but it does suggest that additional work is needed on the variability of thermal infrared data within agricultural fields in order to fully evaluate the aspect of pixel size relative to agricultural management.

Future Directions

Thermal infrared data provide a surface measurement which is directly related to the energy balance and hence the energy exchange of the surface. In

order to fully utilize this measurement it will have to be combined with other spectral data, the visible, near-infrared and microwave portions. These data must be collected in a time resolution sufficient to detect changes in the agricultural or hydrological systems and at a spatial resolution with enough detail to sample within individual fields. The most stringent requirement is that the data be readily available to the user by the most rapid means of communication possible. Jackson (1983) proposed that a high altitude powered platform (HAPP) would be necessary to provide these data for agricultural management. Before we can begin to design this type of system we need to further our body of knowledge in several areas.

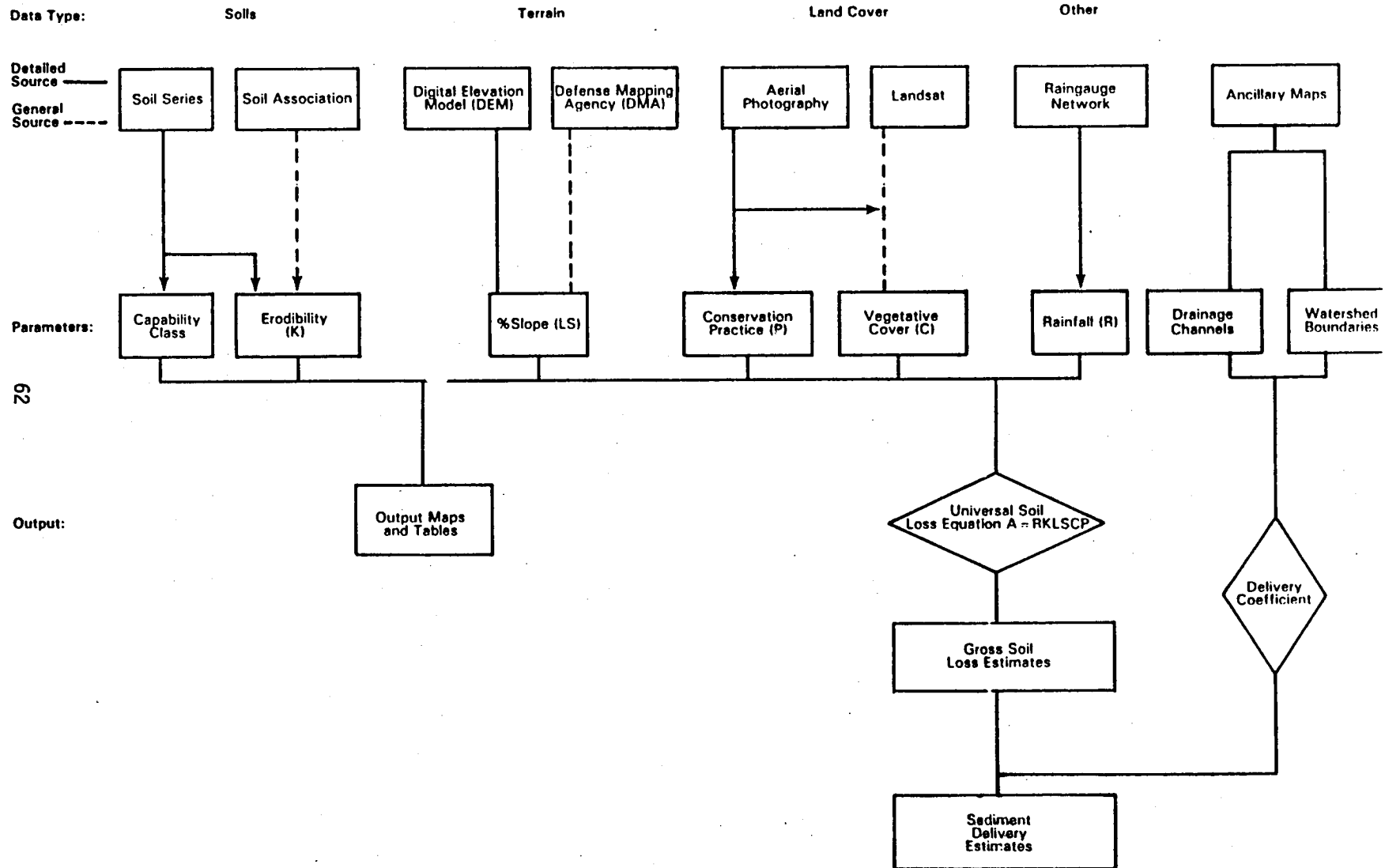
- 1) Evaluation of the spatial resolution necessary for thermal infrared measurements to be incorporated into evapotranspiration models to accurately estimate field and regional evapotranspiration or measure crop stress.
- 2) Evaluation of methods to estimate crop stress and hence yield over large areas and different cultivars within a species to determine if a generalized model could exist.
- 3) Investigate the temporal resolution adequate for detect of stress or inclusion into evapotranspiration models.
- 4) Evaluation of ancillary parameters which could be used to estimate thermal infrared measurements to fill in between acquisition times. These techniques would have to be evaluated over large regions to determine if the same or even similar models exist.
- 5) Evaluate the errors which would be introduced into estimates of soil moisture status from the use of remotely sensed data compared to standard meteorological measurements.

These experiments are only a few which are necessary to further our knowledge of the use of remotely sensed data for agricultural management. We need to increase both our basic understanding of remotely sensed parameters as well as the application of these data in management decisions. To accomplish this we must continue both our ground-based, aircraft, and satellite programs.

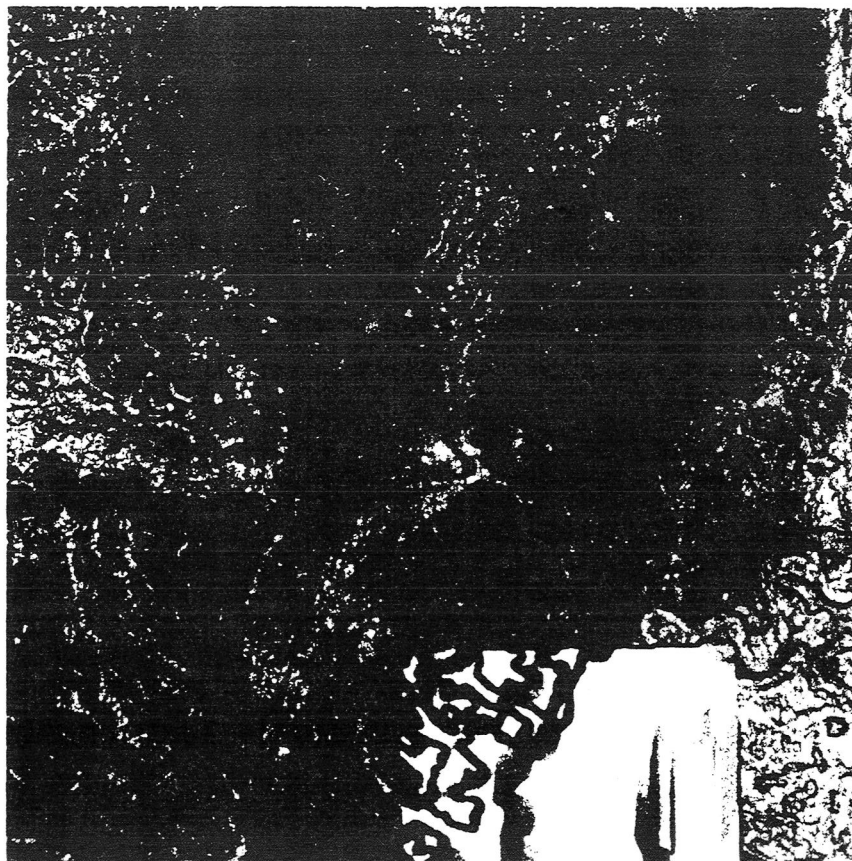
Literature Cited

- Aston, A. R., and van Bavel, C.H.M. 1972. Agron. J. 64:368-373
- Bartholic, J. F., L. N. Namken, and C. L. Wiegand, 1970. USDA-ARS-Bulletin 41-170 14 p.
- Bartholic, J. F., L. N. Namken, and C. L. Wiegand, 1972. Agron J. 64:603-608.
- Blad, B. L., and N. J. Rosenberg. 1976. Agron. J. 68:764-769
- Brown, K. W., and N. J. Rosenberg. 1973. Agron. J. 65:341-347.
- Clawson, K. L. and B. L. Blad, 1982. Agron. J. (In Press).
- Fuchs, M., and C. B. Tanner. 1966. Agron. J. 58:597-601.
- Hatfield, J. L. 1982a. Irrigation Science (Submitted).
- Hatfield, J. L., 1982b. Remote Sensing of Environment (Submitted)
- Hatfield, J. L., J. P. Millard, and P. C. Goettleman. 1982. Photogram. Eng. & Remote Sensing (In Press).
- Heilman, J. L., and E. T. Kanemasu. 1976. Agron. J. 68:607-611.
- Idso, S. B., R. D. Jackson, and R. J. Reginato 1977. Science 196:19-25.
- Idso, S. B., Jackson, R. D., P. J. Pinter, Jr., R. J. Reginato, and J. L. Hatfield. 1981a. Agric. Meteorol. 24:45-55.
- Idso, S. B., R. J. Reginato, D. C. Reicosky and J. L. Hatfield 1981b. Agron. J. 73:826-830.
- Jackson, R. D. 1981. IGARSS '81, International Geoscience and Remote Sensing Symposium, p. 364-374.
- Jackson, R. D. 1983. In Challenging Problems in Plant Health. Amer. Phytopath. Soc. (T. Kommedahl and P. Williams, Eds).

- Jackson, R. D., R. J. Reginato, and S. B. Idso. 1977. Water Resources Res. 13:651-656.
- Jackson, R. D., S. B. Idso, R. J. Reginato, and P. J. Pinter, Jr. 1981. Water Resources Res. 17:1133-1138
- Slack, D. C., K. M. Gieser, K. W. Stange, and E. R. Allerd. 1981. Proc. of Irrig. Sched. Conf. ASAE. p. 116-124
- Soer, G.J.R. 1981. Remote Sensing of Environment 9:27-45.
- Stone, L. R., and M. L. Horton. 1974. Agron. J. 66:450-454.
- Tanner, C. B. 1963. Agron. J. 55:210-211.
- Vauclin, M., S. R. Vieira, R. Bernard, and J. L. Hatfield. 1982. Water Resources Res. (In Press).
- Vieira, S. R., and J. L. Hatfield 1982. Canadian J. Remote Sensing (Submitted).
- Wiegand, C. L. and L. N. Namken. 1966. Agron. J. 58:552-556.



80951-009



KODAK SAFETY FILM

BLK HLS HYDRO STUDY

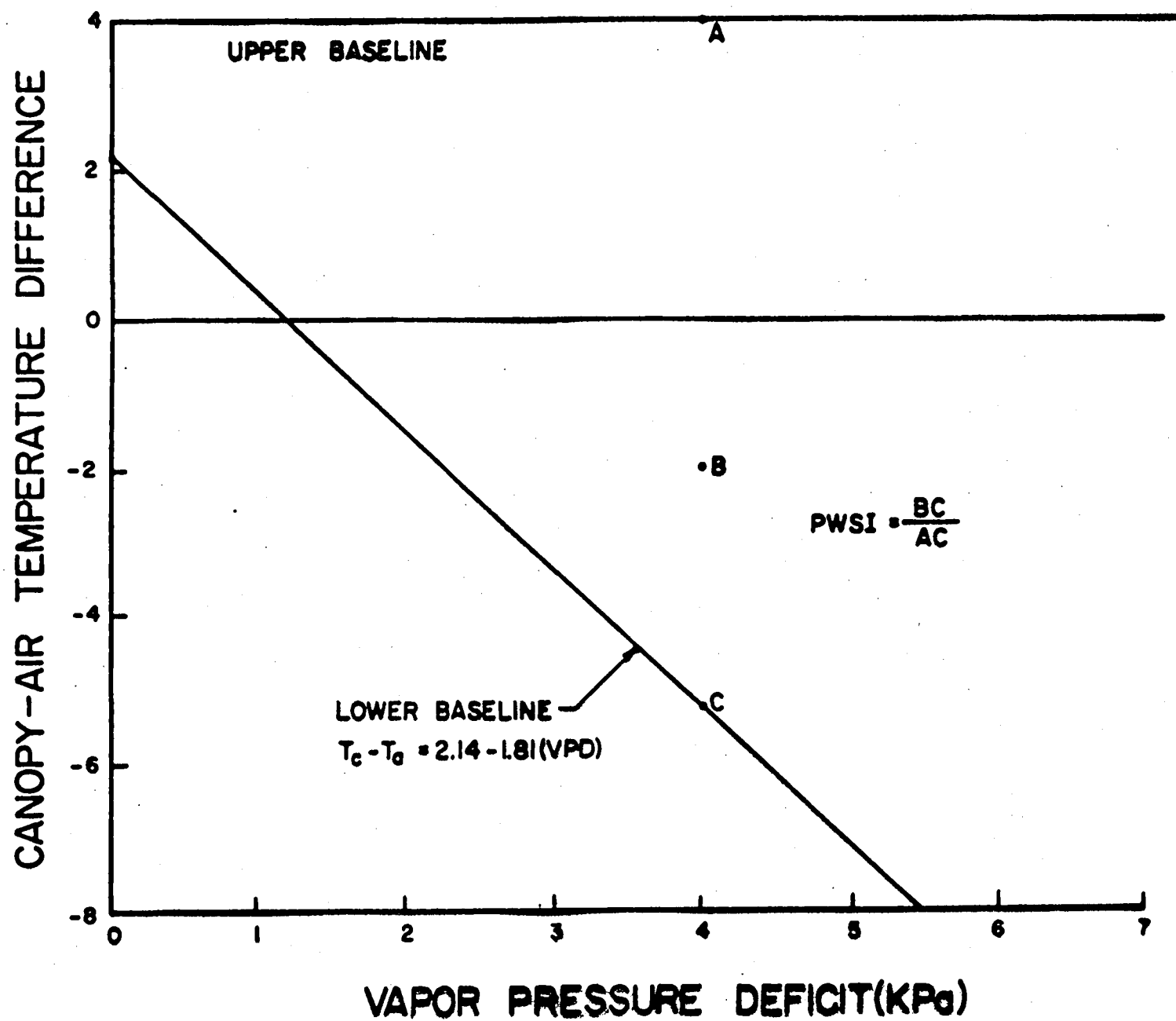
USGS-EDC

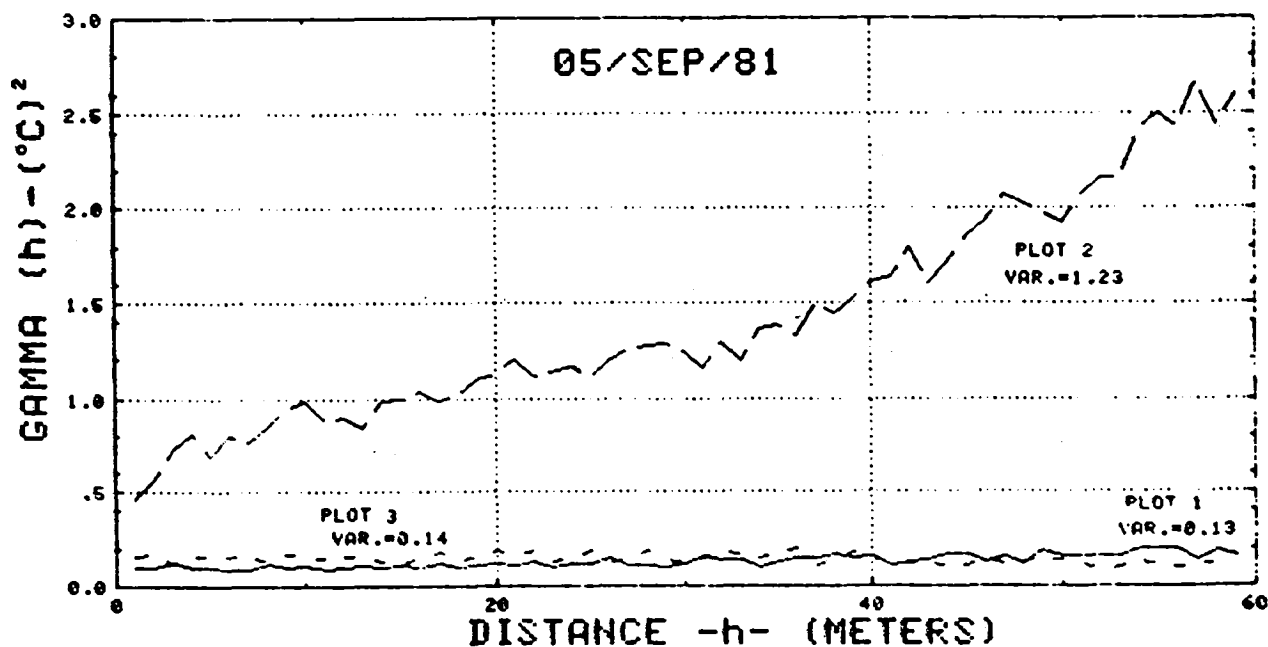
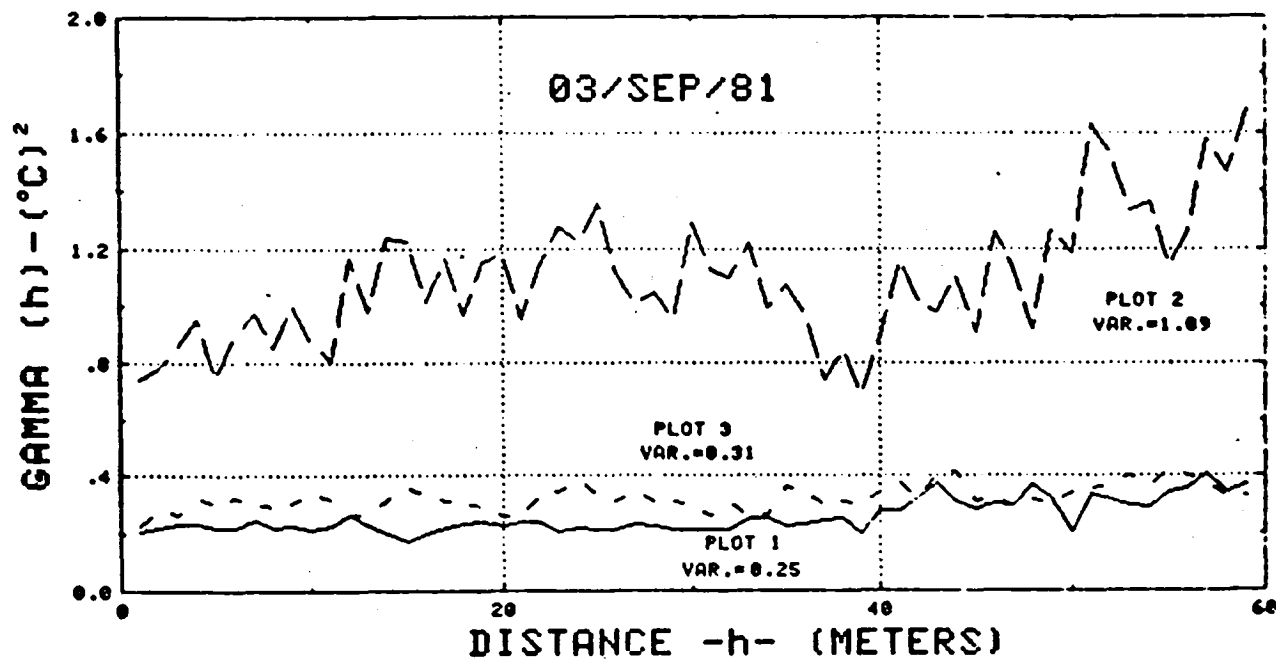
4

HOT SPRINGS, SD

SLOPE MAP

4





CROP STRESS VIA THERMAL IR APPROACHES

1. CANOPY-AIR TEMP.
2. CANOPY (ACTUAL-WELL-WATERED)
3. WITHIN FIELD VARIABILITY

BARTHOLIC ET AL.

$$LE = \frac{-(RN + G)}{1 + \tau \frac{(TA - TC)}{(EA - EO)}}$$

BROWN - ROSENBERG

$$LE = - (RN + G) + CP \frac{(TC - TA)}{R_A}$$

SOER

$$LE = -\theta CP \left(\frac{TA - TC}{R_A} \right) - (L - \phi S) R_S - c(L_P - T_C^4) - G$$

EVAPOTRANSPIRATION METHODS

BARTHOLIC	-	MODIFIED BOWEN RATIO
BROWN & ROSENBERG	-	RESISTANCE
SOER	-	ENERGY BALANCE
CANOPY TEMPERATURES	-	ACTUAL EVAPOTRANSPIRATION

APPENDIX IV

WORKING PAPERS
GEOLOGY SCIENCE TEAM
MULTISPECTRAL IMAGING SCIENCE WORKING GROUP

Lithologic Units Through Analysis of Visible,
Near-infrared, and Mid-infrared Measurements*

by

Lawrence C. Rowan
U.S. Geological Survey
Reston, Virginia 22902

Abstract

One of the main objectives of geological remote sensing is to develop techniques for mapping lithologic units and determining their compositions. During the past 10 years, research has been dominated by analysis of visible and short-wavelength near-infrared (0.4 to 1.3 micrometers) spectral reflectance because of the worldwide availability of digital Landsat Multispectral Scanner (MSS) images. Although MSS images have proved to be very useful for discriminating and mapping lithologic units, as well as structural features, specific mineralogical information is generally limited to Fe^{3+} minerals, collectively referred to as limonite. Lithologic discrimination and identification can be improved markedly by analyzing measurements made in the 1.5 to 2.5 micrometer and 8 to 14 micrometer regions.

As used here, discrimination refers to the separation of lithologic units but without adequate information for determining their mineral contents. Identification is used appropriately where analysis of remote measurements permits the placement of specific boundaries on the mineral composition of a lithologic unit; the range of the boundaries may be broad, but geologically significant or, more rarely, quite narrow and specific.

*This manuscript has not been reviewed and is not approved for publication.

In the visible and short-wavelength near-infrared region, discrimination of lithologic units may be direct in well exposed areas or indirect where variations in vegetation cover reflect underlying lithologic differences; this paper is concerned with direct measurements. Direct lithologic discrimination is generally accomplished through analysis of albedo or spectral reflectance variations. The albedo of terrestrial rocks and soils in this wavelength region is determined mainly by the abundances of opaque minerals and carbonaceous material both as surface coatings and within the rock; texture is of secondary importance. In some well exposed regions where seasonal rains occur, differential moisture content of lithologic units causes albedo differences that permit discrimination of units that are inseparable when they are dry. In spite of the limited mineralogical information that is available directly through albedo analyses, many lithologic units can be distinguished and mapped over large areas. The value of this type of lithologic information increases as knowledge about the areas increases through field and literature studies.

Because of the unique spectral reflectance of limonite and the common association of limonite with hydrothermally altered rocks, analysis of Landsat MSS images has been used as the basis for compiling alteration maps of areas as large as $1^{\circ} \times 2^{\circ}$ quadrangles and as small as individual mining districts. However, this approach to alteration mapping commonly requires extensive field checking, because methods for distinguishing between supergene limonite and limonite produced through normal weathering of mafic and opaque minerals in

MSS images has not been developed. In addition, non-limonitic altered rocks are not consistently distinctive in MSS images.

The 2.2 micrometer channel was proposed and selected for inclusion in the Landsat D Thematic Mapper (TM) in order to overcome the above mentioned limitations of the MSS channels for mapping altered rocks. Numerous studies, particularly the Geosat test case studies, have demonstrated the value of this spectral channel for mapping altered and other OH-bearing rocks. However, in the East Tintic Mountains, Utah, some altered rocks lack a prominent 2.2 micrometer absorption band, and some limestone exposures have a very intense 2.33 micrometer CO_3^{2-} -absorption feature which gives rise to considerable ambiguity between the occurrences of carbonate rocks and altered rocks having an OH-absorption band. Lithologic studies in this area are complicated further by the presence of carbonate rocks having only a very subtle CO_3^{2-} -absorption feature and unaltered argillaceous rocks that display a prominent OH-absorption band. These results indicate that TM images will greatly reduce the extent of field checking in mapping altered rocks and aid in discriminating other rock types, but lithologic identification will be hampered by several ambiguities.

Lithologic identification could be improved substantially by acquiring and analyzing high spectral-resolution images in the 1.5 to 2.5 micrometer region. Preliminary analysis of Shuttle Multispectral Infrared Radiometer (SMIRR) and high spectral-resolution airborne measurements show that, given

some general knowledge of the types of rocks present, several minerals can be identified, including alunite, jarosite, kaolinite, montmorillonite, and carbonates. As these studies progress, I believe that other minerals will prove to be identifiable, and discrimination of subtle lithologic variations should be possible in high spectral-resolution images.

High spectral-resolution images recorded in the visible and short-wavelength near-infrared region might also be useful for identifying and mapping variations among Fe^{3+} minerals in altered rocks. Evaluation of MSS color-ratio composite images of the Goldfield, Nev., mining district suggested that subtle color variations were related to local differences in the Fe^{3+} mineralogy in the altered rocks. These color variations were attributed to a higher MSS 6/7 ratio for hematitic rocks than goethitic rocks. Alternatively, these color variations may be due to a small shift in the position of the crystal field transition band centered near 0.92 micrometers. Studies conducted by S. Sommer (Mobil Oil) and Wm. Buckingham (Gulf Research) have documented that a 24 nanometer shift of this absorption band towards shorter wavelengths is induced by a 33 percent depletion of Al in the acidic environment of hydrothermal alteration.

The mid-infrared (8 to 14 micrometer) region has considerable potential for providing lithologic information that complements the information available in the shorter wavelength regions. Studies conducted in the East Tintic Mountains, Utah, using NASA 24-channel scanner images show that

silicate rocks can be distinguished from carbonate rocks, which results in identification of the latter rock type. In addition, distinctions among the silicate rocks, including quartzite, quartz latite and latite, were possible apparently due to differences in quartz content and, hence, the depth of the reststrahlen band; silicified altered rocks were also discriminated from the other altered rocks. Use of these images alone resulted in some ambiguities, but most of these problems were resolved by using data acquired in the 1.5 to 2.5 micrometer region.

Thermal inertia analysis provides another, independent means of narrowing the mineralogical boundaries for many rock types. Studies using aircraft and satellite measurements in the 8-14 micrometer region show that limestone and dolomite can be discriminated because of the higher thermal inertia of dolomite. Similarly, quartzite and ultramafic rocks are distinctive from most other rock types owing to their high thermal inertias. Also, studies conducted by K. Watson (USGS) using Heat Capacity Mapping Mission (HCMM) data of southwestern Arizona show that the thermal inertias of the igneous rock units are measurably different, indicating a finer discrimination capability than previous laboratory data suggests. A particularly surprising and intriguing result of this HCMM study is the correspondence between lithologic variations and night-time temperature differences in the central Appalachians where vegetation cover is nearly 100 percent.

Integrated analysis of high spectral-resolution reflectance, moderate spectral-resolution emittance, and thermal inertia measurements should permit identification of most exposed rock types and a level of discrimination that is difficult to achieve through conventional mapping methods. Ideally, an airborne system should be designed for acquiring the necessary imagery simultaneously.

RADIOMETRIC CONSIDERATIONS IN REMOTE SENSING SYSTEMS

Alexander F. H. Goetz

Jet Propulsion Laboratory
California Institute of Technology
Pasadena, CA 91109

Introduction

All sensor systems designed to acquire quantitative data undergo radiometric calibration. The following discussion describes the types and potential accuracies of calibration as well as the needs for calibration in the practical application of sensors. The recent and ongoing experience with the Shuttle Multispectral Infrared Radiometer (SMIRR) will be used as a reference.

Definition of Terms

Calibration is defined as the process by which the output of a sensor is related to the input stimulus. In radiometers and radiometric imaging systems using detectors that translate incoming photons into electrical signals, an amplified output voltage is calibrated in terms of measured spectral radiance in $\text{watts m}^{-1} \text{sr}^{-1} \mu\text{m}^{-1}$. The uncertainty of this measurement is dependent on the calibration source and the stability of the detector-electronic sensor system. The sources of spectral irradiance are lamps calibrated by the National Bureau of Standards (NBS) to a standard of spectral radiance such as a high temperature graphite blackbody. The lamps provide a specified spectral irradiance at a given distance from the filament. The absolute accuracies in irradiance under NBS conditions range from 1.4% at 350 nm, 1.1 % at 800 nm and 1.2% at 1600 nm (Slater, 1980). However, international comparison of spectral-irradiance measurements in the 300 - 800 nm range reveal inconsistencies as great as 6.5% (Gillham, 1977).

Although absolute calibration is necessary for establishing standards of comparisons among systems, the present-day requirements for remote sensing of the earth are best served by understanding a spectral sensing system in terms of relative calibration.

Relative calibration means that the output of a sensor under a varying input stimulus maintains the ratio between input and output in all spectral bands. In other words, the spectral character of the reflectance or emittance curves is maintained to the accuracy required for proper interpretation, but the absolute values are not necessarily known. Relative calibration is more readily achieved than absolute calibration and more important for the interpretation of remote sensing data.

Detector response can be either linear or more often non-linear with respect to variation in irradiance. Within a sufficiently small range of irradiance values, depending on the detector type, the output (O) can be described in terms of the input (I) and two constants (a,b) by $O = aI + b$. Over a larger range of values, a series of linear approximations must be used or a power curve of the form $O = aI^c + b$ where c is usually greater than 0.5 and less

than 2. Silicon detectors and photomultiplier tubes have inherent linear responses over a large dynamic range while detectors such as HgCdTe used in sensors for wavelengths beyond 1 μm are notoriously non-linear.

Radiometric sensitivity defines the minimum amount of scene contrast that can be detected by a sensor. Signal-to-noise ratio is another term used to describe the same sensor quality. Present-day practice is to define system sensitivity in terms of the minimum detectable change in reflectance, $n\Delta\rho$ or noise-equivalent change in reflectance for the reflective portion of the spectrum, and $n\Delta T$ or noise-equivalent change in temperature in the mid-IR.

Sensors

The analysis and interpretation of earth-looking data today largely ignores the question of calibration. Data are received from the appropriate agency on computer tape in the form of digital numbers (DN) and they are assumed to be relatively calibrated and linear with respect to irradiance. Papers published on interpreted results do not reveal whether the authors were aware of the nature of the calibration or the consequences of any possible miscalibration. The reasons for this are two-fold.

1. Interpreters have a blind faith in the sensor builders.
2. The variability in the irradiances measured due to atmospheric scattering and absorption, surface slope uncertainty, the inhomogeneities in the surface reflectance or emittance, and the uncertainties in interpretation are much greater than the inaccuracies introduced by faulty calibration.

The blind faith in sensor builders is not misplaced. However, to an interpreter who would like to assure himself that his faith is well placed, precious little data are available on calibration procedures and the results of calibration for the spectral imaging systems in use today. An exception is the Landsat MSS (NASA, 1976).

Aircraft scanners in general have reference blackbodies or calibration lamps that provide data at the end of each mirror rotation or scan. These are useful to set amplifier gains and for comparison among data taken at different times. In most cases engineering measurements are ignored by the interpreter. An exception is the use of thermal scanners to determine radiometric temperatures of surfaces. Here high and low temperature blackbodies scanned during each mirror revolution are set to bracket the temperature range to be measured. A single ground temperature measurement is then sufficient as a reference for low-flying missions over a restricted area.

In all cases the relative response of the detector to an input stimulus must be calibrated and the output linearized either internally to the instrument or the departures from linearity available in an accessible calibration report.

SMIRR

As an example of one calibration procedure, the Shuttle Multispectral Infrared Radiometer (SMIRR) will be discussed (Goetz and Rowan, 1982). It was calibrated with an irradiance standard traceable to an NBS standard (Goetz and Brownell, 1982). The standard consists of a hemisphere containing two, 1000 W quartz-iodide lamps. The hemisphere is coupled with a cone capped with an etched fused-silica face plate. At the base of the cone, in front of the hemisphere exit port is an iris to control the face plate illumination and therefore the irradiance. During calibration runs the output of the hemisphere calibrator is measured with a spot photometer containing a standard traceable to NBS. The relative spectral output was measured with a calibrated spectrometer over the range 0.4 - 2.5 μm . The estimated error in absolute irradiance is 10% while the relative error is probably less than 5%. In comparison the relative calibration using internal reference lamps showed a 10% variation in system response during the flight of SMIRR aboard Shuttle in November 1981. During the three years of intermittent laboratory calibration measurement, the system response decreased by 25% presumably due to detector degradation. The above demonstrates that a one-time, absolute calibration of a sensor is not sufficient and that a continuous relative calibration is necessary if high precision measurements are desired.

Data Interpretation

The necessity for calibration or lack thereof in the interpretation of natural surfaces can be drawn from the experience and the present-day understanding of the process of extracting information from airborne and spaceborne spectral scanners.

The image interpreter is primarily interested in the quality of the image and whether a combination of spectral images will yield the desired identification or at least discrimination of the units of interest. Scanner images should be free of "striping" which means that there should be no variations in response from one image line to the next. With multiple detectors, such as the 6 per band in the Landsat MSS, striping can be a problem if the response curves of the detectors are not matched. The matching can be obtained by accurate relative calibration.

Accurate spectral reflectance curves from a radiometer or an imager are only possible if relative calibration has been carried out. The effect of the atmosphere can be modeled, but normally more parameters need to be known than can be acquired. Therefore the interpreter, for instance in the case of reflectance measurements, is forced to pick a calibration point on the ground and normalize the surrounding data to this point. This procedure has been used with success in the preliminary reduction of data from SMIRR in Egypt (Goetz et al, 1982). Ground samples were collected and measured in the laboratory. The laboratory spectra were used to normalize the data and remove the atmospheric effects. By this means several hundred km of ground coverage could be investigated and spectra obtained. The resulting spectra were interpreted on the basis of the relative inter-band spectral values giving characteristic shape to the curves. The absolute reflectances were of little interest since the surface topography, the major source of overall brightness variations, was unknown.

The use of ratio images (Rowan et al, 1974) immediately obviates the need for absolute calibration but relies on a linear or known detector response. Other techniques such as principal component analysis, in which the maximum contrast is sought for display of an individual scene, does not require knowledge of sensor characteristics but makes the assumption that the detector responses are linear (J. Conel, personal communication).

Conclusion

The interpretation of spectroradiometric information from multispectral sensors to present-day levels of accuracy requires thorough instrument calibration, primarily to determine the response (non-linearity) of the detector, spectral bandwidth and relative response among the spectral bands. Absolute calibration is of value for intercomparison of instruments but does not contribute significantly to data interpretation.

ACKNOWLEDGEMENTS

This research was conducted by the Jet Propulsion Laboratory, California Institute of Technology, under contract with the National Aeronautics and Space Administration.

REFERENCES

- Gillham, E. J., Radiation standards, Applied Optics, 16, 300-301, 1977.
- Goetz, A. F. H., and M. Brownell, SMIRR calibration, JPL Technical Report, in preparation, 1982.
- Goetz, A. F. H., L. C. Rowan, and M. L. Kingston, Shuttle Multispectral Infrared Radiometer: Preliminary results from the second flight of Columbia, Proceedings IEEE, Munich, Germany, 1982.
- NASA, Landsat Data Users Handbook, Goddard Spaceflight Center Report No. 765D4258, 1976.
- Rowan, L. C., P. H. Wetlaufer, A. F. H. Goetz, F. C. Billingsley, and J. H. Stewart, Discrimination of rock types and detection of hydrothermally altered areas in South-Central Nevada by the use of computer-enhanced ERTS images, USGS Professional Paper 883, 1974.
- Slater, P. N., Remote Sensing Optics and Optical Systems, Addison-Welsey Inc., Reading MA, 1980.

On Optimum Design of Remote Sensing and Data Analysis Systems

James E. Conel
Harold R. Lang

Concept of an "optimum" scanner

Improvements in the application of remote sensing methods to geologic and geobotanic problems are likely to occur with development of future sensor systems along the following "optimal" lines. The optimum remote sensing system (1) gathers spectral radiance data at the highest spectral resolution possible, (2) over the greatest spectral interval feasible, and (3) at the highest areal resolution obtainable. The limits in any case are engineering questions that cannot be answered by geologic arguments. The spectral sampling should be to the extent possible statistically unbiased, which is to say equal sampling of all wavelength intervals. Other fundamental problems are: (1) design of statistical separation (clustering techniques), (2) classification schemes (discriminant function), (3) linear reduction methods (principal component or canonical variate) and (4) principles of data display. Applications to particular geologic problems benefit from model studies, which are either: (1) empirical, or (2) deterministic connections between geologic features of interest (lithology, alteration) and the observable remote sensing variable (spectral reflectance).

Areas of future research

To answer this broad array of problems, future research should be directed at (1) engineering studies to improve instrument performance, i.e., the spectral resolution, photometric accuracy and spatial definition of scanner systems, (2) engineering studies to improve the manipulation or handling of data flow, (3) statistical studies to provide optimum methods for reduction, separation and classification, (4) acquisition and analysis of geologic, and field and laboratory reflectance data to provide a sound basis for interpretation which will lead to a classification of geologic materials based on their spectral reflectance characteristics (such a classification must exploit the rock/soil/vegetation system), (5) systematic utilization of color display devices to maximize the number of (just noticeable) differences between spectral groups, i.e., transformations that maximize separability both statistically and perceptually.

Specific Recommendations

Designation of specific band widths, number of bands, radiometric precision, and spacial resolution are presently the result of site/problem specific observations made with available sensor systems. The following comments are primarily the result of research conducted at 5 JPL/Geosat test sites (2 uranium, and 3 oil and gas sites):

- (1) 1-15 m data provides information that may be used to produce the 1:24,000-48,000 maps which are most useful to exploration geologists.

- (2) Utility of multispectral data improves significantly with topographic information. Future multispectral sensor systems must assign elevations (1-3 m range) to every pixel. This requires conventional color photography, stereo multispectral data or some other integrated system (stereo radar, laser sounder, etc.).
- (3) Radiometric precision of 1% is usually sufficient for geologic applications. This requires only 7 bit rather than 8 bit data.
- (4) A strong aircraft observation program ensures rapid engineering and geologic testing of new scanner concepts. The proposed AVIRIS system is an efficient candidate research device for starting such a program.

POTENTIAL OF MULTISENSOR DATA AND STRATEGIES FOR DATA AQUISITION AND ANALYSIS

Diane Evans and Ron Blom, Jet Propulsion Laboratory
Pasadena, California 91109

BACKGROUND

Registration and simultaneous analysis of multisensor images have been found useful because the multiple data sets can be compressed through various image processing techniques to facilitate interpretation. This also allows integration of other spatial data sets, such as geophysical data, in a geographical management approach.

Multisensor image sets have been used for discrimination and, to some extent, characterization of geologic units. In the San Rafael Swell, Utah study area, coregistered Landsat and Seasat images provided better discrimination of geologic units than Landsat or Seasat data alone, due to the complementary effects of the compositional inferences possible from the multispectral data, and the textural and roughness data from the radar (Blom, et al., 1981). In other studies, coregistered Landsat and radar images of Death Valley resulted in less ambiguous discrimination of alluvial units based on albedo variations in Landsat images and roughness variations in the radar images (e.g. Daily, et al., 1978).

New techniques are being developed to analyze multisensor images that involve comparison of image data with a library of attributes based on the physical properties measured by each sensor. This results in the ability to characterize geologic units based upon their similarity to the library attributes, as well as discriminate among them. Refinement of the attributes-library concept may also make it possible to extract intrinsic physical properties from the images, such as dielectric constant and surface roughness in radar images. Once the physical properties can be extracted from the images, other applications for the multisensor images become possible, for example, 1) to use radar images to correct visible and near IR and thermal IR images for effects of surface roughness, and 2) to use near IR images to estimate vegetation cover in order to isolate the effects of partial vegetation cover from intrinsic surface properties in other images.

DETERMINATION OF DATA REQUIREMENTS

There are several studies that will provide information on ways to optimize multisensor remote sensing. Continuation of analyses of the Death Valley and San Rafael Swell image data sets will provide some insight into tradeoffs in spectral and spatial resolutions of the various sensors. The San Rafael Swell data set consists of coregistered Landsat, Seasat and HCMM images. The southern portion of the swell was also covered by the Shuttle Imaging Radar (SIR-A). Part of the SIR-A image has been digitized and

registered to the coregistered Landsat/Seasat/HCMH images. SIR-A images provide more information about small scale surface roughness properties of the units than Seasat because of the larger incidence angle (50 degrees compared to 23 degrees for Seasat). Thus, the SIR-A image provides complementary tonal information to the Landsat/Seasat combination described in Blom, et al. (1981). However, the resolution of SIR-A was lower than Seasat (40 meters compared to 25 meters for Seasat), and the effect of this lower resolution on texture analysis will have to be assessed.

The Death Valley coregistered data set consists of Seasat and Landsat images, as well as aircraft L-band and X-band radar images, and 11 channel VIS-NIR and thermal inertia images. This represents a wide range in both spatial and spectral resolution that can be analyzed. However, these data were obtained at different times, which could introduce some ambiguous results.

It will be very valuable for future multisensor experiments to acquire calibrated images with near-coincident coverage and comparable pixel sizes. It will then be possible to reduce the number of variables, and determine optimized resolution for a combination of sensors. The results might indicate that if one sensor has an optimal resolution for discriminating a given rock type, it may be possible to relax the resolution constraints on the other sensors.

REFERENCES

Blom, R., M. Abrams, and C. Conrad (1981) Rock Type discrimination techniques using Landsat and Seasat image data; IGARSS '81, 597-602.

Daily, M., C. Elachi, T. Farr, W. Stromberg, S. Williams, G. Schaber (1978) Application of Multispectral Radar and Landsat Imagery to Geologic Mapping in Death Valley; JPL Publication 78-19, 47 pgs.

GEOLOGIC UTILITY OF IMPROVED ORBITAL MEASUREMENTS

A. R. Gillespie
Jet Propulsion Laboratory

From a geologist's viewpoint, the most important use of orbital cameras is probably to provide spatial or contextual information in remote areas. This information may be extracted even from broad-band, single-channel images ... provided that the spatial resolution is adequate for the problem at hand. Presently most of the globe has been recorded at 80 m/pixel (Landsat MSS); which is roughly equivalent to a scale of 1:125,000. This is clearly inadequate for some purposes; for example, Holocene or late Quaternary tectonic studies require the identification and measurement of fault-offset features as small as 10 m, or even less. In a recent study of the Red River Fault in southern China the Landsat MSS images were sufficient to locate the main trace of the strike-slip fault, to identify its sense of displacement, and even to measure its cumulative late Cenozoic offset (5-6 km). Using Landsat RBV and SIR-A (shuttle radar) images, with twice the resolution, it was possible to recognize that a minor trace of the fault, inconspicuous on the MSS data, was the one on which recent offset had occurred, and was the one which was seismically dangerous. Using 1:50,000 BW aerial photographs, (~ 2 m resolution) geomorphic features on this new fault were obvious--but even at this scale the smaller features (e.g., inflections in ravine walls) necessary to establish the level of activity were inconspicuous. Thus an increase of resolution of as much as two orders of magnitude could be used in tectonically active areas of the world--especially in China and Russia, where conventional aerial photographs are difficult to obtain.

The second most useful kind of information is topographic, usually provided by stereoscopic images. Most present-day orbital systems do not produce such data, but where stereo images are available they have proven valuable--even with the small base/height ratios of Landsat. Any future satellite system designed to satisfy general geologic requirements must be able to produce stereo images, preferably with large base/height ratios of 0.5 or more.

Stereoscopic images are sufficient for most geologic applications involving only photo-interpretation, but the geometry may not be adequately controlled for geodetic measurements without auxiliary information. During the design of Stereosat it was recognized that although subtle topographic relief could be detected during visual inspection of stereo pictures, it was difficult to measure (resolve). Thus an instrument such as a scanning laser ranger, which would permit accurate and precise measurements at elevations, would have considerable application to geologic studies. Of particular interest in remote sensing would be precise topographic slope information, necessary for the reduction of thermal images and for the removal of photometric effects from all images.

The Landsat program was designed to give periodic coverage of the same scenes at the same local time. This is advantageous for agricultural studies, but not for most geologic studies. For geologic purposes it would be useful to have coverage at different illumination geometries instead. Low sun angles

are advantageous in regions of low relief where topography must be accentuated; high sun angles are desirable in areas of high relief or when multispectral data are to be collected. Thus for geologic studies, a different polar orbit than that of Landsat might be appropriate.

One of the main benefits of the remote sensing program to date has been the extended spectral sensitivity of electronic scanners. For geologists, this is important because it allows inferences of the composition of rocks in the scene to be drawn from the data directly, rather than from contextual clues. The current crop of sensors provides more channels and narrower spectral windows than those of the previous decade, and this welcome trend is likely to continue. Narrow-band sensors at 2.2 μm and multi-channel thermal scanners seem to be the most interesting at the moment. The former permit the recognition and distinction of different clays--an ability required in mineral exploration, but one which may also prove valuable in the relative dating of late Quaternary sediments. Multi-channel thermal images have been used to construct maps showing relative concentrations of silica at Tintic, Utah. This permits remote sensing to be used in the mapping of sedimentary facies as well as compositional variation in plutons, and may mark the advent of a new era of sophistication in geologic applications of remote sensing.

The need for data of high spatial and spectral resolution places a severe burden on the design and operation of the satellite. There are probably two useful approaches: (1) to fly numerous small, inexpensive, instruments designed for different special purposes; and (2) to fly a single complex instrument which may be programmed to select appropriate spectral channels and spatial characteristics. Such a flexible system could entail on-board data processing to minimize the transmission of unneeded data.

MIDDLE INFRARED REMOTE SENSING FOR GEOLOGY

Anne B. Kahle

California Institute of Technology
Jet Propulsion Laboratory
Pasadena, CA 91109

Introduction

The middle infrared (MIR) portion of the spectrum available for geologic remote sensing extends from approximately 3 to 25 μm . The source of energy is thermal radiation from surface materials at ambient terrestrial temperatures. The spectral range of usefulness of the region is limited by both the amount of energy available and by transmission of the energy through the atmosphere. At terrestrial temperatures the maximum black body radiation will be somewhere around 10 to 11 μm , dropping off sharply to shorter wavelengths and less sharply to longer wavelengths (see Fig.1). The best atmospheric window lies between about 8 and 14 μm with poorer windows between 3 and 5 μm and between 17-25 μm (see Fig. 2). The region between 3 and 5 μm is further complicated by overlap with the reflected solar radiation which is dropping rapidly in intensity but still has some contribution in this region. Thus the 8-14 region is by far the easiest spectral region to use and has received most of the effort to date. Fortunately, this is also a spectral region containing diagnostic spectral information on the silicates.

Remote sensing of the earth in the middle infrared is just on the threshold of becoming a valuable new geologic tool. Topics which still need to be studied include 1) the uses and limitations the 8-14 μm region for distinguishing between silicates and non-silicates, for distinguishing among the silicates, and for recognizing other rocks or minerals, 2) a theoretical and experimental understanding of laboratory spectra of rocks and minerals and their relationship to remotely sensed emission spectra, and 3) the possible use of the 3-5 and 17-25 μm portions of the spectrum for remote sensing.

Use of the 8-14 μ region

The recent work at Tintic with multispectral MIR scanner data has demonstrated that there is significant geologic information which can be obtained from surface spectral emissivity data acquired by remote sensors. It was shown that in certain cases even minor differences in rock type could be distinguished, i.e., quartz latite/quartz monzonite could be distinguished from latite/monzonite. At the same time there are numerous excellent collections of laboratory transmission and reflection spectra of minerals and rocks along with explanations of the source mechanisms of the observed spectral features. Fig. 3 through 6, from Hunt are representative. Fig. 3 shows spectra of some silicates and their dependence upon crystal structure. Fig. 4 shows spectra of some non-silicates. Fig. 5 is a diagram summarizing locations of spectral features including Christiansen peaks, transmission minima, and the processes responsible for their origin. In Fig. 6 are shown the spectra of a few common rocks. It is clear from these figures that rocks and minerals

possess abundant spectral features under idealized laboratory conditions. The basic problem is to determine exactly what can and cannot be achieved with remote sensing. Because of the difficulties (discussed in the next section) in relating laboratory transmission and reflection data to emission of natural surfaces, it is not possible to accurately predict the specific capabilities for rock type discrimination which can be realized. Field and aircraft data collection programs need to be undertaken along with both theoretical and experimental laboratory work in emission spectroscopy.

Crude spectra have been derived from the six channels of multispectral aircraft data at Tintic, and field spectra have been acquired with the Portable Field Emission Spectrometer (PFES). Both data sets indicate that the spectral differences are at least as much due to variations in the intensity of the spectral feature as to variations in the position of the bands. See Fig. 7. The bands decrease in intensity and shift to higher wavelength with decreasing quartz content of the rocks in a manner similar to laboratory spectra. Further PFES data taken in the Southern California batholith show these same effects.

A new aircraft scanner, the Thermal Infrared Multispectral Scanner (TIMS), is now complete and undergoing testing. This instrument has six mid-infrared channels: 8.2-8.6, 8.6-9.0, 9.0-9.4, 9.4-10.2, 10.2-11.2 and 11.2 to 12.2. The choice of bands was dictated by instrument constraints, atmospheric effects and laboratory and field measurements of spectral signatures of rocks. Data acquisition with the new TIMS aircraft scanner should begin this summer.

Laboratory data

The most complete set of laboratory spectra of rocks available for the MIR are the transmission and reflection of spectra of Hunt and Salisbury. Their transmission spectra were obtained using two different sample preparation techniques, the conventional method of the powdered specimens being compressed in KBr pellets, and by deposition of thin layers of fine particles onto a mirror. The principal Christiansen peaks appear in the spectra of the deposited particles (with the particles on the mirror in air), but not in the spectra obtained from the samples in the KBr pellets. However, apart from this difference, most of the absorption features are similar. The reflection spectra measured using polished rock surfaces, which should more closely approximate emission spectra, display significant differences from the transmission spectra. Emission spectra, which would be the most applicable to remote sensing of emitted radiance are more difficult to measure and interpret. In order to be able to measure emissivity, the sample must be at a higher temperature than its surroundings, which creates unnatural temperature gradients. Most of the differences between the spectra obtained in the various modes have been shown both theoretically and experimentally to be dependent upon such variables as particle size, surface roughness, packing density, and the near-surface temperature gradients.

Hunt measured emission spectra in the laboratory of some rock samples collected at Tintic. Although he stated that there were still some problems to be resolved with his experimental procedures, he felt the data were illustrative of the problems involved. His emission spectra are shown in Fig. 8, along with transmission spectra of the same samples run by K. Baird, using the

KBr pellet method. Of this work Hunt wrote, "It is obvious that only general agreement exists between transmission and emission spectra for these particular samples and that the agreement is better at longer wavelengths than in the 10 μm region. These preliminary data are presented to emphasize the need for both experimental and theoretical studies to define the spectral characteristics of emission from geologic materials under natural conditions. Of immediate importance is the need to develop appropriate methods for simulating the natural environment in the laboratory and using the data acquired to develop models to relate the spectral emission behavior to the fundamental properties of geologic materials."

Use of the 3-5 and 17-25 μm regions

Not much work has been reported which attempts to use the 3-5 μm region for spectral remote sensing of the earth's surface. Referring to Fig. 2, one sees that there is good atmospheric transmission between about 3 and 4.2 μm and then again from 4.5 to 5 μm , and data from this wavelength region have been used for determination of the surface temperature. Laboratory spectral data, in this wavelength region, however, show a paucity of diagnostic spectral features of rocks and minerals. There is a very strong molecular water band at 2.94 μm which is present in the spectrum of any mineral with adsorbed water. Hovis claims that there are strong carbonate features near 3.5 and 4.0 μm and that the sulphates and nitrates have a number of strong bands between 3 and 4.5 μm . However, examination of several collections of mineral spectra shows only a relatively weak carbonate band at about 4.02 μm , a few weak chlorite features between 3 and 4.4 μm , and relatively weak gypsum bands at 4.48 and 4.72 μm . Most mineral spectra shown in these collections are completely featureless from 3 to 5 μm . Hydrocarbons and vegetation may have important spectral bands in these wavelengths but little data is available in the literature. Perhaps, therefore, laboratory studies directly explicated toward the feasibility of using this spectral region for geologic remote sensing, are warranted.

This spectral region is further complicated by overlap with the reflected solar radiation which must be taken into consideration at the shorter wavelengths. The exact wavelengths where both sources of radiation must be considered will vary with the amount of incoming solar radiation (dependent primarily on solar angle) and amount of emitted radiation from the surface (dependent primarily on surface temperature).

In the 17-25 μm region, numerous diagnostic spectral features exist. Feldspars have extremely characteristic stretching bands between 15 and 20 μm . Mafic minerals also have stretching bands in this region. Above 20 μm deformation and bending modes for numerous minerals exist. However, the intensity of emitted radiation in these wavelengths is low (see Fig. 1) and the atmospheric transmission is very poor (less than 10%) (Fig. 2). It appears that the 17-25 μm region of the middle infrared does not hold much promise for geologic remote sensing in the immediate future, until and unless more sensitive sensors become available.

ACKNOWLEDGEMENTS

The research described was carried out by the Jet Propulsion Laboratory, California Institute of Technology, under contract with the National Aeronautics and Space Administration.

Figure Captions

1. Black body emission for various temperatures.
2. Atmospheric transmission.
3. Midinfrared transmission spectra of some silicate minerals.
4. Midinfrared transmission spectra of some non-silicate minerals.
5. The location of features and the types of vibrations that produce the spectral signatures of silicates in the midinfrared.
6. Midinfrared transmission spectra of a few common rocks.
7. Midinfrared field emission spectra.
8. Quartzite (left) and clay (right) transmission and emission spectra. E-10 is quartzite; E-29 is a quartzite rock with a heavy iron stain; E-38, a silicified rock containing halloysite and quartz; E-55, B-clay altered from latite; E-63, opalized quartz.

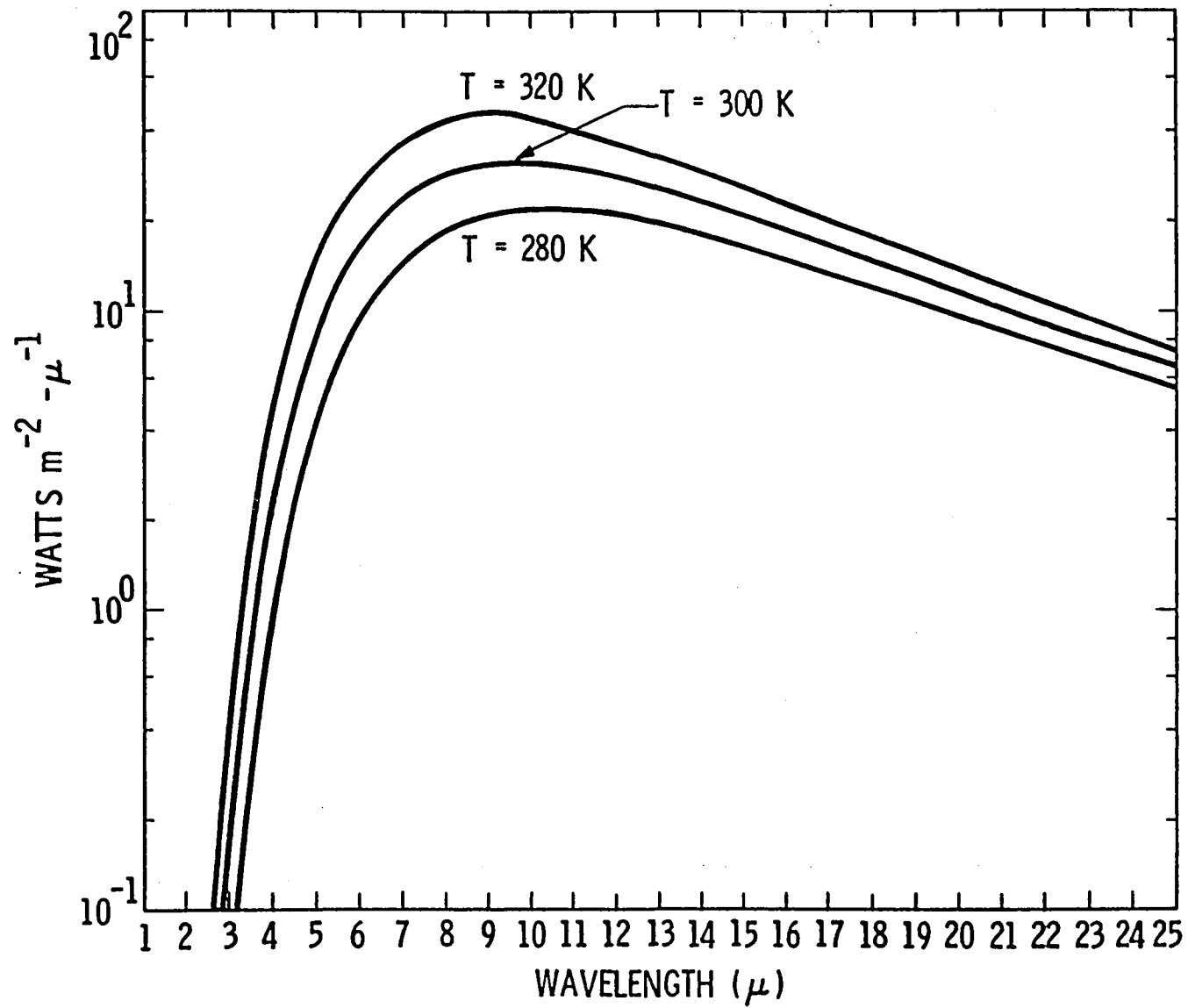


Figure 1

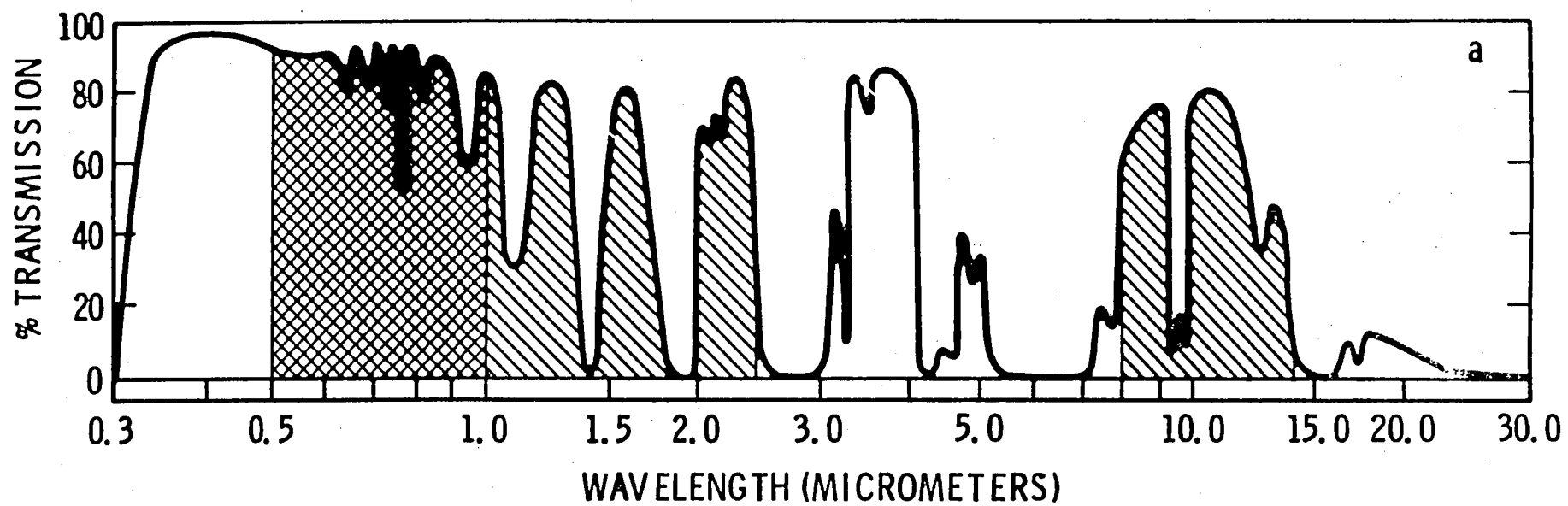


Figure 2.

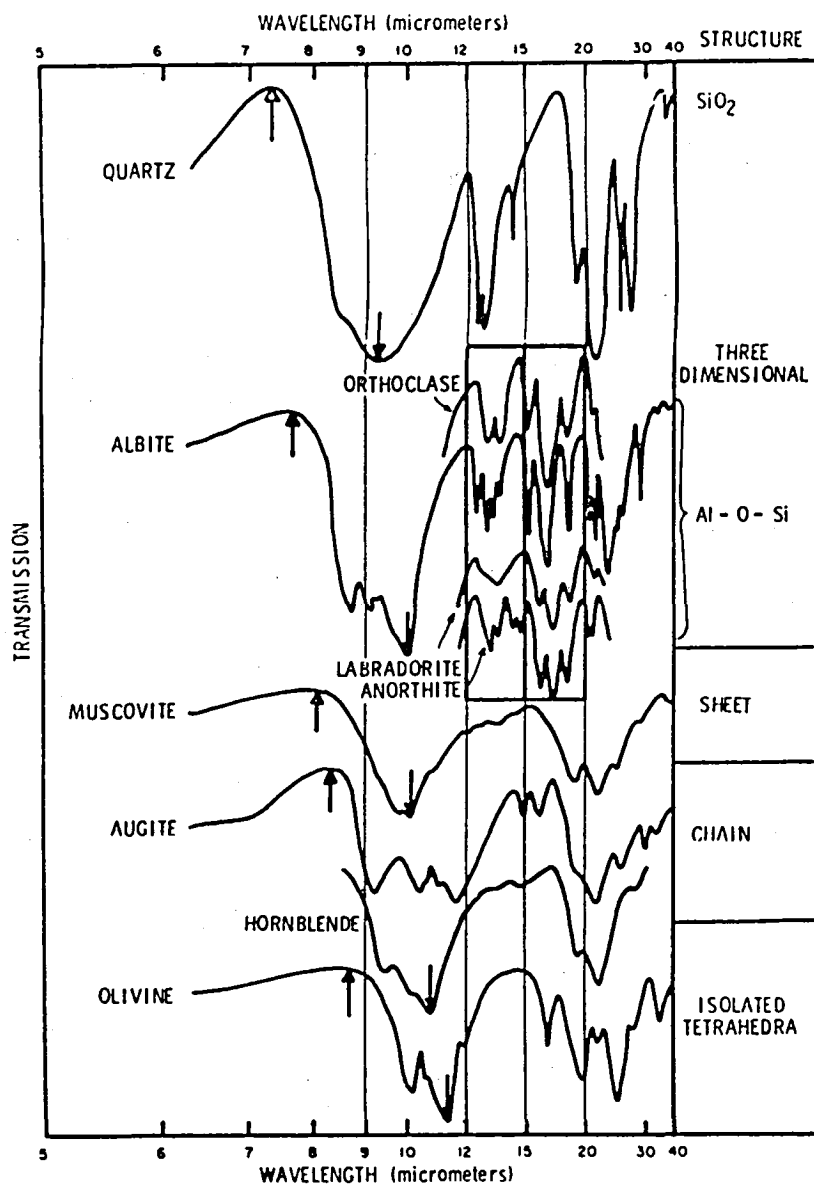


Figure 3.

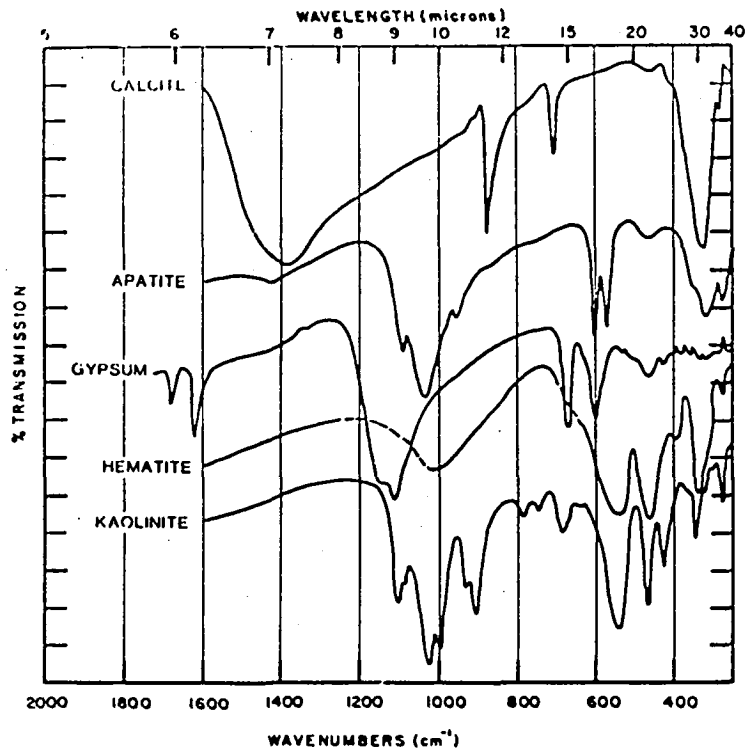


Figure 4.

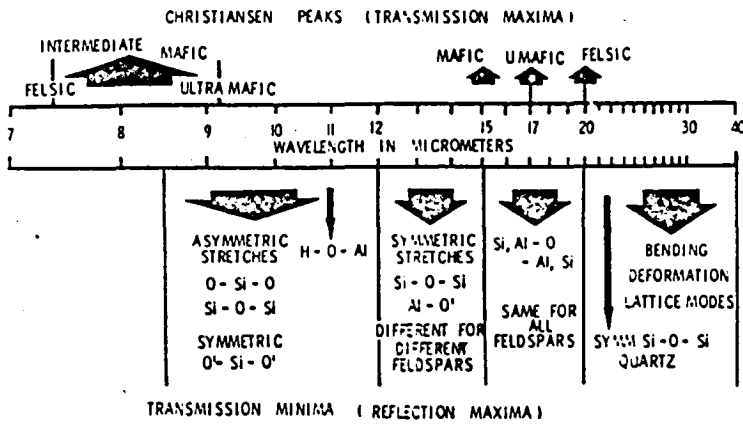


Figure 5.

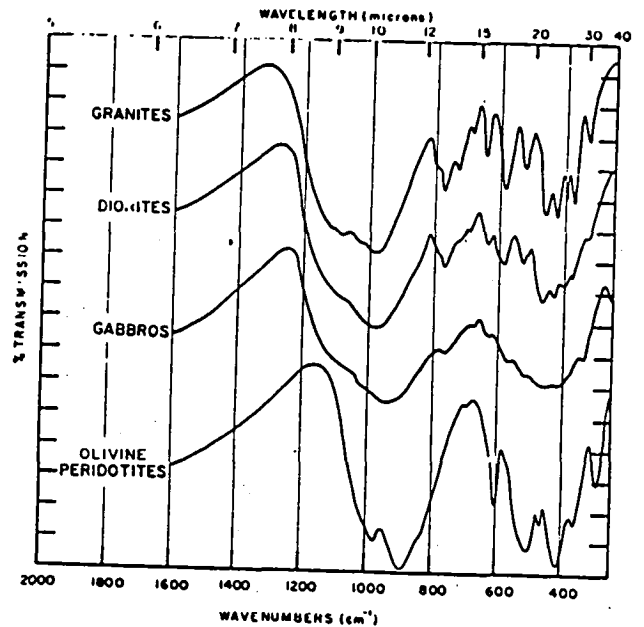


Figure 6.

PFES FIELD SPECTRA TINTIC, UTAH

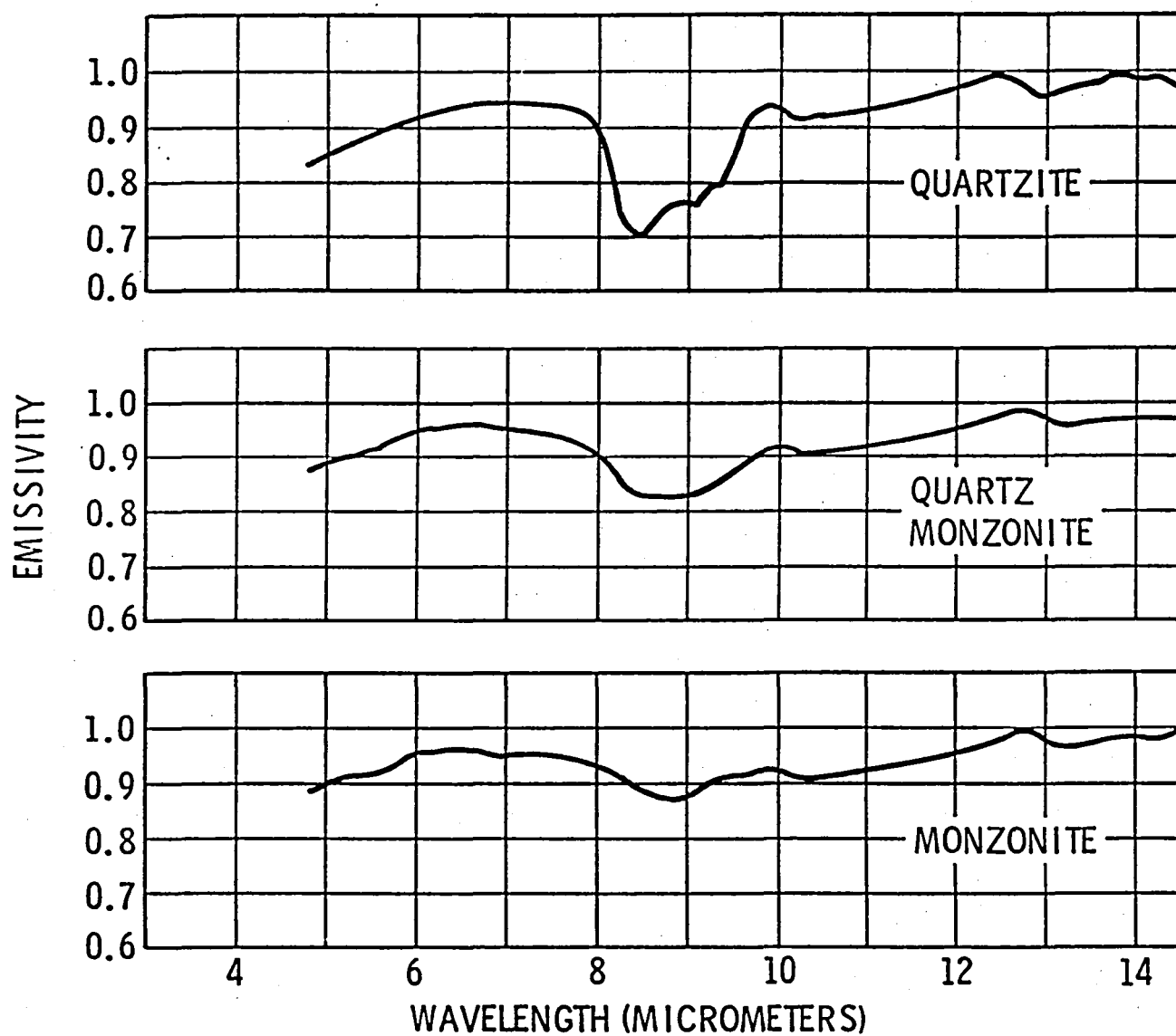


Figure 7.

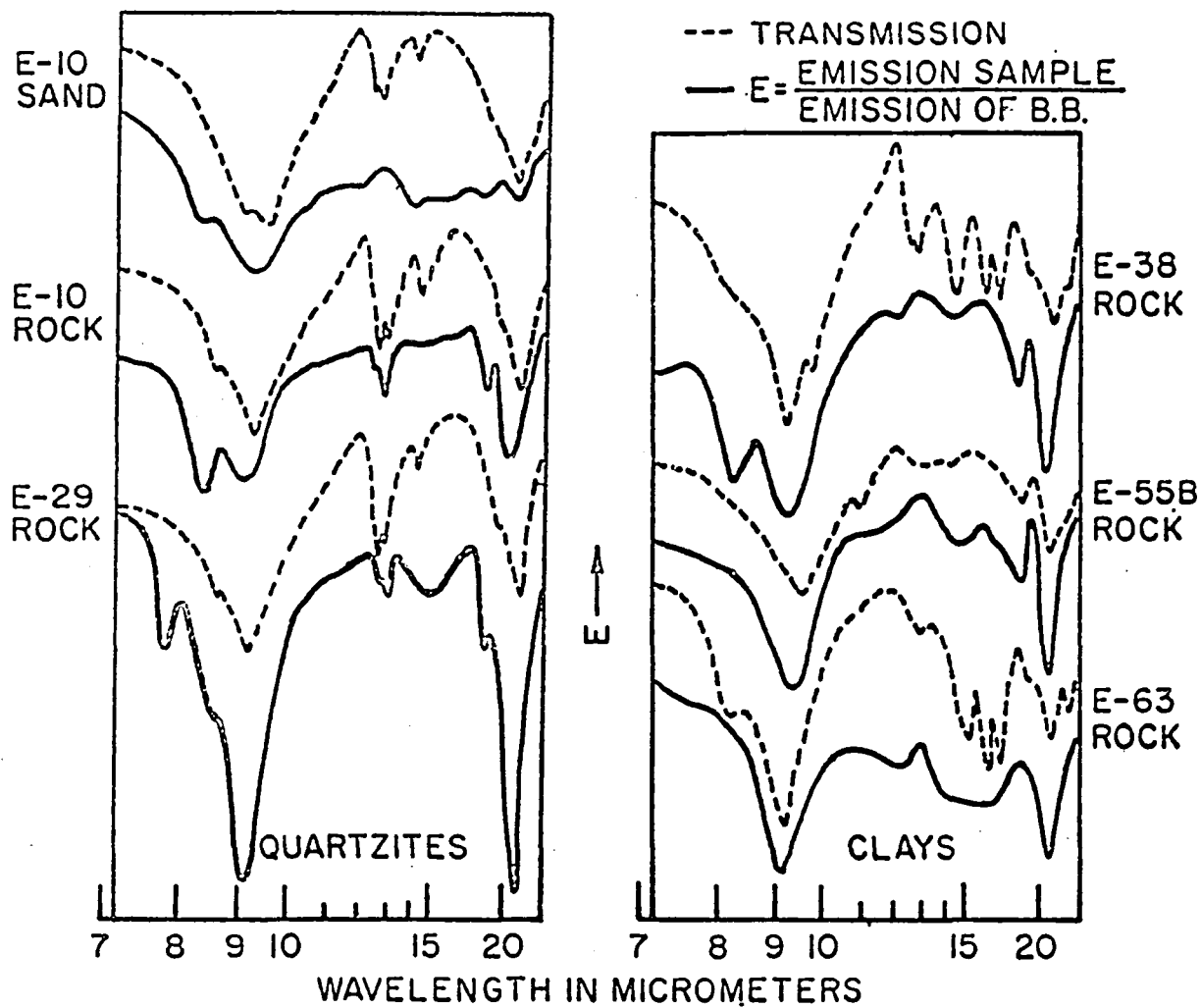


Figure 8.

AIRBORNE INFRARED MINERAL MAPPING
SURVEY OF MARYSVALE, UTAH

WILLIAM COLLINS
SHENG-HUEI CHANG

Aldridge Laboratory of Applied Geophysics
Columbia University
New York, New York 10027

Preliminary report on Marysvale study in cooperation with
U.S. Geological Survey. This paper has not been approved
for publication.

TABLE OF CONTENTS

ABSTRACT.....	i
INTRODUCTION.....	1
Survey Site.....	3
ALTERATION AND MINERALOGIC MAPPING.....	4
Alteration Intensity Analysis.....	5
Spectral Data.....	11
Mineral Mapping.....	12
INFRARED SPECTRAL DATA.....	21
CONCLUSION.....	33

INTRODUCTION

Infrared spectroradiometer survey results from recent flights over the Marysvale, Utah, district show that hydrothermal alteration mineralogy can be mapped using very rapid and effective airborne techniques. The airborne spectroradiometer system is able to detect alteration mineral absorption band intensities in the infrared spectral region with very high sensitivity. The higher resolution spectral features and spectral differences characteristic of the various clay and carbonate minerals are also readily identified by the airborne infrared instrument allowing the mineralogy to be mapped as well as the mineralization intensity.

The Marysvale survey shows very conclusively that high spectral and radiometric resolution systems can perform mineral exploration and mapping functions that have not been possible by any other means. The airborne survey methods acquire much more and comprehensive data than can be obtained by ground sampling and mapping techniques, and the mapping can be accomplished in a matter of days. As an exploration technique, the airborne infrared spectroradiometer is the most sensitive system available. For mapping and developing known mineral properties, the airborne application can save considerable time and expense.

Previous flights by the newly developed infrared spectroradiometer system were designed for quick reconnaissance of several scattered sites in western Nevada (Collins, Chang and Kuo, 1981). These flights were very successful in showing the 2.0 to 2.5 micron infrared spectral properties of various hydrothermally altered sites and other sites of unaltered clay and carbonate lithologies. The present survey over Marysvale marks the first time that a detailed grid survey has been flown over a mineral site using a high spectral resolution infrared system. The present results show that airborne surveys in rectangular grid patterns will provide very good coverage and allow accurate mapping of geologic terrain.

The Marysvale site was flown on October 9, 1981 in a grid pattern as shown in Figure 1. The flight traverse pattern in this case was designed to cover earlier ground traverses by the U.S. Geological Survey. The aircraft was flown at 2000 feet above the terrain and at 110 miles per hour.

The airborne spectroradiometer acquired data in two spectral windows. In the visible and near IR the instrument acquired 512 channels of data in the 350nm to 1.0nm region at 1.3nm bandwidth in each channel. The infrared data was acquired in 64 channels

between 2.0 micron and 2.5 micron. The bandwidth is 8nm in the infrared region. The data are acquired in 20 meter square fields of view in a contiguous sequence along the ground track. Storage is on digital tape. The data are calibrated in radiance received at the front aperture. Data processing and analysis are done on the computer.

Survey Site

The Marysvale district is in south western Utah. It is one of the major volcanic centers that surround the Colorado Plateau. The exposed rocks are mostly oligocene to miocene volcanic flows and tuffs with some quartz monzonite and granite intrusions (Kerr, 1968). Hydrothermal alteration has resulted in heavy alunite mineralization with surrounding kaolinite and montmorillonite. Metallic mineralization is gold, silver, base metals, uranium, and molybdenum.

ALTERATION AND MINERALOGIC MAPPING

The alteration in the Marysvale region has been mapped both for mineralization intensity and mineral type. The intensity is measured with respect to the total absorption intensity in the mineral bands. This absorption intensity can be measured in several ways such as by taking the ratio of bands inside and outside the absorption feature, or by integrating the energy within the absorption band window. These techniques have the disadvantage that, in data taken over natural terrain, there are many spectral and intensity variations that are not related to the mineral bands.

The Marysvale data were analyzed using techniques specially developed for high spectral resolution aircraft data. Spectral variations in the data are recognized using a "waveform analysis" technique in which the spectral curves for each field-of-view measurement in the radiance/wavelength domain are transformed into a series of polynomial terms using the Chebyshev method. The appearance of various absorption features in the data along the aircraft traverses is seen as a change in the polynomial terms. This technique has proven more reliable and noise free than other analysis methods.





The results of the mineralization intensity analysis are mapped on the aerial photo mosaic in Figure 1. The mineralization intensity along each aircraft traverse is mapped in color with yellow and red the most intensely altered areas, as measured by the strength of the mineral bands. The areas mapped in orange show moderately strong absorption features. The areas mapped in brown have weak but still very obvious mineral features. The areas mapped in blue show no mineral features or very weak ones. These areas are considered background.

The mapping results show four hydrothermal cells in the survey area. The outer contours enclose the zone of weak to moderate mineralization as mapped in brown and orange. The inner contours with cross hatching mark the more intensely altered areas mapped in yellow, red, and orange. The more intensely altered zones in each cell are well defined areas within the larger zones of alteration. The mapping results also show that the alteration within each site is quite pervasive.

Alteration Intensity Analysis

The waveform analysis results used to determine the mineral absorption band intensities are shown in Figure 2. These data are from aircraft traverse 5 (Figure 1), which runs north-south through the largest alteration cell in the center of the survey

PHOTO-MAP INDEX
ALTERATION INTENSITY MAP
MARYSVALE, UTAH

<u>COLOR</u>	<u>PATTERN</u>	<u>EXPLANATION</u>
YELLOW		Very Strong Clay Alteration
RED		Strong Clay Alteration
ORANGE		Moderate Clay Alteration
BROWN		Weak Clay Alteration
BLUE		No Clay Alteration

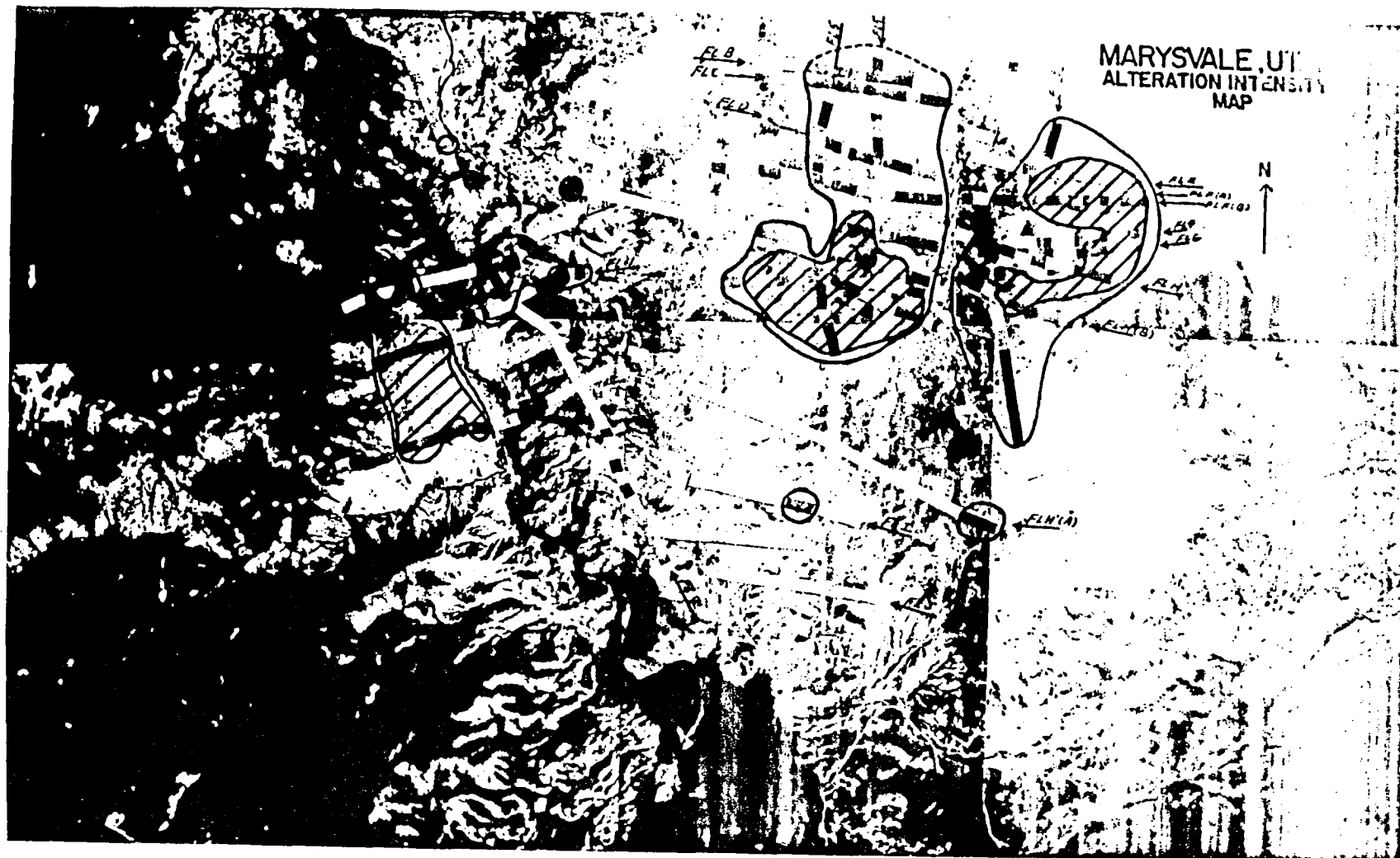


Figure 1. Alteration intensity map of marysvale, Utah. Contures outline four major hydrothermal cells with intently altered cores.

MARYSVALE , UTAH WAVEFORM SPECTRAL ANALYSIS

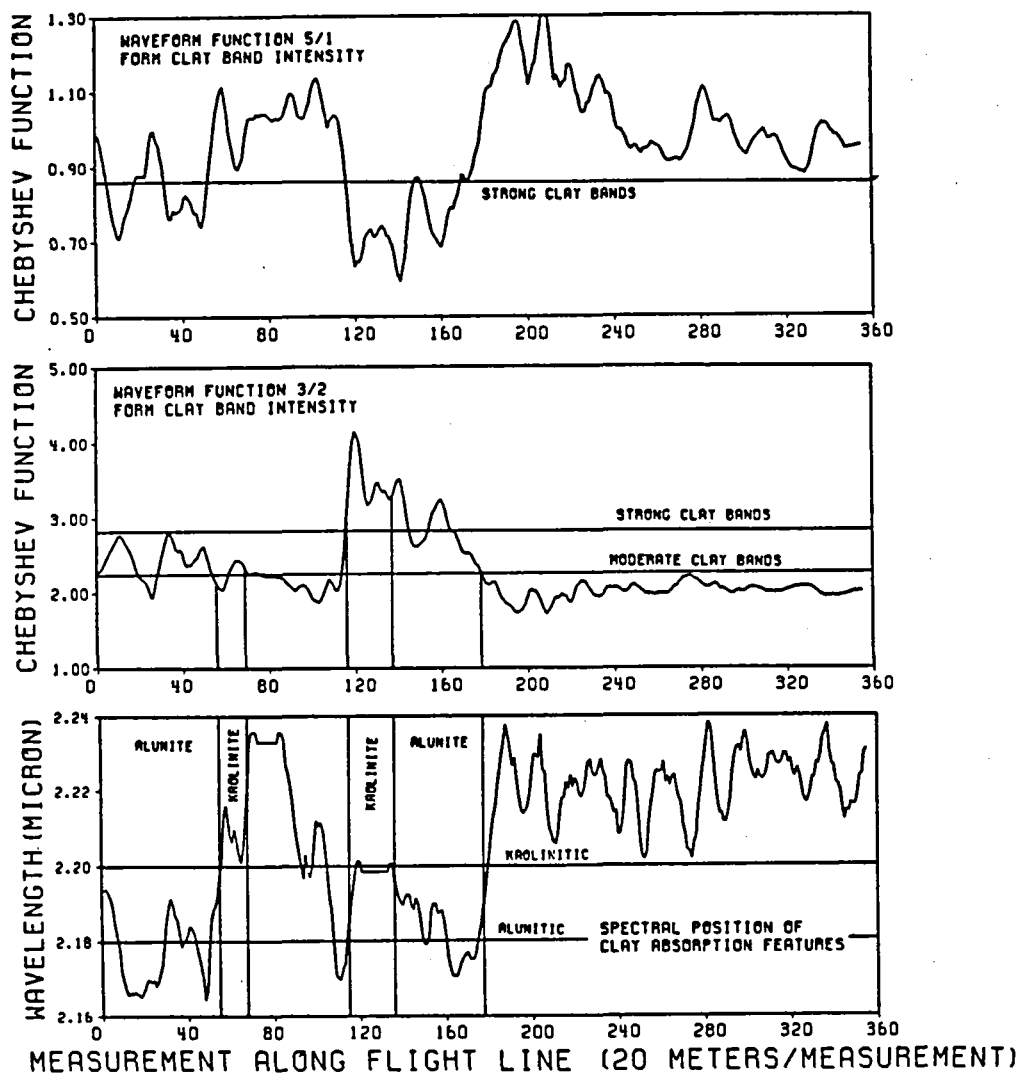


Figure 2. Waveform and mineral analysis along traverse 5. The upper waveform analysis results quantify the clay absorption intensity along the traverse, with the most intense zone near measurement 120. The lower curve shows the spectral position of the clay feature, which can indicate the difference between kaolinite and alunite.

area. The traverse is about four miles long; running from the top of the survey site, through the alteration zone for about two miles, and through background areas of no alteration for the last two miles.

The data in Figure 2 are from 360 measurements taken in sequence along the aircraft traverse each measurement is a 64 channel infrared spectrum of the type shown in Figure 3. Each measurement is made up of the integrated energy, in radiance, reflected from a 20 meter square field-of-view. Waveform functions 5/1 and 3/2 are sensitive to the clay absorption bands. Function 3/2 is used mainly to measure the clay band intensity, while function 5/1 is an indicator of carbonate versus clay features. The 5/1 function when low indicates clay absorption in the 2.15 to 2.2 micron region.

The waveform function 3/2 is very sensitive to the intensity of the clay absorption features. Higher values indicate more intense absorption. The values of waveform function 3/2 show moderate to weak clay mineralization between measurements one and 70 in Figure 2. This area is mapped in orange and brown for the first 3/4 of a mile of traverse 5 on Figure 1. Between measurement 70 and 115, the function 3/2 values are low indicating no alteration. This area is mapped in blue.

AIRCRAFT INFRARED SPECTRA MARYSVALE TRAVERSE-5

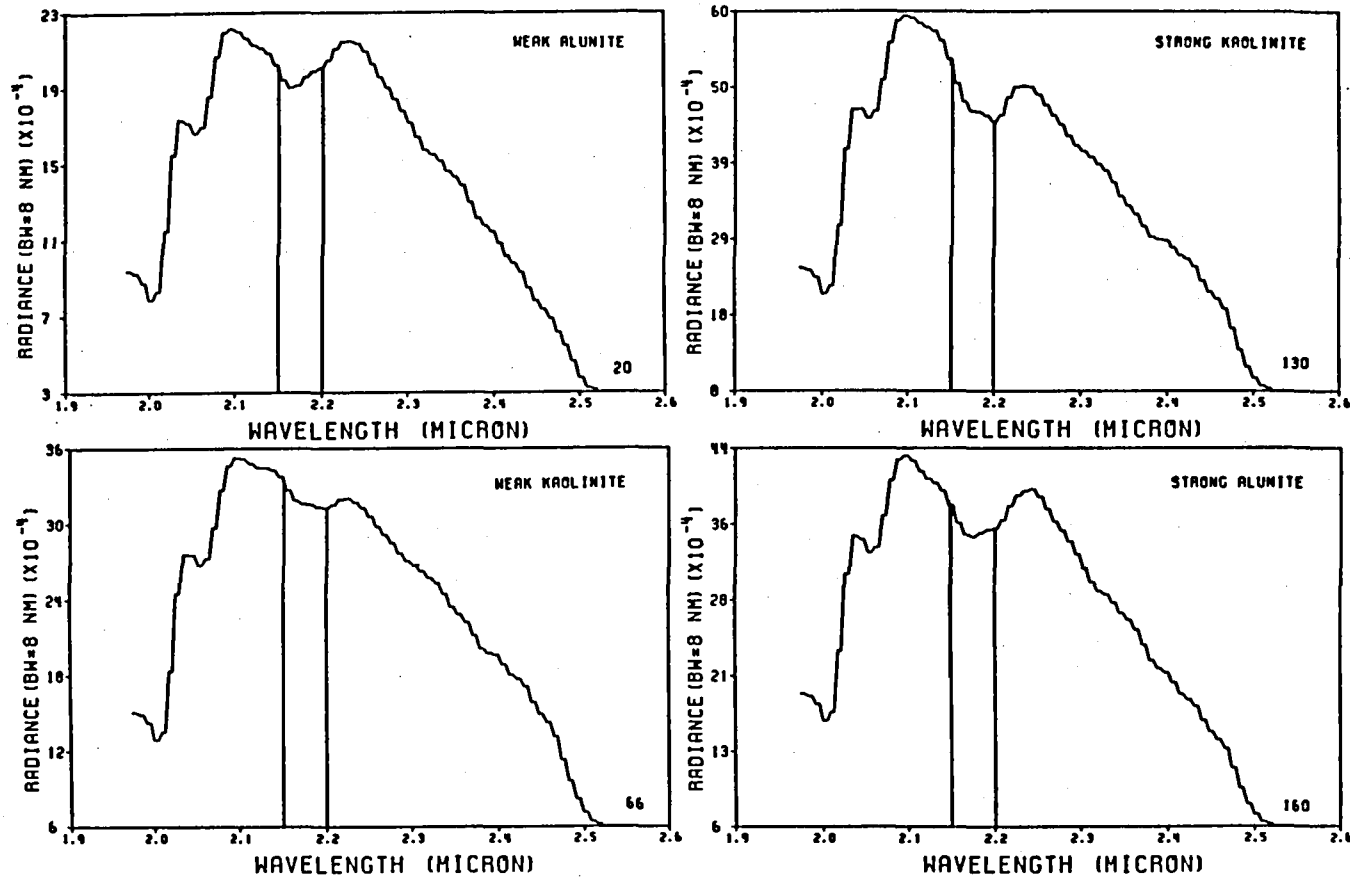


Figure 3. Spectral measurements along traverse 5. The numbers in the lower right corner identify the measurement number. These numbers correlate with the x-axis scale in Figure 2. The spectra show the differences in alteration intensity and mineral species.

From measurement 115 to 180, the waveform results indicate strong alteration. This section of traverse 5 is mapped in red and orange. After measurement 180 the data show no alteration minerals along the traverse. This "background" area has waveform function $3/2$ values well below those over the altered zone.

Spectral Data

Eventually the computer analysis will also include pattern recognition of various mineral spectra based on a stored library of reference curves. This technique, however, will require an extensive data base of known curves, which is now being assembled from the survey data. At present the analysis of aircraft infrared data includes visual inspection.

Selected infrared spectral curves from traverse 5 are shown in Figure 3. The spectra are measured in 64 channels between 2.0 and 2.5 microns. The numbers in the lower right corner of each diagram indicate the measurement number along the flight path. In Figure 3 the spectra are from measurements 20, 66, 130, and 160 along the traverse. These numbers can be related back to the flight line measurement in Figure 2 and to the mapping in Figure 1.

The two spectra labeled weak alunite and weak kaolinite are from the beginning section of traverse 5, which is mapped in brown and orange in Figure 1. This is the northern section of the hydrothermal cell where the alteration appears weaker. The mineral bands, as can be seen in Figure 3, are less intense in this zone of the alteration cell. The spectra from measurements 130 and 160 show strong absorption features between 2.15 and 2.20 microns. These measurements are from the zone in Figure 2 with high waveform function 3/2 values and low function 5/1 values. The spectra are from the areas mapped in red in Figure 1, and where the traverse crosses the strongly altered zone in the southern part of the hydrothermal cell.

Mineral Mapping

Identification of mineral species can be accomplished using infrared spectral data providing that the instrument spectral resolution is sufficient to resolve the spectral features that distinguish the various minerals. The 8nm band width of the airborne system is quite adequate to allow mineral identification. This identification at present is being accomplished by comparison of the airborne results with known laboratory measurements (for example Hunt, 1979) and with airborne surveys over known terrain (for example Collins, Chang, Kuo, 1981).

PHOTO-MAP INDEX

MARYSVALE, UTAH

MINERAL MAP





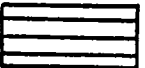
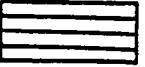
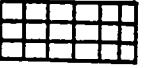

<u>COLOR</u>	<u>PATTERN</u>	<u>EXPLANATION</u>
YELLOW		Alunite
RED		Kaolinite
ORANGE		Mixed Alunite and Kaolinite
CHERRY RED		Montmorillonite
BLUE		Clay plus Gypsum
GREEN		Alunite/Kaolinite plus Gypsum
VIOLET		Kaolinite/Montmorillonite plus Jarosite?
BROWN		Kaolinite/Montmorillonite



Figure 4. Mineral map of Marysvale, Utah. The various hydrothermal alteration minerals are mapped in each of the four cells.

The results of the mineral identification and mapping are shown in the map overlay of Figure 4. The mineral mapping was done only within the hydrothermal cells. The main hydrothermal mineralogy of alunite, kaolinite, and montmorillonite occurs in a very interesting pattern that is well defined by the infrared spectral mapping.

The alunitic zones are mapped in yellow with single cross hatched pattern, and the kaolinitic zones are mapped in red with single cross hatching pattern. The montmorillonite zones are mapped in cherry red with double cross hatching. Some smaller areas that contain other minerals as well are mapped in other colors and patterns, as explained in the index for Figure 4. The other minerals appear to be gypsum and possible jarosite or chlorite. Ground measurements and sampling are required to establish this mineralogy.

The alunite and kaolinite infrared spectral properties can be seen in the spectra of Figure 3 from traverse 5. The kaolinite clays have a well defined doublet absorption band with the minimum at 2.2 microns and a shoulder feature at 2.17 microns. The alunite band has a strong minimum at 2.1 to 2.18 microns and is generally broader than the kaolinite band. The variations in the position of the absorption minima along traverse

5 are shown in the lower diagram of Figure 2. The upper horizontal line through the wavelength value of 2.20 microns, and labeled kaolinitic, marks the wavelength position of the kaolinite minimum. The lower horizontal line through 2.18 microns marks the approximate limit of the minimum shift in alunite spectra. The mineral determination is done within the limits of significant alteration intensity as indicated by the waveform function $3/2$ values (vertical boundary lines). The data in Figure 2 have been smoothed in the flight direction. This brings out the general trend in alteration. The point-to-point variation in mineralogy is greater than is indicated by the curves in Figure 2. The finer variations would be useful in mapping specific sites on a much more expanded scale.

The mineralization in the two larger, eastern, cells occurs in a well defined pattern of three alunite "core zones" with outer zones of kaolinite. Two of the alunite zones fall within the zones mapped as intense alteration in Figure 1. The largest alunite zone occurs in the northern section of the larger central cell. The mineralization appears less intense in this area. In summary the two eastern hydrothermal cells show a more or less central zone of intense alteration with alunite zones coinciding with the more intense mineralization. A third zone of

alunite does not correlate with the most intense alteration. The two eastern cells are current molybdenum prospects.

The two western cells show a different mineralogy; which is dominantly montmorillonite, or a similar clay. This preliminary classification of montmorillonite from the spectral data requires ground sampling for initial correlation of infrared spectral properties as measured from the air. The spectral data are shown in the following section. The pattern of distribution of montmorillonite indicates that the western cells, at the surface level, are zones of lower temperature alteration.

INFRARED SPECTRAL DATA

Inspection of the infrared spectral data shows conclusively that there are very distinct and consistent differences in the high spectral resolution features of the alteration minerals. The following data show these spectral features of the Marysvale site. Many additional and distinctive spectral properties have been observed over other sites (Collins, Chang, Kuo, 1981). These results from the airborne infrared spectroradiometer surveys indicate that a wide variety of information is available in applying this survey technique.

The spectral curves from traverse G are shown in Figures 5, 6, and 7. The spectra in Figure 5 are from the first 40 measurements where the traverse crosses the medium to strongly altered zone of kaolinite and alunite on the east edge of the eastern hydrothermal cell.

The spectra in Figures 6 and 7 are from traverse G across the central hydrothermal cell. The traverse is broken because of the offset in the photo mosaic. Traverse G is the straight east/west traverse that begins as the second traverse up from the southeast corner of the hydrothermal cell. The lower traverse crosses G near traverse 5. Traverse G extends the farthest west

AIRCRAFT INFRARED SPECTRA MARYSVALE TRAVERSE-G

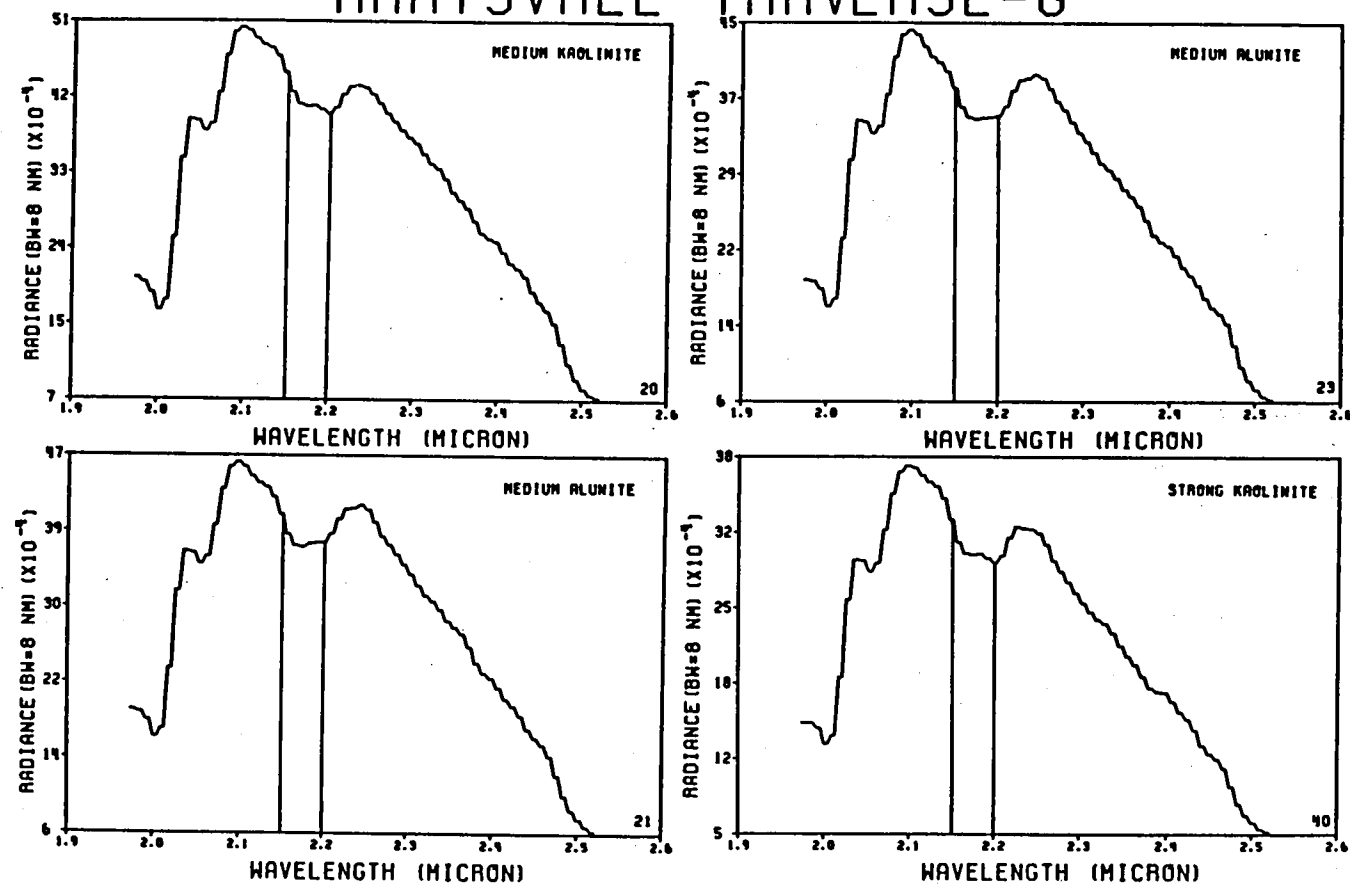


Figure 5. Spectra from traverse G where it crosses medium and strong intensity kaolinite and alunite mineralization in the large eastern hydrothermal cell.

AIRCRAFT INFRARED SPECTRA MARYSVALE TRAVERSE-G

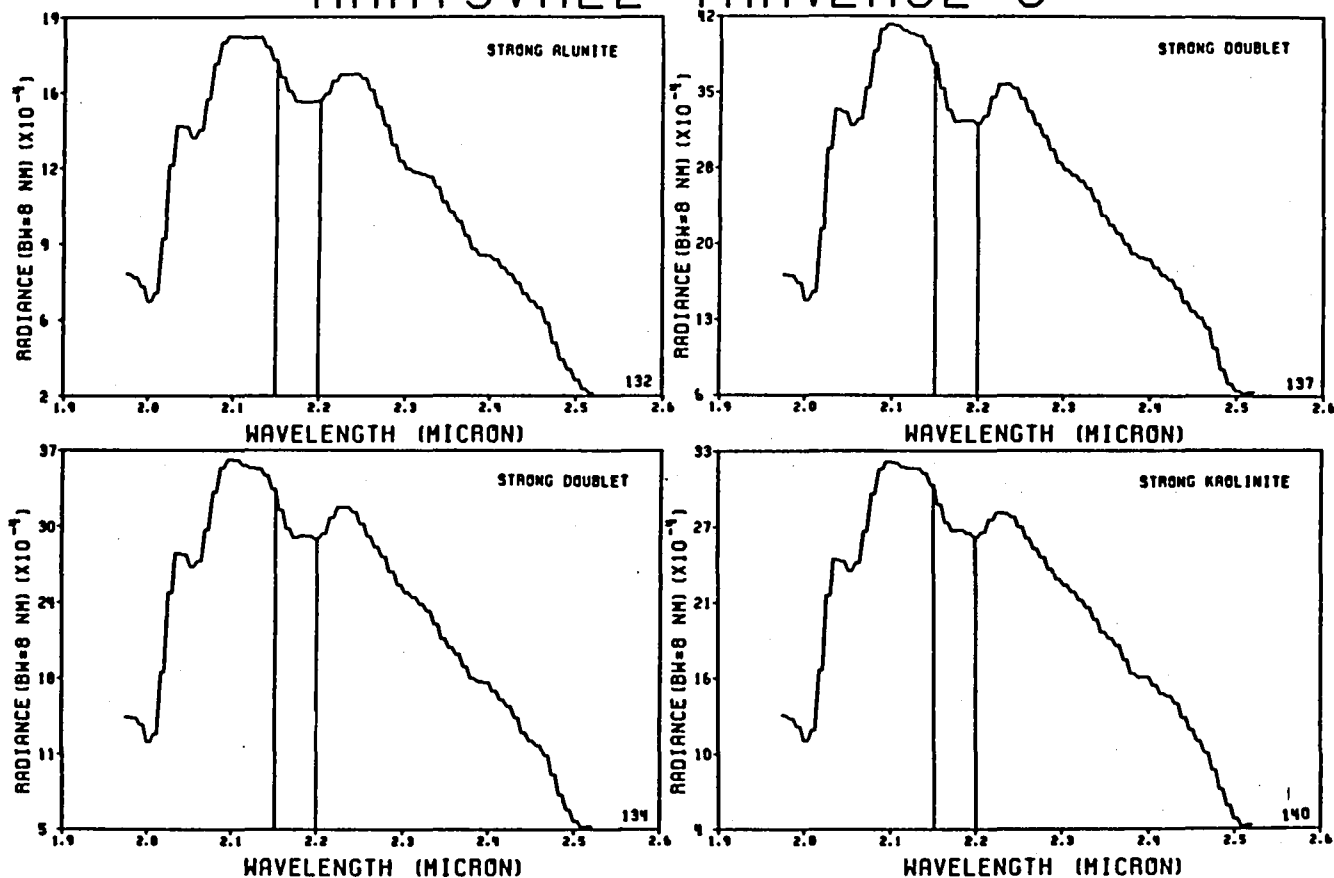


Figure 6. Spectra from traverse G where it crosses strong alunite and kaolinite mineralization in the central hydrothermal cell. Spectra labeled strong doublet appear to be a mixture of kaolinite and alunite. These areas are mapped in orange on the mineral map.

AIRCRAFT INFRARED SPECTRA MARYSVALE TRAVERSE-G

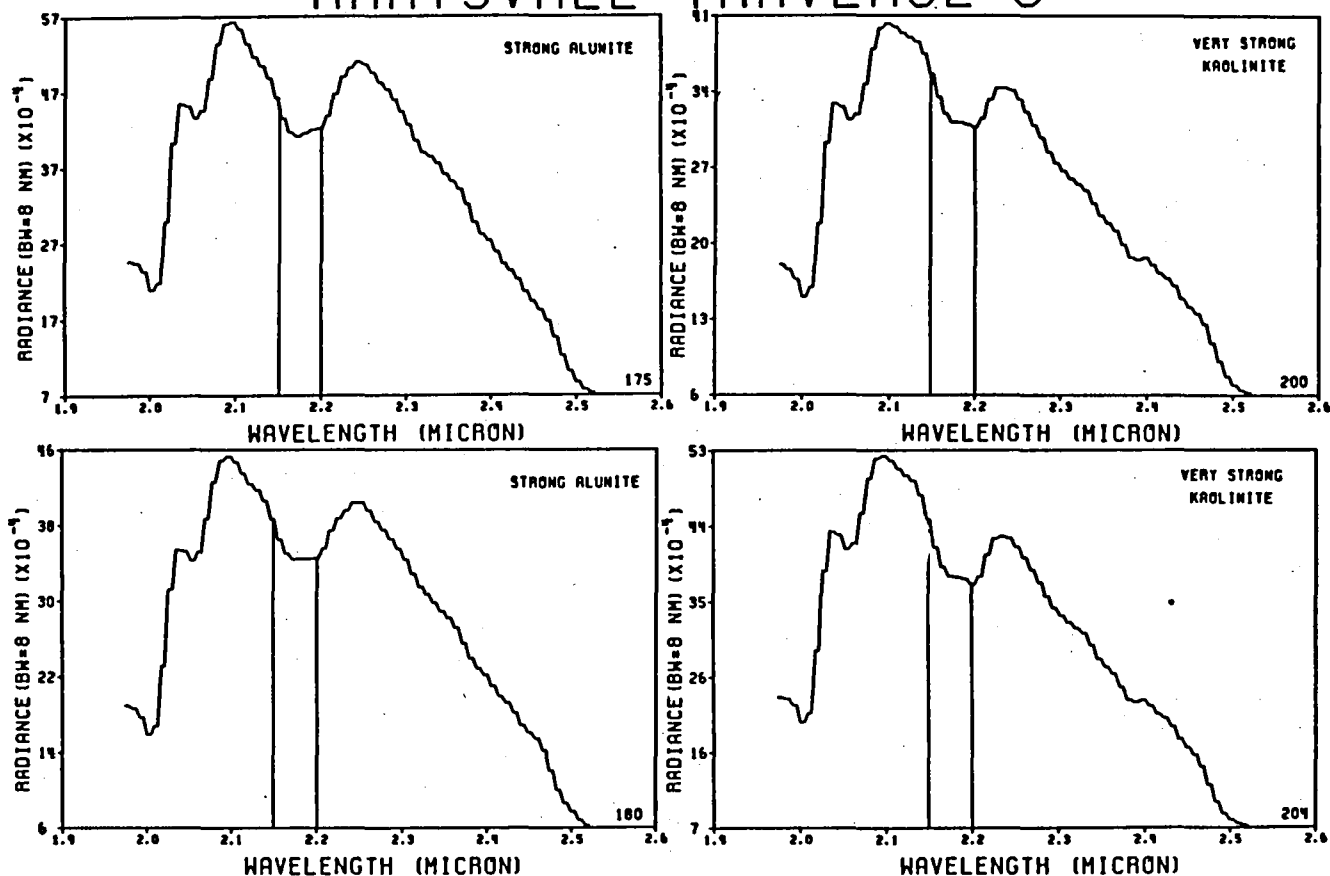


Figure 7. Spectra from the intensely altered zone of the central hydrothermal cell. The kaolinite and alunite bands are strongest in this zone. In addition to the minimum shift in the alunite band, there is a widening of the shoulder between 2.10 and 2.15 microns.

and is the southern most traverse at the southwestern corner of the hydrothermal cell.

The spectra in Figure 6 show a predominant strong doublet of mixed kaolinite and alunite. This area is mapped in orange (Figure 4) at the southeast edge of the hydrothermal cell. The traverse then passes into an area of strong kaolinite mapped in red. A spectrum from this zone is shown in Figure 6, measurement 140.

Traverse G crosses the eastern side of the intensely altered alunite zone (Figure 4) in the area of measurements 175 and 180. These spectra are shown in Figure 7. Near measurements 200 and 204, (Figure 7), the traverse crosses one of the zones in which the kaolinite bands are noticeably more intense than in other kaolinitic zones. These areas are mapped in yellow in Figure 1.

The infrared spectral features of the other traverses through the two large eastern cells are very consistent and similar to the spectral features shown for traverse G.

Outside of the two eastern cells, the spectral properties change markedly. The spectra in Figure 8 are from the background

AIRCRAFT INFRARED SPECTRA MARYSVALE TRAVERSE-9

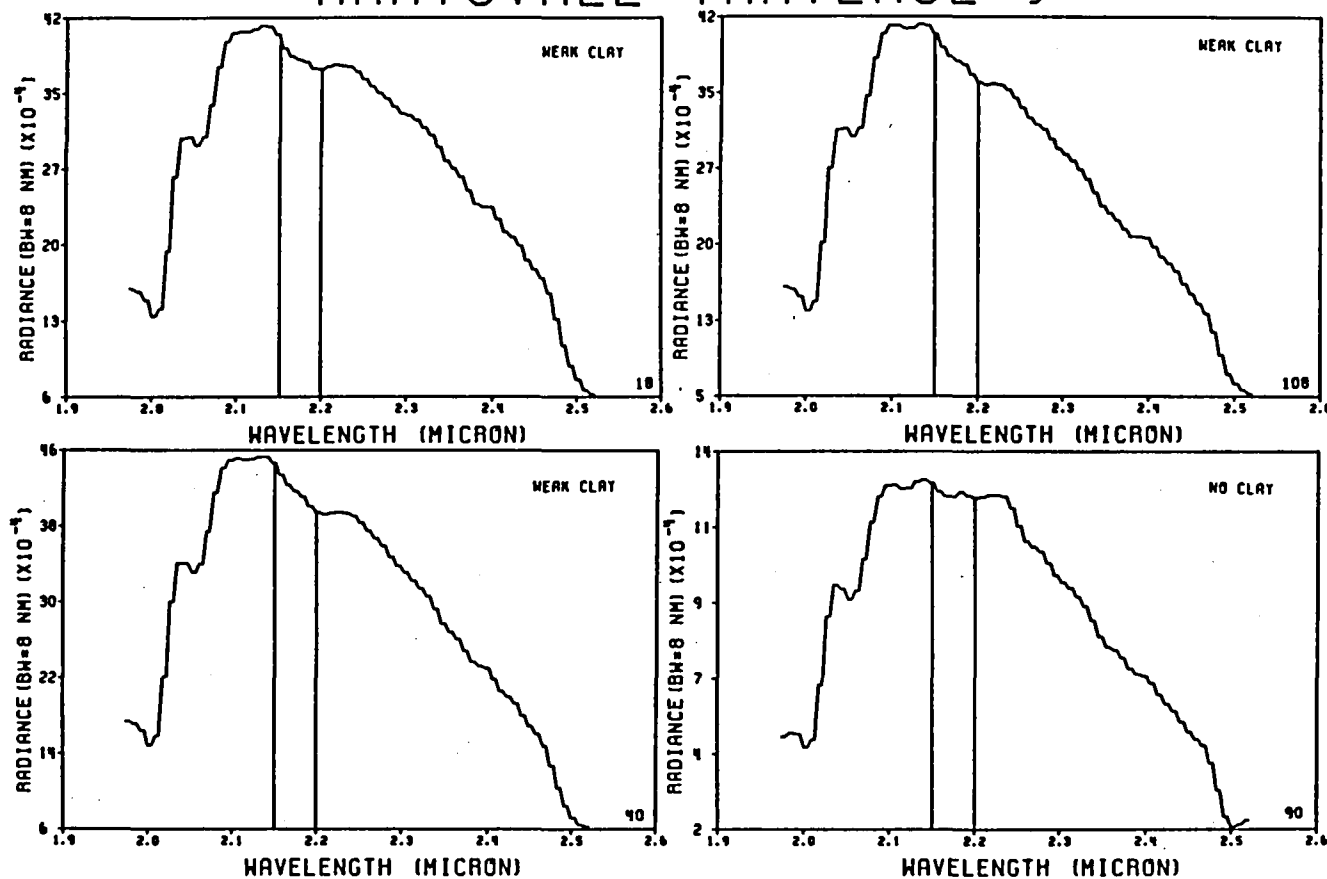


Figure 8. Spectra from the first half of traverse 9, which crosses background terrain of no alteration. The spectra show mostly very weak 2.2 micron clay bands.

area in the southern half of traverse 9. This area is mapped in blue in Figure 1. The spectral features in these areas are predominantly very weak clay bands. Spectrum 90 shows a strong shoulder at 2.25 microns and no clay bands.

The spectra in Figures 9 through 12 show a very different alteration pattern and mineralogy. These data are from the two smaller western hydrothermal cells. The mineralogy in these cells is very mixed, but mostly a clay mineral with a strong 2.21 feature that appears to be montmorillonite. The spectra in Figure 9 are from traverse 11 along the eastern section across the smaller alteration cell. The spectra show a mineral with strong absorption at 2.25 to 2.3 microns. Jarosite has a strong band in this region (Hunt, 1979). Ground measurements and sampling are required, however, to establish the correlation. This zone also shows some strong kaolinite (spectrum 18). Spectrum 21 shows the strong 2.21 micron feature of montmorillonite. In this spectrum the long wavelength shoulder is suppressed and there are weak features at 2.25 and 2.35 microns. This appears to be gypsum mineral mixed with the clay. Stronger gypsum can be seen in Figure 12. Figure 10 shows measurements along traverse 9 where it crosses traverse 10 at measurements 176 and 177. In this area there appears to be mixed strong jarosite and strong

AIRCRAFT INFRARED SPECTRA MARYSVALE TRAVERSE-11

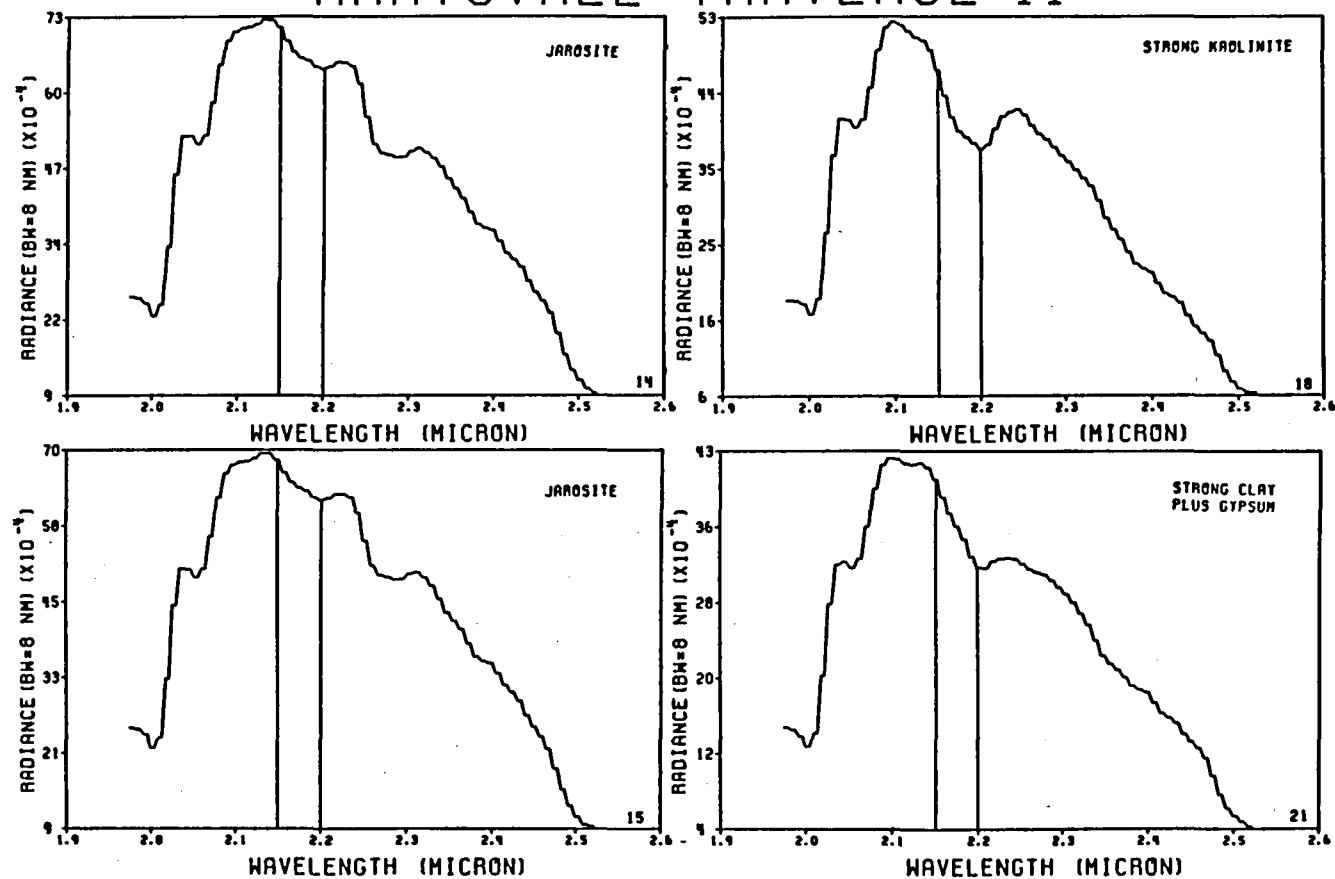


Figure 9. Spectra from the section of traverse 11 where it crosses the smaller of the two western alteration cells. This zone shows very mixed mineralogy.

AIRCRAFT INFRARED SPECTRA MARYSVALE TRAVERSE-9

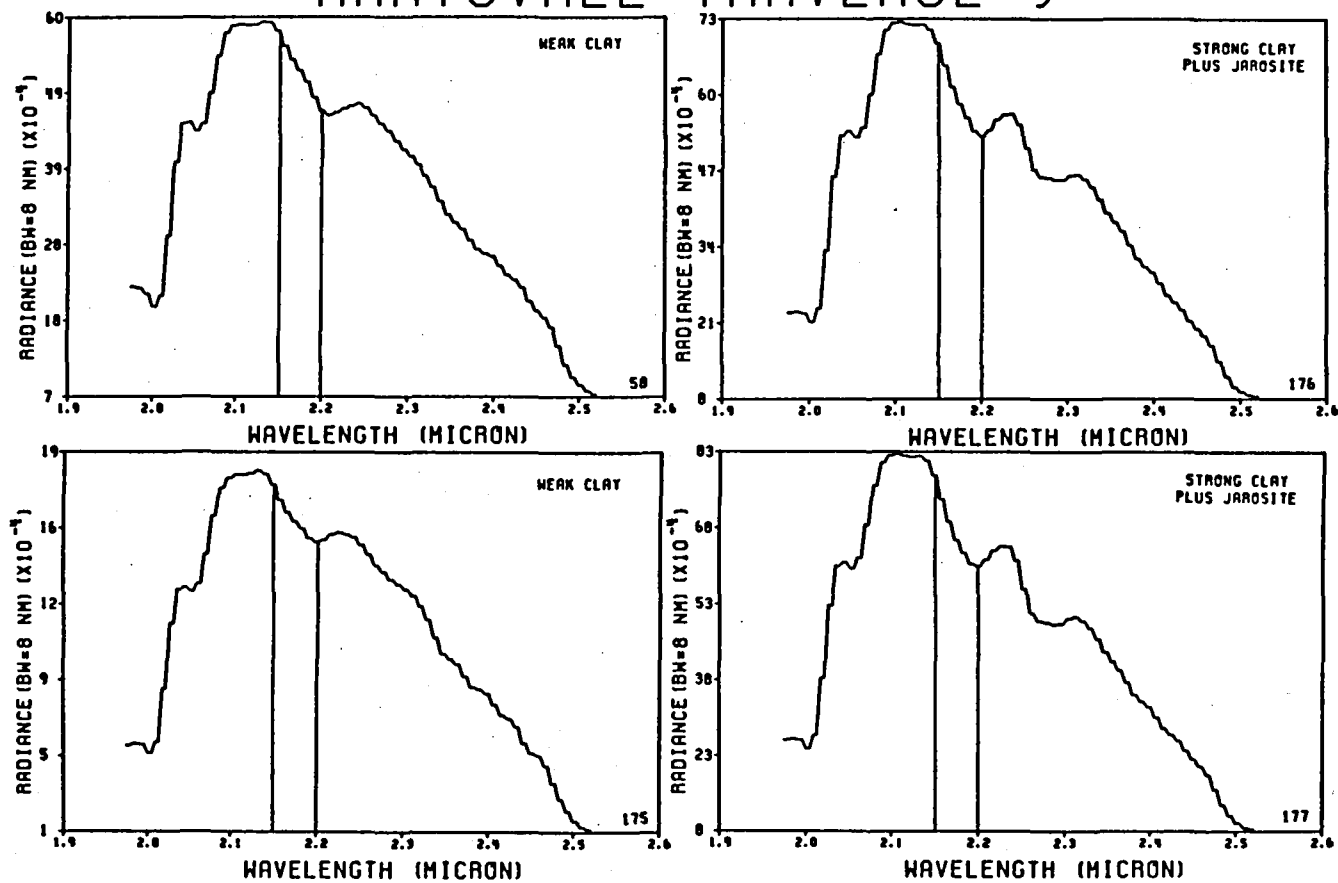


Figure 10. Spectra from traverse 9 where it crosses the smaller western alteration cell. Spectra 176 and 177 are from the area where this traverse crosses traverse 11. The spectra are similar to spectra 14 and 15 in Figure 9.

AIRCRAFT INFRARED SPECTRA MARYSVALE TRAVERSE-11

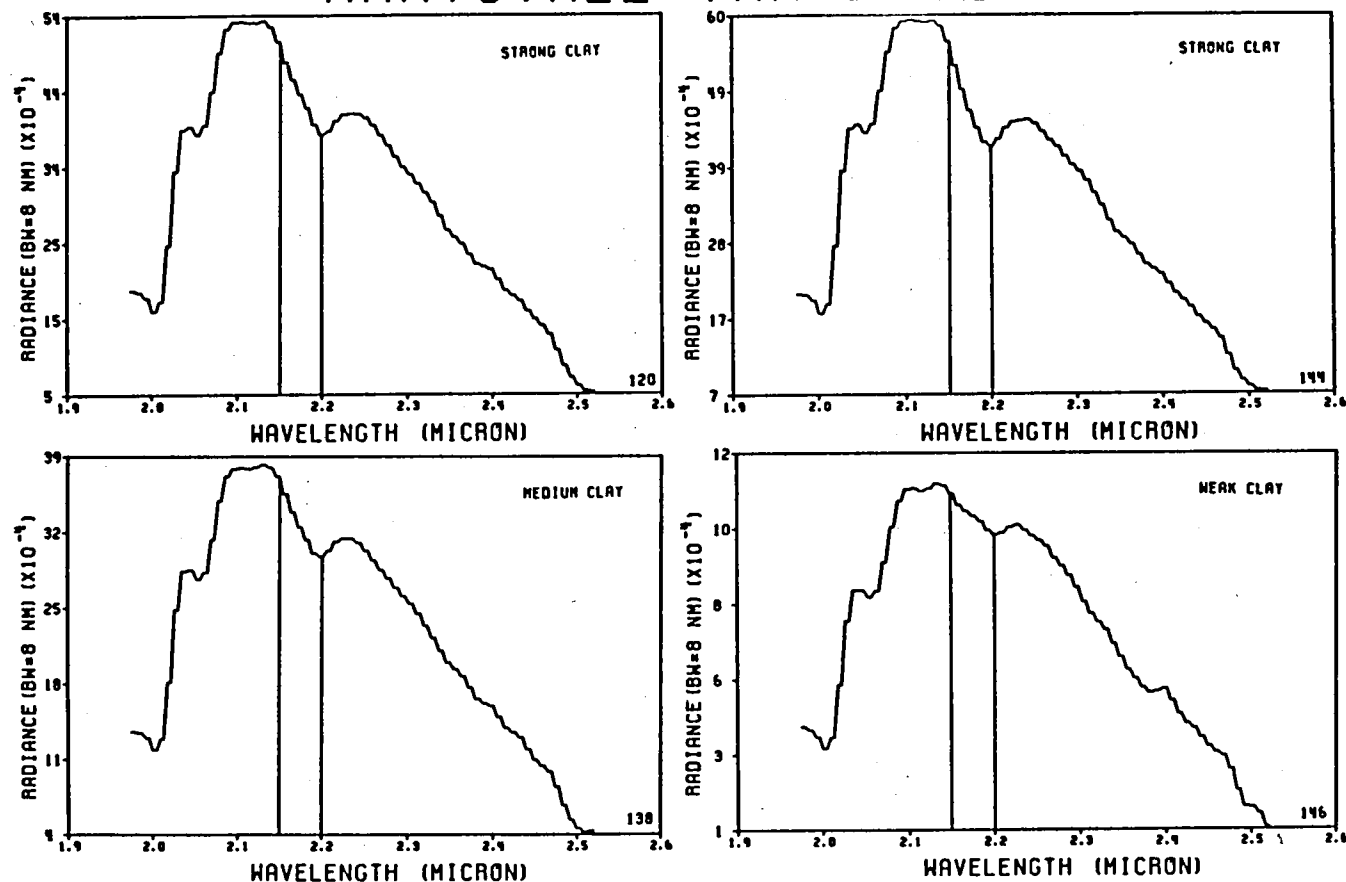


Figure 11. Spectra from the western section of traverse 11 where it crosses the western most alteration cell. The mineralogy appears to be uniformly montmorillonite clay.

AIRCRAFT INFRARED SPECTRA MARYSVALE TRAVERSE-12

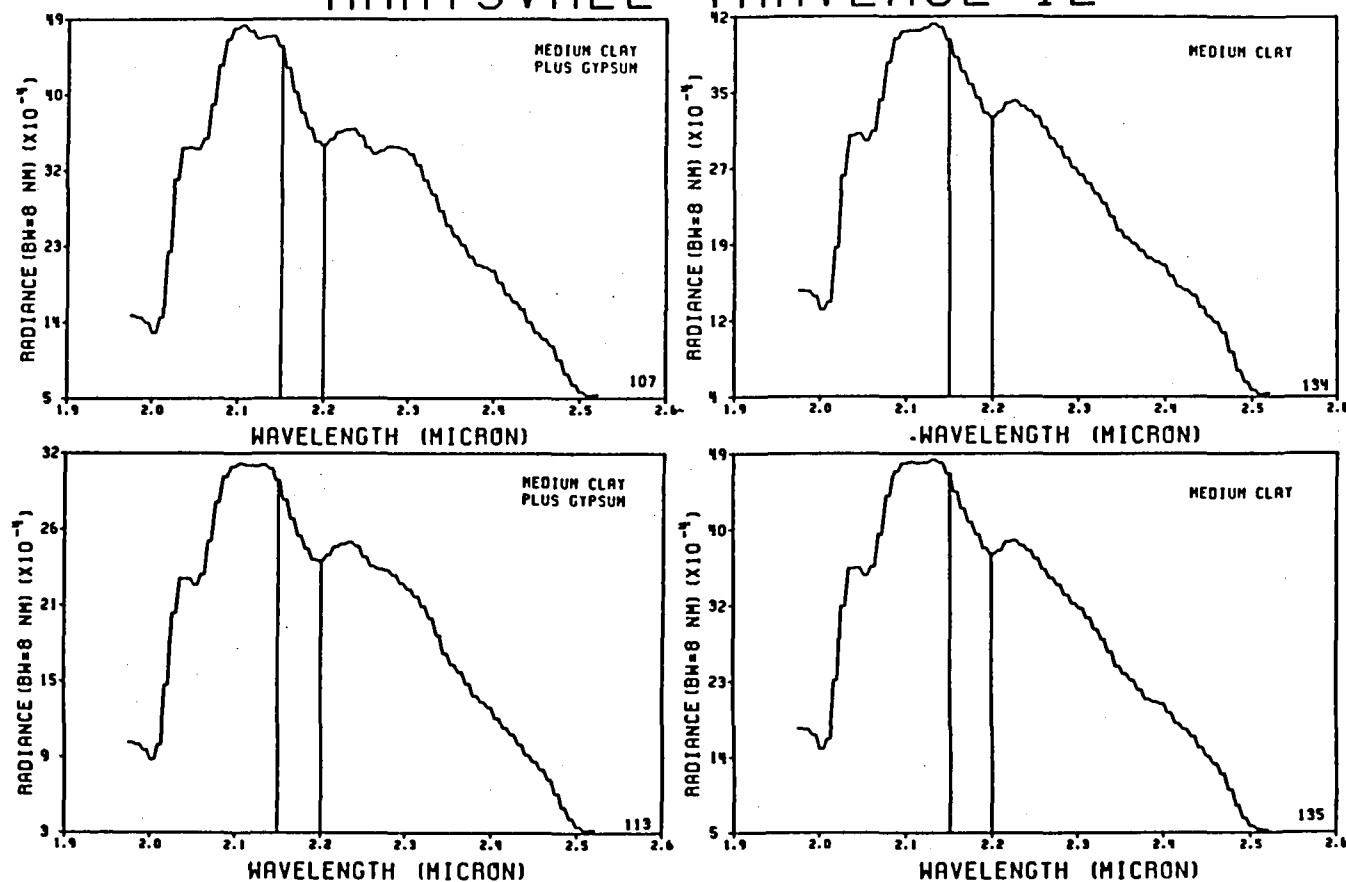


Figure 12. Spectra from the western section of traverse 11 where it crosses the western most alteration cell at the northern end. The mineralization appears to be uniformly montmorillonite clay with a mixture of gypsum.

montmorillonite. The smaller cell is characterized by a very mixed mineralogy including the montmorillonite clay and the "jarosite" mineral with the strong 2.25 to 2.30 micron bands.

Traverse 11 continues to the west where it crosses the center part of the western most alteration cell in the area of Big Rock Candy Mountain. This section is mapped as solid cherry red in Figure 4. Typical spectra from this section of traverse 11 are shown in Figure 11. The spectra show medium to strong 2.21 micron montmorillonite bands. The alteration intensity in this section is mapped as alternating medium to strong intensity in Figure 1. Spectrum 146 in Figure 11 shows the typical background signal where the traverse crosses out of the alteration zone.

Traverse 12 crosses the northern edge of the western most alteration cell. The spectra in Figure 12 show again quite uniform montmorillonite with some mixed gypsum. The northern half of this alteration cell is distinctive in showing uniformly medium to strong montmorillonite alteration.

The spectra in Figures 13 and 14 are from traverse 10(B) across the southern section of the western most alteration cell.

AIRCRAFT INFRARED SPECTRA MARYSVALE TRAVERSE-10 (B)

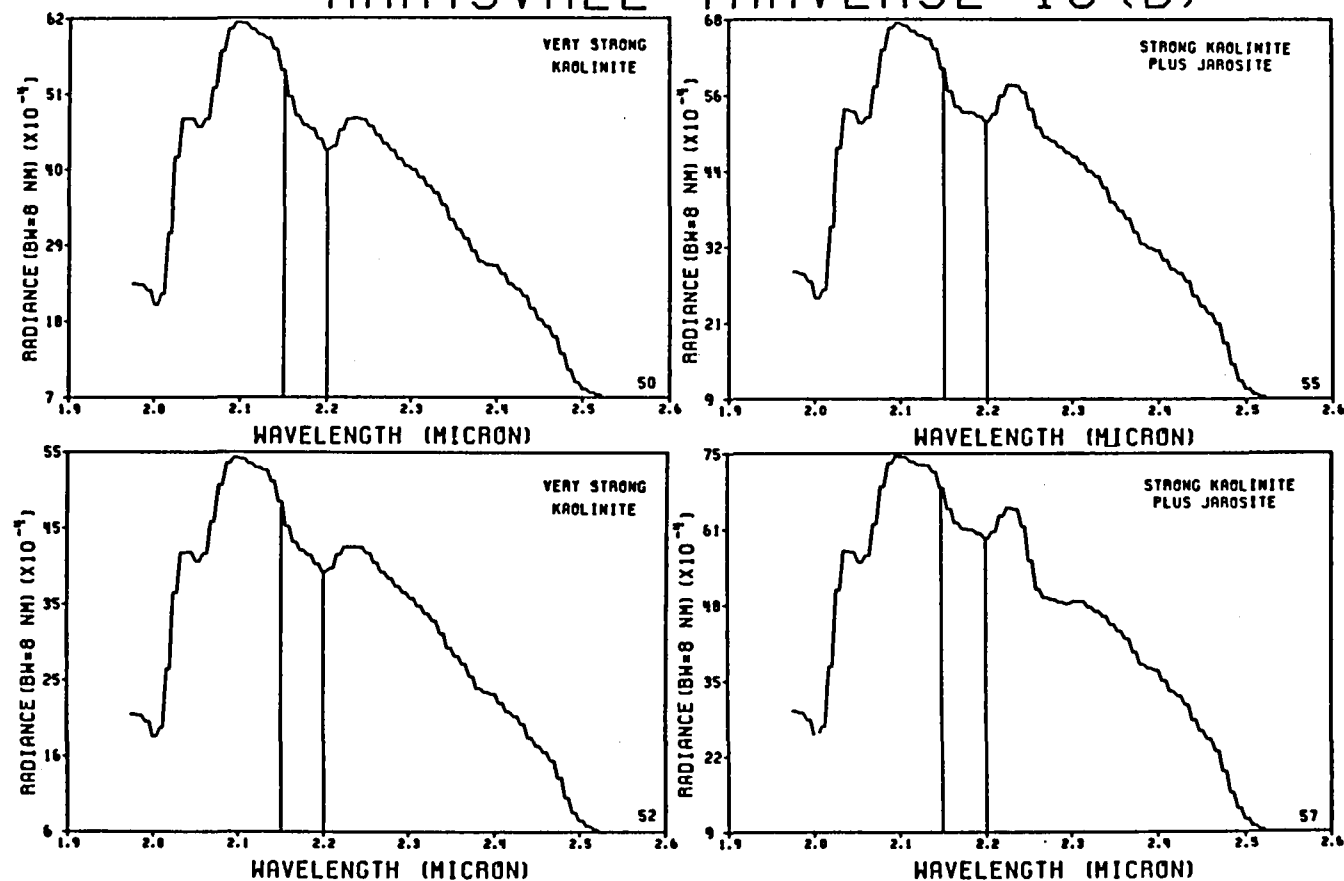


Figure 13. Spectra from the southern section of the western most alteration cell. The mineralogy in this zone is distinctly kaolinite with a mixture of the "jarosite like" mineral.

AIRCRAFT INFRARED SPECTRA MARYSVALE TRAVERSE-10 (B)

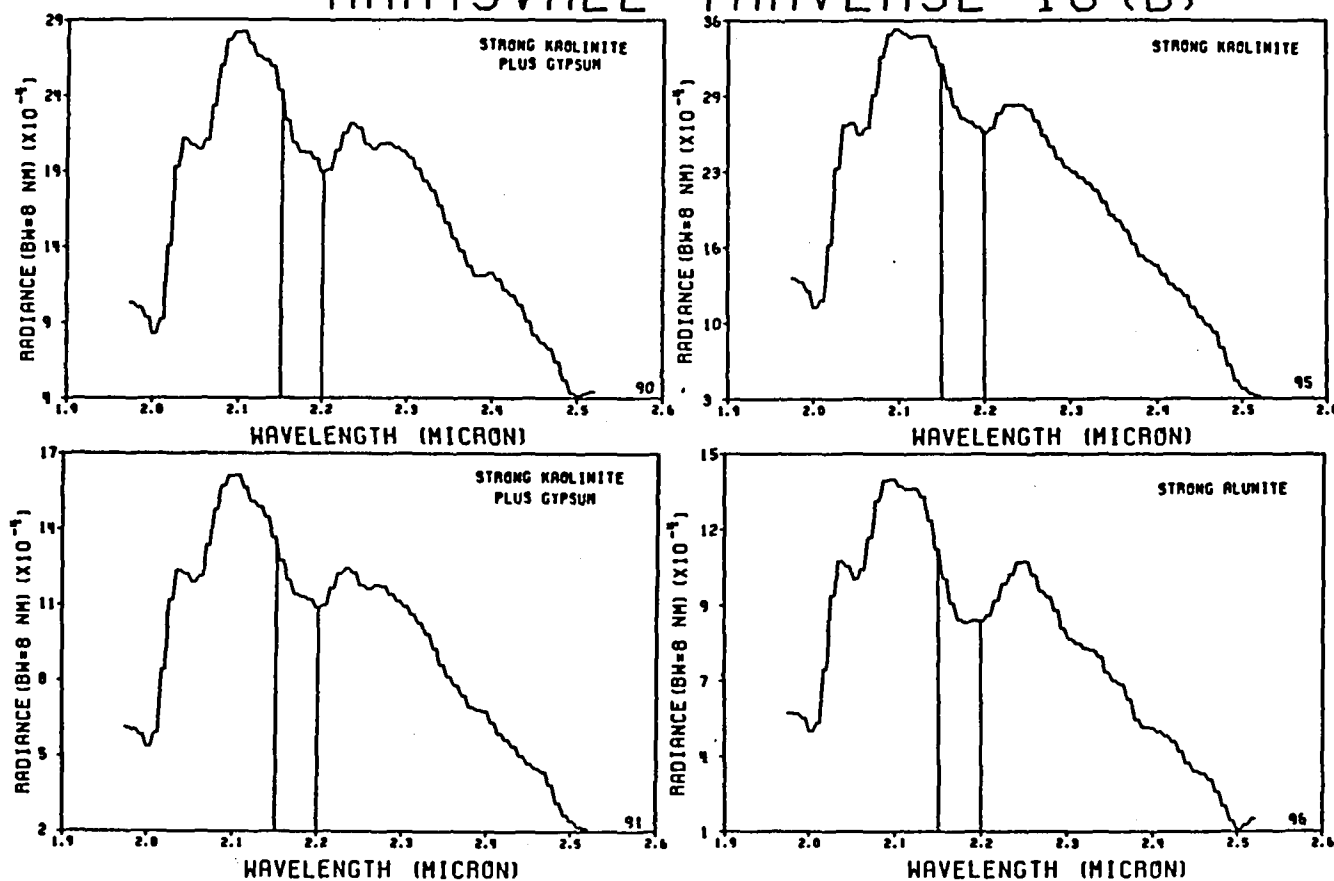


Figure 14. Spectra from the southern section of the western most alteration cell. The mineralogy is distinctly kaolinite with some alunite. A mixture of gypsum is present in some of the kaolinite areas.

This zone of the cell is distinctly different from the northern zone. There is no montmorillonite mineralization. The mineralization is predominantly very strong kaolinite with some very strong alunite. The gypsum and "jarosite like" spectral features are superimposed on some of the kaolinite spectra. The southern part of the cell, then, is a zone of kaolinite/alunite mineralization similar to the two eastern zones with the exception of gypsum and the "jarosite like" mineral mixture.

CONCLUSION

The airborne infrared spectroradiometer, at 8nm spectral bandwidth, functions very effectively in mapping the intensity and species of minerals with bands in the 2.0 to 2.5 micron region. The 8nm bandwidth is a critical factor in this application because it is near the lower limit of the natural bandwidths of the mineral features. With less spectral resolution, the capacity to identify specific minerals would rapidly disappear. Survey tests at 16nm bandwidth show that much of the resolution is already lost. At 8nm bandwidth, however, we achieve an optimum spectral resolution of the infrared mineral bands with still wide enough bandwidths to also achieve very good signal to noise ratio.

The survey over Marysvale shows that detailed airborne mineral mapping can be achieved rapidly over large areas. This type of mapping has been very difficult in the past using ground techniques. The airborne technique can substantially improve exploration effectiveness and reduce the costs and time involved in initial site evaluation and development.

EFFECTS OF SPATIAL RESOLUTION

Michael Abrams, JPL

I. Introduction

Studies of the effects of spatial resolution on extraction of geologic information are woefully lacking. This writer was unable to find even a single systematic, quantitative study bearing on this problem, though there has been a never-ending hue and cry for better spatial resolution. Figures of 10-30 m are often mentioned, with little substantive evidence to support these demands. However, pieces of various reports do have bearing on this subject, and they will be discussed as appropriate.

Spatial resolution effects can be examined as they influence two general categories: detection of spatial features per se; and the effects of IFOV on the definition of spectral signatures and on general mapping abilities.

II. Detection of Spatial Features

Mapping of lineaments and curvilinear features from remote sensing images has been one of the most widely pursued uses of these data. Lineaments can be manifestations of faults, fractures, and joints which may be of geologic significance. Or they may be caused by fortuitous topographic alignments or by a wide range of culturally-related phenomena, such as roads, fence lines, etc.

Lambert and others (1975) examined detectability of lineaments on Landsat images (80 m resolution), Skylab S190A photography (40 m resolution) and Skylab S190B photography (~20 m resolution) for the area of Alice Springs, Australia, and compared these to faults shown on a 1:250,000 scale geological map (Table 1).

Table 1. Number of faults identified

<u>Source</u>	<u>>10km</u>	<u><10km</u>	<u>Total</u>
Map	26	39	65
Landsat	48	26	74
S190A	48	4	52
S190B	72	71	143

Two to three times as many faults were identified from the 20 m data compared to the 40 or 80 m data. Similar results have been reported by other investigators.

The two features which are improved by better spatial resolution are:
1) detection of short lineaments, which may represent joint systems. Landsat data at 80 m do not have the necessary resolution to detect any but the grossest joint patterns; 2) fine structure of large lineaments which have

complex surface expression. Again, Landsat is inadequate for detecting these features. The Landsat Follow-on Working Group (Billingsley and others, 1976) concluded that the 30 m resolution of Landsat-D would provide a large improvement in the ability to map lineaments.

Mapping of geomorphic features is another area where spatial resolution is a critical factor. Billingsley and others (1976, p. III-17) reported that the threefold increase in resolution of Landsat-D compared to Landsats 1, 2 and 3 would "significantly improve the capability to map glacial (individual drumlins, isette lakes, eskers), fluvial (drainage boundaries, meanders, terraces, fans), desert (dune types) and permafrost (pingoes, polygonal ground) features, which are marginally observable or below the limits of detection on earlier Landsat imagery."

III. Definition of Spectral Signatures and Mapping Abilities

Measurement of spectral reflectance characteristics is accomplished at widely varying scales, ranging from laboratory analyses of 1 cm^2 powders or chips, to km size areas from orbital scanners. Conel (1982) examined the effects of spatial resolution at three different IFOV's: 1 cm^2 , 200 cm^2 , and 225 m^2 . Spectral reflectance curves for a variety of rock types in the 0.45 to $2.45 \text{ }\mu\text{m}$ region are shown in Figures 1 and 2. Figure 1 depicts hemispherical reflectance curves obtained in the laboratory for 1 cm^2 samples using a Beckman UV 5240 Spectrophotometer. Figure 2 depicts: a) the upper and lower range of Portable Field Reflectance Spectrometer (PFRS) in situ measurements. These spectra are normalized bi-directional reflectance measurements of a 200 cm^2 area on the ground; and b) image spectra from the NS-001 Thematic Mapper Simulator. These data were calibrated to reflectance using ground control measurements; the IFOV of the instrument is about 15 m (225 m^2 area). The laboratory measurements display sharp, well-defined absorption features characteristic of the samples' mineralogical composition. Cutler unbleached (#1), for example, has bands at 0.9, 1.4, 1.9, 2.2 and $2.35 \text{ }\mu\text{m}$ due to the presence of ferric iron, water, water, kaolinite, and carbonate respectively (confirmed by X-ray analyses). Besides the absorption features, the general shapes of the curves and overall brightnesses provide diagnostic information relating to composition.

Field acquired reflectance data for these same materials reveal several effects of increasing the IFOV of the measurement. The most obvious effect is the inclusion in the 200 cm^2 IFOV of a wider variety of materials than is represented by a tiny laboratory sample. In addition to rock materials, such materials as soil and vegetation contribute their spectral properties to the measured spectrum. Only rarely do the two measuring systems observe the same materials. A major effect is to reduce the intensity of absorption bands in many cases. There is a fair similarity between the Beckman and PFRS spectra for Wingate, bleached; Kayenta; and Upper Chinle Sandstone. Cutler Formation PFRS represents samples of both bleached and unbleached Beckman samples; Moss Back MBR, Chinle PFRS curves include the three types of Beckman Moss Back samples. PFRS curves show absorption bands at 2.35, 2.2, 0.9, and $0.65 \text{ }\mu\text{m}$. All of these features are seen in the Beckman curves, though not all are present in any individual curve. The effect of increasing the IFOV is to average and include a greater diversity of materials. In the PFRS curve for Navajo Sandstone, the $2.2 \text{ }\mu\text{m}$ band is not visible; the area sampled in the field included some dry vegetation and soil which tend to mask this feature.

Increasing the resolution one step further is crudely shown by the aircraft scanner image spectra on Figure 2. For most of the rock types, the image spectra fall within the range of PFRS values. The Cutler formation shows the effects of the inclusion of a significant vegetation component in the spectral signature - albedo is depressed and falls below the range of PFRS measurements, which excluded piñon-juniper prevalent on this rock type. Again the same types of effects are seen going from the ground (20 cm^2) to aircraft (225 m^2) as from laboratory (1 cm^2) to the ground. More heterogeneous materials are included in the field of view, contributing a mixture of spectral signatures to the reflectance measurements.

Mapping capability is probably the bottom line for remote sensing. Landsat data with 80 m IFOV are usable to produce maps equivalent to 1:250,000 geological maps. Landsat-D resolution (30 m) is expected to allow mapping at 1:100,000 scale (Billingsley and others, 1976). Systematic studies of resolution for mapping are scarce. Vincent of GeoSpectra Corp. used 7.5 m IFOV aircraft scanner data to produce spatial resolution simulations of different IFOV's. An area near Knoxville, Tennessee was overflowed, and false color infrared composites were produced. Figure 3 shows: (1) quick-look 7.5 m data, (2) 10 m, (3) 20 m, (4) 30 m, (5) 40m, and (6) 80 m simulations. It is instructive to examine the appearance of small roads, houses, fields, and treed areas as a function of spatial resolution. At 10 m they are all visible. At 20 m, there is little loss of detail. At 30 m, small streets are less clear, individual houses can no longer be resolved; fields and treed areas are still distinct and boundaries between them are still detectable. At 40 m only the larger streets are detectable; houses are unrecognizable; field boundaries are starting to break down, though some are visible. At 80 m, individual fields are no longer detectable; only the largest roads and building complexes are discernible.

Abrams and Brown (1982) compared Landsat data to high resolution aircraft scanner data over the Silver Bell copper deposit in Arizona; the scanner data were acquired at 12 m resolution, and were then degraded via computer processing to 30 m and 80 m resolution. Figure 4 shows the same strip of area for: (1) 12 m scanner ratio composite data, (b) 30 m degradation, (c) 80 m degradation, (d) Landsat 80 m false color infrared composite, and (e) Landsat ratio composite. At 12 m resolution, small drainages, cross-cutting dikes and roads on the dump are visible. At 30 m these features are barely visible; and by 80 m, they are indistinguishable. The detail visible on the degraded 80 m resolution aircraft scanner image is the same as on the Landsat image.

At about 1:125,000 scale, the 80 m data appears grainy, as the individual pixels are about 0.5 mm in size. At 1:50,000 scale, the pixels are about 1.5 mm each, and the images start to become unusable due to the appearance of grain due to the large pixel size.

The 30 m data at 1:50,000 scale is similar in appearance to the 80 m data at 1:125,000 scale: the pixels are starting to be discernible. At higher enlargements, no additional information is visible; the pixels merely get larger.

This little exercise, perhaps provides some quantitative feel for the useful scale of various resolutions; i.e., digital data can be displayed at a scale of 1500 X the IFOV in meters. With sophisticated image processing, this can probably be increased by a factor of 2.

IV. Recommendations for Future Work

It is obvious that there is a crying need for detailed, systematic studies of effects of spatial resolution on information extraction. These studies should be conducted over a wide variety of geological terrains, and examine a range of problems. The field of geology encompasses many subdisciplines, each of which has its own requirements for the scale of information necessary to address key problems. Global or continental tectonics needs data at scales on the order of $1:10 \times 10^6$. Geological mapping is done at various scales, from 1:250,000 to 1:2,000. Resolution requirements are grossly different: 50-100 m may be adequate for small scale mapping; ~1 m resolution for detailed mapping. Therefore, the requirements are to a large extent problem or site specific. Nevertheless, detailed studies of the effect of decreasing resolution on information content should be done.

Similarly, the effects of resolution on spectral signatures should be systematically studied. One experiment would be to examine a heterogeneous area, measuring spectral reflectance at increasingly larger FOV's (Perhaps using the PFRS in a helicopter). Characterizing the resulting mixed signatures and developing satisfactory methods for estimating components would be fruitful.

REFERENCES

- Abrams, M., and Brown, D, 1982, "The Silver Bell Porphyry Copper Test Site Report" in the Joint NASA/Geosat Test Case Study, JPL publication, Pasadena, CA, in preparation.
- Billingsley, F., Helton, M., O'Brien, V., 1976, "Landsat Follow-on: A Report by the Application Survey Groups", JPL Technical Memorandum 33-803, Pasadena, CA.
- Conel, J., 1982, "Lisbon Valley Uranium Test Site Report", in Joint NASA/Geosat Test Case Study, JPL Report, Pasadena, CA, in preparation.
- Lambert, B., Benson, C., et al., 1975, "A Study of the Usefulness of Skylab EREP Data for Earth Resources Studies in Australia", NASA CR-144493, Washington, D.C.

EFFECT OF ALUMINUM SUBSTITUTION ON THE REFLECTANCE SPECTRA OF HEMATITE

Richard V. Morris¹, Howard V. Lauer, Jr.², and Wendell W. Mendell¹

¹ Code SN7, NASA/Johnson Space Center, Houston, TX 77058

² Lockheed Engineering and Management Services Co., Houston, TX 77058

INTRODUCTION

Terrestrial remote sensing makes extensive use of multispectral imagery. Geologic units or terrains frequently are found to be delineated in false color representations or band ratio images. Generally, ground truth is required to identify dominant minerals and rock types in a particular unit. In some cases, regional rock types are known, and spectral units can be correlated with known spectra from laboratory experiments.

Iron oxides and oxyhydroxides are a class of minerals important in remote sensing applications. Spectra of supposedly pure iron oxides and oxyhydroxides are prevalent in the literature, although usually the compounds studied are not well-characterized as to chemical purity, particle size and shape, and other factors which may affect their spectral behavior. In addition to pure compounds, it is also important to know the extent impurity-ion substitution in these minerals affects their spectral properties. In the natural environment, aluminum substitution for ferric iron is likely to occur. Sommer and Buckingham (1981) report that the near-IR crystal field band of hematite and goethite shifts to longer wavelengths with aluminum substitution. On the other hand, Evans and Adams (1980) concluded that aluminum content does not have a significant effect on the reflectance spectra of synthetic gels containing ferric iron and aluminum. We report here some results of our study of the changes in the spectral properties of hematite due to aluminum substitution.

EXPERIMENTAL

Our approach was to conduct parallel synthesis of hematite and aluminous hematite under nominally the same conditions so that in as much as possible, aluminum content was the only variant in the starting materials and procedures. Briefly, two solutions were prepared from iron and aluminum sulfate salts; one had Al/Fe = 0 and the other Al/Fe = 0.25. Addition of excess base caused a precipitate to form. After repeated washings with neutral water, they were hydrolyzed in neutral water at ~100°C. The precipitates were again washed, then dried in air, and finally heated in air at ~560°C.

The diffuse reflectance spectra were recorded on a Cary-14 configured with a 9-inch diameter integrating sphere.

RESULTS AND DISCUSSION

The diffuse reflectance spectra of the two powders are shown in the

EFFECT OF ALUMINUM SUBSTITUTION...

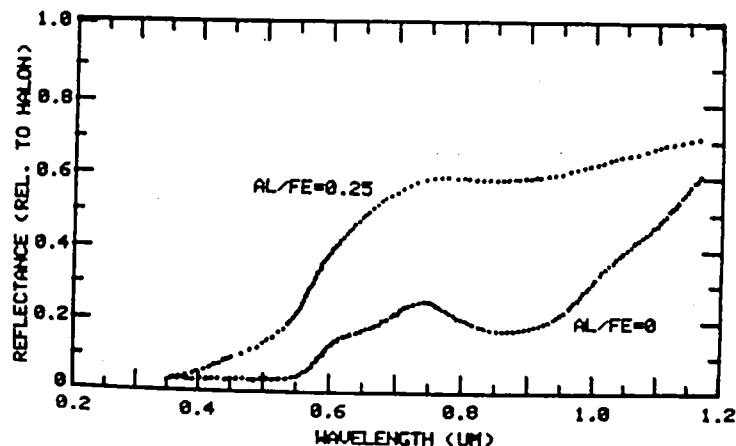
Morris, R.V. et al.

figure for the region between 0.35 and 1.20 μm ; they are labeled according to the Al/Fe ratio. They are very different in their spectral signatures; visually, the Al/Fe = 0 powder is a very dark red while the Al/Fe = 0.25 powder is tan. The spectral features for the Al/Fe = 0 powder correspond to those for hematite, and X-ray diffraction confirms this phase. The near-IR based minimum for the Al/Fe = 0.25 powder is shifted longward by about 0.02 μm and is much more shallow; this powder is amorphous to X-rays so we cannot confirm the phase by this method. The longward shift of the band minimum is in agreement with Sommer and Buckingham (1981). The Al/Fe = 0.25 powder is considerably more reflective shortward of $\sim 0.55 \mu\text{m}$ where the Al/Fe = 0 powder is very strongly absorbing. This is important since the visible slope and the red shoulder are often used in the construction of false color and band ratio images.

In conclusion, our studies confirm the findings of Sommer and Buckingham (1981) that the reflectance spectrum of hematite can be modified (very strongly for our case) by aluminum substitution. Thus, the aluminum content of target media should also be considered as a variable in the interpretation of their spectral properties.

REFERENCES

- Evans D. L. and Adams J. B. (1980) Amorphous gels as possible analogs to martian weathering products. Proc. Lunar Planet. Sci. Conf. 11th, 757-763.
- Sommer S. E. and Buckingham W. F. (1981) The role of geological surfaces in determining visible-near infra red spectral signatures. IEEE IGARSS, June 8-10, Washington, D. C., 603-607.



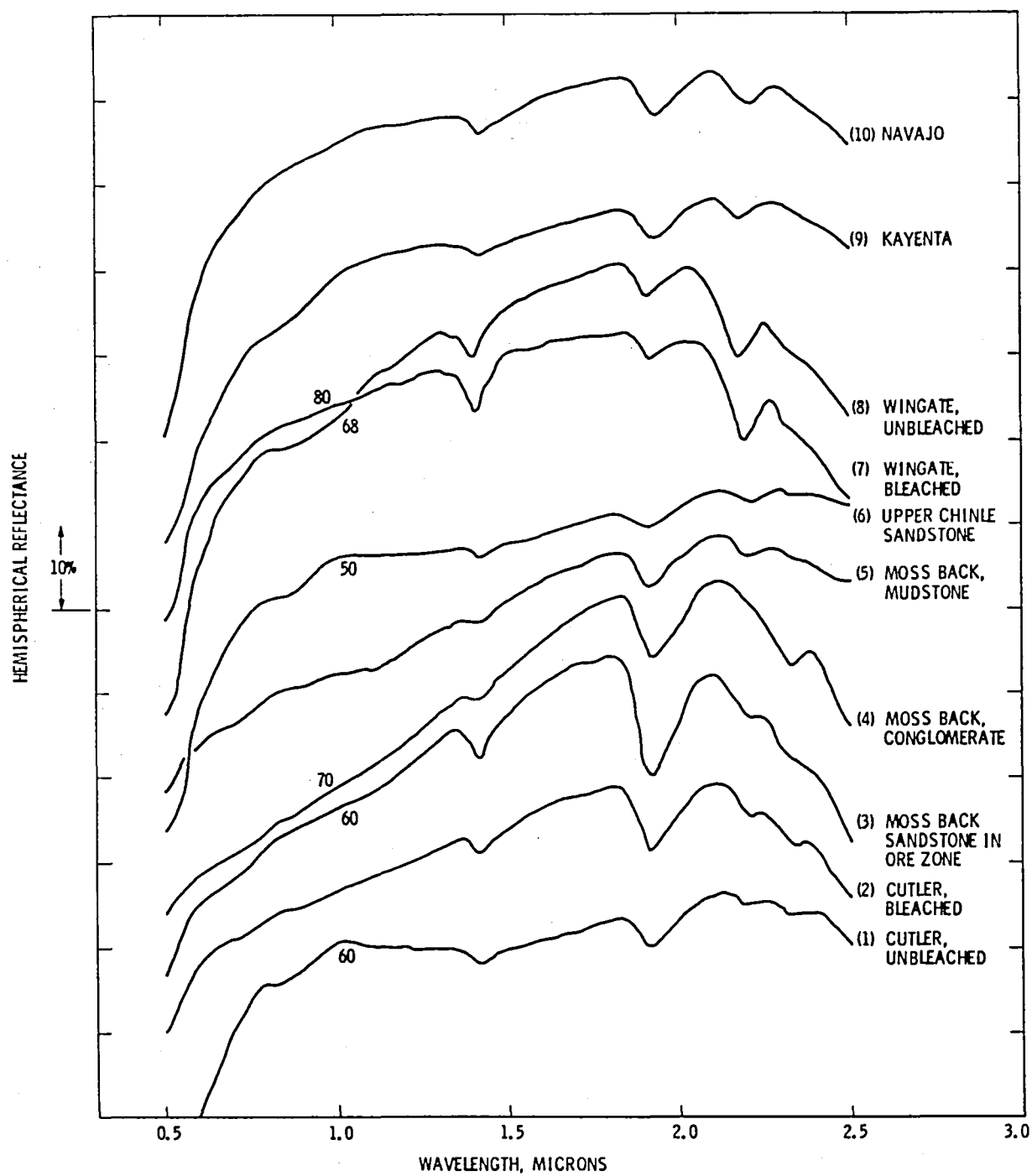


Figure 1

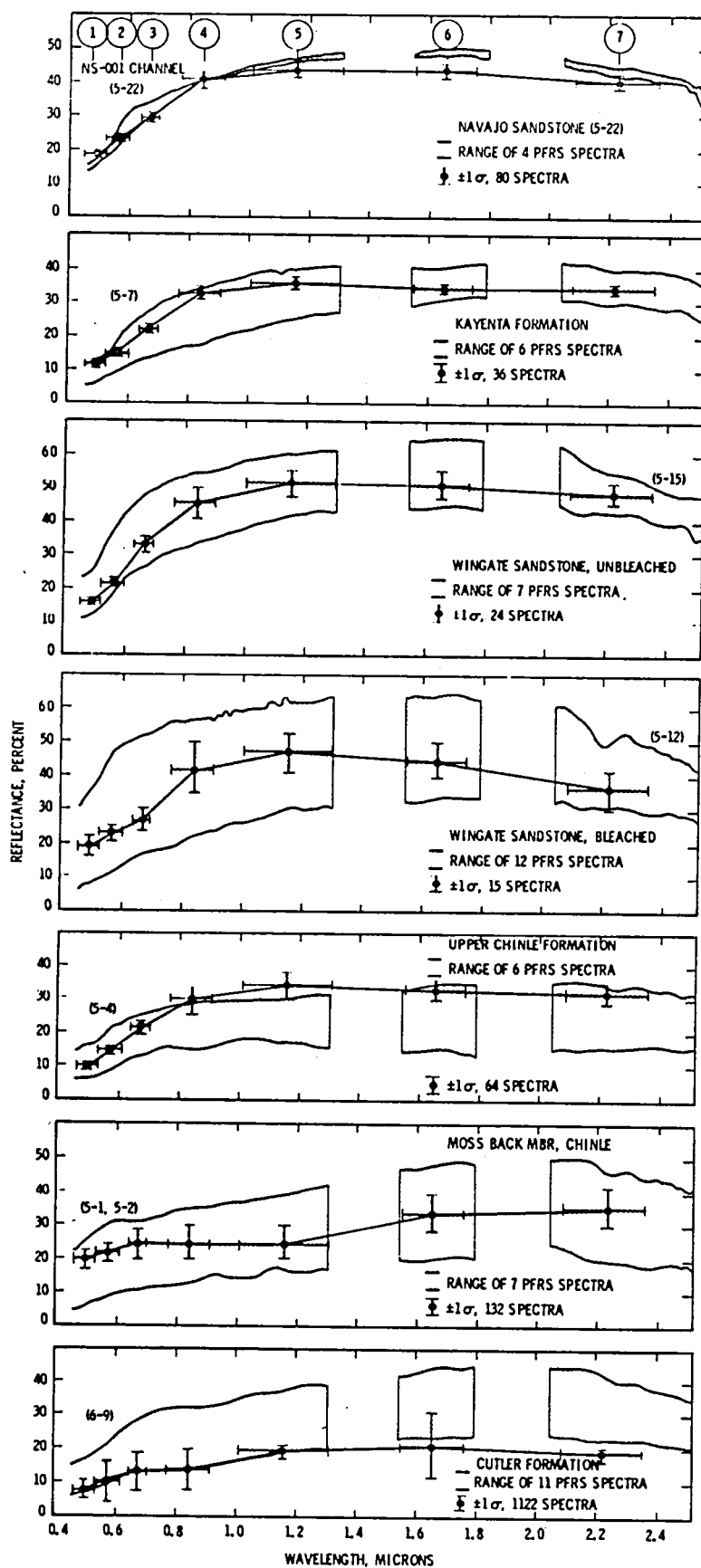


Figure 2

VISIBLE AND NEAR-IR SPECTRAL REFLECTANCE OF GEOLOGICALLY IMPORTANT MATERIALS

A SHORT REVIEW.

Robert B. Singer

Planetary Geosciences
Hawaii Institute of Geophysics
2525 Correa Rd.
Honolulu, HI 98822

INTRODUCTION

A number of extensive surveys of the reflectance properties of geologically interesting materials exist in the literature. The purpose of this paper is to provide a short review and to serve as a resource for readers interested in further details. Excellent review papers have been written by Adams (1975) and Hunt (1977). A library of reflectance spectra of many phases was published in a series of papers by Hunt and Salisbury (1970, 1971) and Hunt et al. (1971, 1973a,b,c, 1974). While the utility of these data is somewhat limited by the lack of chemical and/or other characterizations of the samples, this series of papers provides a good starting point for more detailed studies. Spectra obtained in the field of plutonic igneous rocks have been published by Blom et al. (1980). Burns (1970) and Burns and Vaughan (1975) provide detailed discussion of some of the physical mechanisms which control spectral reflectance.

A note of caution is appropriate at this point: the researchers referenced above obtained their data using different equipment, illumination geometries, and sample preparations. A discussion of some grain size and geometry effects is provided by Adams and Felice (1967). In general the measurements of Adams are diffuse reflectance of powders, those of Hunt and his co-workers are bidirectional reflectance of powders, those of Blom et al. are bidirectional reflectance of natural rock surfaces, and those of Burns are mainly transmission of polarized light

through oriented crystals. The relationships among data taken in these various ways are not totally understood, and must be considered for each application.

SOURCES OF SPECTRAL FEATURES

1) Charge Transfers and Conduction Bands.

A charge-transfer feature is generated when incident radiation is of the proper energy (wavelength) to cause an electron to hop between neighboring ions. Common ion pairs include $\text{Fe}^{3+} \rightarrow \text{O}^{2-}$ and $\text{Fe}^{3+} \rightarrow \text{Fe}^{2+}$. Absorption bands of the former are centered in the near-U.V. (relatively high energy) and are quite intense, while the latter occur between 0.55 and 0.80 μm (somewhat lower energies) and are less intense (Burns et al., 1976).

For some materials, particularly semiconductors, visible or near-IR photons have enough energy to boost electrons into a conduction band, where they are no longer bound to a specific ion. Sulphur and sulphur compounds are examples. They have a steep absorption edge in the visible, with high reflectance at longer wavelengths (lower energies) and strong absorption at shorter wavelengths (higher energies).

2) Crystal Field Absorptions.

Crystal field absorptions are intralelectronic events in which anion electrons are excited into a higher energy orbital by incident radiation. Orbital energy levels

are modified by electrostatic repulsion from the surrounding anions. Different crystal structures, with varied cation site symmetries and cation-anion distances, have different "crystal fields" which control the location, strength, and width of the absorption bands. Most important crystal-field absorptions are due to elements in the first transition series, most notably ferrous iron, in somewhat distorted octahedral coordination with oxygen. Many of the Fe^{2+} crystal field bands are relatively broad and occur near $1\ \mu\text{m}$. A detailed discussion of mineralogic applications of crystal field theory is provided by Burns (1970).

3) Vibrational absorptions.

Stretching and bending vibrations of molecular bonds have discrete excitation energies, corresponding to specific wavelengths of radiation. This fundamental mode for most bonds of geologic interest (Si, Al, Mg to oxygen) occurs at wavelengths beyond the near-infrared, with overtone absorptions too weak to observe in this spectral region. While the fundamentals for OH (near $2.75\ \mu\text{m}$) and H_2O (near 3 and $6\ \mu\text{m}$) are also beyond this region, various overtones and combinations can be prominent in the near-IR. Overtones and combination vibrations of the C-O bond are also seen in the near-IR for carbonate minerals. These various absorptions will be discussed further in the context of specific minerals. An excellent discussion of vibrational spectral features can be found in Hunt (1977).

DISCUSSION BY MINERAL GROUP

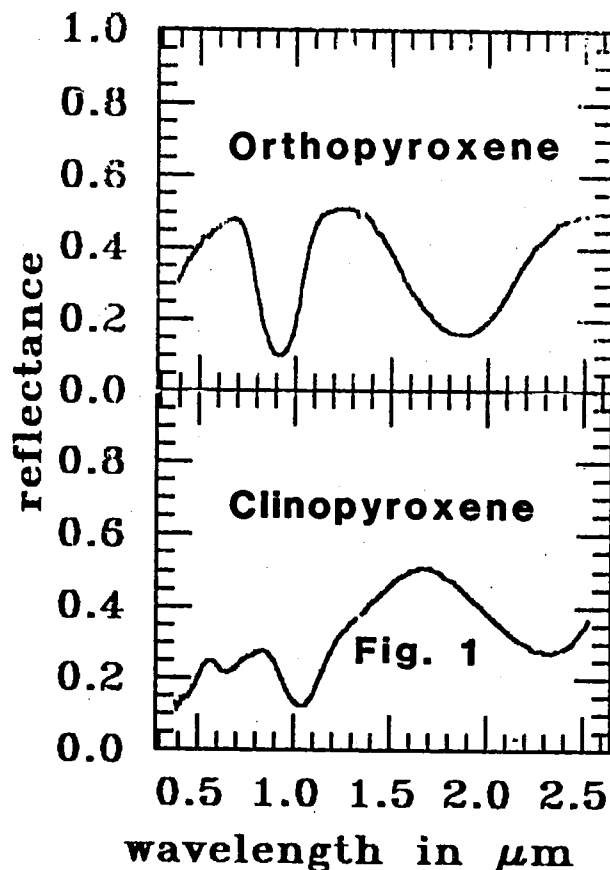
Examples of reflectance spectra of various mineral groups are presented here. Unless otherwise noted, spectra are of particulate samples observed with a bidirectional instrument.

1) Pyroxenes

The prominent spectral characteristic of most pyroxenes is the occurrence of two ferrous iron crystal-field absorptions, one near $1\ \mu\text{m}$ and the other near $2\ \mu\text{m}$.

Adams (1974) demonstrated a strong empirical relationship between center position of these two bands and pyroxene composition. Cations occur in pyroxene in 6-fold coordination with oxygen in two separate mineralogic sites: a relatively undistorted site (M1) and a more highly distorted site (M2).

Figure 1a shows the spectrum of an orthopyroxene in the hypersthene range, En_{88} (Singer, 1981). The two major bands are centered near 0.92 and $1.87\ \mu\text{m}$. The Fe^{2+} preferentially occupies the more distorted (and thermodynamically more stable) M2 sites (Burns, 1970). With increasing iron content in orthopyroxenes

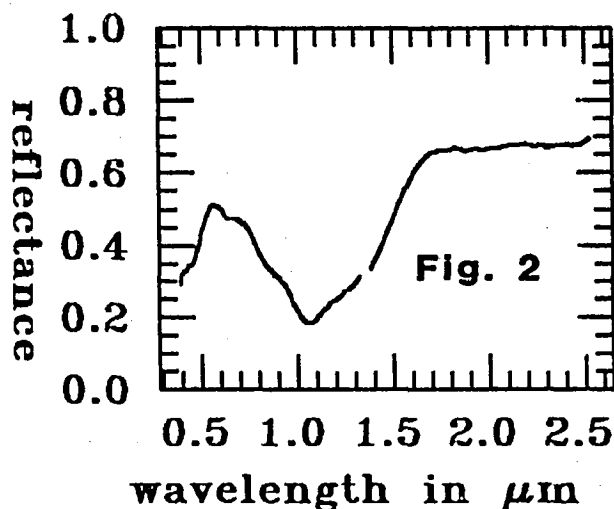


both absorptions shift to longer wavelengths. The reflectance dropoff from the red to the U.V. is most likely caused by $\text{Fe}^{2+} \rightarrow \text{O}^{2-}$ charge transfers. The narrow, weak bands superimposed on this slope are spin-forbidden Fe^{2+} crystal-field absorptions.

The spectrum of a diopsidic-augite clinopyroxene ($\text{Wo}_{41}\text{En}_{51}\text{Fs}_8$) is shown in Figure 1b (Singer, 1981). The sample contains small amounts of Al, Ti, and Fe^{3+} . The two prominent crystal-field absorptions are centered near 1.03 and 2.31 μm , consistent with the Adams (1974) relationship. Clinopyroxenes have cation sites analogous to orthopyroxenes, but Ca^{2+} preferentially fills the more distorted M2 sites, increasing the occupancy of the less distorted M1 sites by Fe^{2+} . These changes and the modified crystal structure account for the occurrence of clinopyroxene absorptions at longer wavelengths than for orthopyroxene and cause a different dependence of band location on composition (Burns et al., 1972; Adams, 1975). The shallower band located near 0.65 μm is probably either an $\text{Fe}^{2+} \rightarrow \text{Fe}^{3+}$ charge transfer or a crystal-field absorption caused by a small amount of chromium.

2) Olivine

The spectrum of an olivine with composition Fo_{85} is shown in Figure 2. The three overlapping Fe^{3+} crystal-field absorptions, located at 0.86, 1.06, and 1.33 μm , are diagnostic for this mineral. The weaker side bands appear as shoulders on the more intense central absorption. Assignments of these components to specific crystallographic sites and electronic transitions is



vis abs refl olv01 t=0 c 1/27/82
ir abs refl olv01 t=0 c 1/28/82

provided by Burns (1970). With increasingly fayalitic composition all three absorptions shift to slightly longer wavelengths and increase in depth, with a larger proportional increase of the shoulders, leading to an overall broadening of the absorption envelope, especially on the long wavelength side (Burns, 1970; Hunt and Salisbury, 1970; Adams, 1975).

3) Phyllosilicates

The distinguishing characteristics of layered silicates are relatively sharp, asymmetric bands in the near-IR caused by structural OH and often molecular H_2O . As discussed above these are overtones and combinations of stretching and bending vibrational modes which have fundamentals further in the infrared. Absorptions near 1.9 μm are due to a combination of the H-O-H bend and the asymmetric O-H stretch, and are therefore indicative of adsorbed molecular water. Absorptions in the 1.4 μm region arise from O-H stretch in molecular water and/or structural OH. Band in the 2.2 - 2.4 μm region are attributed to combination overtones of structural OH stretches with lattice modes, and therefore are dependent on the cation present. For di-octahedral clay minerals (Al^{3+} bearing) a band occurs near 2.2 μm , with a weaker band frequently present near 2.3 μm . For tri-octahedral minerals (Mg^{2+} bearing) analogous absorptions appear near 2.3 and 2.4 μm .

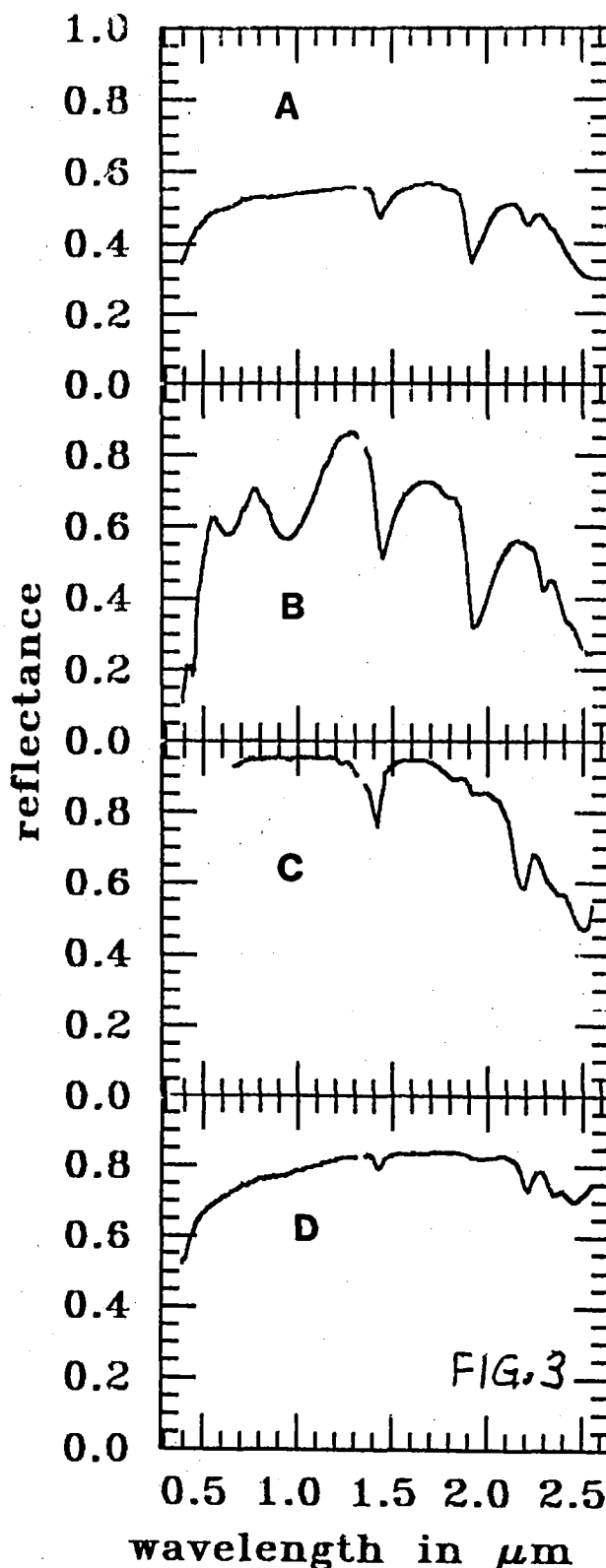
Figure 3a is the spectrum of a montmorillonite (a di-octahedral smectite clay). Smectites generally contain a large amount of physically adsorbed molecular H_2O in interlayer sites, and therefore have a prominent absorption near 1.9 μm . The band near 1.4 μm arises from both this molecular water and the structural OH in the clay structure. The weaker band near 2.22 μm is due to the Al - OH combination mode discussed above. The reflectance falloff towards longer wavelengths is the wing of more intense water absorptions further in the infrared. The very weak structure and reflectance dropoff in the very near-IR and the visible is due to a few percent ferric iron in this sample.

The spectrum of a tri-octahedral smectite with Fe^{3+} substituting for most of the Al^{3+} , known as nontronite, is shown in Figure 3b. The 1.4 and 1.9 μm bands are the same as discussed above. The longer wavelength band is shifted slightly compared to the montmorillonite, to 2.3 μm , because of the change in cation in coordination with the structural OH. The three bands at 0.44, 0.63, and 0.95 μm are crystal-field absorptions of the ferric iron, and the steep slope in the visible is caused by $\text{Fe}^{3+} \rightarrow \text{O}^{2-}$ charge transfers.

The spectrum of kaolinite, a non-smectite di-octahedral clay, is shown in Figure 3c. Like montmorillonite this mineral has aluminum in octahedral coordination with oxygen and hydroxyl, but lacks the interlayer water sites of the smectites. Accordingly, kaolinite displays characteristic OH and Al-OH bands near 1.4 and 2.2 μm , but lacks a well developed molecular water band near 1.9 μm . The weak band at this location is caused by physical adsorption of a small amount molecular water to the fine-grained clay particles.

Figure 3d shows the spectrum of serpentinite, the tri-octahedral (Mg^{2+} bearing) analog of kaolinite. Like kaolinite it displays OH absorptions at near 1.4 and beyond 2.2 μm , but has only a very weak signature of physically adsorbed water. The spectrum in the 2.2 to 2.5 μm region is somewhat complicated, showing at least three distinct bands; I have not studied this sample in great enough detail to propose an explanation.

Minerals in the mica family generally show OH absorptions near 2.2 μm and beyond, and sometimes also the 1.4 μm OH band, although Adams (1975) suggests that sometimes iron absorptions are intense enough to mask the 1.4 μm band. The molecular water absorption at 1.9 μm is absent or very weak.



4) Amphiboles

Amphiboles are hydroxylated double chain minerals somewhat analogous to the pyroxenes (single chain, non-hydroxylated). The general shape of the spectrum is often low in the visible and very near-IR due to iron absorptions, with a dramatic increase in reflectance to a spectrum peak near 1.8 to 2.0 μm . The 1.4 μm OH band is sometimes visible, apparently largely masked by the iron absorptions. A double or single absorption due to the combination of hydroxyl stretching modes and lattice modes is generally prominent at 2.3 to 2.4 μm . This family of minerals has not been studied in detail by our research group. The reader is referred to Hunt and Salisbury (1970) and Adams (1975) for examples and more in-depth discussion.

5) Feldspars

While pure feldspars are spectrally very neutral, naturally occurring samples generally exhibit spectral features due to trace amounts of Fe^{2+} or Fe^{3+} , as well as liquid water inclusions. Generally K-spar accepts Fe^{3+} substitution in aluminum sites, while plagioclase more readily accommodates Fe^{2+} in calcium sites (Adams, 1975). Examples are shown in Figure 5, which was copied from Adams (1975). Trace Fe^{2+} gives plagioclase a broad absorption in the 1.1 to 1.3 μm region. There is an apparent relationship between the position of this absorption band and the albite/anorthite ratio of the plagioclase. K-spars tend to show a weak band at 0.86 μm and a relatively sharp absorption edge in the visible, both caused by trace Fe^{3+} (Adams, 1975). Because of the great transparency of most feldspars, these features are generally masked in mixtures with other minerals; the Fe^{2+} plagioclase band is often visible as a weak shoulder on the long-wavelength side of the 1 μm pyroxene band in basaltic assemblages, if there is no olivine present to hide the feldspar signature.

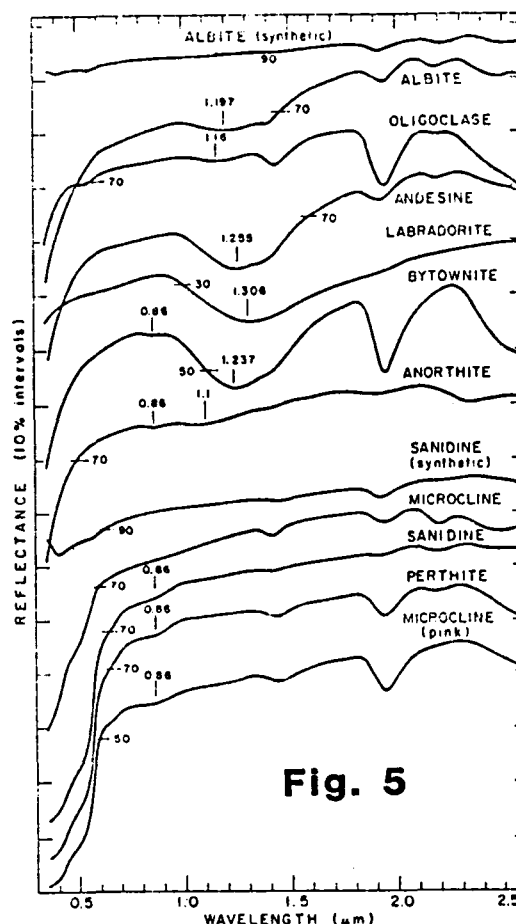


Fig. 5

6) Oxides and Hydroxides

Iron oxides and hydroxides are ubiquitous on earth and are a major source of color in rocks and soils. A few of the more common types are reviewed here.

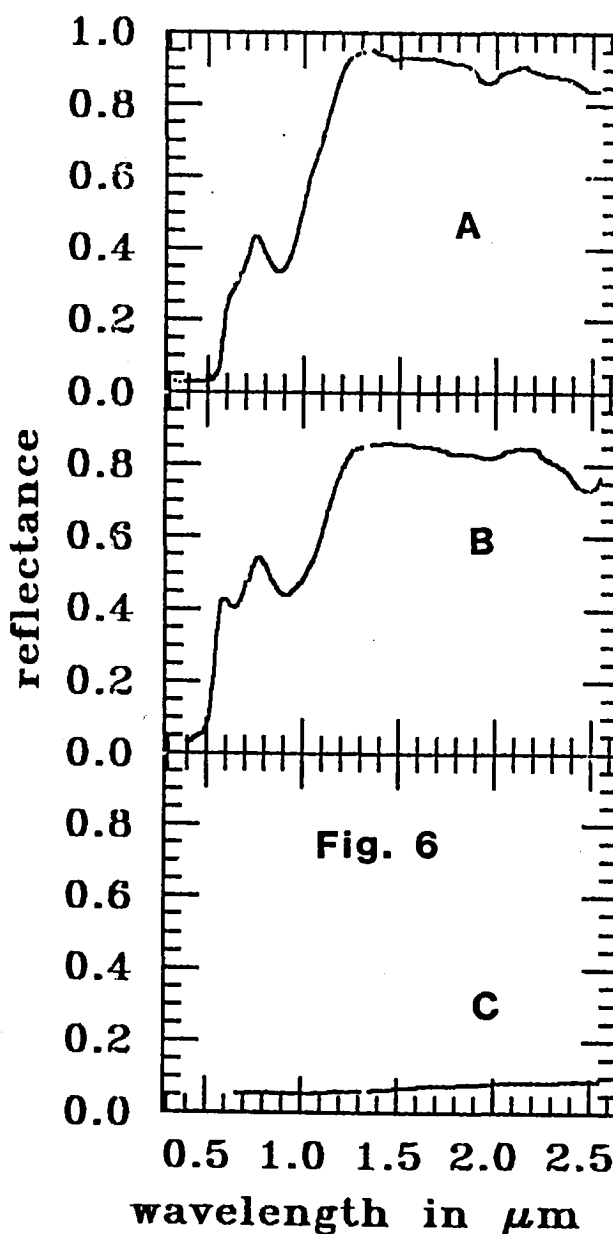
Hematite, $\alpha\text{Fe}_2\text{O}_3$, (Figure 6a) has Fe^{3+} ions in octahedral coordination with oxygen. Goethite, αFeOOH , (Figure 6b) also has Fe^{3+} in octahedral coordination, although with different site distortions and oxygen ligands (OH^-), resulting in a different crystal field. Common to all reflectance spectra of fine-grained ferric oxides is strong absorption in the visible region coupled with rather high reflectance in the near infrared. The greatest contributors to this visible absorption are a pair of $\text{Fe}^{3+} \rightarrow \text{O}^{2-}$ charge-transfers centered in the near UV at 0.34 and 0.40 μm (Loefer et al., 1974).

Both hematite and goethite display band saturation at and below $0.4\ \mu\text{m}$. The long wavelength band edge of the charge-transfers extends through the visible and into the very near infrared. Superimposed on this band edge are spin-forbidden crystal-field absorptions of Fe^{3+} . Depending on the relative positions and strengths some of these absorptions appear as shoulders or inflections on other band edges. There is a sharp unresolved doublet located at $0.53\ \mu\text{m}$ in hematite and $0.45\ \mu\text{m}$ in goethite. The long wavelength position of this absorption in hematite coupled with the strong charge transfer lead to a distinctive flat low reflectance profile throughout most of the visible, accounting for the intense red coloration. In goethite this crystal-field absorption occurs at a shorter wavelength and with less intensity, leading to the characteristic yellow to orange color. A second crystal-field absorption occurs for crystalline ferric oxides centered near 0.62 to $0.64\ \mu\text{m}$. In pure goethite this band is well defined; for hematite it appears only as a shoulder superimposed on the edge of the combined bands discussed above. A third crystal-field band produces a reflectance minimum at wavelengths as short as $0.86\ \mu\text{m}$ for hematite to $0.89\ \mu\text{m}$ or longer for goethite.

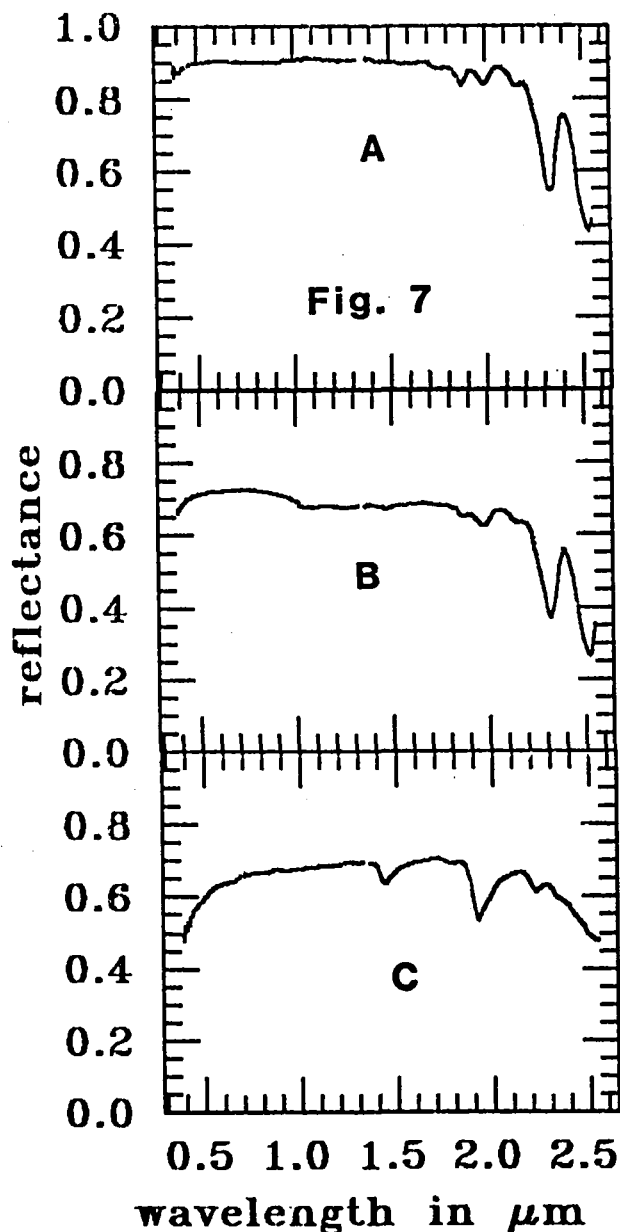
Magnetite, Fe_3O_4 , (Figure 6c) is very opaque but does exhibit a shallow, broad absorption near $1\ \mu\text{m}$ and a general increase in reflectance with increasing wavelength. The $1\ \mu\text{m}$ band has been attributed to ferrous iron, while the continuum optical absorption has been attributed to high rate very intense charge transfers between Fe^{3+} and Fe^{2+} (Adams, 1975). The effect of opaque minerals in mixtures with other minerals will be discussed later.

7) Carbonates.

The spectral properties of carbonates are discussed in some detail by Hunt and Salisbury (1971). In this spectral region the observed absorptions occur longward of about $1.6\ \mu\text{m}$ and are overtones or combinations of various modes of the CO_3^{2-} ion. As demonstrated by Figure 7a, a calcite spectrum, and Figure 7b, a dolomite,



the strongest absorption occurs at a wavelength of about $2.55\ \mu\text{m}$, while the next strongest is centered near $2.35\ \mu\text{m}$. A number of additional weaker overtones occur at shorter wavelengths. An ongoing research project in our group is to investigate the systematics and uniqueness of carbonate absorption features. The calcite and dolomite examples presented here, for instance, are distinguishable by slight differences in the wavelengths of the



vibrational features. Both these samples show little absorption in the visible, which indicates that they are relatively free of color producing contaminants such as iron.

Figure 7c is the spectrum of a half-and-half mixture of fine grained calcite and montmorillonite. It can be seen that in this particular mixture the clay spectral features mask most of the carbonate bands. Mixtures using coarser carbonate grains retain the features of both phases,

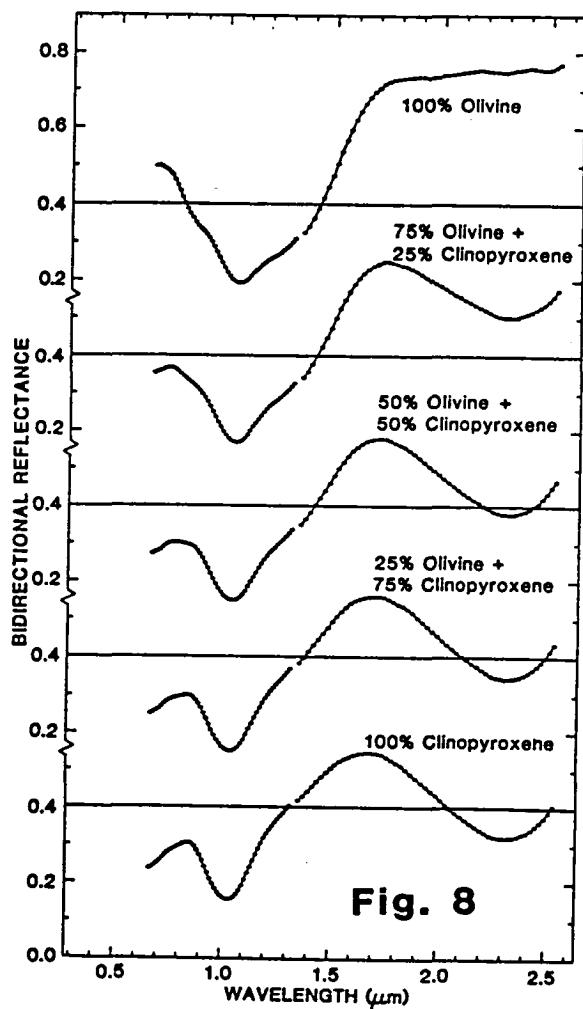
but interpretation is still not straightforward. The deconvolution of clay and carbonate features is another area of emphasis in our current research.

MIXTURES OF MINERALS

Large scale mixing of multiple spectral components, where discrete patches of surface materials are centimeter size or larger, can be accurately treated with a simple additive or "checkerboard" model (Singer and McCord, 1979). However, intimate mixtures of several mineral components produce a net reflectance spectrum that is considerably more complicated than a simple additive or multiplicative combination of individual spectral characteristics. Investigations of lunar analog mixtures (pyroxene, plagioclase, and an opaque) have been published by Pieters (1973) and Nash and Conel (1974). Examples of laboratory mineral combinations involving two pyroxenes and a pyroxene and olivine have been presented by Adams (1974, 1975). Some discussion of qualitative and quantitative analysis of spectra for mineral mixtures is also provided by Adams (1974, 1975), Gaffey (1978), and Gaffey and McFadden (1977). More recently Singer (1981) presented results for laboratory mixtures of pyroxenes, olivine, and iron oxides. A few representative examples will be reviewed here.

Figure 8 shows the results of a series of weight-percent mixtures of the olivine and the clinopyroxene discussed earlier in this paper. The maximum band depth or contrast in the spectral reflectance of powders occurs when the grain size is about one optical depth (Adams and Felice, 1967). Here the overall more opaque clinopyroxene is closer to that condition than is the olivine, and therefore the spectra of mixtures are dominated by pyroxene characteristics. Because the band minima near $1 \mu\text{m}$ for these two minerals are close, there is little change in the locations of the mixture band minima. The shape and width of the total absorption envelope, however, change dramatically as

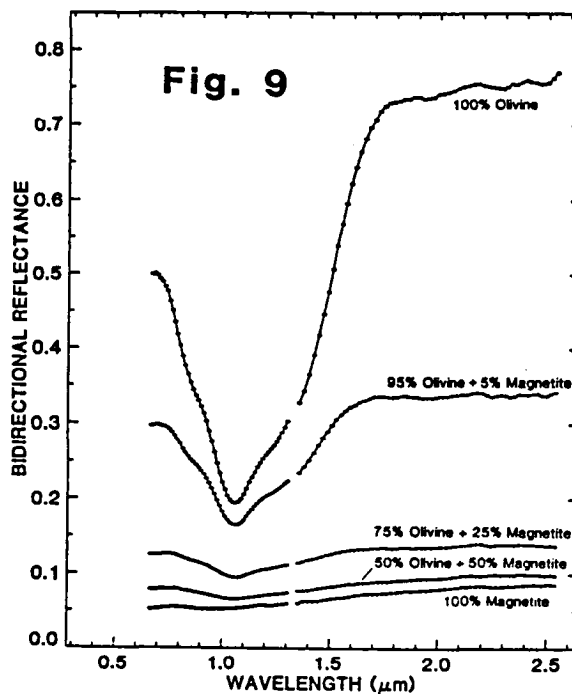
the olivine sidebands are masked by increasing pyroxene content. With pyroxene contents of 50% and greater the main indication of olivine is the depression or shoulder centered near $1.3\ \mu\text{m}$.



An example of a mixture with an opaque phase is demonstrated in Figures 9 and 10. The albedo and spectral contrast of olivine is lowered drastically by admixture of even a small amount of magnetite. However, as shown in Figure 10, the characteristic olivine spectral shape is recognizable even in a half-and-half mixture. This behavior, which holds for pyroxenes, clays, and other phases with diagnostic spectral features, demonstrates the desirability of high precision and low noise in remotely sensed data.

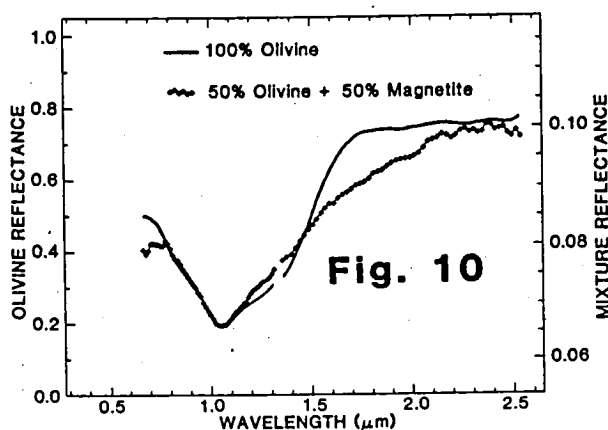
Theoretical modeling of the spectral properties of mineral mixtures has advanced substantially in the last year or two. Johnson (1982) has developed a computational scheme, based on the reflectance theory published by Hapke (1981), which yields reasonable approximations to the measurements of Singer (1981). At this stage the model works somewhat better for materials of similar extinction coefficients, such as olivine and pyroxene, than it does when one component is an opaque, such as olivine and magnetite.

Another mixing geometry that is routinely encountered in the field is that of surface weathering or coatings on rocks. This problem is currently being investigated for application to Mars as well as the earth. Initial work shows that thin colored coatings, such as those bearing Fe^{3+} , exhibit wavelength dependent transmission and do not completely hide the spectral characteristics of the underlying rock (Evans et al., 1981; Singer, 1982). Laboratory work is now in progress to facilitate more quantitative modeling of this reflectance geometry.



PRIORITIES FOR THE FUTURE

At present laboratory investigations of mineral and rock spectral behavior, while incomplete, outstrip our ability to make high quality remote observations in the real world. This is not to say that there isn't need for continuing laboratory research; I would, however, suggest two



complementary research directions which could over the next few years greatly enhance our abilities in geologic remote sensing:

- 1) Perhaps the most important laboratory research now is to refine our qualitative and especially our quantitative models of how mineral signatures combine to produce "real-world" spectral properties. This work is essential to the sophisticated capabilities for which we are all striving.

- 2) More on the technological side, we need to refine our remote observing techniques in terms of more complete spectral coverage, higher spectral resolution, better data precision, and more accurate calibration and atmospheric correction.

REFERENCES

Adams, J.B., Visible and near-infrared diffuse reflectance spectra of pyroxenes as applied to remote sensing of solid objects in the solar system, *J. Geophys. Res.*, 79, 4329-4336, 1974.

Adams, J.B., Interpretation of visible and near-infrared diffuse reflectance spectra of pyroxenes and other rock forming minerals, in *Infrared and Raman Spectroscopy of Lunar and Terrestrial Minerals*, edited by C. Karr, Jr., Academic, New York, 91-116, 1975.

Adams, J.B., and A.L. Felice, Spectral reflectance 0.4 to 2.0 microns of silicate rock powders, *J. Geophys. Res.*, 72 5705-5715, 1967.

Blom, R.G., M.J. Abrams, and H.G. Adams, Spectral reflectance and discrimination of plutonic rocks in the 0.45 to 2.45 micron region, *J. Geophys. Res.*, 85, 2638-2648, 1980.

Burns, R.G., *Mineralogical Applications of Crystal-Field Theory*, Cambridge University Press, New York, 1970.

Burns, R.G., R.M. Abu-Eid, and F.E. Huggins, Crystal field spectra of lunar pyroxenes, *Proc. Lunar Sci. Conf. 3rd*, 1, 533-543, 1972.

Burns, R.G., and D.J. Vaughan, Polarized electronic spectra, in *Infrared and Raman Spectroscopy of Lunar and Terrestrial Minerals*, edited by C. Karr, Jr., Academic, New York, 39-68, 1975.

Burns, R.G., K.M. Parkin, B.M. Loefer, I.S. Leung, and R.M. Abu-Eid, Further characterization of spectral features attributable to titanium on the moon, *Proc. Lunar Sci. Conf. 7th*, 2581-2578, 1976.

SPATIAL AND SPECTRAL RESOLUTION NECESSARY FOR REMOTELY SENSED VEGETATION STUDIES

Barrett N. Rock
Jet Propulsion Laboratory

The following is an outline of the required spatial and spectral resolution needed for accurate vegetation discrimination and mapping studies as well as for determination of state of health (i.e. detection of stress symptoms) of actively growing vegetation.

A. Spatial Resolution

The spatial resolution required for accurate vegetation discrimination and mapping is directly related to the complexity of the canopy being studied. A relatively homogeneous canopy (crop plantings, conifer forests consisting of one or two species, etc.) requires less spatial resolution for accurate mapping than does a more heterogeneous canopy (conifer/hardwood mixes, multiple species of hardwoods, etc.) which contains greater scene variation. The Lost River NASA/Geosat test site in eastern West Virginia (ridge and valley province of the Appalachians) represents one of the most complex areas for vegetation discrimination and mapping available in the United States.

The Lost River test site is heavily forested (approximately 80%), representing a typical eastern mixed deciduous/evergreen (Oak-Hickory-Pine) cover type. The non-forested areas of the sites are generally under cultivation (lawns, pastures and field crops such as corn or hay) and thus surface reflectance data are totally dominated by vegetation. The vegetation cover occurring at Lost River is typical of the entire ridge and valley portion of West Virginia.

As a product of the recently completed NASA/Geosat study, highly accurate supervised vegetation classifications for the Lost River area have been produced. A total of seven forest tree classes (species or species associations) are recognized with approximately 90% accuracy of class assignment. Data used to produce these images are from Johnson Space Center's NS-001 airborne scanner (Thematic Mapper Simulator), acquired with an instantaneous field of view (IFOV) of 15 m (11 m resolution over center of the field). A recent over-flight (October, 1981) has provided NSTL Thematic Mapper Simulator data for the same area acquired with an IFOV of 30 m. In terms of accuracy of vegetation discrimination, these data provide a background for assessing the degree of spatial resolution required for a given level of accuracy.

Degradation of NS-001 Lost River data (15 m IFOV), using a low-pass, 3 x 3 filtering produced data corresponding to that acquired with approximately 45 m resolution. A vegetation classification, produced using these degraded data and the same training areas used for the 15 m data, proved less than optimal. Although the produced image was never field checked, considerable loss of usable information resulted in less precise (i.e. detailed) vegetation discrimination and mapping than is possible with the 15 m data. Clearly, 15 m spatial resolution represents an upper limit necessary for accurate analysis of a heterogeneous vegetation canopy.

In study of crop type and maturation as well as stress symptoms in plants growing over mineralized soils (containing heavy metals such as copper, lead and zinc), good success (Collins, 1978; Collins et al., 1981) has been achieved using a 500 channel spectroradiometer with an 18 m IFOV. This spatial resolution allows for detection of the so-called red-shift of .007 to .010 μm in the chlorophyll absorption band in homogeneous crop canopies (this red shift has been related to metal-induced stress).

Based on these results and the degree of accuracy possible in vegetation mapping at the Lost River test site, using 15 m resolution, it is my opinion that an instrument delivering spatial resolution ranging from 10 to 15 m is required for accurate geobotanical study in the future. While improved spatial resolution may be possible, I am of the opinion that the increased amount of data made available is likely unnecessary and may in fact create additional problems related to excessive amounts of data (varying reflectance data from separate portions of a single tree crown, for example) leading to amplification of scene "noise."

B. Spectral Resolution

Broad-band spectral data (NS-001) for the Lost River test site are available for two phenologic periods; September (near the end of the growing season for woody species) and October (period for fall foliage display, selected to afford maximum species discrimination data). NS-001 bands 3 (0.63 - 0.69 μm), 4 (0.76 - 0.90 μm), 5 (1.00 - 1.30 μm), 6 (1.55 - 1.75 μm) and 7 (2.08 - 2.35 μm) are the most useful in providing accurate vegetation discrimination and classification of forest species and species associations using October foliage display data.

The analysis of NS-001 spectral data acquired over the Lost River test site provides insight into the utility of these broad-band data in mapping densely vegetated terrain. The work of Harold Lang (at JPL - Final Geosat Report) shows that based on an evaluation of interband correlation matrices, principal components analyses, and stepwise discriminant analyses for the supervised vegetation classifications produced for the Lost River study, in order of decreasing utility for vegetation discrimination, the four most important NS-001 VNIR bands may be ranked in the following order: band 6 (1.55 - 1.75 μm), band 3 (0.63 - 0.69 μm), band 5 (1.00 - 1.30 μm), band 4 (0.76 - 0.90 μm). The somewhat surprising absence of the bands at 0.45 - 0.52 μm (band 1) and 0.52 - 0.60 μm (band 2) is attributed to their high positive correlation with the 0.63 - 0.69 μm band. The high ranking of the 1.00 - 1.30 μm band is significant, since data will not be acquired in that wavelength range by the Landsat-D TM. NS-001 bands at 0.52 - 0.60 μm (band 2), 0.63 - 0.69 μm (band 3) and 0.76 - 0.90 μm (band 4) were of considerable value in the process of vegetation discrimination and mapping since they may be used to produce images which mimic aerial CIR photography, an image format with which field botanists and photointerpreters are familiar.

Certain spectral regions, when studied with high resolution, are seen to contain a great many fine spectral features that may well provide useful data for improved vegetation discrimination studies. Based on laboratory studies (reflectance data from the Beckman 5240 spectrophotometer) the 0.80 to 1.30 μm region contains the greatest amount of fine spectral structure (both reflectance and absorbance features; note Table 1), data which relate to leaf struc-

ture. The 1.50 to 1.75 μm and 2.00 to 2.40 μm regions also contain fine spectral structure, in this case relating to leaf moisture content (Gausman et al., 1978; Tucker, 1980) and thus, state of health (senescence vs. active growth). Table 1 lists areas of fine spectral structure in the VNIR, SWIR, and TIR, which will be of use in both vegetation discrimination and stress detection.

According to the work of Collins et al. (1981) and others, the spectral region most affected by mineral-induced stress lies between .550 μm and .750 μm , with the symptomatic red-shift occurring on the far wing of the red chlorophyll absorption band centered at approximately .680 μm (principal absorption peak for chlorophyll-a molecules associated with the photosynthetic light trap). As stated previously, the red-shift consists of a .007 to .010 μm shift of the chlorophyll shoulder to slightly longer wavelengths (.690 to .700 μm).

In the study of phenologic changes (ontogenetic or maturation stages), crop plants such as corn, wheat, and sorghum demonstrate a similar red-shift in the chlorophyll-a absorption band (Collins, 1978). The red-shift (again .007 to .010 μm) occurs along the entire length of the absorption wing, but is most pronounced on the chlorophyll shoulder centered at about .740 μm (ranging from .700 to .750 μm). In both cases (mineral-induced stress and progressive maturation) the red-shift may be related to a decrease in chlorophyll production.

The instrumentation used by Collins (1978) in his study of crop canopies was an airborne 500 channel spectroradiometer with .0014 μm spectral resolution, collecting data in the .400 to 1.100 μm spectral region. Collins noted that the red-shift can be measured with .010 μm -wide spectral bands centered at .745 μm and .785 μm . These two bands plus one centered at .670 μm provide enough information to identify a variety of crop plants as well as detect the symptomatic red-shift. Tucker and Maxwell (1976) have demonstrated that wide spectral bands of .050 μm or more do not provide adequate information in the 700 to 750 μm range for detection of the chlorophyll absorption edge.

C. Summary

Good success has been achieved in vegetation discrimination and mapping of a heterogeneous forest cover in the ridge and valley portion of the Appalachians using multispectral data acquired with a spatial resolution of 15 m (IFOV). A sensor system delivering 10 to 15 m spatial resolution is needed for both vegetation mapping and detection of stress symptoms.

Based on the vegetation discrimination and mapping exercises conducted at the Lost River site, accurate products (vegetation maps) are produced using broad-band spectral data ranging from the .500 to 2.500 μm portion of the spectrum. In order of decreasing utility for vegetation discrimination, the four most valuable NS-001 VNIR bands are: 6 (1.55-1.75 μm), 3 (0.63-0.69 μm), 5 (1.00-1.30 μm) and 4 (0.76-0.90 μm). Spectral data acquired in the 1.00-1.30 μm range is essential. Finer spectral detail from certain wavelength regions (0.80-1.30 μm , 1.50-1.75 μm , and 2.00-2.40 μm) will supply additional useful information for vegetation mapping and monitoring, provided that 10-15 m spatial resolution is possible.

References

- Collins, W. 1978. Remote sensing of crop type and maturity. Photogrammetric Engineering and Remote Sensing. 44(1):43-55.
- Collins, W., S. H. Chang, and J. T. Kuo. 1981. Detection of hidden mineral deposits by airborne spectral analysis of forest canopies. Final Report to NASA, Contract NSG-5222.
- Gausman, H. W., D. E. Escobar, J. H. Everitt, A. J. Richardson, and R. R. Rodriguez. 1978. Distinguishing succulent plants from crop and woody plants. Photogrammetric Engineering and Remote Sensing. 44(4):487-491.
- Tucker, C. J. 1980. Remote sensing of leaf water content in the near infrared. Remote Sensing of Environment. 10:23-32.
- Tucker, C. J., and E. L. Maxwell. 1976. Sensor design for monitoring vegetation canopies. Photogrammetric Engineering and Remote Sensing. 24(11):1399-1410.

TABLE 1. FINE STRUCTURE OF PLANT
SPECTRA IN THE VNIR, SWIR AND TIR

Wavelength (μm)	Type of Feature	Value
.440-.500	Absorbance	Detection of changes in chlorophyll/carotenoid ratios (related to stress).
.650-.700	Absorbance	Detection of chlorophyll states as well as tannin and anthocyanin content. Initial stress detection.
.700-.750	Reflectance	Senescence detection. Dead or dormant vegetation.
.800-.840	Absorbance	Possibly related to leaf anatomy and/or state of hydration.
.865	Reflectance	Height of feature may be useful in species discrimination.
.940-.980	Absorption	Shifts in this minor water absorption band may be useful in species discrimination and determination of hydration state.
1.060-1.100	Reflectance	Shifts in peaks may be related to leaf anatomy and/or morphology. May be useful for species discrimination.
1.140-1.220	Absorbance	Shifts in this minor water absorption band may be useful in species discrimination and determination of hydration state.
1.250-1.290	Reflectance	Height of this feature very useful for species discrimination of senescent forest species. A ratio of this feature with the one at 1.645 μm offers a good indication of moisture content and thus stress.
1.630-1.660	Reflectance	An indication of moisture content of leaf. May also be an indicator of variation in leaf anatomy. May be useful for species discrimination. An indicator of leaf moisture content when used as a ratio with the 1.270 μm data above.
2.190-2.300	Reflectance	An indicator of moisture content. May also be of value in species discrimination.
3.000-5.000; 8.000-14.000	Reflectance	Little is known concerning the value of thermal IR data in the study of vegetation. This is an area that needs further study.

Analysis of Lithology - Vegetation Mixes in Multispectral Images

John B. Adams¹, Milton Smith¹, Jill D. Adams²

1) Department of Geological Sciences

2) Department of Botany
University of Washington

Abstract

Discrimination and identification of lithologies from multispectral images become more challenging with increasing density of vegetative cover. Although hyperarid areas such as parts of the Sahara have virtually no vegetation a greater part of the earth's surface, including much of the Western U.S., shows reflectance from some mixture of rock/soil and vegetation. Rock/soil identification can be facilitated by removing the component of the signal in the images that is contributed by the vegetation. Conversely, in some studies it is desirable to isolate the vegetation signal and to suppress the rock/soil signal. Work to date suggests that at least for some areas unmixing techniques provide unique and useful information.

Our approach relies heavily on the results of laboratory studies of the spectral reflectance of minerals, rocks, weathering products, soils, and vegetation. We have developed mixing models to predict the spectra of combinations of pure end members, and have tested and refined those models using laboratory measurements of real mixtures. Models in use include a simple linear (checkerboard) mix, granular mixing, semi-transparent coatings, and combinations of the above.

We also rely on interactive computer techniques that allow quick comparison of the "spectrum" of a pixel stack (in a multiband set) with laboratory spectra. To make these comparisons we recalculate the laboratory spectra to the values that would be expected if the sample were being viewed by the imaging device. Solar, atmospheric, and instrumental corrections are applied. This approach has

been used successfully to identify lithologies in Viking Lander and Orbiter images, and using LANDSAT images.

There are two main objectives of the pixel-by-pixel spectral analysis. First a rapid check can be made of the laboratory spectra for correspondence with pure materials or mixtures; and their distribution can be displayed on the image by alarming like pixels. Second, whether or not there is correspondence with any laboratory spectra, the "pixel spectra" can be analyzed and classified according to their ranking as end members or as part of a mixture of end members. Displayed on the image these data show unique units (rock, soil, vegetation, mixes, etc.), and the mixing relations between units. In ideal cases where a continuous gradation exists between end members A and B, the proportions of the mixtures of A and B can be contoured on the image. We have studied a LANDSAT image of part of the Western Desert of Egypt where there is continuous spectral mixing between dark lag chert and lighter drifting sand. Pixels that fall on the mixing line between A and B can with some confidence be assigned the percentages of spectra of the two contributing components (chert and sand) even though neither component is spatially resolved by LANDSAT.

The spectral response of green vegetation is more complex. There are, of course, important differences between species in both pigmental and leaf/stem surface characteristics. In addition the architecture of the plant (arrangement of leaves, stems, etc.) and the multi-layered nature of a plant community introduce factors of shading and shadow which when coupled with the reflectance of detrital components, often make the signatures of plant assemblages difficult to interpret.

Working with field and laboratory vegetation data and LANDSAT MSS images in two semi-arid areas, Arizona (Tucson Mtns.) and Hawaii (Mauna Kea-Mauna Loa saddle), we find little evidence of simple mixing of vegetation and the rock/soil substrate. That is, changes in vegetation density do not usually involve simple changes in the proportions of spectral components A and B (vegetation and rock/soil) seen in

the images. Instead image analysis, confirmed by field work, typically defines several vegetation and rock/soil zones that are spectral end members. These do not mix appreciably with one another, even though the type of rock/soil is constant throughout the image. These observations are consistent with ecological theory. For example, plant density changes which often follow altitudinal or moisture gradients typically are accompanied by changes in numbers of species or in the relative proportions of those species.

To isolate (and possibly remove) the spectral signature of vegetation requires an understanding of the types of vegetation present in an area, as well as an estimate of the percent cover. This may be a difficult task, depending on how much is known about the area in the image that is being studied. Given some knowledge of the likely vegetation types and their distribution in an area we can isolate the vegetation signal after working through an iterative process that progressively narrows the model (species and percent cover) for a vegetation zone. The steps are: first, to define the zone (spectrally unique end member that does not mix with other zones); second, to model in the computer the composite spectral signature of the vegetation (which does involve mixtures of the spectra of the vegetation species within the zone); third, to model the percent cover of the vegetation. With field data and laboratory spectra on the main kinds of vegetation that occur in altitudinal zones in the Tucson Mtns. and on Mauna Loa we can reconstruct the complex vegetation signal. In these areas a limited field traverse provides data that allows correct analysis of large surrounding areas. With proper modeling of the complex vegetation signal we can then isolate the component from the rock/soil and more readily map lithologies:

The techniques described here have been developed using LANDSAT MSS data. We conclude that future advanced multispectral imaging systems with many band-passes will greatly facilitate identification of rock/soil and vegetation, and will substantially improve the reliability of mixing models. At the same time the increased data load will force the use of selective strategies for discriminating, identifying

and mapping, and will make less attractive "brute force" approaches for classifying. We propose that spectral mixing techniques will become increasingly useful as the instrument technology advances.

GEOLOGIC UTILITY OF IMPROVED ORBITAL MEASUREMENT
CAPABILITIES IN REFERENCE TO NON-RENEWABLE
RESOURCES

H. Stewart, S. Marsh

The following is an abbreviated attempt at defining spectral and spatial characteristics for future orbital remote sensing systems. These conclusions are based on the past decade of experience in exploring for non-renewable resources with reference to data from ground, aircraft, and orbital systems. This turns out to be a difficult task in that the final decisions concerning discriminability of features and basic interpretability are really subjective decisions. In terms of spectral band selection, we have extensive laboratory spectroscopy data to point our decisions.

Spatial Resolution Requirements

Based on the experience of the Geosat test case program as well as the Aircraft Thematic Mapper Group Shoot, we have gained a good deal of experience in non-renewable resource areas using various scanner systems at various ground resolutions. Using the approximate thematic mapper bands as they will be seen on Landsat D as a spectral case, we can make comparisons from original 10 meter resolution data using the 24 channel scanner or thematic mapper simulator (NS001) up to any resolution simply by a pixel averaging method. For our discussion, we will use two principle areas of investigation. A structural interpretation in a basin area for hydrocarbon exploration, and a discrimination of altered areas in the Cuprite district in Nevada.

Hydrocarbon Basins

The first case is really a subjective decision based on examination of several basins using remote sensing data with ground resolutions of from 8 meters to 80 meters. There are obviously many variables involved in mapping structural elements which may or may not contribute to their identification. Lineaments in particular may be detected by any or all of several attributes including changes in slope, physical offset, changes in soil or rock material, changes in soil moisture, or changes in vegetation cover. Then correspondingly different scanners or radar systems more or less sensitive to these attributes will do a highly variable job in discriminating them. Fortunately, there seems to be a basic ability of the eye-mind system to integrate pixel displays into a smooth image, which based on the general scale of intra basin lineaments, seems to be optimal at about 20 meter resolution. Based on experiences from 1:50,000 scale images and looking at examples at 10, 20, 30, and 80 meter resolutions; 30 meter resolution is quite nearly as interpretable as 10 meter resolution while a reduction of resolution to 80 meters loses considerable information. This conclusion should be quantified if possible.

Goldfield (Cuprite Area)

An example of the spatial resolution requirements for the accurate delineation of alteration zones can be presented from a study of the Cuprite mining district in western Nevada. Figure 1 (from Abrams and others, 1977)

demonstrates the successful discrimination of silicified, opalized, and argillized rocks employing 10 meter resolution 24-channel scanner data. Figure 2 is a nearly equivalent color ratio composite (1.6/0.48, 1.6/2.2, 0.6/1.0 = g,r,b) employing 30 meter resolution airborne thematic mapper (ATM) data. Though the color rendition with the ATM data at 30 meters is not identical, under close study the discrimination and mapping of the three alteration zones is nearly equal. Figure 3 is the same ATM data after having averaged the pixels to 90 meter resolution. At this resolution accurately distinguishing the opalized and silicified zones is far more difficult, and our ability to recognize the argillized zone is severely reduced, as the geologic environment is less clear.

Nevertheless, recognition of the separate alteration phenomena at Cuprite is still possible, if not as accurate at 90 meter resolution. This obviously re-inforces the importance of the 1.6 and 2.2 bands to improved mapping of surface mineralogy even at poor spatial resolutions.

Spectral Resolution Requirements

The value of improved spectral resolution to non-renewable resource exploration can be enormous. Our objectives are improved discrimination of vegetation stress, lithology, and soil type and identification of specific surface mineralogy. Exploration for base metals and hydrocarbons can be facilitated by the recognition of: 1) vegetation stress caused by abnormal soil mineralogy or gas content as opposed to normal environmental water stress; 2) recognition of surface carbonates or gypsum; and 3) identification of specific

alteration iron-oxides or hydroxides (goethite, limonite, jarosite, hematite) and clays (alunite, sericite, kaolinite, montmorillonite, pyrophyllite, chlorite). However, to accomplish these goals future scanners must be at the forefront of technology in filter and detector development.

Based upon our objectives and current technology an ideal scanner system is proposed with approximately 50 nanometer resolution in the visible, 100 nanometer resolution in the near-ir, and 2000 nanometer resolution in the thermal infrared. Table 1 lists the bands of this ideal system. These proposed bands are based upon our previous experience with high spectral resolution field and airborne systems. However, detailed simulation studies employing these or other bands must be performed and studied if our next generation system is to be designed intelligently.

For geologic purposes, we tend to lean toward a C band (10 cm) radar to provide optimal information on texture variability which could be related to rock type discrimination. Based on experience with X band systems, L band systems and the radar equation, maximum variability in back scatter energy return vs wavelength radar vis-a-vis erosional geometry of sedimentary surfaces points toward the need for maximum sensitivity to particle size variations around 2-3 cm. which would correspond to a C band radar. Naturally to define geologic surfaces for topographic information using radar systems we need variable look angle. The Seasat experience illustrated the utility of a small angle off Nadir ($\sim 23^\circ$) as being very effective in topographically flat areas. For mountain areas, we need larger angles ($\sim 70^\circ$). Unfortunately the middle range at 45° while providing faithful information on geometry is almost useless for texture information, or small scale slope variability.

Table 1

<u>Channel</u>	<u>Bandwidth (nm)</u>	<u>Objective</u>
1	400-450	Iron-oxide minerals
2	450-520	Iron-oxide minerals
3	520-600	Spectral response
4	630-690	Spectral response
5	680-730	Vegetation stress
6	760-900	Vegetation vigor
7	850-950	Iron-oxide minerals
8	1000-1300	Igneous rock types
9	1550-1750	Spectral ratioing
10	2050-2150	Clay minerals
11	2100-2200	Clay minerals
12	2200-2300	Clay minerals
13	2300-2400	Clay minerals
14	8000-10,000	Thermal/Silicates
15	10,000-12,000	Thermal/Silicates
16	C Band Radar tunable at $\sim 25^\circ/70^\circ$	Texture/Geometry

CONSIDERATIONS CONCERNING FUTURE SATELLITE EXPERIMENTS

Gary L. Raines
U.S. Geological Survey
Denver, Colorado
April, 1982

Considering future satellite systems, I believe there are three general areas of importance that will produce significant results. These three areas are (1) refinement of spectral data in the .4 to 2.5 um region, (2) systematic research in spatial resolution, and (3) better data for geologic structural studies. My bias in selection of these three areas is my primary interest in the application of remote sensing to mineral exploration. These three areas are clearly interrelated; therefore research in one will contribute to the other two.

The area of better data for structural studies is probably the simplest area of the three. Two types of data would clearly contribute in a major way to this problem, radar and stereoscopic data. The radar data should be available in digital format, but this is probably not critical for the stereoscopic data, which could be photographic. It is not clear to me that radar has any great advantage over stereoscopic images or photographs in the visible and near infrared except in areas of cloud cover. Therefore I would place higher priority on stereoscopic photographs or images.

The spatial resolution area is a more complex problem. Part of the complexity has to do with differing perceptions of the rationale for using satellites as opposed to aircraft systems.

In my opinion, the major rationale for using satellites is for synoptic coverage under essentially identical conditions. The importance of this is demonstrated in the large regional structures and subtle lithologic variations that have been easily observed with Landsat images.

The significant question is basically what new geologic insights might be derived from coarser resolution data that can only be obtained from satellite systems; as opposed to can satellite systems replace aircraft systems? An interesting example is the structural features being reported on by Ken Watson with HCMM 0.5 km resolution images. An underlying problem is that increased resolution increases the data volume geometrically; this significantly hinders one's ability to study large areas. Furthermore, the mixing rules are not well understood; so it is not a trivial matter of numerically degrading high resolution data to lower resolution data. Thus, systematic research is needed to assess the utility of various spatial resolutions in order (1) to determine the trade-offs and (2) to assess the utility of these differing perspectives.

The third area, refinement of spectral bands in the .4 to 2.5 μ m region is possibly the most beneficial area. The Landsat and TM data have resulted from and stimulated a tremendous increase in our knowledge of spectral properties. As a result of these data it is now possible to map geologic materials that were at best very difficult to differentiate in the past. New avenues of attack are now open in solution of such a broad spectrum of geologic problems that the full significance is just

beginning to be accessed. However, significant spectral differences are possible using higher spectral resolution. Several important differences that should be practical to measure are the following: hematite/goethite/ferrihydrite, alumite/kaolinite/montmorillonite, carbonate, sulfates, and possibly ferrous absorption bands.

A part of the problem in accessing and refining present capability and future potential is the lack of well calibrated data. The problem of calibration is hindering present research in understanding the results that have been obtained and the problems that have been encountered. Calibration has the potential of significant refinement in potential and should be considered for future systems.

Finally, mineral stress in vegetation has been demonstrated by Bill Collins to produce a small shift on the infrared plateau near .7 μm . This offers the potential for mapping mineralized areas in heavily vegetated terrains. Much research is needed on this problem. Important areas are the following: (1) is there an optimal season, (2) is there a species dependency or is this a universal property of chlorophyll-bearing plants, (3) what exactly causes the phenomenon, (4) are there ways to map this phenomenon in image format, and (5) can such minor differences be detected from space or only from lower altitude aircraft? I believe this to be of critical importance because extensive land areas are covered with dense vegetation and are essentially unexplored for mineral deposits, and there is no reason to expect

these areas to have less mineral potential than the more arid,
better explored areas of the world.

A NEXT-GENERATION MAPPING SPECTROMETER

R.B. Singer, Planetary Geosciences,

University of Hawaii

The following recommendations represent my view of the desirable characteristics for a remote-sensing instrument for aircraft and orbital use, as was discussed at the Multispectral Imaging Science Working Group, Geology Team (Cal Tech, April 20-21, 1982). I make no particular claim to the originality of these ideas, nor can I say that this summary represents the consensus of the entire team. These are my thoughts on the matter, following that very productive meeting.

1) General

The ideal instrument would be based around two-dimensional detector arrays, silicon for the visible and very-near infrared (0.4 to 1.0 microns) and InSb or PbS for the rest of the near-infrared (out to about 2.6 microns). Spectral information would be dispersed along one axis. Thus one exposure or frame would simultaneously record a full spectrum for each pixel in a row perpendicular to the ground track. The instrument should be "smart" and versatile, with extensive pre-processing capability programmable from the ground.

2) Spatial Resolution

The general consensus of the team was that current Landsat resolution (about 80m) was not adequate, but that 30m would be quite acceptable, without leading to a serious data-rate problem. From the standpoint of deconvolving spectral endmembers, as discussed by John Adams, the smaller the pixel, the more successful we are likely to be in applying simple mixing models.

3) Spectral Resolution

Spectral dispersion should be designed so that individual array

elements provide a resolution of about 1% ($\frac{\Delta\lambda}{\lambda}$). This resolution has been demonstrated to be useful and/or necessary for identification and discrimination of certain geologically and agriculturally important features. Retention of all spectral elements for each pixel would lead to problems with on-board data storage and transmission. Because the instrument would be computerized, however, data from selected spectral elements could be averaged or deleted, as programmed by the users for specific measurements. It seems likely that a repertoire of "standard" combinations of averages and deletions, optimized for different groups of users, could be developed based on experience from laboratory and field work as well as from hands-on experience with the actual instrument(s).

When used in a mode where only information in certain bandpasses is retained, it would probably prove useful to record a complete spectrum for at least the track directly below the instrument, and possibly also for a track on each side, near the extremes of coverage. This detailed spectral information would help resolve possible ambiguities in regions of abbreviated spectral coverage, and might alert researchers to interesting spectral features which would otherwise have gone unnoticed.

4) Signal-to-Noise and Data Precision

These are really two different issues which were somewhat confused during part of the meeting. Signal-to-noise, or sensitivity, is a property of the detector and its associated analog electronics. My opinion is that we should shoot for a S/N of 100 for surface materials with 10% reflectivity (typical of many basalts, for instance). This corresponds to an uncertainty of only 1.0% of the measured signal, which would provide excellent interpretability of mafic mineralogy. If this goal cannot be met due to engineering realities, 2-3% noise for these dark materials would be servicable. A noise level of 5% (S/N = 20) or worse would seriously compromise our ability to interpret mineralogy or even discriminate among low albedo surface materials.

By "data precision" I refer to the number of bits used to digitize, process, store, and transmit the observed information. Experience with Landsat and various planetary missions has shown that 8 bit (256) or less is not satisfactory for digitilization. A minimum of 10 bits (1024) is required to meet the requirements discussed above, and this only suffices if the signal from a perfectly reflective target is carefully matched to full scale. I would suggest 12 bits (4096) for digitizing the detector signal because it provides reasonable margin for scaling without losing information at either the high or low end. The processing step I envision as serving two purposes: averaging and dumping of channels as discussed above (3), and applying some type of compression scheme to the 12 bit data. While I am not familiar with the details of data compression techniques, the engineers here tell me that a clever scheme might require as little as 8 bits, or at most 10 bits, for onboard data storage and transmission to ground stations.

5) Calibration and Atmospheric Corrections

I am willing to agree with Alex Goetz that absolute calibration of the sensor system is not necessary. We don't really need numbers in units such as watts/square meter. However, knowledge of the response of the various channel relative to each other, and as a function of time, is very important. We need to be able to make direct comparisons between the remotely sensed observations and laboratory and field observations. The great difficulty of calibrating Landsat data to reflectance substantially limits its utility for compositional mapping. I disagree with the opinion put forth at the meeting that it is not worth keeping albedo information. Many people are used to thinking in terms of ratio type analyses primarily because this is required for Landsat data. It would be a shame to not calibrate new instruments well enough to provide albedo measurements.

The first type of calibration required is to look at solar

illumination either through a diffusive filter or off of some standard surface. In either case the calibration device should be covered when not in use to reduce deterioration. (This sort of calibration has of course been used on many spacecraft instruments.) The next aspect of calibration is to have an effective computational way of removing atmospheric effects, primarily water absorptions, from the data. A number of groups have come almost simultaneously to the idea that some kind of real-time atmospheric sounding from the spacecraft is highly desirable. It is not clear yet whether data in the visible and near-IR will suffice, or whether there will need to be a few separate channels further in the IR specifically for this purpose.

The last major aspect of calibration is to develop certain areas (or materials) in the observed regions as known calibration standards. Traditionally this is done by sampling and laboratory measurement. Based on our experience comparing laboratory samples to measurements of the same unit in the field, I feel that certain units or areas are too heterogeneous, on a scale of centimeters to meters, to be characterized by laboratory measurements of small samples. For these types of areas field measurements from the ground (ala PFRS) or aircraft, using artificial calibration standards, are likely to be much more useful.

6) Miscellaneous

A number of people at the Geology Team meeting expressed their frustration at not being able to locate in the field the position of single pixels in Landsat data. It was suggested that a broadband very high spatial resolution data set be obtained concurrently with multispectral observations, preferably using the same optics. This sounds like a desirable feature but I do not have a feel or how difficult it might be to implement.

It was also suggested that topographic information be collected

by the new instrument, either through laser ranging or radar. This would allow a fairly accurate removal of photometric and shadowing effects, and therefore would be a great aid during analysis of the multispectral data. Again, I do not know how feasible this might be, but it should certainly be considered.

DETECTION OF SMALL THERMAL FEATURES BY MEANS OF TWO-BAND RADIOMETRY

Hugh H. Kieffer, U.S. Geological Survey, Flagstaff, Ariz.

Simultaneous radiometry in the 3-5- and 8-12- μm bands can be useful in estimating the temperature and area of thermal features that are smaller than the spatial resolution of the radiometer. This technique, which has been used for forest fire detection is now being used to study geothermal features on the volcanoes of the Cascade Range. Observations in both these bands were obtained of Mount St. Helens during the 1980 eruptive sequence and, during 1981, of many other active volcanic areas; typical resolution was 2 to 5 m. Many geothermal features are smaller than this spatial resolution and yield unrealistically low temperatures in both bands.

The ability to invert the brightness temperatures in these two bands to the temperature and area of a small feature depends on the nonlinearity of radiance as a function of temperature. The relatively strong nonlinearity of the 3-5- μm band between 0 and 100°C, in comparison with the 8-10- μm band, allows useful determination of the temperature and area of subpixel sources when thermal contrasts are greater than about 30°C. This condition is commonly met for small vents where steam reaches the surface.

Measurements of geothermal areas should be made at night to avoid the sensitivity of the 3-5- μm band to reflected solar radiation. This technique is limited by the necessary assumption that the small hot source is isothermal. Most atmospheric effects, apart from localized water vapor or fog from the geothermal feature itself, can be removed by using observations of adjacent unheated ground to determine the relative atmospheric transmission in the two bands. For scenes in which the natural variation of radiance is much greater than the system noise (as in the Cascade survey), simultaneous use of

these two bands yields a manyfold increase in the system's sensitivity to small heated areas.

The U.S. Forest Service has developed a real-time airborne system based on this principle that processes data from the 3-5- and 8-12- μm bands and triggers on differences in brightness temperature. This system has been tested on small controlled ground fires and is used in an operational mode to direct firefighting efforts.

APPENDIX V

WORKING PAPERS

IMAGE SCIENCE AND INFORMATION SCIENCE WORKING GROUPS

MULTISPECTRAL IMAGING SCIENCE WORKING GROUP

REGISTRATION WORKSHOP REPORT

H. K. Ramapriyan

NASA/GSFC

I. INTRODUCTION

The following is a brief report on the NASA Workshop on Registration and Rectification held in Leesburg, Virginia during November 17-19, 1981. Sponsored by NASA Headquarters, the workshop was attended by over a hundred representatives from NASA and other government agencies, universities and private industry. The purpose of the workshop was to examine the state-of-the-art in registration and rectification of image data for terrestrial applications and make recommendations for further research in these areas.

The workshop was organized into plenary session presentations and panel/subpanel meetings. There were three panels-Registration, Rectification and Error Analysis-with seven subpanels as shown below.

- o Registration - Image Sharpness, Feature Extraction, Inter-Image Matching

- o Rectification - Remapping Procedures, Resampling Functions
- o Error Analysis - Error Characterization and Error Budgets, Methods of Verification

Initially, presentations were made on user's needs, space and ground segment errors, and systems. Representatives from each of the subpanels provided tutorial presentations on their respective topics. Separate subpanel meetings were held to identify the state-of-the-art and make recommendations on further work needed in each of the subareas. These recommendations were then presented to the members-at-large by the respective subpanel chairmen to pursue general discussions. Next the subpanels reconvened and reworked the recommendations accounting for inputs from the members-at-large. The results of these meetings were again presented in a final plenary session.

The following is a summary of the information gathered during the workshop. It is not meant to be comprehensive. It will probably not provide equal emphasis to all the topics covered. It is, rather, a condensation of my notes from the workshop and the information from a number of references handed out. The list of handouts referred to in preparing this report is given in Section IX. A more complete bibliography on registration will be available with the detailed workshop report (to appear in Spring 1982)

II. USER'S NEEDS

The requirements of the users are dependent on the discipline and applications. The following disciplines were represented at the workshop with corresponding applications:

1. Land Use, Land Cover and Hydrology:

- a. Generation of land use and land cover maps
- b. Merging with ancillary data in a geographic information system
- c. Finding the effect of land use on hydrological budget
- d. Estimation of water usage via modelling
- e. Identification of residential land use.

2. Agriculture and Forestry

- a. Foreign crop forecasting
- b. Domestic crop acreage estimation
- c. Forestry information

- d. Rangeland evaluation

3. Geology

- a. Structural mapping
- b. Material type identification
- c. Linear mapping
- d. Generation of small (quadrangle size) and large (state/country wide) mosaics
- e. Hydrological studies
- f. Comparison of mosaics with topographic maps
- g. Monitoring temporal changes in vegetation for soil type information and soil erosion.
- h. Albedo monitoring in arid lands
- i. Land slide/erosion potential mapping

4. Oceanography

- a. Sea-ice dynamics and ice-flow tracking

- b. Ocean pattern analysis
- c. Motion measurements
- d. Biological estimates

5. Meteorology

- a. Severe storms prediction
- b. Measuring atmospheric motion and cloud growth
- c. Generation of time-lapse displays
- d. Cloud height estimation

Typical requirements indicated by the users are:

1. Accuracy

- a. It is sufficient if the "system" (i.e., the central data distribution facility) performs as well as the users themselves do, so that the users can avoid spending the effort in registering their images.

- b. Root-mean-squared errors of less than one pixel are satisfactory in applications involving extraction of summary data for polygons.
- c. Many Landsat users are satisfied with fitting the data to standard maps at 1:250,000 or 1:500,000 scale (implying errors less than 127 or 254 meters at more than 90% of the locations).
- d. Errors of less than .5 pixel at (90% of the location) for temporal registration and digital mosaicking are satisfactory for most applications in geology and meteorology.
- e. For applications involving visual interpretation (for example, making linears from large area mosaics) errors of the order the "width of a pencil line" (1.5 pixels) are acceptable.
- f. One forestry application involving combination of Landsat data with other data for regions containing irregular features required an absolute accuracy of 20 meters at more than 95% of the locations.
- g. It is necessary to have 50% of the "multitemporal energy" from the same ground area. This implies that (in the

absence of rotational errors) the shift in the X (or Y) direction should be less than or equal to $(\sqrt{2}-1)/\sqrt{2} = .29$ pixels.

2. Other

- a. The "system" should provide information on image geometry, such as listings of ground control points.
- b. The "system" should provide more quality information.
- c. Software for transformation of coordinates from one projection to another and a convenient means of converting from geodetic to image coordinates and vice versa should be available.
- d. The images should be rotated to north to facilitate inclusion into geographic information systems.
- e. Pixel sizes which are multiples (and submultiples) of 50 meters are preferred.
- f. For oceanographic applications, a well organized, easily accessible file of coastline and landmarks is useful.
- g. Applications-specific, rather than data-source-specific, packaging of techniques for users is needed.

It is to be noted that there were no user-expressed needs for band-to-band registration. It was assumed that this was easily satisfied as in the case of Landsat MSS and was considered a non-problem. Also, some of the needs were obviously tempered by the user's perceptions of the capabilities of the present Landsat systems.

There are at least two recent quantitative studies addressing this topic. The first, by Swain (1980) uses simulated Thematic Mapper data sets using aircraft multi-spectral scanner data. Classification accuracies are evaluated for various simulated band-to-band registration errors. It is found that a misregistration of .3 pixel causes a classification change of over 10%. The second study, by Billingsley (1981) treats band-to-band and multitemporal registration similarly. Using a first order analysis and modeling the multispectral classification process, this study concludes that the difference between .3 and .5 pixel errors in registration are insignificant and greater gains will be realized with increased spatial resolution than with increased registration accuracy at a given resolution.

III. SYSTEM ERRORS

Several presentations were made regarding the sources of distortions in images from various types of sensors. The sensors considered were space- and air-borne scanners, Synthetic Aperture Radar and Multispectral Linear Array. Of primary interest is the error remaining after correcting for

known/measured system-induced distortions. This represents the error that can only be removed using ground control points.

In the presentation by Ungar, examples of simulated aircraft scanner errors, their effects on images, and the correction of those errors were shown. However, no quantitative estimates of the residual errors after systematic corrections were given (even though in an experiment with ground control points and systematic corrections an RMS error of .29 pixel was obtained at a pixel size of 30 meters).

The main sources of error in such "Systematic Corrections" are the uncertainties in measuring ephemeris and attitude of the spacecraft and the alignment of the sensor relative to the spacecraft body. The present Landsats (up to 3) use the Goddard Spacecraft Tracking and Data Network (GSTDN) for deriving the ephemeris data. The accuracy of the attitude measurement system is .1 degree. The initial operation of Landsat-D will use GSTDN for ephemeris. Even though the operational post-processing of the ephemeris data can reduce the error to 105m (Root-Sum Squared of along-track, across-track and radial 1σ errors), the ground processing is designed for the worst case errors of 510 meters associated with two-day predicts of orbit data. It is expected that with TDRSS in operation, the RSS error will be reduced to 90 meters and with the Global Positioning System the error will be further reduced to 12 meters (1σ with 4 satellites in view) to 60 meters (with poor visibility). The presentation on GPS indicated, however, that the ephemeris data may be intentionally degraded to greater errors than indicated here. The attitude measurement accuracy on Landsat-D is .01 degree. Table I shows the approximate errors in the systematic correction data for Landsats.

Tests on Seasat SAR processing have indicated that systematic corrections leave residual errors in the neighborhood of 200 meters.

Note that the errors remaining after systematic corrections, even with the better ephemeris and attitude measurements anticipated, are greater than acceptable as indicated by user's needs. This clearly implies that some amount of ground control (or relative control for multitemporal registration) will be required at least for the foreseeable future.

IV. GEODETIC ERRORS

Given that it is necessary to use ground control to achieve the required geodetic accuracy, it is relevant to examine the availability and accuracy of geodetic data throughout the world. Presentations on geodetic data indicated that within the U.S., the geodetic control data were quite good with datum points known to within 15 meters (absolute accuracy) (per NAD27) and expected to be known to within .5 meters (per NAD83). The estimated absolute accuracy in the worldwide geodetic data, however, was 200 meters. Also, the data are generally not available due to security classification and the available data are not current. It may well prove that, for many of the non-U.S. areas, the satellite data will provide better mapping information than currently available and relative registration will be the best that can be expected.

The U.S. National map accuracy standards call for "errors of less than 0.02" (90%) at any scale smaller than 1:20,000. This is equivalent to approximately 12.2 meters at the scale of 1:24,000 used for the 7 1/2 minute quadrangle sheets. This means that many of the control points used for geodetic registration could be in error by as much as 0.4 pixels at the TM resolution. Therefore, to achieve the desired 1/2 pixel accuracy, (i) all the other procedures used in registration must have a tight subpixel error budget, and (ii) unless the errors tend to compensate each other the accuracy may not be achievable.

V. REGISTRATION

The tutorial papers on registration addressed the issues related to automatic matching of images and the preprocessing needed to achieve better results. Preprocessing steps useful for manual determination of control point coordinates from a displayed image are: enlargement using cubic convolution, least-squares estimation for given (or assumed) modulation transfer function (MTF) and noise characteristics and other enhancements to sharpen the image. Even though enlargement, as a preprocessing step, may be useful in automatic matching of local image areas, it has not been used much.

The most common approach to image matching is to:

- (i) Store a local patch (control point chip) from a reference image in a control point library

- (ii) Extract a neighborhood, from the registrant image, large enough to assure inclusion of the control point chip
- (iii) Preprocess the chip and the neighborhood using gradient filters and/or binary edge determination
- (iv) Compute a "correlation surface" to define the match between the chip and neighborhood for all integral pixel displacements of the chip.
- (v) Find the integral coordinates of the location of maximum correlation.
- (vi) Interpolate the correlation surface around its maximum using a linear or quadratic model and estimate the fractional coordinates of the correlation peak.
- (vii) Repeat the procedure for several patches and find displacements between expected and actual locations of match.
- (viii) Find a global mapping function to fit the registrant image to the reference image.

Studies have shown that matching gradient or edge images, rather than grey level images directly, is more likely to succeed especially in cases of multitemporal scenes. It is important to suppress cloudly areas prior to

matching and techniques exist to find matches in slightly cloudy neighborhoods. Various correlation methods have been used including Fast Fourier Transforms, binary "AND" and bit counting, Sequential Similarity Detection, etc.

Generally, criteria are needed for automatic rejection of control points so that the final mapping will not be affected by erroneous matches. The usual criteria are: peak threshold, primary to secondary peak ratio, offset magnitude threshold, errors in least squares fitting to find the global mapping function.

Since control point correlation is a computationally intensive process, it is desirable to minimize the number of control points required. The number of control points necessary to achieve a given registration accuracy depends on the accuracy with which their individual locations are known, their distribution and the accuracy to which the physical model used to describe the imaging process is known.

The above image-matching procedure assumes that the local patches suffer only translational errors. This is a reasonable assumption over small neighborhoods of multitemporal satellite imagery. However, for matching aircraft images or multisensor images where local distortions can be significant, or for direct "full-image matching" other techniques are used. Of note in this regard are (i) finding affine distortions in the Fourier domain and (ii) least-squares estimation of the coefficients of a parametric distortion model.

VI. RECTIFICATION

The problems associated with handling large quantities of image data and the fidelity of resampled digital images were the major topics considered by the rectification panel and its tutorial presentations.

Alternatives to representing "output space to input space" mapping functions are: direct functional method gridded approximation, dope vectors and combinations thereof. The direct functional method is suitable only for simple transformations applied to small images (for example, affine transformation and images less than 1000 by 1000). The more common approach is to use a gridded approximation taking advantage of the low spatial frequency of the mapping functions. The functions are fully evaluated over a very sparse grid. The mapped coordinates for non-grid points are computed by suitable interpolation using the nearest grid-points. When the distortions are functions of a single variable (for example, the non-linear mirror velocity profile on the Landsat MSS, or the earth skew offsets and sensor readout delay) they can be stored in "dope vectors" and used as table-look-up corrections to computed coordinates. When high-frequency corrections are present (such as jitter on Landsat-D TM) it is necessary to use combinations of the above methods.

Data handling is a significant problem in the rectification of images. For example, the rotation of a 2340x3240 MSS image by 14.4 degree (the approximate angle to orient to North a Landsat 3 image at 35 degree latitude) requires 835 lines of input image to generate one line of output. The problem is worse with TM images where the nominal line length

is 6176 pixels. It is for this reason that the ground processing systems for Landsat have chosen not to orient the images to North, but use a fixed angle from North for all images of a given scene such that the buffer size for resampling is minimized. In general, it is necessary to segment an input image, resample and reassemble the output image. The strategies for doing this are varied depending on the hardware configuration.

Geometric transformations involving small angles of rotation can be treated as separable and the horizontal and vertical resampling can be performed independently with no significant difference in the output image values. Separable transformations also have the potential of being implemented with intermediate 90 degree rotations (or transpositions) for which efficient methods exist.

Nearest neighbor, bilinear, cubic convolution, $\sin x/x$ interpolation, spline interpolation, and least-squared error with respect to a desired point-spread function are among the approaches to deriving the resampled output images.

The advantages and disadvantages of these methods are discussed sufficiently in the literature. The cubic convolution method is used in the ground processing systems for Landsat due to its balance between performance and computational complexity.

VII. VERIFICATION AND VALIDATION

The error analysis panel was concerned about the procedures for characterizing the errors as well as verification and validation of geometrically corrected products. It was indicated that in the present production system for Landsat images there was insufficient verification of geometric accuracy.

Verification can be a labor-intensive process depending on the extent of output images to be checked. Geodetic accuracy of an image can be verified by converting the geodetic coordinates of selected points within a scene to image coordinates, displaying neighborhoods of these points, comparing them with maps, and checking whether features on the map and the image overlay as expected. The tools needed for this are identical to those for building a Control Point Library. The task is simplified if sections of maps are available in digital image format.

Verification with such digital maps (and verification of registration of two images) can be performed by using flickering displays. Registration can also be verified automatically by correlation of several test segments from the reference image with the corresponding segments of the resampled image registered to it. Such a procedure would, however, be insensitive to high frequency distortions.

VIII. RECOMMENDATIONS

The recommendations made by the various panels and the members-at-large can be summarized under three major headings:

1. Verification and Validation: It is necessary to have a capability to verify achieved registration accuracies and validate techniques appropriate to a given sensor using simulations. It is necessary to define the amount of quality control required and to design a system which permits efficient verification.
2. Advanced Registration System: Advanced concepts in registration such as sensors with inherent registration accuracy, pointable sensors with selectable/multiple resolution, on-board processing for registration, and "creation" of a few very accurate, possibly "active" ground control points per orbit should be studied. Analyst's capabilities should also be enhanced through interactive terminals with image enhancement and manipulation software, especially related to remapping to various projections. Such software should be modular and transportable.
3. Universal Control Point Library: A control point library system should be developed which receives, verifies and enters data from various sources. The library should be applicable to several sensors. It should provide world-wide coverage and have a database management system permitting distributed input/output access to users. Potential use of non-image format "control point patterns" should be considered.

IX. REFERENCES

Workshop Presentations (November 17-19, 1981)

1. Allen, R., USDA Registration and Rectification Requirements.
2. Ananda, M., Navstar/Global Positioning Systems.
3. Ando, K. J., MLA Imaging Systems.
4. Anuta, P. E., Image Sharpness.
5. Beyer, E., Geometric Error Characterization and Error Budgets (Landsat-D Thematic Mapper Processing).
6. Billingsley, F. C., Data Versus Information: A System Paradigm.
7. Chavez, P. S., Jr., Registration and Rectification Needs of Geology.
8. Curlander, J. C., Geometric and Radiometric Distortion in Spaceborne SAR Imagery.
9. Dalton, J. T., Data Registration and Integration Requirements for Severe Storms Research.
10. Driver, J. M., A Case for Inherent Geometric and Geodetic Accuracy in Remotely Sensed VNIR and SWIR Imaging Products.
11. Dye, R. H., A Quantitative Assessment of Resampling Errors.
12. Engel, J., Thematic Mapper Performance.
13. Gaydos, L., Needs for Registration and Rectification of Satellite Imagery for Land-Use and Land-Cover and Hydrologic Applications.
14. Grebowsky, G. J., Geometric Verification.
15. Haralick, R., Feature Extraction.
16. Heuberger, H., Spacecraft Induced Error Sources.
17. Nichols, D., Oceanographic Satellite Remote Sensing: Registration and Data Integration Requirements.
18. Prakash, A., Spaceborne Scanner Imaging System Errors.
19. Ungar, S. G., Aircraft Scanner Imagery System.
20. Wolfe, R. H., Jr., and R. D. Juday, Inter-Image Matching.
21. Zobrist, A. L., Computational Aspects of Remapping Digital Imagery.

Other

1. Anuta, P. E. and C. D. McGillem, A Two-Dimensional Filter Design for Isotropic Reconstruction of Track-Type Airborne Geophysical Surveys, IEEE Acoustics, Speech and Signal Processing Conference, Washington, D. C., April 1979.
2. Billingsley, F. C., Modeling Misregistration and Related Effects on Multispectral Classification, JPL Report #81-6, 1981.
3. Colvocoresses, A. P., Control and Stability of Earth Sensing Satellites, Memorandum for the Record, U.S. G.S., Reston, VA, July 9, 1980.
4. McGlone, J. C., and E. M. Mikhail, Accuracy, Precision and Reliability of Aircraft MSS Block Adjustment, to be published in Photogrammetric Engineering and Remote Sensing.
5. McGlone, J. C., and E. M. Mikhail, Geometric Constraints in Multispectral Scanner Data, Presentation at the Annual Convention of the American Society of Photogrammetry, 1982.
6. McGillem, C. D., et al, Resolution Enhancement of ERTS Imagery, Symposium on Machine Processing of Remotely Sensed Data, Purdue University, 1975.
7. McGillem, C. D., and N. Y. Chu, A Simplified Design Procedure for Image Restoration and Enhancement Filters, LARS Technical Report 091577, Purdue University, 1977.
8. Mikhail, E. M., and J. C. McGlone, Current Status of Metric Reduction of (Passive) Scanner Data, 14th Congress of the International Society of Photogrammetry, Hamburg, July 1980.
9. Snyder, J. P., Map Projections for Larger Scale Mapping, Presentation at the Workshop (adapted from paper in Proceedings of the 1981 ACSM Fall Technical Meeting).
10. Svedlow, M., et al, Experimental Examination of Similarity Measures and Preprocessing Methods Used for Image Registration, Symposium Machine Processing of Remotely Sensed Data, Purdue University, 1976.
11. Swain, P. H., A Quantitative Applications - Oriented Evaluation of Thematic Mapper Specifications, LARS Grant Report 121680, Purdue University, Dec. 1980.

TABLE I

APPROX. ERRORS (METERS, 1σ) IN
SYSTEMATIC CORRECTION DATA

	LANDSAT-2	LANDSAT-D <TDRSS	LANDSAT-D >TDRSS, <GPS	LANDSAT-D >GPS
EPHEMERIS				
A.T.	500	500	80	10*
C.T.	100	100	30	6*
ATTITUDE				
A.T.	1580	125	125	125
C.T.	1580	125	125	125
ALIGNMENT				
A.T.	-	855	205+	205+
C.T.	-	427	205+	205+
RSS	2292	1098	350	340
RSS/80	28.7	13.7	4.4	4.2
RSS/30	-	36.6	11.7	11.3

*VALUES MAY BE GREATER DUE TO INTENTIONAL DEGRADATION
+EXPECTED AFTER POST-LAUNCH CALIBRATION

REGISTRATION WORKSHOP SUMMARY

- o NASA HQ SPONSORED (A. VILLASENOR)
- o N. BRYANT (JPL) CHAIRMAN
- o LEESBURG, VA.
- o NOVEMBER 17-19, 1981

H.K. RAMAPRIYAN
NASA GSFC
CODE 932

o PRESENTATIONS

- USER NEEDS
- SPACE SEGMENT ERRORS
- GROUND SEGMENT ERRORS
- SYSTEMS
- PROCESSING & VERIFICATION

o PANEL MEETINGS

- REGISTRATION
- RECTIFICATION
- ERROR ANALYSIS

o DISCUSSIONS AND RECOMMENDATIONS

TYPICAL REQUIREMENTS

o ACCURACY

- GOOD IF SYSTEM CAN DO AS WELL AS USERS
- RMS ERROR ≤ 1 PIXEL; EXTRACTION OF PIXELS IN A POLYGON
- FITTING TO A MAP - 1:250,000 OR 1:500,000 SATISFACTORY TO MANY USERS ($<127\text{M}$ OR 254M ; 90%)
- ($<1/2$ PIXEL; 90%) SATISFACTORY FOR TEMPORAL REGISTRATION & DIGITAL MOSAICS
- "WIDTH OF PENCIL LINE" FOR VISUAL INTERPRETATION
- ONE FORESTRY APPLICATION - (20M ; 95%)
- 50% MULTITEMPORAL ENERGY FROM SAME GROUND AREA ($\Delta X, \Delta Y \leq (\sqrt{2}-1)/\sqrt{2} = .29$ PIX.)
- NO "USER ANSWERS" ON BAND-TO-BAND REGISTRATION
- SWAIN STUDY: BAND-TO-BAND REGISTRATION ERROR OF .3 PIX. SIGNIFICANT
- BILLINGSLEY STUDY: BAND-TO-BAND & MULTITEMPORAL REGISTRATION ERRORS TREATED SIMILARLY; INSIGNIFICANT DIFFERENCE BETWEEN .3 & .5 PIXEL REGISTRATION FROM CLASSN. POINT OF VIEW

o OTHER

- INFO. ON GEOMETRIC CORRECTIONS (PROJECTION CONVERSIONS, QUALITY, ETC.)
- GCP LISTS
- ROTATION TO NORTH
- COAST-LINE & LANDMARKS FILE FOR OCEANOGRAPHY

APPROX. ERRORS (METERS, 1σ) IN
SYSTEMATIC CORRECTION DATA

	LANDSAT-2	LANDSAT-D <TDRSS	LANDSAT-D >TDRSS, <GPS	LANDSAT-D >GPS
EPHEMERIS				
A.T.	500	500	80	10*
C.T.	100	100	30	6*
ATTITUDE				
\approx A.T.	1580	125	125	125
C.T.	1580	125	125	125
ALIGNMENT				
A.T.	-	855	205+	205+
C.T.	-	427	205+	205+
RSS	2292	1098	350	340
RSS/80	28.7	13.7	4.4	4.2
RSS/30	-	36.6	11.7	11.3

*VALUES MAY BE GREATER DUE TO INTENTIONAL DEGRADATION
+EXPECTED AFTER POST-LAUNCH CALIBRATION

RECTIFICATION

o RESAMPLING

- RESTORATION
- RESOLUTION ENHANCEMENT
- NN, BL, CC, SPLINE, PSF
- USER ACCEPTANCE

o DATA HANDLING

- RESAMPLING GRIDS
- SEPARABILITY (HORIZ. & VERT.)
- EFFICIENT I/O

VERIFICATION

- o CHECKING SATISFACTION OF SPECS.
- o LACIE SEGMENTS FOUND TO SATISFY SPECS. MOST OF THE TIME
- o USERS HAVE COMPLAINED ABOUT MDP REGISTRATION
- o HOW EXTENSIVE SHOULD QUALITY CHECKS BE?
- o WHAT KIND OF VERIFICATION SYSTEM?

IMAGE MATCHING

- o LOCAL NEIGHBORHOODS (SHIFT WILL DO)
- o CONTROL POINT CHIPS-SIZE & DISTRIBUTION
- o CLOUD SUPPRESSION
- o CORRELATION
 - GRAY LEVEL
 - GRADIENT
 - EDGE
 - FFT, SSDA, 'AND' + BIT COUNT
 - NORMALIZED/UNNORMALIZED
 - SUBPIXEL PEAK FINDING
 - PEAK REJECTION
- o MAPPING FUNCTIONS
 - SENSOR MODELS
 - AFFINE/POLYNOMIALS
 - COMBINATION

IMAGE MATCHING (CONT)

- o OUTLIER REJECTION
 - LEAST SQUARES & HIGH RESIDUAL
 - "ALL-BUT-ONE" SOLUTIONS
 - RANDOM SAMPLE CONSENSUS
- o FULL-IMAGE MATCHING (ACCOUNT FOR WARP)
 - AFFINE (FOURIER TRANSFORM)
 - PARAMETER ESTIMATION (LEAST SQUARES)

RECOMMENDATIONS

MAIN AREAS NEEDING ATTENTION:

- o VERIFICATION & VALIDATION
 - DEFINITION OF EXPERIMENTS
 - HOW MUCH QUALITY CONTROL?
 - SYSTEMS TO HELP EFFICIENT VERIFICATION
- o ADVANCED REGISTRATION CONCEPTS
 - BUILD SENSORS WITH INHERENT REGISTRATION ACCURACY
 - ON-BOARD PROCESSING
 - POINTABLE SENSORS, SELECTABLE RESOLUTION
 - SYSTEM SIMULATION MODELS TO HELP ERROR ANALYSES
- o UNIVERSAL CONTROL POINT LIBRARY
 - FEASIBILITY STUDY
 - MULTISENSOR
 - NON-IMAGE FORMATS
 - DISTRIBUTED ACCESS
 - ACHIEVABLE ACCURACIES

NON-NASA SENSORS

MULTISPECTRAL IMAGING SCIENCE WORKING GROUP

IMAGE SCIENCE TEAM

INFORMATION EXTRACTION SCIENCE TEAM

MAY 10, 1982

MARVIN S. MAXWELL

"METEOR" EARTH OBSERVATION (AND METEOROLOGY) SPACECRAFT

LAUNCHED BY THE USSR IN JUNE 1980

589→678 KM ALTITUDE, 98° INCLINATION

BASIC PARAMETERS ON THE METEOR SATELLITE SENSORS INSTRUMENTS

PARAMETER	BIK-E		"FRAGMENT"	RTVK	
	MSU-E	MSU-SK		MSU-S	MSU-M
FOV (KM)	30	600	85	1,400	2,000
IFOV (M)	30	170	80	240	1,000
BANDS (μM)	0.5-0.7	0.5-0.6	0.4-0.8	0.5-0.7	0.5-0.6
	0.7-0.8	0.6-0.7	0.5-0.6	0.7-1.0	0.6-0.7
	0.8-1.0	0.7-0.8	0.6-0.7		0.7-0.8
		0.8-1.0	0.7-0.8		0.8-1.0
			0.7-1.1		
			1.2-1.3		
			1.5-1.8		
			2.1-2.4		
	ELECTRON- ICALLY SCANNED ARRAYS	CONICAL IMAGE SCANNER	OPTICAL- MECHANICAL SCANNER	OPTICAL- MECHANICAL SCANNER	OPTICAL- MECHANICAL SCANNER

MODULAR OPTOELECTRIC MULTISPECTRAL SCANNER - MOMS

SCHEDULED TO FLY ON SHUTTLE PALLET SATELLITE (SPAS-01) ON STS FLIGHT #7, MARCH 1982

TWO CHANNELS - 575 TO 625 NM, 825 TO 975 NM

6.912 PIXELS/LINE, IFOV - 67.5μ RAD, FOV - 26.2°

NOMINAL ALTITUDE - 296 KM, IFOV - 20 M, FOV - 140 KM

OPTICALLY BUTTED - 2 LENSES AND FILTERS PER SPECTRAL BAND

ON BOARD CORRECTION OF GAIN AND OFFSET OF THE DETECTORS

ON BOARD STORAGE OF 30 MINUTES OF DATA

7 BITS ENCODING, DATA RATE = 2 X 2.8M BYTE/SEC

	<u>OPTICS MODULE</u>	<u>POWER BOX</u>	<u>LOGIC BOX</u>	<u>RECORDING SYSTEM</u>	<u>CONTAINER</u>
SIZE (CM)	39X42X43	22X40X13	22X36X13	21X33X16	72X69X49
WEIGHT (KG)	48	24	15	54	35
TOTAL POWER - 350W					

BUILT BY MEBSERSCHMITT-BÖLKOW-BLOHM GMBH (MMB)

FOR GERMAN MINISTRY OF RESEARCH AND TECHNOLOGY (BMFT)

HIGH RESOLUTION VISIBLE (HRV) IMAGER

SCHEDULED TO FLY ON THE FRENCH SPOT SATELLITE IN 1984

832 KM ALTITUDE, 98.7° INCLINATION, SUN SYNCHRONOUS, 10:30 AM EQUATOR CROSSING

TWO HRV INSTRUMENT ON SPACECRAFT, 2 TAPE RECORDERS

EACH HRV INSTRUMENT INDEPENDENTLY PROGRAMMED

FIELD OF VIEW - 60 KM, OFF NADIR POINTING $\pm 27^\circ$ (± 525 KM) ALLOWS
SIDE LAP STEREO AND OBSERVATIONS EVERY 5 DAYS ON SELECTED SITES

34

EACH INSTRUMENT - TWO MODES:		<u>MULTISPECTRAL</u>	<u>PANCHROMATIC</u>
		(HRV-XS)	(HRV-P)
SPECTRAL BANDS		.50-.59 μM	.51-.73 μM
		.61-.68 μM	
		.79-.89 μM	
FOV		4.13°	4.13°
Ifov		20m X 20m	10m X 10m
PIXELS/LINE		3,000	6,000
PIXEL CODING		8 BITS	6 BITS, DPCM
DATA RATE		25 MB/S	25 MB/S

REAL TIME AND STORED TRANSMISSIONS - XBAND - SIMILAR TO LANDSAT-D.

COMMERCIAL SALE OF PRODUCTS - IMAGES AND DIGITAL TAPES

IMAGES ON 241 MM FILM - SCALE - 1:400,000

RADIOMETRIC CALIBRATION IS ROUTINE, GEOMETRIC AND TERRAIN RELIEF COMPENSATION AVAILABLE.

MULTISPECTRAL ELECTRONIC SELF SCANNING RADIOMETER - MESSR

SCHEDULED TO FLY ON THE MARINE OBSERVATION SATELLITE (MOS-1) IN 1985 -
FOR LAND AND OCEAN OBSERVATIONS

909 KM ALTITUDE, INCLINATION 99.1° , 17 DAY COVERAGE CYCLE, SUN SYNCHRONOUS,
10 AM TO 11 AM DESCENDING NODE

THE MOS-1 ALSO CARRIES:

A VISIBLE AND THERMAL INFRARED RADIOMETER TO MEASURE SEA SURFACE TEMPERATURE

MICROWAVE SCANNING RADIOMETER TO ALSO MEASURE ATMOSPHERIC WATER VAPOR

THE MESSR CONSISTS OF FOUR GAUSS TYPE TELESCOPES (LENSES)

A PRISM DICHROIC BEAM SPLITTER IMAGES TWO SPECTRAL BANDS

ON TWO 2048 CCD DETECTOR ARRAYS

EACH TELESCOPE HAS A FIELD OF VIEW OF 100 KM

TWO PAIRS OF TELESCOPES ARE CANTED TO PROVIDE A 200 KM FOV, 50 M IFOV, 4 BAND SENSOR

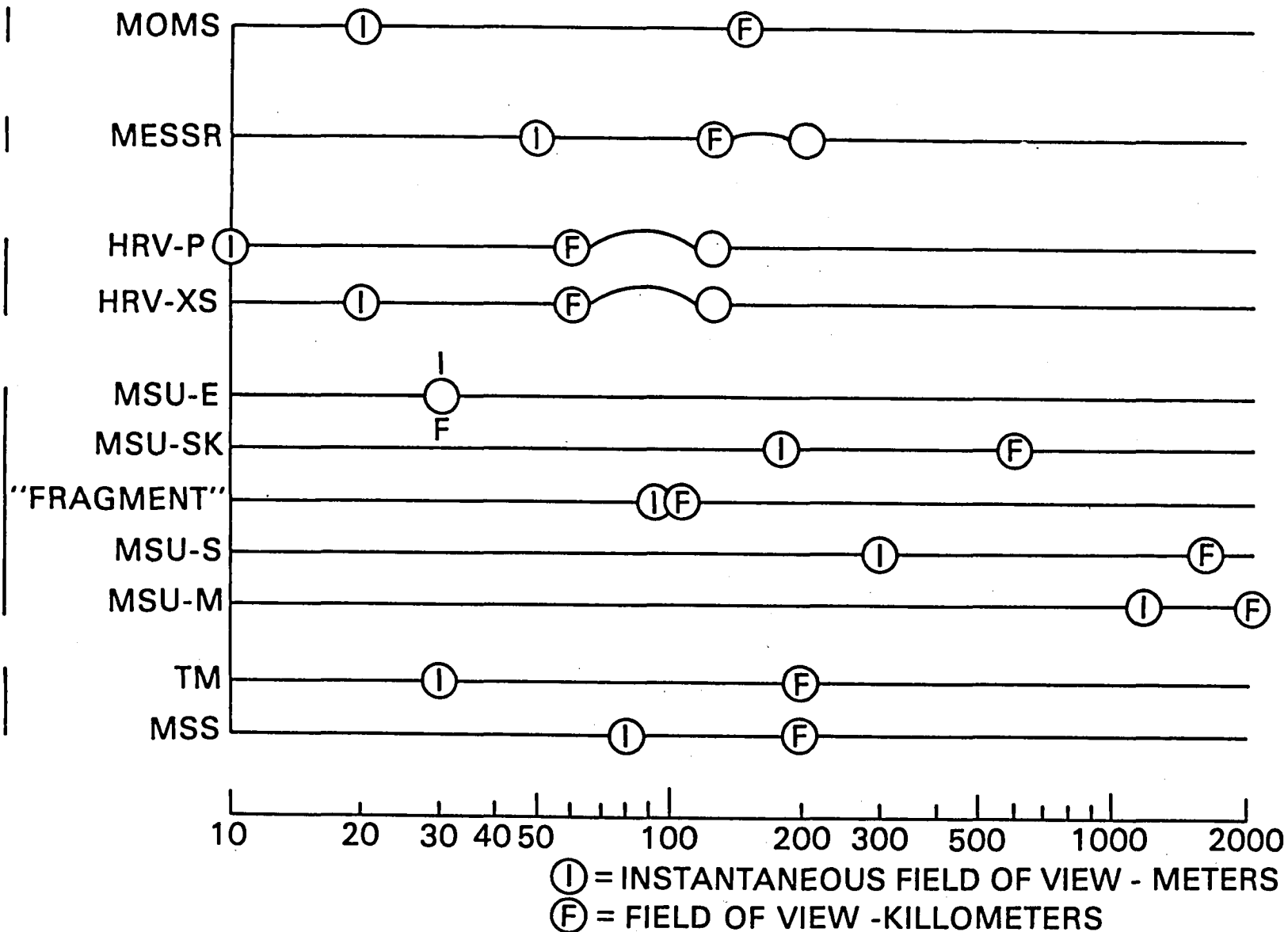
SPECTRAL BANDS (NM)	0.51-0.59
	0.61-0.69
	0.72-0.80
	0.80-1.10

RADIOMETRIC RESOLUTION	39 DB (90 TO 1)
------------------------	-----------------

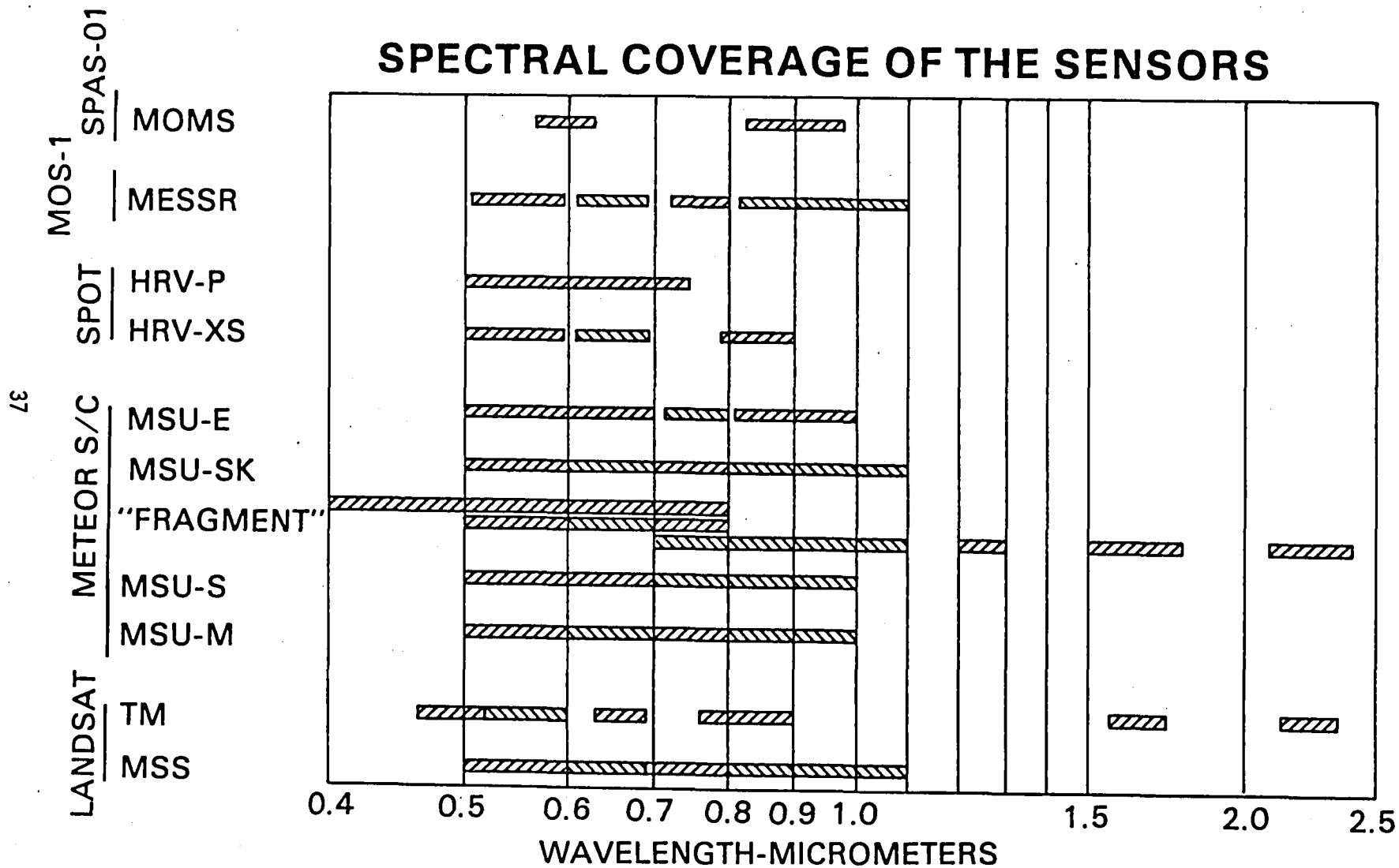
IFOV (M)	50
----------	----

LANDSAT METEOR S/C
SPOT
MOS-1
SPAS-01

"RESOLUTION"- (I FOV) AND FIELD OF VIEW OF THE SENSORS



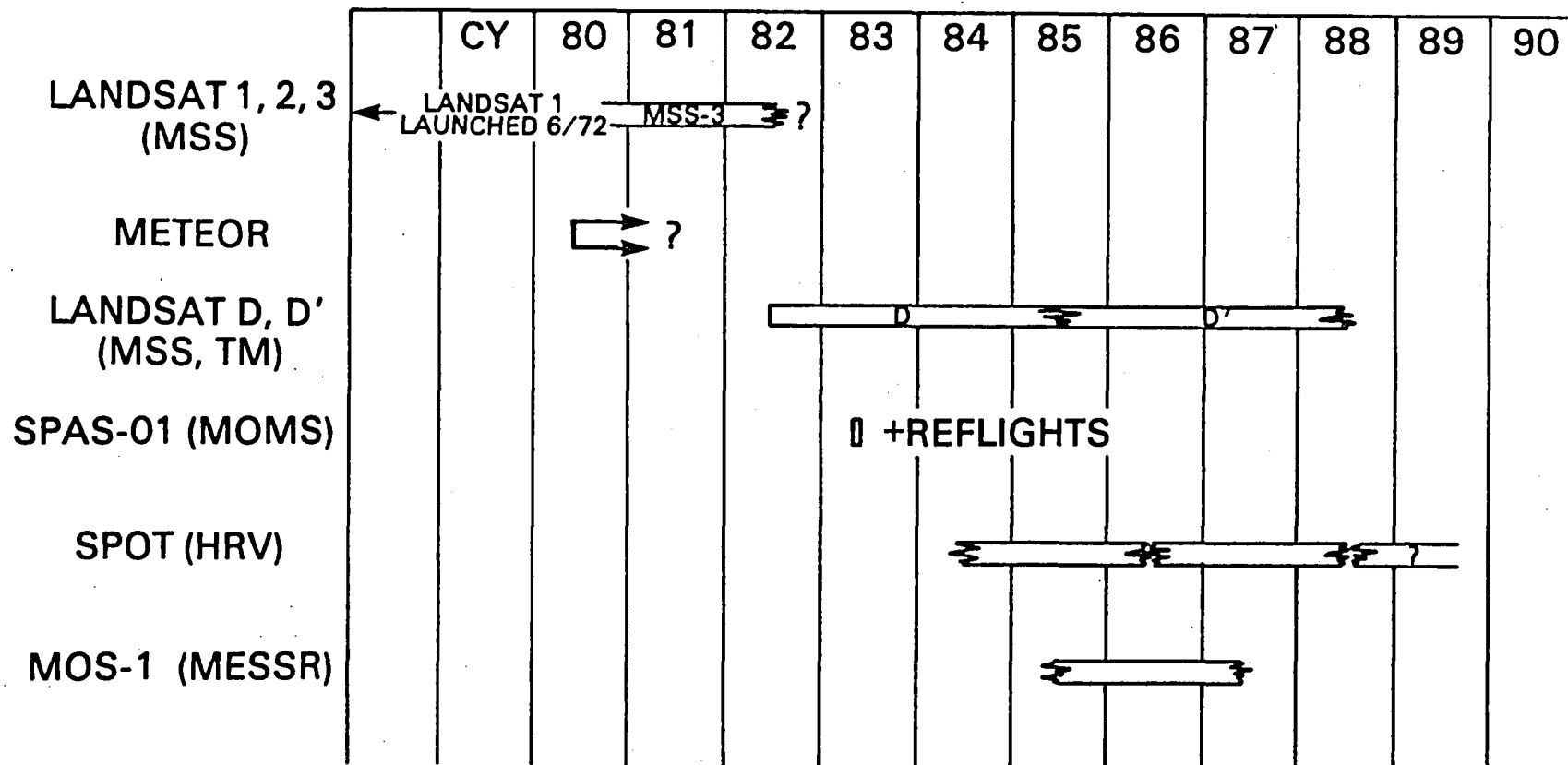
SPECTRAL COVERAGE OF THE SENSORS



- Jackson, T. J., and Ragan, R. M., 1977, Value of Landsat in Urban Water Resources Planning, Journal of the Water Resources Planning and Management Division, ASCE, Vol. 103, No. WR1, pp. 33-46.
- Jackson, T. J., and Ragan, R. M., and Fitch, W. N., 1977, Test of Landsat-Based Urban Hydrologic Modeling, Journal of the Water Resources Planning and Management Division, ASCE, Vol. 103, No. WR1, pp. 141-158.
- McKeon, J. B., Reed, L. E., Rogers, R. H., Ragan, R. M., and Wiegand, O. C., 1978, Landsat Derived Land Cover and Imperviousness Categories for Metropolitan Washington: An Urban/Non-Urban Computer Approach, Proceedings of the ASCM-ASP Annual Meeting, Washington, D.C.
- Price, J. C., 1982, Estimation of Regional Scale Evapotranspiration through Analysis of Satellite Thermal Infrared Data, to be published in Transactions of the IEEE.
- Ragan, R. M., and Jackson, T. J., 1980, Runoff Synthesis Using Landsat and the SCS Model, Journal of the Hydraulics Division of the ASCE, Vol. 106, No. HY5, pp. 667-678.
- Slack, R. B., and Welch, R., 1980, Soil Conservation Service Runoff Curve Number Estimates from Landsat Data, Water Resources Bulletin, Vol. 16, No. 5, pp. 887-893.

SCHEDULE OF PAST AND PROPOSED FLIGHTS

39



MAPSAT COMPARED TO OTHER EARTH-SENSING CONCEPTS*

Alden P. Colvocoresses

U.S. Geological Survey
National Center-MS 522
Reston, Virginia 22092 USA

ABSTRACT

During 1980 ITEK Corporation in conjunction with TRW conducted a feasibility study of a U.S. Geological Survey (USGS) proposed satellite system known as Mapsat. Mapsat differs from other proposed systems as follows:

- o It does not involve existing constraints such as transmission through the Tracking and Data Relay Satellite System or the 705-km orbital altitude of Landsat D.
- o It retains the orbit and basic transmission system of Landsat 1, 2, and 3.
- o It involves three- as well as two-dimensional mapping with up to three spectral bands.
- o It is designed for simplified (one-dimensional) data processing, long life, and overall cost effectiveness.

The ITEK study has established feasibility, so it is now appropriate to compare Mapsat with other candidates for an operational Earth-sensing mission. The task of defining the operational system rests with the National Oceanic and Atmospheric Administration (NOAA) of the Department of Commerce. However, the USGS as a major user agency has a large stake in any such system. Moreover, many Earth resource agencies throughout the world in the fields of geology, hydrology, and mapping look to the USGS as the key U.S. Government organization to represent their professional interests. Thus the USGS proposes Mapsat as an operational Earth-sensing system.

BACKGROUND

On September 21, 1966, Secretary of the Interior Stewart Udall announced the creation of the Earth Resources Observation Systems program to study the earth, its natural resources and environment from space. Secretary Udall and USGS Director William Pecora proposed an appropriate satellite system and NASA responded by building, launching, and operating the Landsat series.

Since 1966, the USGS through its EROS program has played a key role in the development and utilization of Earth-sensing systems. Moreover, the EROS Data Center of the USGS is the U.S. sales facility that distributes Landsat data on a global basis. The USGS has actively encouraged the Earth-sensing concept with the expectation of the evolution of an operational system. However, no government agency, until recently, has had the authority to define an Earth-sensing system other than for experimental purposes, and this is one reason why no operational system has evolved.

On November 16, 1979, Presidential Directive NSC-54 was issued. It assigned the management responsibility for civil operational land remote sen-

*Presented at the Fifteenth International Symposium on Remote Sensing of Environment, Ann Arbor, MI, May 1981.

sing activities to NOAA of the Department of Commerce. While the governmental responsibility for operational systems has been assigned to NOAA, the USGS and other concerned agencies should make vital contributions to define such operational systems, which according to NSC-54 should be based on Landsat technology.

For nearly 9 years Landsat satellites (originally designated ERTS) have been imaging the Earth from space. The Landsat program is well documented (1,2,3) and has established remote sensing from space as a recognized discipline throughout the world. The latest Landsat (Landsat-3) carries return beam vidicon (RbV) cameras of 30-m resolution* as compared to 80+ m for Landsat-1 and -2; even so, Landsat is a relatively low-resolution system and is thus limited with respect to making detailed studies of the Earth. Moreover, Landsat lacks the stereoscopic mode essential to the delineation of elevations of the Earth's surface. The acceptance and use of Landsat products clearly indicates that there is a need for a truly operational Earth-sensing system, and that this need is considered to be global and not restricted to any one country or group of countries. Whether or not the United States develops a truly operational system depends on many unanswered questions. It should be noted that several foreign governments (France, Japan, Germany, India) and agencies (European Space Agency, United Nations) are considering the development of an operational Earth-sensing satellite system or systems. From all indications some such system will evolve during the 1980's. Because of the high cost involved, it is hoped that such systems will be international in nature--perhaps similar organizationally to the global communications systems--rather than each interested country developing its own system.

Landsat D (4,5) is scheduled for launch during 1982, but because of its limitations (very low production capabilities for Thematic Mapper data, and no stereo capability) the USGS does not view Landsat D as an operational system or even as an operational prototype.

On December 3, 1980 NASA issued a request for proposal (RFP) for an MLA (multispectral linear array) Instrument Definition Study (6). The MLA described is "to potentially support an Operational Land Observation System (OLOS)." Awards, not to exceed \$450,000 each, are called for by the RFP. Four successful proposers (Ball Bros., Honeywell, Eastman, and Hughes) were announced on April 7, 1981, and the study is expected to be of 6-months duration after awards are made. This study addresses linear array technology, but does not include the geometric constraints of a mapping satellite that to many, including the USGS, should be an integral part of an operational system. The MLA study calls for two "short-wave" infrared bands (1.55 to 1.75 μm and 2.08 to 2.35 μm). However, the cost and complexity of recording such bands with solid-state linear arrays plus their limited use to date, make them unlikely candidates for flying on any operational system during the 1980's.

SYSTEMS COMPARISONS

There are two primary modes for imaging the Earth--by aircraft in the atmosphere and by satellites in space. For single-country coverage the aircraft mode probably holds the economic edge, but for global coverage satellites have a definite advantage. Many of today's problems related to energy, natural

*The term resolution as used herein refers to the effective resolution element which is defined as the instantaneous field-of-view of the sensor element coupled with the estimated spread function of the sensing and primary processing system.

and cultural resources, and the quality of environment are clearly of a global nature. Thus if man is to properly understand and monitor both the natural and manmade occurrences on this planet he must utilize a space system.

The options related to space sensor systems fall into three groups, namely film cameras, electro-optical systems, and microwave radars. Film cameras represent a proven technology, especially for topographic mapping, but they are not suited for the multispectral continuous monitoring of the Earth so successfully demonstrated by Landsat. The third group, microwave radars, are needed where illumination limitations or atmospheric opacity preclude the use of optical sensors that use the Sun as their imaging energy source. This leaves electro-optical sensors, which again subdivide into three groups; vidicons (TV), opto-mechanical scanners, and solid-state detector arrays.

Vidicons are represented by the RBV's of Landsat 1, 2, and 3 and the opto-mechanical scanners by the MSS of Landsat 1, 2, and 3; the Thematic Mapper (TM) planned for Landsat D and/or D'; and the conical scanner flown on Skylab as experiment S192. The vidicons are relatively poor radiometers and, therefore, not well suited for multispectral applications. The opto-mechanical scanners of Landsat utilize oscillating parts which create geometric problems and are subject to mechanical failure. The conical scanner of Skylab moves in a simple uniform rotation, but the processing of conical data, as opposed to the linear data of the MSS and TM, poses problems which have weighed against this type of imaging system. However, it is interesting to note that a new type of laser scanner, designed for the mapping of shallow sea areas from aircraft uses the same conical scanning system (7).

The sensors remaining to be considered are the solid-state detector arrays (8). They can be fabricated in either a two- or one-dimensional configuration. The two-dimensional form can, in theory, produce an instantaneous image similar to that of a frame film camera, except that each element is discrete and normally quantified in digital form. However, a continuous imaging system which is devoid of the discontinuities created by framing cameras is highly desirable, and such continuous imaging can best be obtained by one-dimensional (linear) array sensors.

The advantage of solid-state linear arrays for a space sensor system are manifold. A few of these include: light weight, low power use, long sensor life, no moving parts, high geometric fidelity, compatibility with stereo system and one-dimensional processing of data. These advantages all add up to high cost effectiveness, an essential element in the consideration of any operational system.

Two of the advantages of linear arrays warrant amplification--namely stereo compatibility and one-dimensional processing. Landsat's inability to provide adequate stereo coverage and thus provide for the delineation of height is a serious deficiency. Elevation data are required for an ever-increasing list of applications, and for most of these applications, elevation data in digital form are required. Digital elevation data (digital terrain data, digital elevation models) geometrically define the Earth's surface in three dimensions and in a form from which the following types of products can be computer generated:

- o topographic contours and topographic derivatives such as slope maps, profiles, drainage areas, and elevations of key points or areas.

- o relief depiction under any desired condition of illumination, vertical exaggeration, or perspective. This has obvious application to those geoscientists concerned with the size, shape, and distribution of Earth surface features. This relief depiction capability also permits terrain data to be stored on-board an aircraft or other platform where it can be correlated with "live" radar response and thus used in the automation of navigational systems.
- o terrain aspect correction algorithms to normalize radiometric responses distorted by slopes and thus aid in the automated classification of the Earth's surface and its cover.
- o cartographic products composed of or derived from two or more data sets of which one is elevation data.

Equal to the stereo capability in importance, is one-dimensional data processing. Existing systems involve two-dimensional storage and analysis of data. A Landsat image for example (one band) involves about 10,000,000 picture elements (pixels), and a thematic mapper image (one band), nearly 100,000,000 pixels. Data processing has been the Achilles' heel of all remote sensing systems, including photographic systems from which data compilation, particularly in the stereo mode, is both slow and costly. With linear arrays it is possible to reduce data processing from a two- to one-dimensional problem, and this applies to the stereo as well as the monoscopic mode.

Thus, linear arrays were selected as the logical sensor design for an operational system, but there are two major limitations which must also be considered. The first limitation is detector calibration, since thousands of detectors are involved for each waveband. No two detectors respond identically and thus the radiometric calibration of a linear array is a sizeable task. If one demands very fine radiometric precision to a fraction of a percent, linear arrays are not the answer. However, the sensing of any specific feature or phenomenon on the Earth's surface generally involves "noise" from various sources which add up to a few percent of the signal itself. It is believed that linear arrays can be calibrated to within one percent of expected signals, and this should be adequate for general purpose remote sensing of the Earth.

The second limitation is that available detectors and optics limits waveband response to about 1.05 μm . Longer waves generally require cooled detectors and reflective rather than refractive optics and, moreover, the available energy in the 1 to 5 μm range (short-wave infrared) is quite low. Recording the Earth's response in that range is both costly and technically difficult. It is known that certain vegetation and rock types, under suitable conditions, will give unique signatures within this range but the overall utility of such sensing has yet to be established.

MAPSAT

Mapsat is the result of a USGS effort to define an operational Earth-sensing system. It is based on Landsat technology, and includes the following concepts:

- o Global coverage on a continuous basis.
- o Open data dissemination in reasonable time and at reasonable cost.

- o Variable resolution, swath-width, stereoscopic and multispectral capabilities.
- o Capability of 1:50,000-scale image mapping with a 20-m contour interval.
- o Continuity with respect to Landsat-1, -2, and -3 including the same basic data transmission and reception system.
- o Cost effectiveness including one-dimensional data processing.

Details relative to Mapsat are covered in other papers (8,9,10) but a few points warrant elaboration.

- o Mapping geometry. The name Mapsat implies a mapping system, but this does not mean its primary function is to serve the mapmaker. Disciplines such as geology, hydrology, agriculture, geography, and engineering, to name a few, require multispectral data in accurate mappable form. Raymond Dideriksen (written commun., 1976) of the U.S. Soil Conservation Service has stated, "Until the geometric accuracy and resolution are greatly improved we cannot consider Landsat or LFO (Landsat Follow-On) to be competitive cartographic tools when compared with either high-altitude photography or cameras such as those that were demonstrated in Skylab." Here a Department of Agriculture spokesman is calling for a space system of higher geometric fidelity and resolution, and it is hard to conceive of any other serious user to whom geometry is not important. Geometric precision, which is essential to the cartographer, is also the key to an operational Earth-sensing system, and thus the name "Mapsat" has been applied. The products envisaged from Mapsat are by no means limited to conventional planimetric and topographic maps but include thematic displays and other products which can be derived from digital elevation data.

The high geometric fidelity of Mapsat is achieved by defining a spacecraft and sensor system having virtually no moving parts and very precise position and attitude determination. The sensor system is based on rigid solid-state linear arrays rather than mechanical scanners such as used on Landsat. Moreover, the antennas are defined to remain rigid as are the solar panels during periods of data acquisition.

- o Resolution and data transmission. Mapsat is designed to use up to three spectral bands at various resolutions and swath widths. Areas requiring high resolution may be so covered with an effective resolution element as small as 10-m. Fortunately areas requiring such relatively high resolution are generally of limited extent. The selection of the spectral band and stereo combinations would also depend on the type of area to be covered. However, a limitation on the data transmission rate is considered essential. By using on-board data compression techniques and data storage, and minor modifications to the existing Landsat receiving stations to increase their capacity, the existing S-band Landsat transmission system should be adequate. However, a single centrally located receiving station, such as near Sioux Falls, S. Dak., would reduce the number of data transmissions and thus improve the efficiency of the system for coverage of the conterminous United States.
- o Spectral bands. The Landsat multispectral scanner (MSS) uses four basic spectral bands. A fifth thermal band was added on Landsat-3 but failed soon after launch. Of the four MSS bands, two are in the near infrared

and are largely redundant. In order to optimize data acquisition against demonstrated practical use, the two near-infrared bands have been consolidated into one for Mapsat. The three bands selected are a blue-green (0.47 to 0.57 μm), a green-red (0.57 to 0.70 μm) and a near-infrared (0.76 to 1.05 μm) band. While the importance of a thermal band is recognized, it is considered suitable for Mapsat, which records reflected solar energy. The thermal emissions from the Earth's surface can best be measured before dawn and afternoon to separate the Sun's effects. Thus a sun synchronous satellite other than Mapsat is needed for thermal sensing.

- o Stereoscopic capability. As previously stated, the delineation of the Earth's surface in three dimensions is essential for many uses, and Mapsat will be able to do this at two different base-height ratios (0.5 and 1.0) depending on the type of topography involved.
- o One-dimensional data processing. One attribute of solid-state linear arrays is that they generate one-dimensional streams of data. For a single-optic vertically oriented sensor system this is easy to see, but for the stereo mode the generation of one-dimensional data is rather difficult to visualize.

The two dimensions of image acquisition and processing are normally defined as x (direction of forward motion) and y (cross-track direction). For any given Mapsat optic the y component is fixed by the linear array itself and all data sets are generated in what is basically the x direction. In space it is also possible to define two or more sets of linear arrays using two or more sets of optics looking forward, vertical, and/or aft to create stereo imagery. Moreover, it is feasible (10) to control the spacecraft so that corresponding detectors in two separate optics will track each other as the satellite circles the Earth. This creates epipolar planes which produce one-dimensional (x direction) sets of stereo data. If one assumes that such data will correlate (the same image points identified and located on the two data sets by their radiometric signature) then data processing in stereo as well as monoscopic mode is greatly simplified and can in fact be automated. In so far as is known linear arrays provide the only defined sensor system that can generate the epipolar planes in space.

For precise mapping ground control is needed, however, with the expected stability and positional accuracy expected of Mapsat, such control need only be and spaced on the order of 1,000 km along any given ground track. The correlated data can be processed by automated means and thus can provide the basis for an automated mapping system. The proper implementation of this concept would greatly reduce data processing time and costs.

On April 3, 1980, the USGS awarded a contract to ITEK Corporation (with TKW as subcontractor) for a feasibility study of the conceptual design for an automated mapping system (Mapsat). ITEK's final report (10) confirmed the feasibility of the Mapsat concept, and clearly indicates that if the U.S. Government decides now to move ahead on Mapsat, such a satellite could be launched in the 1986-88 time frame. Moreover, the system can be built and operated for a 7-year period at an estimated cost of \$215,000,000 (1979 dollars). This figure is considered highly reasonable and cost effective when compared to other proposed systems and to the value of the expected products.

CONCLUSIONS

Parameters for Mapsat were first published in April 1979 (9). Since then some modifications have developed as a result of the recent feasibility study. The basic concepts have now been validated and the following conclusions reached:

- o The orbital parameters of Landsat 1, 2, and 3 are considered optimum for an Earth-sensing satellite, and the Landsat data transmission system, with minor modifications, is considered adequate.
- o Solid-state linear arrays promise to simplify the problem of multispectral imaging of the Earth from space.
- o The epipolar plane condition can be achieved with a properly designed Earth-sensing satellite, and this will permit the delineation of the third dimension of height using linear arrays which produce one-dimensional data flows. Moreover, this condition will permit the automated processing of stereo data into topographic information.
- o An Earth-sensing satellite can now be built with virtually no actuated parts and thus achieve a very high stability, expected long life, and increased cost effectiveness as compared to existing and other proposed systems.
- o ITEK's report indicates first launch could be as early as 1986 and at a reasonable cost.

In light of these considerations the USGS proposes that the Mapsat concepts be developed into an operational Earth-sensing satellite system.

REFERENCES

- (1) U.S. Geological Survey, 1979, Landsat data users handbook, [rev. ed.]: U.S. Geological Survey.
- (2) Short, N.M., Lowman, P.D., Freden, S.C., and Finch, W.A., 1976, Mission to Earth: Landsat views the World: NASA SP-36.
- (3) Williams, R.S., and Carter, W.D., 1976, A new window on our planet: U.S. Geol. Survey Prof. Paper 929.
- (4) Goddard Space Flight Center, 1977, Specifications for the Landsat-D System: NASA (GSFC-430-D-100), July 1977.
- (5) Solomonson, V.V., 1981, The early 1981 view of Landsat-D progress: SPIE Tech. Symposium East '81, April 20-24, 1981, Washington, D.C. (SPIE v. 278)
- (6) Goddard Space Flight Center, 1980, MLA Instrument Definition Study Statement of Work: NASA, (RFP 5-31522/230) Dec. 3, 1980.
- (7) Enabnit, D.B., 1980, Airborne Laser Hydrography (FY 1982): National Ocean Survey, U.S. Dept. of Commerce, Issue paper, May 1980.

- (8) Colvocoresses, A.P., 1981, Solid-State Sensors for Topographic Mapping: SPIE Tech. Symposium East '81, April 20-24, 1981, Washington, D.C. (SPIE v. 278)
- (9) Colvocoresses, A.P., 1979, Proposed parameters for Mapsat: Photogrammetric Engineering and Remote Sensing, v. 45, no. 4, April 1979, p. 501-506.
- (10) ITEK Corp., 1981, Final Report, Conceptual Design of an Automated Mapping Satellite System (Mapsat): Natl. Tech. Inf. Serv. PB 81-185555.

September 30, 1981

AN AUTOMATED MAPPING SATELLITE SYSTEM (MAPSAT)*

Alden P. Colvocoresses
U.S. Geological Survey
National Center, Mail Stop #520
Reston, Virginia 22092

Abstract

Throughout the world, topographic maps are compiled by manually operated stereoplotters that recreate the geometry of two wide-angle overlapping stereo frame photographs. Continuous imaging systems such as strip cameras, electro-optical scanners, or linear arrays of detectors (push brooms) can also create stereo coverage from which, in theory, topography can be compiled. However, the instability of an aircraft in the atmosphere makes this approach impractical. The benign environment of space permits a satellite to orbit the Earth with very high stability as long as no local perturbing forces are involved. Solid-state linear-array sensors have no moving parts and create no perturbing force on the satellite. Digital data from highly stabilized stereo linear arrays are amenable to simplified processing to produce both planimetric imagery and elevation data. A satellite, called Mapsat, including this concept has been proposed to accomplish automated mapping in near real time. Image maps as large as 1:50,000 scale with contours as close as 20-m interval may be produced from Mapsat data.

Background

The geometry of stereo mapping photographs, whether taken from aircraft or satellite, is well known and documented. Transforming such photographs into topographic maps is a relatively slow and expensive process that for many critical steps defies automation. Compared to an aircraft, a satellite offers the unique advantages of much greater stability and uniform velocity.

Utilizing these advantages, a sensing system in space can now provide imagery of mapping quality, even though a continuous electro-optical imaging system is used instead of a mapping camera with its inherent high geometric fidelity. The next generation of space sensors will include solid-state linear arrays (fig. 1) that involve no moving parts. By continuous imaging with very high geometric fidelity they will permit, at least in part, the automated mapping of the Earth from space in three as well as two dimensions. The fundamental difference between conventional and continuous stereo methods is illustrated by figure 2.

* Approved for publication by Director, U.S.G.S.

At least four papers have been published that relate directly to automated three-dimensional mapping. In 1952, Katz (1) showed how height measurements could be made with a stereoscopic continuous-strip camera. The geometry of such a strip camera and stereo linear arrays is basically the same. In 1962, Elms (2) elaborated on the strip camera concept and indicated its advantages over frame cameras as a possible component of an automated mapping system. In 1972, Helava and Chapelle (3) described the development of instrumentation by which a conventional stereomodel can be scanned using the epipolar-plane* principle, and thus reducing image correlation from a two-dimensional to a basically one-dimensional task.

In 1976 Scarano and Brumm (4) described the automated stereo-mapper AS-11B-X which utilizes the epipolar-scan concept and one-dimensional digital image correlation described by Helava and Chapelle. Thus the concept of reducing photogrammetric data stereo correlation from two to one dimension is well established. The cited literature, however does not describe the possibility of imaging the Earth directly in stereoscopic digital form suitable for one-dimensional processing.

Beginning in 1977 a serious effort to define a stereo satellite or Stereosat (5) was undertaken by NASA. The Stereosat concept calls for linear-array sensors, looking fore, vertical and aft, but its principal objective is to provide a stereoscopic view of the Earth rather than to map it in automated mode. There are other ways of obtaining stereo imagery with linear arrays. The French SPOT (6) satellite can look left or right of the track and thus achieves stereo by combining imagery from nearby passes of the the satellite. NASA's Multispectral Linear Array (MLA) concept (7), as so far defined, calls for fore and aft looks through the same set of optics by use of a rotating mirror. However, neither the SPOT nor NASA's MLA approach are considered optimum for stereo mapping of the Earth, as neither is designed to acquire data in continuous form.

Mapsat Geometric Concept

Linear arrays represent a relatively new remote sensing concept. Five papers on this subject were presented at the ASP/ACSM annual convention during March 1978 (8,9,10,11,12). These papers concentrated on detector

*An epipolar plane is defined by two air or space exposure (imaging) stations and one point on the ground.

technology and the application of linear array sensors in a vertical imaging mode. Welsh (13) recently described the geometry of linear arrays in stereo mode, although his error analysis for such a system is based on measurements made from images rather than computations based on the digital data.

By combining the technology of linear arrays, the concept of epipolar-plane scanning, and the experience gained from Landsat and other space sensing systems, Mapsat was defined (14), and its proposed parameters are listed in Table 1. The Mapsat concept was the work of several individuals, but perhaps the single most important contribution was that of Donald Light (verbal communication), then of the Defense Mapping Agency, who first suggested that epipolar planes, as described by Helava (3) and used in the AS-11B-X plotter, could be achieved directly from space and that topographic data might then be extracted in real time. There are several feasible configurations by which linear array sensors can continuously acquire stereo data. It was decided that the system must permit selection from the three spectral bands, provide for two base-to-height ratios of 0.5 and 1.0 and be compatible with the epipolar concept. Figure 3 illustrates the configuration selected to accomplish the stereoscopic as well as monoscopic functions.

Acquiring stereo data of the Earth in epipolar form directly from space is the fundamental geometric concept of Mapsat. The epipolar conditions shown in Figure 4 implies that five points--the observed ground point P , the two exposure stations S_1 and S_2 , and the two image detectors f_1 and a_1 --lie in a single plane. If this epipolar condition is maintained as the satellite moves along its orbit, every point P observed by detector f_1 in the forward looking array will also be observed subsequently by detector a_1 in the aft looking array. Thus image correlation can be obtained by matching the data stream from detector f_1 with that from a_1 --a one-dimensional correlation scheme. This description applies equally to the use of the vertical with either the fore-or aft-looking array but involves a weaker (0.5) base-to-height ratio than the described use of the fore and aft arrays (base-to-height ratio of 1.0). In practice the data streams from more than one detector may be involved since there will normally be some offset in the path of a given pair of detectors. Moreover under certain conditions, correlation may be improved by a limited expansion of the correlation function to two dimensions.

Because each detector array is looking at a different portion of the Earth at any given time, Earth rotation complicates the epipolar condition. As shown in figure 5, this complication can be overcome by controlling the spacecraft attitude. This description is obviously simplified; further complications involve such factors as the ellipsoidal shape of the Earth, variations in the orbit, spacecraft stability, and even very large elevation differences. The spacecraft position and attitude must be precisely determined by such systems as the Global Positioning System (GPS or NAVSTAR) and frequent stellar referencing. Satellite attitude control involves gyros and inertial wheels, and, when a satellite is free of perturbing forces created by moving (actuated) parts, attitude can be maintained for reasonable periods to the arc-second.

Of course, the sensing system must retain precise geometric relationship to the attitude control system. Defining the correct satellite attitude and the rates in yaw, pitch, and roll to maintain the epipolar condition requires precise mathematical analysis. Two independent analyses, one by Howell of ITEK (15) and the other by Snyder (16) of U.S. Geological Survey, confirm Mapsat's geometric feasibility, and a U.S. patent has been allowed on the concept. Table 2 indicates the maximum deviations from the epipolar condition caused by the various expected error sources. This table is based on a half orbit (50 minutes) which covers the daylight portion to which imagery is basically limited. Attitude rate errors would be considerable if only corrected once every 50 minutes but, as the table indicates, 10-minute intervals based on stellar reference reduce the errors to a reasonable amount. Ten-minute stellar referencing using star sensors as described by Junkins et al., (17), is considered reasonable. Computer programs have been developed that result in the epipolar plane condition being maintained as long as adequate positional and attitude reference data are available and properly utilized. Figure 6 illustrates the simplicity of elevation determination in an epipolar plane which is the key element of Mapsat.

Obviously, the Mapsat concept can be effectively implemented only if stringent specifications regarding orbit, stability, reference, and sensor systems are met. Table 3 lists the Mapsat geometric requirements as defined to date, and each is considered to be within the state of the art.

Mapping Accuracy

By meeting the geometric requirements indicated and achieving stereo correlation, the resulting map accuracy is compatible with scales as large as 1:50,000 and contours as close as 20 m interval based on U.S. National Map Accuracy Standards. Reference 15 covers this analysis in some detail. Such accuracies result from the indicated geometric requirements and the following factors:

- o Linear array detectors are positioned with sub-micron accuracy.
- o Optical distortion effects, when accounted for by calibration, are negligible.
- o Atmospheric refraction, because of the steep look angles, is of a very low order and is reasonably well known; air-to-water refraction is also known where underwater depth determination is involved.
- o Relative timing, which is referenced to data acquisition, is accurate to within the microsecond.
- o Digital stereo correlation, where uniquely achieved, provides three dimensional root-mean-square (rms) positional accuracy to within half the pixel dimension.

These considerations result in relative positional errors for defined points of only 6 to 7m (rms) both horizontally and vertically. This vertical accuracy requires the 1.0 base-to-height ratio. Such accuracy is adequate for the mapping indicated but assumes that control is available for reference to the Earth's figure. As indicated by ITEK (15) and the author (19), control points of 1,000 km spacing along on orbital path will be adequate for such a purpose. Where no control exists the absolute accuracy of the resultant maps, with respect to the Earth's figure, may be in rms error by 50 to 100 m although their internal (relative) accuracy remains at the 6 to 7 m rms level.

Stereocorrelation

The determination of elevations from stereo data requires the correlation of the spectral response from the same point or group of points as recorded from two different positions. In the aerial photography case these two positions are the camera stations, whereas with linear arrays in space the two recording positions are constantly moving with the satellite. In the photography case, correlation is achieved by orienting the two photographs to model the acquisition geometry. Once this is done, correlation can be achieved by the human operator, or the image stereomodel can be scanned and correlated by automated comparison of the signal patterns from the two photographs. A system such as the AS-11B-X (3,4) generates one-dimensional digital data in epipolar planes from the model. In theory, epipolar data should be correlated much faster than that from a system that must search in two dimensions to establish correlation. In practice, the automated correlation of digital data has been only partially successful; and, as Mahoney (18) has recently pointed out, correlation by either manual or automated systems is still a slow and costly process. To date, no one has acquired original sensor data in epipolar form. Thus, no one can really say how well such data can be

automatically correlated, until a satellite such as Mapsat is flown. Simulation using digitized aerial photographs or linear-array stereo-sensing of a terrain model are relevant experiments worth conducting. However, they will provide only partial answers, since the degree of correlation will depend on the area involved. The characteristics of the Earth's surface, coupled with related conditions, such as the atmosphere and Sun angles, are highly varied; which means that the degree of correlation will also be highly varied. This problem does not imply that the Mapsat concept has not been validated. Having stereo data organized in linear digital form is of obvious advantage to create the three-dimensional model of the Earth's surface. Many areas will correlate in one-dimensional mode, others will require two-dimensional treatment, and still other areas may not correlate at all. By properly defining the satellite parameters and data processing, the correlation function can be optimized and raised well above that obtainable from wide-angle photography systems. For example, digital data can readily be modulated to enhance contrast or edges that make up the patterns on which correlation depends. Photography can also be modulated, but it is far more difficult (and less effective) than digital-data modulation, as film lacks the dynamic range and sensitivity of solid-state detectors. Mapsat will acquire data in an optimum form for automated correlation, which will expedite the precise determination of elevations and create digital elevation data that are becoming a basic tool for many disciplines.

Acquisition Modes and Products

As previously described (14), Mapsat is designed to be operated in a wide variety of modes. These include variation in resolution (10-m elements on up), spectral bands, swath width, and stereo modes. Such flexibility permits optimum data acquisition without exceeding a specified data-transmission rate that is now defined at 48 megabits per second (Mb/s).

The Earth's surface is highly varied, and data product requirements are likewise highly varied. By varying the acquisition modes and, in turn, producing a variety of products, the data management problem becomes complicated as compared to existing systems such as Landsat which produces only two basic types of data. However, solving this data management problem is a small price to pay for a system that can meet a wide variety of requirements for remotely sensed data of the Earth. Only four primary products are expected from Mapsat as follows:

- (a) Raw-data digital tapes from which quick-look images can be displayed in near real time.
- (b) Processed digital image tapes calibrated both radiometrically and geometrically to a defined map projection. Such data will be two-dimensional (planimetric) but describe the Earth's radiance (brightness) in multispectral form as is now accomplished by Landsat Multispectral Scanner tapes.

- (c) Processed digital tapes, again calibrated both radiometrically and geometrically, but which now describe the Earth's surface in three dimensions (topographically) with an associated radiance value. Such tapes are, in effect, digital elevation data sets of the Earth's surface.
- (d) Standardized images, both black-and-white and in color, which include geometric corrections and radiometric enhancements. Such corrections and enhancements will be of recognized general value and of a type that can be performed without undue delay or excessive cost. The images would also be of standardized scale.

From these four basic products, a wide variety of derivatives can be made which include the following:

- (a) Black-and-white and multicolor image maps and mosaics at scales as large as 1:50,000, or even 1:25,000 (1:24,000) where map accuracy standards are not required.
- (b) Thematic displays and maps involving such subjects as land cover and land use classification.
- (c) Maps which depict the Earth's topography by such means as contours (as close as 20-m interval), slopes, elevation zones, shaded relief, and perspective display.

Conclusion

Mapsat will not meet all anticipated remote sensing requirements, and it will in no way replace those air-photo surveys required to meet mapping requirements for scales larger than 1:50,000 and contour intervals of less than 20 m. What it will do, is provide a precise three-dimensional multispectral model of the Earth at reasonable resolution and in digital form. Moreover, the satellite will record the changing responses of the Earth's surface as long as it is in operation.

Mapsat can be built today at what is considered to be a reasonable cost (15) as it is based on available components and technology. Moreover, it is designed for simplified operation and data processing. Assuming that an operational Earth-sensing system will be flown, surely Mapsat is a deserving candidate for such a job.

Mapsat Parameters

- o Orbit—Same as Landsat 1, 2 and 3 (919 km alt).
- o Sensor—Linear Arrays—Three optics looking 23° forward, vertical and 23° aft. Three spectral bands:
 - blue green 0.47 - 0.57 μ m
 - red 0.57 - 0.70 μ m
 - near IR 0.76 - 1.05 μ m
- o Swath—180 km or portion thereof.
- o Resolution—Variable—Down to 10 m element.
- o Transmission—S (or X) band, compatible with Landsat receivers modified for data rates up to 48 Mb/s.
- o Processing—One dimensional, including stereo.

TABLE 1

Mapsat Epipolar Condition
Maximum Deviation (\pm) in Half Orbit--(50 Minutes)
(Meters on the Ground)

Case 1. Vertical plus
For or Aft--B/H = 0.5

Case 2. Fore and
Aft--B/H = 1.0

o Optimum condition:	1.3 m	0.3 m
o Attitude errors (yaw and pitch) of:		
10 arc seconds	0.7	1.6
100 arc seconds	5.0	12
o Attitude rate errors of:		
10^{-6} deg./sec.	11 (2)*	22 (4)*
10^{-5} deg./sec.	110 (22)*	230 (46)*
o Elevation differences of:		
1,000 m	2.3	0.5
10,000 m	22	1.8

* () Values obtained by 10 minute rather than 50 minute stellar reference intervals.

Mapsat Geometric Requirements

- o Positional Determination of Satellite—10 to 20 m^{1/} in all three axes.
- o Pointing Accuracy—Within^{2/} 0.1° of vertical.
- o Pointing Determination—Within^{2/} 5 to 10 arc seconds
- o Stability of Satellite—Rotational rates within^{2/} 10⁻⁶ degrees/second.

1/ rms. (1σ)

2/ very high probability (3σ)

TABLE 3

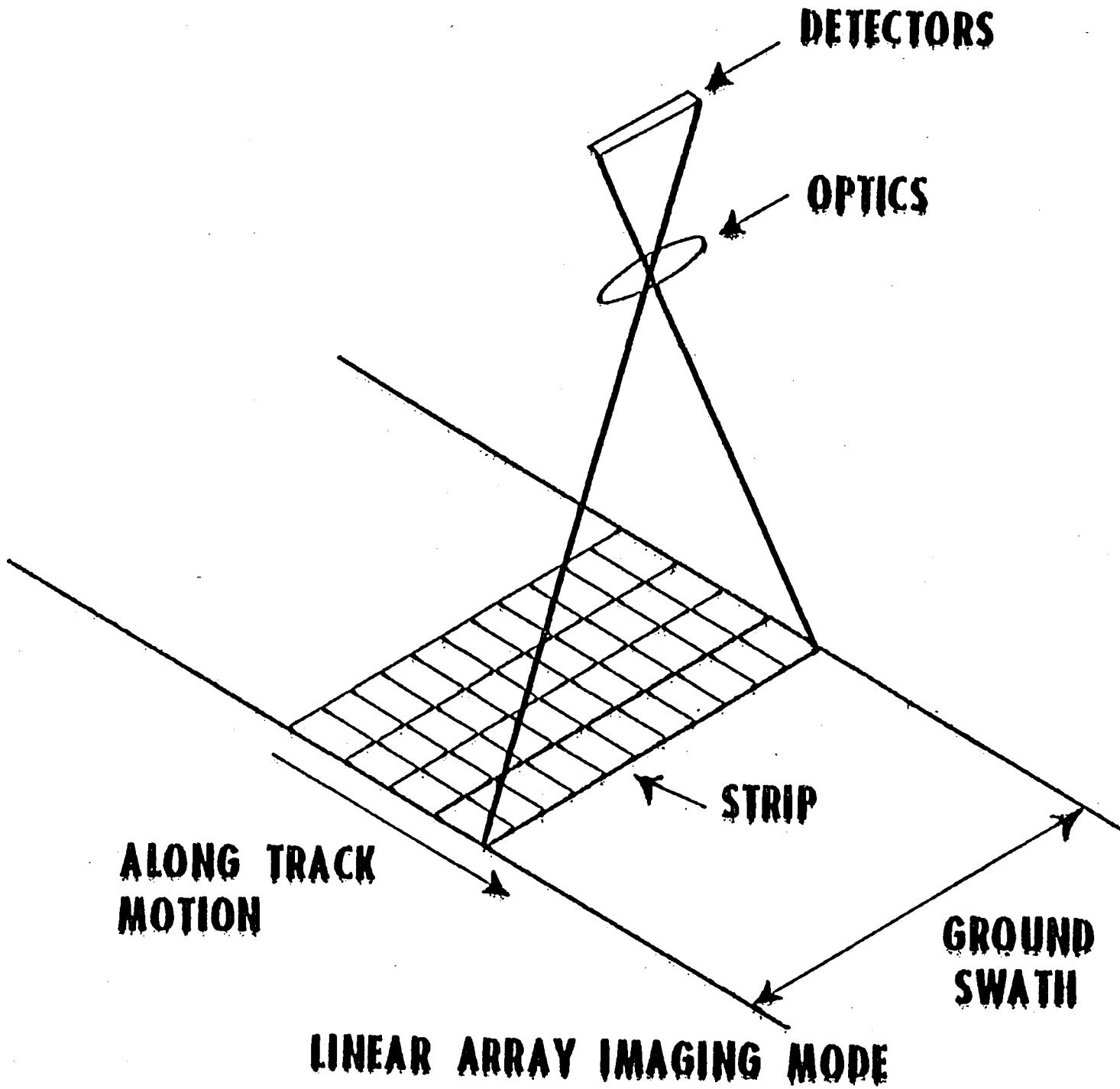
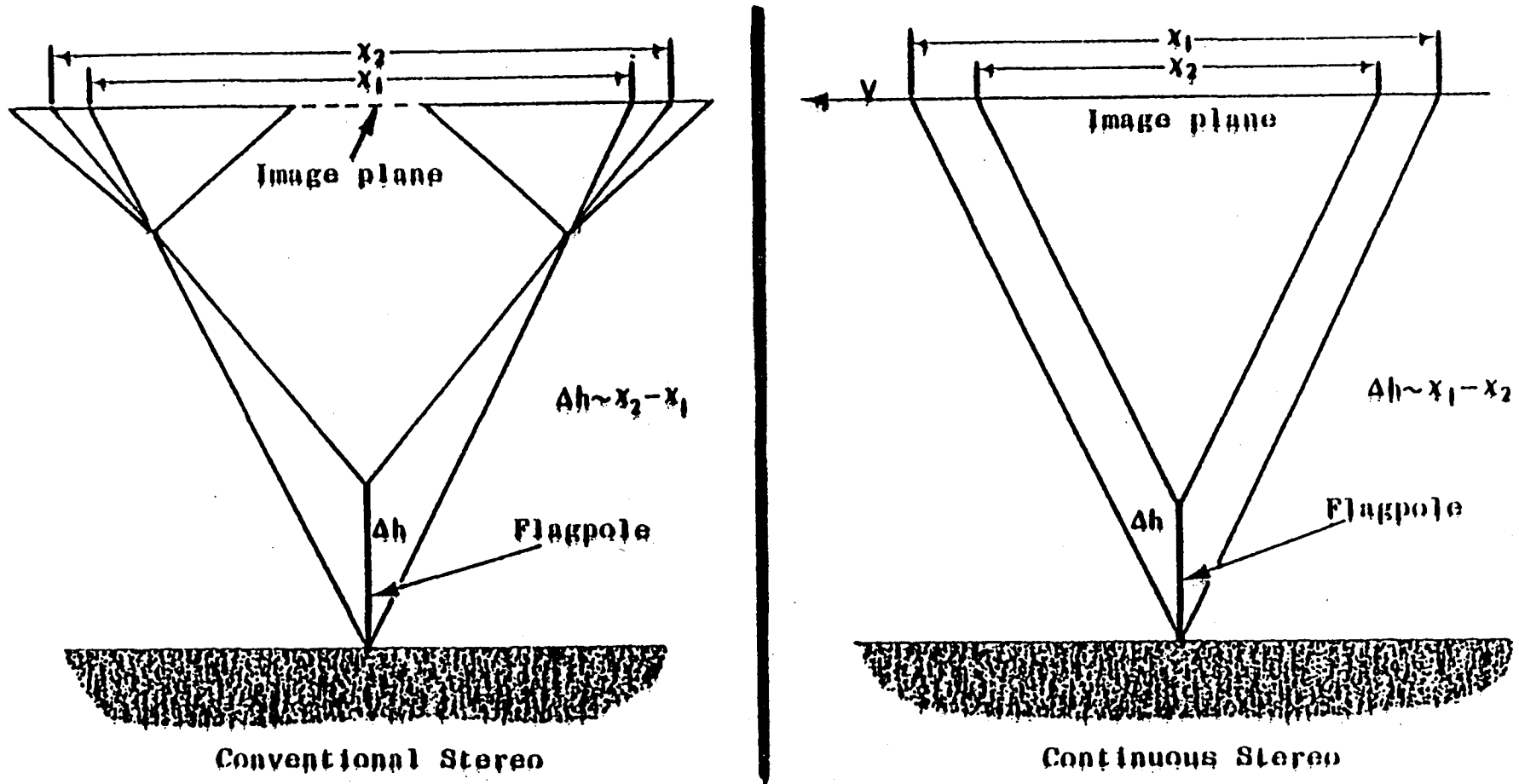
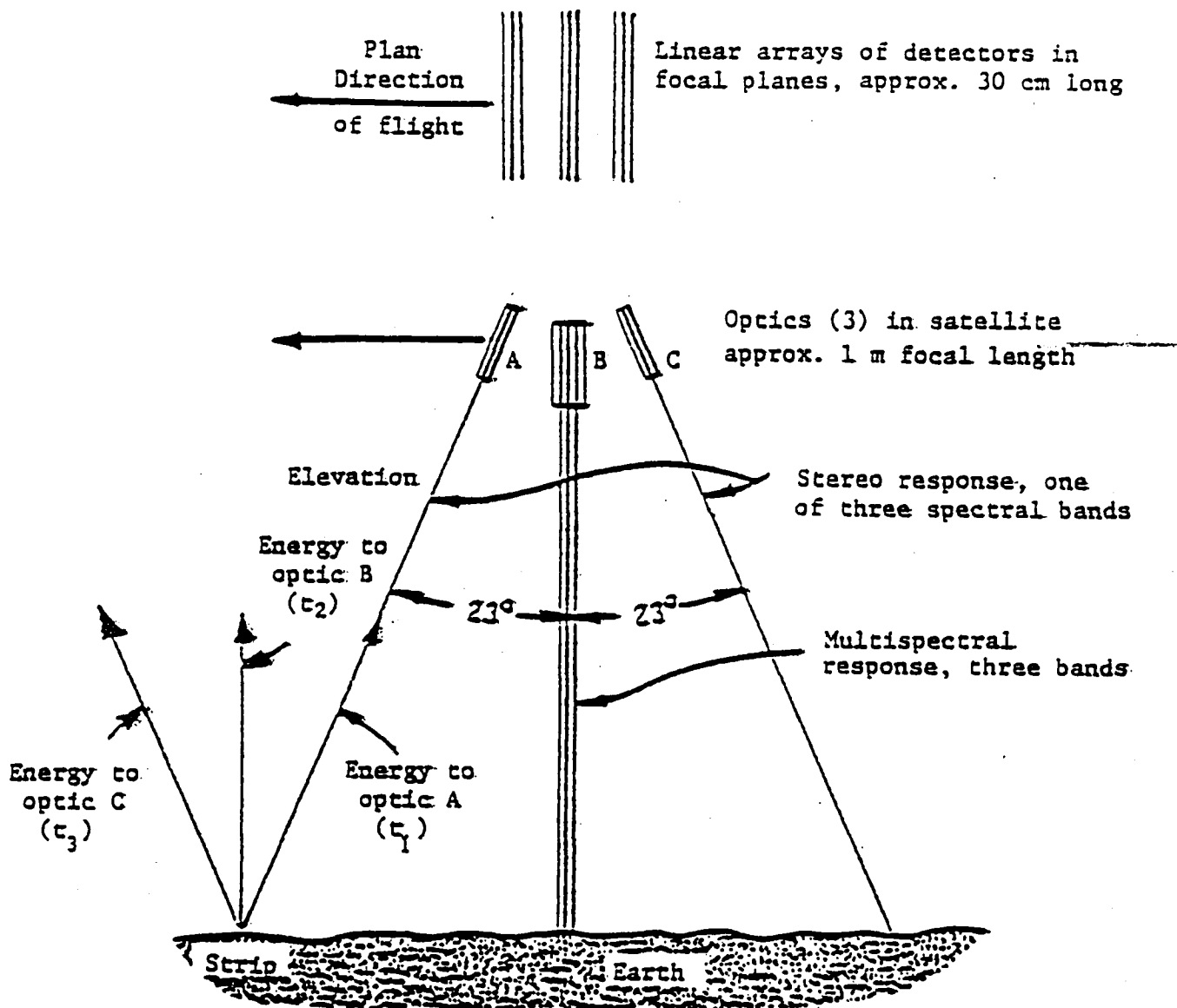


FIGURE 1

CONVENTIONAL VS. CONTINUOUS STEREO IMAGING MODES



- Both modes resolve elevation differences
- Conventional mode involves discontinuities based on each stereo pair
- Continuous mode involves no discontinuities but requires very stable platform of known uniform velocity (V)
- Conventional mode involves 2 dimensional data processing
- Continuous mode permits 1 dimensional data processing from 2 data sets



Mapsat Sensor Configuration (not to scale).

Optics A, B, and C are a rigid part of the satellite. Optic B senses the same strip 60 seconds after A; optic C, 120 seconds after A. Any combination of A, B, and C produces stereo. Optics A and C are of about 10% longer focal length to provide resolution compatible with optic B.

FIGURE 3

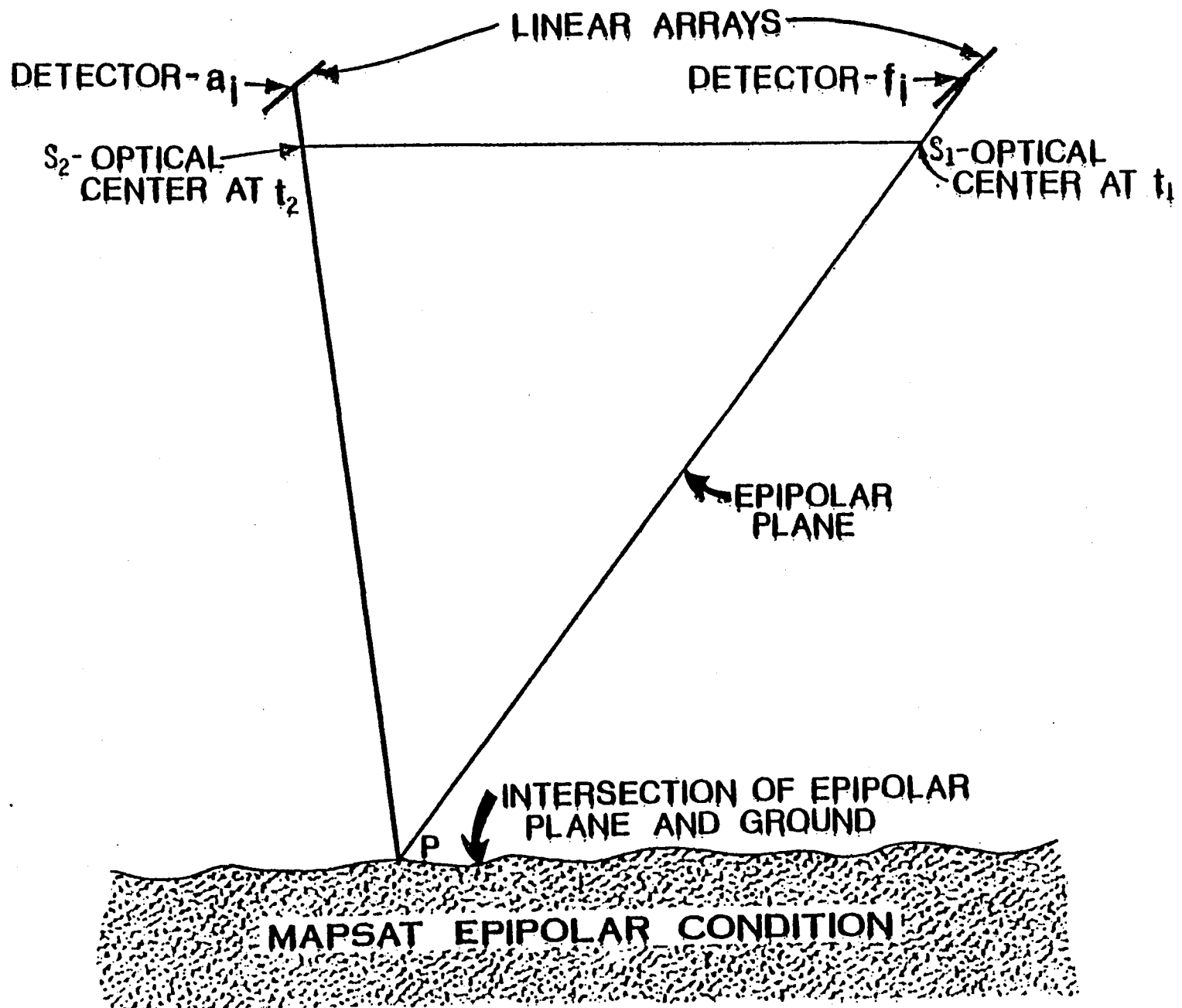
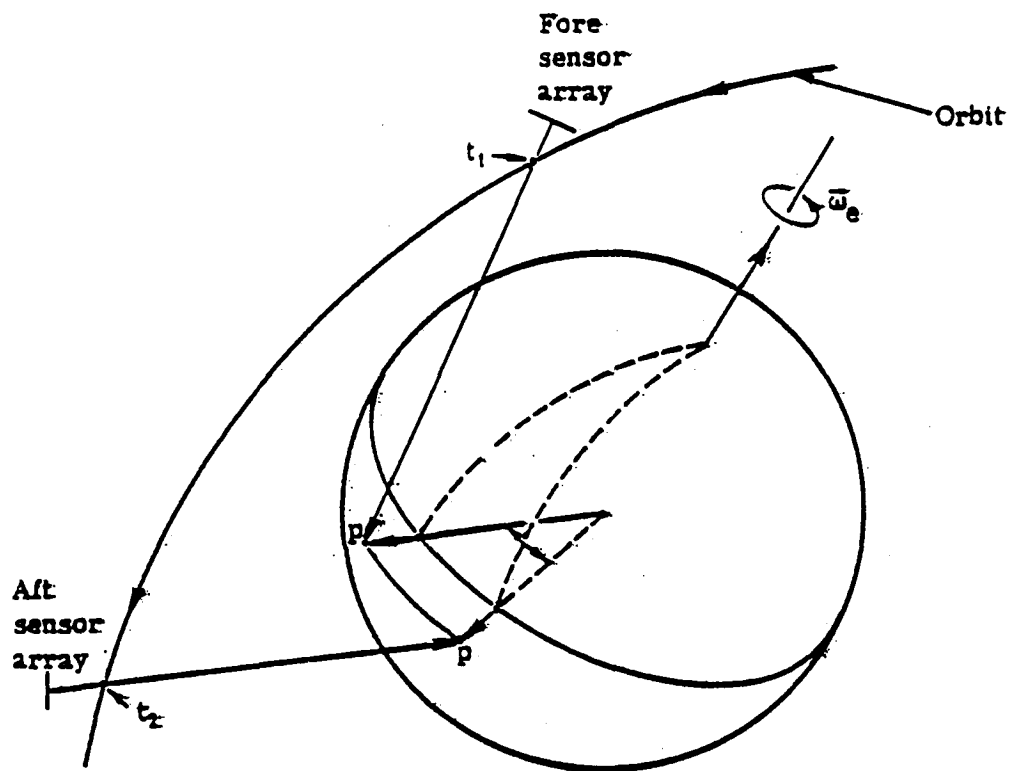


FIGURE 4

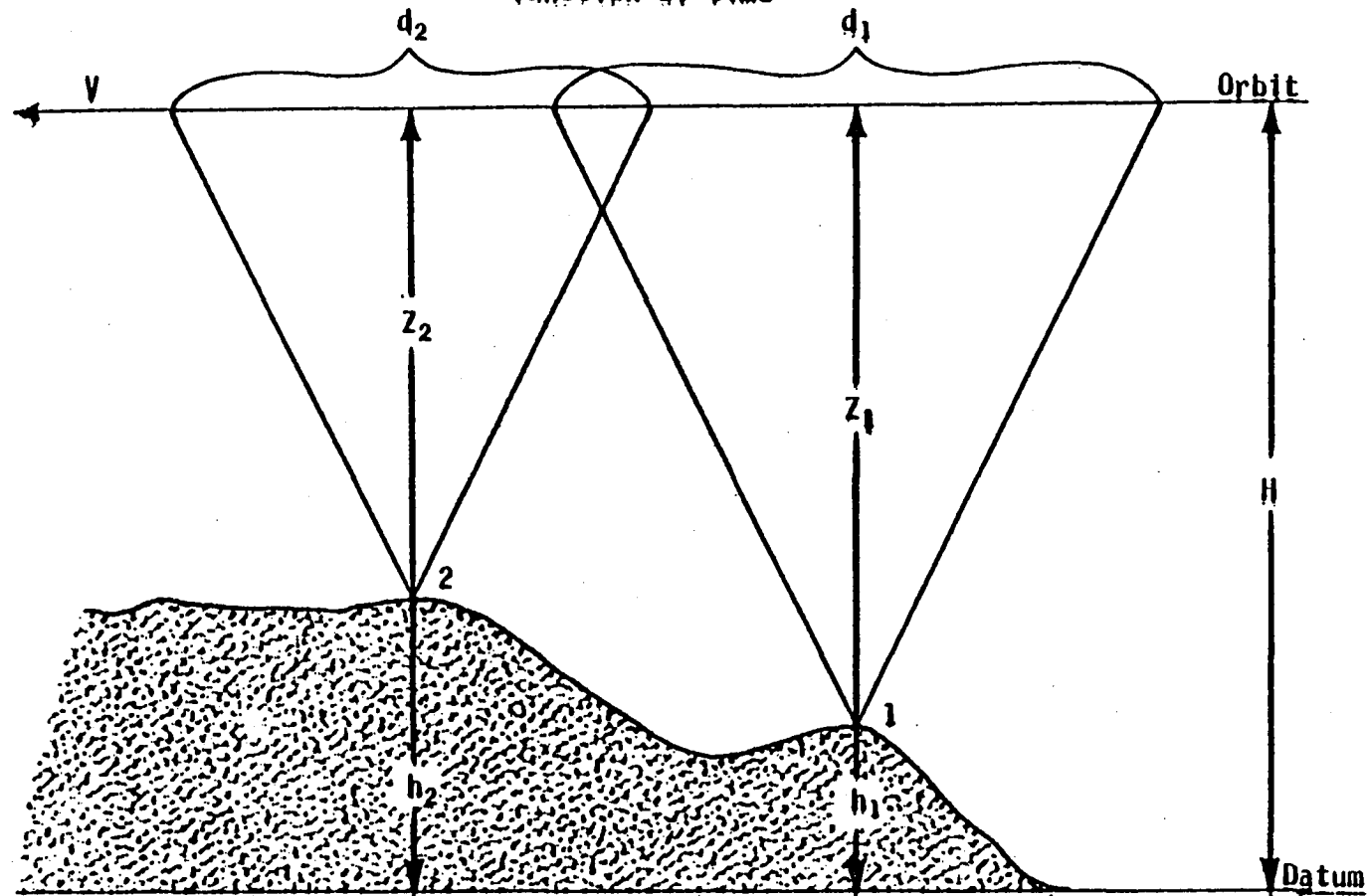


Mapsats Epipolar Acquisition Geometry

FIGURE 5

Mapsat Epipolar Plane Geometry

Elevation difference as a function of time



V = satellite velocity (constant)
 t_1, t_2 = time to stereo image points 1 and 2
 $d_1 = V \cdot t_1$ dist. moved to acquire stereo
 $d_2 = V \cdot t_2$ data of points 1 and 2

H = satellite altitude above datum (constant)
 h_1, h_2 = elevation of points 1 and 2 above datum
 Z_1, Z_2 = distance from orbit to points 1 and 2

k, K = constants
 $h_1 = H - Z_1 = H - k \cdot d_1 = H - k \cdot V \cdot t_1$
 $h_2 = H - Z_2 = H - k \cdot d_2 = H - k \cdot V \cdot t_2$
 $h_2 - h_1 = K \cdot (t_2 - t_1)$

$\Delta h, \Delta t$ = elevation and time differences, points 1 and 2
 $\Delta h = K \cdot \Delta t$

References

1. Katz, A. H., 1952, "Height Measurements with the Stereoscopic Continuous Strip Camera," Photogrammetric Engineering, Vol. 18, No. 1, pp. 53-62, March 1952.
2. Elms, D. G., 1962, "Mapping with a Strip Camera," Photogrammetric Engineering, Vol. 28, No. 4, pp. 638-653, September 1962.
3. Helava, U. V., and Chapelle, W. E., 1972, "Epipolar-Scan Correlation," Bendix Technical Journal, pp. 19-23, Spring 1972.
4. Scarano, F. A., and Brumm, G. A., 1976, "A Digital Elevation Data Collection System," Photogrammetric Engineering and Remote Sensing, Vol. 42, No. 4, pp. 489-496, April 1976.
5. Welch, R., and Marko, Wayne, 1981, "Cartographic Potential of a Spacecraft Linear-Array Camera System: Stereosat," Photogrammetric Engineering and Remote Sensing, Vol. 47, NO. 8, pp. 1173-1185, August 1981.
6. Chevrel, M., Courtois, M., and Weill, G., 1980, "The Spot Satellite Remote Sensing Mission," Photogrammetric Engineering and Remote Sensing, Vol. 47, pp. 1163-1171, August 1981.
7. NASA, Goddard Space Flight Center, 1980, MLA Instrument Definition Study Statement of Work: NASA (RFP5-31522/230) December 3, 1980.
8. Welch, R., 1979, "Acquisition of Remote Sensor Data with Linear Arrays," Photogrammetric Engineering and Remote Sensing, Vol. 45, No. 1, pp. 44-46, January 1979.
9. Thompson, L. L., 1979, "Remote Sensing Using Solid-State Array Technology," Photogrammetric Engineering and Remote Sensing, Vol. 45, No. 1, pp. 47-55, January 1979.
10. Tracy, R. A., and Noll, R. E., 1979, "User-Oriented Data Processing Considerations in Linear Array Applications," Photogrammetric Engineering and Remote Sensing, Vol. 45, No. 1, pp. 57-61, January 1979.
11. Wight, R., 1979, "Sensor Implications of High Altitude Low Contrast Imaging," Photogrammetric Engineering and Remote Sensing, Vol. 45, No. 1, pp. 63-66, January 1979.
12. Colvocoresses, A. P., 1979, "Multispectral Linear Arrays as an Alternative to Landsat-D," Photogrammetric Engineering and Remote Sensing, Vol. 45, No. 1, pp. 67-69, January 1979.
13. Welch, R., 1980, "Measurements from Linear Array Camera Images," Photogrammetric Engineering and Remote Sensing, Vol. 46, No. 3, pp. 315-318, March 1980.

References (Con't)

14. Colvocoresses, A. P., 1979, "Proposed Parameters for Mapsat," Photogrammetric Engineering and Remote Sensing, Vol. 45, No. 4, pp. 501-506, April 1979.
15. Itek Optical Systems, Div. of Itek Corp., 1981, "Conceptual Design of an Automated Mapping Satellite System (MAPSAT)," Final Technical Report, Feb. 3, 1981, prepared for U.S. Geological Survey: U.S. Department of Commerce, National Technical Information Service, PB81-185555.
16. Snyder, J. P. 1981, "Geometry of a Mapping Satellite" Photogrammetric Engineering and Remote Sensing _____ 1982.
17. Junkins, John, Strikwerda, T. E., and Kraige, L. G., 1978, "Star Pattern Recognition and Spacecraft Attitude Determination, Phase 1," Prepared for U.S. Army Engineering Topographic Laboratories (ETL-0173), Virginia.
18. Mahoney, W. C. 1981, "DMA Overview of MC&G Application of Digital Image Pattern Recognition" Presented at SPIE Tech. Symp East, April 1981.
19. Colvocoresses, A. P., 1981, "Mapsats Compared to Other Earth-Sensing Concepts," Proceedings of the Fifteenth International Symposium on Remote Sensing of the Environment", Ann Arbor, Mich., May 1981.

DESIGN TRADEOFFS FOR A MULTISPECTRAL LINEAR ARRAY (MLA) INSTRUMENT

Aram M. Mika
Santa Barbara Research Center, Goleta, CA

Abstract

The heart of the MLA design problem is to develop an instrument concept which concurrently provides a wide field-of-view with high resolution, spectral separation with precise band-to-band registration, and excellent radiometric accuracy. Often, these requirements have conflicting design implications which can only be resolved by careful tradeoffs that consider performance, cost, fabrication feasibility and development risk. The key design tradeoffs for an MLA instrument are addressed in this paper, and elements of a baseline instrument concept are presented.

Background

The NASA Landsat program has been thoroughly successful to date, based on the imagery produced by the Multispectral Scanner. Currently, with spacecraft integration underway for the Thematic Mapper protoflight instrument, the second generation of Landsat is approaching fruition. In light of these developments, the design challenge for a third-generation MLA sensor is to conceive an instrument that will provide extraordinary benefits that are well worth the development cost.

The strength of the MLA concept emanates from the pushbroom image-formation approach, which offers some fundamental improvements over opto-mechanically scanned instruments. A dramatic advantage of the MLA sensor is the increased dwell time that can be used to improve signal-to-noise, spectral resolution and spatial resolution simultaneously. The design latitude in all three parameters is such that only the optical blur circle need constrain the spatial resolution. Thus, an outstanding optical design is required to exploit the pushbroom approach. However, higher resolution by itself is a modest justification for a new development program. To fully realize the potential benefits of the MLA concept, the instrument design must be mechanically simple, with a minimal number of moving parts. Otherwise, the promised reliability advantage of the pushbroom approach may not be achieved.

Moreover, the instrument must provide excellent spatial (band-to-band) registration and radiometric accuracy, as well as minimum geometric distortion. Spectral registration and geometric fidelity are essential for accurate color-composite imagery. Object-space registration is also extremely important for successful crop assessment and classification, since the precise radiometric accuracy required for this task is significantly degraded by misregistration. That is, radiometric performance and band-to-band registration are cross-coupled. With inherent band-to-band registration at the instrument, a large segment of the user community might be served by data that come directly from the spacecraft, or with a minimal amount of expensive and time-consuming ground processing that delays delivery of data to the customer. This capability is pivotal for many applications, such as crop-yield assessment or evaluation of transient-pollution phenomena, where the utility of Landsat data declines sharply with time.

Quantitative performance goals have been established for MLA by the NASA Goddard Space Flight Center, which has been guiding MLA design studies at several companies, including SBRC.¹ These design objectives, summarized in Table 1, serve as a point of departure for the tradeoffs discussed in the following section.

Table 1. MLA Design Objectives

Spectral Bands (μm)	IFOV ^A (m)	SNR (min)	MTF ^B	Field-of-View	15° Cross-Track 1+20 IFOV In-Track
1. 0.45 - 0.52	10-15	73	>0.30	Spectral-Band Registration	<20 IFOV In-Track Separation (Bands 1 + 6) ± 0.1 IFOV Pixel Position ± 0.2 IFOV Parallelism Within Bands (1-4) and (5, 6) ± 0.5 IFOV Parallelism Bands (5, 6) W.R.T. (1 + 4)
2. 0.52 - 0.60	10-15	149	>0.30		
3. 0.63 - 0.69	10-15	126	>0.30		
4. 0.76 - 0.90	10-15	158	>0.30		
5. 1.55 - 1.75	20-30	54	>0.30		
6. 2.08 - 2.35	20-30	77	>0.30		
Notes: A. Detector IFOV at 705 km. Altitude B. At Nyquist Frequency				Pointing Modes: $\pm 30^\circ$ Cross-Track 0, $\pm 26^\circ$ In-Track (Stereo)	

Table 1. MLA Design Objectives (Continued)

RADIOMETRIC ACCURACY	$\pm 5\%$ ABSOLUTE W.R.T. NBS STANDARDS $\pm 1\%$ RELATIVE INTERBAND $\pm 0.5\%$ RELATIVE INTRABAND
DATA COMMUNICATION	2 x 150 MBPS VIA TDRSS 1 x 100 MBPS DIRECT DOWNLINK
SPACECRAFT INTERFACE	COMPATIBLE WITH MULTIMISSIION SPACECRAFT (MMS), STS LAUNCH

Design tradeoffs

The system-level tradeoffs, which translate mission requirements into a baseline instrument configuration, establish the basic design parameters and design philosophy for the MLA instrument. The heart of the MLA design problem is to develop a design approach that embodies the following features:

1. Wide field-of-view with high resolution
2. Spectral separation and precise band-to-band registration
3. Stereo and cross-track pointing modes
4. Radiometric accuracy
5. On-board signal/data processing
6. High reliability - minimum number of moving parts.

Any one of these objectives might be straightforward to attain, but it is challenging to provide all these features in a single instrument, because these requirements have conflicting and interdependent design implications. For example, the optical design strongly influences the spectral separation-registration technique, the stereo/cross-track pointing method and the design of the on-board calibration source. Before delving into the details of these hardware tradeoffs, we shall begin by presenting the first-order sizing parameters for the instrument.

Instrument sizing

Detector pitch, optical focal length, aperture size and integration time are the basic parameters that determine the physical size and radiometric performance of the instrument. These numbers follow directly from the IFOV, MTF and SNR specifications. Since detector technology is the dominant feasibility driver for the MLA instrument, detector size and density constraints are a good place to begin the sizing analysis. For a given ground-sampling interval and IFOV, the focal length (and instrument size and cost) is reduced in direct proportion with detector pitch and size. Although SNR is degraded as detector size is decreased, this is not a driving constraint on MLA where ample dwell time is available to build SNR. Therefore, the smallest detector size and pitch, consistent with acceptable processing yield and cost, are desirable for MLA.

Once the optimal detector pitch is selected, the focal length is immediately determined from IFOV and sampling interval requirements. Then, the optical aperture size (and hence f-number) is chosen to meet MTF and SNR requirements. This instrument-sizing procedure is illustrated in Figure 1. These sizing tradeoffs lead to an instrument with 12 μm square detectors on 15 μm centers (bands 1 to 4), 705 mm focal length, a 190.5 mm aperture diameter, and other parameters as shown in Table 2. Additionally, the 705 mm focal length yields a fortuitous relationship between dimensions on the ground and on the focal plane: 1m on the ground corresponds to 1 μm on the focal plane (for the 705 km orbit).

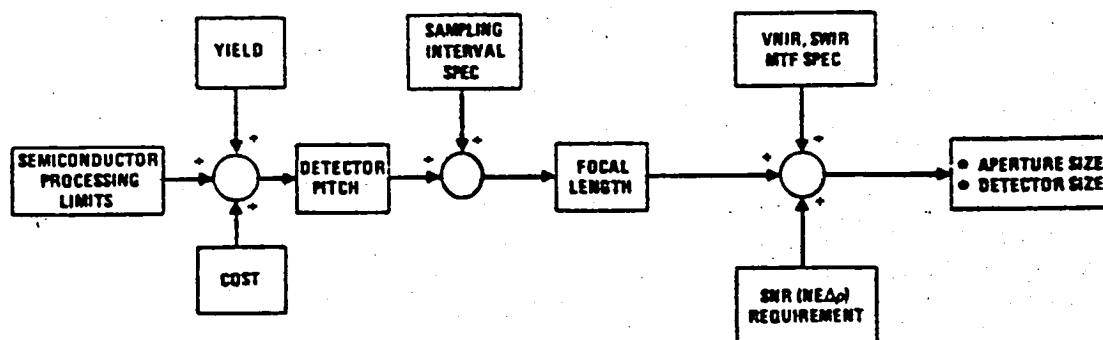


Figure 1. Instrument sizing procedure

Table 2. System Parameter Summary

Aperture Diameter	190.5 mm
Focal Length	705 mm
f/No.	3.7
IFOV at 705 km	12m (17.0 μ rad) Bands 1 + 4
	25m (35.5 μ rad) Bands 5, 6
Sampling Interval	15m (21.3 μ rad) Bands 1 + 4
	30m (42.6 μ rad) Bands 5, 6
Number of Detectors	61,440
Data Rate (Uncompressed)	208-570 MRPS

Configuration tradeoffs

The sizing parameters established above set the stage for configuration tradeoffs. This section summarizes the principal packaging considerations, identifies the most promising candidate, and presents the rationale for that selection.

The overall instrument configuration appears to be most strongly influenced by the following factors, listed in the order of their importance to the selection process:

1. Stereo mode implementation
2. Cross-track mode implementation
3. Radiative cooler field-of-view
4. Spacecraft structural integration

Three generic configurations are possible, with optical systems whose principal axes are oriented along the orbital track, cross track, and nadir directions. Figure 2 illustrates these alternatives, and the relative merits and flaws of each approach are also noted in the figure.

	STEREO MODE IMPLEMENTATION A	CROSS TRACK MODE IMPLEMENTATION B	RADIATIVE COOLER IMPLICATIONS C	SPACECRAFT INTEGRATION D	COMMENTS
OPTICAL AXIS ALONG TRACK					<ul style="list-style-type: none"> • DIFFICULT TO TEST • POOR STRUCTURAL COUPLING TO SPACECRAFT • CROSS PRODUCT OF INERTIA DIFFICULT TO MINIMIZE
OPTICAL AXIS CROSS TRACK					<ul style="list-style-type: none"> • EASIER TO TEST THAN (1) • CONSTRICTION NEAR FPA • BETTER STRUCTURE THAN (1)
OPTICAL AXIS ALONG NADIR					<ul style="list-style-type: none"> • REQUIRES EXTERNAL PUPIL • MIRRORS LARGER THAN (3)
					<ul style="list-style-type: none"> • WORST CONFIGURATION • RADIATOR MOVES ON 2 AXIS

Figure 2. Configuration tradeoffs

Configuration number three (with the optical axis in the cross-track direction), when coupled with an optical design having a convenient entrance-pupil location, was selected. This configuration provides an excellent combination of simplicity and compactness; articulated radiators, rotating sensors, oversized mirrors and other undesirable features are absent.

Optical design tradeoffs

Performance requirements in the areas of pointing capability, field of view (FOV), resolution, spectral coverage, radiometric accuracy and spectral registration are highly coupled and contain important implications for the MLA optical form. As presented in Table 3, a variety of additional optical system characteristics strongly affect the design of other MLA subsystems. For example, a flat focal plane will greatly facilitate detector-array assembly and alignment. The use of a relayed optical form will improve stray light rejection and simplify on-orbit detector calibration. The optical form should permit compact system packaging consistent with MMS payload capabilities, and fabrication and alignment tolerances must be realistic in order to guarantee satisfactory on-orbit optical-system resolution. An unobscured system with adequate performance margin will simplify scaling to sensors with improved resolution, and an all-reflective telescope will permit future inclusion of LWIR spectral bands. Minimal geometric distortion will reduce post-processing requirements for some applications. Finally, telecentricity (normal incidence for all chief rays in the field of view) is an extremely important feature, since it eliminates angular variations in coating performance (for dichroic and spectral-bandpass filters).

Table 3. MLA Optical System Desired Characteristics

Desired Feature	Motivation
Flat Focal Plane	Simplified alignment and assembly for FPA detectors
Telecentricity	Low focal plane angles of incidence, simplified spectral separation, uniform filter performance
Relayed Optical Form	Intermediate image: simplified on-orbit calibration and stray light rejection
Real Entrance Pupil	Reduced Stereo mirror size
Unobscured Aperture	Improved optics MTF
Compact Packaging	Maintain compatibility with MMS
Feasible Optical System Tolerances	Simplify sensor integration, reduce risk
All-Reflective Telescope	LWIR growth capability
Performance Margin	Simplify scaling to 10m/20m system
Minimal Geometric Distortion	Reduced post-processing requirements

A variety of telescope design forms have been considered for use in the MLA sensor. These optical designs have been evaluated against the set of performance requirements and desired features listed above. The design form options considered for MLA are depicted in Figure 3. The various Schmidt designs and the four-mirror telecentric system are the principal design candidates. However, the Schmidt approaches have serious flaws ranging from non-telecentricity and curved focal surfaces (for some variants), to unfavorable pupil locations and intractable pointing-mirror sizes. For a complete exposition of the key tradeoff issues, the reader is directed to Reference 2.

The four-mirror telecentric design (Figure 3.1-5c) has been selected as the MLA optical system baseline because of its excellent combination of optical performance and desirable features. Main advantages of this form are its real entrance pupil, intermediate image, flat focal plane, and telecentricity. The folded version of this telescope provides compact packaging, and image quality (10-12 μ rad 80% blur diameter in band 3) is better than MLA specifications. Moreover, this all-reflective design has an unobscured aperture. Although the as-designed optical performance of this system is outstanding, fabrication feasibility, alignment sensitivity and on-orbit alignment stability are also important. Each of these issues has been addressed in depth, as discussed in Reference 2. This work has shown that the four-mirror telecentric system is a thoroughly workable design for MLA. Hughes has demonstrated (with hardware) a similar four-mirror system with off-axis aspheric elements, and the measured performance of this system is as predicted for the design. A key factor in achieving the designed performance for these systems is a Hughes-developed computer-aided optical alignment method which ensures optimal alignment of the mirrors and permits relaxation of figure tolerances.

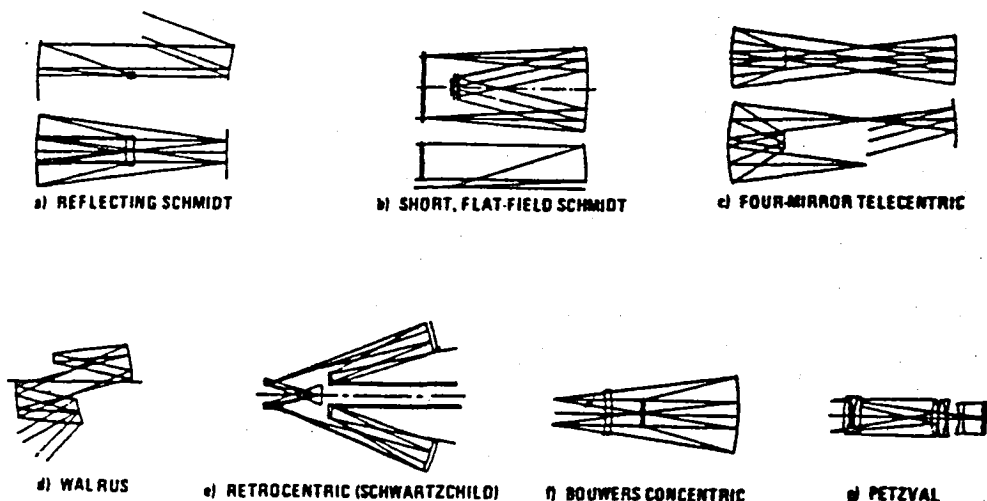


Figure 3. Telescope design alternatives

Spectral separation and registration

The requirements for spectral separation and band-to-band registration are significant considerations for the MLA instrument. The spectral-separation approach has implications that ripple through the system, in the areas of optical design, detector packaging, cooling, structural design and signal/data processing.

Two fundamental points of departure for selecting a spectral-separation approach hinge on the desirability of maintaining true object-space registration and on the location of the visible-near infrared (VNIR) and short-wave infrared (SWIR) focal planes. The key tradeoff in achieving spectral registration centers on how the detectors are mounted. The mounting of the detectors is affected by the choice between the two different philosophies for registration of the MLA bands; time delay between parallel rows of detectors or spectral beam-splitting of the incoming energy.

The time-delay approach leads to a misregistration of 0.2 IFOV at the edge of the field of view, even with ideal (constant focal length) optics. Thus, object-space registration is not achieved, and extensive corrective data processing would be required to produce the registered imagery needed for many applications. Therefore, a beamsplitter utilizing dichroic filters has been selected, as illustrated in Figure 4. This approach provides coincident images in all six bands.

The preferred tilted-plate beamsplitter approach leads to the next major tradeoff; to mount all the detectors on a common substrate and cool the entire assembly or to cool only the two SWIR bands. If only the SWIR bands are cooled then they must be registered with an ultra-low hysteresis mount or servoed into a position of registration with the visible detectors. Cross-track registration becomes another issue because the cooled detectors may have a coefficient of expansion that is large enough to misregister detectors along the length of the array relative to the corresponding warm VNIR arrays. For these and other reasons it appears that cooling all the detectors on a common, isothermal substrate minimizes misregistration due to structural compliance and differential thermal effects.

Radiometric accuracy and calibration tradeoffs

Achieving the required radiometric precision for MLA raises several important issues regarding detectors, signal-processing, and calibration approach. Much of the radiometric-accuracy issue hinges on the performance of the detectors, particularly for the SWIR bands, so this is a good place to begin the discussion. The detector material and temperature directly affect radiometric performance because responsivity and $1/f$ noise (which are material and temperature dependent) influence SNR and calibration frequency. Moreover, the selection of a SWIR detector material is tightly coupled to other aspects of the instrument design, since the operating-temperature requirements influence the cooler size, mechanical layout and spectral-registration approach.

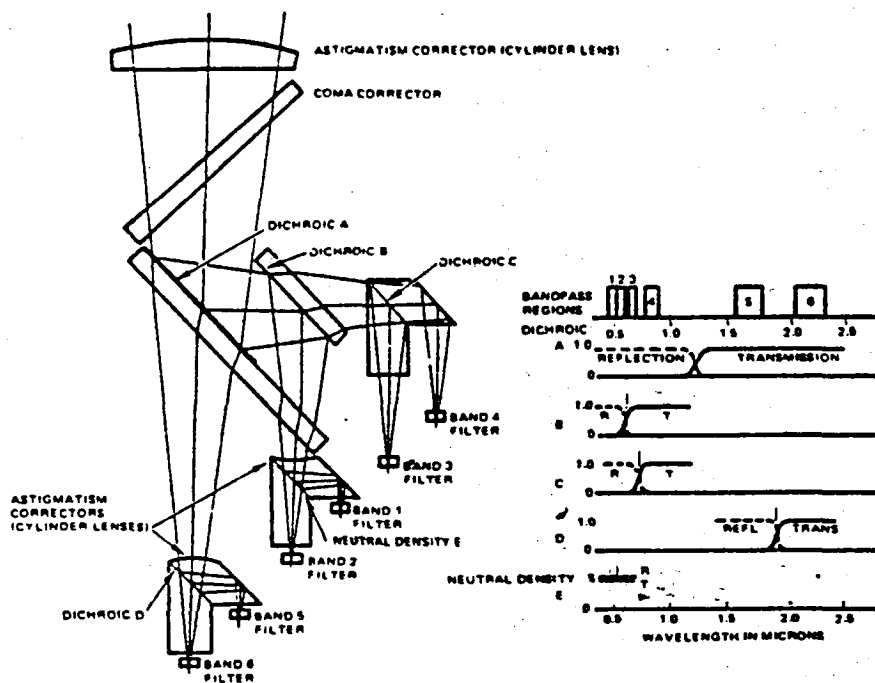


Figure 4. Beamsplitter concept

The preferred spectral-separation/registration approach, with a six-band colocated, isothermal focal-plane assembly, poses some temperature restrictions, if reasonably-sized radiative coolers are employed. Specifically, a complete six-band focal-plane assembly requires on the order of 5W of cooling capacity, including the parasitic heat loads due to cables, supporting structures, and the like. With a tractably-sized radiator, say with an area of 0.2 m^2 , focal-plane temperatures as low as 155K are achievable. In this operating-temperature regime, the detector material of choice is HgCdTe. Palladium silicide, another candidate detector material, requires a much lower temperature (circa 110K) and has poor responsivity. However, if the $1/f$ noise properties of HgCdTe introduce radiometric-drift errors that must be corrected by frequent recalibration — or even a chopper assembly — then the attractiveness of the isothermal-FPA approach and HgCdTe SWIR detectors comes into question.

The crux of this issue is the potential requirement for an opto-mechanical chopper. Incorporating a chopper would violate the no-moving-parts design philosophy of MLA. While an MLA instrument without a chopper would still have movable pointing mirrors, the fundamental imaging operation of the instrument would not depend on any rotating or oscillating components. Indeed, if a chopper were necessary, the entire issue of a scanned versus pushbroom instrument would merit reexamination, since the perceived reliability advantage of the pushbroom design might be eliminated. In addition to the severe reliability issue inclusion of a chopper would reduce SNR in proportion to the effective transmission loss caused by periodic blanking of the detectors.

In view of the pivotal nature of this issue, a comprehensive analysis of drift and $1/f$ noise was undertaken. This analysis was verified by measured data, and the results of this work indicate that drift in the SWIR (as well as the VNIR) bands will be less than 0.05% of full scale during an orbital period when HgCdTe detectors are operated at 175K. This drift level is well within the GSFC radiometric-accuracy specification. The predicted drift is also well below the even more stringent ~ 0.2% uniformity required to avoid cosmetic defects (striping) in the imagery. Thus, a chopper mechanism is unnecessary.

Other tradeoffs affecting radiometric accuracy, including the design and location of calibration sources, the precision of A/D quantization and subsequent on-board calibration correction, have also been addressed.

Instrument concept

The design tradeoffs outlined above have led to the instrument concept illustrated in Figure 5. This figure is a photograph of a full-scale mockup fabricated at SBRC as an aid for visualizing the key elements of the instrument. Figure 6, which is a cutaway drawing

corresponding to the mockup photo, reveals the internal details of the sensor. The mockup does not show the instruments' covers or stereo mirror module, and these additional items are depicted in Figure 7.

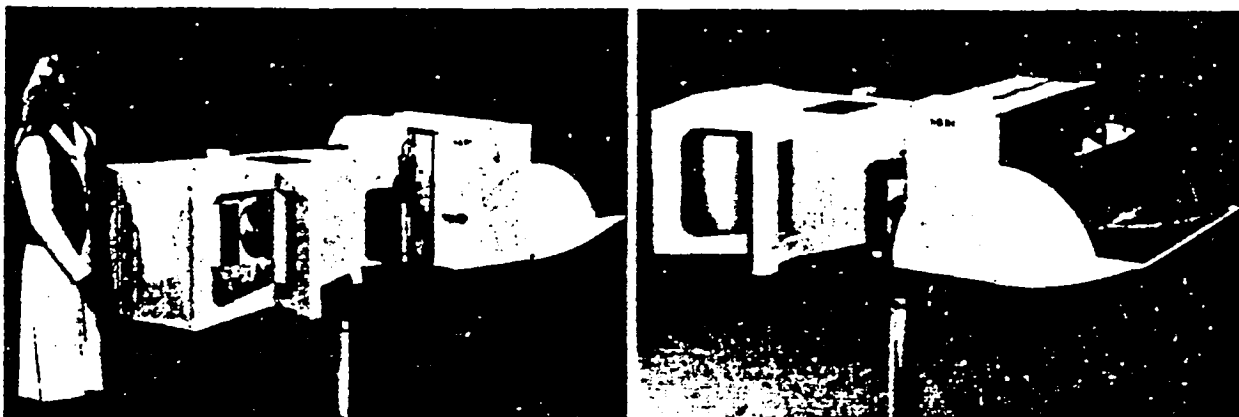


Figure 5. Multi-spectral linear array (MLA) instrument full-scale mock-up

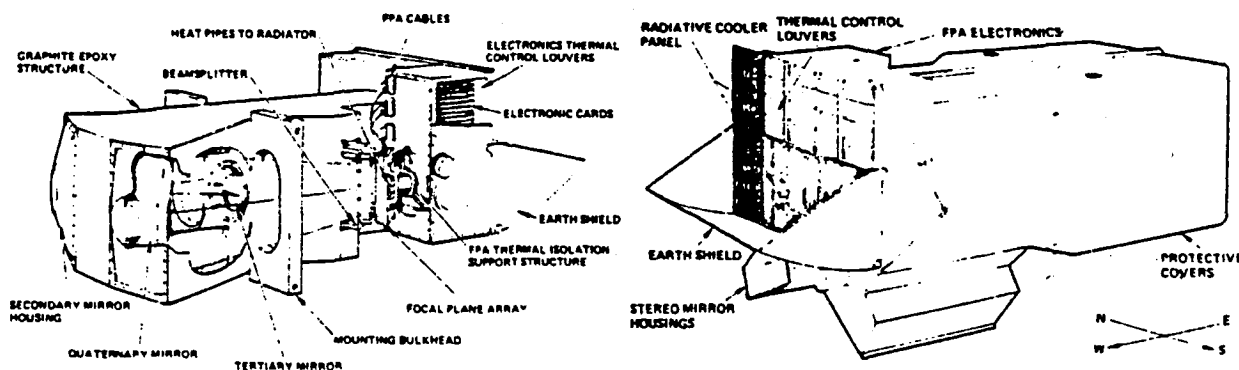


Figure 6. MLA instrument cutaway view

Figure 7. MLA instrument with covers and stereo module

The telescope and beamsplitter have been described in the preceding section; highlights of other subsystems are presented below.

Focal plane assembly

The baseline focal-plane design consists of six color bands arranged in stairstep fashion as dictated by the beamsplitter design. The focal plane is modular at the band level, with each assembly electrically independent of the others, as illustrated in Figure 8. Thus, the band assemblies can be functionally tested separately and in parallel. With special tooling, the detector modules are precisely located on a substrate, and these completed band assemblies in turn mount to a monolithic staircase structure which has diamond-machined mounting surfaces that provide the required positioning accuracy for the detector arrays. The staircase is thermally coupled to the radiative cooler via two redundant heat pipes. Although the focal-plane temperature is controlled at 175K, the cooler has sufficient design margin to achieve temperatures as low as 155K with the nominal 5W total heat load, as discussed earlier.

On the focal plane, bands 1 through 4 employ silicon photodiodes, while HgCdTe photodiodes are used for bands 5 and 6. The two SWIR detector arrays each consist of 6,144 detectors, and the four VNIR detector arrays each have 12,288 detectors. Each of the six band-level assemblies are composed of precisely-buffed modules. To read out all the more than 60,000 detector signals, each module has a corresponding multiplexer (MUX). In the VNIR bands, the MUX and detector array are a monolithic unit. In the SWIR bands, a hybrid structure is used: HgCdTe detectors with a silicon MUX chip.

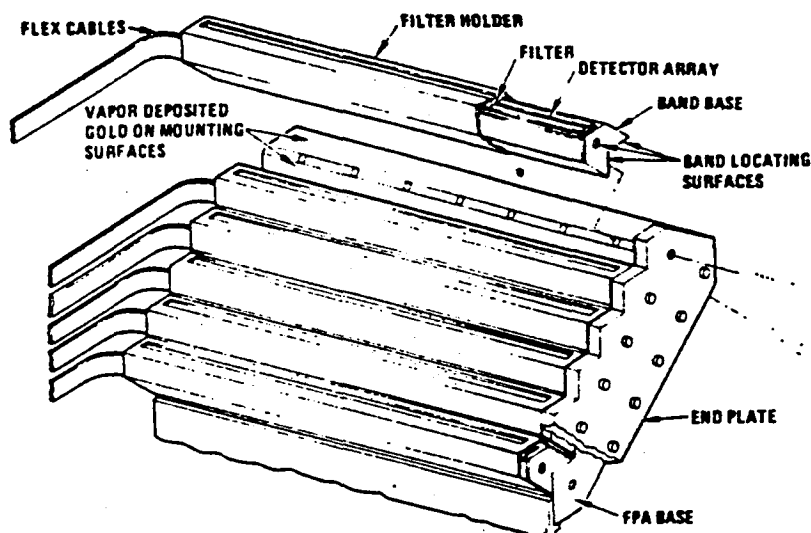


Figure 8. Focal plane assembly

Electronics

The existence of a large array of detectors and simultaneous signal output from many modules pose significant problems in signal processing, such as speed and reliability. An attractive solution is a highly distributed hardware design, involving many replicated electronic systems working in parallel. For the purposes of signal processing, the focal plane was organized into 48 sections, or "slices," each containing its own independent processing chain. Each slice consists of the aforementioned output multiplexing devices, as well as associated analog-to-digital converters, and digital signal processing circuits. This distributed approach is the key to meeting reliability objectives while fulfilling the high-speed signal-processing requirements for MLA. The architecture provides additional benefits in terms of low power dissipation with correspondingly simple thermal control. Moreover, the parallel approach yields thoroughly tractable data rates through the signal-processing chain illustrated in Figure 9.

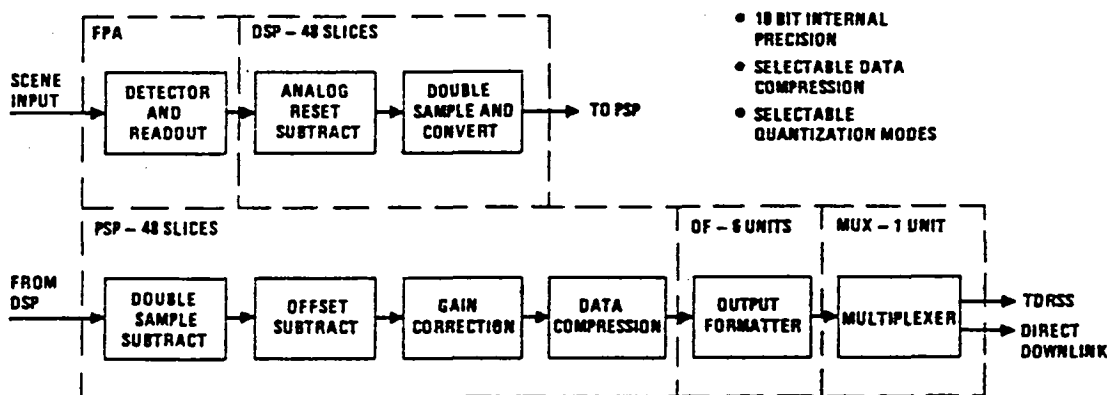


Figure 9. Distributed signal processing from FPA to output

The processing starts at the FPA, with the first-level multiplexing. Under the supervision of ten timing and control (TC) circuits, all 48 FPA slices are processed simultaneously. From the FPA, signals enter the detector signal processor (DSP), where ten-bit A/D conversion is performed in an interleaved fashion that obviates the need for buffer memory. Under microprogram control, the DSP/TC provides the variable-rate timing for different orbits.

The digital signals from the DSP can be transmitted uncompressed at full ten-bit resolution from the 705 km orbit. However, at the lower orbits (283 and 470 km), the short detector sample time leads to data rates that exceed TDRSS capacity. Therefore, in addition to detector gain and offset correction, the programmable signal processor (PSP) provides data compression. Selectable compression modes include standard differential pulse code modulation (DPCM) as well as a Hughes-developed advanced DPCM (ADPCM), which combines DPCM with a

predictive coder. ADPCM will provide lossless data compression for many scenes. Various quantization modes are available which take advantage of the ten-bit A/D converter precision. For example, one mode allows increased precision over a reduced dynamic range. From the PSP, the 2.3 to 6.3 MHz parallel data (depending on the orbit) enter the output formatter where they are organized for serial transmission. Additionally, there is a command processor which orchestrates control and telemetry for the entire instrument.

On-board calibration

The on-board calibration concept includes a controlled calibration source at the intermediate image plane between the folding mirror and the secondary mirror, a movable solar diffuser that can be positioned in front of the entrance pupil, and a backup collimator located within the stereo-mirror module. The location of the source allows for system calibration from the secondary mirror to the video output, while the solar diffuser provides an end-to-end calibration reference that also encompasses the mirrors that precede the controlled calibration source. However, the reflectance properties of these mirrors will change slowly, so relatively-infrequent solar calibration will be adequate.

The principal on-board calibrator is a cylindrical integrating source (CIS), which consists of a metal cavity with thirty incandescent lamps distributed along the length of the cylinder. The interior of the cavity, which has a diffuse surface coating, serves to average or "integrate" the lamp illumination, so that nearly uniform radiance appears at the exit slit. During calibration, the folding mirror near the intermediate image plane is rotated so that the CIS illuminates the focal-plane assembly (FPA). A closed-loop silicon-photodiode sensor circuit controls the CIS at six discrete light levels, which are obtained by activating different numbers of lamps.

Summary

The principal design tradeoffs for an MLA instrument encompass the opto-mechanical layout, spectral separation/registration approach, detector selection and signal-processing architecture. These tradeoffs led to an instrument concept employing a four-mirror-telecentric telescope, coupled with a six-way beamsplitter, an isothermal focal-plane assembly and highly distributed signal processing. Key features of the concept include object-space registration of all six spectral bands, stereo and cross-track pointing via compact mirrors, and a small overall envelope compatible with the multimission spacecraft.

Acknowledgements

The MLA instrument study represents the cooperative effort of over forty people at Hughes/SBRC, as listed below, and it is this collective work that has been summarized in the preceding paper. The work reported here was supported in part by NASA Contract No. NAS5-26591, under the technical direction of Mr. H.L. Richard of the Goddard Space Flight Center.

MLA Study Contributors

Cliff Adams	Brian Cohn	Jim Hesson	Tony Schoepke
Ray Amador	Lacy Cook	Dave Hitzelberger	Carl Schueler
Gary Barnett	Bob Cooley	Roger Hoelter	Ken Shamordola
Ron Blumenthal	Loren Criss	Ron Kimmel	George Speake
Steve Botts	Roland Davis	Jim Kodak	Irv Sperling
Jack Brooks	Brent Ellerbroek	Lisa Krone-Schmidt	Rich Thom
Elliot Burke	Donna Evett	Jack Lansing	Robert Turtle
Terry Cafferty	Brent Froquet	Dana Morrison	Bert Warren
Dick Chandos	Steve Gaalema	Virginia Norwood	Milt Waxman
Art Chapman	Fred Gallagher	Smitty Preston	Roger Withrington
Still Chase	Ellen Gerardis	Jim Randolph	Jim Young
Dick Cline	George Hershman	Cesar Rodil	

References

1. H.L. Richard, "Solid State Instrumentation Concepts For Earth Resource Observation, Proceedings of the Twentieth Goddard Memorial Symposium, Greenbelt, Maryland, American Astronautical Society, March 1982.
2. "Multispectral Linear Array Optical System Design Study," Santa Barbara Research Center, NASA/GSFC Contract No. NAS5-26591, March 1982.

High density Schottky Barrier IRCCD sensors for SWIR applications at intermediate temperature

H. Elabd, T. S. Villani
RCA Laboratories, Princeton, NJ 08540
J. R. Tower
RCA Advanced Technology Laboratories, Camden, NJ 08102

Abstract

Monolithic 32 x 64 and 64 x 128 palladium silicide (Pd₂Si) interline transfer IRCCDs sensitive in the 1-3.5 μ m spectral band have been developed. This silicon imager exhibits a low response nonuniformity of typically 0.2-1.6% rms, and has been operated in the temperature range between 40-140K.

Spectral response measurements of test Pd₂Si p-type Si devices yield quantum efficiencies of 7.9% at 1.25 μ m, 5.6% at 1.65 μ m and 2.2% at 2.22 μ m. Improvement in quantum efficiency is expected by optimizing the different structural parameters of the Pd₂Si detectors. The spectral response of the Pd₂Si detectors fit a modified Fowler emission model. The measured photo-electric barrier height for the Pd₂Si detector is ~ 0.34 eV and the measured quantum efficiency coefficient, C_1 , is 19%/eV.

The dark current level of Pd₂Si Schottky barrier focal plane arrays (FPAs) is sufficiently low to enable operation at intermediate temperatures at TV frame rates. Typical dark current level measured at 120K on the FPA is 2 nA/cm².

The Pd₂Si Schottky barrier imaging technology has been developed for satellite sensing of earth resources. The operating temperature of the Pd₂Si FPA is compatible with passive cooler performance. In addition, high density Pd₂Si Schottky barrier FPAs are manufactured with high yield and therefore represent an economical approach to short wavelength IR imaging.

A Pd₂Si Schottky barrier image sensor for push-broom multispectral imaging in the 1.25, 1.65, and 2.22 μ m bands is being studied. The sensor will have two line arrays (dual band capability) of 512 detectors each, with 30 μ m center-to-center detector spacing. The device will be suitable for chip-to-chip abutment, thus providing the capability to produce large, multiple chip focal planes with contiguous, in-line sensors.

Introduction

The ambitious goals charted for the next generation of space-borne sensors challenge the state-of-the-art in solid state imaging technology. Next generation satellite surveillance and earth resources sensors will call for visible and infrared focal planes with thousands of detector elements, attendant high fill-factors, and low blemish densities. The requirements are further compounded for infrared focal planes by the desire to operate these large arrays with passive cooling at intermediate temperatures of 120-140K.

The Schottky barrier infrared technology is now at a level of demonstrated performance and maturity that makes it an attractive choice for next generation space-borne sensors. This technology is suitable for Earth sensing applications where moderate quantum efficiency and intermediate operating temperatures are required. Palladium silicide (Pd₂Si) infrared charge coupled device, IR-CCDs, can operate between 40 and 140K and are sensitive in the short-wave infrared band (1-3.5 μ m), whereas platinum silicide (PtSi) IRCCDs, require cooling below 90K but are sensitive in both SWIR and thermal bands (1-5.5 μ m). (A paper on PtSi IR-CCDs is presented in the IR Sensor Technology Session of this conference).

The main advantage of this infrared sensor technology is that it is fabricated using standard integrated circuit (IC) processing techniques and commercial IC grade silicon. It is therefore possible to construct high yield Schottky barrier area and line arrays with high density designs and large numbers of blemish-free elements (>8000). A second principal advantage is that Schottky detectors provide inherently high uniformity. Typical photoresponse non-uniformity is on the order of 0.5% RMS for Pd₂Si detectors. This high uniformity reduces the complexity of electronic compensation, and indeed obviates the need for compensation in many imaging applications. The sensor also exhibits high dynamic range, inherent blooming control, and high linearity at low, as well as, high illumination levels.

The Pd₂Si technology has been evaluated for NASA Multispectral Linear Array sensor applications.* This IR-CCD technology is well matched to the operational requirements of the MLA instrument. [1,2,3]

Schottky barrier sensor technology

The Schottky barrier detector is a photon detector, which utilizes the internal photoemission of "hot" carriers (holes) from metal or metal silicide electrodes into silicon for the detection of optical radiation. Fig. 1 depicts the energy band diagram for the Schottky barrier junction with a simplified one dimensional demonstration of the hole emission process. The back illuminated Schottky barrier detector operates in the spectral window between the band gap of silicon (E_g) and the barrier height (ψ_{ms}). Photons with energies between the bandgap and the barrier height

$$E_g > h\nu > \psi_{ms} \quad (1)$$

will be transmitted through the silicon substrate and will be absorbed in the metal electrode of the junction. The photon energy will increase the potential and kinetic energies of some hole carriers within the metal electrode. Holes traveling in a direction almost normal to the interface with energies larger than the barrier height have a high probability of emission into the silicon substrate.

*Pd₂Si testing and MLA sensor studies funded in part by Ball Aerospace Systems Division as part of the BASD "Multispectral Linear Array Instrument Definition Study", NASA GSFC Contract NAS5-26590, March 1982.

To enhance the number of photocarriers injected in the substrate for a certain Schottky barrier height, it is important to thin down the silicide layer to below the attenuation length of the photoresponse. Improvement in the injection efficiency is usually achieved with thin silicide layers typically in the range between 20-100Å. The improvement is the result of reflections of excited carriers by the back surface at the silicide-dielectric interface, minimal reflection of incident radiation at the silicon-silicide interface and enhanced optical absorption within the attenuation length by the multiple pass induced by an aluminum reflector.

The barrier height determines the cut-off wavelength (λ_c), dark current (J_D), maximum operating temperature (T_{max}), quantum efficiency (Y) and the responsivity (R) of the Schottky barrier detector at low temperature according to the following equations:

$$\lambda_c = 1.24/\psi_{ms} \quad \text{microns} \quad (2)$$

$$J_D = A^* T^2 e^{-q\psi_{ms}/kT} \quad \text{A/cm}^2 \quad (3)$$

$$T_{max} \sim 425 \psi_{ms} \quad \text{K} \quad (4)$$

(for $J_{Dmax} = 10^{-7} \text{ A/cm}^2$)

$$Y = C_1 [h\nu - \psi_{ms}]^2 / h\nu \quad \text{electrons/photon} \quad (5)$$

$$R = C_1 [1 - \psi_{ms} \lambda / 1.24]^2 \quad \text{A/W} \quad (6)$$

where ψ_{ms} is the barrier height in eV, A^* is the Richardson constant, T is the absolute temperature in degrees Kelvin, q is the electronic charge, k is the Boltzmann constant, C_1 is the quantum efficiency coefficient of the modified Fowler emission model, $h\nu$ is the photon energy and λ in the wavelength in microns.

There is a trade-off between the maximum operating temperature and the cut-off wavelength as shown in equations (2) and (4). The maximum operating temperature is calculated from equations (3) and (4) assuming a dark current density of 10^{-7} A/cm^2 , estimated from typical thermal imaging dynamic range and dark current shot noise considerations. This trade-off is demonstrated in Table 1 for different silicide electrodes. Fig. 2 is a graphical representation of this trade-off. The locus of the maximum operating temperature for different wavelengths may be approximated by $\lambda_c T_{max} \sim 527$. Pd_2Si arrays with a $3.5 \mu\text{m}$ cut-off wavelength can operate up to 145K, whereas two types of PtSi arrays with $5.5 \mu\text{m}$ and $6.0 \mu\text{m}$ cut-off wavelength have maximum operating temperatures of 90K and 85K respectively. NiSi , WSi_2 , and TiSi_2 Schottky barrier detectors have cut-off wavelengths around $2.5 \mu\text{m}$ and maximum operating temperature in the range between 180 and 200K. Extended long-wavelength spectral response can be achieved at temperatures below 77K by using IrSi electrodes or shallow barrier lowering p-type implants.

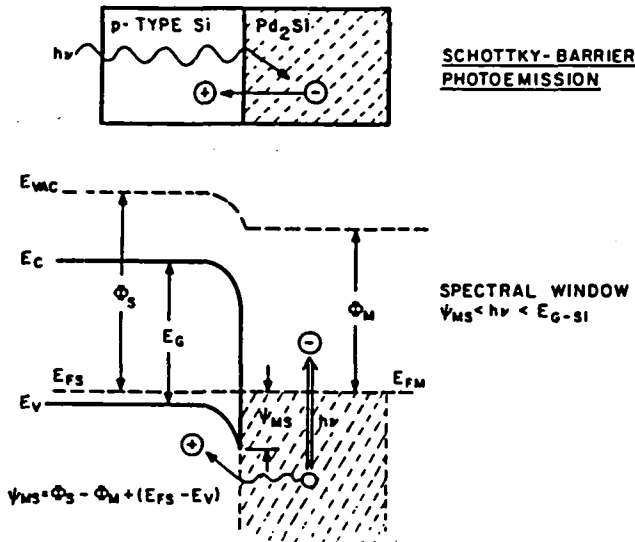


Fig. 1. Energy band diagram.

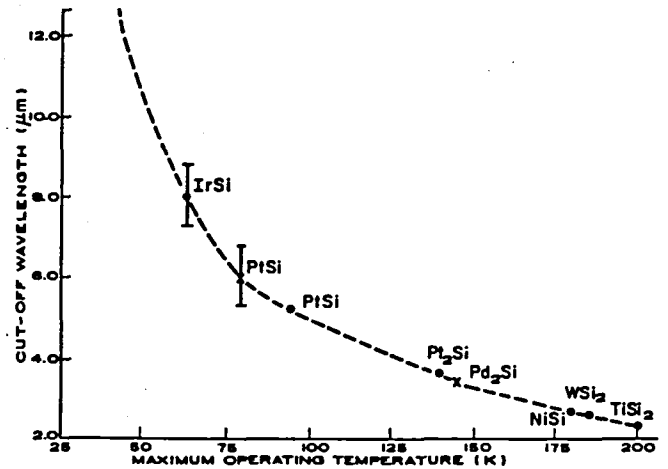


Fig. 2. Maximum operating temperature of various Schottky Barrier technologies

Detector and FPA responsivities

The detector responsivity model (equation 6) corresponding to the modified Fowler emission is shown to fit the measured spectral response of PtSi and Pd_2Si Schottky barrier detectors presented on Fig. 3. By comparing the responsivity data, it is evident that, at the present time, the PtSi detectors are more sensitive in the SWIR band than Pd_2Si -detectors by a factor of 3 or higher. A typical value of the C_1 coefficient of the PtSi detectors is 54.2% as compared to a C_1 coefficient of 19.1% for the first generation Pd_2Si detectors. Further optimization of the quantum efficiency of the Pd_2Si detectors is possible. This should be achieved by improving the C_1 coefficient, which is dependent on the stoichiometry, thickness of the silicide layer, and the junction depth. We project the following quantum efficiencies for Pd_2S detectors in the MLA-SWIR bands: 20.0% at $1.25 \mu\text{m}$, 14.0% at $1.65 \mu\text{m}$ and 5.5% at $2.2 \mu\text{m}$.

TABLE 1. SCHOTTKY BARRIER SPECTRAL RESPONSE - OPERATING TEMPERATURE TRADE-OFF

SILICIDE	MEASURED VALUES OF ϕ_{BN} (eV)	MEASURED OR CALCULATED VALUES OF		
		ψ_{MS} (eV)	λ_c (μm)	MAX. OPERATING TEMP (K) $J_D = 1.0 \times 10^{-7} A/CM^2$
IRSi	0.93-0.94	<0.18	>7.0	55-65
PtSi	0.88	0.19-0.20	~6.0	<90
Pt ₂ Si	0.78	0.35	3.65	140
Pd ₂ Si	0.74	~0.34	~3.6	145
NiSi	0.66	0.46	2.7	180
WSi ₂	0.65	0.47	2.64	185
TiSi ₂	0.60	0.52	2.4	200

The Schottky barrier focal plane (FPA) responsivity, R_{FPA} in Volts/Watt and Volts/Photon can be calculated from the following equations:

$$R_{FPA} = R \frac{t_{int} \tau_o \eta_{ff} G}{C_{FD}} \quad V/W \quad (7a)$$

$$R \text{ (Volts/Photon)} = R_{FPA} \text{ (V/W)} / h\nu \text{ (Joule)} \quad (7b)$$

where R is the detector responsivity as calculated from equation (6), t_{int} is the optical integration time, τ_o is the transmission of the optics, η_{ff} is the fill factor (the ratio of the detector area to the pixel area), G is the gain of the output amplifier and C_{FD} is the capacitance of the floating diffusion amplifier. The FPA responsivity is reduced by the duty factor of the detector if the integration time is less than the frame time.

The high responsivity attained with the 32×64 PtSi-SB area array is demonstrated in Fig. 4. This interline transfer array has a 25% fill factor and operates at a 60 frames per second rate, $G = 0.5$ and $C_{FD} = 0.16$ Pf. For comparison we note here that PtSi SB-FPA responsivity is comparable to that of the InSb-line array with higher fill factor and longer frame time ($t_{int} = 40$ m sec). The InSb-FPA voltage responsivity at $\lambda = 2.65 \mu m$ is 9×10^9 V/W.[4] Whereas the PtSi-FPA responsivity is 3×10^9 V/W at the same wavelength. The PtSi-FPA voltage responsivity in the thermal band is lower and typically in the range between 1.5×10^9 and 1.5×10^8 V/W. This responsivity is still sufficient to resolve $0.1^\circ C$ temperature difference in the PtSi-FPA thermal imagery.

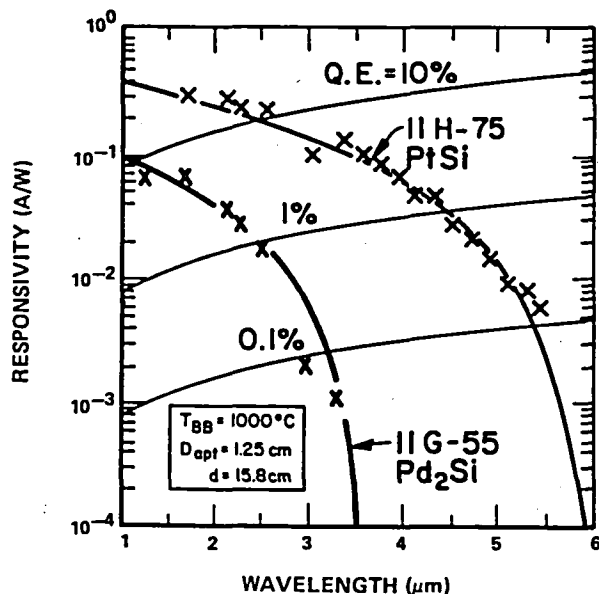


Fig. 3. Measured responsivity of first generation Pd₂Si and recent PtSi detectors.

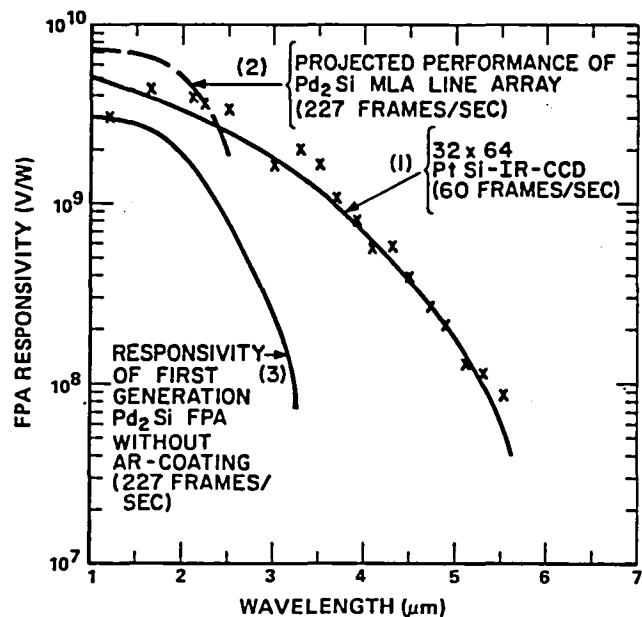


Fig. 4. FPA responsivity for PtSi and Pd₂Si arrays.

flowing from HgCdTe detectors to a CCD in the direct injection mode result in increased sensitivity to CCD input nonlinearity and nonuniformity. Therefore, gate coupling is a preferred readout technique for compound semiconductor SWIR detectors [6] in spite of the inherent fixed pattern noise and nonlinearity associated with that CCD input technique.

The measured optical transfer characteristics for Schottky barrier detectors with vidicon mode readout is illustrated in Fig. 6. This measurement was performed with a 32 x 64 PtSi array (3-5 μm band) at 77K. The net optical densities (τ_0) of the neutral density filters used in the test are indicated below the curve. The change in the output voltage above the value corresponding to the thermal background is linear with irradiance (slope = 1) from the noise equivalent irradiance, until the saturation irradiance of the detector.

Electrical characteristics

The Pd₂Si Schottky barrier detector exhibits ideal electrical characteristics below 200K. Typical Pd₂Si dark current density at 120K is 2 nA/cm² (at a transfer voltage of ~ 10 volts). The dark current of the Pd₂Si detector at 120K is considerably less than that of PtSi at 77K.

The measured dark current-temperature characteristic of PtSi and Pd₂Si Schottky barrier detectors fit the Richardson thermionic emission model (equation (3), as shown in Fig. 7. The curves are fitted to equation (3) to evaluate the electrical barrier height (activation energies): 0.20 eV for PtSi and 0.37 eV for Pd₂Si.

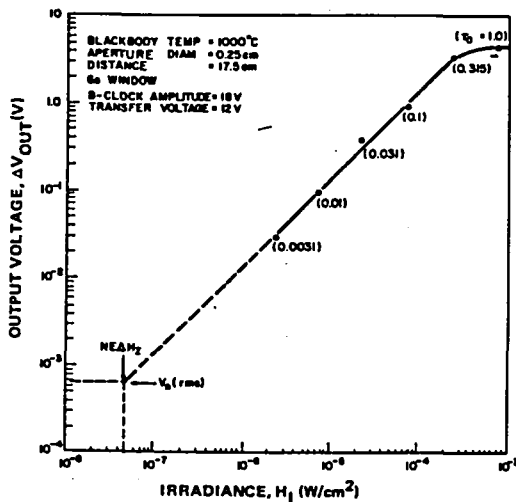


Fig. 6. Photoresponse linearity of Schottky barrier FPAs with vidicon readout mode.

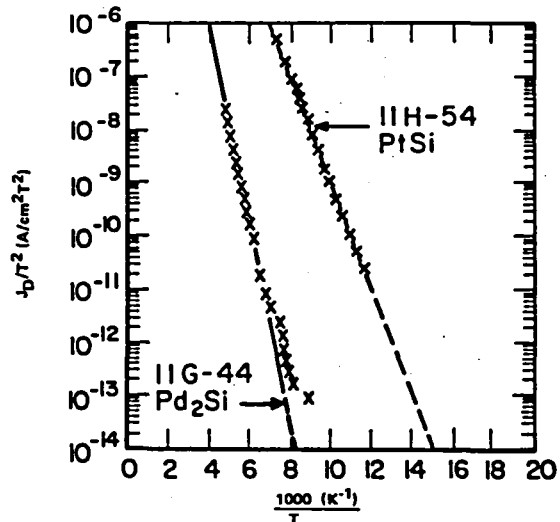


Fig. 7. Measured dark current-temperature characteristics for Pd₂Si and PtSi detectors.

Test imagery

The rms non-uniformity, g , of the output video of the SWIR array may be approximately estimated from this empirical formula:

$$g = \frac{\Delta V_{p-p}}{6 V_{out}} = \frac{\Delta V_{p-p}}{6 m V_m} \quad (10)$$

where ΔV_{p-p} is the peak-to-peak nonuniformity in a frame of video displayed on a scope under uniform illumination, V_{out} is the mean output voltage at the same exposure, m is the filled fraction of the detector well, and V_m is the output voltage corresponding to a full detector well. Measurements made on the 32 x 64 Pd₂Si-FPA at 120K indicate high response uniformity, $g = 0.2\%$ at $m = 0.16$, $g = 0.4\%$ at $m = 0.008$.

Figs. 8 and 9 demonstrate SWIR-Pd₂Si imagery obtained without electronic compensation at 130K. These images were produced with a blemish-free 32 x 64 (>2000 detectors) area array (Fig. 9) and an array with one defective diode (Fig. 8). The images were sensed in the dark with a remote SWIR radiation source (1-3 μm) directed towards the objects. The Pd₂Si-FPA operating behind variable aperture Si optics ($f/\# \sim 1.5$) was used to detect the radiation reflected from the skin. This skin reflectance at room temperature is above 30% between 1.0 μm and 1.5 μm and drops below 10% for longer wavelengths. In addition a video tape was recorded of outdoor imagery in the SWIR band using daytime reflected sun light. The scene contrast changed depending on the time of the day and intensity of solar radiation. Similar SWIR imagery have been produced by 64 x 128 FPAs.

The charge integration process in the vidicon readout mode is self-limiting and no blooming occurs during optical overload. The difference in the turn-on voltage of the Schottky detector and the parallel n^+p junction is 0.3-0.5 volt. Therefore the CCD channel will not be flooded with electrons even if the Schottky detector is forward biased during optical overload. In addition, the Pd₂Si detector with vidicon readout has high dynamic range, 70 dB, and high MTF, 65%, calculated for the proposed MLA sensor array. The high MTF of the Schottky barrier array imagery is the result of the fact that the carrier generation and collection occur in the same thin silicide layer (no carrier diffusion to adjacent detectors occurs as in some visible CCD imagers). The resulting imagery tends to be of higher quality than expected from a 32 x 64 element array.



Fig. 8. Pd₂Si SWIR imagery of a man smoking a cigar (uncompensated at 130K).

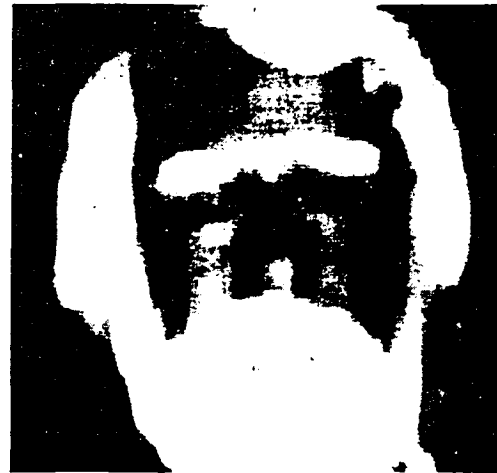


Fig. 9. Pd₂Si SWIR imagery of a face (uncompensated at 130K).

MLA application

The MLA instrument [3] will have several distinct advantages compared to present satellite-borne remote sensing systems [Table 2]. For comparison, the current imaging systems in the Landsat program, the Multispectral Scanners (MSS) and the Thematic Mapper (TM), use mechanical scanner technology to provide image information in the cross-track direction. The MLA however will use the satellite's motion to scan large solid state detector line arrays in a 185Km wide swath on the earth's surface as shown in Fig. 10. This "pushbroom" mode of operation will have the obvious benefits of increased dwell time, potentially higher spatial resolution, and inherent reliability. Furthermore, by simply adjusting the sensor read-out rate (i.e., variable integration time), multi-altitude capability is achieved, which is something inconceivable in mechanical scanned system due to loss of contiguity between stripes of data. Table 2 compares the system capabilities of the MSS, TM, and MLA sensors [7, 8, 9]. It is planned that there will be six spectral bands in the MLA instrument, four bands in the visible (VIS) and near-IR (NIR) and two bands in the SWIR. An additional thermal IR band (TIR) may be added. The desired ground resolution across the 185Km swath is 15 meters in the visible/near-IR bands and 30 meters in the SWIR bands. These specifications call for 12,288 detectors per band in the visible/near-IR and 6,144 detectors in each of the two SWIR bands. Furthermore, it may be desirable that both SWIR bands be placed in close proximity on the same substrate in order to attain maximum band-to-band alignment accuracy. The two SWIR bands will be chosen from the three bands currently under study, 1.25 μ , 1.65 μ , and 2.22 μ .

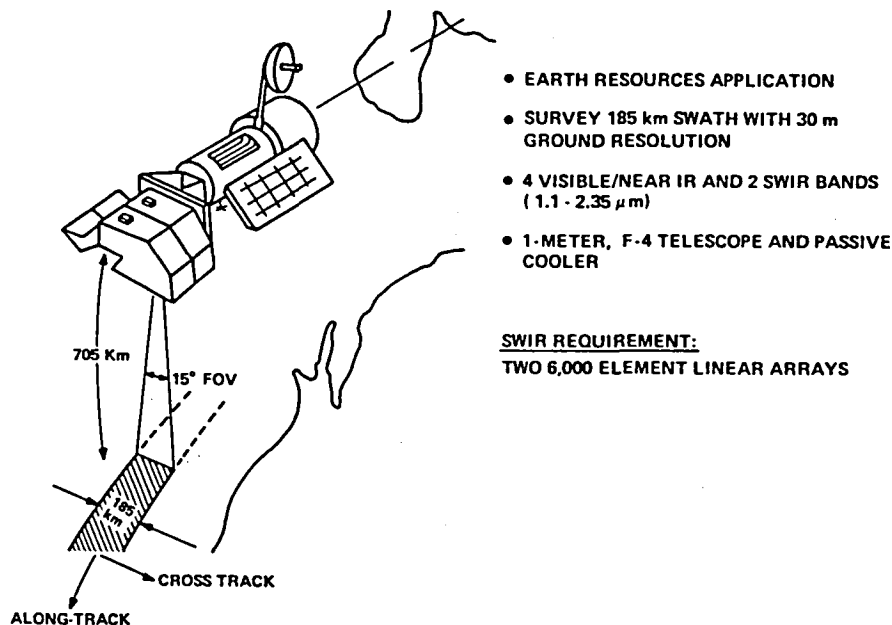


Fig. 10. MLA instrument system concept.

TABLE 2. COMPARISON OF MSS, TM, AND MLA SENSORS

	MSS		TM	MLA
Nominal Altitude	918 km		705 km	705 km (free flyer, current design)
Multialtitude capability	Loss of contiguity of data strips			Yes
Scene Scan	Oscillating mirror, image in forward sweep only		Oscillating mirror image in forward and back sweep	Staring array - Pushbroom
Dwell time at 705 km orbit	> 10 μ sec		VIS/NIR/SWIR 10 μ sec TIR 40 μ sec	4.4 m sec
Spectral bands (μ m)	VIS 0.5 - 0.6 0.6 - 0.7 0.7 - 0.8 NIR 0.8 - 1.1 SWIR TIR	0.45 - 0.53 0.52 - 0.60 0.63 - 0.69 0.76 - 0.90 1.55 - 1.75 2.08 - 2.35 10.4 - 12.5	0.45 - 0.52 0.52 - 0.60 0.63 - 0.69 0.76 - 0.90 1.55 - 1.75 2.08 - 2.35 (10.0 - 12.0)	
Detectors per band	6		16 VIS/NIR/SWIR 4 TIR	12,288 VIS/NIR 6,144 SWIR (1,843 TIR)
Ground resolution	80 m		30 m VIS/NIR/SWIR 120 m SWIR	15 m VIS/NIR 30 m SWIR (120 m TIR)
Quantization	1.56% 6 bits		0.39% 8 bits	< 0.39% > 8 bits
Sensor pointing modes	Nadir		Nadir	- Nadir - Fore-aft stereo - Cross-track

Pd₂Si staring FPA cameras may be used as radiometers in different SWIR spectral windows to measure target reflectance. The voltage response, V_λ , of the FPA at wavelength λ for reflected radiation from a resolved target is:

$$V_\lambda = R_{FPA,\lambda} \left[\frac{W \rho \tau_a A}{4\pi f/\#^2} \right] = p\rho \quad (11)$$

where $R_{FPA,\lambda}$ is the voltage responsivity of the FPA at wavelength λ , W is the scene illumination intensity in W/cm^2 , ρ is the target reflectivity, τ_a is the atmospheric transmission, $f/\#$ is the optics focal ratio, A is the pixel area and p is the voltage-reflectance proportionality factor.

The output voltage of the camera is proportional to the target reflectivity. Thus, target reflectivity, ρ , can be estimated by calibrating the FPA output in response to several targets of known reflectance at the identical illumination intensity. In this case, the $NE\Delta\rho$, the rms noise equivalent reflectance change from a background reflectance p at a scene illumination W , is determined by the IRCCD noise equivalent signal, NES, in rms electrons, at the same exposure

$$NE\Delta\rho = \left[\frac{4\pi q f/\#^2}{R t_{int} \tau_o \tau_a W A \eta_{ff}} \right] (NES) \quad (12)$$

Clearly $NE\Delta\rho$ is a function of the atmospheric transmission and scene illumination at the time of the measurement. The noise equivalent signal (NES) is the rms summation of: (1) the signal generated shot noise, (2) KTC noise sources, (3) MOSFET noise, and (4) CCD noise. The NES signal, at or above the working level irradiance (WLI), is dominated by the signal photon generated shot noise and some CCD low temperature transfer loss noise (for long CCD arrays). Equation (12) neglects the radiometric error generated by the temperature uncertainty between the time of calibration and the time of the measurement as well as the quantization errors. Table 3 demonstrates the required radiometric resolution [10], for the SWIR bands. These calculations assume typical working level irradiance in the image plane, and the corresponding scene illumination based on $f/\# = 3$, $\tau_o \tau_a = 60\%$ and 100% scene reflectance. $NE\Delta\rho$ values are calculated based on $t_{int} = 4.4$ msec, $A = 9 \times 10^{-6} cm^2$, $\eta_{ff} = 0.85$, NES values of 721, 638 and 414 (electrons) in SWIR bands 1 to 3 respectively, and the Pd₂Si projected quantum efficiency. Clearly the projected $NE\Delta\rho$ for the Pd₂Si arrays is better than the required ($NE\Delta\rho$) radiometric resolution.

Alternatively, the target reflectivity, ρ , can be evaluated by comparing the output of the FPA corresponding to the target, V_T , to that due to a reference surface, V_r , of known reflectivity ρ_r [11]:

$$\rho = \frac{V_T - V_D}{V_r - V_D} \rho_r \quad (13)$$

where V_D is the dark level voltage. Equation (13) assumes that both the target and the reference are illuminated by the same irradiance.

TABLE 3. RADIOMETRIC PERFORMANCE OF Pd₂Si SENSOR

Band	Required NEΔρ	WLI (μW/cm ²)	Scene Radiance (W:mW/cm ² .Sr)	Projected (NEΔρ)	Limit Error in Relative Measurement of 10% Reflectance
1.2–1.3 μm (1)	1.0%	9.2	0.55	0.19%	0.1±0.0015
1.55–1.75 μm (2)	1.0%	7.2	0.43	0.22%	0.1±0.002
2.08–2.35 μm (3)	2.4%	3.5	0.21	0.56%	0.1±0.006

The maximum fractional uncertainty in the reflectance measurement described above is given by:

$$\frac{\Delta\rho_{\max}}{\rho} = (S/N)_T^{-1} + (S/N)_r^{-1} + \left(\frac{1}{V_r} + \frac{1}{V_T}\right) (2\bar{Q} + \text{DNES}) + \text{TCE} \quad (14)$$

where $(S/N)_T$ and $(S/N)_r$ are the signal-to-noise ratio of the target and reference measurements, \bar{Q} the quantization error in the A/D converter, DNES is the noise equivalent signal at no illumination and TCE is the radiometric error due to temperature calibration uncertainty between the reference and the target measurements (calibration uncertainty between the reference and target measurements caused by changes in the level and shot noise of detector dark current). For the Pd₂Si-FPA operating at 120K with 1°C temperature uncertainty, this TCE error is negligible.

At the photon shot noise limit for short line arrays with negligible detector 1/f noise, neglecting DNES error in comparison to the noise equivalent signal under illumination (NES), the limit uncertainty is given by:

$$\frac{\Delta\rho_{\max}}{\rho} = \sqrt{\frac{qG}{C_{FD}p}} \left[\frac{1}{\sqrt{\rho}} + \frac{1}{\sqrt{\rho_r}} \right] + \frac{2\bar{Q}}{p} \left[\frac{1}{\rho} + \frac{1}{\rho_r} \right] + \text{TCE} \quad (15)$$

Using equation (15) we calculate the limit fractional uncertainty in a 10% target reflectance measured by comparing to a 100% reflectance, assuming 1 Volt: 4096 quantization. In Table 3 we show these maximum fractional error values calculated for this relative measurement. Increasing the A/D resolution reduces this maximum fractional uncertainty.

MLA sensor design

The sensor envisioned for the MLA application would consist of multiple chips placed end-to-end to produce the desired two linear arrays of 6,144 detectors each. Each chip would consist of two rows of detectors with on-chip CCD multiplexers and associated output amplifiers. The overall module configuration for this monolithic integrated circuit is shown in Fig. 11. A 512 x 2 dual band device is thought to be the optimum choice considering yield, data-rates, and focal plane complexity. This would result in a twelve chip MLA focal plane. There is confidence in proposing this 1024 detector module based upon the demonstrated yield in the technology. Of particular note is that blemish-free 64 x 128 Schottky-barrier area arrays have been fabricated [12].

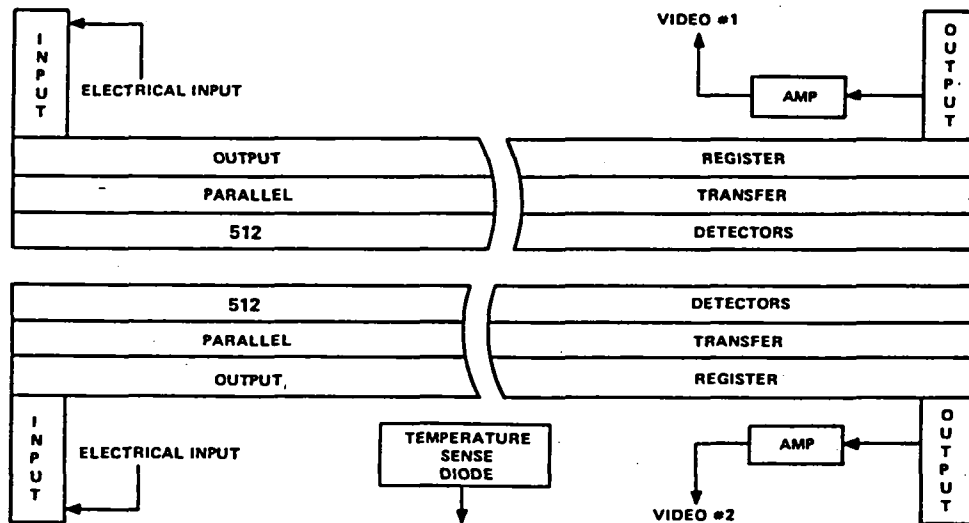


Fig. 11. MLA dual band sensor design.

Mechanical end-to-end butting is the preferred butting technique. It avoids the vignetting and optical/mechanical alignment problems found in optically butted systems, as well as, the tight chip packaging (along-track) and data reformatting required in staggered offset configurations. Experiments indicate that end-to-end butting may be done with less than $40\ \mu$ inactive area across the abutment seam ($20\ \mu$ on each chip edge). This would permit a minimal loss of image data at the eleven abutment seams required for a twelve chip focal plane.

The packaging concept for an MLA focal plane may be seen in Fig. 12. The chips are back-side illuminated through a baffled aperture. The cold mount would be attached to the package cover. The package material studied has an excellent match of thermal expansion coefficient to that of the silicon chips. Based on experience with visible CCD imagers [13] operating at room temperature, and calculations of low temperature induced stresses, it appears that this packaging concept would maintain $5\ \mu$ alignment tolerances (chip-to-chip).

The desirable detector pitch (center-to-center spacing) for the MLA instrument is $30\ \mu$. This pitch would result in a focal plane with a $7.25''$ active scanning dimension. This aggressive pitch is coupled with a fill-factor requirement of 85% active area per $30\ \mu \times 30\ \mu$ detector.

The power dissipation and operating temperature of the dual band sensor are important figures of merit. The dissipation of the 2×512 sensor is projected to be 11 mW at the nominal data rate. Thus, the full twelve chip focal plane would dissipate 132 mW, which is well within the passive cooler performance range (typically 1 Watt at 120K operating temperature).

Table 4 summarizes the projected performance for an MLA dual band Pd_2Si sensor.

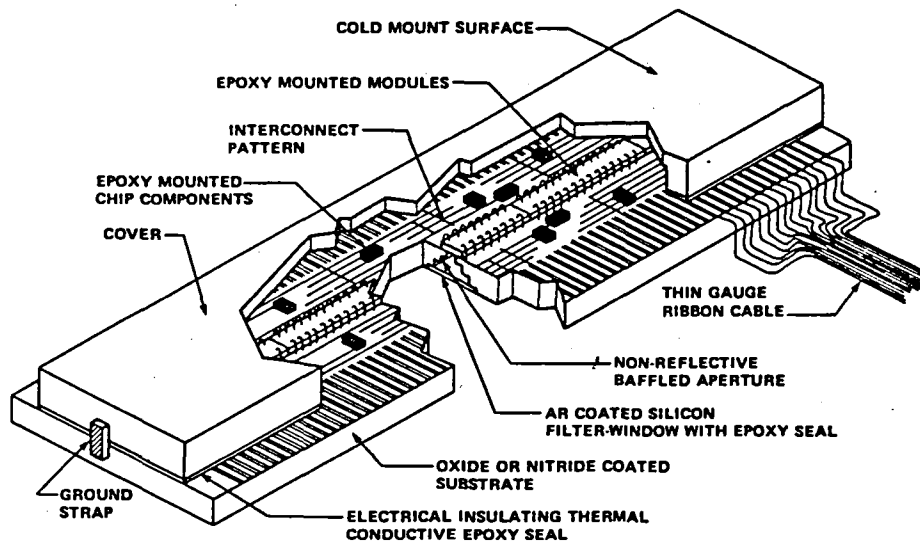


Fig. 12. MLA focal plane concept.

TABLE 4. DUAL BAND SENSOR DESIGN

Number of Detectors	2×512
Center-to-Center Spacing	$30\ \mu$
Fill Factor	80-90%
Projected Quantum Efficiency	
$\lambda = 1.25$	20%
$\lambda = 1.65$	14%
$\lambda = 2.22$	5.5%
Operating Temperature	120K
Dark Current (120K)	$2\ \text{nA/cm}^2$
Signal-to-Noise Ratio (at 705 Km altitude) [†]	200-555
Pixel Loss at Seam	2
MTF at Nyquist Frequency	65%
X, Y, Z Alignment Tolerances	$< 5\ \mu/\text{Chip}$
Power Dissipation (On-Chip)	11 mW

[†]Employing NASA specified nominal irradiance/integration time.

Summary

In addition to the PtSi-Schottky barrier IR-CCD which we have previously developed for thermal imaging (NEAT) applications; we have presented here our recent results on first generation Pd₂Si IR-CCDs. The Pd₂Si-FPA is intended for NEAT applications in the SWIR spectral range at intermediate temperatures. The Pd₂Si-FPA may also be used in the NEAT application of hot target detection and discrimination in early warning satellites [14].

Table 5 demonstrates the different staring FPA technologies available. From the point of view of adequacy to space applications requiring passive cooling the Schottky barrier and HgCdTe technologies offer feasibility. Monolithic Schottky barrier arrays, however, are more suitable for high density sensors with large numbers of elements. We have demonstrated that the responsivities of Schottky barrier arrays meet the NEAT requirements for accurate classification of earth resources features. We have detailed our concept for an MLA instrument SWIR focal plane utilizing high-density dual band Pd₂Si detector arrays.

TABLE 5. STARING FPA TECHNOLOGIES

	IR BAND	OPERATING TEMPERATURE	TYPE OF FPA	TYPICAL NUMBER OF ELEMENTS
(Hg, Cd) Te	3 – 5 μ m 8 – 10 μ m	77 (to 190) K 77K	HYBRID MONOLITHIC CID (area) CCD (line)	32 x 32 64 x 64
InSb OR InAsSb	3 – 5 μ m 3 – 4 μ m	77K	HYBRID MONOLITHIC CID (area) CCD (line)	32 x 32 64 x 64
EXTRINSIC In:Si Ga:Si	3 – 5 μ m 8 – 14 μ m	45K 25K	HYBRID MONOLITHIC CCD	32 x 32 64 x 64
PtSi SCHOTTKY	3 – 6 μ m	77K (40 – 90K)	MONOLITHIC CCD	32 x 64 64 x 128 256 x 1
Pd ₂ Si SCHOTTKY	1 – 3.5 μ m	40 – 145K	MONOLITHIC CCD	32 x 64 64 x 128

Acknowledgment

The authors wish to acknowledge the basic IR-CCD technology development supported by the Air Force Rome Air Development Center, Hanscom AFB, MA, Dr. F. Shepherd contract monitor.

The encouragement of F.B. Warren, Manager of the Systems Laboratory of the Advanced Technology Laboratories is appreciated. The assistance of the RCA Automated Systems Division, Burlington, MA, in producing the test imagery is gratefully acknowledged.

References

1. H. Elabd, T. Villani, and W.F. Kosonocky, "Palladium-Silicide Schottky-Barrier IR-CCD For SWIR Applications at Intermediate Temperatures," IEEE ED Letters, 3, April (1982)
2. H. Elabd, "Multispectral Earth Imaging: Applications of Metal Silicide Schottky-Barrier Mosaic Sensors," presented at the AAS - 20th Goddard Memorial Symposium Meeting, March (1982).
3. D.D. Norris and J.B. Wellman, "Earth Sensing Technology" GOMAC Digest of Paper, 74 (1980).
4. R.D. Thom, T.L. Koch, J.D. Langan, and W.J. Parrish, "A Fully Monolithic InSb Infrared CCD Array," IEEE ED Trans. 27, 160 (1980).
5. K. Chow, J.D. Blackwell, J.P. Rode, D.H. Sieb, W.N. Lin, "Source-Coupling for Hybrid Focal Planes," SPIE, Vol. 282, Tech. Issues in FPA Development, 60 (1981).
6. J. Stobie, S. Iwasa, "1.0 to 2.5 micrometer Short Wavelength Infrared (SWIR) Linear Array Technology For Low Background Applications," SPIE Vol. 282, Tech. Issues in FPA Development, 98 (1981).
7. Herbert Richard, "Solid State Instrumentation Concepts for Earth Resource Observation," AAS-20th Goddard Memorial Symposium, March (1982).
8. Paul Heffner, et al., "Advanced Technology for Earth Observation Data Processing AAS," AAS-20th Goddard Memorial Symposium, March 1982).
9. Private communications with Mr. Oscar Weinstein, NASA, GSFC.
10. J.L. Engel, "Thematic Mapper - An Interim Report on Anticipated Performance," AIAA Publications, "Sens. Syst. for the 80's Conference," Colorado Springs Co., 25, December (1980).
11. B.F. Robinson, R.E. Buckley, and J.A. Burgess, "Performance Evaluation and Calibration of a Modular Multiband Radiometer for Remote Sensing Field Research," SPIE, Vol. 308, Contemporary Infrared Standards and Calibration, 146 (1981).
12. W.F. Kosonocky, H. Elabd, H. Erhardt, F. Shallcross, T. William, J. Groppe, M. Cantella, J. Klein, "Design and Performance of a 64 x 128 PtSi Schottky-Barrier IRCCD Focal Plane Array," SPIE Sym. - Infrared Sensor Technology Session, May (1982).
13. S. Goldfarb, D. Colvin, "A Large Hybrid Electro-optical Array," Int. J. For Hybrid Microelectronics, Vol. 3, 75 (1980).
14. R.D. Hudson and J.W. Hudson, "The Military Applications of Remote Sensing by Infrared," Proceedings of the IEEE, 63, 104 (1975).

MULTISPECTRAL LINEAR ARRAY (MLA)

SCIENCE AND TECHNOLOGY PROGRAM

GODDARD SPACE FLIGHT CENTER
GREENBELT, MARYLAND 20771

W. L. BARNES

MAY 10, 1982

ABSTRACT

This document summarizes a Goddard Space Flight Center program of science studies, and research and technology development to provide the basis for future earth observation sensors employing multispectral linear array (MLA) technology.

SCIENCE ACTIVITIES INCLUDE:

1. Science Requirements Study
2. Establishment of MLA Performance Parameters
3. Performance Modeling to Assess MLA Instrument Parameter Recommendations

CRITICAL TECHNOLOGIES BEING DEVELOPED INCLUDE:

1. Short-Wave Infrared (SWIR) Detector Arrays:
 - a. Primary Approach (HgCdTe)
 - b. Alternate Approach (monolithic Schottky barrier)
2. Visible/and Near Infrared Detector Arrays
3. Passive cryogenic coolers

SUPPORTING ACTIVITIES INCLUDE:

1. Test and Field Instrument Development
2. Focal Plane Research and Assessment Laboratory
3. System Simulation Laboratory
4. Calibration Sources and Techniques
5. Optics
6. Thermal Infrared Arrays (TIRA)

INTRODUCTION

This document summarizes a set of science studies, and research and technology developments which will provide the basis for future land observing research mission sensor systems utilizing multispectral linear array (MLA) technology. These sensors will support important research in agriculture, forestry, geology, water resource analysis, urban management, and environmental assessment. MLA technology provides the potential for significant advances in performance beyond the Thematic Mapper. An MLA sensor can provide very high spatial and spectral resolution data, improved mapping, multispectral stereoscopic data, and capability for multi-altitude operations.

An MLA sensor will be developed in the near future for a land observing remote sensing research program. Science studies are being initiated to establish objectives for the land observing research mission and to convert these scientific objectives to a set of required MLA sensor parameters. A technology development program in selected areas is being generated to permit the sensor to be brought to fruition with reasonable technical risk to the mission objectives. Finally, a laboratory and field research program is being conducted to provide a base of expertise at GSFC in the reduction and analysis of MLA sensor data and in the complexities of detector array technology.

This program is managed by the Earth Observation Systems Division of the Goddard Space Flight Center. Major supporting roles are provided by other divisions within the Applications Directorate, by the Engineering Directorate, and the Mission and Data Operations Directorate.

Objectives:

1. Perform studies to provide an improved science basis for earth resource applications of a future MLA type sensor.
2. Develop and demonstrate focal plane array technology for the visible near infrared, shortwave infrared, and thermal infrared spectral regions.
3. Design and fabricate field test instruments, conduct evaluation tests and provide data for scientific assessment.
4. Perform engineering studies in technical areas critical to MLA instrument development.

Justification

An MLA sensor operating in the pushbroom scan mode can meet difficult research requirements. A pushbroom mode sensor provides:

- a. Long dwell times which permit high spatial resolution and radiometric sensitivity.
- b. Fixed detector array and optics geometry which result in improved mapping.
- c. compact optics which allow a pointable field-of-view to conduct atmospheric effects and stereographic experiments.

The key technical advancements that are necessary for a land observing research mission will be addressed by this program.

Approach

Instrument and mission requirements are being defined based on science and engineering studies. Principal technology drivers have been identified, and development activities are being initiated to assure timely availability of critical MLA technology.

An in-house capability is being developed to evaluate sensor concepts, assess advanced detector arrays, conduct field test experiments and provide a calibration capability.

Expected Results:

1. Science and engineering studies, including feasibility and risk assessments, will be provided for use in defining experimental and technological objectives for MLA sensors.
2. Visible, NIR, SWIR and thermal IR focal plane arrays for MLA type sensors will be developed, tested and evaluated.
3. Data from airborne field test instruments will be used to develop and test science algorithms.
4. Studies in other technology areas critical to MLA development will assess the state-of-the-art, identify required technology developments, and provide potential design solutions. These studies will include:
 - a. passive cryogenic coolers.
 - b. wide-field-of-view, broad spectral range optics.
 - c. narrow-band stripe interference filters deposited on silicon detector arrays.
 - d. dichroic beam splitting techniques.
 - e. calibration techniques.

A Focal Plane Research and Assessment Laboratory as well as a System Simulation Laboratory will be completed. Advanced detector arrays will be evaluated and end-to-end hardware/software MLA instrument simulations will be conducted

1.0 SCIENCE ACTIVITIES

Science support for the MLA development program is focused on three areas:

- (a) further the basic science of remote sensing,
- (b) establish the initial scientific basis for selection of performance parameters for a land observing research mission, and
- (c) establish relationships and trade offs between experimental sensor/system/mission alternatives.

1.1 SCIENCE REQUIREMENTS

The design of an optimum land observing research mission requires a thorough understanding of the current state-of-the-art in remote sensing, and of the additional capabilities offered by available new and developing techniques (e.g., MLA). A thorough review of available documentation and associated R&D activities is therefore being performed to provide a basis for the mission design.

A Multispectral Imaging Science Working Group has been established, with representation from NASA centers, other federal agencies, universities and not-for-profit industry. This working group will provide in-depth review and analysis of current remote sensing techniques. Potential future research and experimental approaches for the detection, identification, and measurement of renewable and nonrenewable resources will be examined using new technologies as required. These efforts will be directed toward definition and prioritization of experimental objectives for the proposed land observing research mission.

1.2 PERFORMANCE PARAMETERS

The short term science goal is the establishment of the scientific justification for a land observing research mission payload. Initial efforts have concentrated on identifying instrument parameters, and performing critical research activities where definitive parameter selection is not yet supportable. This research will build on present knowledge and will include field experiments as appropriate. The schedule of this activity will be coordinated with the mission schedule and will provide the latter with the necessary inputs. Major instrument parameters being considered are:

SPECTRAL: Band location and width, spectral band information content and redundancy.

SPATIAL: Instantaneous field-of-view (IFOV), sampling rate, registration, textural information, mixed resolution utility.

TEMPORAL: Revisit frequency, illumination conditions, global coverage.

RADIOMETRIC: Calibration, atmospheric correction, adjacency effects, quantization, polarization.

OFF-NADIR: Bi-directional reflectance, atmospheric correction, ground resolution and registration, height resolution, and base-to-height ratio (stereo)

The interrelationships and tradeoffs between these parameters are also being studied.

1.3 PERFORMANCE MODELLING

Preliminary identification of the performance parameters will allow work to start on the definition of parameter extraction algorithms. These algorithms will form the basis for performance modelling and simulation. The work will begin on existing image analysis/geographic information facilities while other alternatives, for instance, the Landsat Assessment System, will be examined for suitability for use in the future. Integration of target emission/reflectance models, atmospheric path models, sensor/system/mission performance parameters, accuracy and position requirements, classification techniques, and test data bases will allow trade-off analyses to be conducted using the experimental objectives and the payload and mission alternatives. Results will be used to define further research activities and field experiments. Performance modeling will allow verification of the initial instrument/payload parameters and the refinement of the system and mission capabilities. This activity will be coupled with that of the System Simulation Laboratory in the Engineering Directorate, to provide an overall sensor/science/requirements modeling capability in support of the land observing research mission. It is anticipated that the land observing research mission will be a very flexible/versatile tool for numerous remote sensing applications. These simulation activities will hence eventually provide the capability for assessing the feasibility of new experiments prior to the implementation on future missions.

2.0 TECHNOLOGY DEVELOPMENT

Emphasis is being placed in two areas: (1) high priority development of technologies critical to MLA sensor development; and (2) engineering studies and hardware development in related important technical areas.

2.1 CRITICAL TECHNOLOGIES

2.1.1 SWIR Focal Plane (1.0-2.4 micrometers)

The preferred configuration consists of photovoltaic HgCdTe detector arrays coupled to a silicon multiplexer. Key Parameters:

- (1) Spectral region 1.0-2.4 μm ;
- (2) pitch-30 micrometer;
- (3) number of detectors - 6200;
- (4) temperature - 130K (nominal);
- (5) sensitivity - $NE\rho = 0.5\%$ (for scene reflectivity of 50%)

Items to be developed: Detector material, module (100 to 500 detectors), 5 module Test Assembly and a 6200 element Focal Plane Assembly. Proposals have been submitted to GSFC.

Two contractors will be chosen to conduct parallel 42-month development efforts. Anticipated starting time is early CY 1983.

The programs will involve two phases and will include the following: Phase I --Study followed by material, module and Test Assembly development. The Test Assembly will incorporate five modules. Phase 2 - a fully populated Focal Plane Assembly of 6200 detectors will be developed.

The modules, Test Assembly, and Focal Plane Assembly will also be delivered to GSFC for in-house test and evaluation

2.1.2 Alternate SWIR Array (1.0-2.4 μm)

Because of the importance of the SWIR spectral bands to a future MLA sensor, an alternate array technique will also be developed. Proposals have been submitted to GSFC to develop a monolithic PdSi Schottky barrier diode array. Key parameters are the same as stated in 2.1.1, except that the nominal operating temperature is 110K and the 6200 element Focal Plane Assembly will not be provided.

The proposed 24-month program will design, develop, test, and evaluate monolithic Schottky barrier SWIR chips and a 5-module Test Assembly

2.1.3 VIS/NIR Array (0.4-1.0 μm)

Although VIS/NIR arrays are not considered a technological problem for the MLA, there are very few off-the-shelf devices to choose from, and

those that are available have not been optimized to meet MLA requirements. The purpose of this activity is to develop a VIS/NIR integrated silicon circuit (chip) optimized for an MLA sensor. The chip would be available in time for incorporation into an MLA sensor. Proposals have been received and are being evaluated.

The proposed 24-month program is to design, develop, test and evaluate a VIS/NIR chip with 4 parallel arrays each having an interference filter in close proximity and a 5-chip Evaluation Focal Plane.

2.1.4 Passive Cryogenic Cooler Study

The SWIR detectors will require cooling in the 110 to 190K temperature range, with thermal loads on the order of 1.0 watt. A passive cooler of this capacity is substantially larger than those NASA has flown to date. The potential development risks and problems associated with such a cooler need are being addressed in a detailed study. The study is a 9-month effort to size a passive cooler for an MLA sensor and to fabricate a breadboard heat transfer device.

3.0 SUPPORTING ACTIVITIES

3.1 TEST/FIELD INSTRUMENT DEVELOPMENT

In order to assess technology capability, evaluate radiometric properties and examine calibration and information extraction techniques, pushbroom type airborne sensors will be developed and flown. The first of the GSFC radiometers was flown in CY1979. Sensors near completion include an advanced visible sensor and a short wave infrared sensor. Sensors planned for the FY1983 through FY1985 time period will utilize area SWIR and VIS/NIR arrays in an imaging spectrometer mode to provide multispectral data for algorithm development. The main effort will be to develop an airborne MLA Experiment Simulator. Sensor definition is underway. The aircraft sensors are built in-house. These include:

- (a) LAPR-I (3 VIS/NIR channels);
- (b) LAPR-II (4 VIS/NIR bands with selectable spectral channels);
- (c) SWIR/LAPR (1 band, 1 - 3 micrometers);
- (d) MLA Experiment Simulator.

Laboratory instrument developments include both SWIR and TIR pushbroom array sensors. The laboratory instruments include the following:

1. 9-element HgCdTe array, TIR imager (10 - 12 micrometers)
2. 90-element HgCdTe array, TIR imager
3. 64-element PbS, SWIR imager

Each of the laboratory sensors is complete. They are being used in several in-house studies.

3.2 FOCAL PLANE RESEARCH AND ASSESSMENT LABORATORY

The purpose of this laboratory is to perform science and engineering studies to validate characteristics of detectors and detector arrays, post-amplifiers, multiplexers, etc. during the device research and development phase, and to evaluate modules and arrays operating in the visible, NIR, SWIR, and TIR spectral regions.

Emphasis will be placed on achieving accurate measurements of detector radiometric properties, stability, sensitivity, spectral and temporal response. This laboratory is required to provide an independent assessment of MLA detector performance.

3.3 SYSTEM SIMULATION LABORATORY

The purpose of this laboratory is to perform end-to-end hardware/software simulations to support MLA flight and/or ground system trade-off, optimization and evaluation studies. The simulation activity will concentrate on the electro-optical signal processing chain and will provide a capability for technology development, assessment, and evaluation of critical subsystem elements in a "system" environment. The MLA focal planes and optical breadboards as well as signal processing breadboards developed in the technology program will be utilized in the simulations. This laboratory will: provide MLA "hands-on" experience; provide capability for independent testing, assessment and validation of instruments and subsystems; lead to realistic instrument specifications; and lead to improved techniques for synthesizing and evaluating focal plane assemblies, signal processing electronics, wide field of view optics, spectral separation concepts, and high data rate information handling systems.

3.4 CALIBRATION SOURCES AND TECHNIQUES

The MLA requirement for high radiometric accuracy (+5% absolute and +1% relative between spectral bands) requires frequent on-orbit calibration of detectors using sources of high stability. High quality sources for ground calibration traceable to NBS are also required. GSFC has traditionally provided ground sources to calibrate earth viewing sensors, and this capability is being extended to support the MLA requirements.

3.5 OPTICS

A requirement generated by the need for MLA type sensors is for wide field collecting optics (up to 15° FOV) that are achromatic over the spectral region from 0.4 to 2.5 micrometers. An in-house capability to design and analyze complex optical systems has been developed over several years and a variety of sophisticated computer programs are available (ACCOS-V, GENOPTICS, CODE V). These are being used to examine potential

optical systems for MLA sensors. Extensive work has already been done which indicates that an all reflective Swarzschild is one desirable candidate. However, other optical forms need to be examined and optimization studies performed. A breadboard optical system of one or more of these designs will be fabricated and tested.

Another key technology item in the optics area is the problem of spectral band selection. Techniques such as dichroic beam splitting, use of narrow stripe interference filters deposited directly on the linear arrays are also being addressed.

3.6 THERMAL INFRARED ARRAYS (TIRA)

Thermal Infrared Arrays will be required for research in resource applications such as geology and/or hydrology.

A program has been underway for several years to develop Thermal Infrared Array (TIRA) technology. The major thrust has been directed towards hybrid HgCdTe structures. Up to this time, 9 element and 90 element photoconductive array imagers have been fabricated and successfully tested.

The present thrust of the program is the development of a hybrid photovoltaic HgCdTe module capable of being assembled into large linear arrays.

A program is underway to develop the photovoltaic HgCdTe module with the Honeywell Electro-Optics Center. The study phase of the program has been completed and the fabrication phase is underway.

MULTISPECTRAL LINEAR ARRAYS FOR TERRESTRIAL REMOTE SENSING 677-27-01

OBJECTIVES:

- DEMONSTRATE REQUIRED MLA FOCAL PLANE TECHNOLOGY FOR RESOURCE OBSERVATIONS
- DEVELOP A SCIENTIFIC BASIS FOR SYSTEM PERFORMANCE CRITERIA.
- DEVELOP CRITICAL ASSOCIATED TECHNOLOGIES.



MLA SCIENCE PROGRAM

OBJECTIVE:

TO PROVIDE A SCIENTIFIC BASIS FOR THE SELECTION OF MLA
SENSOR, SYSTEM AND MISSION PARAMETERS FOR FUTURE
SATELLITE-BASED LAND REMOTE SENSING

APPROACH:

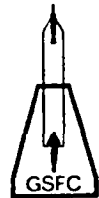
IN-HOUSE STUDIES AND FIELD EXPERIMENTS UTILIZING SUPPORT
CONTRACTORS TO EXAMINE:

- SPATIAL PARAMETERS: IFOV, MIXED RESOLUTION, TEXTURE
- SPECTRAL PARAMETERS: LOCATION, WIDTH, SHAPE,
SELECTION
- ATMOSPHERIC CORRECTION: ATTENUATION, PATH RADIANCE,
ADJACENCY
- OFF-NADIR PARAMETERS: BI-DIRECTIONAL, REFLECTANCE,
STEREO
- OTHER ISSUES: CALIBRATION, REGISTRATION

STATUS:

ALL ACTIVITIES UNDERWAY

PRELIMINARY RESULTS AVAILABLE FROM SPATIAL, SPECTRAL,
OFF-NADIR



HYBRID SWIR TECHNOLOGY DEVELOPMENT

OBJECTIVE:

TO DEVELOP AND DEMONSTRATE A SWIR FOCAL PLANE DETECTOR/
MULTIPLEXER ARRAY.

APPROACH:

- TWO PARALLEL 42-MONTH CONTRACTS TO DEVELOP A HYBRID HgCdTe DEVICE.
- PHASE I—DEVELOP 256-ELEMENT MODULE AND 5-MODULE TEST ASSEMBLY.
- PHASE II—DESIGN, FABRICATE AND TEST 6200-ELEMENT FOCAL PLANE ASSEMBLY.

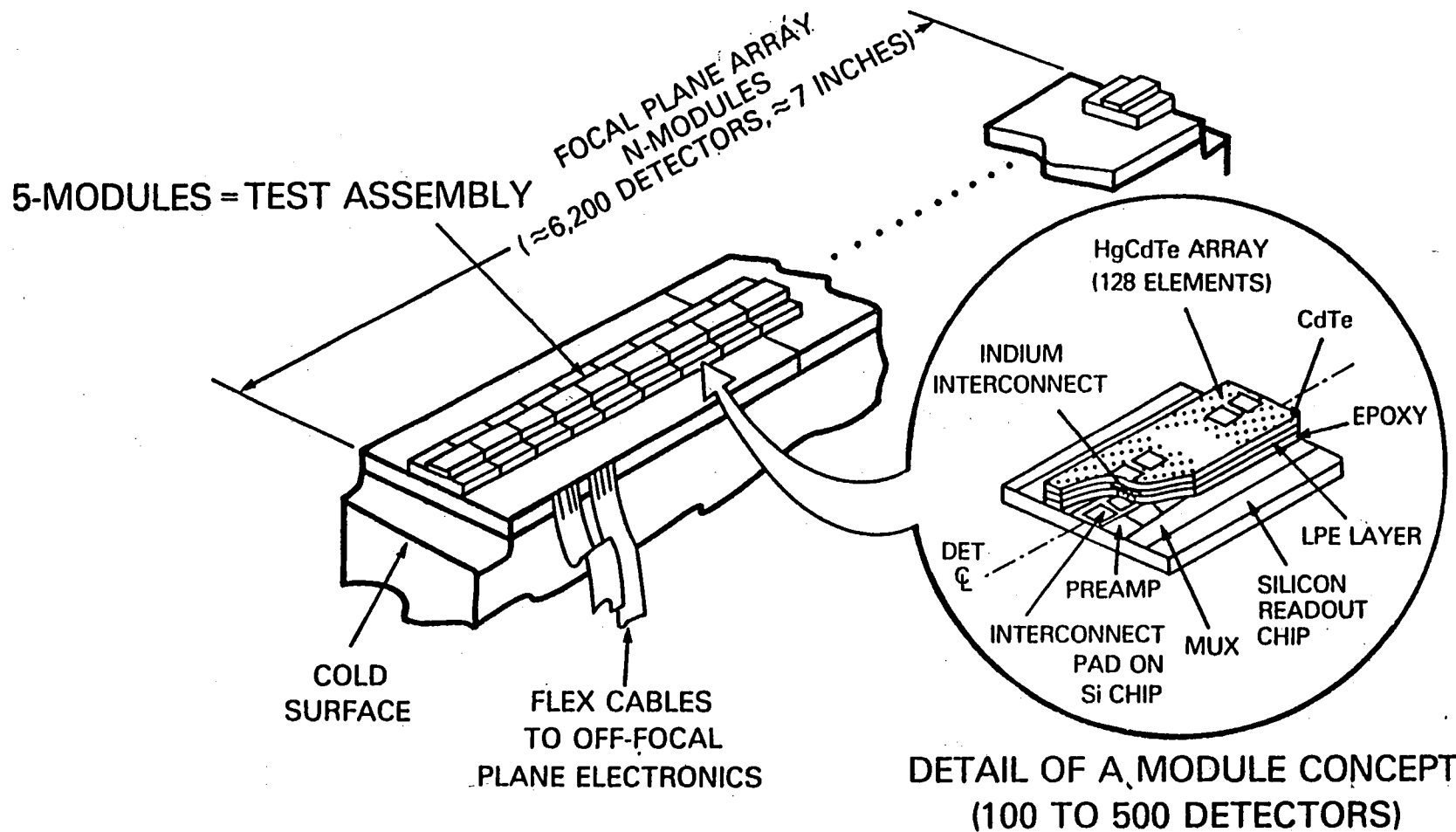
STATUS:

- PROCUREMENT PACKAGE COMPLETE.
- RFP RELEASE 2/82.
- CONTRACTS 1/83.



A CONCEPT HYBRID SWIR ARRAY

66



SWIR FPA

KEY CHARACTERISTICS

- SPECTRAL REGION 1.1 TO 2.4 μM
 - BANDS 1.2, 1.6, 2.2 μM , <10% BW
 - DETECTOR SIZE 30 μM PITCH
 - ARRAY \approx 6200 DETECTORS
 - BLEMISHES LESS THAN 1%, INCLUDING BUTTS
 - SIGNAL-TO-NOISE 100 P-P/RMS AT WORKING LEVEL IRRAD
 - STABLE LESS THAN 1% DRIFT IN 25 SEC
 - UNIFORM LESS THAN 10% STANDARD DEVIATION
 - MULTIPLEXING FIRST LEVEL ON FOCAL PLANE
 - OPERATING TEMPERATURE 130K OR WARMER
 - HEAT LOAD 40 μW PER DETECTOR
- RELIABLE
 - TESTABLE
 - REPAIRABLE
 - AFFORDABLE
 - TIMELY



MONOLITHIC SWIR TECHNOLOGY DEVELOPMENT

OBJECTIVE:

TO DEVELOP AND DEMONSTRATE A MONOLITHIC SCHOTTKY BARRIER
DETECTOR/MULTIPLEXER MODULE AS A BACK-UP TO THE HgCdTe
DEVELOPMENT.

APPROACH:

- 24-MONTH CONTRACT TO DEVELOP AND TEST PdSi/Si MONOLITHIC
DEVICE.
- DEVELOP MODULES AND 5-MODULE TEST ASSEMBLY.

STATUS:

- RFP RELEASE..... 11/81.
- PROPOSALS DUE..... 2/2/82.
- CONTRACT AWARD..... 7/82.



VIS/NIR DETECTOR ARRAYS

OBJECTIVE:

DEVELOP A VIS/NIR DETECTOR ARRAY DEVICE THAT WILL SERVE AS THE BASIC UNIT FOR A MLA FOCAL PLANE.

APPROACH:

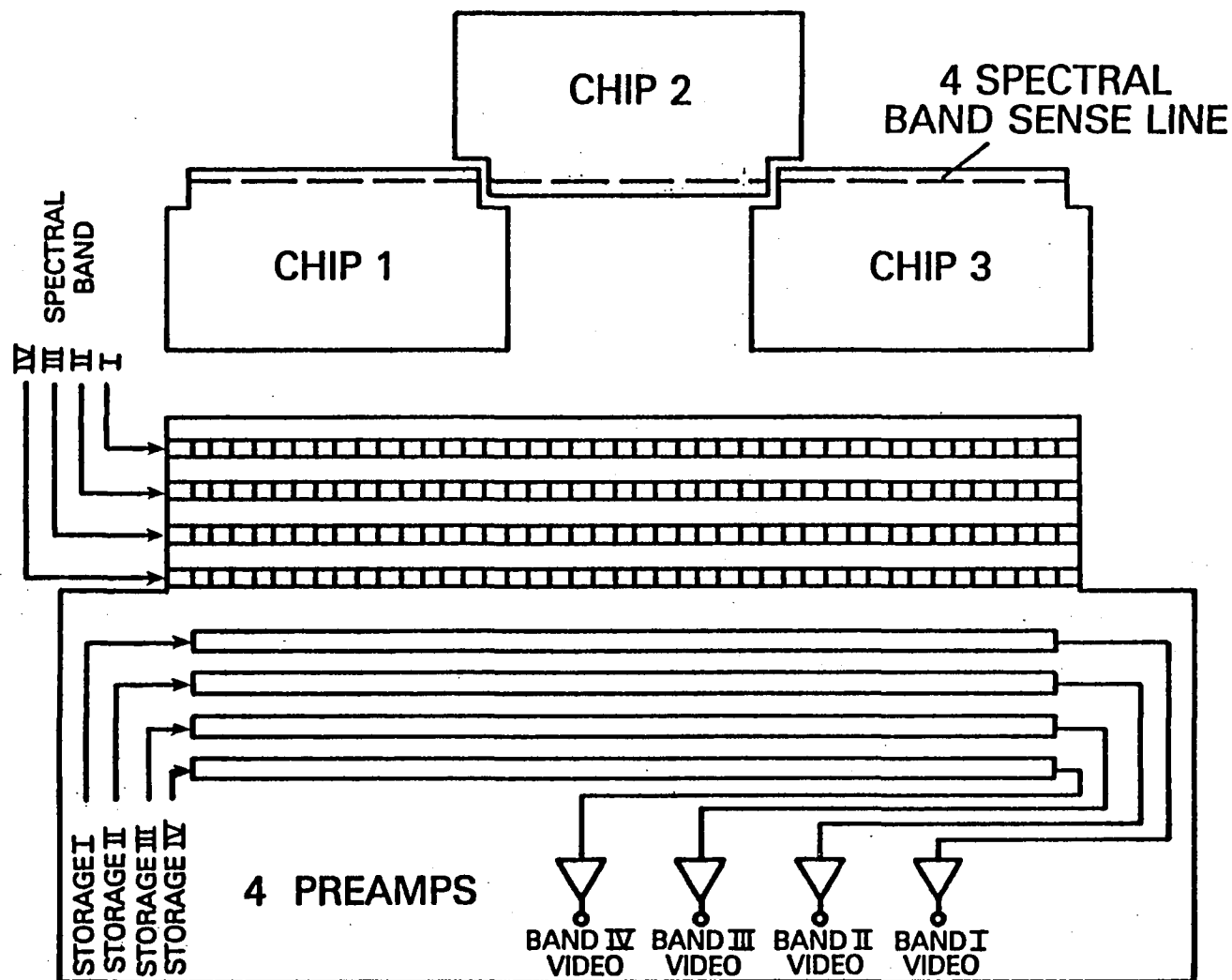
- 24-MONTH CONTRACT TO DEVELOP A SILICON DETECTOR ARRAY DEVICE.
- EACH CHIP—FOUR 1024-ELEMENT DETECTOR ARRAYS, FOUR SPECTRAL FILTERS AND ASSOCIATED ELECTRONICS.
- DEMONSTRATE BUTTABILITY.

STATUS:

- PROPOSALS DUE 2/8/81
- CONTRACT AWARD 7/82

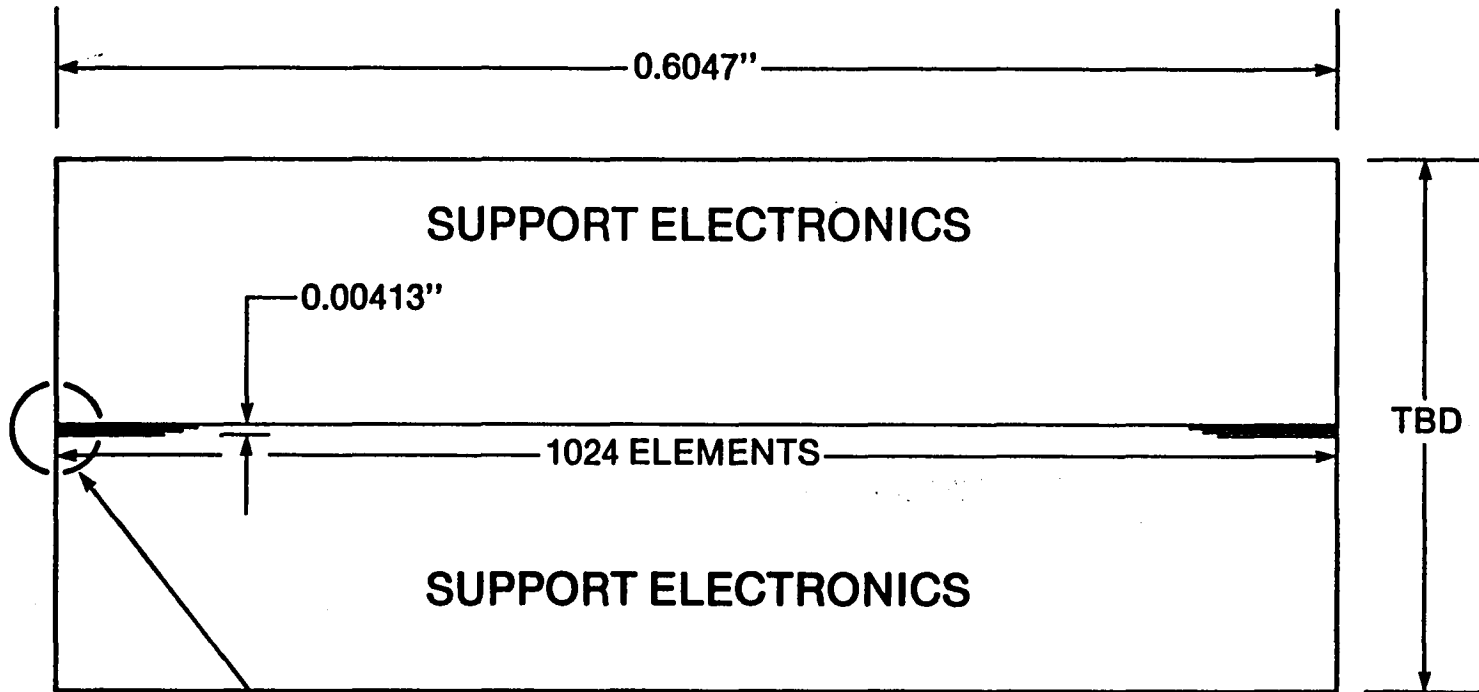


CONCEPTUAL VIS/NIR DETECTOR ARRAY

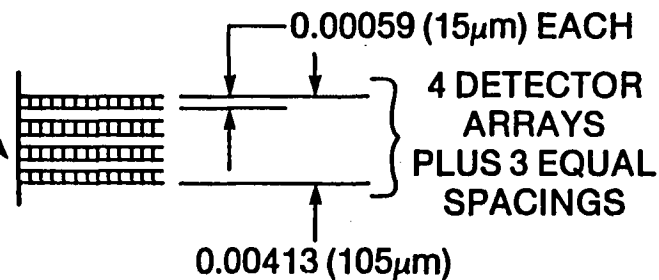


4 SPECTRAL BANDS PER CHIP WITH SPECTRAL FILTERS
 1024 ELEMENTS PER BAND (NOMINAL)
 DETECTOR SPACING 15 μm
 < 2 MISSING ELEMENTS/BUTT JOINT

VIS/NIR DEVICE LAYOUT



DEVICE:
 1024 DETECTOR
 ELEMENTS/ARRAY
 4 ARRAYS/DEVICE
 4096 ELEMENTS/DEVICE



FOCAL PLANE:
 12 DEVICES LONG (7.256")
 12,288 ELEMENTS/ARRAY
 49,152 ELEMENTS/
 FOCAL PLANE

OPTICS DESIGN AND FABRICATION

OBJECTIVE:

DESIGN, FABRICATE AND TEST CRITICAL OPTICAL COMPONENTS REQUIRED FOR MLA SENSOR.

APPROACH:

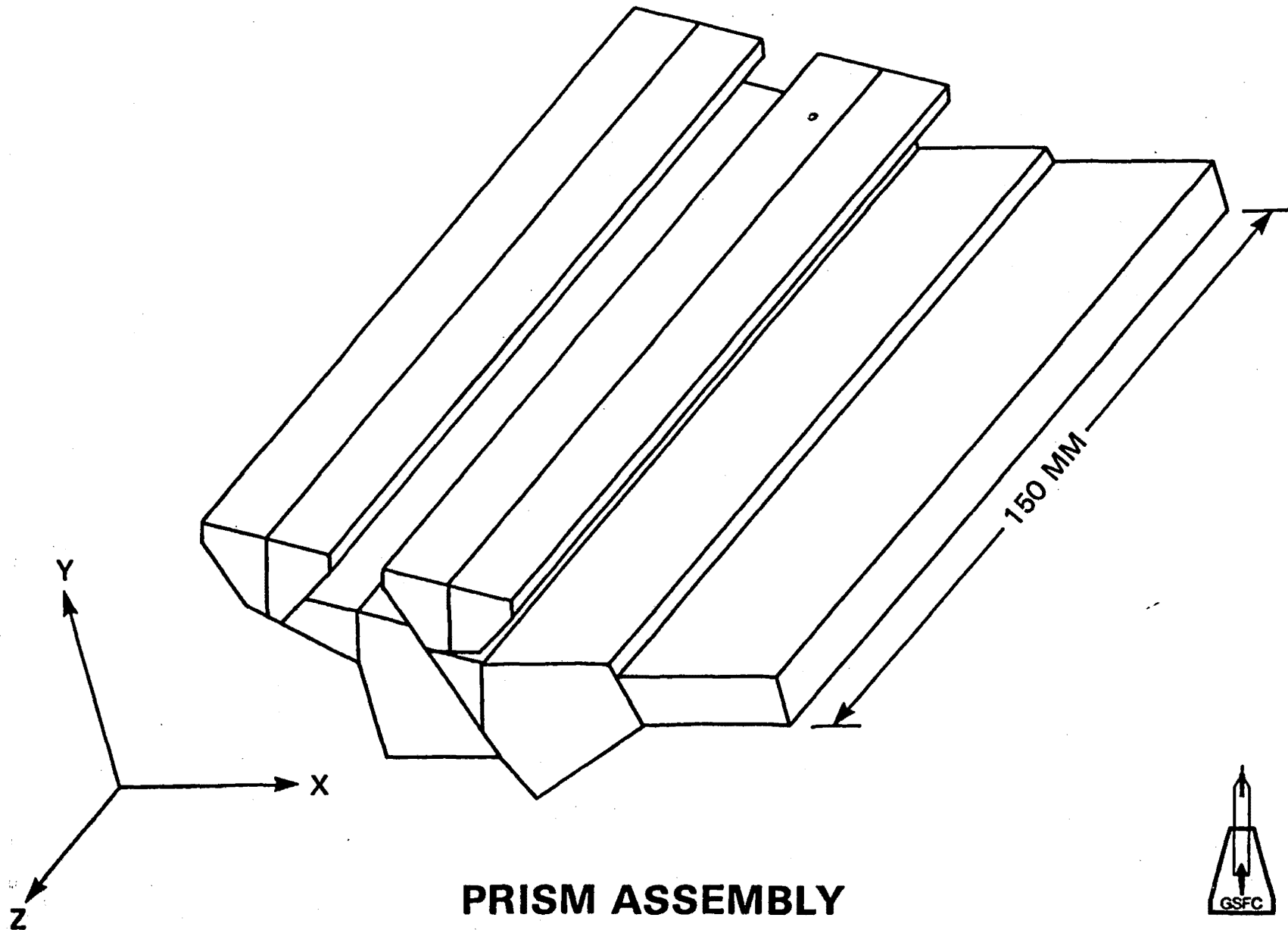
- NINE-MONTH \$100K STRIPE FILTER DEVELOPMENT AND EVALUATION.
- FOUR-MONTH \$45K STUDY OF MLA DICHROIC BEAM-SPLITTERS.
- IN-HOUSE ASSESSMENT OF IDS OPTICAL SYSTEM DESIGNS AND DEVELOPMENT OF GSFC DESIGN.

STATUS:

- STRIPE FILTER CONTRACT/WESTINGHOUSE COMPLETE 2/82
- DICHROIC FILTER STUDY/PERKIN-ELMER COMPLETE 9/81

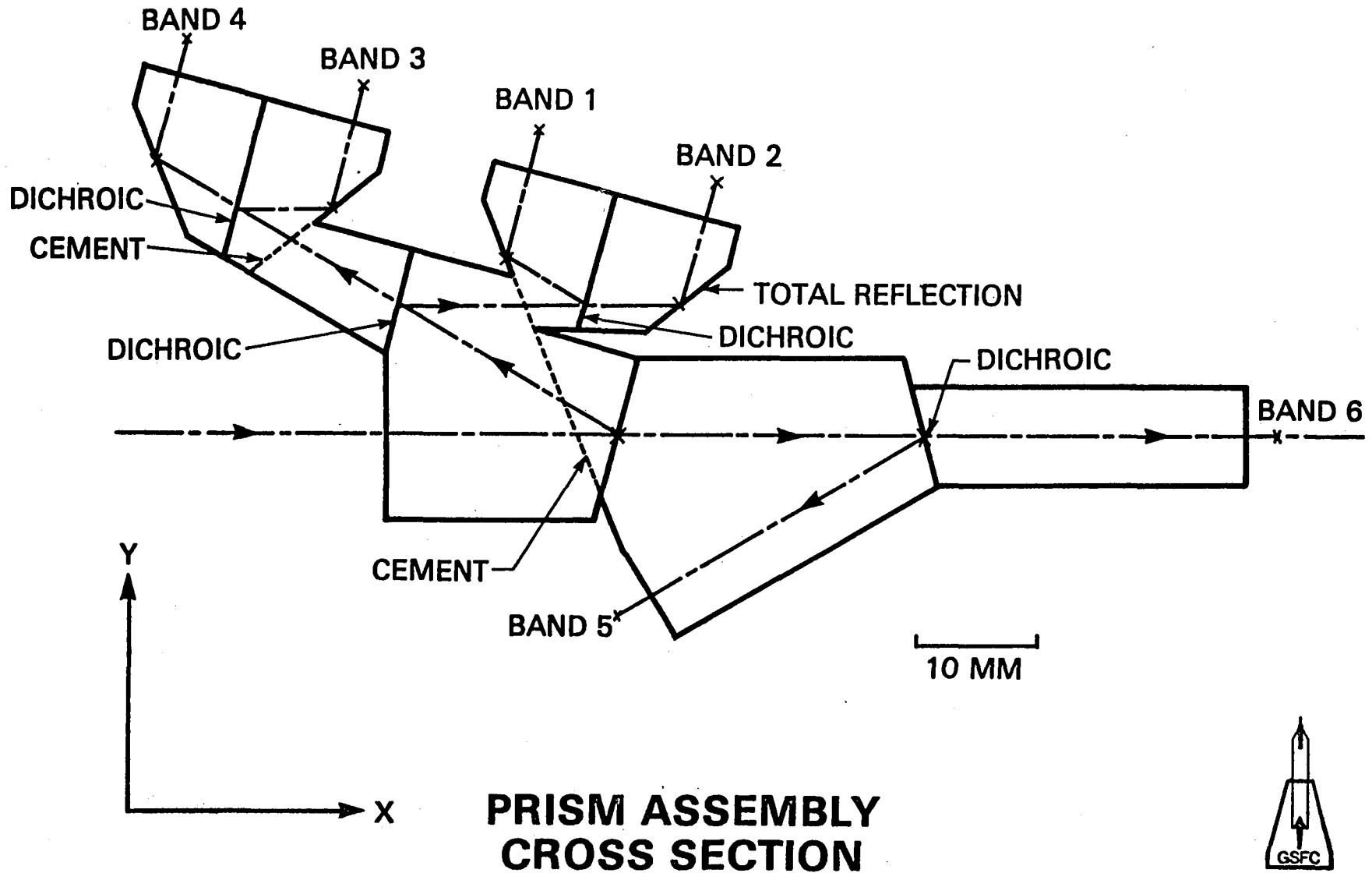


MLA BEAMSPLITTER DESIGN STUDY



MLA BEAMSPLITTER DESIGN STUDY

107



PASSIVE COOLER DESIGN

OBJECTIVE:

DEVELOP A DETAILED DESIGN FOR A PASSIVE RADIATIVE COOLER
THAT WILL FULFILL THE REQUIREMENTS GENERATED BY A MLA SENSOR.

APPROACH:

\$100K CONTRACT FOR RADIATIVE COOLER DESIGN TO MEET IDS
REQUIREMENTS

REQUIREMENTS:

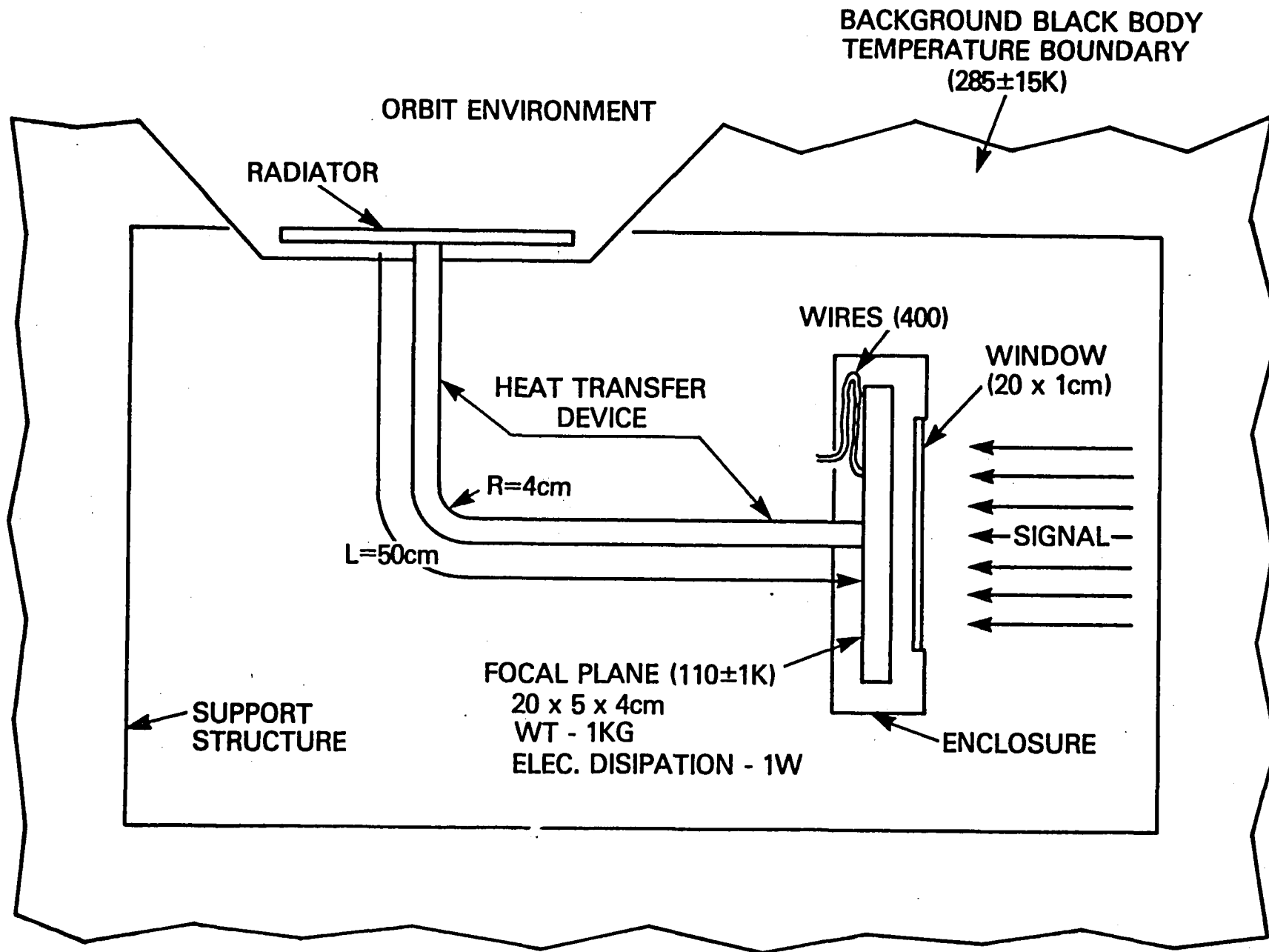
1W ELECTRICAL DISSIPATION AT 125K.
400 SIGNAL LEADS.
50 CM HEAT TRANSFER DEVICE.

STATUS:

RFP RELEASE 11/81.
CONTRACT START 1/82.



MLA COOLER STUDY

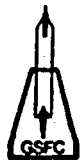


SENSOR SYSTEM SIMULATION

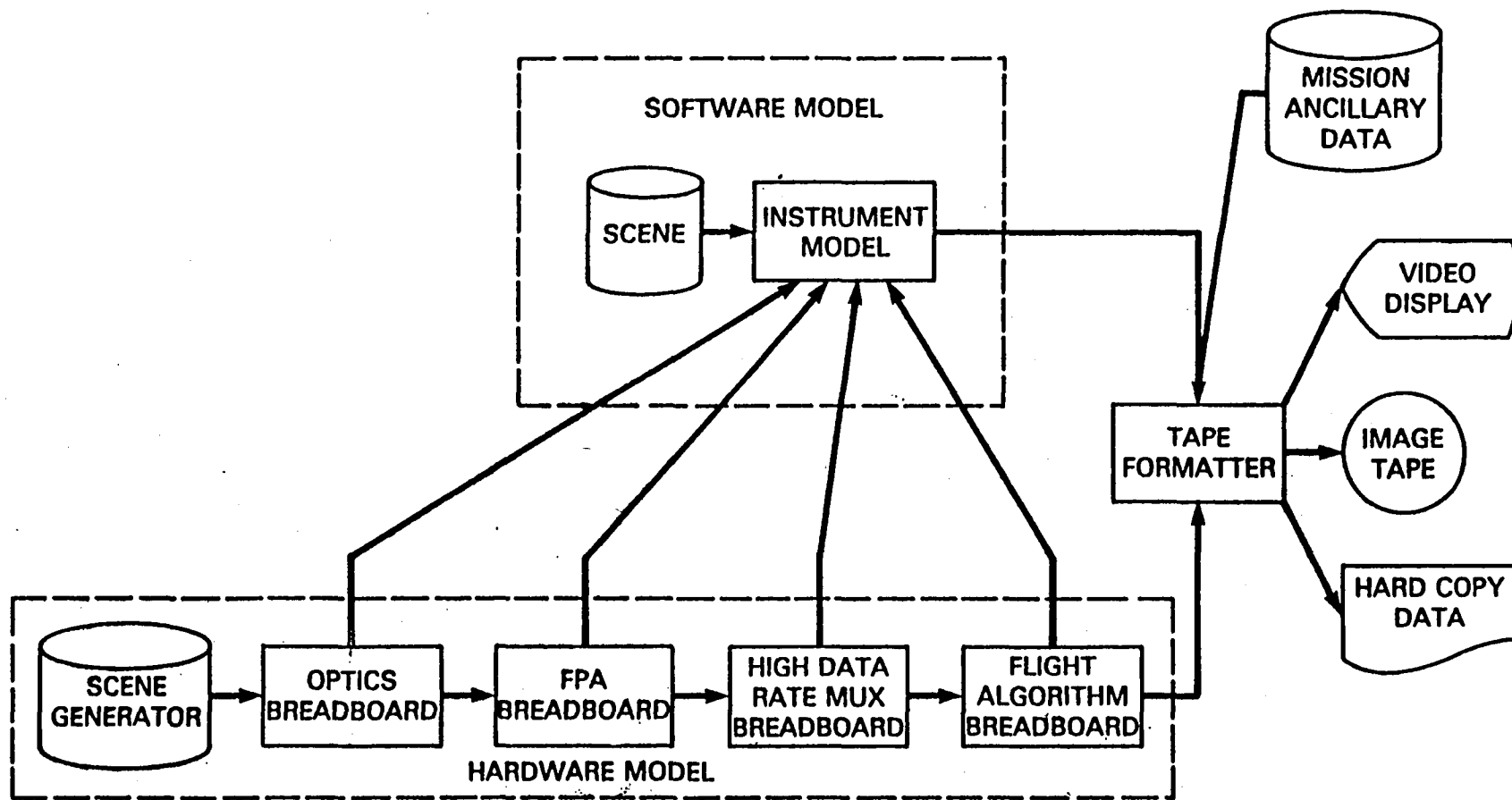
OBJECTIVE: EVALUATE MLA FLIGHT AND/OR GROUND SYSTEM TRADE-OFFS
VIA AN END-TO-END HARDWARE/SOFTWARE SYSTEM
SIMULATOR.

APPROACH: COMBINE OUTPUTS FROM BREADBOARD HARDWARE AND
SOFTWARE SYSTEM SIMULATOR.

STATUS: NEW TASK START FY82



SENSOR SYSTEM SIMULATION



MLA END-TO-END INSTRUMENT MODEL



ASSESSMENT AND CALIBRATION LABORATORY

OBJECTIVE:

CHARACTERIZATION OF THE RADIOMETRIC, SPECTRAL AND ELECTRONIC RESPONSE OF DETECTOR ARRAY MODULES AND FOCAL PLANE ASSEMBLIES

APPROACH:

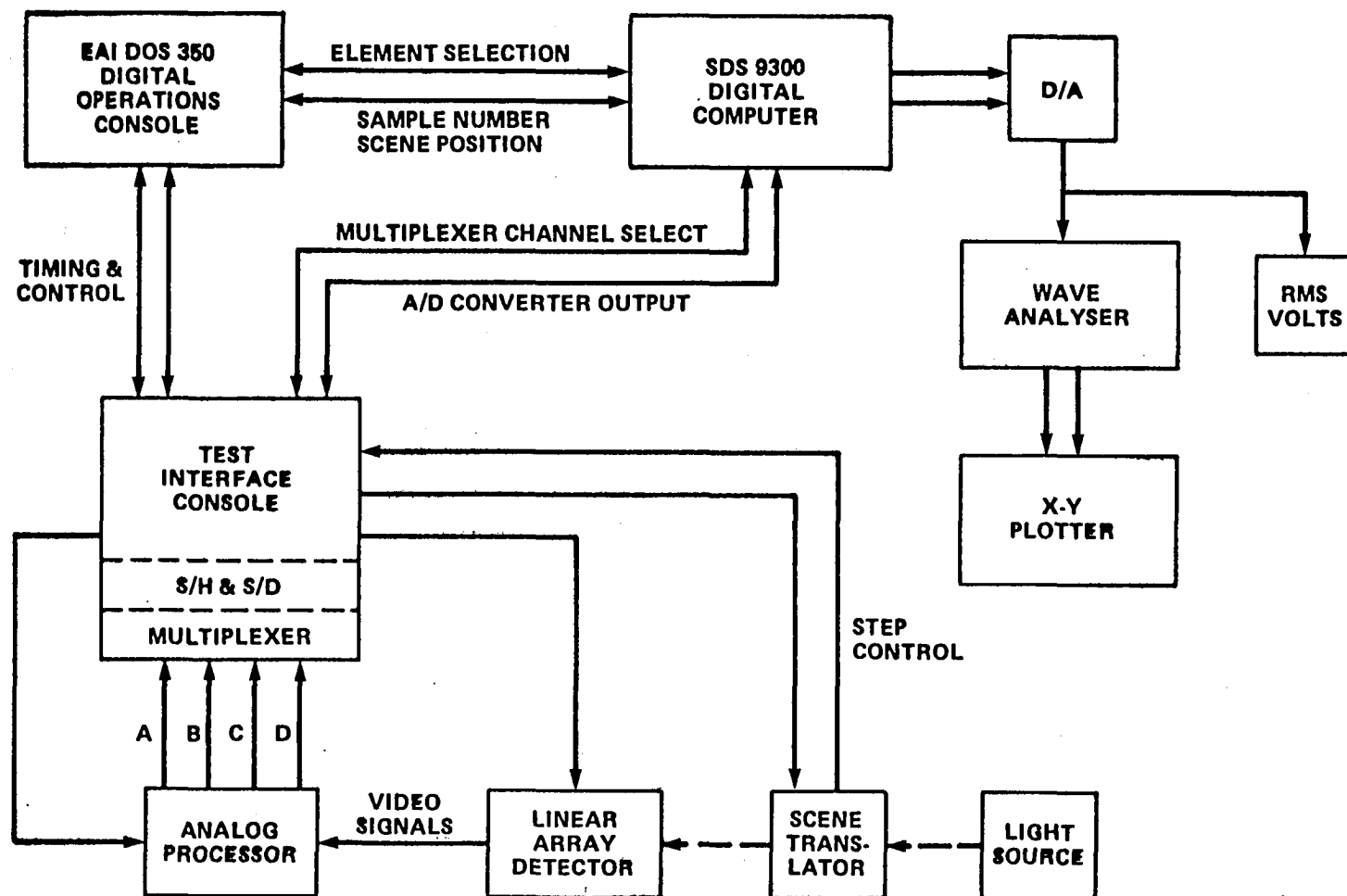
- EXPAND EXISTING FACILITY WITH VIS/NIR CAPABILITY TO SWIR AND TIR SYSTEMS.
- MEASURE ANGULAR AND SPATIAL VARIATIONS IN RADIANCE OF RADIOMETRIC CALIBRATION STANDARDS.
- IMPROVE ABSOLUTE ACCURACY OF EXISTING RADIOMETRIC STANDARDS.

STATUS:

- INTEGRATING SPHERE RADIANCE MAPPER COMPLETE.
- LABORATORY EXPANSION PLAN UNDER DEVELOPMENT.



ASSESSMENT AND CALIBRATION LABORATORY



AIRBORNE MLA SENSORS

OBJECTIVES:

- DEVELOP EXPERTISE IN THE DESIGN CALIBRATION AND TESTING OF MLA REMOTE SENSORS.
- EXAMINE TECHNIQUES TO CALIBRATE AND REMOVE SENSOR ARTIFACTS FROM MLA DATA.
- SUPPLY CALIBRATED MLA DATA TO THE SCIENTIFIC USERS.

APPROACH:

DEVELOP AIRBORNE LINEAR ARRAY PUSHBROOM RADIOMETERS (LAPR) AND ELOS SIMULATOR(S)

STATUS:

- | | | |
|------------|----------------------|--------|
| ● LAPR I | — RETIRED | — 9/81 |
| ● LAPR II | — DELIVERY | — 9/82 |
| ● ELOS/SIM | — PRELIMINARY DESIGN | — TBD |



THE IMAGING SPECTROMETER APPROACH

Executive Summary

John B. Wellman
Jet Propulsion Laboratory
California Institute of Technology
May 11, 1982

SUMMARY OF CONCLUSIONS

(1) A need for advanced multispectral capabilities has been defined by a significant segment of the discipline groups. Needs include multiple spectral bands, high spectral resolution, and the ability to tailor the band choices for the research application.

(2) Two important design drivers are the requirement for spatial registration of the spectral components and the implementation of the advanced multispectral capability, including spectral band width, number of bands and programmability.

(3) The dispersive approach, fundamental to the Imaging Spectrometer concept, achieves these capabilities by utilizing a spectrometer to disperse the spectral content while preserving the spatial identity of the information in the cross-track direction. Area array detectors in the spectrometer focal plane detect and store the spatial and multispectral content for each line of the image. The choice of spectral bands, image IFOV and swath width is implemented by programmed readout of the focal plane. These choices in conjunction with data compression are used to match the output data rate with the telemetry link capability.

(4) Progress in the key technologies of optics, focal plane

detector arrays, onboard processing and focal plane cooling supports the viability of the Imaging Spectrometer approach. Continued support of the current technology development activities will permit the implementation of a space flight system in the late 1980's.

THE NEED FOR ADVANCED MULTISPECTRAL CAPABILITIES

Differing observational requirements of the several discipline groups combine to justify an advanced capability. Several disciplines, which can be individually satisfied with a few spectral bands, require different sets of bands, thereby necessitating a wide variety of bands to choose from. Other measurement goals are optimized by making the spectral bands narrow. The problem of removing atmospheric effects from multispectral data sets may necessitate additional spectral bands to characterize the atmospheric contribution. Finally, there is a need to explore the accessible spectral regions to determine the most useful bands. These needs can be met by a programmable sensor which possesses sufficient granularity in spectral band selection to exploit the known spectral signatures and to explore new spectral characteristics.

KEY DESIGN DRIVERS

The parameters of IFOV, swath width, radiometric sensitivity (NE δ R), and data rates determine the system design of land remote sensing systems in general. Spatial registration of the multispectral samples is extremely critical in discriminating among instrument approaches. In critically sampled MLA-type systems a fundamental loss in multispectral information occurs when the misregistration exceeds about 0.3 pixels. In the range from 0.3 to 1.0 pixels, resampling will not produce a significant improvement. For misregistration greater than 1.0 pixel, resampling will improve quality, but not the level of completely registered data.

For advanced multispectral systems with high spectral resolution capability, three considerations are critical -- the spectral band width (or granularity), the number of spectral bands, and the spectral programmability

of the instrument. With the NEdR specification, spectral band width determines the required system aperture, a major determining factor in instrument size and cost. The number of bands directly influences data rate. Programmability implies complexity in the onboard electronics.

THE DISPERSIVE IMAGING APPROACH

A variety of Imaging Spectrometer instrument concepts are under study ranging from aircraft instruments with limited imaging capability (Airborne Imaging Spectrometer) to free-flying spacecraft-borne systems capable of meeting both research and operational needs. An intermediate design suitable for space shuttle and possible space platform application is described in the attached viewgraphs and paper (Imaging Spectrometer Technologies for Advanced Earth Remote Sensing, Wellman, et al, Paper No. 345-04, Proceedings of the Society of Photo-Optical Instrumentation Engineers, May 6, 1982).

The instrument provides 20 nanometer spectral resolution over the wavelength range from 0.4 to 2.5 micrometers with 10m IFOV in the VNIR and 20m IFOV in the SWIR. A 60 km swath width is obtained from 300 km. Although internal data rates are high, a wide variety of multispectral imaging modes can be commanded within the data rate constraints imposed by the Shuttle and TDRSS.

PROGRESS IN KEY TECHNOLOGIES

As part of this program the key technologies of optics, focal plane detector arrays, onboard processing and focal plane cooling are being developed.

An optical design concept centered on a multiple-pass Schmidt system has been shown to satisfy the spatial and spectral resolution requirements. Linearization of prism dispersion is accomplished by using a multiple element prism. Breadboarding of critical elements is planned.

Planar hybrid HgCdTe area arrays of 32 by 32 format have been fabricated and tested. Development of 64 by 64 element mosaickable arrays for the 1.0 to 2.5 micrometer region has begun. An alternative technology using InSb has been demonstrated with 128 element linear arrays. The extension to area arrays is planned.

The Block Adaptive Rate Controlled (BARC) data compression algorithm implemented for the Galileo mission to Jupiter has been modified and demonstrated with representative terrestrial scenes. Electronics for the programmable readout of area array detectors and real-time radiometric calibration restoration are being breadboarded for use with the existing HgCdTe SWIR arrays.

A radiative cooler suitable for free-flying missions has been designed and analyzed. A new approach -- the adsorption refrigerator -- has been chosen for study in connection with a shuttle mission. This cooler provides closed cycle cooling over a wide range of temperatures without the concern of limited lifetimes attendant to mechanical compressors.

Progress in these technologies is sufficient to project flight readiness in the late 1980's.

THE IMAGING SPECTROMETER APPROACH

- o MAJOR CONCLUSIONS
- o THE REGISTRATION ISSUE
- o DESIGN SPACE FOR I. S. SYSTEMS
- o AN EXAMPLE: SHUTTLE IMAGING SPECTROMETER
- o REMARKS ON TECHNOLOGY READINESS

MAJOR CONCLUSIONS

- o NEEDS FOR ADVANCED MULTISPECTRAL CAPABILITIES NOTED:
 - MULTIPLE BANDS
 - HIGH SPECTRAL RESOLUTION
 - PROGRAMMABILITY
- o SPECTRAL CAPABILITY KEY DESIGN DRIVER
 - REGISTRATION
 - DEFINITION OF SPECTRAL SELECTION FEATURES
- o VIABLE DISPERSIVE IMAGING APPROACH UNDER DEVELOPMENT
- o PROGRESS IN KEY TECHNOLOGIES SUPPORTS THE APPROACH

ISSUES

SPATIAL REGISTRATION OF MULTISPECTRAL DATA SETS

QUESTION: BY WHAT AMOUNT CAN SEPARATE SPECTRAL SAMPLES BE MIS-REGISTERED WITHOUT DEGRADING THE INHERENT QUALITY OF THE DATA

SUGGESTED ANSWER:

- (1) FOR MISREGISTRATION LESS THAN 0.1 TO 0.3 PIXELS THE DATA MAY BE USED DIRECTLY FOR CLASSIFICATION WITH LITTLE DEGRADATION FROM 0-PIXEL MISREGISTRATION
- (2) FOR MISREGISTRATION OF THE ORDER 0.3 - 1.0 PIXELS A SIGNIFICANT LOSS IN CLASSIFICATION ACCURACY (10%) WILL OCCUR. RESAMPLING WILL NOT PRODUCE A SIGNIFICANT IMPROVEMENT

ISSUES (CONT)

- (3) FOR MISREGISTRATION GREATER THAN 1 PIXEL, RESAMPLING CAN IMPROVE CLASSIFICATION ACCURACIES TO THE LEVEL INDICATED IN (2), WITHOUT RESAMPLING ERRORS OF 10 TO 30% WILL OCCUR.

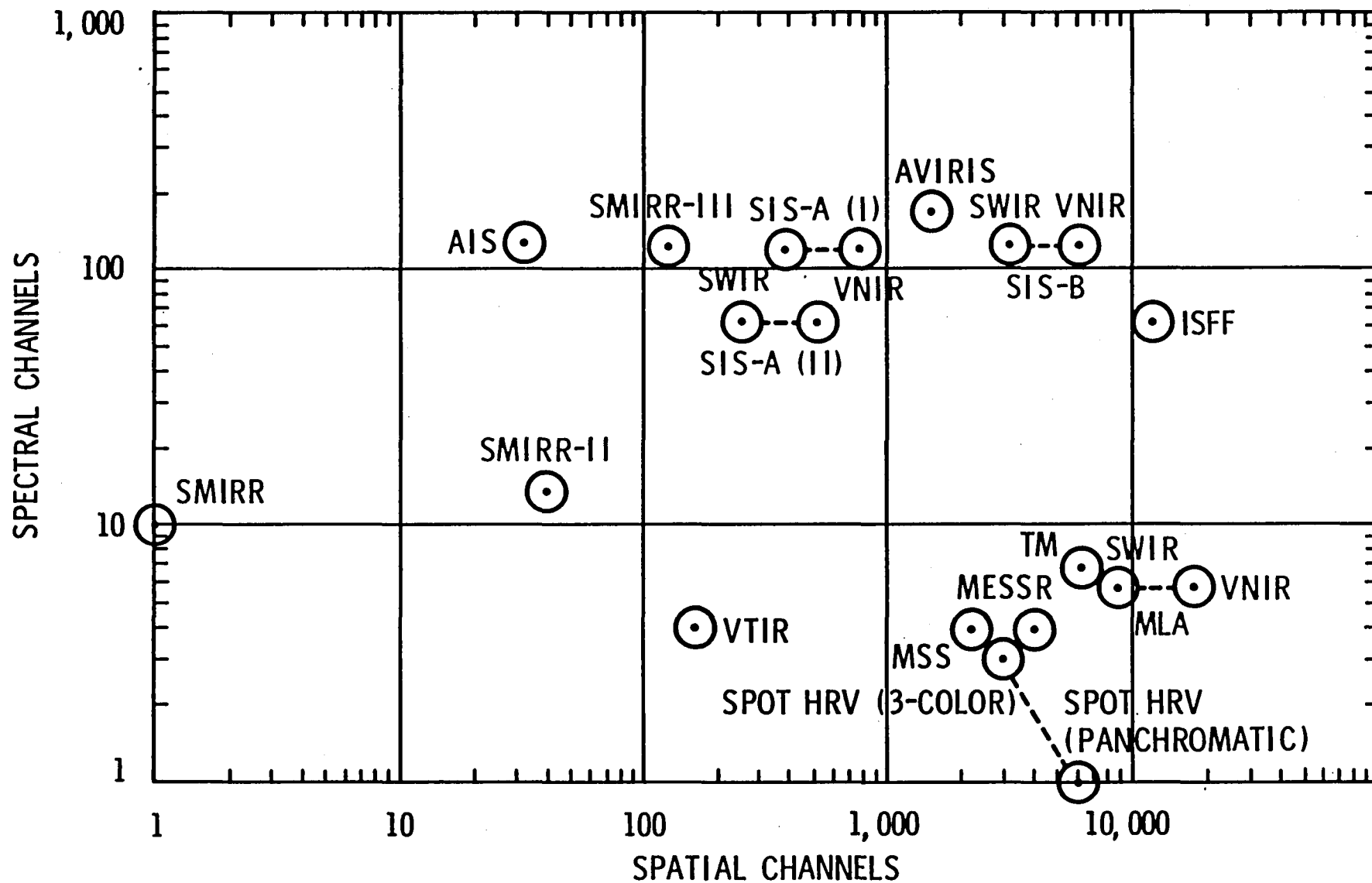
REFERENCES:

- (1) SWAIN, P. H., VANDERBILT, V. C., JOBUSCH, C. D.,
"A QUANTITATIVE APPLICATIONS-ORIENTED EVALUATION OF
THEMATIC MAPPER DESIGN SPECIFICATIONS," 1981
INTERNATIONAL GEOSCIENCE AND REMOTE SENSING SYMPOSIUM,
WASHINGTON, D.C., JUNE 8-10, 1981, P820.
- (2) ROOT, G. R., "REGISTRATION BETWEEN SPECTRAL BANDS,"
APPENDIX A, IN APPLICATION OF SOLID STATE ARRAY
TECHNOLOGY TO AN OPERATIONAL LAND-OBSERVING SYSTEM,
JPL DOCUMENT 715-82, OCT 31, 1980.



COMPARISON OF LAND REMOTE SENSING SYSTEMS

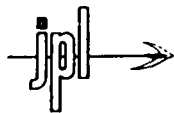
123





LAND REMOTE SENSING SYSTEM INDEX

INSTRUMENTS FLOWN	INSTRUMENTS UNDER DEVELOPMENT	INSTRUMENT CONCEPTS	AIRCRAFT INSTRUMENTS
MSS – MULTI- SPECTRAL SCANNER SYSTEM (LANDSATS 1-3)	TM – THEMATIC MAPPER (1982)	MLA – MULTI- SPECTRAL LINEAR ARRAY (1987-)	AIS – AIRBORNE IMAGING SPECTRO- METER (1982)
SMIRR – SHUTTLE MULTI- SPECTRAL RADIOMETER (SHUTTLE OSTA-2)	SPOT – HRV – SYSTEME PROBATOIRE d'OBSERVA- TION DE LA TERRE (1984)	SIS – SHUTTLE IMAGING SPECTRO- METER (A: 1987-) (B: 1989-)	AVIRIS – ADVANCED VISUAL AND INFRARED IMAGING SPECTRO- METER (1985)
	MESSR – MULTI- SPECTRAL ELECTRONIC SELF-SCAN- ING RADIO- METER (1985)	ISFF – IMAGING SPECTRO- METER FREE- FLYER (1980-)	
	VTIR – VISIBLE AND THERMAL INFRARED RADIOMETER (1985)	SMIRR – SHUTTLE MULTI- SPECTRAL INFRARED RADIO- METER (II: 1985-) (III: 1987-)	

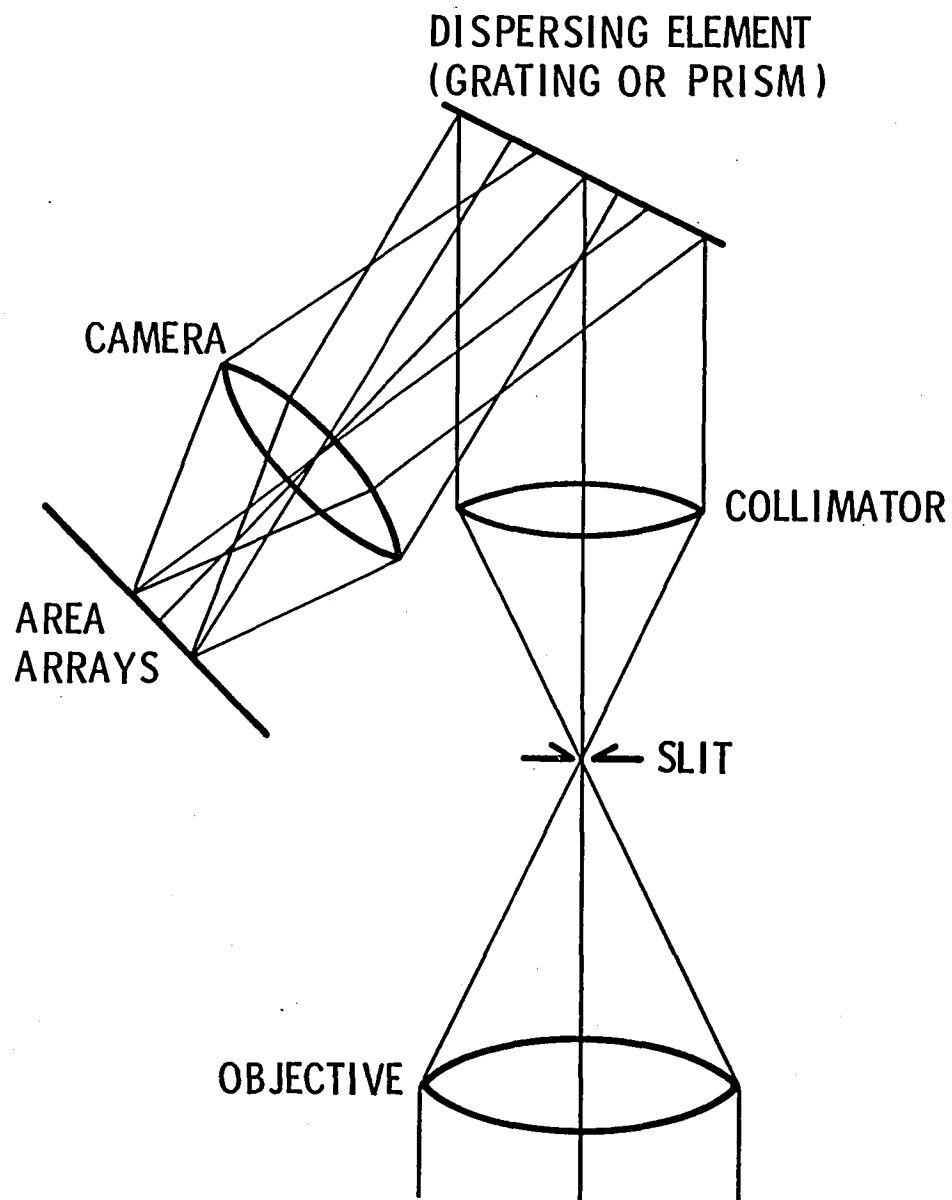


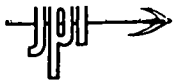
PERFORMANCE REQUIREMENTS

PARAMETER	VALUE	
	VNIR	SWIR
GROUND IFOV, m	10	20
SPECTRAL RESOLUTION, nm	20	20
SWATH WIDTH, km	60	60
RADIOMETRIC PRECISION, PERCENT	0.5	1.0



DISPERSIVE IMAGING TECHNIQUE





IMAGING SPECTROMETER CONCEPT



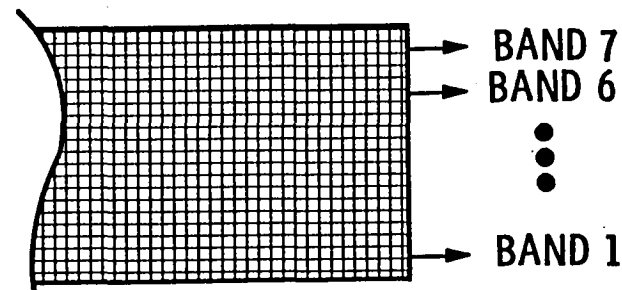
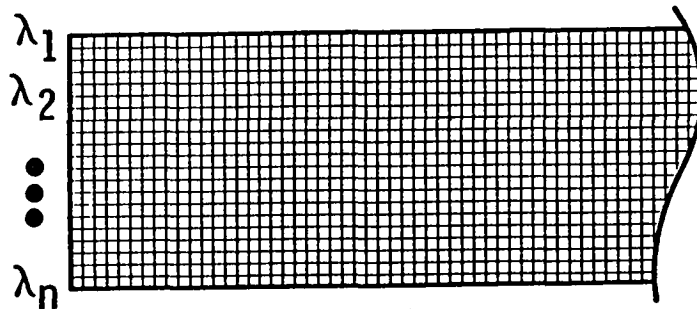
OBJECT SPACE

DURING ONE LINE TIME: ONE LINE OF THE SCENE IS TRANSFORMED INTO MANY LINE IMAGES AT DIFFERING WAVELENGTHS

← SPATIAL INFORMATION →

x_1, x_2 ----

---- x_n



BAND 7

BAND 6



BAND 1

IMAGE SPACE



IN-FLIGHT FUNCTIONAL CAPABILITIES

- **SPECTRAL BAND SELECTION**

THE NUMBER, CENTRAL WAVELENGTH AND SPECTRAL BANDWIDTH OF THE CHANNELS MAY BE SELECTED AND VARIED ACCORDING TO USER CHOICES

- **ONBOARD RADIOMETRIC CORRECTION AND REGISTRATION**

DATA COMPRESSION AND ADVANCED INFORMATION PROCESSING CAN BE APPLIED TO THE DATA, PRODUCING INFORMATION-INTENSIVE TELEMETRY

- **SELECTABLE IFOV**

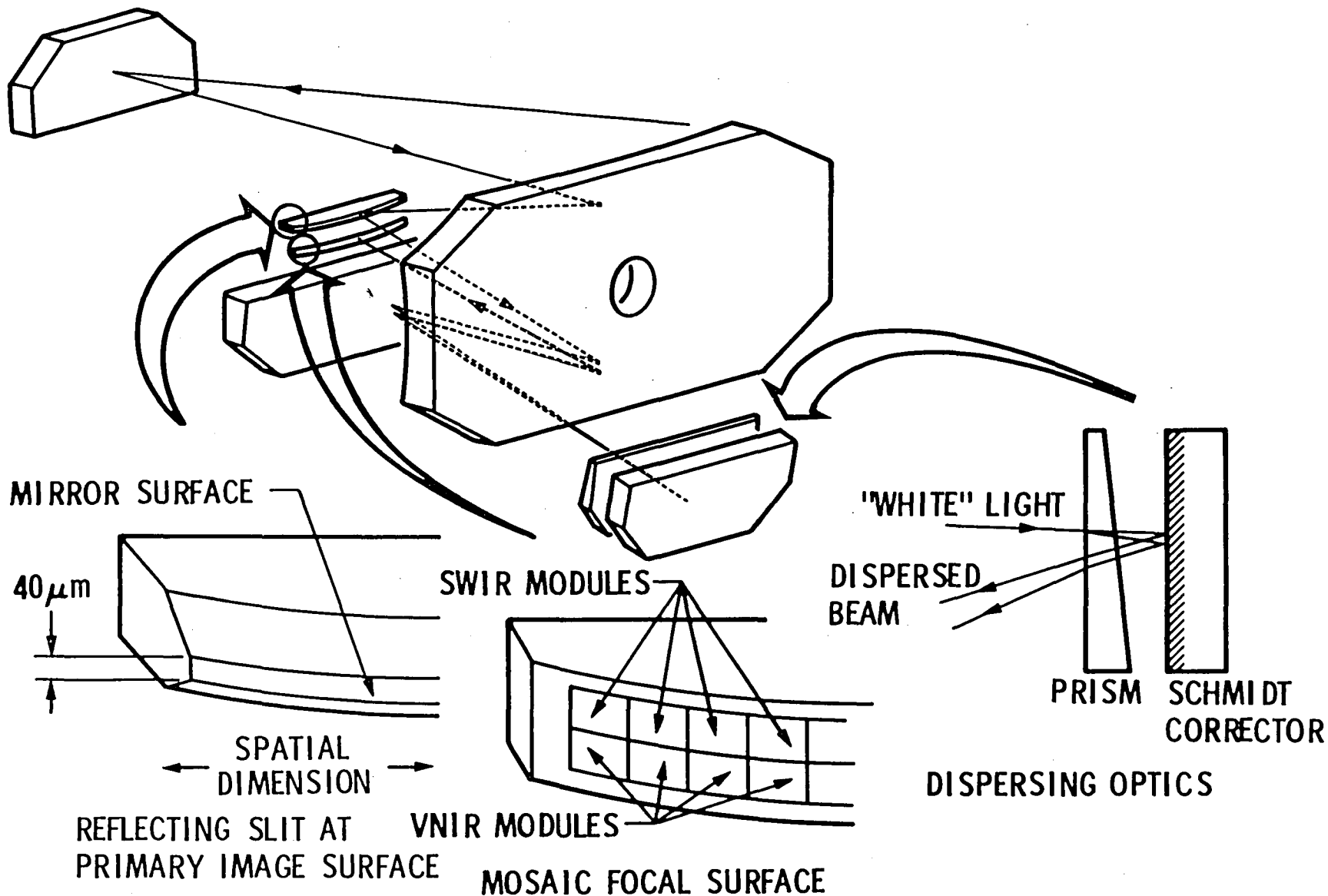
VARIOUS IFOV'S MAY BE COMMANDED TO INVESTIGATE DIFFERING RESOLUTIONS, TO MATCH TELEMETRY CAPABILITIES, OR TO PROVIDE A LOW-RESOLUTION LOW DATA RATE CHANNEL

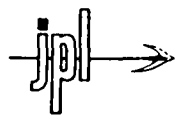
- **SELECTABLE SWATH WIDTH**

COMBINED WITH SELECTABLE SWATH WIDTH A VARIETY OF TARGET CHOICE AND VIEWING PARAMETER SELECTIONS CAN BE MADE WITHIN A LIMITED TELEMETRY CAPABILITY



IMAGING SPECTROMETER OPTICAL CONCEPT





DESIGN CHARACTERISTICS

PARAMETER	VALUE
EQUIVALENT APERTURE DIAMETER, cm	30
TELESCOPE FOCAL LENGTH, cm	120
PHYSICAL SLIT WIDTH, μm	40
GROUND-PROJECTED SLIT WIDTH, m	10
ALTITUDE, km	300
SWATH WIDTH, km	61.44
DETECTOR SIZE (pixel), μm	40 x 40
LINE TIME (FOR 10 m IFOV), ms	1.385
ENCODING, bits/pixel	8
RAW DATA RATE (VNIR), bits/s	2.27×10^9
(SWIR), bits/s	0.57×10^9
(Total), bits/s	2.84×10^9

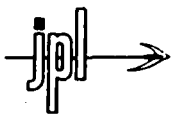
SAMPLE IMAGING MODES AND DATA RATES

VNIR		VNIR		SWATH WIDTH (KM)	DATA RATES (1)	
CHANNELS	IFOV (M)	CHANNELS	IFOV (M)		@ 8 BITS/PIXEL (MB/s)	@ 3.2 BITS/PIXEL (2) (MB/s)
1	10	-	-	60	35.5	14.2
-	-	1	20	60	8.9	3.6
4	10	2	20	60	159.8	63.9
3	10	3	20	60	133.2	53.3
2	10	4	20	60	106.6	42.6
4	10	2	20	45	117.4	46.9
6	20	-	-	60	53.4	21.4
(3) 12	30	-	-	60	47.3	18.9

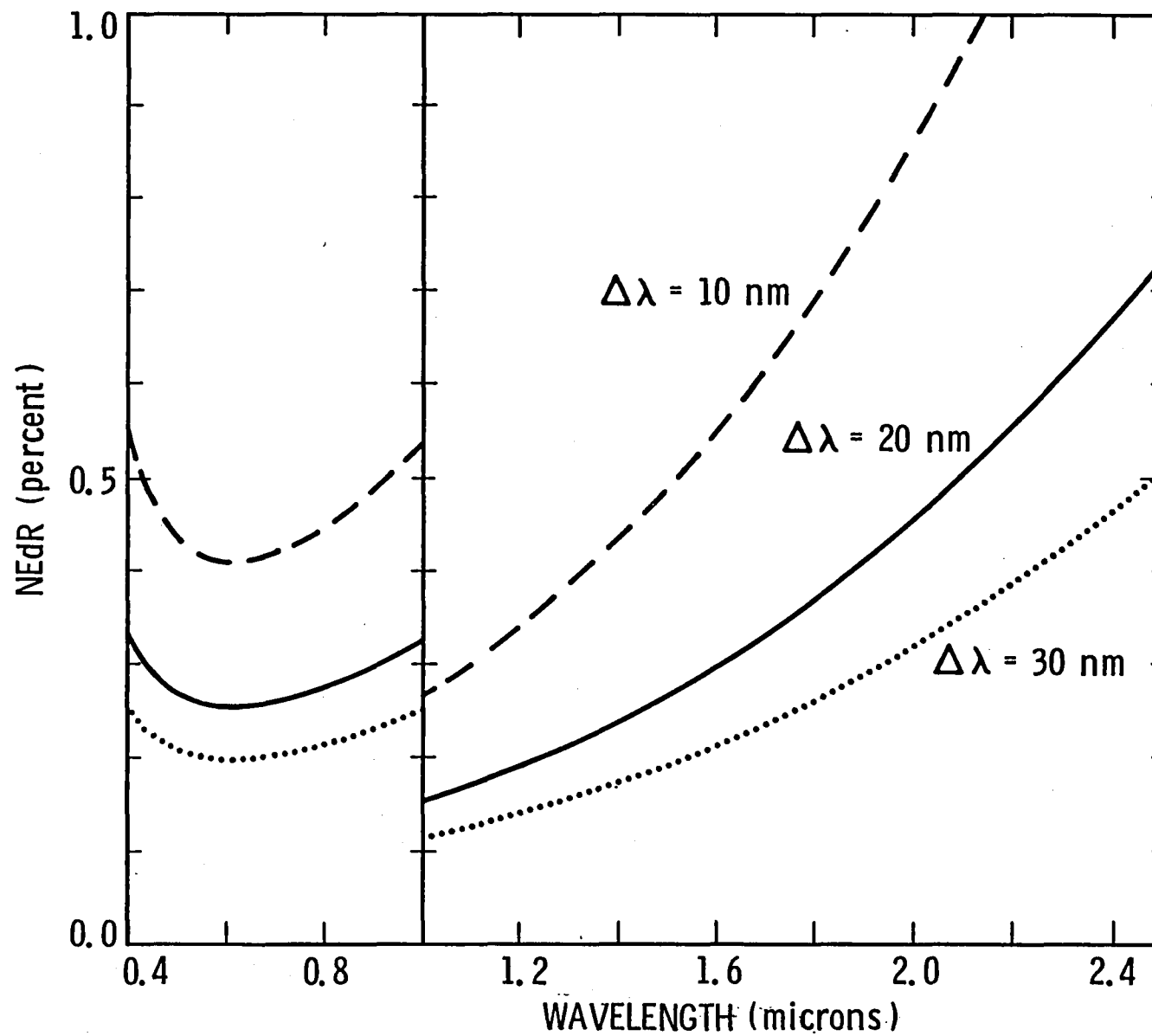
(1) LIMIT FOR FREE-FLYER WITH TDRSS IS 300 MB/s; FOR SHUTTLE, 50 MB/s

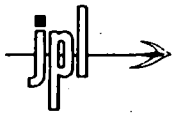
(2) BLOCK ADAPTIVE RATE CONTROLLED (BARC) DATA COMPRESSION OF 2.5:1 ASSUMED

(3) REQUIRES CHANGE TO IMAGING SPECTROMETER BASELINE DEFINITION

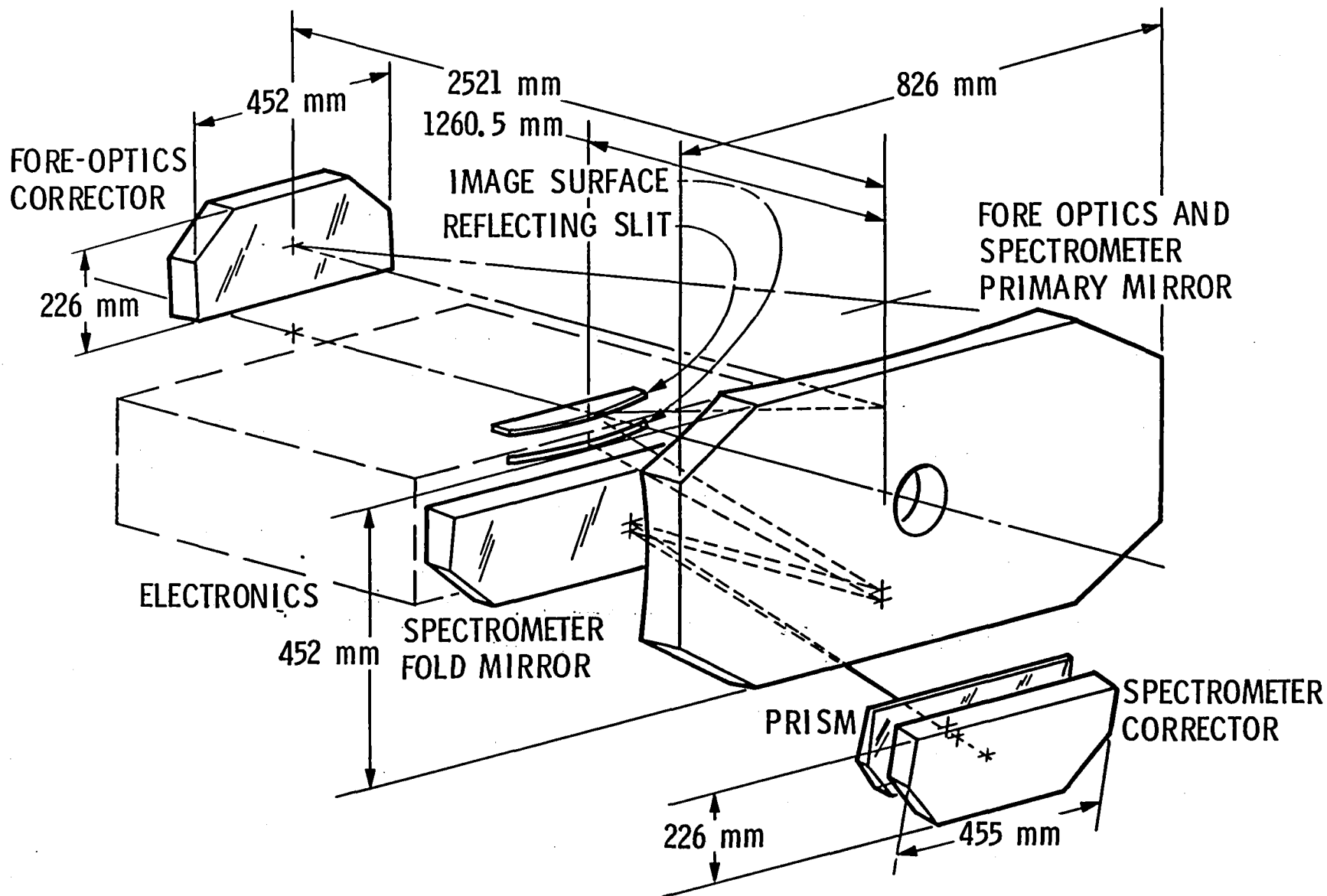


RADIOMETRIC PERFORMANCE CHARACTERISTICS OF THE SIS



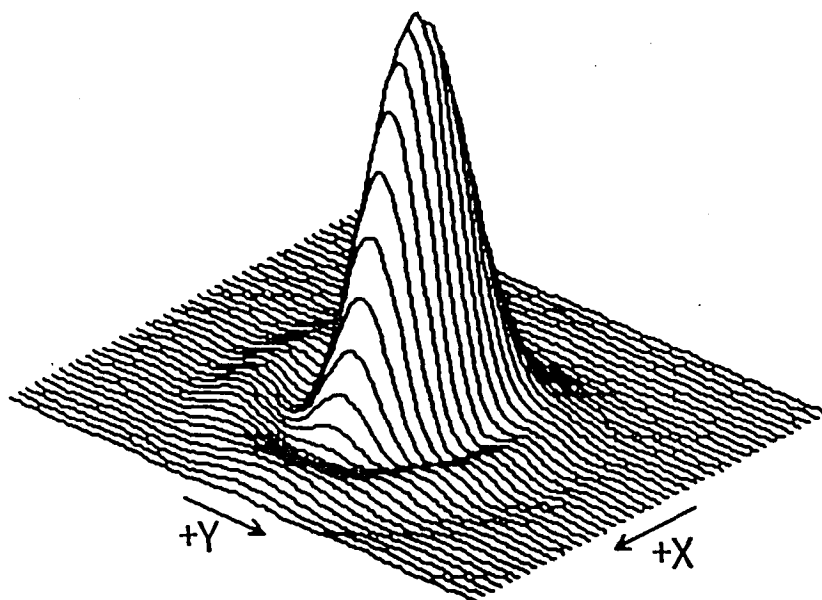


OPTICAL CONFIGURATION

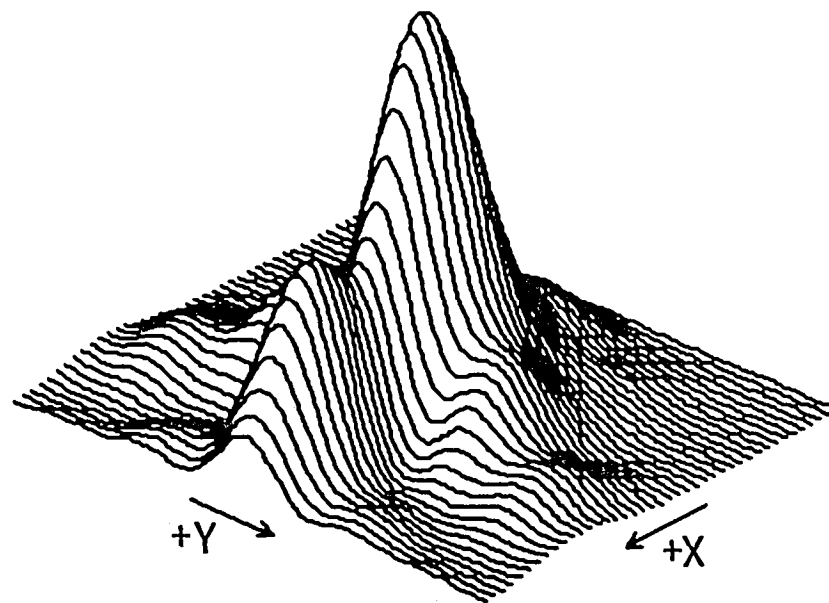




OPTICAL POINT SPREAD FUNCTIONS



ON AXIS



FULL FIELD

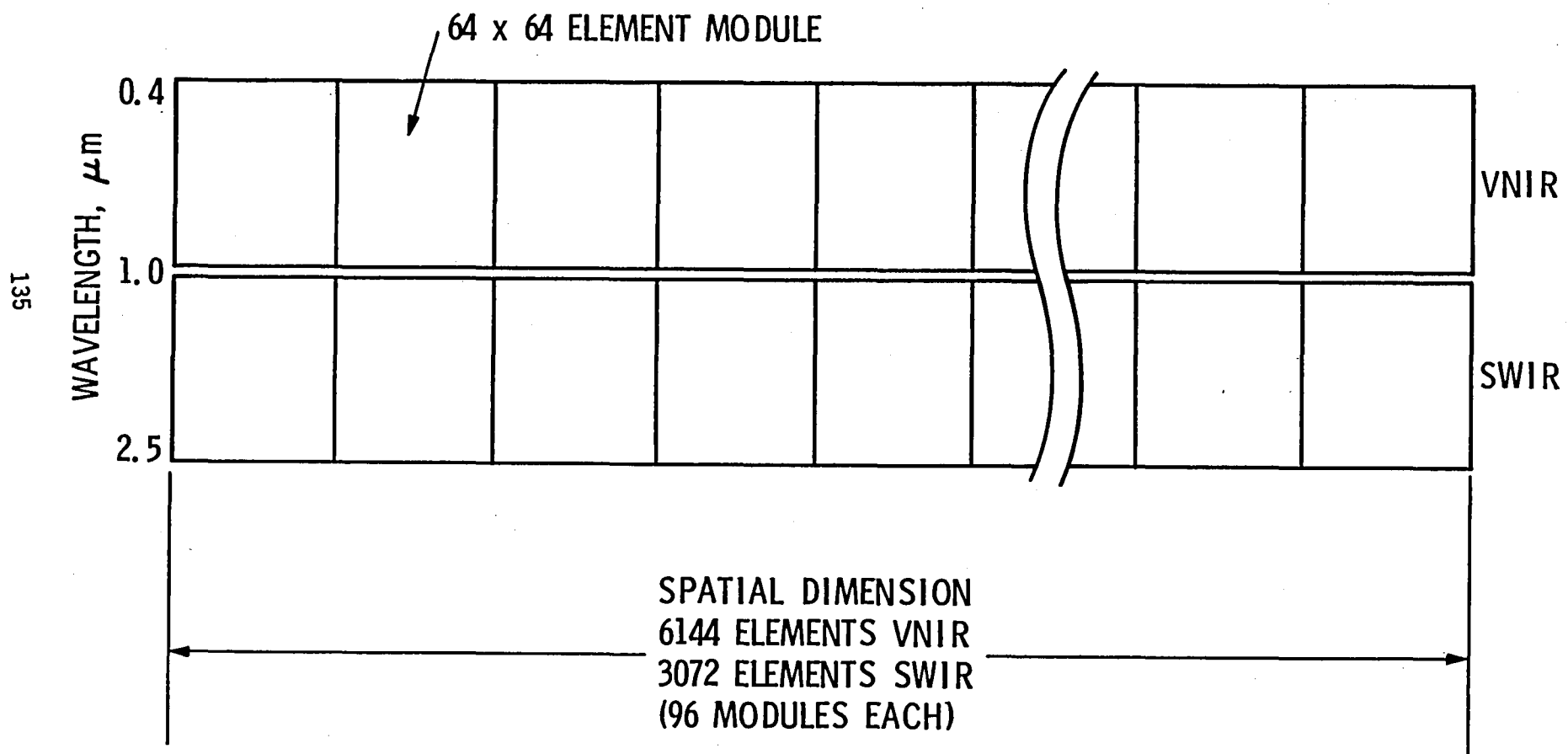
X IS THE SPECTRAL DIMENSION

Y IS THE SPATIAL DIMENSION

PLOT BOUNDARIES DEFINE 40 x 40 μm PIXEL

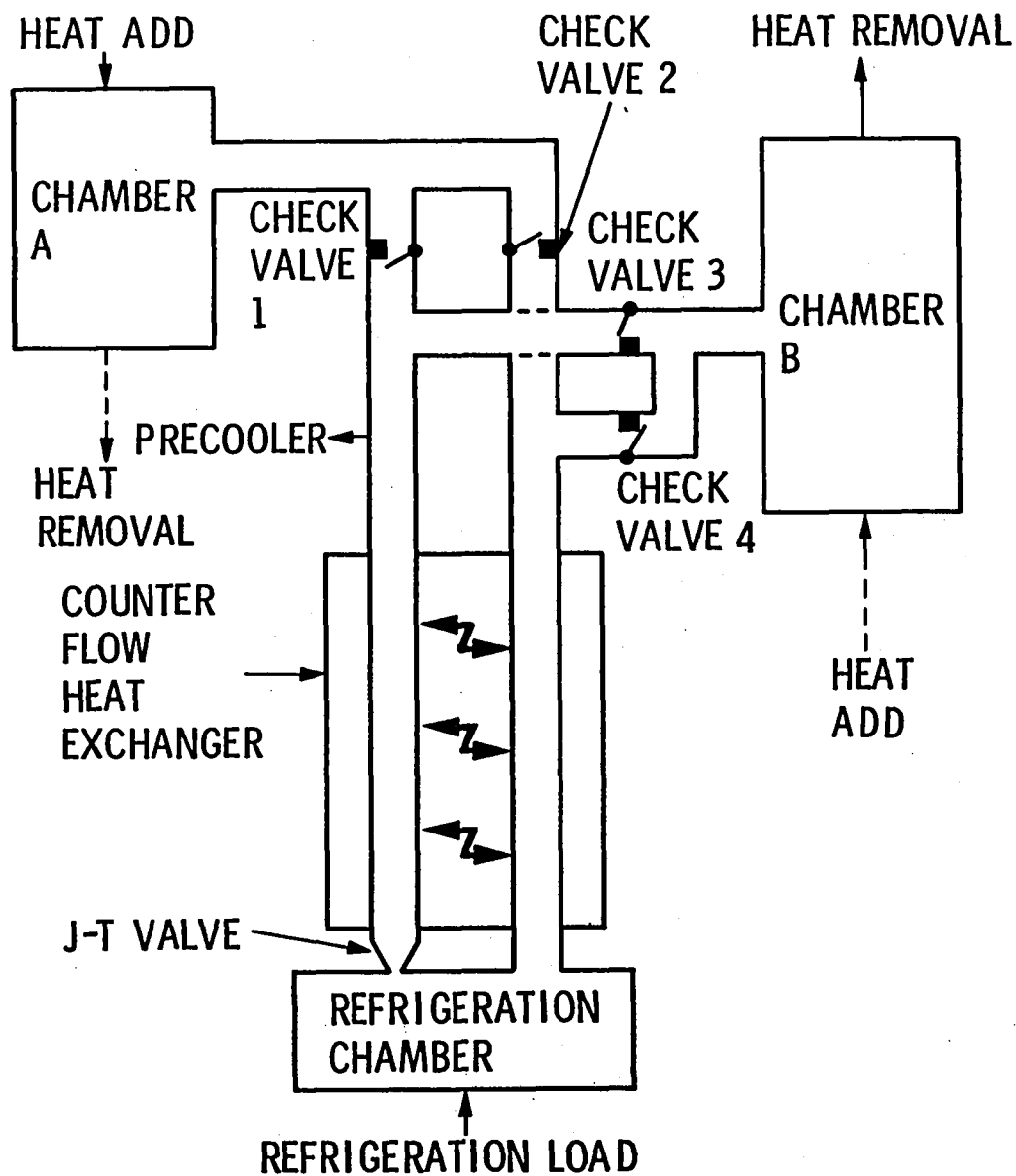


SHUTTLE IMAGING SPECTROMETER FOCAL PLANE





ADSORPTION REFRIGERATOR BLOCK DIAGRAM



Imaging spectrometer technologies for advanced Earth remote sensing

J. B. Wellman, J. B. Breckinridge, P. Kupferman, R. P. Salazar, and K. B. Sigurdson

Jet Propulsion Laboratory, California Institute of Technology
4800 Oak Grove Drive, Pasadena, California 91109

Abstract

A major requirement of multispectral imaging systems for advanced Earth remote sensing is the provision for greater spectral resolution and more versatile spectral band selection. The imaging spectrometer instrument concept provides this versatility by the combination of pushbroom imaging and spectrally dispersing optics using area array detectors in the focal plane. The Shuttle Imaging Spectrometer concept achieves 10- and 20-meter ground instantaneous fields of view with 20-nanometer spectral resolution from Earth orbit. Onboard processing allows the selection of spectral bands during flight; this, in turn, permits the sensor parameters to be tailored to the experiment objectives. Recent advances in optical design, infrared detector arrays, and focal plane cooling indicate the feasibility of the instrument concept and support the practicability of a validation flight experiment for the Shuttle in the late 1980s.

Introduction

The broad range of user requirements for advanced land remote sensing is addressed in a companion paper.¹ From this study and others, the need for greater versatility in spectral coverage and spectral isolation within the 0.4- to 2.5- μm region emerges as a significant consideration in the design of future systems. The application of spectrometric techniques to pushbroom imaging^{2,3,4} offers a method by which versatility in defining the individual spectral bands and the utilization of narrow spectral bands (high spectral resolution) can be realized.

Instrument concepts suitable for free-flying spacecraft, Shuttle-attached payloads, potential space platforms, and research aircraft have been studied. These concepts provide inherent registration of the many spectral channels in addition to the spectral versatility. Implementation of the imaging spectrometer concept requires technological advances in area array detectors for the visual and near-infrared (VNIR) and short-wavelength infrared (SWIR) spectral bands, in optical systems that provide imaging and spectral dispersion over the broad wavelength region, in focal plane cooling necessary for the achievement of acceptable signal-to-noise ratios, and in onboard electronics.

In the following presentation, we describe the Shuttle Imaging Spectrometer (SIS) as a prototypical example of the instrument system technology, discuss its performance capabilities, and review three supporting subsystem technologies: optics, focal-plane arrays, and focal-plane cooling.

Shuttle Imaging Spectrometer design

The formulation of observational requirements and needs for the SIS is based on the need for an instrument that would serve both as a research tool and a mechanism for verifying the technology. The constraints imposed on the SIS design include compatibility with the Shuttle, low cost in comparison to a free flyer (in consideration of the short duration missions), and a corresponding decrease in complexity. The intent was to develop a simple design that retained the major technological elements and fundamental performance capabilities, but dispensed with the operational requirements, most notably, swath width and complete global coverage.

From our analysis of the broad range of user's needs, a basic set of performance requirements was derived⁴. They are shown in Table 1. The spatial resolution of the system is specified by the ground instantaneous field of view (IFOV), an idealized measure defined by the cross-track geometric projection of a detector element or the along-track distance corresponding to the integration time (following the usual convention, these distances are designed to be equal). The radiometric precision is expressed as the noise equivalent change in reflectance (NE Δ R), which is defined as that change in ground reflectance that produces a change in detected signal equivalent to the instrument system noise level.

The dispersive approach, the key to the imaging spectrometer concept, uses area array detectors and accomplishes spectral separation by use of a spectrometer section added after the imaging optics. The concept is illustrated in Figure 1. Radiation from the scene is imaged upon a slit (oriented normal to the plane of the figure). The slit defines

Table 1. Shuttle Imaging Spectrometer Performance Requirements

Parameter	Value	
	VNIR	SWIR
Ground IFOV, m	10	20
Spectral resolution, nm	20	20
Swath width, km	60	60
Radiometric precision, %	0.5	1.0

the system field stop and determines the footprint on the ground. Radiation passing through the slit is dispersed within a spectrometer and reimaged at the camera focal plane. Since the spectrometer is designed to maintain the spatial resolution present at the slit, the image at the spectrometer camera focal plane is a series of images of the line in object space, but displaced orthogonally in the spectral dimension as shown in Figure 2. This mapping of spatial and spectral

information corresponds to a single line on the ground. The data to be transmitted by the instrument is read out from the focal plane in a short period of time. Within this time

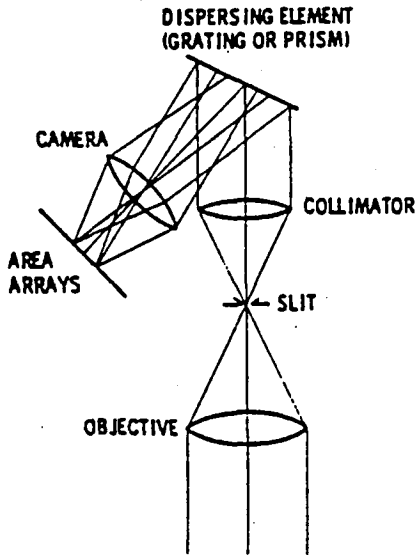


Figure 1. Imaging spectrometer optical concept

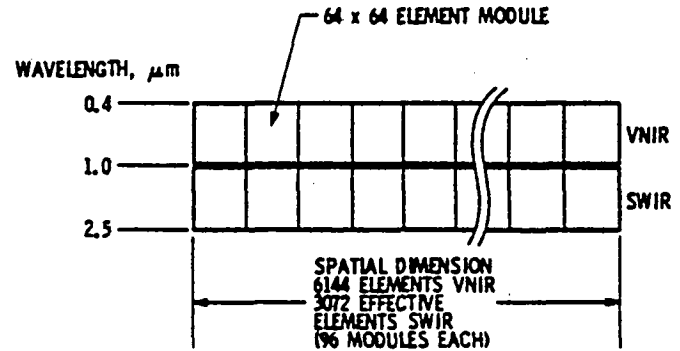


Figure 2. Shuttle imaging spectrometer focal surface arrangement

interval, the spacecraft motion moves the line image into the next position so that the imaging process can be repeated. The procedure is repeated continually to build up an image in the pushbroom manner.

With the information arranged in the focal plane as shown in Figure 2, considerable selectivity can be employed in the readout process. Individual spectral channels are confined to single rows within the detector; thus they can be extracted individually. Furthermore, the ability to sum adjacent rows in the readout structure of a charge-coupled device (CCD) permits broad spectral bands to be collected on the focal plane and read out as a single channel.

This dispersive approach offers several advantages over linear array approaches discussed elsewhere.^{2,3} So long as the area arrays are oriented perpendicularly to the slit image, spectral registration is assured. The spectral dimension is typically one to two orders of magnitude smaller than the spatial dimension; thus the alignment problems are reduced by the corresponding factor when compared to the line array approaches. The dispersive approach provides higher spectral resolution and the opportunity to select a variety of spectral and spatial modes simply by varying the readout process. This degree of control can be exercised by ground command.

The significant disadvantage of the dispersive approach is complexity. The optical system is potentially larger and contains more elements. To preserve the desired radiometric precision at the narrower spectral channels, the aperture size must be increased, resulting in a weight penalty. The development of area array detectors is generally more difficult than that of line arrays. The supporting electronics must process more data at higher rates, which suggests increases in the power requirements. Although these penalties exist, the design efforts indicate that an instrument using the dispersive approach is technically and economically feasible, and that its performance advantages commend it for further development.

An iterative system design process was used to develop the instrument parameters that satisfy the stated performance requirements. The key detector parameters of element size

and noise performance were determined on the basis of experience with state-of-the-art detector arrays and feasibility studies for advanced array capability. The instrument aperture is sized to permit the achievement of the required NEdR. The resulting design characteristics are listed in Table 2.

Table 2. SIS Design Characteristics

Parameter	Value
Equivalent aperture diameter, cm	30
Telescope focal length, cm	120
Physical slit width, μm	40
Ground-projected slit width, m	10
Altitude, km	300
Swath width, km	61.44
Detector size (pixel), μm	40 \times 40
Line time (for 10-m IFOV), ms	1.38
Encoding, bits/pixel	8
Raw data rate (VNIR), bits/s	2.27 \times 10 ⁹
(SWIR), bits/s	0.57 \times 10 ⁹
(Total), bits/s	2.84 \times 10 ⁹

SIS performance analysis

Major constraints on choice of system parameters arise because of limitations in the data rate, maximum size and speed of the optics, length and flatness of the focal plane, limitations in the butting of detector arrays, maximum detector array format and minimum pixel sizes, development of a linear prism disperser, and maximum integration times determined by the limitations imposed by pushbroom imaging. The design, developed in adherence to these constraints and summarized in Table 2, must satisfy the radiometric precision specification. The radiometric analysis is described in the following paragraphs.

We define NEdR to be that change in ground reflectance that produces a change in detected signal equivalent to the noise. The signal source is considered to be a perfectly diffusing target on Earth that reflects sunlight, which is attenuated by the atmosphere, towards the instrument. The NEdR is based on a reflectance scale of 100 percent, and the noise is a combination of signal and background shot noise and detector array readout noise.

The performance requirements in Table 1 call for differing spatial resolutions for the VNIR and SWIR. Since both arrays have the same format and physical size, the instantaneous footprints for the detectors are equal and designed to be 10 m. The 20-m IFOV for the SWIR channels is created by integrating for twice the basic line time and by summing the pixels in pairs during the readout process. These summations increase the signal-to-noise ratio because they occur prior to the readout amplifier. The data rate is reduced by a factor of four by these processes.

The working equations that incorporate these concepts are defined below. Equation (1) gives the signal per detector as a function of system parameters, Equation (2) the scene radiance at the instrument, Equation (3) the definition of noise, and Equation (4) the definition of NEdR.

$$S_{\lambda} = A \omega t \eta_{\lambda} T_{\lambda} N_{\lambda} d_{\lambda} \quad (1)$$

where

S_{λ} = signal in electrons for each band

A = effective primary area

ω = angular FOV subtended by the ground IFOV

t = integration time derived from given IFOV and spacecraft altitude

η_{λ} = detector quantum efficiency

T_{λ} = optical transmission of the system

N_{λ} = radiance of source at the aperture results from the solar irradiance attenuated by the atmosphere, isotropically scattered by a ground target of a given reflectance, and again attenuated by the atmosphere (Although not included here, the contribution to the signal from upwelling atmospheric radiance may be included in the design.)

$$N_{\lambda} = \frac{F_{\lambda}}{\pi} R_{\lambda} \cos i \ln \left[\left(1 + \frac{1}{\cos i} \right) \phi_{\lambda} \right] \quad (2)$$

where

πF_{λ} = solar irradiance outside the atmosphere

R_{λ} = ground reflectance

i = solar zenith angle

ϕ_λ = atmospheric transmission

$$N = \sqrt{S_\lambda + B + R^2} \quad (3)$$

where

N = rms noise in electrons

S_λ = signal in electrons

B = background signal in electrons. B is a function of background (instrumental) temperature and detector area, and is integrated over the entire detector spectral bandwidth. It is negligible for the 0.4- to 1.0- μm region

R = read noise in electrons (taken as 300 for the VNIR and 1000 for the SWIR)

$$\text{NEdR} = \frac{NR_\lambda}{S_\lambda} \quad (4)$$

where N , S_λ , and R_λ are defined above.

Using these relations, the NEdR as a function of wavelength is shown in Figure 3. The solid curve corresponds to the design spectral bandwidth of 20 nm. The dotted curve indicates the improvement in performance (smaller NEdR) gained by increasing the spectral bandwidth to 30 nm. The dashed curve shows the degraded performance (larger NEdR) achieved by decreasing the spectral bandwidth to 10 nm. The discontinuity at 1.0 μm results from the change from 10 m IFOV at shorter wavelengths to 20 m IFOV at longer wavelengths and the change in the detector noise figure from VNIR to SWIR values. The primary reason for the use of differing IFOVs for the VNIR and SWIR is to maintain the desired NEdR with a modest aperture dimension. Based on this analysis, the required NEdRs of 0.5 percent for the VNIR and 1.0 for the SWIR are met by all of the 20-nm spectral bands.

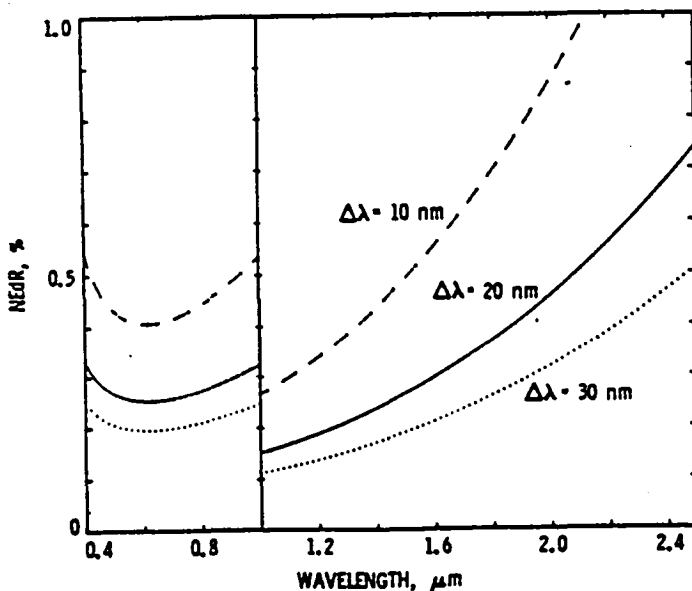


Figure 3. Radiometric performance characteristics of the SIS

This analysis assumes that the spectral dispersion is uniform across the spectral range. This condition does not generally hold for a prism spectrometer. A current design activity is to choose a combination of prism materials that will minimize the variation in spectral resolution over the 0.4- to 2.5- μm region.

Optical design

The most challenging optical design requirements are the field of view and spectral range over which the imaging performance is to be achieved. For the SIS requirements, a field of view of 8.6 deg must be provided over a spectral range from 0.4 to 2.5 μm . These requirements resulted in the design of an all-reflecting system with the single exception of the dispersing element. The wide spectral range, spanning three octaves in wavelength, combined with the low dispersion required and the high optical throughput goal, strongly argued for the use of a prism rather than a diffraction grating. Based on a careful tradeoff study, the Triple Reflecting Schmidt, Littrow Prism design⁵ developed for the free-flyer instrument was selected. The design presented in this paper is a scaled version of the original design.

The optical design approach for the Shuttle Imaging Spectrometer, shown in Figure 4, consists of three reflecting Schmidt cameras, one for the foreoptics and two for the

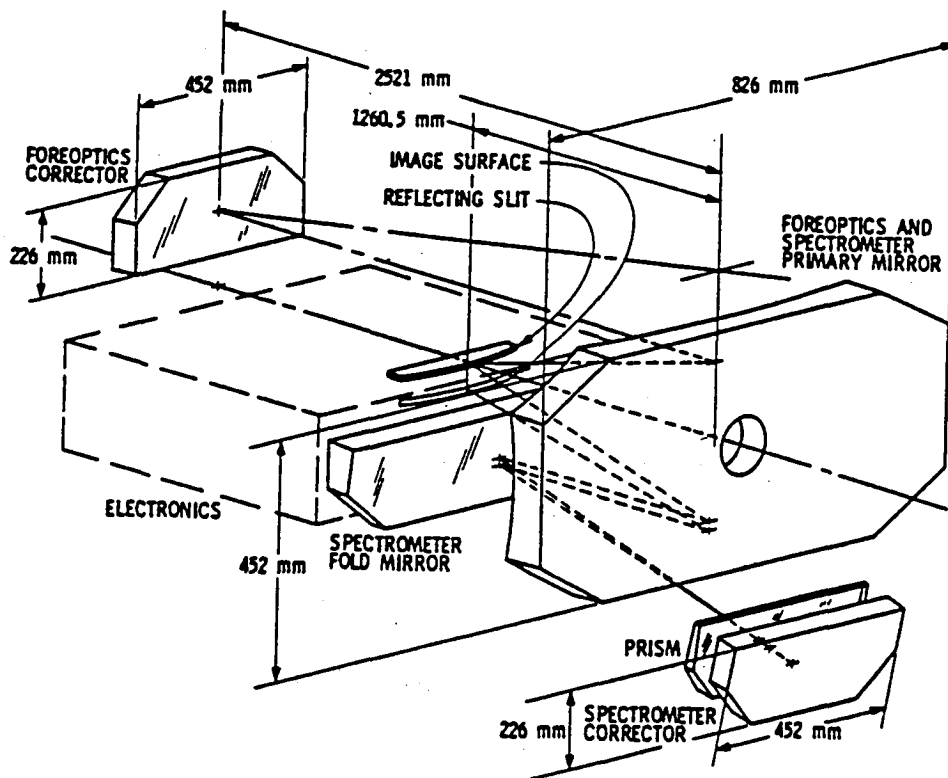


Figure 4. Shuttle imaging spectrometer optical configuration

spectrometer. The large primary mirror is shared by the three systems. Radiation enters the instrument through an aperture directly above the large primary mirror and strikes a D-shaped reflecting Schmidt corrector plate, located near the center of curvature of the spherical primary mirror. The corrector has the surface figure of a circular aspheric plate, but with the axis of symmetry passing below the bottom edge of the element. Radiation reflecting from the aperture corrector illuminates the upper portion of the primary mirror to produce an image at the primary focal surface, which is a sphere.

At the primary focal surface, a reflective slit defines the field stop and serves as the entrance slit for the spectrometer section. Serving also as a field flattener, the reflecting slit illuminates the lower portion of the primary, which now serves as the spectrometer collimator. A plane folding mirror directs the beam to the shallow prism. Radiation passing through the prism is reflected by another Schmidt corrector plate similar to the one used at the entrance to the foreoptics. The radiation is further dispersed as it makes its return pass through the prism, is folded back to the lower portion of the primary, which now serves as the spectrometer camera, and is imaged at the spectrometer focal surface. A small tilt in the spectrometer corrector displaces the spectrometer focal surface below the primary image focal surface, thereby leaving room for the detector arrays that populate the spectrometer focal surface.

The use of the fold mirror provides a large unobscured volume immediately behind the focal plane; this volume facilitates detector cooling and the convenient location of the supporting electronics.

The optics were ray-traced for design, tolerances, and focal-plane metrology using the ACCOS V interactive computer-aided design program. The focal surface lies on a spherical surface of 2.5-m radius. It is curved slightly with a deviation from the chord of 0.63 mm at the short wavelength end. This slight curvature can be accommodated by adjusting the locations of the detector arrays in the alignment of the focal plane. Designs that reduce this curvature are currently being evaluated.

The image quality of the system can be inferred from the isometric views of the point spread functions shown in Figure 5. The boundaries of each plot define the 40- μm -square pixel size. The spatial coordinate is indicated by Y; the spectral by X. The polarization of the instrument is less than one percent and is probably limited by the residual polarization present in thin-film mirror coatings.

Focal-plane implementation

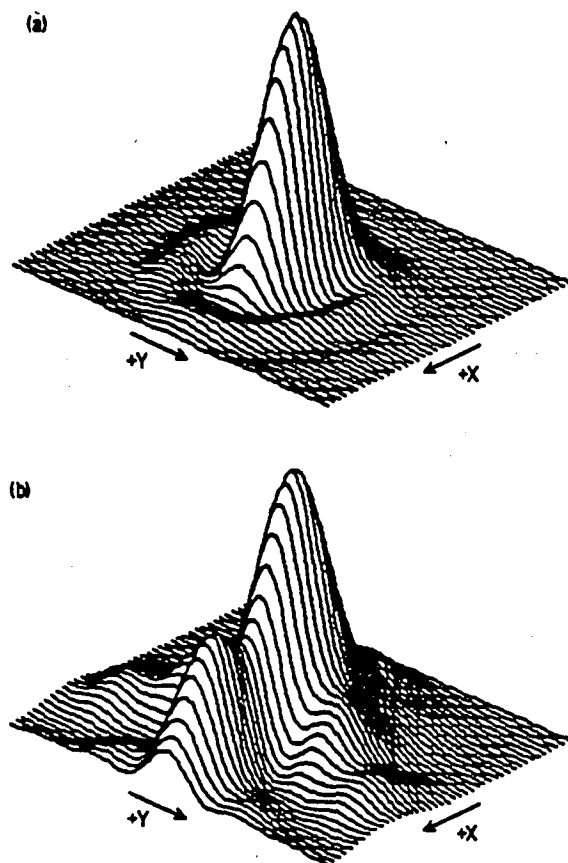


Figure 5. Optical point spread functions: (a) on-axis; (b) full-field

The most significant challenge in the implementation of the SIS is the short-wavelength infrared focal plane. Detector arrays of the performance and format needed do not presently exist, although a major development program is underway. Based on an assessment of the several IR technologies being developed, the hybrid approach using mercury-cadmium-telluride photodiodes with a 2.5- μm cutoff wavelength has been selected for this design. The arrays consist of two parts: a photodiode array made of the appropriate IR detecting material, and a CCD multiplexer, which collects the photogenerated charge and transfers it to an on-chip amplifier for readout. The two elements are interconnected with an array of indium column bonds, one for each pixel. This technology has been demonstrated, but not for the specific wavelength performance characteristics and format needed by SIS.

Development of mercury-cadmium-telluride detector arrays for imaging spectrometer applications has been underway at the Rockwell International Science Center.⁶ Three 32×32 element hybrid arrays with 68- μm -square pixels and a 4.5- μm cutoff wavelength have been fabricated and tested prior to delivery to the Jet Propulsion Laboratory for characterization and use in the Airborne Imaging Spectrometer.⁷ Indium column interconnect yields of 100% have been achieved. A significant improvement in pixel-to-pixel uniformity of response can be seen in the detectivity histogram of Figure 6. Arrays with a 2.5- μm cutoff wavelength will be developed and evaluated in the next phase of the effort.

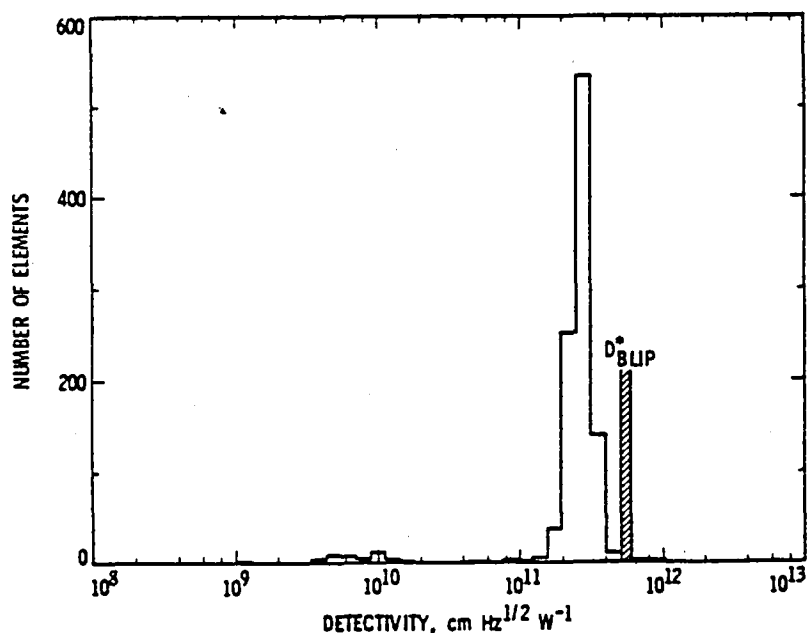


Figure 6. Detectivity (D^*) histogram for 32×32 HgCdTe hybrid detector array at 77 K and high background (5×10^{15} photons $\text{cm}^{-2}\text{s}^{-1}$).

Forecasts of the technology suggested that a development goal of a 64-by-64 element format with a 2.5- μm cutoff wavelength could be met within the next few years, and that flight quality arrays could be produced with sufficient yield to support a space flight program in the latter half of the decade. Accordingly, the SIS design was developed around this building block.

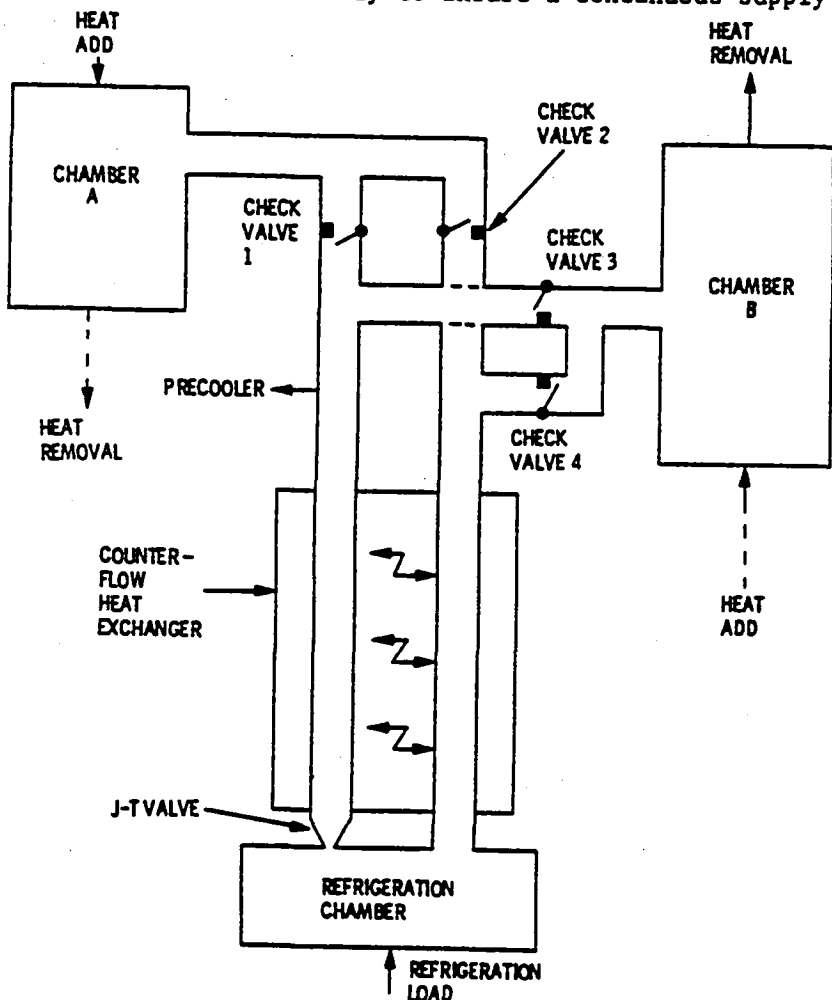
The visual and near-infrared detectors, covering the 0.4- to 1.0- μm spectral range, chosen were silicon CCD imagers. By comparison to the SWIR arrays, the silicon CCDs do not represent a major technology challenge. For the purposes of this design, the detectors were defined as having the same format and dimensions as the SWIR arrays. The focal plane configuration shown in Figure 2 is a mosaic of both types of array. The arrays are mosaicked or butted on two sides to create a focal plane with 6144 elements in the spatial dimensions and 64 elements in each of the SWIR and VNIR spectral dimensions. A total of 96 arrays in each wavelength group is needed to populate the focal plane.

An alternative approach for detection in the SWIR wavelength range is the relatively mature indium-antimonide photodiode technology (developed by Cincinnati Electronics Corp.) coupled with a novel multiplexed readout technique.^{8,9,10} A 128-element linear array with good uniformity and more than adequate detectivity for the application has been demonstrated. A 512-element linear array is under development using the same technique. Use of multiple linear arrays in place of area array detectors offers the possibility of a near-term demonstration of the imaging spectrometer technique prior to commitment to the full-scale development of the SIS.

Focal-plane cooling

To perform properly, the infrared detector arrays must be cooled to temperatures on the order of 130 K. (The alternative focal-plane technology using indium-antimonide detectors requires temperatures below 90 K.) Studies conducted in conjunction with the free-flyer design indicate that the required temperatures could be attained using an advanced, passive, radiative cooler.¹¹ A Shuttle mission poses different problems, most notably the inability of a radiator to view cold space. The alternative that appears to offer the best potential for meeting temperature and heat-load requirements reliably for long Shuttle or platform missions is the adsorption refrigerator.¹² In this system, high-pressure gas is supplied to a Joule-Thomson refrigerator by an adsorption compressor. In the compressor, the working gas is adsorbed by a solid at low temperatures and pressures. Low-quality heat, either waste or solar, is utilized to desorb the gas. The resulting high-pressure gas is then passed through a Joule-Thomson valve, which cools the gas. The heat load from the detectors is transferred to the gas, which flows back to the compressor/adsorber (exchanging heat with the incoming gas along the way) where it is readsorbed upon cooling of the compressor. This results in a closed system that has only self-operating check valves for moving parts. It is thus expected to be inherently reliable for long-life applications.

A conceptual diagram of this system is shown in Figure 7. The two compressors shown would be used alternately to insure a continuous supply of cold gas to the refrigeration



chamber. A heat source and sink must be alternately connected and disconnected from the compressor for the system to operate. The two heating sources envisioned are solar heating, using electrically actuated louvers to cycle the heat supply, or waste electrical heat, using thermal switches. Both approaches would have few moving parts and would be inherently reliable.

The adsorption refrigerator offers the strong advantages of reliability, a lower power requirement, and insensitivity to spacecraft configuration and orbit over a broad range of operating temperatures. This device is applicable to large space platforms, whereas radiators are unlikely to be usable because of geometry problems. It can also be used in an evolutionary manner on short Shuttle flights by replacing the adsorption compressor with a mechanical compressor or an expendable supply of high-pressure gas.

Conclusions

The SIS instrument design is responsive to the future requirements of both research- and applications-oriented users. As an experimental tool, the SIS provides a great deal of versatility with which the spectral domain can be explored at high resolution. The

Figure 7. Adsorption refrigeration block diagram

technology elements on which the SIS concept depends are being pursued both within this program and on related efforts.

The optical design presented here and several variations under study are capable of satisfying the performance requirements and can be implemented with standard optical fabrication processes. The reflecting slit poses some unusual fabrication challenges, which will be addressed in future work. Further exploration of linearizing the spectral dispersion and correcting the focal-plane curvature are expected to simplify the focal-plane mosaic implementation.

The required SWIR performance levels have been achieved with two materials - mercury cadmium telluride and indium antimonide - and suitable multiplexing techniques have been demonstrated. Challenges remain in optimizing the performance for the 1.0- to 2.5- μ m spectral region and in developing structures suitable for mosaicking into large focal-plane arrays.

Cooling methodologies for both Shuttle and free-flyer instrument concepts have been examined. Both the adsorption refrigerator and radiative coolers are capable of providing focal-plane operation at temperatures as low as 80 K; thus the detector choices need not be severely restricted by temperature constraints. The development of a breadboard adsorption refrigerator sized for the SIS application is planned.

We conclude that the performance requirements identified in this paper can be met and that continued progress in the supporting technologies will permit a space-flight verification of the imaging spectrometer approach in the latter half of the 1980s.

Acknowledgements

The authors wish to acknowledge the efforts of the Imaging Spectrometer Design Team at JPL, the contributions of Professors R. R. Shannon and R. V. Shack and their students at the University of Arizona in optical design, and the detector array development efforts led by Dr. J. Rode of Rockwell International Science Center and B. Fehler of Cincinnati Electronics Corporation.

The research described in this publication was carried out by the Jet Propulsion Laboratory, California Institute of Technology, under contract with the National Aeronautics and Space Administration.

References

1. Vane, G., Billingsley, F. C., and Dunne, J. A., "Observational Parameters for Remote Sensing in the Next Decade," Paper No. 345-06, in Proceedings of the Society of Photo-Optical Instrumentation Engineers, May 4-7, 1982.
2. Wellman, J. B., "Multispectral Mapper: Imaging Spectroscopy as Applied to the Mapping of Earth Resources," Paper No. 268-19, in Proceedings of the Society of Photo-Optical Instrumentation Engineers, D. D. Norris, ed., 268, February 10-11, 1981.
3. Wellman, J. B., "Technologies for the Multispectral Mapping of Earth Resources," in Proceedings of the Fifteenth International Symposium on Remote Sensing of Environment, Vol. 1, Environmental Research Institute of Michigan, Ann Arbor, Michigan, May 11-15, 1981.
4. Wellman, J. B., Breckinridge, J. B., Kupferman, P. N., and Salazar, R., "Imaging Spectrometer: An Advanced Multispectral Imaging Concept," 1982 International Geoscience and Remote Sensing Symposium, Munich, Federal Republic of Germany, June 1-4, 1982.
5. Breckinridge, J., Page, N., and Shannon, R., Applied Optics, 1982 (in preparation).
6. Vural, K., Acceptance Test Report, Contract No. 955940, Rockwell International Science Center, Thousand Oaks, California, 1982.
7. Wellman, J. B., and Goetz, A. F. H., "Experiments in Infrared Multispectral Mapping of Earth Resources," Paper No. 80-1930, AIAA Sensor Systems for the 80's Conference, Colorado Springs, Co., December 2-4, 1980.
8. Bailey, G. C., "Design and Test of the Near Infrared Mapping Spectrometer (NIMS) Focal Plane for the Galileo Jupiter Orbiter Mission," in Proceedings of the Society of Photo-Optical Instrumentation Engineers, 197, August 29-30, 1979.
9. Bailey, G. C., "An Integrating 128 Element Linear Imager for the 1 to 5 μ m Region," in Proceedings of the Society of Photo-Optical Instrumentation Engineers, 311, 1981.
10. Bailey, G. C., "An Integrating 128 Element InSb Array: Recent Results," Paper No. 345-23, in Proceedings of the SPIE, May 4-7, 1982.
11. Bard, S., Stein, J., Petrick, S., "Advanced Radiative Cooler with Angled Shields," Paper No. 81-1100, AIAA 16th Thermophysics Conference, Palo Alto, Calif., June 23-25, 1981.
12. Chan, C. K., "Cryogenic Refrigeration Using a Low Temperature Heat Source," Cryogenics, 391-399, July 1981.

IR AREA ARRAY STATUS

JON RODE



Rockwell International
Science Center

AGENDA

- IR FOCAL PLANE OVERVIEW: THE CHOICES
- STATUS OF HCT HYBRID FOCAL PLANES
- AREAS OF DEVELOPMENT



Rockwell International
Science Center

TRADE-OFFS FOR APPLICATION COMPLEX

OPERATING TEMPERATURE

QUANTUM EFFICIENCY

FILL FACTOR

WAVELENGTH

UNIFORMITY (λ_c, η)

COMPLEXITY

YIELD

COST

CELL SIZE

ARRAY SIZE

SPEED OF READOUT

INTEGRATION TIME

DYNAMIC RANGE

POWER

SIGNAL PROCESSING

BUTTABILITY



IR ARRAYS BASED ON PHOTON DETECTION

DETECTION

INTRINSIC (PV, MIS, PC)

- HgCdTe
- InSb
- InAsSb
- PbSnTe
- PbSSe
- HgMnTe

SCHOTTKY BARRIER

- PtSi
- PdSi

EXTRINSIC

Si: As, G, In, S, Zn, —



FOCAL PLANE ARCHITECTURE

**BACKSIDE ILLUMINATED
(EPITAXY, THINNED)**

**FRONT-SIDE
ILLUMINATED**

MONOLITHIC

**CHARGE INJECTION
DEVICE**

SPRITE

HYBRID

Z-PLANE



Rockwell International
Science Center

LEADING ARRAY TECHNOLOGIES

- EPITAXIAL HgCdTe HYBRIDS (EXTEND TO Z PLANE)
- EXTRINSIC (As, Ga, In, S) SILICON (MONOLITHIC AND HYBRID)
- MONOLITHIC AND CID HgCdTe (ALSO InSb)
- SCHOTTKY BARRIER MONOLITHIC DEVICES (Pt AND Pd)

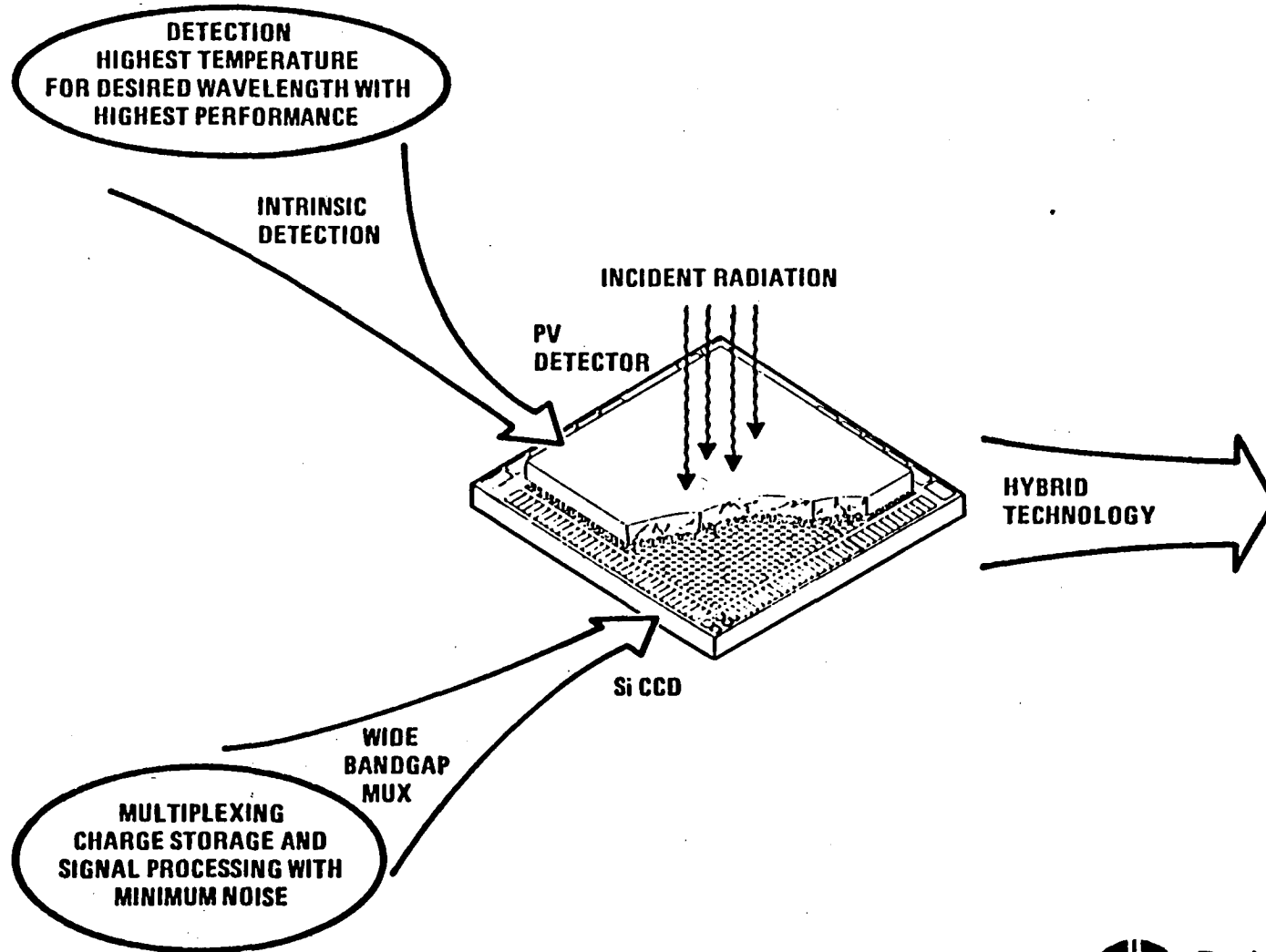


Rockwell International
Science Center

HYBRID TECHNOLOGY

SC80-7335

151



Rockwell International
Science Center

EPITAXIAL HgCdTe HYBRID FOCAL PLANE

- SPECTRAL RANGE 1-12 μm
 - 3-5 μm MOST MATURE
 - 1-3 μm RIPE FOR DEVELOPMENT
 - 8-12 μm MOST DIFFICULT FOR MATERIALS AND SIGNAL PROCESSING

- ARRAY SIZE
 - 64 x 64 DEMONSTRATED; 128 x 128 FEASIBLE
 - DETECTOR SIZE AT 25 x 25 μm , CAN GO TO 15 μm x 15 μm
 - CELL SIZE AT 50 μm x 50 μm , CAN GO TO 30 μm x 30 μm

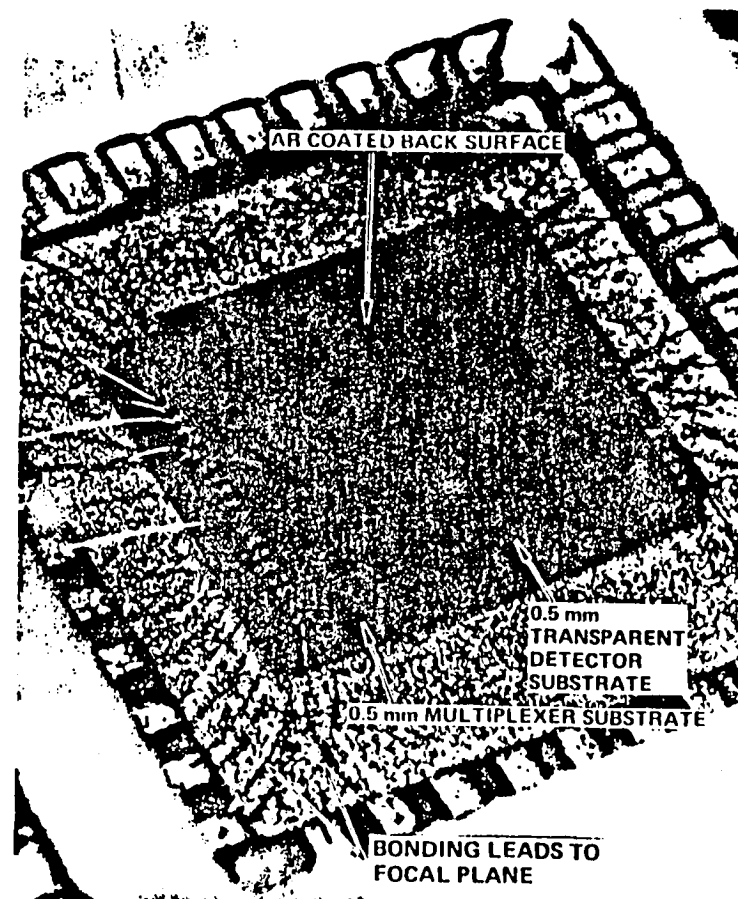
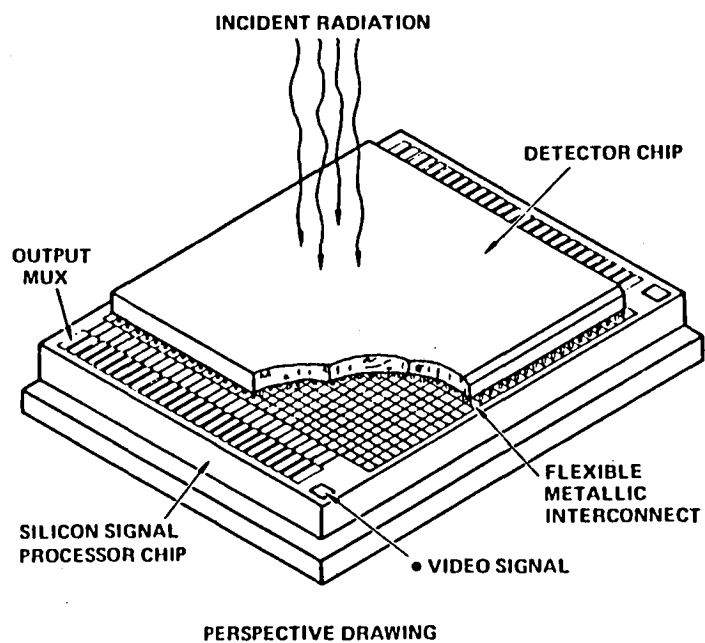
- SIGNAL PROCESSING
 - DIRECT INJECTION WITH DC SUPPRESSION AND GAIN REDUCTION
 - GATE MODULATION (DC SUPPRESSION)
 - AC COUPLED CIRCUITS IN DEVELOPMENT



Rockwell International
Science Center

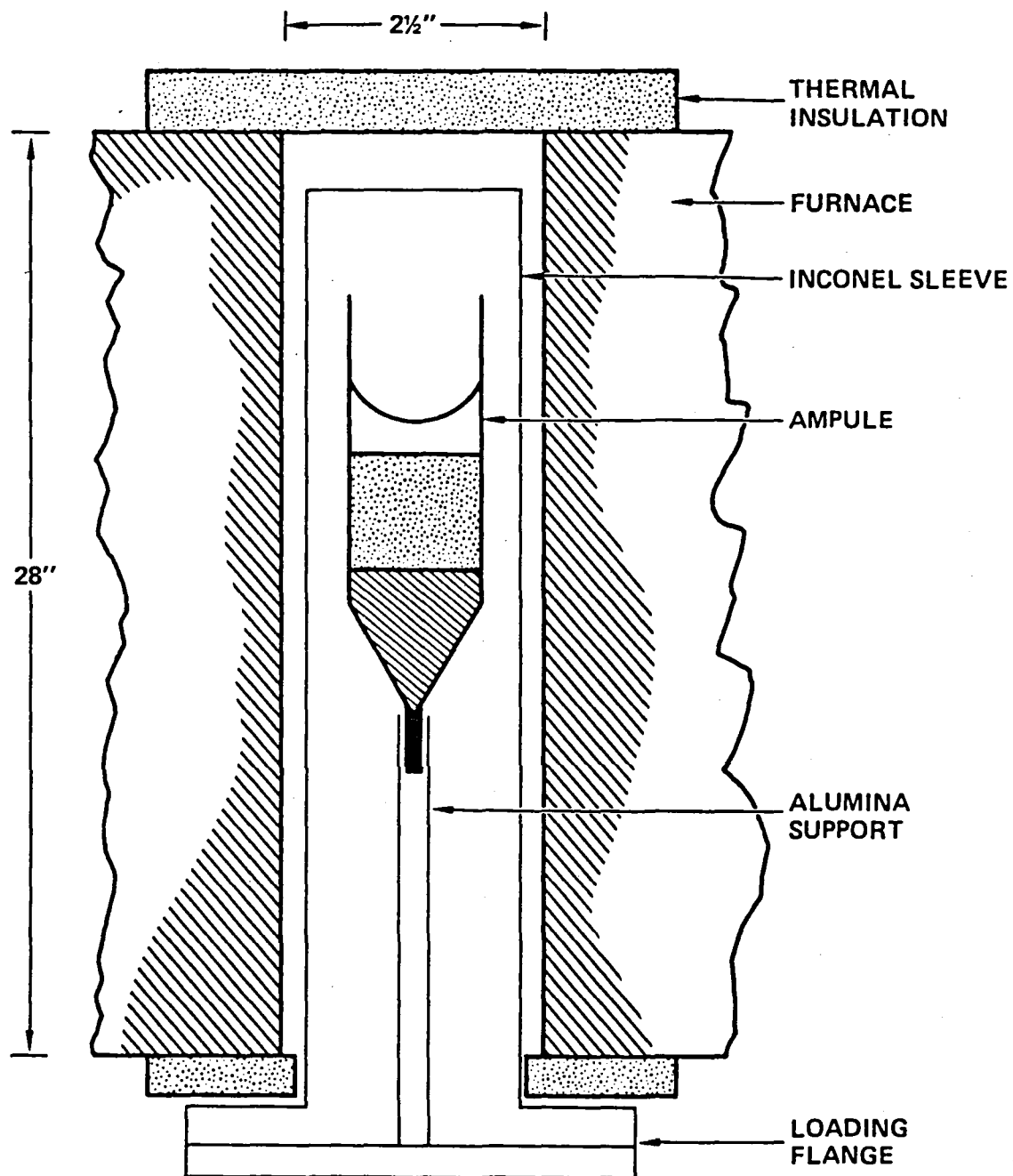
PLANAR HYBRID FOCAL PLANE

SC81-13051



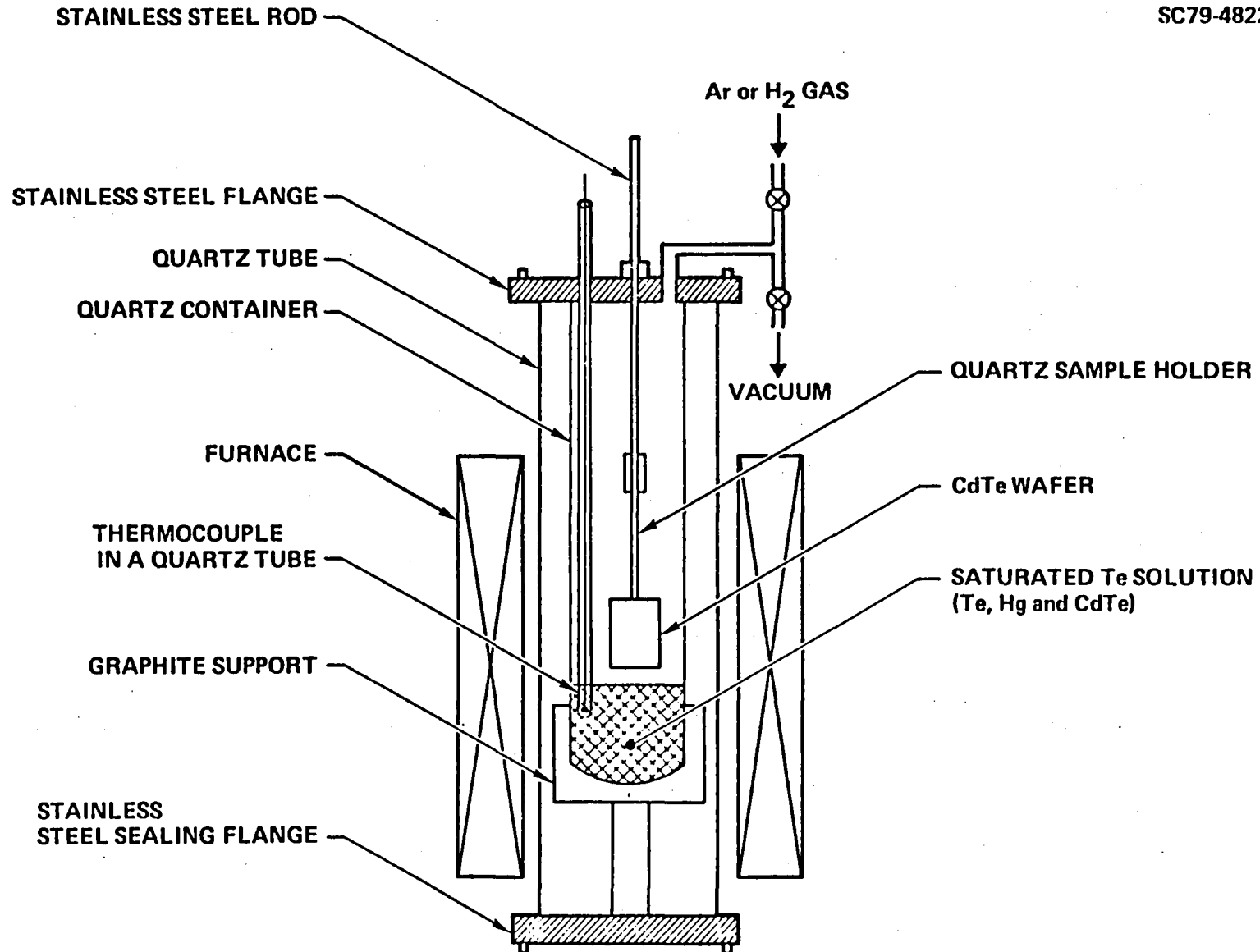
Rockwell International
Science Center

SC81-13778



HgCdTe LPE SYSTEM

SC79-4822



24 CM² HgCdTe MWIR LPE

GOALS ADDRESSED: LARGE ELEMENT NUMBER, LOW DEAD SPACE
VERSATILITY, PRODUCIBILITY

<u>PARAMETER</u>	<u>TYPICAL VALUE</u>
GROWTH AREA	> 15 CM ²
THICKNESS	15 μm
MORPHOLOGY	SUITABLE FOR DEVICE PROCESSING
λ_c UNIFORMITY (ACROSS WAFER)	$\sigma = 0.035 \mu\text{m}$
λ_c REPRODUCIBILITY (FOR > 200 LAYERS)	$\sigma = 0.056 \mu\text{m}$
HOLE CONCENTRATION	$3 \times 10^{16} \text{ cm}^{-3}$
MOBILITY	300 cm ² /V-sec
DEVICE QUALITY	EXCELLENT

- LPE HgCdTe CAN BE FABRICATED IN SIZES AND GEOMETRIES
COMPATIBLE WITH S1 PROCESSING
- 35 MEDIUM ARRAYS/WAFER POSSIBLE WITH OPTIMIZATION OF
GROWTH



Rockwell International
Science Center

HgCdTe DIODE ARRAYS

GOALS ADDRESSED: COST, LARGE ELEMENT NUMBER,
LOW DEAD SPACE PRODUCIBILITY VERSATILITY

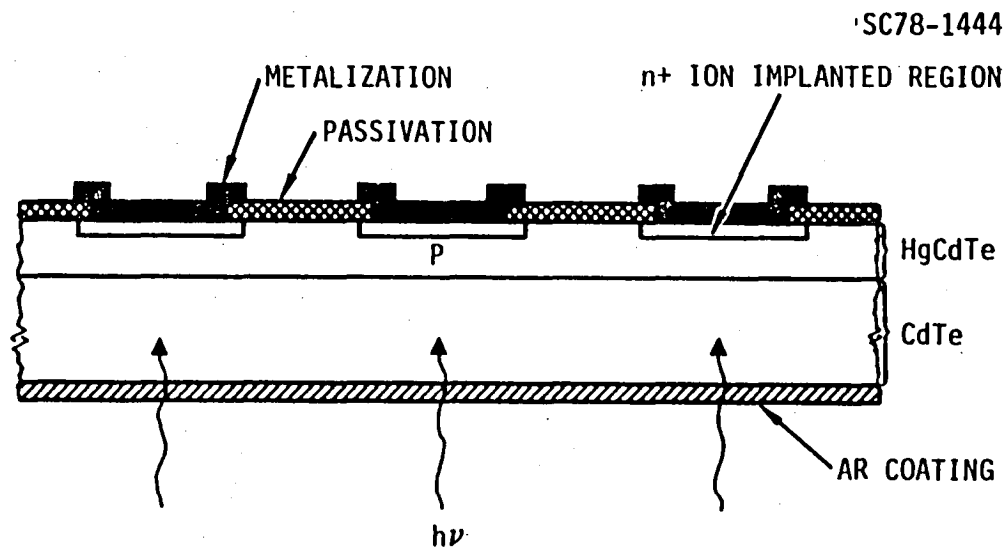
ARRAY CHARACTERISTICS

- PLANAR (MAXIMIZES USEFUL AREA, SIMPLIFIES PROCESSING)
- PROCESS COMPATIBLE WITH Si PROCESSING
- HIGH UNIFORMITY FROM IMPLANT PROCESS
- PROCESS ADAPTABLE TO PRODUCTION FOCAL PLANES



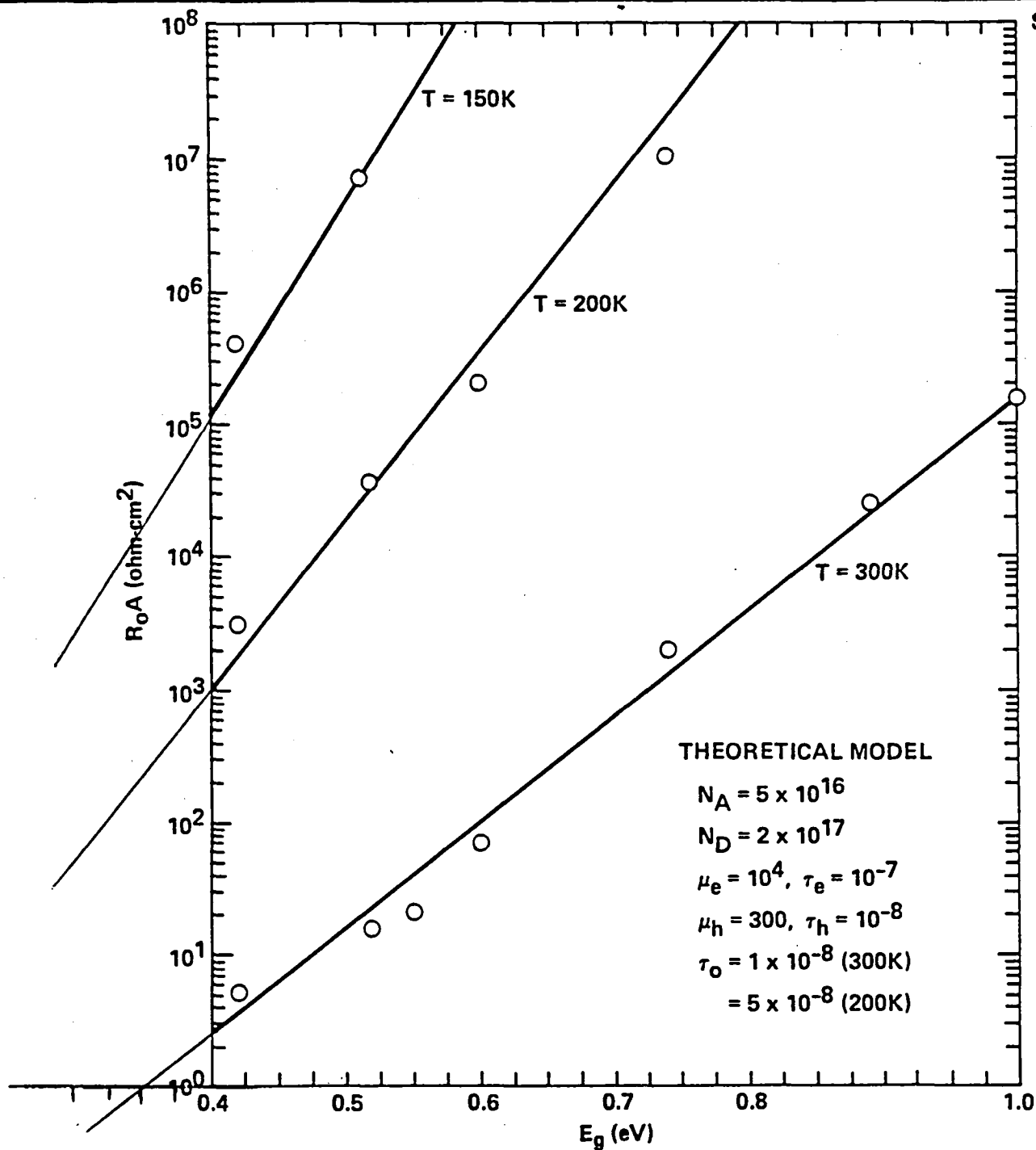
Rockwell International
Science Center

SCHEMATIC VIEW OF HgCdTe/CdTe DETECTOR ARRAY



R₀A PRODUCTS OF SWIR PHOTODIODES AS A FUNCTION OF E_g

SC80-11276



Rockwell International
Science Center

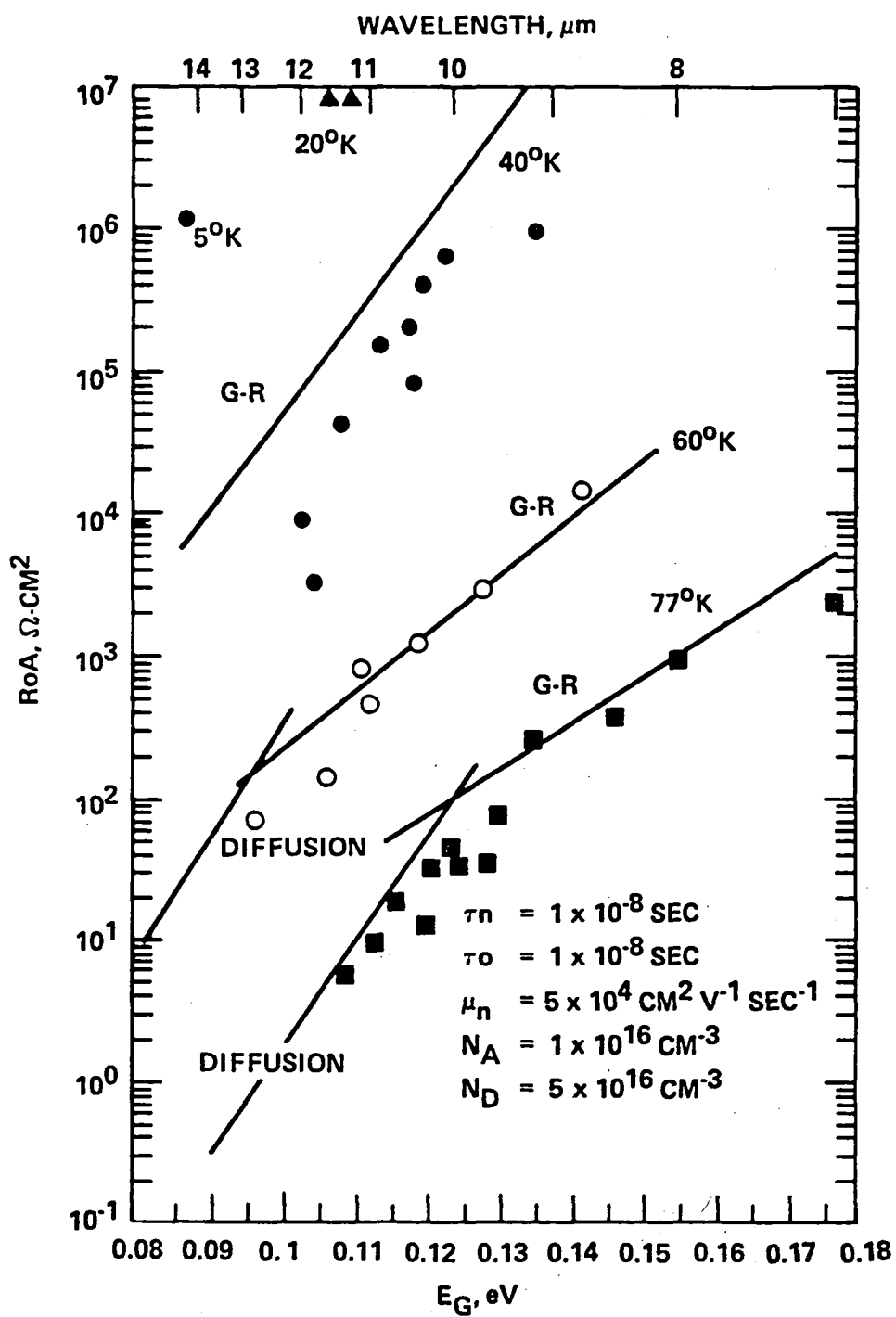
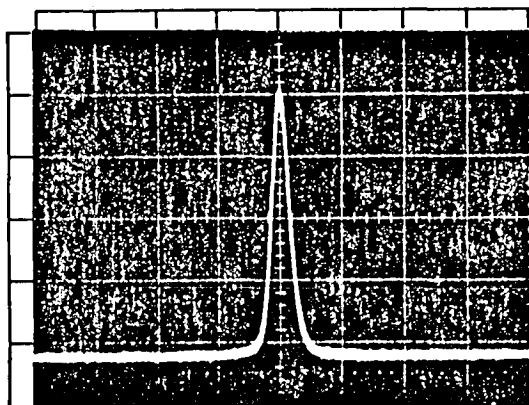


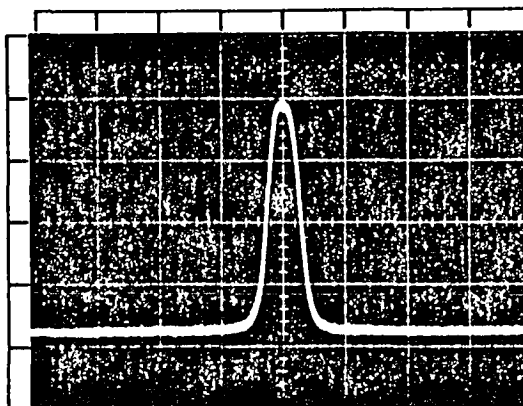
Fig. 3 Calculated and experimental results of R_0A versus energy bandgap for LPE-grown PV HgCdTe devices.

SPOT SCAN OF DIFFERENT AREA HgCdTe DETECTORS

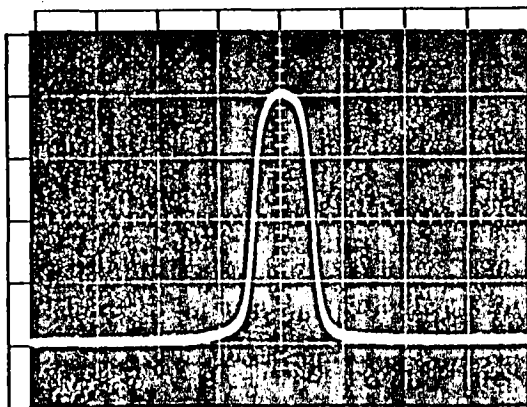
SC81-12755



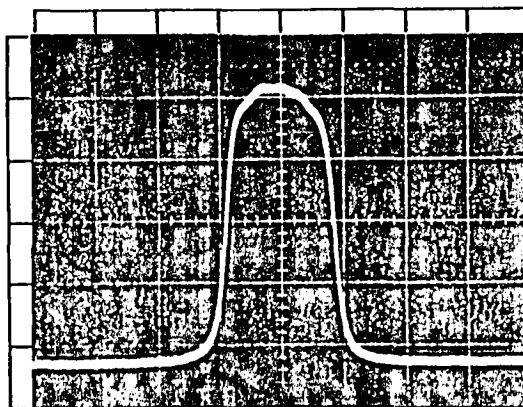
A. (0.5 x 0.5)



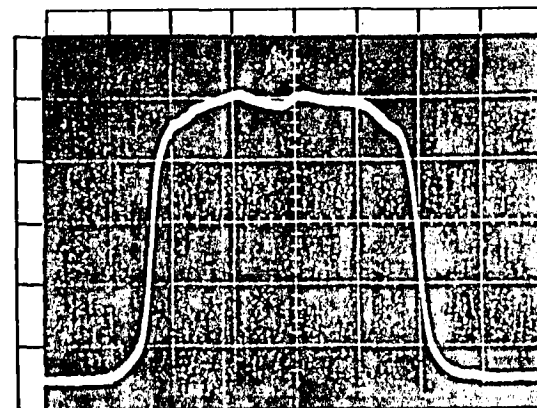
B. (1.0 x 1.0)



C. (2.0 x 2.0)



D. (4.0 x 4.0)



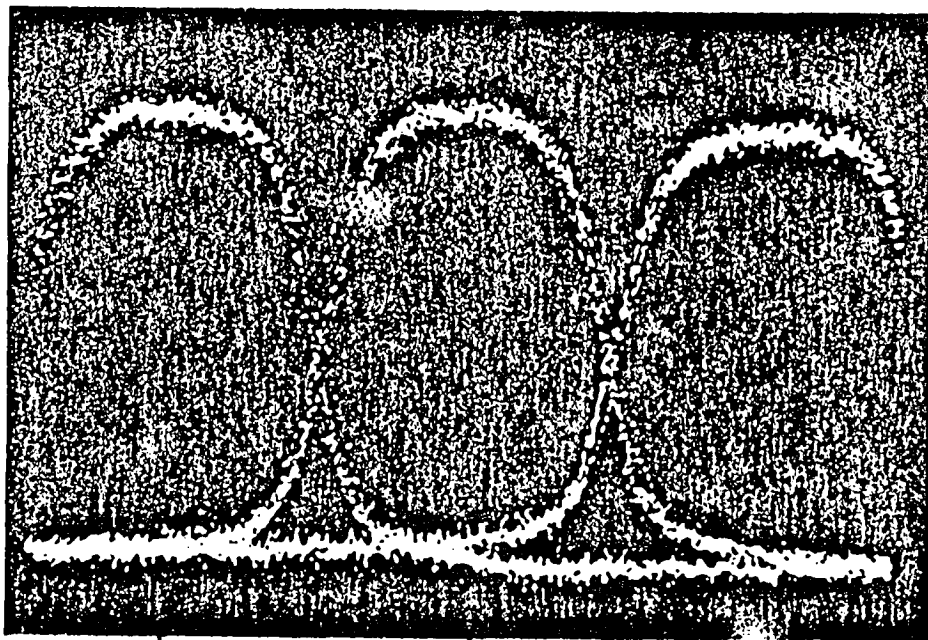
E. (10.0 x 10.0)

- PLANAR, BACKSIDE ILLUMINATED PV DETECTORS AT 77K
- 1 DIVISION = 2.40 MILS
- IMPLANT AREA (MILS)
 - A. 0.5 x 0.5
 - B. 1.0 x 1.0
 - C. 2.0 x 2.0
 - D. 4.0 x 4.0
 - E. 10.0 x 10.0



SPOT SCAN OF MWIR DEVICE 149N01-2C5

SC81-12340



DEVICE No. 149N01-2C5

$T = 77K$

$\lambda_c = 4.7 \mu m$

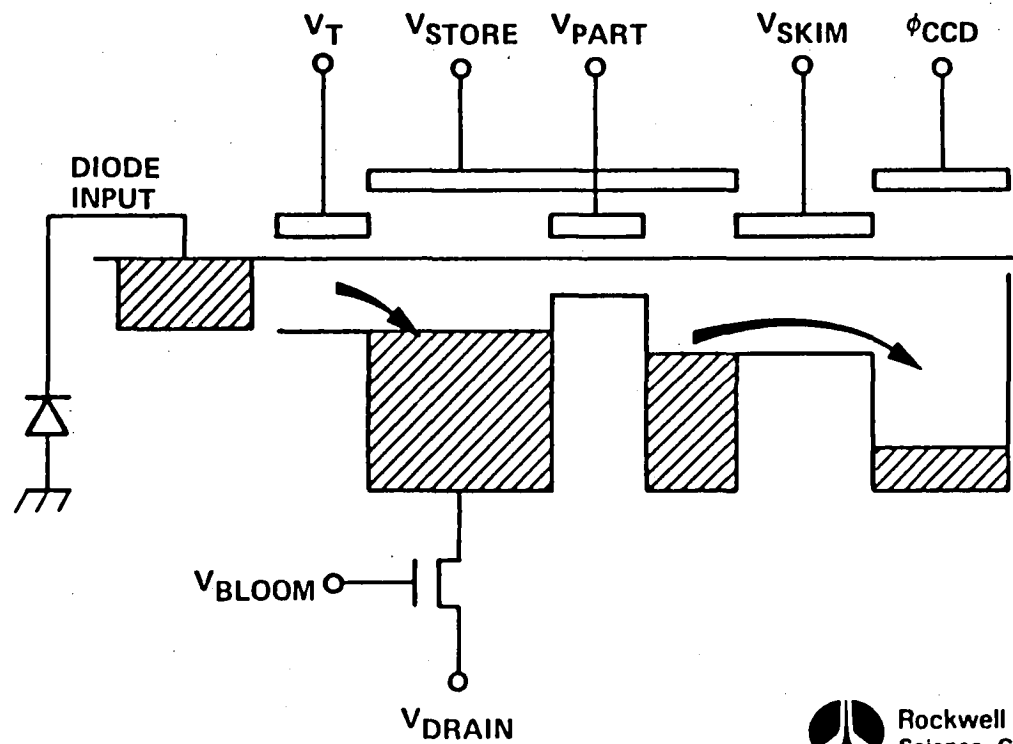
68 μm UNIT CELL



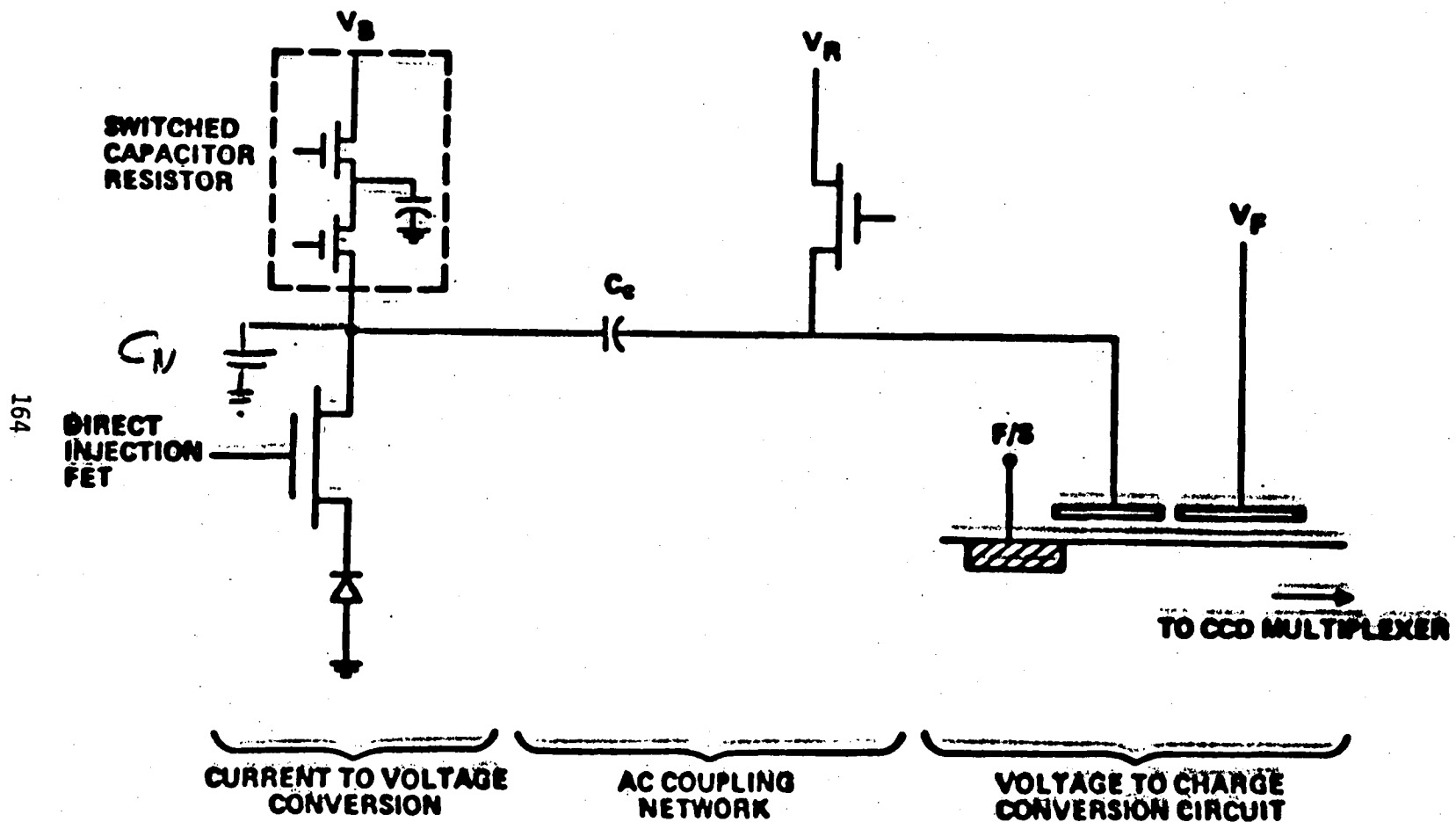
Rockwell International
Science Center

BACKGROUND SUPPRESSION OF DIRECT INJECTION INPUT

SC80-9371A

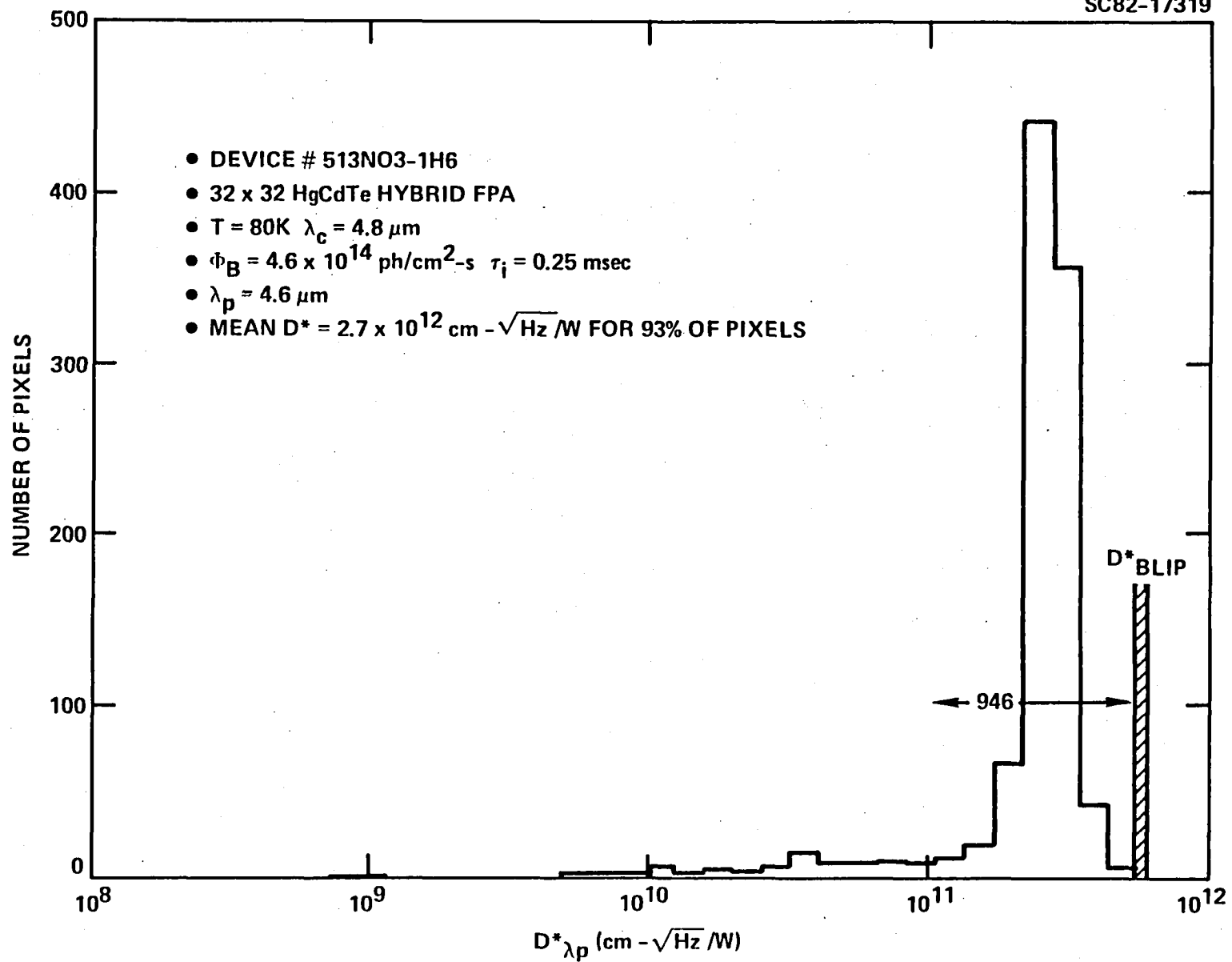


INPUT CIRCUIT DESIGN FOR AC COUPLED MULTIPLEXER

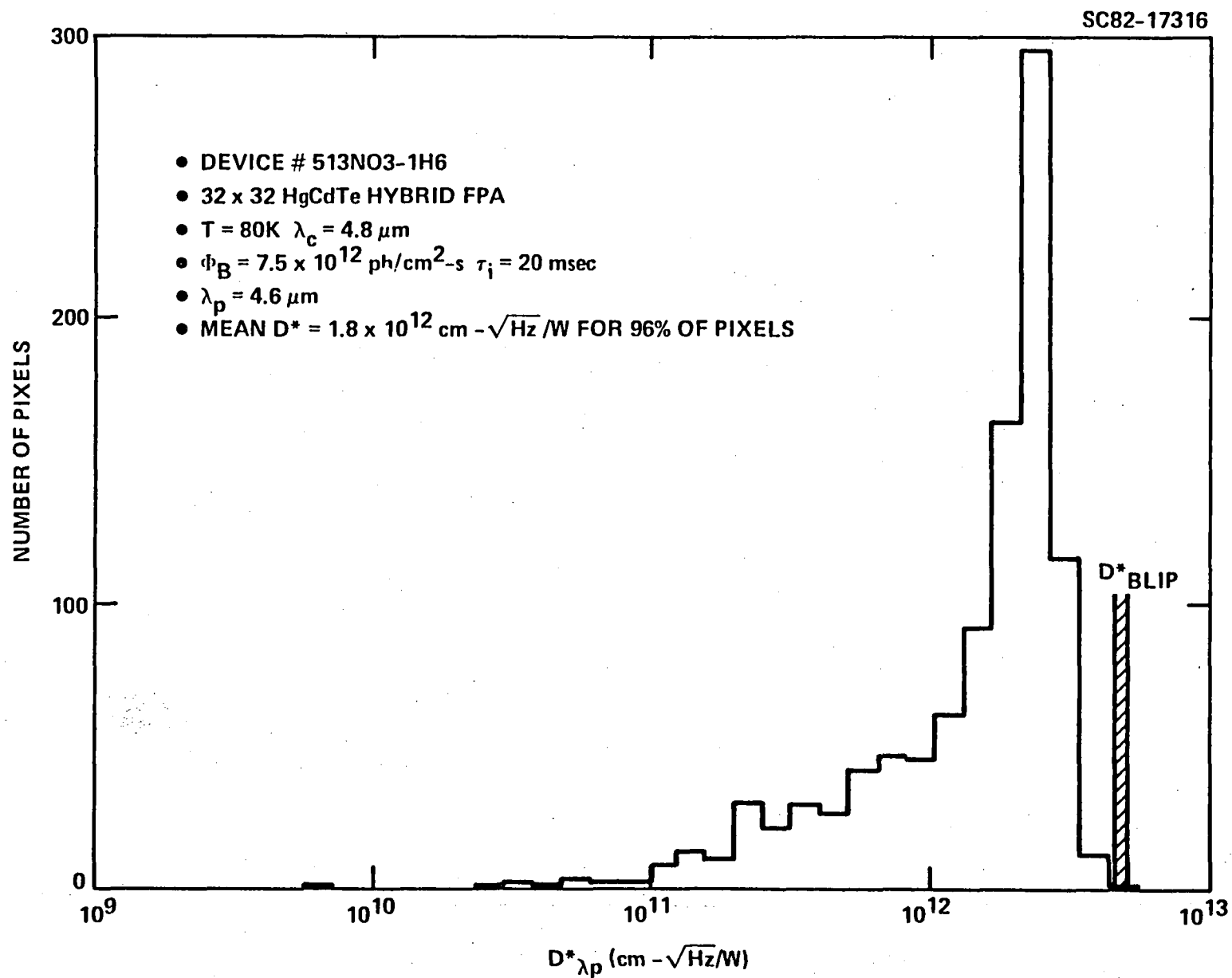


$D^* \lambda_p$ HISTOGRAM

SC82-17319

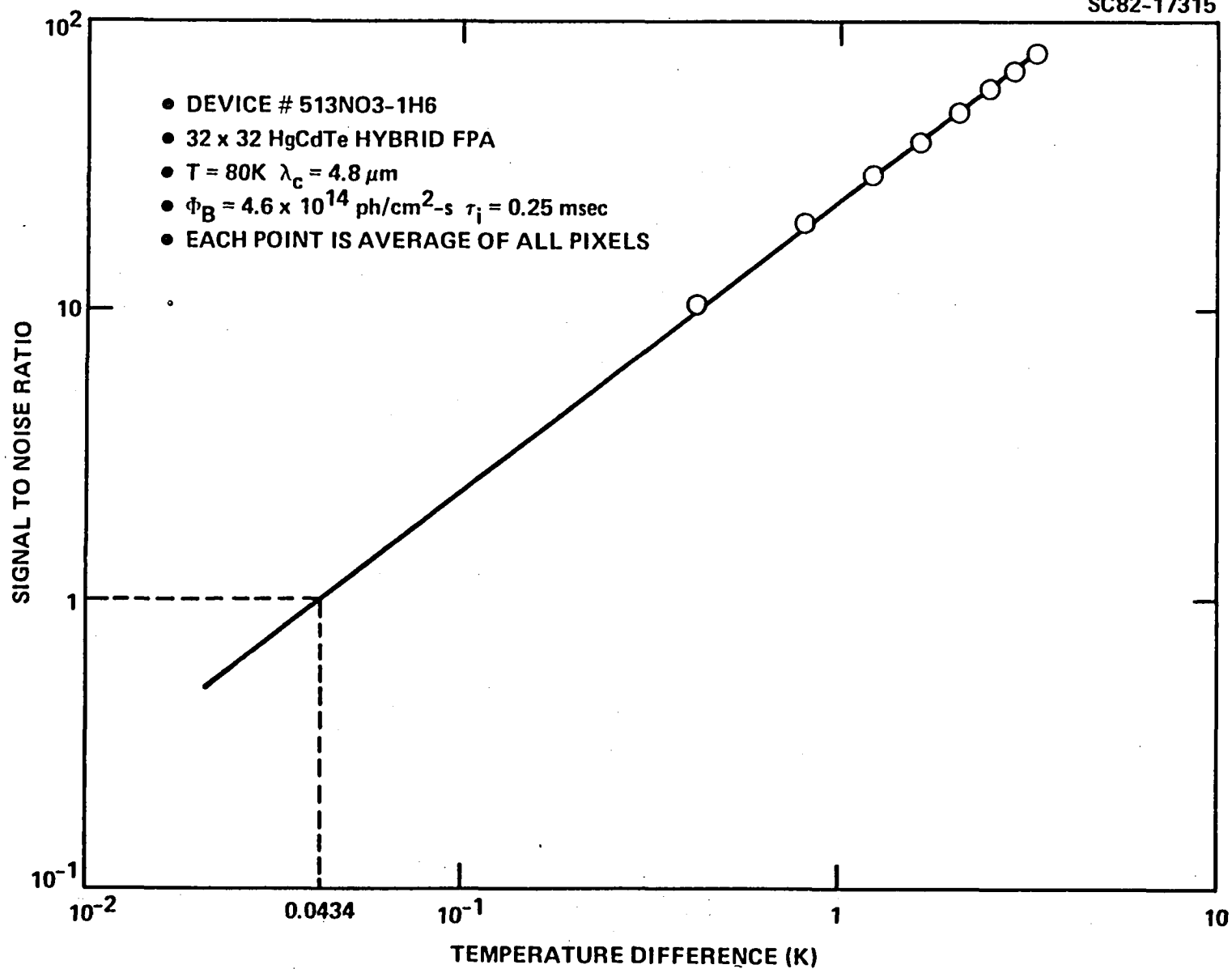


$D^* \lambda_p$ HISTOGRAM



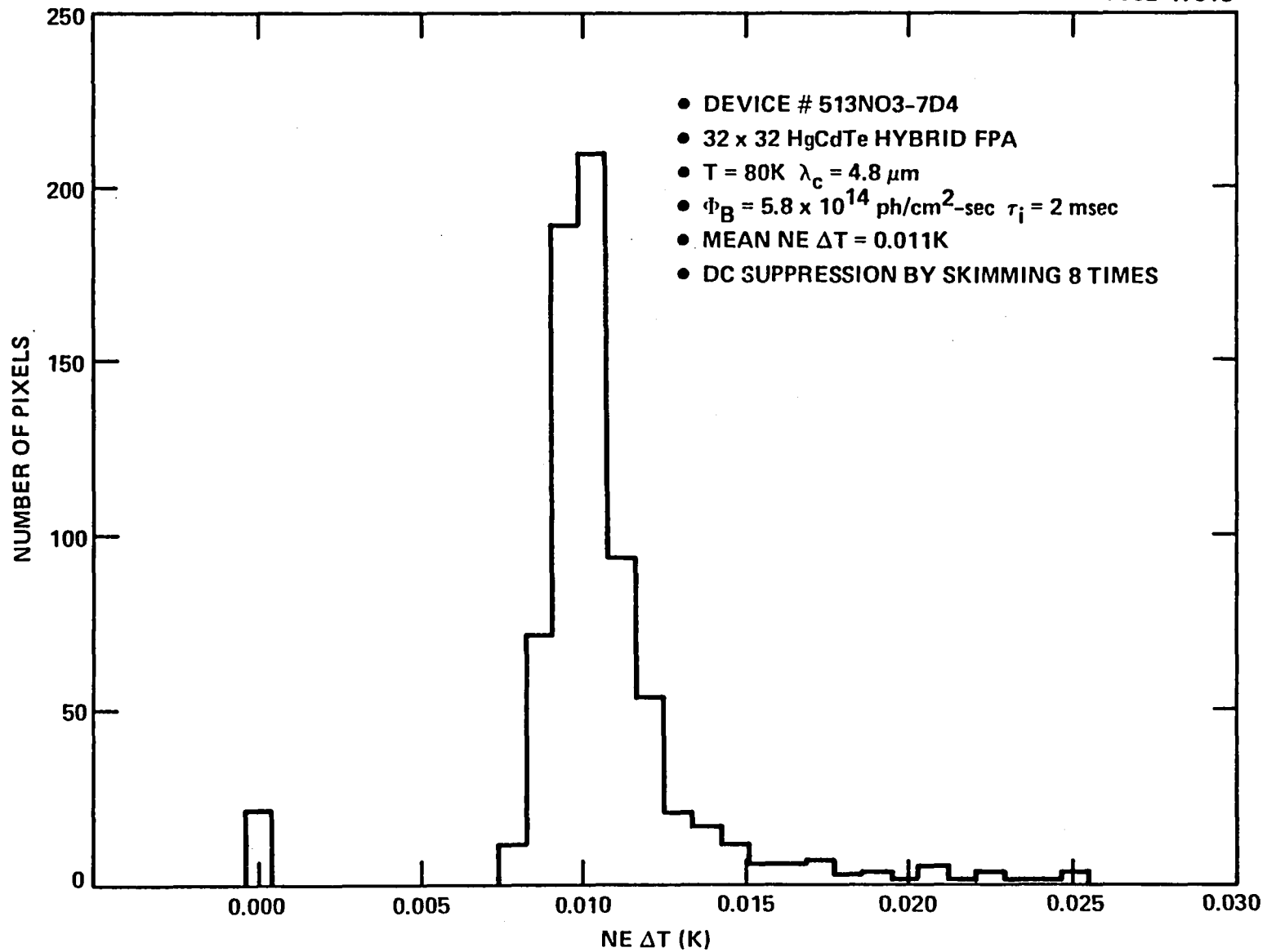
NOISE EQUIVALENT TEMPERATURE DIFFERENCE

SC82-17315



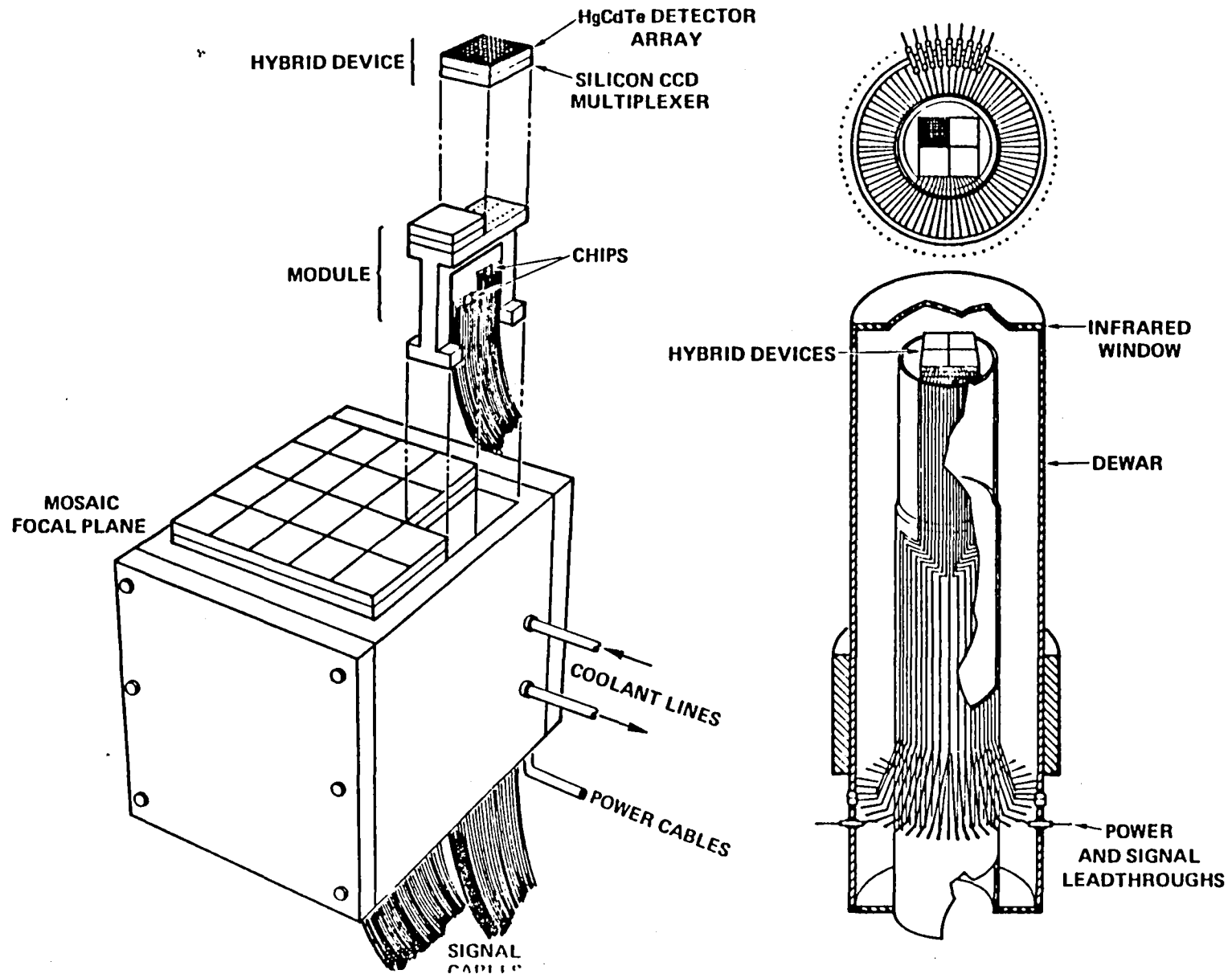
NOISE EQUIVALENT TEMPERATURE DIFFERENCE HISTOGRAM

SC82-17318



FOCAL PLANE MODULES

SC80-7285A



DEVELOPMENT OF HgCdTe FOCAL PLANES

MATERIALS

- ALTERNATE SUBSTRATES (CHEAP, STRONG, UNIFORM)
- ALTERNATE GROWTH TECHNIQUES (IMPROVE MORPHOLOGY)

PROCESSING

- PASSIVATION
- YIELD

UNIT CELL

- NEW INPUT STRUCTURES (ESPECIALLY LWIR)
- IMPROVE SIGNAL PROCESSING
- INCREASE DYNAMIC RANGE

FOCAL PLANE ARCHITECTURE

- LOW DEAD SPACE
- Z-PLANE
- MONOLITHIC



Rockwell International
Science Center

ABSOLUTE RADIOMETRIC CALIBRATION OF ADVANCED REMOTE SENSING SYSTEMS

P. N. Slater

Committee on Remote Sensing
Optical Sciences Center
University of Arizona

ABSTRACT

The distinction between the uses of relative and absolute spectroradiometric calibration of remote sensing systems is discussed. The advantages of detector-based absolute calibration are described, and the categories of relative and absolute system calibrations are listed. The limitations and problems associated with three common methods used for the absolute calibration of remote sensing systems are discussed.

Two methods are proposed for the in-flight absolute calibration of advanced multispectral linear array (MLA) systems. One makes use of a sun-illuminated panel in front of the sensor, the radiance of which is monitored by a spectrally flat pyroelectric radiometer. The other uses a large, uniform, high-radiance reference ground surface. The ground and atmospheric measurements required as input to a radiative transfer program to predict the radiance level at the entrance pupil of the orbital sensor are discussed, and the ground instrumentation is described.

Key words: Radiometry; Calibration; Remote Sensing.

1. SPECTRORADIOMETRIC CALIBRATION—WHO NEEDS IT?

For purposes of this discussion, the community of remote sensing data users can be divided into two groups:

1. Users requiring relative, but not necessarily absolute, spectroradiometric sensor calibration. These include workers in computer-aided scene classification, cartographers, image processors, photointerpreters, and people concerned with composing large mosaics.

2. Users requiring absolute spectroradiometric calibration. These include physical scientists concerned with relating ground-measured parameters and/or atmospheric characteristics to the spectral radiance at the entrance pupil of the space sensor.

The distinction can be drawn that the former are concerned primarily with taking an inventory or compiling a map of ground features. The latter are concerned primarily with understanding and characterizing the physical interactions taking place, usually through models and often with a view to optimizing (for example an irrigation schedule) or to predicting a change in a particular process

(for example an agricultural yield). Expressed differently, those concerned with relative calibration use data described in digital counts, while those needing absolute calibration use data referenced in terms of radiance units at the entrance pupil of the sensor (in this case, the radiometric calibration of the sensor is invoked to convert the digital value to spectral radiance). We must emphasize that the radiance value is of no more worth to the average user than the digital value, as both refer to an incident radiance level at the sensor over broad, unequal spectral passbands, over which the spectral reflectance of the feature being observed can change by a significant but unknown amount. However, there are two reasons for converting the digital value to radiance: first, in multitemporal sensing, to account for any documented changes of radiometric calibration with time; second, to test or utilize physical models in which the ground reflectance and atmospheric effects are measured and/or calculated over identical spectral passbands as employed by the space sensor.

Perfect relative radiometric response occurs when the outputs from all detectors in a band are equal or can be adjusted during preprocessing to be equal, when the incident spectral radiance is constant across the sensor's field of view. (Note that the number of detectors in a band can be as few as six for the Multispectral Scanner System (MSS) on Landsat and as many as 18,500 on future MLA systems.) This condition must be met independently of the spectral content of the scene. When this condition is not met, the image appears striped. If it is not scene-dependent, striping often can be completely removed by the histogram equalization method; thus, relative radiometric precision can be high even though the accuracy involved may be low. In this equalization procedure the histogram of each detector output is compared with that of every other detector, after a large number of data samples ($\sim 2 \times 10^5$) have been recorded. It is assumed that, if the scene is spatially and spectrally random, the histograms for a large number of samples will be identical. If the histograms are not identical, adjustments are made during the preprocessing step to make them so. This procedure can be repeated for scenes of different average radiance, and the relative responses can then be equalized over the dynamic range of the detectors. This procedure does not work if the striping is scene-dependent (Ref. 1). Fortunately the design and the spectral band location for the Thematic Mapper and future MLA sensors will not give rise to a scene-dependent

striping problem of the magnitude of that in the MSS.

Inadequately corrected relative detector-to-detector response causes unsightly striping in the imagery. Striping can cause inaccuracies in automated scene classification. In addition, even though the human photointerpreter is usually more forgiving than a computer, if the striping is severe it can cause errors in photointerpretation. Uncorrected striping can be aggravated by the application of some image processing algorithms. Thus, it is important to reduce striping as much as possible for image processing and classification purposes. The relative response of the individual detectors is also important for ratioing purposes. However, once the in-band tolerance has been met, the concern is with the relative stability of response because many applications utilize the comparison of multitemporal band ratios.

The utilization or verification of physical models usually requires the use of data calibrated in an absolute sense. Until recently the highest in-orbit absolute radiometric accuracy has been little better than 10%. This low accuracy has been due to: (a) the fact that the calibration in orbit has often been for the focal plane only, not for the complete system; (b) the loss in accuracy accompanying the transfer of calibration from the standard source at the national laboratory to the factory or laboratory calibration site; (c) the use of source-based calibration procedures.

As described later, the use of detector-based calibration promises to reduce the approximately 10% error to 1%. To what extent we can afford to relax or strive to exceed the 1% potential can best be determined from a set of well-coordinated measurement and modeling exercises conducted as part of an experimental MLA mission. The results of work to date on this subject are in disagreement. On one hand we know that natural or scene variability is seldom less than 1% and we also know from atmospheric modeling work (not yet experimentally verified) that we can expect considerable atmospheric-scatter-induced spectral radiance crosstalk between neighboring ground samples owing to the so-called adjacency or boundary effect (Refs. 2-5). On the other hand, the sensor simulations made to date (Ref. 6) indicate there is an improvement in classification accuracy in going from 6-bit to 8-bit quantization. Eight-bit quantization is available on most future sensors. A purist might contend that, if 8-bit radiometric resolution is really justified, it should, for maximum utility, be associated with commensurate (<0.4%) error in absolute radiometric accuracy!

In summary, we know that spectroradiometric calibration is important and that the need for relative or absolute calibration depends on the application for the data. However, we do not know how accurate the calibrations should be, particularly the absolute calibration. The most encouraging aspect of the situation is that we now have the potential of utilizing 8-bit quantization resolution with commensurate absolute radiometric accuracy in an orbital imager at least over the 400 to 900 nm range. This potential should be exploited as fully as possible as an important component of any system and applications research associated with an experimental land-observing system having an 8- to 10-bit quantization capability.

2. DETECTOR-BASED RADIOMETRIC CALIBRATION

The recent work at the US National Bureau of Standards on self-calibrated photodiodes is described only briefly here. For more details the interested reader is referred to references 7-12.

The calibration of the photodiode is accomplished by either of two differently applied biasing procedures, depending on the wavelength region of interest. At short wavelengths, a negative bias is applied to remove the recombination centers at the Si-SiO interface at the front of the detector. To do this, a contact is made with the front surface using an electrode immersed in a conducting liquid, or the surface can be exposed to a corona discharge. For long wavelengths, a back-bias is applied to extend the depletion region to a depth beyond which incident flux penetrates. The experimental procedure is to irradiate the detector with a constant monochromatic flux level and to increase the bias voltage until further increase no longer gives rise to an increase in output signal. For both the short and the long wavelength ranges, the internal quantum efficiency saturates at a value extremely close to unity, as shown in Fig. 1. Thus the maximum increase in signal output obtained as a result of biasing can be used to determine the internal quantum efficiency of the detector without biasing, as it will be used in practice.

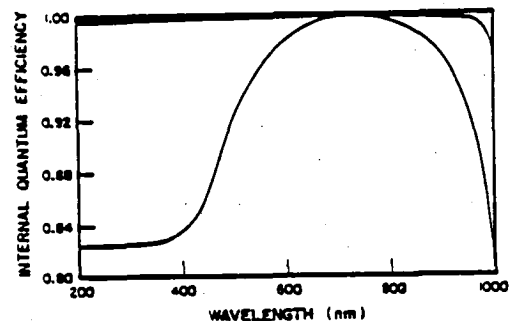


Fig. 1. Typical photodiode internal quantum efficiency without biasing (lower curve) and with biasing (upper curve), reference 9.

The only significant loss in the external quantum efficiency of the photodiode is caused by reflection. This can be reduced to insignificance by making use of three photodiodes according to the geometry sketched in Fig. 2.

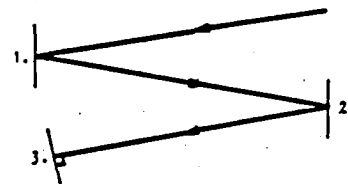


Fig. 2. A three-diode arrangement to minimize specular reflection losses.

The output signals from the three diodes are summed to provide the signal corresponding to a black detector of overall quantum efficiency that

can be assumed to be unity. The second diode reflects the specular reflection from diode 1 to diode 3, which acts as a retroreflector. The incident flux thereby undergoes five reflections, and at a 10% value the final specular reflectance is down to 10^{-5} of the initial incident radiance. It is claimed (Ref. 12) that the diffuse reflectance losses for clean detectors are typically much less than 1%. The photodiodes used in similar calibration facilities at NBS and at the University of Arizona, Optical Sciences Center, are EGG UV 444R.

The discussion at the end of this paper refers to the use of self-calibrating NBS detectors for the spectroradiometric calibration of an MLA system. However, as shown in Fig. 1, the unbiased quantum efficiency is wavelength dependent. Because of possible changes in the passband position of spectral filters during long duration space flights, it may be advisable to use the NBS detectors to calibrate a spectrally flat pyroelectric detector, at the 0.1-0.2% level, and for that to be used in the in-orbit calibration.

3. BROAD CLASSIFICATION OF CALIBRATION PROCEDURES

Some of the most commonly used procedures for the calibration of remote sensing systems are referred to in Fig. 3. The two major divisions in the figure are between relative and absolute calibration and between the static macro-image response and the dynamic micro-image response of the system. Some aspects of relative calibration were discussed in the first part of this paper and together with dynamic micro-image response will not be discussed further, beyond remarking that the dynamic micro-image response is of vital interest in any pixel-by-pixel analysis of remotely collected imagery. The rest of this paper deals with the absolute calibration of remote sensing systems, and only the static macro-image response will be considered in this context, as is usually the case.

The procedures for the absolute calibration of a remote sensing system fall into the three categories shown in the bottom right of Fig. 3:

(1) The absolute calibration of the system is made only before launch. In flight the calibration is checked by irradiating the focal plane with a

radiometrically calibrated source and optical system. The drawbacks to this procedure are that any change in the transmission of the image-forming optics of the sensor system, due to the condensation of outgassed contaminants, will be undetected and the on-board calibration system is also assumed to be stable through launch and unaffected by the vacuum, high energy particle irradiation, and zero-g environment at orbital altitudes. The Thematic Mapper and the Multispectral Scanner System on Landsat-D are examples of remote sensing systems calibrated in this manner.

(2) The sun or an on-board calibrated source can be used to irradiate the focal plane through the image-forming optics. The drawbacks to this approach are the uncertainty in the knowledge of (a) the irradiance of the sun above the atmosphere and (b) the output of the calibrated source system, for the reasons mentioned earlier. Furthermore, in examples of the use of this procedure (MSSs 1, 2 and 3 and SPOT), the calibration beam passes through only a small portion of the aperture of the system, thus not simulating the actual operation of the system. When imaging the ground, the system entrance aperture is irradiated over its entire area by flux incident over a roughly three steradian solid angle. In the imaging mode there is much more stray light present in the system and incident on the focal plane. If this additional flux level is unknown, it may introduce a substantial uncertainty into the absolute calibration of the system.

(c) Reference can be made in-flight to a ground area of known spectral radiance. If at the time the sensor system is imaging the known area, measurements are made of the atmospheric conditions, these data can be used with an atmospheric radiative transfer program to predict the spectral radiance at the entrance pupil of the sensor. The main uncertainty in this approach is that of determining the atmospheric aerosol content well enough. The approach is also limited to scenes having large uniform areas of high radiance. For example, although many water bodies are of sufficient size and uniformity, they are not appropriate for calibration purposes because their radiance is too low to provide a calibration of sufficient accuracy or to cover much of the dynamic range of the sensor. Fortunately, some suitable areas do exist, particularly in the arid regions of

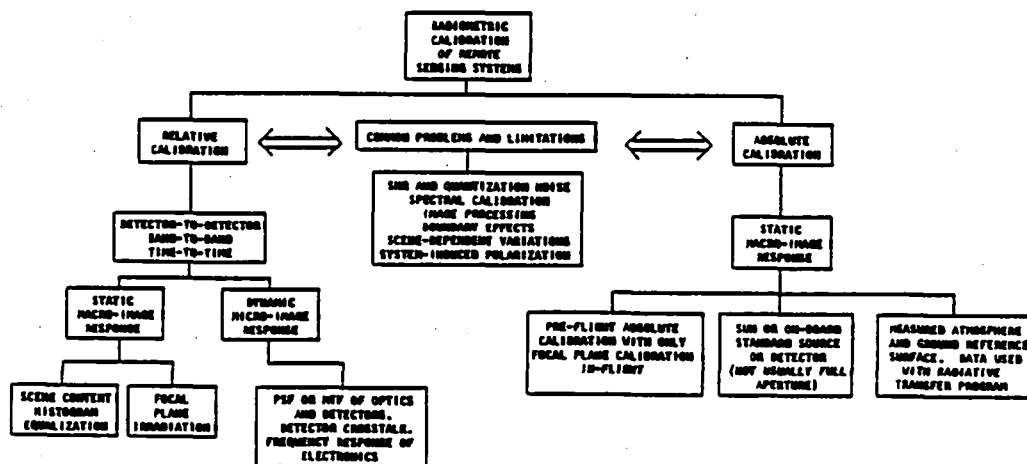


Fig. 3. Classification of radiometric calibration procedures.

the world, for example at White Sands, New Mexico, in the United States.

The rest of this paper is devoted to discussion of the factory and in-flight calibration of an MLA system using the self-calibrated photodiode approach and the use of a ground reference area for calibration purposes.

4. CALIBRATION IN THE FACTORY AND IN ORBIT

The concept proposed for the factory calibration is similar to the proposed orbital procedure, the main difference being that an artificial source is used in the factory and the sun is used in orbit—simply a matter of convenience in the former case and of convenience and reliability in the latter case. In the factory, redundancy is not at a premium and our requirements for a source are simply power, spectral flatness, and stability. We do not need a standard source although an array of standard NBS FEL tungsten halogen lamps could be used, if their polarization characteristics can be tolerated (Ref. 13). A xenon arc selected for minimum arc wander and with a highly stable power supply and a feedback loop would suffice.

The source would be used to irradiate a near-Lambertian, near-unity-reflectance, white-surfaced panel perhaps 1 m x 0.5 m in size in front of the system. (An integrating sphere could be used, but it would have to be very large, and uniformity checks can sometimes themselves introduce non-uniformities.) A self-calibrating NBS-style radiometer, with the incident beam perhaps defined by two or three apertures, and using spectral bandpass filters matching those used in the MLA, would be used to determine the radiance of the panel in each band. The MLA would image the panel out of focus, but being an extended object, its image would have exactly the same irradiance in or out of focus. The arrangement is sketched in Fig. 4.

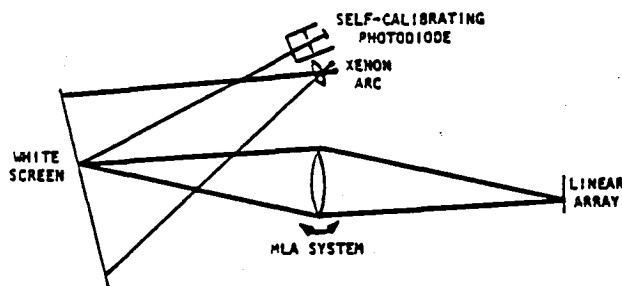


Fig. 4. The factory procedure for absolute spectroradiometric calibration.

To avoid problems due to the nonuniform irradiation of the panel, the MLA should be rotated to sequentially irradiate the focal plane with the image of the same small area that is sampled by the radiometer. The reason for a large panel is to simulate the viewing conditions from space in which, depending on the baffle design, significant out-of-the-field-of-view stray light could be incident on the image plane to modify the calibration. For this reason it would be worthwhile to conduct at least one calibration using a white panel several meters in diameter. To

check for linearity of response, several different irradiance levels on the panel should be used. This irradiance level can be changed conveniently by inserting heat-resistant neutral density filters in front of the stabilized xenon arc source.

The profiles of the spectral filters should be measured in a spectrophotometer using the same F/No. beam as the MLA. If they are integral with the array, they should be measured using a double monochromator, again with the MLA F/No., before installation in the focal plane. Care should be taken to cover the whole wavelength sensitivity range of the detectors, the off-band suppression being particularly important for detectors with the wide spectral response of silicon.

The procedure proposed here for in-flight calibration is similar to the panel method sketched in Fig. 4, but it uses the sun as the source. We believe that the irradiance over the panel can then be considered to be uniform and known spectrally to better than 1% absolute. (Several solar measurement programs are currently being conducted with this accuracy as a goal. However, if the uncertainty is thought to be greater than 1%, a pyroelectric detector could be used to measure the direct solar flux in orbit, over the wavelength intervals of interest and at the same time that the system is being calibrated.) The calibration would be carried out in the few minutes while the spacecraft is sun-illuminated but before it images the sun-illuminated earth. The absolute radiometer containing the pyroelectric detector would now be needed only to check for any deterioration in the reflectance of the panel owing to exposure to the space environment and short exposures to unattenuated UV and other high energy radiation from the sun and from space. In this last respect, the panel would usually be stowed in a well-shielded compartment and exposed only during actual calibration checks. Also, when deployed, it would not interfere with normal operation of the system, as it would be viewed by the stereo mirror in one of its extreme positions. In this respect it is fail-safe.

5. WHITE SANDS AS A CALIBRATION REFERENCE

To keep the description of the theory of the method brief, spectral dependencies are not included in the following discussion. In all cases the spectral dependence is implied, the spectral value having the same wavelength dependence as the spectral response of each band of the sensor being calibrated. The theoretical basis for the calibration method is straightforward.

The radiance at the sensor, L_s , is determined with respect to the ground radiance, L_0 , the reduction of this radiance by the upward path through the atmosphere, $\tau'_{\text{ext}} \sec \theta$ (where τ'_{ext} is the atmospheric extinction and θ is the nadir scan angle), and $L_{g,\phi}$, the atmospheric path radiance (where ϕ is the azimuth angle of the observation). Thus,

$$L_s = L_0 \exp(\tau'_{\text{ext}} \sec \theta) + L_{g,\phi}$$

The path radiance term, $L_{g,\phi}$, in the equation is unknown and can be determined only by the use of a radiative transfer calculation. Such calculations require a knowledge of τ'_{ext} , ground reflectance, the irradiance incident at the top of the atmosphere, the aerosol optical depth and phase

function, the optical depth due to ozone and water vapor, the solar zenith angle, the nadir angle of the sensor, and its azimuthal angle with respect to the sun's direction. These radiative transfer calculations assume an infinite, flat, Lambertian reflecting surface with an atmosphere composed of plane homogeneous layers. Although these assumptions are never exactly met, they are closely approximated by the nearly Lambertian flat surface of the qvosum at White Sands and the small field of view of the space sensors.

The quantity r'_{ext} can be determined from the solar radiometer data in the following way. The solar radiometer records the irradiance E_{θ_z} at the ground as a function of the solar zenith angle during the morning of the overpass. If the atmospheric conditions are steady during that period, the Langley plot of $\ln E_{\theta_z}$ against $\sec \theta$ is a straight line of slope r'_{ext} . The extrapolation of the line to a $\sec \theta_z$ value of zero gives the value of the irradiance above the atmosphere in the measurement passband. The value of the ground radiance L_0 is determined at the time of the overflight by the solar radiometer looking at the ground at the same θ and ϕ angles as that of the space sensor. The ground radiance value can be converted into the reflectance required as input to the radiative transfer program in one of two ways. First, the global irradiance can be measured by the solar radiometer with either a horizontal cosine diffuser or an integrating sphere, with horizontal entrance port, placed over the entrance aperture of the solar radiometer. Or second, the solar radiometer can be pointed down at a horizontal, diffusing, white surface such as $BaSO_4$ or Halon. The cosine diffuser approach is preferred because its small surface can be conveniently stored to minimize contamination. Intercomparisons will be made, during the six monthly recalibrations of the field equipment, between the cosine diffuser global irradiance and the Lambertian white reference surface measurements of the ground reflectance. The nadir angle from the satellite to the ground observation point, the solar zenith angle, and the azimuth of the satellite nadir angle to the sun's direction are all readily determinable. Such quantities as atmospheric pressure, humidity, surface and air temperature, etc., are routinely monitored by the Atmospheric Sciences Laboratory at White Sands. These data will be formatted with the radiation data and telemetered to Wallops Island, Virginia, United States.

The difficult quantities to determine for radiative transfer calculations are the characteristics of the atmospheric aerosols. Fortunately, we can make reasonable assumptions regarding their values based on prior results. For example, 79 aerosol profiles have been measured at White Sands (Ref. 14) to establish an atmospheric model; the effects of aerosol complex refractive index and size distribution on extinction and absorption for the wavelength range 0.55 to 10.6 μm for desert atmospheres are reported in reference 15; and reference 16 reports that the imaginary refractive index is 0.007 at 0.6 μm and shows little dependence on wavelength over the range 0.3 to 1.1 μm .

We intend to investigate some new techniques for determining aerosol characteristics that are under development and that make use of sky polarization measurements. We also intend to explore methods of monitoring the aerosol size distribution from inversion of the spectral optical

depth measurements (Ref. 17) and aureole measurements (Ref. 18). Some of these measurements and analyses, particularly the polarimetric, fall into the research category. They represent attempts to improve the accuracy of the calibration procedure and, because of their untested nature, require validation. However, without them we anticipate an overall accuracy of about $\pm 3\%$ absolute. This represents an improvement over the $\pm 5\%$ value claimed in reference 19, and is due to our anticipated $\pm 1\%$ absolute accuracy of calibration of the ground instrumentation.

The proposed basic design of the instrumentation is similar to that being designed and built at the University of Arizona for the investigation of solar irradiance variations over a 23-year period. It employs a precision alt-azimuth tracking stand, with stepper motors to drive the two axes, so that it can be pointed in almost any direction or be held in alignment with the sun. A microprocessor based computer system will be used to control the motors as well as the data acquisition and processing system. A conceptual view of the instrument is shown in Fig. 5, further details of its design will be presented at the symposium.

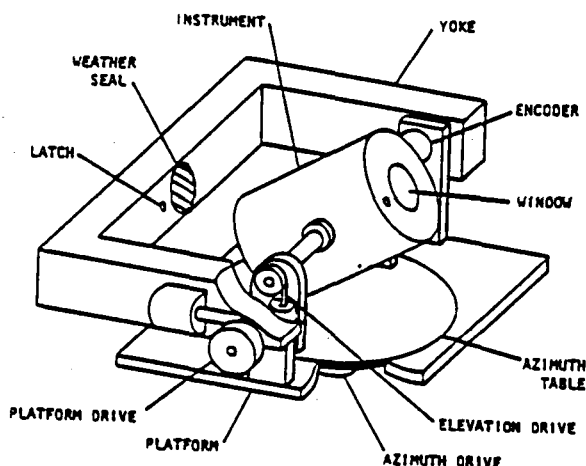


Fig. 5. Conceptual view of spectroradiometer for ground and atmospheric measurements.

6. ACKNOWLEDGEMENTS

I wish to thank J. Geist, S.J. Martinek, J.M. Palmer and E.F. Zalewski for the benefit of useful discussions. This work was supported under grant number NAG 5-196.

7. REFERENCES

1. Slater P N 1980, *Remote Sensing: Optics and Optical Systems*, Reading, Mass., Addison-Wesley, 481-484.
2. NASA Contract NAS5-23639 1977, *A study of the effects of the atmosphere on thematic mapper observations*, by Pearce W A.
3. Dave J V 1980, Effect of atmospheric conditions on remote sensing of a surface non-homogeneity, *Photogram Eng & Remote Sensing* 46(9), 1173-1180.

4. NASA Tech Memo 83818 1981, *The effect of finite field size on classification and atmospheric correction*, by Kaufman Y J & Fraser R S.
5. Tanre D et al 1981, Influence of the back-ground contribution on space measurements of ground reflectance, *Appl Opt.* 20(20), 3676-3684.
6. Environmental Res Inst of Michigan Final Report E77-10057 1976, *Investigation of Landsat follow-on thematic mapper spatial, radiometric and spectral resolution*, by Morgenstern J P et al.
7. Geist J 1979, Quantum efficiency of the p-n junction in silicon as an absolute radiometric standard, *Appl Opt.* 18(6), 760-762.
8. Geist J 1980, Silicon photodiode front region collection efficiency models, *J Appl Phys.* 51(7), 3993-3995.
9. Geist J et al 1979, Spectral response and self-calibration and interpolation of silicon photodiodes, *Appl Opt.* 19(22), 3795-3799.
10. Geist J & Zalewski E F 1979, The quantum yield of silicon in the visible, *Appl Phys Lett.* 35(7), 503-506.
11. Zalewski E F & Geist J 1980, Silicon photodiode absolute spectral response self-calibration, *Appl Opt.* 19(8), 1214-1216.
12. Zalewski E F 1981, private communication.
13. Kostuk R K 1981, Polarization properties of a 1000-W FEL type filament lamp, *Appl Opt.* 20(13), 2181-2184.
14. Air Force Cambridge Research Laboratories Environmental Research Papers No 285 1968, *UV visible and IR attenuation for altitudes to 50 km*, by Elterman L.
15. Jennings S G et al 1978, Effects of particulate complex refractive index and particle size distribution variations on atmospheric extinction and adsorption for visible through middle ir wavelengths, *Appl Opt.* 17(24), 3922-3929.
16. Lindberg J D & Laude L S 1974, Measurement of the absorption coefficient of atmospheric dust, *Appl Opt.* 13(8), 1923-1927.
17. King M D et al 1978, Aerosol size distribution obtained by inversion of spectral optical depth measurements, *J Atmos Sci.* 35, 2153.
18. Twitty J T 1975, The inversion of aureole measurements to derive aerosol size distributions, *J Atmos Sci.* 32, 584.
19. Kriebel K T 1981, Calibration of the METEOSTAT-VIS channel by airborne measurements, *Appl Opt.* 20(1), 11-12.

JPL AIRBORNE INSTRUMENTS ACTIVITIES

AN OVERVIEW

Gregg Vane

Two instruments intended for flight aboard aircraft for research in advanced remote sensing of the earth are under development at JPL: the Airborne Imaging Spectrometer (AIS) and the Airborne Visible-Infrared Imaging Spectrometer (AVIRIS). The AIS utilizes a Rockwell 32 x 32 element HgCdTe CCD array to gather 10nm spectral data, initially in the 1.2 - 2.4 μ m range, with 32 pixels of cross-track spatial data. The instrument acquires 128 channels of spectral data by using a grating spectrometer whose grating is stepped through four positions during a fraction of an IFOV time on the ground. With an IFOV of 2 mrad, the GIFOV at the design altitude of 3 km is 6m. The instrument has several on-board processing capabilities including $ax+b$ corrections for detector calibration, cross-track and down-track pixel summing, spectral band summing, and variable integration time to allow flight at various altitudes and velocities. Flights are planned for September 1982, over the Coaldale Mining District, Nevada in a mineral identification study, and in November 1982, over the Pico Anticline area, Los Angeles County, California in a geobotany study. Because the detector array used has a cutoff wavelength of 4.5 μ m, the instrument can potentially be reconfigured to cover the mid IR region as well.

The AVIRIS instrument concept is an outgrowth of the study by Vane, Billingsley and Dunne appended at the end of this paper, in which leaders of the various remote sensing research communities were asked for their appraisal of spectral and spatial resolution needs for the next generation of spaceborne systems. The fundamental conclusion of that study was that while there are promising, and in many cases proven uses for high

spectral and spatial resolution data, the data base itself is too limited to specify which combinations of spectral bands and IFOVs will provide the optimum data sets within the constraints of data transmission, handling and storage capabilities to be available by the time such a spaceborne system might be launched. Hence there is a considerable need for such a data set at this time, to allow such trade-off studies to be made in a systematic manner.

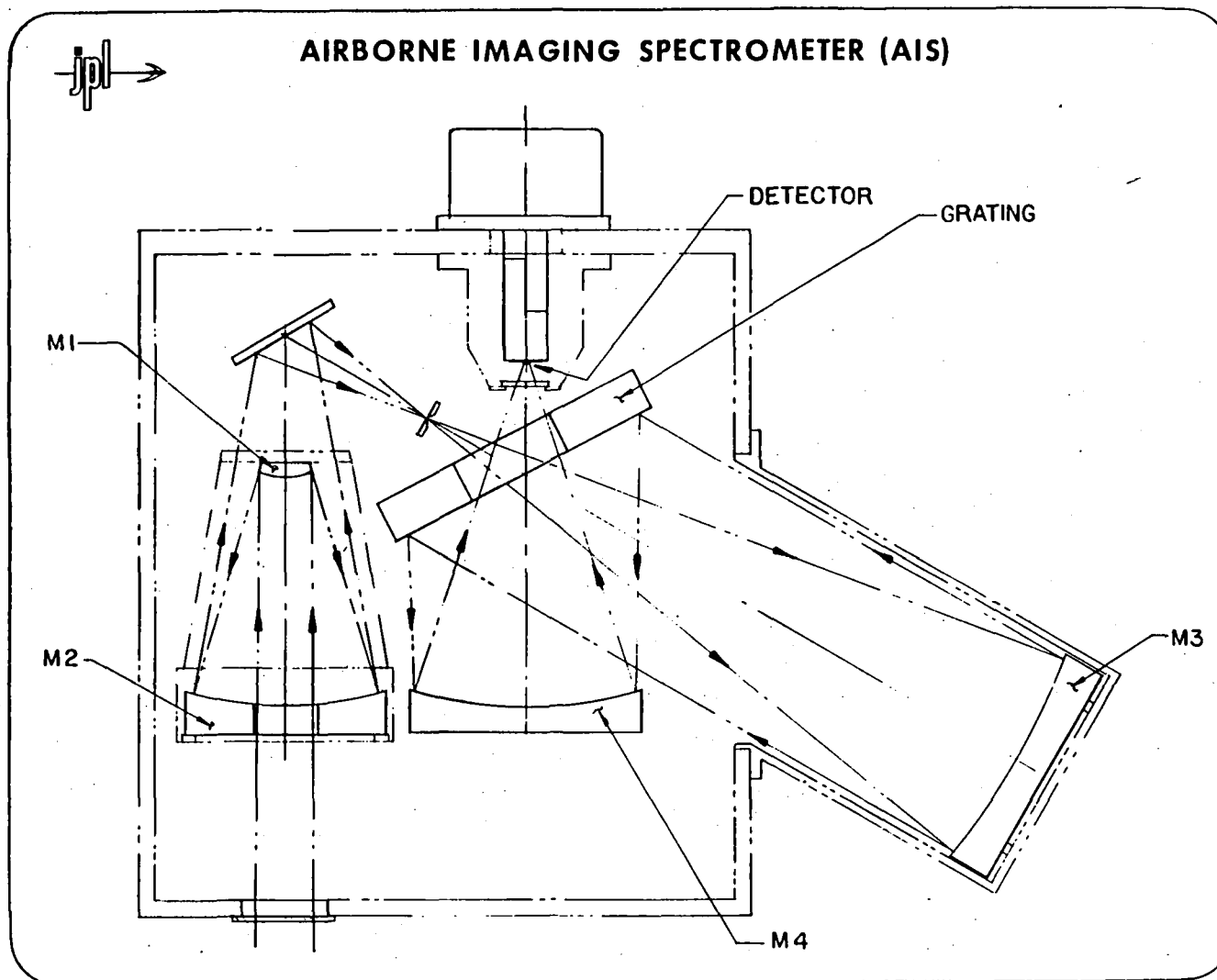
The purpose of AVIRIS then is to gather data, as distinct from demonstrating advanced technology. Hence its design is conservative, using off-the-shelf technology. The heart of the instrument design is the InSb line array detectors made by Cincinnati Electronics, for the short wavelength infrared. Area array technology is not sufficiently well developed yet to make it an option for AVIRIS, whereas the line arrays made by CE are extremely stable, linear in response, and are readily available. Indeed, it is the availability of such detectors that make such an instrument concept possible at this time. For the visible portions of the spectrum silicon reticon line arrays are equally well-developed.

With the existence of high quality line arrays in the visible and SWIR, the design of choice for AVIRIS uses a proven scanning mechanism to acquire the spatial data in a whisk broom mode, obviating expensive and difficult to build wide angle optics. The line arrays are oriented in the spectral direction at the focal plane of a spectrometer, covering the entire spectrum from 0.35 to 2.5 μm at bandwidths ranging from 10 to 20nm. The instrument IFOV is 0.5 mrad giving a GIFOV of 5m at the design altitude of 10km. Variable integration time is provided to permit flying higher or lower than this for atmospheric studies or for a more stable platform (e.g., the ER-2). The scan angle is 60 degrees so that data can be collected for the assessment of off-nadir viewing. Finally, because InSb has a cutoff wavelength of 5.2 μm , the instrument can be configured to acquire spectral data in the mid IR. Instrument design activities are currently underway at JPL and a proposal will be submitted to NASA in August 1982.



AIRBORNE IMAGING SPECTROMETER (AIS) INSTRUMENT DESCRIPTION

- DETECTOR: ROCKWELL 32 x 32 HgCdTe CCD
- TELESCOPE OPTICS: F/3 SCHWARZCHILD CONCENTRIC OBJECTIVE
WITH 70.7 mm EFL
- SPECTROMETER OPTICS: SLIT - 4.23 mm x 142.24 μ m
COLLIMATOR - 300 mm EFL F/3 PARABOLOID
GRATING - 42 G/mm, BLAZE 1.05-3.16 μ m
CAMERA - 150 mm EFL F/1.5 PARABOLOID
- ELECTRONICS: AX + B CORRECTION ALGORITHM FOR EACH
PIXEL WITH UPGRADING TO MORE SOPHISTICATED
ALGORITHM IF NECESSARY
CROSS-TRACK AND DOWN-TRACK PIXEL
SUMMING
SPECTRAL BAND SUMMING
VARIABLE INTEGRATION TIME





AIRBORNE IMAGING SPECTROMETER (AIS) OBSERVATIONAL CAPABILITIES

- SPECTRAL RANGE: 1.2 - 2.4 μm
- SPECTRAL BANDWIDTH: 9.6 nanometers
- SPECTRAL CHANNELS: 128
- IFOV: 1.9 mrad
- GIFOV AT 3 km: 5.7 meters
- SWATH WIDTH AT 3 km: 183 meters
- DATA RATE: 100 kbps IN EACH OF 4 CHANNELS



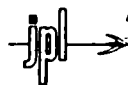
AIRBORNE IMAGING SPECTROMETER (AIS) FLIGHT OPERATIONS FOR 1982

SEPTEMBER

AIRCRAFT: C130, AMES
ALTITUDE: 15,000 feet
GIFOV: 8 meters
AREA: COALDALE MINING DISTRICT, NEVADA
APPLICATION: GEOLOGY - MINERAL STUDIES

NOVEMBER

AIRCRAFT: DC3, DRYDEN
ALTITUDE: 7,500 feet
GIFOV: 4 meters
AREA: PICO ANTICLINE, LOS ANGELES COUNTY
APPLICATION: GEOBOTANY



AIRBORNE VISIBLE — INFRARED IMAGING SPECTROMETER (AVIRIS)

PROGRAM OBJECTIVES

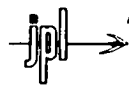
- **EXPLORE THE UTILITY OF HIGH SPECTRAL AND SPATIAL RESOLUTION DATA AND DEVELOP NEW EXPERIMENT METHODOLOGIES FOR USING THESE DATA**
- **PROVIDE HARD EXPERIMENTAL GUIDANCE FOR FUTURE OBSERVATIONAL REQUIREMENTS FOR SPACEBORNE SENSORS. SPECIFICALLY:**
 - **ESTABLISH OPTIMUM SPECTRAL CHANNELS FOR THE MAJOR REMOTE SENSING DISCIPLINES**
 - **ESTABLISH THE EFFECTS OF SPATIAL RESOLUTION ON SYSTEM PERFORMANCE.**
 - **ASSESS THE EFFECTS OF OFF-NADAR VIEWING.**
 - **ASSESS THE EFFECTS OF THE ATMOSPHERE ON SYSTEM PERFORMANCE.**



AIRBORNE VISIBLE – INFRARED IMAGING SPECTROMETER (AVIRIS)

PROGRAM FUNCTIONAL DESCRIPTION

- AS A RESEARCH INSTRUMENT DEDICATED TO ACQUIRING DATA, AVIRIS IS DESIGNED FOR MAXIMUM RELIABILITY, USING PROVEN TECHNOLOGY
- AVIRIS IS A SCANNING INSTRUMENT USING SILICON AND INDIUM ANTIMONIDE LINE ARRAYS TO COVER THE 0.4 TO 2.5 μm REGION
- THE INSTRUMENT WILL PROVIDE IN-FLIGHT CALIBRATION
- AVIRIS WILL BE CAPABLE OF OPERATION AT SEVERAL ALTITUDES
- DATA PROCESSING PLANS WILL BE GENERATED IN ADVANCE TO PROVIDE 4-8 WEEK DATA OUTPUT IN A FORMAT USEABLE AT THE RESEARCHER'S HOME INSTITUTION



AIRBORNE VISIBLE — INFRARED IMAGING SPECTROMETER (AVIRIS)

INSTRUMENT DESCRIPTION

INSTANTANEOUS FIELD OF VIEW	0.5 mrad
DESIGN ALTITUDE	10 km
GROUND IFOV AT 10 km	5 meters
SCAN ANGLE	60 degrees
SWATH WIDTH AT 10 km	11.5 km
NUMBER OF BITS PER PIXEL	8
SPECTRAL COVERAGE	0.35-2.55 μm
SPECTRAL BANDWIDTH	10-20 nm
NUMBER OF SPECTRAL CHANNELS	170
DATA RATE AT 200 knots, 10 km ALTITUDE	55 Mbps



**AIRBORNE VISIBLE – INFRARED IMAGING SPECTROMETER
(AVIRIS)**

SPECTRAL COVERAGE

<u>SPECTRAL BAND (micron)</u>	<u>SPECTRAL RESOLUTION (nm)</u>	<u># OF SPECTRAL CHANNELS</u>	<u>DETECTOR MATERIAL</u>	<u>NEdR %</u>
0.35 - 0.70	10	35	Si	0.5
0.70 - 1.00	10	30	Si	0.5
1.00 - 1.40	10	40	InSb	1.0
1.40 - 1.85	15	30	InSb	1.0
1.85 - 2.55	20	35	InSb	1.5

ADVANCED COPY

Airborne Multispectral Linear Array Instruments

at

Goddard Space Flight Center

James R. Irons
James C. Smith
William L. Barnes

The fabrication of airborne instruments is contributing to the development of multispectral linear array (MLA) technology at NASA's Goddard Space Flight Center (GSFC). GSFC's first MLA instrument, the Linear Array Pushbroom Radiometer (LAPR-I), was built in 1979 to demonstrate capabilities for acquiring digital image data using linear arrays (Fig. 1). LAPR-I employed three arrays of 512 silicon photodiodes each to simultaneously acquire three channels of data for spectral bands within the visible and near-infrared portions of the spectrum. LAPR-I was operated from aircraft during 1979 to 1981 and useful imagery and thematic maps were derived from the digital image data (Wharton et al., 1981).

A second instrument, LAPR-II, is being built to enhance data acquisition capabilities for scientific investigations (Fig. 2). LAPR-II will use four arrays each consisting of 512 silicon detectors. A filter wheel containing six spectral filters will be used in conjunction with each array to allow filter changes in flight. This capability will facilitate studies into the utility of various bands within the visible and near infrared portions of the spectrum (0.4-1.0 μm). LAPR-II's aircraft mounting will allow off-nadir pointing (plus-or-minus 50° fore-and-aft and side-to-side) which will enable investigations of the radiometric and geometric effects of off-nadir viewing. The spatial and spectral characteristics of LAPR-II will be quantitatively characterized and the radiometric response of each detector will be calibrated before the instrument is flown in 1983 (Irons et al., 1982). Fabrication will be completed and test flights will be conducted in the late summer of 1982. LAPR-II will provide investigators with a well-described, flexible source of digital image data for scientific research.

A third linear array instrument has recently been completed for sensing energy within an additional portion of the spectrum. The Short Wave Infrared Radiometer (SWIR) will use a single array of 64 lead-sulfide detectors to acquire data for spectral bands within the 1.0 μm to 2.6 μm region (Fig. 3). An 80-hertz chopper blade is used to minimize electrical noise and drift. A filter wheel provides a selection of three spectral filters which can be switched in flight. SWIR has been operated in the laboratory and test flights are planned for the late summer 1982.

In the future, consideration will be given to the development of an airborne area array instrument (Fig. 4). This instrument would employ a two-dimensional array of detectors where each row of detectors would sense a narrow spectral band. An investigator could select data from any combination of detector rows or could integrate the signal from several adjacent rows to create a spectral band configuration which meets the requirements of a specific mission.

The creation of the airborne instruments is developing expertise in the design, fabrication, calibration, and operation of multispectral linear array systems. Furthermore, the instruments will provide investigators with a versatile source of digital image data. The instruments will familiarize both scientists and engineers with the attributes of MLA technology.

REFERENCES CITED

Irons, J. R., J. C. Smith, L. R. Blaine, and M. W. Finkel. 1982. A Plan for the Characterization, Calibration, and Evaluation of LAPR-II. NASA Technical Memorandum 83915. Goddard Space Flight Center, Greenbelt, MD.

Wharton, S. W., J. R. Irons, F. Huegel. 1981. LAPR: An Experimental Pushbroom Scanner. Photogrammetric Engineering and Remote Sensing, Vol. 47, No. 5. pp. 631-639.

LAPR-I

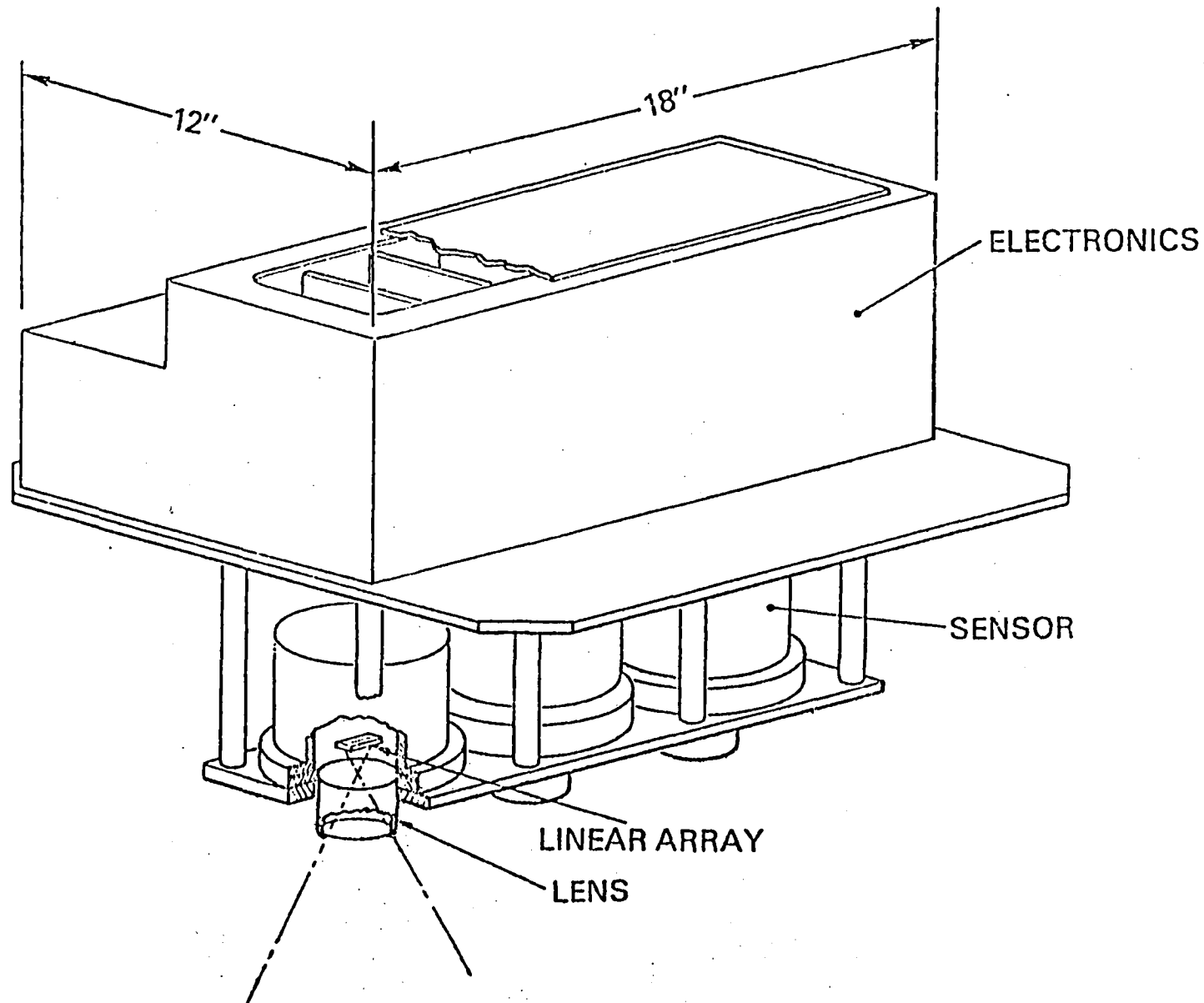


Figure 1. The First Linear Array Pushbroom Radiometer

LAPR-II

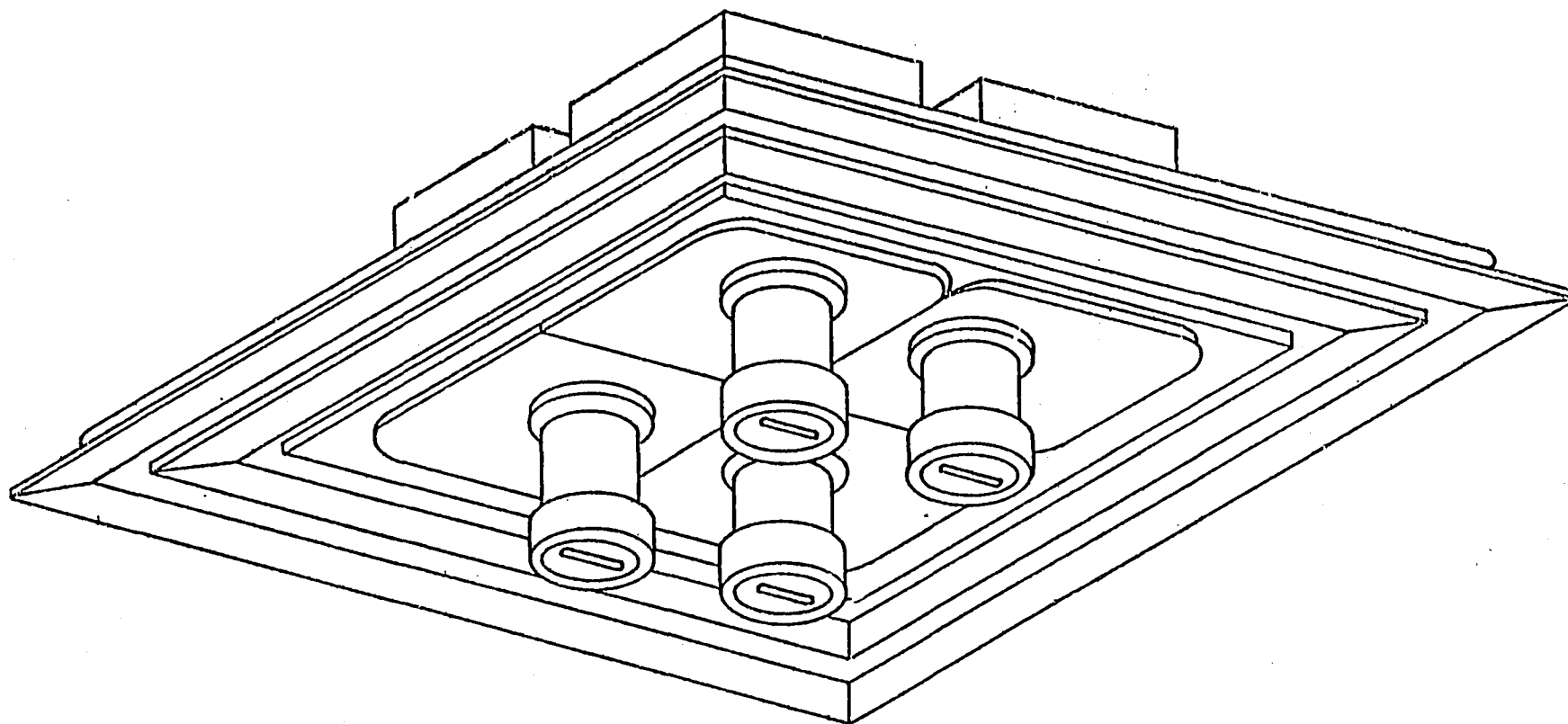


Figure 2. The Second Linear Array Pushbroom Radiometer

LAPR-SWIR

FILTER WHEEL
MOTOR

FILTER WHEEL

DETECTOR

LENS

CHOPPER
BLADE

CHOPPER
MOTOR

ELECTRONICS

Figure 3. The Short Wave Infrared Radiometer

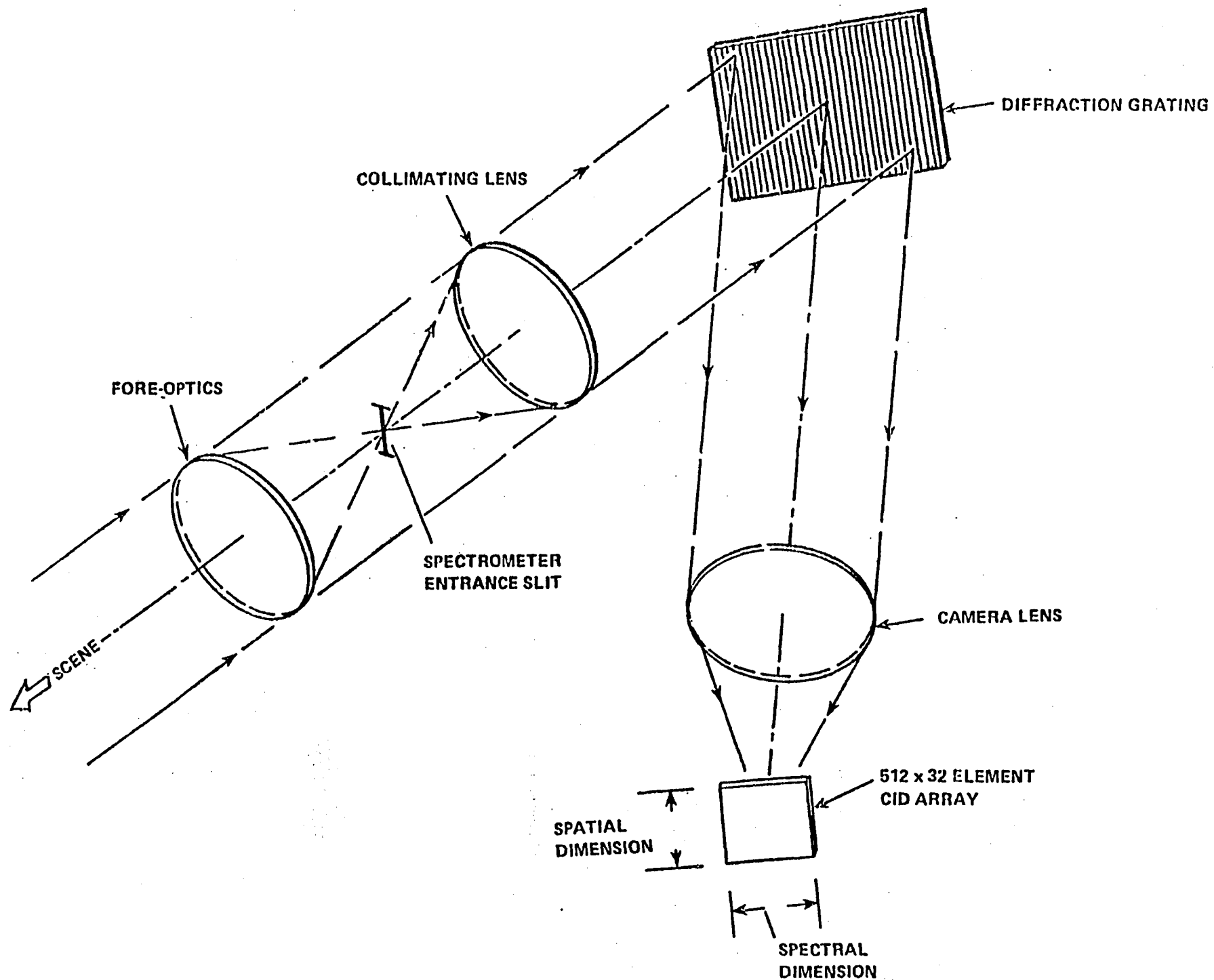


Figure 4. Configuration of an Airborne Area Array Instrument

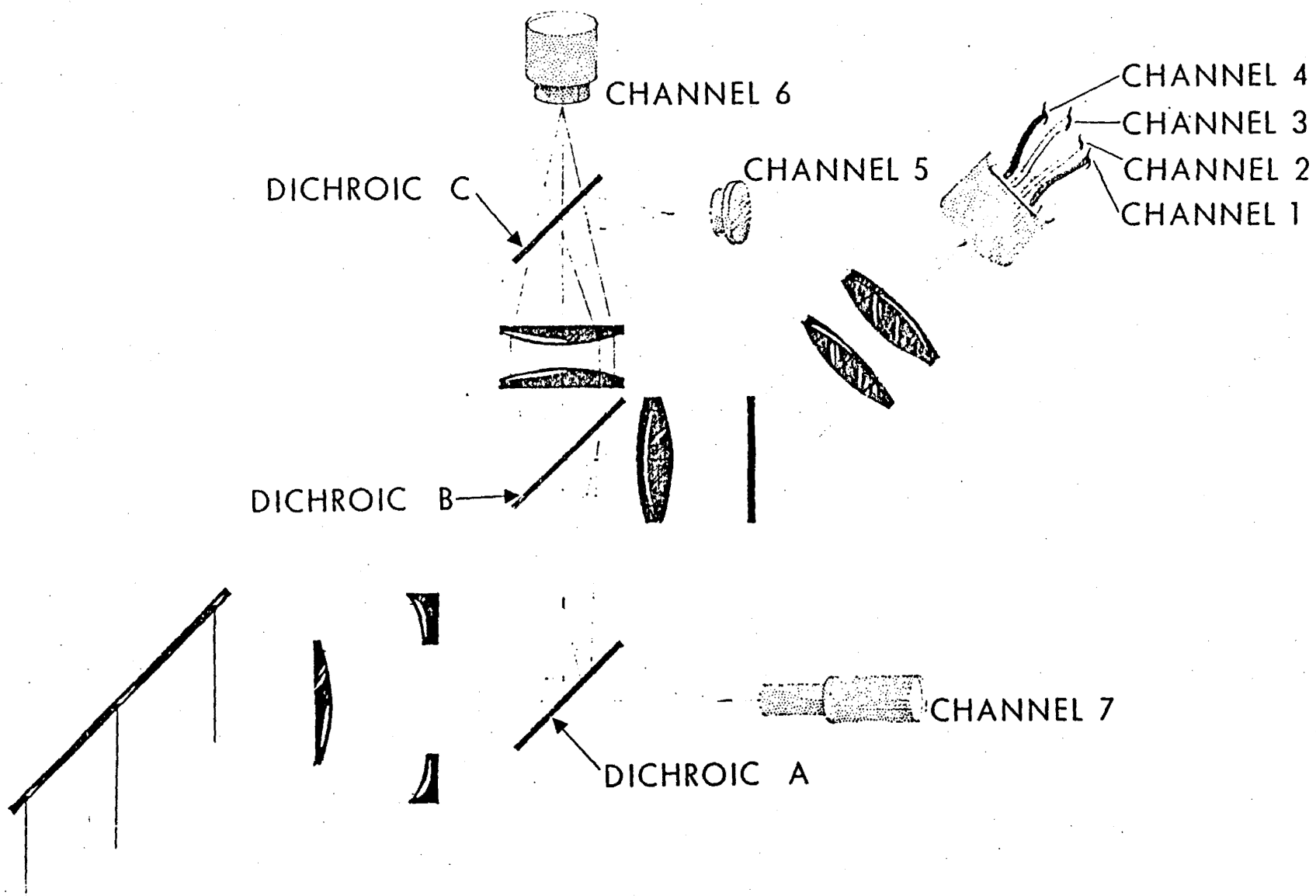
NASA - NSTL EARTH RESOURCES LABORATORY
SENSOR DEVELOPMENT
OVERVIEW

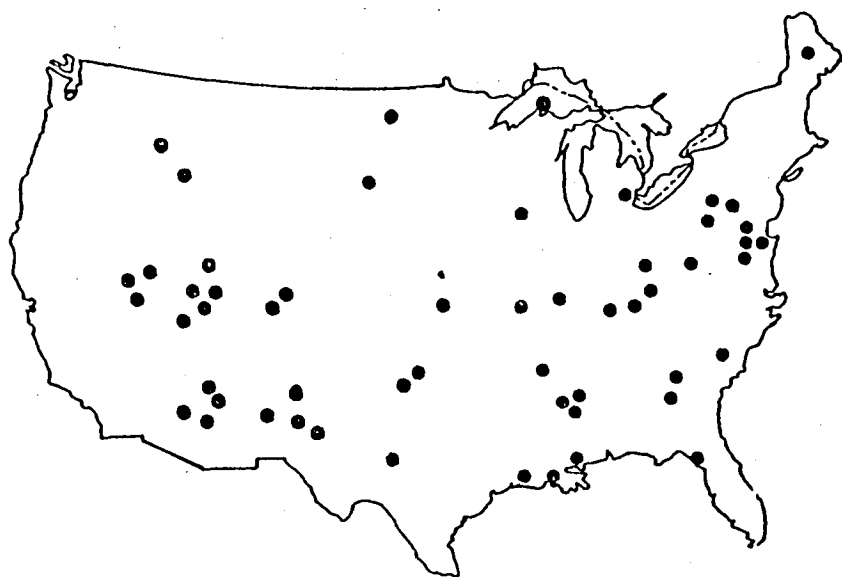
- OPERATIONAL SENSORS
 - * ● THEMATIC MAPPER SIMULATOR (TMS) ($0.46\mu - 12.3\mu$)
 - S-191 FIELD SPECTROMETER ($0.45\mu - 2.5\mu$)
 - THEMATIC MAPPER RADIOMETER ($0.45\mu - 0.90\mu$)
- DEVELOPMENTAL SENSORS
 - * ● THERMAL INFRARED MULTISPECTRAL SCANNER (TIMS) ($8.2\mu - 12.2\mu$)
- DESIGN STUDIES
 - * ● VARIABLE RESOLUTION MULTI-LINEAR ARRAY PUSHBROOM SCANNER
($0.45\mu - 1.10\mu$)
 - ACTIVE (TARGET - ILLUMINATING) MULTISPECTRAL SCANNER ($0.45\mu - 1.10\mu$)
 - SCANNING TERRAIN PROFILER
 - MICROPROCESSOR CONTROLLED SPECTROMETER ($0.40\mu - 14.0\mu$)

THEMATIC MAPPER SIMULATOR (TMS)

- SINGLE CHANNEL THERMAL SCANNER (ANALOG) PURCHASED FROM TEXAS INSTRUMENTS IN 1971.
- CONVERTED TO FIVE BAND (LANDSAT MSS + THERMAL) SCANNER (DIGITAL) IN 1974.
- CONVERTED TO SEVEN BAND (LANDSAT D THEMATIC MAPPER) SIMULATOR IN 1980.
 - CONVERSION TO TMS ACCOMPLISHED IN-HOUSE FOR \$42K
- FIRST FLIGHT ON MAY 30, 1980, WITH FLIGHT EVALUATION JUNE-SEPTEMBER, 1980.
 - 12 MISSIONS CONDUCTED OVER 6 TEST SITES, INCLUDING DOS TEST SITES.
- SYSTEM OPERATIONAL OCTOBER, 1980.
- SPECTRAL/SPATIAL CAPABILITIES.

BAND	LANDSAT-D SPATIAL	TM SPECTRAL	NSTL SPATIAL	TMS SPECTRAL	LANDSAT-D SPECTRAL	TM SPEC
1	30M	.45 - .52 μ	5-33M	.46 - .52 μ	.45 - .52 μ	.52 μ
2	30M	.53 - .61 μ	5-33M	.53 - .60 μ	.52 - .60 μ	.60 μ
3	30M	.62 - .69 μ	5-33M	.63 - .69 μ	.63 - .69 μ	.69 μ
4	30M	.78 - .91 μ	5-33M	.77 - .90 μ	.76 - .90 μ	.90 μ
5	30M	1.57 - 1.79 μ	5-33M	1.53 - 1.73 μ	1.55 - 1.75 μ	1.75 μ
7	30M	2.10 - 2.35 μ	5-33M	2.06 - 2.33 μ	2.08 - 2.35 μ	2.35 μ
6	120M	10.40 - 11.60 μ	5-131M	10.30 - 12.30 μ	10.40 - 12.50 μ	12.50 μ





DISTRIBUTION OF FY81 TMS
DATA ACQUISITION FLIGHTS
IN CONTINENTAL UNITED STATES

FY81: 86 MISSIONS (7 REIMBURSABLE)
367 AIRCRAFT FLIGHT HOURS

FY82: (OCT - MAR)
18 MISSIONS (9 REIMBURSABLE)
112 AIRCRAFT FLIGHT HOURS

TMS DATA USERS

NASA - NSTL

GSFC (R)

JPL (R)

JSC

DEPT OF STATE

USDA - USFS (R)

USGS - EROS (R)

LOUISIANA STATE UNIVERSITY

MISSISSIPPI STATE UNIVERSITY

MURRAY STATE UNIVERSITY (KY)

OKLAHOMA STATE UNIVERSITY

UNIVERSITY OF GEORGIA

UNIVERSITY OF MICHIGAN (R)

TAC-UNIVERSITY OF NEW MEXICO

WASHINGTON UNIVERSITY (MO)

ST. REGIS PAPER COMPANY

MEXICO (R)

COLOMBIA (R)

LAND COVER CLASSIFICATION ACCURACIES

<u>SURFACE COVER</u>	<u>TMS ACCURACY (%)</u>
INERT	97.62
OLD FIELDS	91.95
MARSH	89.29
RIVER BOTTOM	95.54
MIXED FOREST	92.54
PINE	91.58
HAY/GRASS	98.19
WATER	100.00
OVERALL	92.30

DATA ACQUIRED OVER PEARL RIVER, MISSISSIPPI TEST SITE WITH NASA TMS.

THERMAL INFRARED MULTI SPECTRAL SCANNER (TIMS)

- SPECTROMETER DESIGN - JPL/DAEDALUS (AUGUST, 1980 - \$66K)
- SCANNER DESIGN, SPECTROMETER/SCANNER FABRICATION - NSTL/DAEDALUS (DECEMBER, 1980 - \$761K)
- SYSTEM LABORATORY ACCEPTANCE TEST - MAY 10-12, 1982.
- SYSTEM FLIGHT ACCEPTANCE TEST - MAY 13, 1982.
- SCHEDULE:

FLIGHT EVALUATION - MAY 14-24

CALIBRATION TESTS - MAY 25 - JULY 18

OPERATIONAL FLIGHTS - JULY 19 - AUGUST 1

DATA EVALUATION - AUGUST 2-31

OPERATIONAL FLIGHTS - SEPTEMBER 1

- SPECIFICATIONS:

		<u>BAND</u>	<u>SPECTRAL COVERAGE</u>	<u>NEΔT</u>
FOCAL LENGTH	13.0 INCHES	1	8.2 μ m - 8.6 μ m	0.09 ⁰ C
CLEAR APERTURE	7.5 INCHES	2	8.6 μ m - 9.0 μ m	0.09 ⁰ C
SYSTEM IFOV	2.5 MR	3	9.0 μ m - 9.4 μ m	0.09 ⁰ C
GROUND RESOLUTION	5-33 METERS	4	9.4 μ m - 10.2 μ m	0.12 ⁰ C
SWATH WIDTH	1.3 - 8.3 MILES	5	10.2 μ m - 11.2 μ m	0.14 ⁰ C
SCAN SPEEDS	7.3, 8.7, 12.0, 25.0 SCANS/SECOND	6	11.2 μ m - 12.2 μ m	0.32 ⁰ C

SPECTROMETER

AADS1285 (TIMS) SCAN HEAD
CROSS SECTIONAL DIAGRAM

PARABOLIC
MIRROR

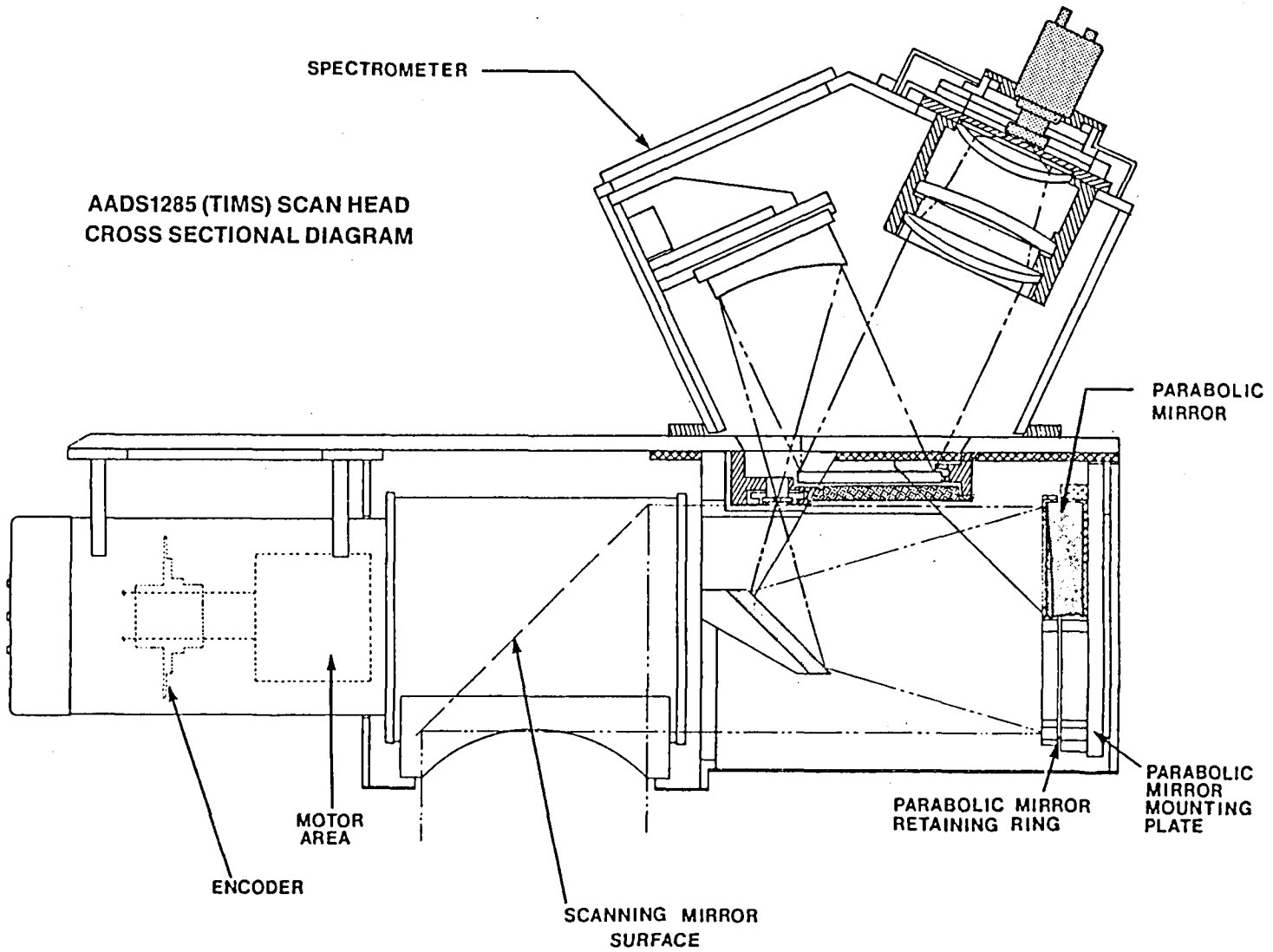
PARABOLIC MIRROR
MOUNTING
PLATE

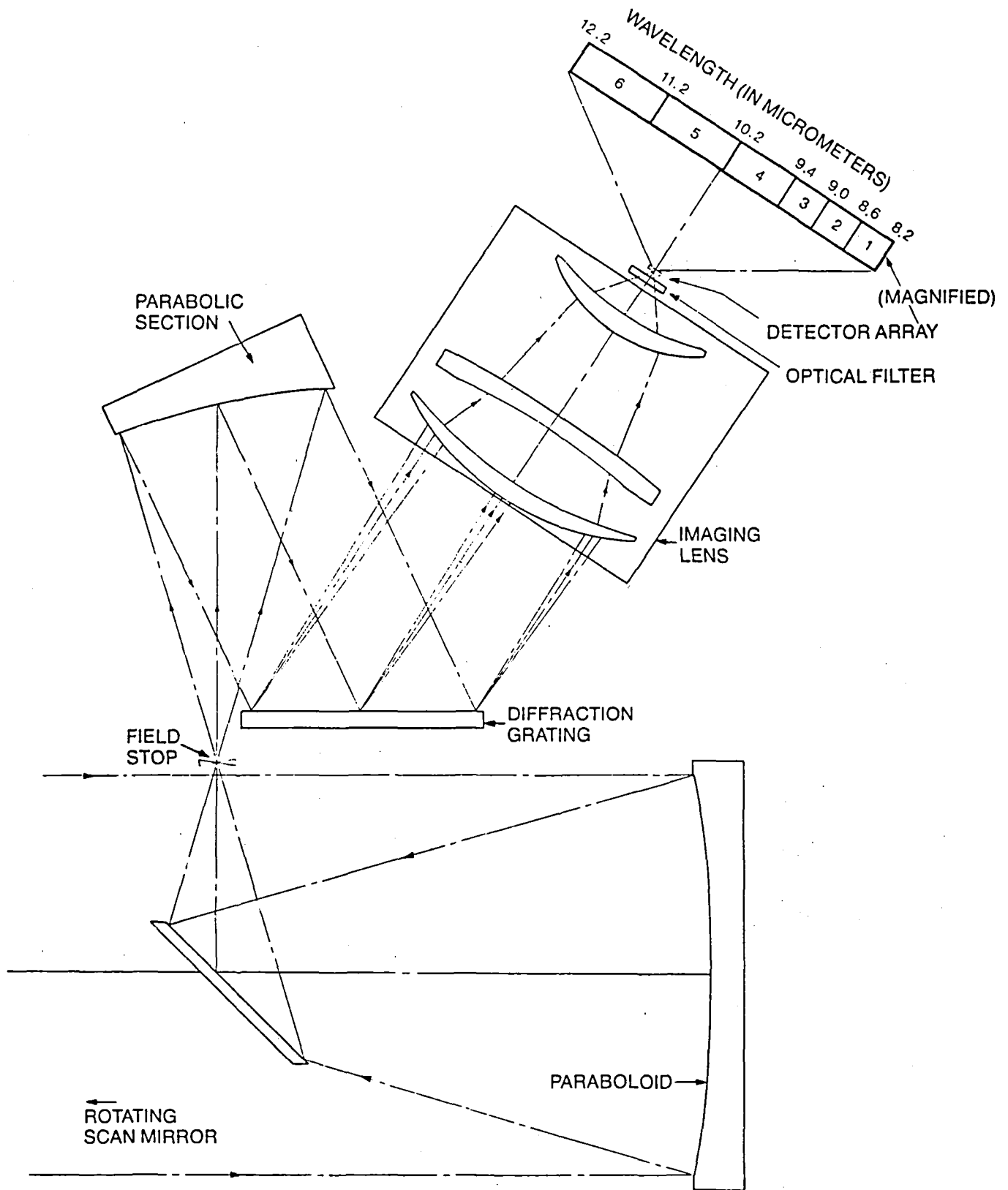
PARABOLIC MIRROR
RETAINING RING

SCANNING MIRROR
SURFACE

MOTOR
AREA

ENCODER





NSTL SPATIAL RESOLUTION ANALYSIS SYSTEM

- BACKGROUND: 7 BAND TM SIMULATOR DATA WAS ACQUIRED AT 30, 25, 20, 15, 10, AND 5 METER RESOLUTIONS BY OPERATING AIRCRAFT AT DIFFERENT ALTITUDES. ANALYSIS EXTREMELY DIFFICULT DUE TO ATMOSPHERIC PATH LENGTHS AND RESULTING DATA PERTURBATIONS.
- OBJECTIVE: TO DESIGN AND BUILD A VERY LOW COST VARIABLE RESOLUTION (SPATIAL) MULTI-LINEAR ARRAY DEVICE TO PRODUCE 5-30 METER DATA FROM 40,000 FT.
- FEATURES:
 - 4 DISCRETE CHANNELS WITH 512 ELEMENT ARRAYS
 - 3-30 METER RESOLUTION FROM 40,000 FEET
 - FORE-AFT OFF NADIR VIEWING WITH VARIABLE LOOK ANGLE
 - MULTIPLE SPECTRAL BANDPASS FILTER SELECTION
 - ON-BOARD ELECTRONIC ROLL COMPENSATION
 - ON-BOARD ARRAY PARAMETER (RADIOMETRIC) CORRECTION
 - IN-HOUSE DESIGN AND FABRICATION
- FUND SOURCE: DISCRETIONARY FUNDS - \$25 K FOR FLIGHT PROTOTYPE

IMAGE DATA COMPRESSION
APPLICATION TO IMAGING SPECTROMETERS

A Progress Report

Robert F. Rice

Jun-Ji Lee

August 1981

IMAGE DATA COMPRESSION

INTRODUCTION

JPL has long been involved in the development of imaging data compression concepts and techniques primarily aimed at space program applications. A subset of these techniques will be key elements of the Galileo and Voyager (Uranus) imaging systems as well as in a ground based application to the transmission of IR weather data for the National Oceanic and Atmospheric Administration (NOAA). This year's efforts have focussed on investigations of the potential of these techniques to satisfy the anticipated mission requirements of Imaging Spectrometer missions as currently defined.

Background

Noiseless Coding. Noiseless coding of data sources means compression techniques which allow exact bit for bit reconstruction of the original data. This is illustrated in Fig. 1.

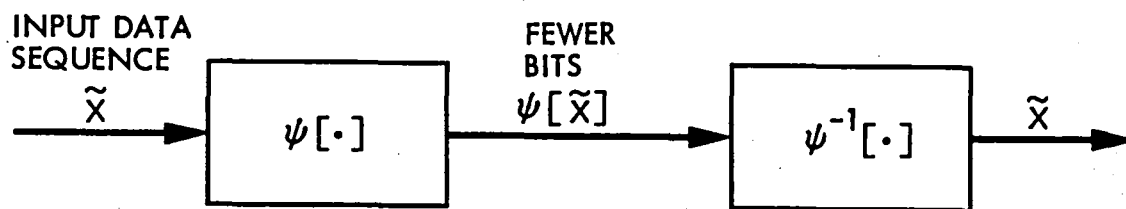


Fig. 1. Noiseless Coding

Coder $\psi[\cdot]$ maps data sequence \tilde{X} into coded sequence $\psi[\tilde{X}]$ from which \tilde{X} can be retrieved precisely using a decoder or inverse, $\psi^{-1}[\cdot]$. Typically, $\psi[\tilde{X}]$ will require many fewer bits than input sequence \tilde{X} . The average number of bits required by $\psi[\tilde{X}]$ will vary depending on a "data activity" term called entropy. $\psi[\tilde{X}]$ is generally considered to perform efficiently if the average number of bits required by $\psi[\tilde{X}]$ is close to the entropy. JPL developed "universal noiseless coders"^{[1]-[3]} which adapt to changing data statistics to ensure that such efficient performance occurs at all entropies. The general result is illustrated in Fig. 2.

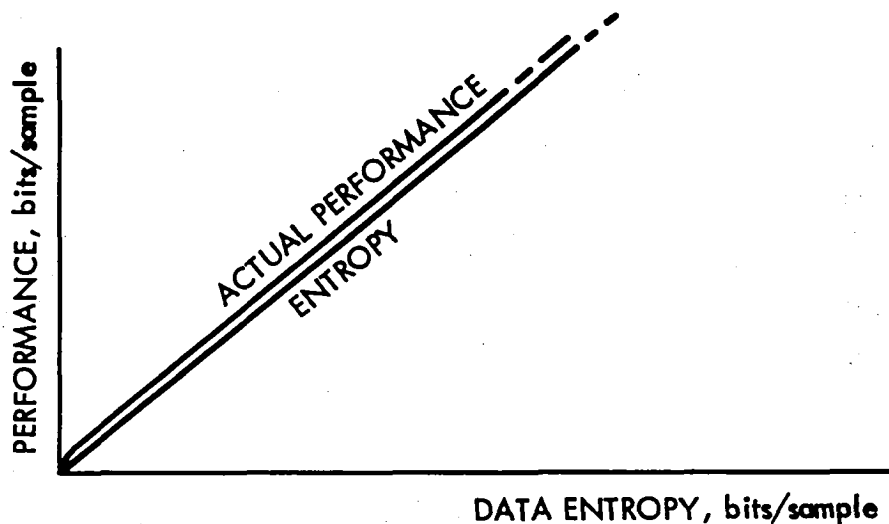


Fig. 2. Universal Noiseless Coder Performance

In image applications to deep space photos and NOAA IR weather satellite images^[4] noiseless coding could be expected to reduce 8 bits/picture element (bits/pixel or b/p) by, typically, 2:1 to 4:1. However, some military reconnaissance photos required over 5 bits/pixel.

Rate Controlled Compression. The variability of the compression factor derived by noiseless coding poses an operational problem for some applications. Further, the noiseless constraint was unnecessarily restrictive in many situations, limiting the compression factors obtainable to the range noted above. These factors led to the development of rate controlled compression with the general characteristics noted in Fig. 3. A graph of image quality vs. rate in bits/pixel is shown in the figure. The two points discussed thus far are shown for no compression and noiseless coding where the abscissa (rate) for the latter is data dependent. The new feature is to be able to specify the rate: per image for a two-dimensional algorithm called RM2^{[5]-[6]} or per line for a one-dimensional algorithm called BARC.^[7] If a selected rate is above what is required for

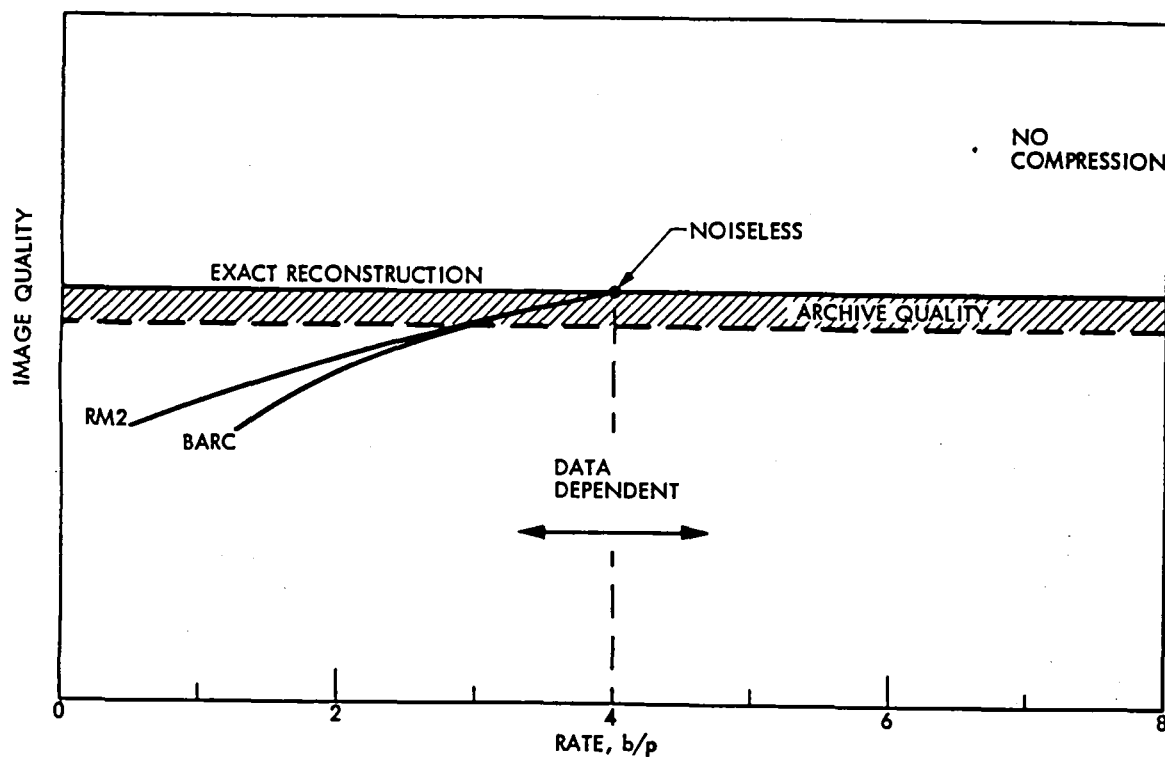


Fig. 3. Basic Rate/Quality Tradeoff

noiseless coding (\approx entropy) then BARC or RM2 will return coded data which will allow exact reconstruction.

A gradual reduction in selected rate below what is required for noiseless coding will yield reconstructions with a corresponding gradual decrease in quality. At selected rates above 3 bits/pixel the relative performance between RM2 and BARC have generally been observed to be small, whereas at much lower rates (below 2 bits/pixel) RM2 clearly performs much better. On an absolute scale, either RM2 or BARC yield what might generally be considered "archive" quality at selected rates above 3 b/p. Here "archive" quality generally means that all objectives for which the data is intended, subjective and quantitative, can still be accomplished. If there is a constraint for archive quality or no need to achieve compression factors much beyond the 3 bits/pixel range then the simpler BARC should provide a more practical solution. The real potential advantage for RM2 and imaging spectrometer missions is the broad user controlled rate/quality tradeoff that could be applied both spatially and across multi-spectral bands to

properly emphasize features of primary interest. This is discussed further in a later section.

CCA.^[8] Another development in data compression and processing at JPL which should, in some form, be applicable to the IS program is a process called the Cluster Compression Algorithm (CCA). CCA obtains data compression by working directly on multi-spectral vectors as a multi-dimensional adaptive quantizer. It has the unique property that standard supervised spectral classification procedures can be performed directly on the data in compressed form. While one might operate CCA with a 4:1 to 6:1 compression factor, the computation required to obtain classifications can be reduced by factors of 1000:1 or more. This enables such classification in real-time using low-cost computer terminals rather than special purpose hardware. While CCA has produced excellent rate/quality performance in earlier studies its most significant advantage may be on the ground as a preprocessor for classification.

FY81 Direction

The primary emphasis in data compression investigations for Imaging Spectrometer missions has been devoted to further development of the BARC algorithm concept. The primary motivations have already been alluded to in prior discussions and are noted below:

- 1) Link requirements for near term demonstration missions suggest that compression factors of 2 to 3:1 would adequately match instrument data rates (for primary modes) with the expected downlink capabilities.
- 2) Sophisticated adaptive modes involving user directed rate/quality tradeoffs had not been adequately studied to incorporate in demonstration missions (with high probability). Archive quality on all data would preclude user objections. The groundwork for understanding the potential usefulness of RM2 or CCA should be established, however.
- 3) Implementations at expected 300 megabit/sec input rates was a far more likely practicality for the simpler BARC.

DATA COMPRESSION INVESTIGATIONS

This section first treats our primary efforts to improve BARC and then investigates the potential impact of a more powerful RM2 to IS missions. Time did not also permit an investigation of CCA which seems best suited for ground application.

Efforts to Improve BARC

The original BARC algorithms are described in Ref. 7 as well as Galileo design documents. Efforts to make BARC a realizable element of a 300 Mbit/sec Imaging Spectrometer (IS) mission dealt with several issues: 1) Attempts to supplement basic BARC with sub-sample modes to extend its efficient rate-quality performance to lower per pixel rates (recall the drop off at rates much below 3 bits/pixel in Fig. 3; 2) modifications to BARC which provide more modularity and ease of parallelism needed for high rate implementations; 3) modifications which provide more accurate rate allocation procedures to enable the modularity improvement; 4) investigations of correlation detection/correction procedures to minimize the impact of channel errors on compressed data; 5) quality evaluations on data relevant to IS mission objectives.

Improvements at Low Rate. As noted earlier, if the number of bits allowed for an image line equals or exceeds the requirements of noiseless coding then a BARC coded line can be exactly reconstructed. If the number allowed is inadequate to enable such noiseless coding then the basic BARC algorithm achieves the needed reduction in bits by selectively reducing the linear quantization in blocks of 64 pixels across the line. This is a fruitful operation until the remaining entropy in a block drops below roughly 3 bits/pixel. Further reductions begin to yield contouring effects. This fact leads to the increasing disparity in performance between RM2 and BARC at low selected rates (Fig. 1). In an effort to extend the one-dimensional BARC operation to lower rates we investigated supplementing the quantization reductions with small decrements in spatial resolution as illustrated in Fig. 4.

As shown, the subsampler preceeding BARC deletes 1 of $E = n + 1$ pixels (in a staggered line by line pattern). As a result, an overall rate of R' is achieved with BARC operating at a higher rate of ER' . Missing pixels are replaced by linear interpolation.

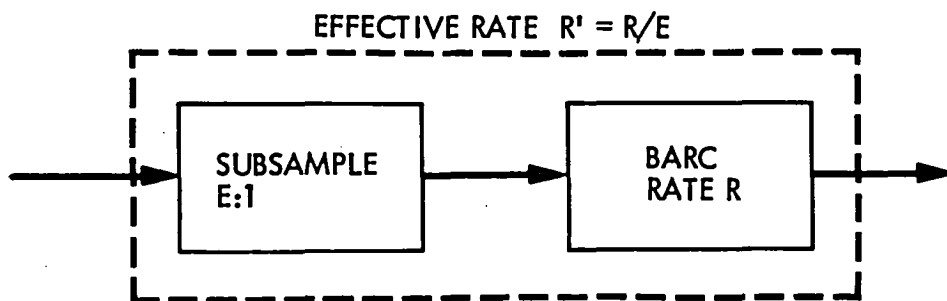


Fig. 4. BARC with Subsample

We considered E values of 1.0, 1.2, 1.25, 1.33, 1.5 and 2.0. The results are shown in Fig. 6 for two deep space Voyager images: a rather inactive Jupiter image and an active image of the satellite Callisto (we did not at the time have data which more closely modeled IS characteristics). The graph plots selected rate in bits/pixel vs. root-mean-squared-error (rmse).[†]

For the less active Jupiter image the subsampling modes were quite effective in lowering the rmse of BARC at per pixel rates of 2 and less. However, the combination was still in general much less effective than RM2, particularly at rates of 1 bit/pixel and less. Subsampling provided little advantage to the more active Callisto image which is closer in characteristic to IS data. The conclusions are then:

- a) Subsampling could improve BARC performance at low rates for some applications if an adaptive mechanism for selecting subsample modes can be found.
- b) It probably is of no value to IS missions.

Improved modularity, BARC2. The basic BARC performs quantization reductions over blocks of 64 pixels whereas the noiseless coding functions are performed over 16. This was partly to minimize the overhead associated with identifying the choice of quantization as well as with assuring adequate operation of the procedure for determining how quantization is determined in each block.^[7]

[†]The standard deviation of the pixel errors in data numbers, DN.

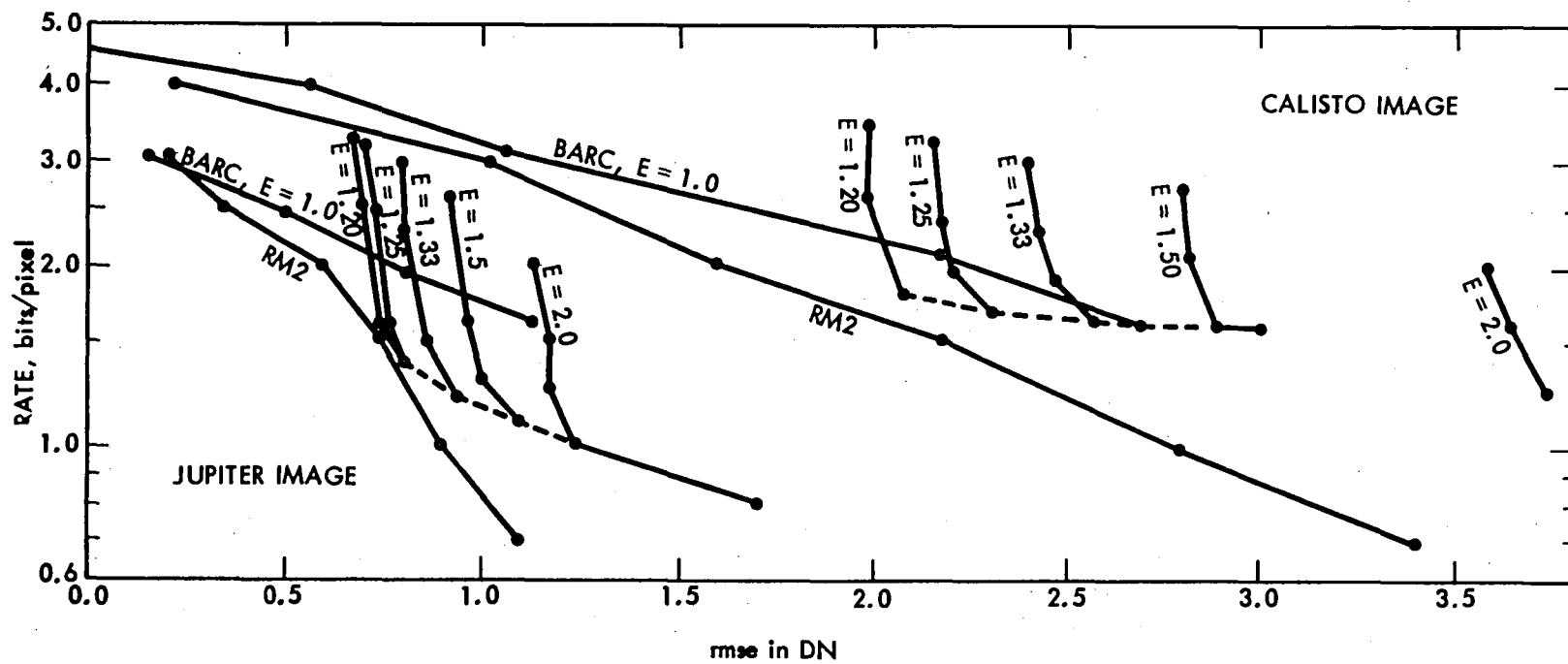


Fig. 6. BARC/Subsample RMSE vs Rate

Experience in the Galileo design suggested that performing both quantization reductions and noiseless coding functions over the same block of 16 pixels could effect simplifications in implementation, particularly in high rate applications such as IS missions. A new method of determining block quantizations needed to be devised to avoid excessive variance in the actual number of bits used over a prescribed data span (e.g., a line). The solution has turned out to be not only simpler and actually more accurate than the old method used on blocks of 64. Compression performance is essentially the same for either approach.

Henceforth, we will assume this new approach and call the overall algorithm BARC2.

Error Protection. The effect of communication errors on compressed data such as from RM2, BARC2 or noiseless coding is much more severe than on uncompressed data. For BARC2 or pure noiseless coding the effect is a propagation of the error across a line until interrupted by a known sync word or other mechanism for a restart. For RM2 the loss may be several two-dimensional blocks of data until restart. If error events are very infrequent then the real damage is minimal. The solution for deep space is the implementation of a concatenated Reed-Solomon/convolutional-Viterbi channel. [5],[9]-[11] This channel produces "virtually error free" ($<10^{-10}$) communication at the same link signal-to-noise ratio that an uncoded link would have error rates higher than 1/100. NASA is considering the application of these same Reed-Solomon codes to high rate earth orbit communications. However, the exact characteristics of communication links for IS missions is not totally defined at this time. Hence we considered the question of what could be done to accomodate errors when they occurred, however rare. Whether further error protection coding would be desirable could be answered at another time.

We first developed a normalized measure of correlation between lines (and defined for each pixel) which tends to hover about unity for the data sets we have thus far investigated. Applying this measure to decompressed BARC2 data will yield similar results, unless a communication error occurs. In the latter case, the correlation measure will eventually diverge, usually very quickly, thus detecting an error event.

The simplest use of this error detection information is the replacement of subsequent data (up to the next restart) with either the line immediately above or or perhaps the average of the line above and the line below. When error events are extremely rare this is probably a completely adequate solution. However, by projecting back to the point where the correlation began to diverge one can consider correcting the error by alternately changing bits and preceding forward until the correlation measure no longer diverges. These observations are illustrated in Fig. 7.

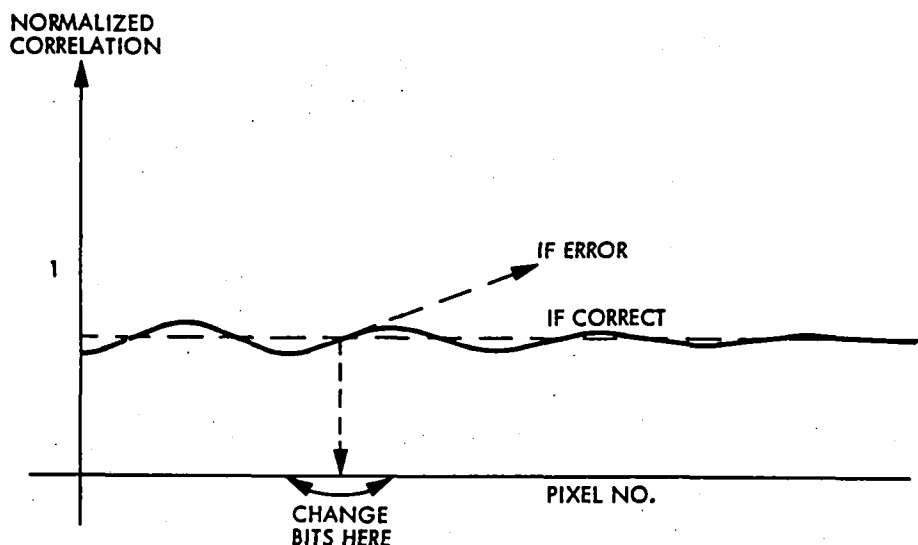


Fig. 7. Correlation Detection/Correction

We are still in the process of developing the error correction procedures. However, an example of automatic line replacement resulting from error detection is shown in Fig. 8. The image on the left is the result of an error rate of roughly $P_e = 10^{-5}$ affecting an image compressed 2:1. The right hand image is the result after detection and replacement.

We anticipate that a sophisticated combination of detection/correction/replacement should enable effective BARC2 operation at much higher error rates but are focussing on the simpler task of $P_e \leq 10^{-5}$ which probably bounds IS mission requirements.

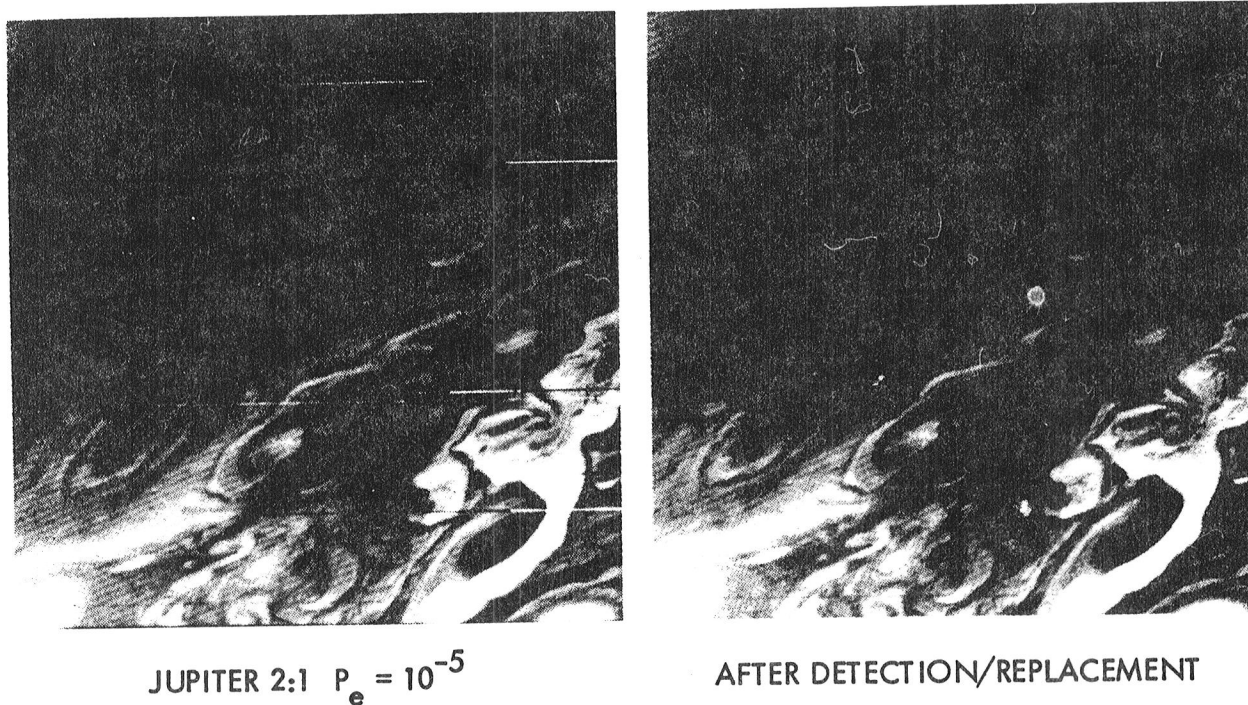


Fig. 8. Detection/Replacement

Application to 15m Multi-spectral Data. Band 4 of a selected aircraft derived 7-band multi-spectral image of Ventura County, CA., is shown in Fig. 9. The 2410 pixel by 956 line, 8 bits/pixel image shown provides 15 meter resolution and covers the spectral range of $0.52 \mu\text{m}$ to $12.5 \mu\text{m}$. Band 4 represents the range from $1.0 \mu\text{m}$ to $1.3 \mu\text{m}$. The four regions enclosed by white borders are 512×512 subsets selected for computer processing.

BARC2 runs at 3.24 bits/pixel (or 2.5:1) on bands 1-7, subset 2, produced an overall rmse of 1.79. This is a quite accurate representation for an image with an average band entropy of just over 5 bits/pixel and a standard deviation about the data mean of nearly 30. The pictorial representation of these results is given in Fig. 10. The image in the upper left is the original Band 4 of 512×512 Subset 2 in Fig. 9 whereas the upper right is the BARC2 result at 3.24 bits/pixel (2.5:1). It is impossible to see the difference. The 128×128 bordered region in both images is severely blown up directly below. These results should support the "archive quality" assumption made earlier.

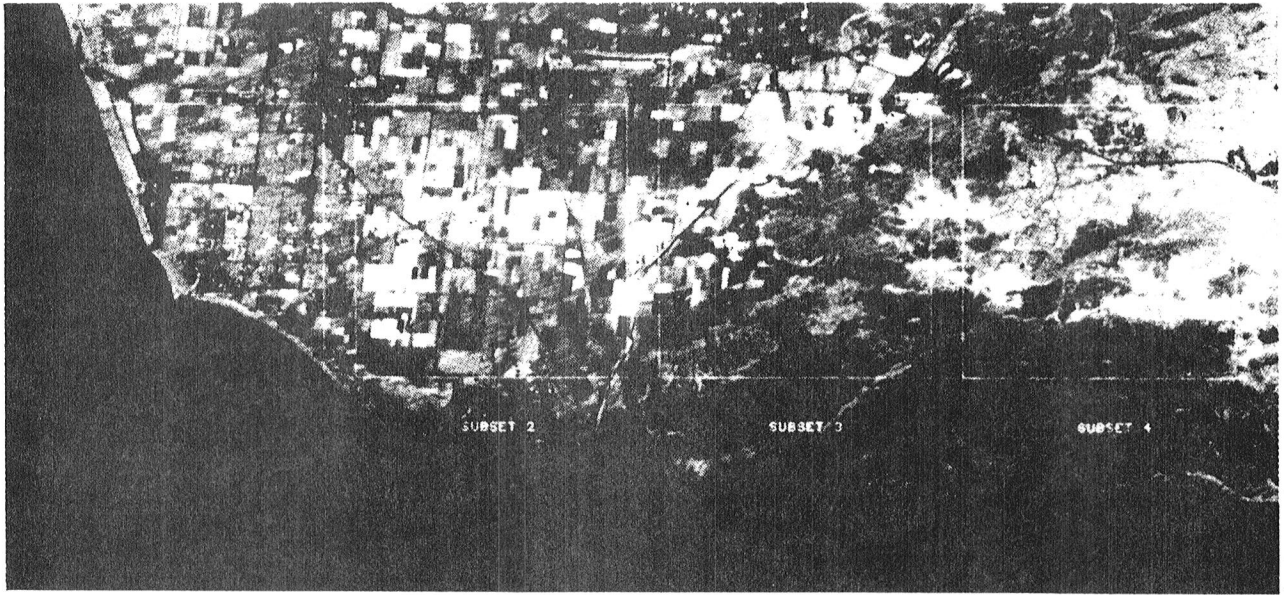


Fig. 9. Ventura County, Band 4

RM2 Application to 15m Ventura

The RM2 algorithm noted earlier was also run on the high resolution multi-spectral image of Ventura County, CA. The results are illustrated in the pictures of Fig. 11-13 and the rate vs. rmse graphs in Fig. 14. The images deal again with Band 4, Subset 2 whereas the rmse plots are composites over all 7 bands.

An original 8 bit/pixel (b/p), 512 x 512 rendition of Subset 2 (Fig. 9), band 4 is shown in Fig. 11 along with RM2 results at 2.0 b/p (4:1), 1.33 b/p (6:1) and 1.0 b/p (8:1). This is followed in Fig. 12 with the corresponding "diff-pics" which display the error between the original and compressed images shifted to an average value of 128. Selected blowups at 256 x 256 appear in Fig. 13.

Degradation is difficult to observe in the more realistic 512 x 512 displays for rates down to 1.33 b/p. Image quality is quite good but probably not of

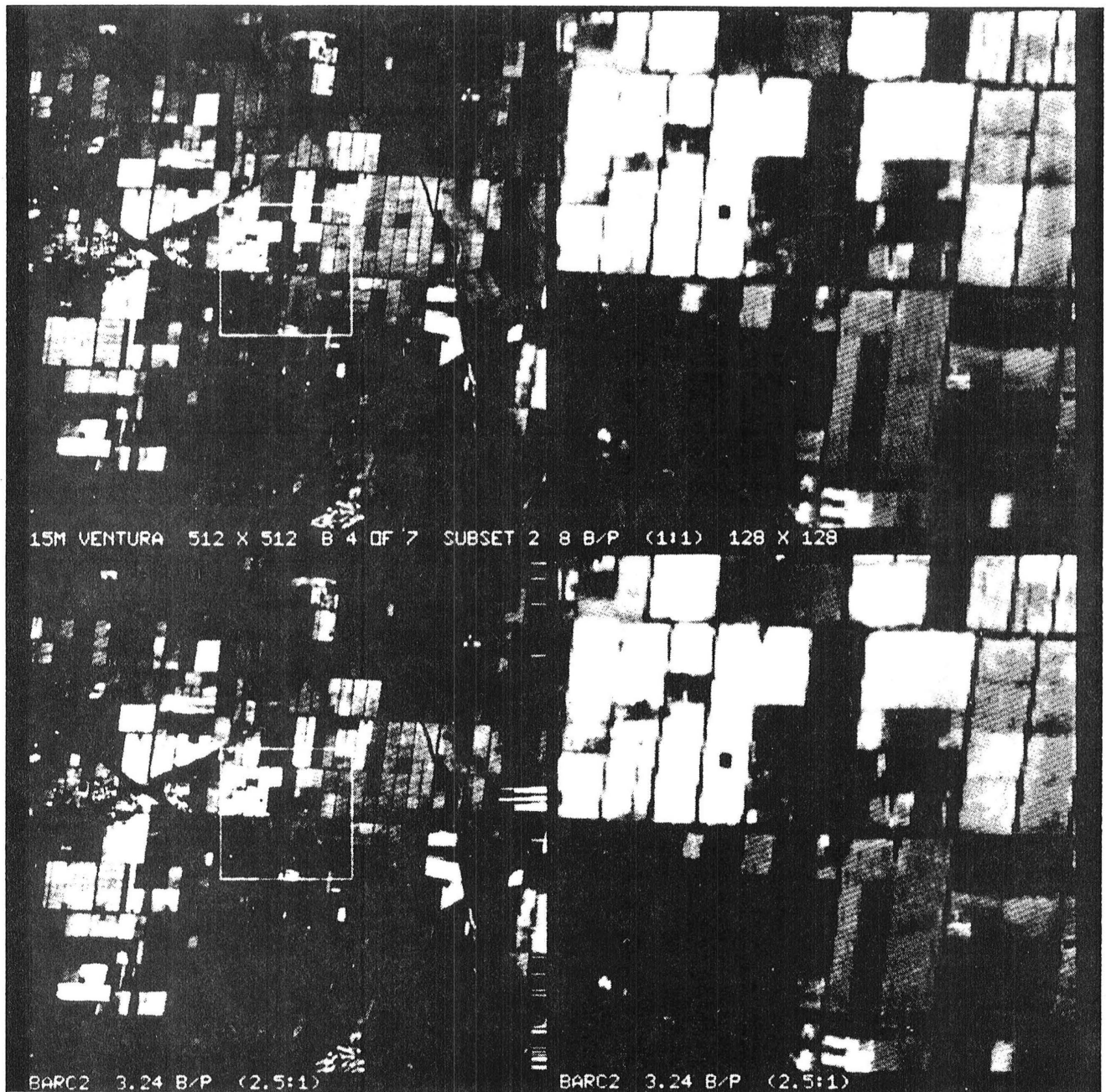


Fig. 10. BARC2 on Ventura, Band 4, Subset 2

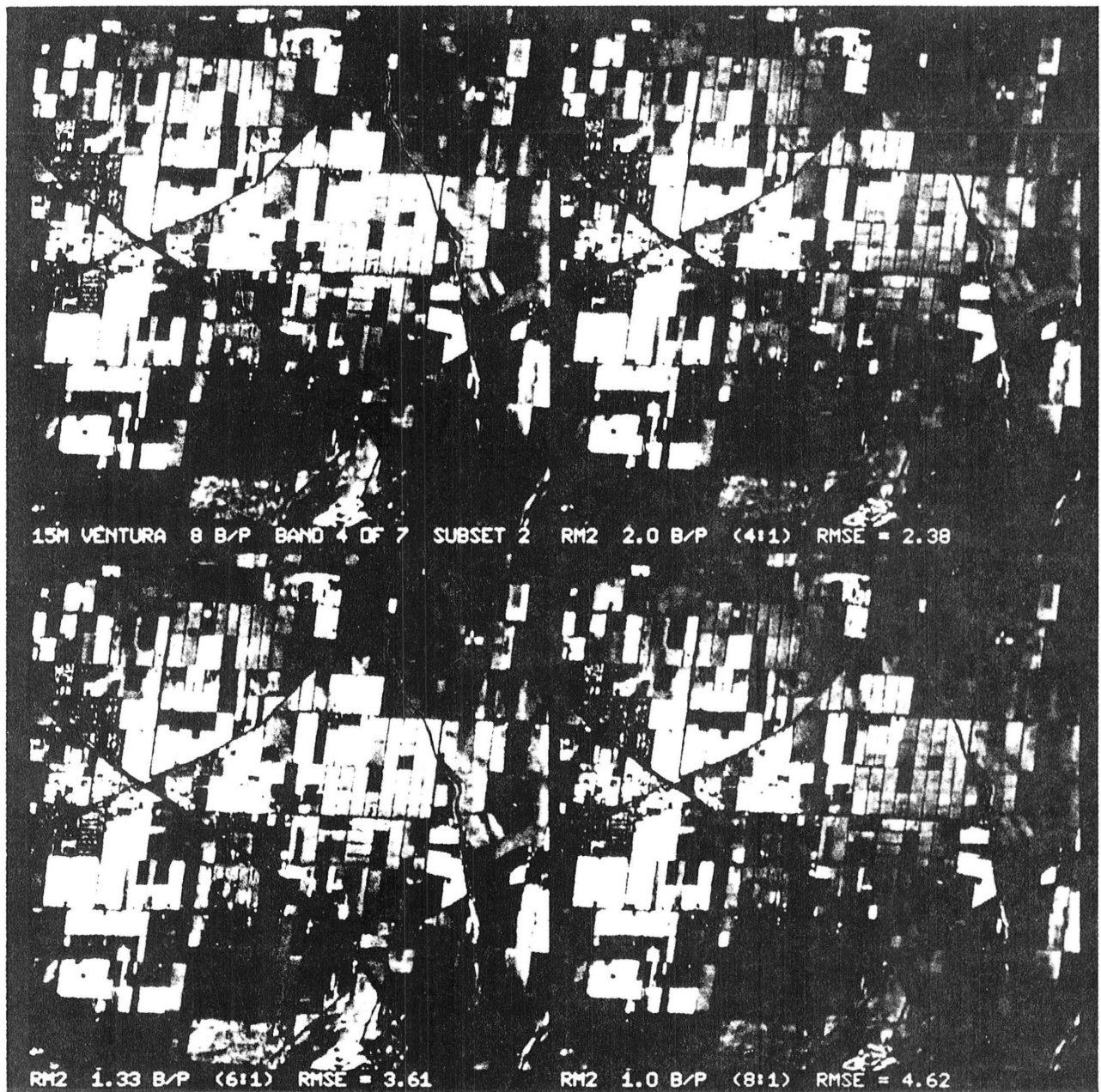


Fig. 11. RM2 on Subset 2, Band 4

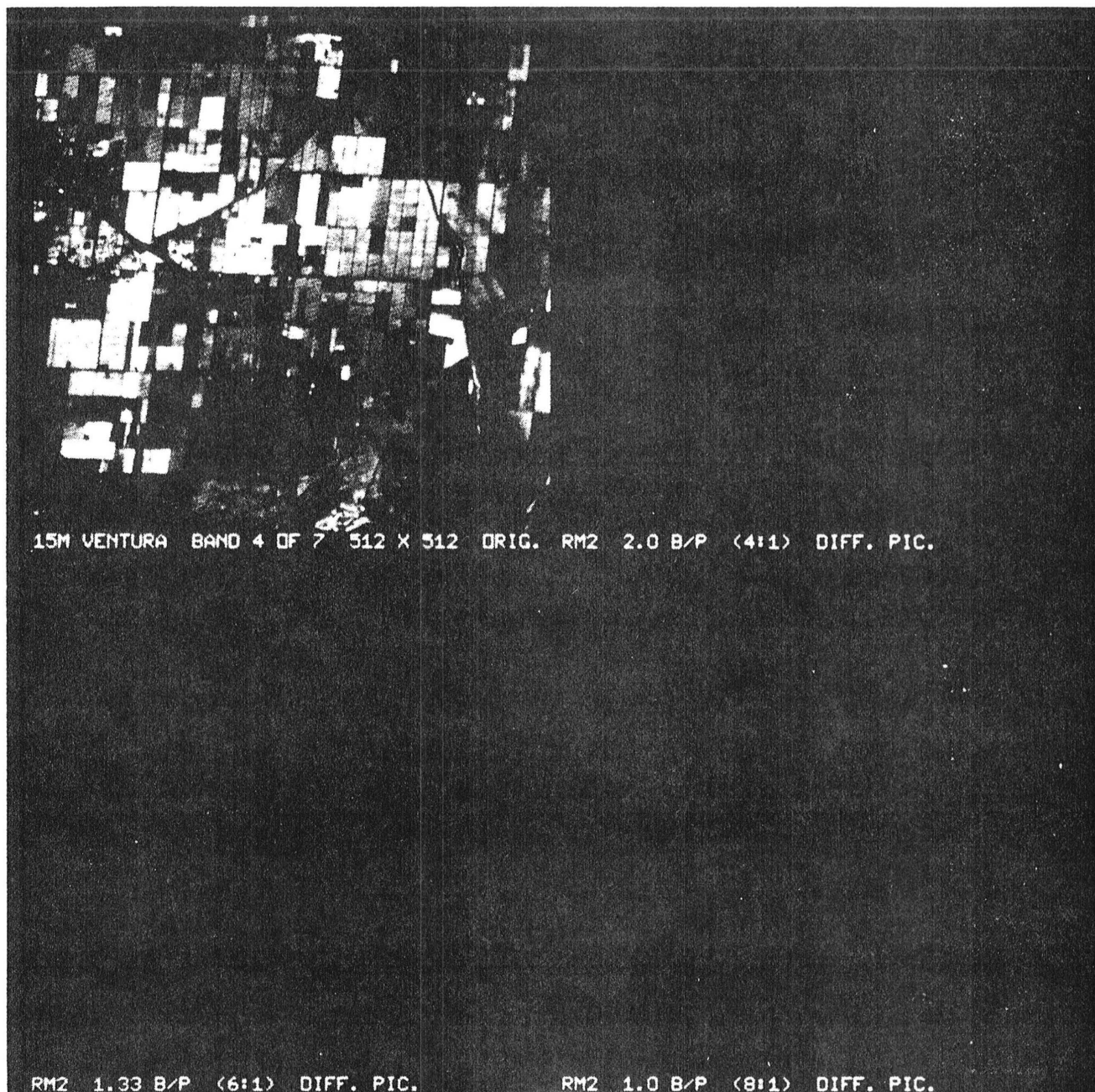


Fig. 12. RM2 Diff Pics on Subset 2, Band 4

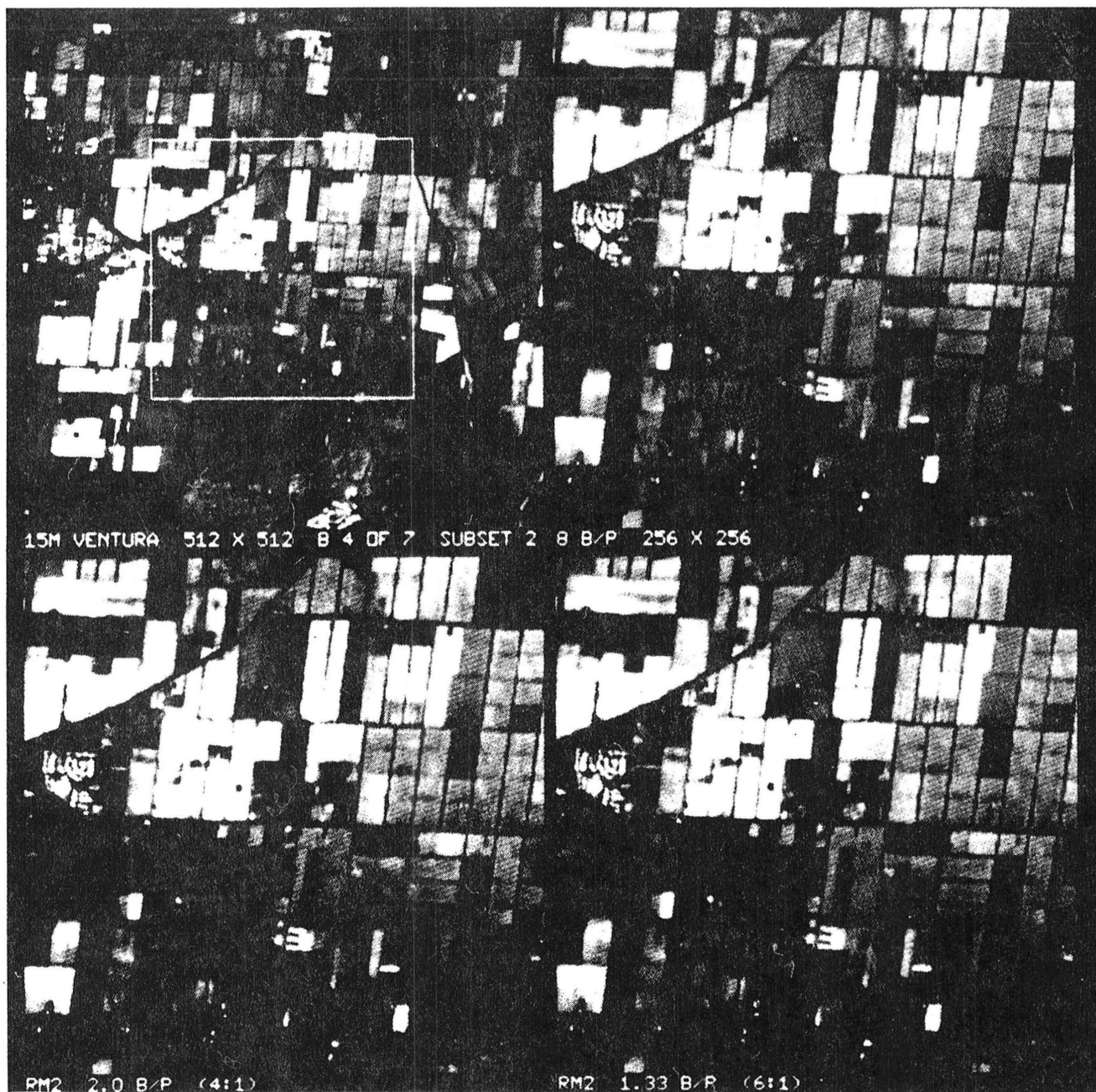


Fig. 13. RM2 256 x 256 Blowups

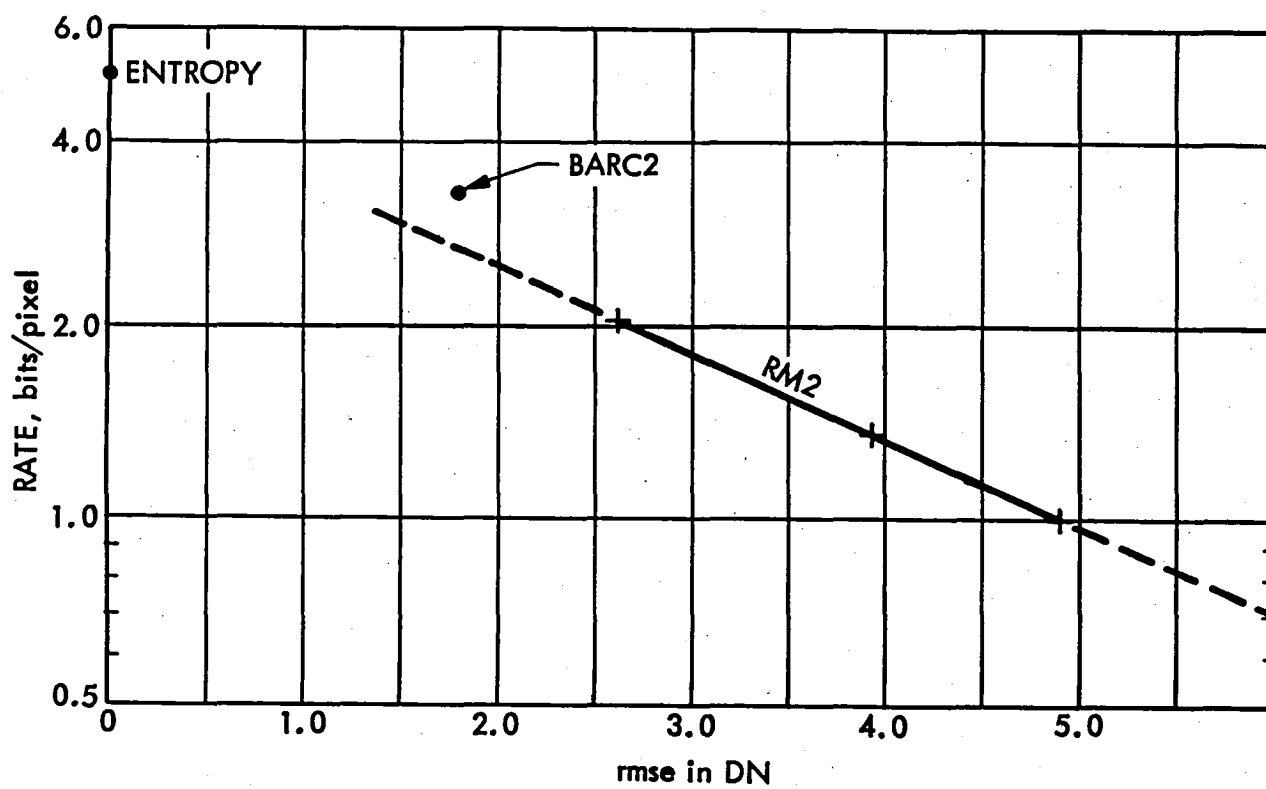


Fig. 14. RM2 rmse results, Subset 2

archive quality at 2.0 b/p. Note that rmse data points in Fig. 14 lie along a straight line which roughly extrapolates back to the data entropy, which for band 4 is 5.03 b/p (a completely random field would have an entropy of 8 b/p). This extrapolated graph will lie slightly below the data point for BARC2 at 3.24 b/p (and illustrated in the pictures of Fig. 10). The results are consistent with the introductory discussions.

It is important to note that the rate/quality tradeoff evidenced by these images and rmse graphs is a continuous one and is not limited to only the selected sample points presented here. A user could arbitrarily tradeoff spatial quality for spectral coverage in virtually any combination, and change his options at any time.

RM2 Global Rate Allocation. Additional gains are potentially possible if one looks further into the rate control structure of RM2. RM2 partitions a single band image into subpictures of size 32 x 32 or 64 x 64, and determines an activity measure for each. This results in an array of activity numbers as shown in Fig. 15 for an N subpicture image. The activity numbers reflect the relative need of each small area for bits. Given B total bits to use in an image an RM2 rate allocation procedure utilizes this information to designate B_i bits to be used to code the i^{th} subpicture (where $i = 1, 2, \dots, N$) so that[†]

$$\sum_{i=1}^N B_i = B \quad \text{where } B \text{ arbitrary} \quad (1)$$

Subpictures with larger activity measures tend to receive more bits than the less active subpictures. Such allocations could in principle be applied across spectral bands or even sequences of images.

Geographic Boost. This global rate allocation procedure thus focusses bits and hence quality towards regions based on a natural measure of activity. The next potential step in performance might be obtained by simply fooling the rate allocator. Suppose for example that a certain geographic area of say 256 x

[†]A subpicture to be completely edited (not sent) receives zero bits by this procedure.

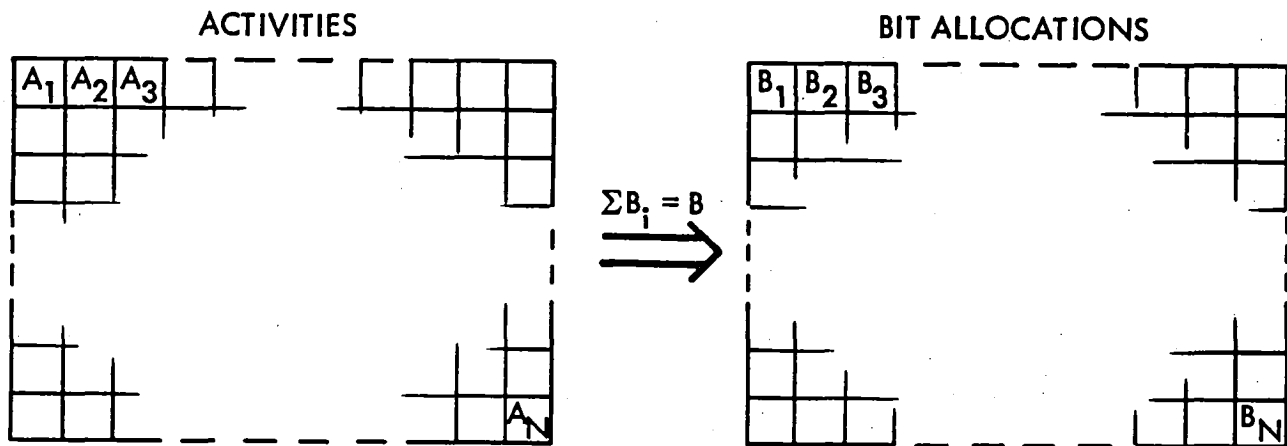


Fig. 15. Rate Allocation

256 size within a very large image (e.g., 2048 x 2048) was known to be of critical importance to a user. He desired 7 full bands at very high quality in this region but the link could support all 7 bands only at an average of 1 bit/pixel. If the position of this region could be (roughly) designated then the user's problems are easily solved. By artificially boosting the natural activity numbers, A_i , of the subpictures in the designated region, the rate allocator would unknowingly allocate a greater number of bits (and hence quality) to those subpictures at the expense of the remaining regions. Since the selected region is only $1/64^{\text{th}}$ of the total this would have little impact on remaining regions. In general, the amount of boost would reflect the relative importance and perhaps size of the selected region over other areas. This is illustrated in Fig. 16.

Auto Boost. More generally, artificial boosts to activities might be determined by independent pattern recognition devices which looked for special features of interest. When certain features were found to be present in a subpicture i the

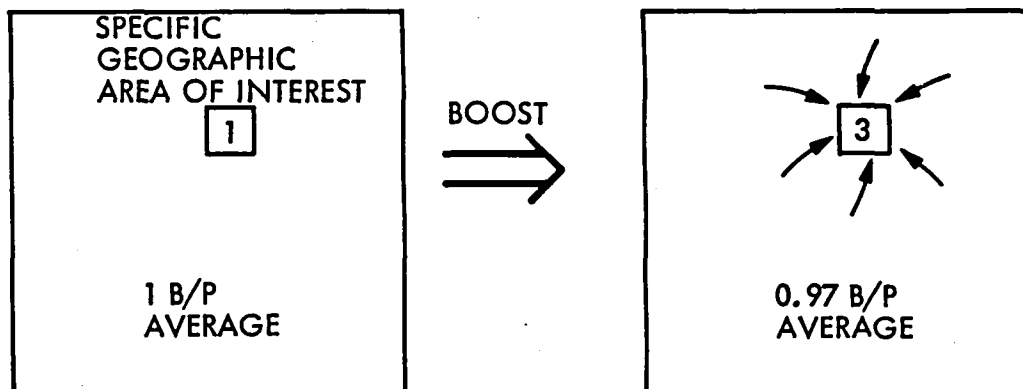


Fig. 16. Geographic Boost to Activity (\Rightarrow quality)

device(s) would call for a boost to the natural activity measure A_i leading to additional bits and hence quality into subpicture i .

These considerations are summarized in Fig. 17 where $\beta_i \geq 1$ is the user generated geographic boost associated with subpicture i (a user would not pinpoint subpictures but whole regions), and $\gamma_i \geq 1$ is the corresponding artificial boost determined by some pattern recognition device. Note that these two forms of added direction to a limited number of bits has no impact on RM2 itself and could be developed or considered as later supplements.

Principal Components. The following investigation is incomplete but offers the possibility of better performance at low rates. We now proceed RM2 with a spectral transformation which maps each multi-spectral pixel onto a new set of basis vectors which are the eigenvectors of the data covariance matrix. Such a transformation is called "principal components," or Karhunen-Loève (K&L) and other names as well. We will stick with the name principal components.

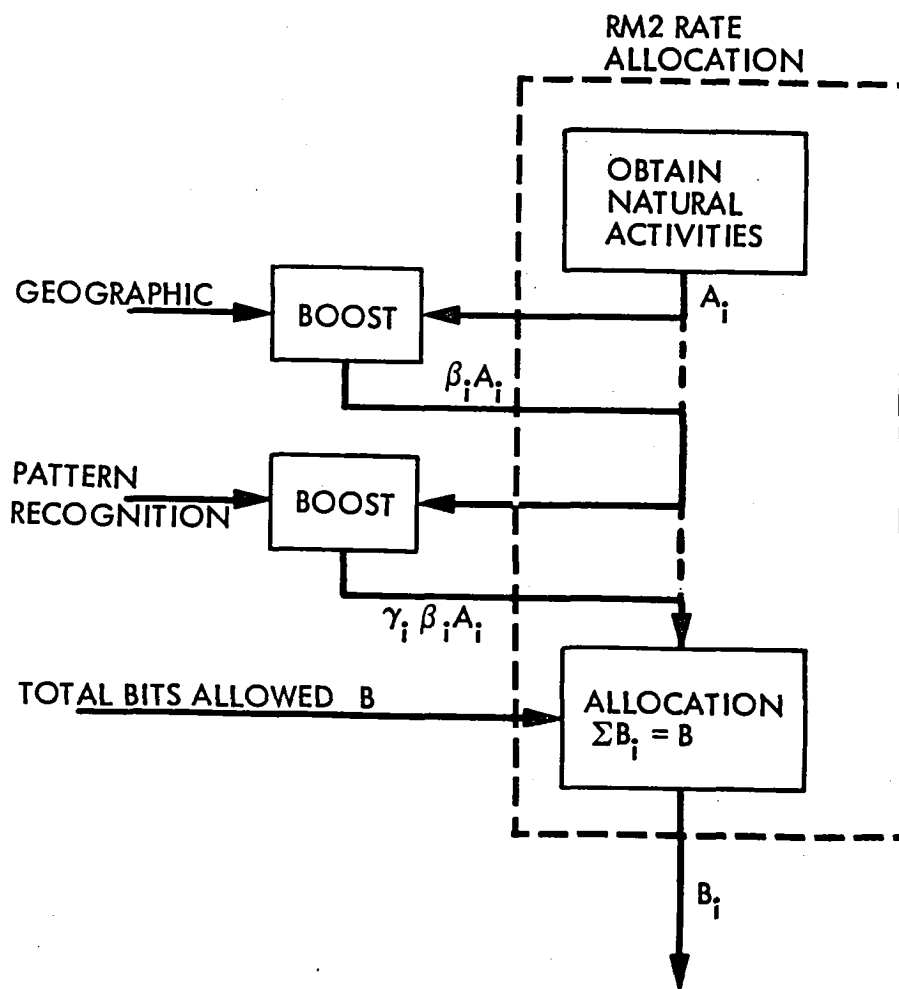


Fig. 17. Generalized Global Rate Allocation

Ideally the result of this transformation is a set of new spectral bands which are no longer correlated and for which most of the image energy has been concentrated in only a few of the new bands. The real hope for improved compression is that principal components makes use of band-to-band correlation which we have so far ignored. Ready and Wintz^[12] obtained some encouraging results using less sophisticated spatial compression than RM2. However, their test sets were significantly less active than the Ventura image, Fig. 9.

RM2 Conclusions. It would seem clear that the RM2 concept offers the potential for significant increases in real information transfer rates. This would come from sophisticated user and autonomous direction of the rate/quality trade-off provided by the RM2 rate control structure. How and if that flexibility fits within the spectrum of IS missions needs to be considered. A more thorough investigation of RM2 capabilities as well as implementation assessments should be completed.

REFERENCES

1. R. F. Rice, "Some Practical Universal Noiseless Coding Techniques," JPL Publication 79-22, Jet Propulsion Laboratory, Pasadena, CA., March 15, 1979.
2. R. F. Rice, "Practical Universal Noiseless Coding," SPIE Symposium Proceedings, Vol. 207, San Diego, CA., Aug. 1979.
3. R. F. Rice, A. P. Schlutsmeier, "Software for Universal Noiseless Coding," Proceedings of 1981 International Conference on Communications, Denver, Colorado, June 1981.
4. R. F. Rice, A. P. Schlutsmeier, "Data Compression for NOAA Weather Satellite Systems," Vol. 249, Proceedings 1980 SPIE Symposium, San Diego, CA., July 1980.
5. R. F. Rice, "An Advanced Imaging Communication System for Planetary Exploration," Vol. 66, SPIE Seminar Proceedings, Aug. 21-22, 1975, pp. 70-89.
6. R. F. Rice, "A Concept for Dynamic Control of RPV Information System Parameters," Proceedings 1978 Military Electronics Exposition, Anaheim, CA., Nov. 1978.
7. R. F. Rice et. al., "Block Adaptive Rate Controlled Image Data Compression," Proceedings of 1979 National Telecommunications Conf., Washington, D.C., Nov. 1979.
8. E. E. Hilbert, "Joint Pattern Recognition/Data Compression Concept for ERTS Multi-Spectral Imaging," Proceedings SPIE Seminar, Vol. 66, pp. 122-137, Aug. 1975.
9. R. F. Rice, "Channel Coding and Data Compression System Considerations for Efficient Communication of Planetary Imaging Data," Chapter 4, Technical Memorandum 33-695. Jet Propulsion Laboratory, Pasadena, CA., June 15, 1974.
10. R. F. Rice, "Potential End-to-End Imaging Information Rate Advantages of Various Alternative Communication Systems," JPL Publication 78-52. Jet Propulsion Laboratory, June 15, 1978.

11. K. Y. Liu, J. J. Lee, "An Experimental Study of the Concatenated Reed-Solomon/Viterbi Channel Coding System Performance and its Impact on Space Communications," JPL Publication 81-58. Jet Propulsion Laboratory, Aug. 15, 1981.
12. P. Ready, P. Wintz, "Information Extraction, SNR Improvement and Data Compression in Multispectral Imagery," IEEE Trans. Commun., Vol. COM-21, No. 10, Oct. 1973.

On-Board Image Compression

Thomas J. Lynch, NASA GSFC

On-board image compression has seen limited use on NASA spacecraft. An example of successful on-board compression was the system designed at the Goddard Space Flight Center and flown on the Radio Astronomy Explorer in lunar orbit (RAE-2) in 1973. In this case, the image compressed was that of the long flexible radio-astronomy boom antennae that also provided gravity-gradient stabilization. The requirement for compression in this case came about because of the mismatch between the output data rate of the on-board camera system and the down-link communication channel. As data rates from future imaging sensors increase, the need for on-board compression will become a more common requirement.

An obvious first approach to on-board image compression is to find a compression algorithm that will provide the highest possible compression ratio. But the compression ratio cannot be increased beyond a certain point without introducing some distortion in the reconstructed, or decompressed, image. For a given image, this point is defined as the entropy, which is really the average information expressed in bits-per pixel. From the statistics of the image, one can compute the entropy and from it obtain a prediction of the maximum compression ratio (for example, if the entropy is 4 bits/pixel and the uncompressed system would normally use 8 bits/pixel then the maximum compression ratio is 2:1). The utility of computing the entropy is that it tells one when to stop increasing the compression ratio if only little or no distortion is a system requirement. Because of the fact that the entropy represents a critical point, the maximum compression ratio, data compression schemes have been classified

into two basic types: redundancy reduction (RR) and entropy reduction (ER). The former produce compression ratios below the theoretical maximum, and the latter, above it. In actual practice, there are also compression schemes which are combinations of RR and ER.

In selecting, designing and implementing an on-board compression scheme, a number of considerations and tradeoffs have to be investigated. As indicated above, the compression ratio must be traded off against the allowable residual distortion in the reconstructed image. The type and magnitude of this allowable distortion depends directly on the particular application of the imagery that is planned. An included question is the effect of this distortion on radiometric and geometric correction. The compression ratio also has to be traded off against the complexity of the on-board design. This includes such considerations as adaptive vs non-adaptive compression, the number of arithmetic operations per pixel, buffer storage and the need for error-control coding to protect the compressed data from communication channel errors.

ON-BOARD IMAGE COMPRESSION

THOMAS J. LYNCH

INFORMATION EXTRACTION DIVISION

NASA GODDARD SPACE FLIGHT CENTER

TOPICS

- o BRIEF HISTORY OF ON-BOARD IMAGE COMPRESSION
- o THE THEORETICAL MAXIMUM COMPRESSION RATIO
- o CLASSES OF DATA COMPRESSION
- o TRADEOFF ISSUES

WHAT IS DATA COMPRESSION?

DATA COMPRESSION IS THE REDUCTION OF:

- DATA VOLUME (SUCH AS IN A STORAGE MEDIUM)
- DATA TRANSMISSION TIME (SEC.)
- DATA TRANSMISSION RATE (BITS/SEC.)

WHERE VOLUME = \int (TIME X RATE)

DATA COMPRESSION IS ALSO CALLED:

- DATA COMPACTION
- SOURCE CODING

EXAMPLES:

- FACSIMILE - TIME REDUCTION
- VOICE - RATE (BANDWIDTH) REDUCTION

CLASSES OF DATA COMPRESSION

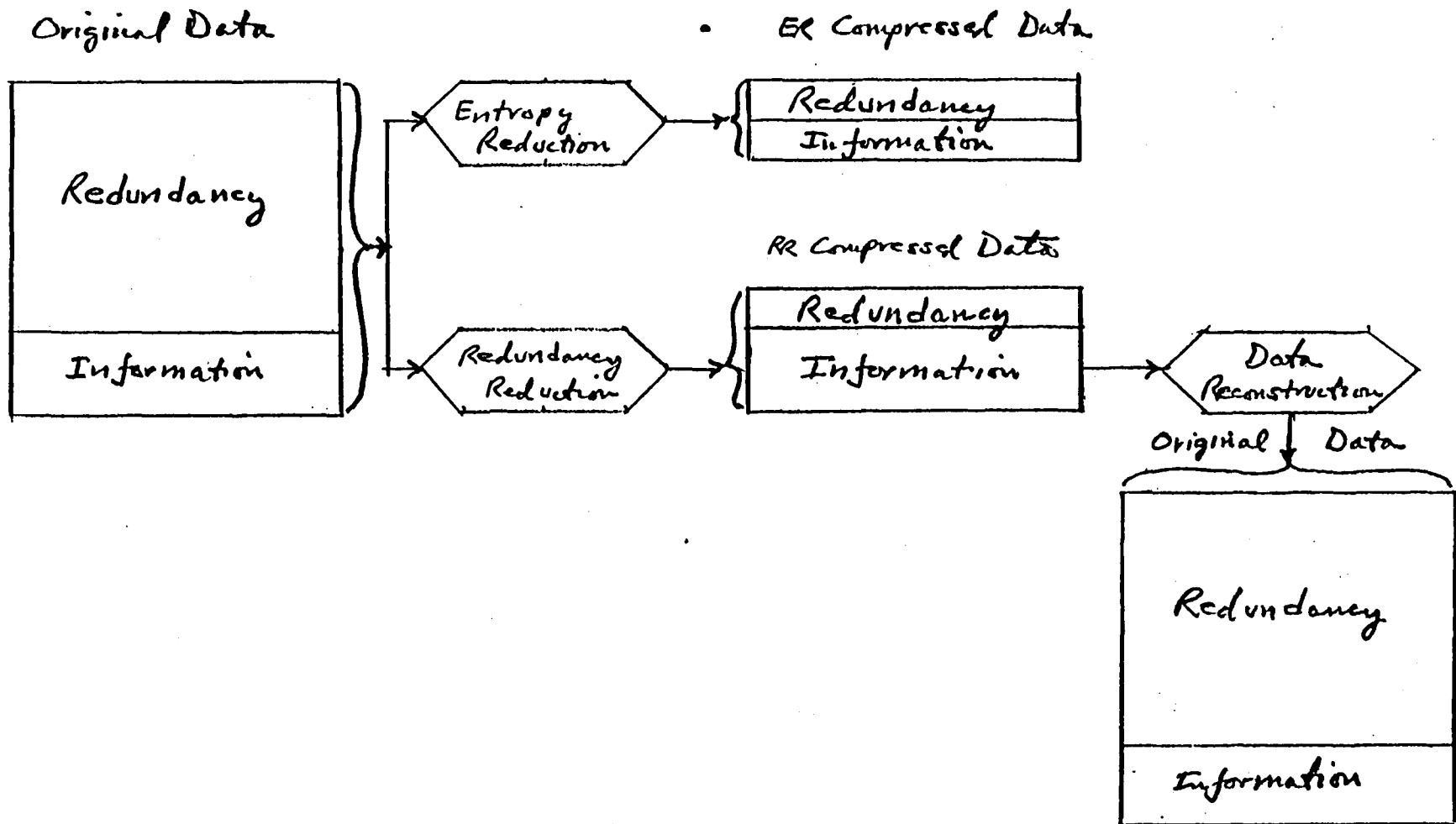
THERE ARE TWO CLASSES OF DATA COMPRESSION:

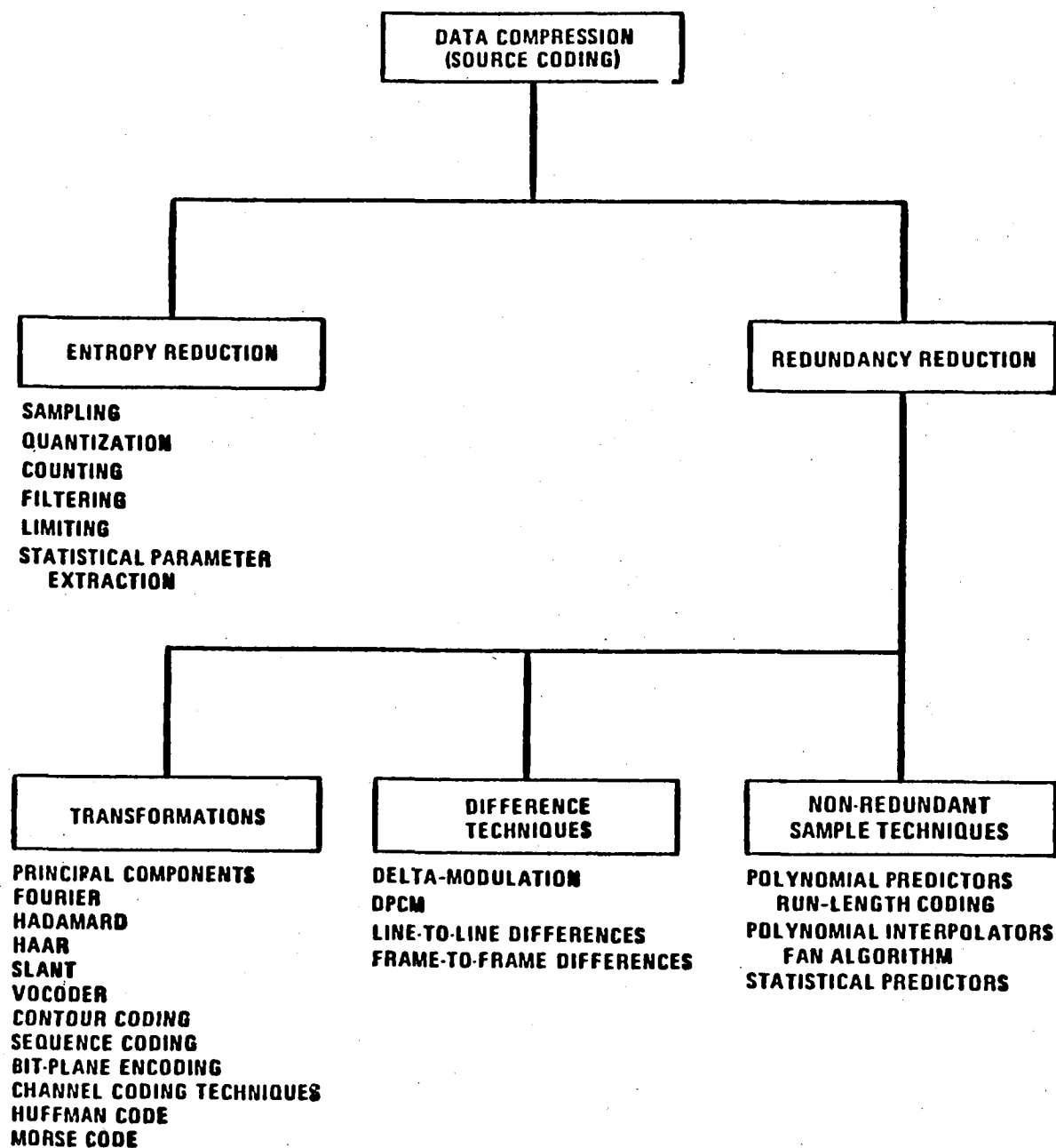
- ENTROPY REDUCTION
- REDUNDANCY REDUCTION

ENTROPY REDUCTION REDUCES THE AVERAGE INFORMATION IN THE DATA. THE INFORMATION THAT IS LOST CANNOT BE RECOVERED, SO THAT ENTROPY REDUCTION IS IRREVERSIBLE.

REDUNDANCY REDUCTION REDUCES OR REMOVES THE REDUNDANCY IN THE DATA IN SUCH A WAY THAT IT CAN BE PUT BACK AT A LATER TIME. IN THIS WAY, REDUNDANCY REDUCTION IS REVERSIBLE.

TWO TYPES OF DATA COMPRESSION





Classes of Data Compression

THE RADIO ASTRONOMY EXPLORER -2 ON-BOARD COMPRESSION

- o ON RAE-2 IN LUNAR ORBIT - 1973
- o COMPRESSED PANORAMIC CAMERA IMAGE OF ANTENNA BOOMS AND MOON*
- o REQUIRED COMPRESSION RATIO: 32:1
(CAMERA OUTPUT: 20,000 BPS; DOWN LINK: 625 BPS)
- o USED A COMBINATION OF:
ENTROPY REDUCTION: SKIP 3 OUT OF 4 SCAN LINES (4:1)
REDUNDANCY REDUCTION: ADAPTIVE RUN-LENGTH CODING OF SAVED LINE (8:1)
- o CONVOLUTIONALLY ENCODED FOR CHANNEL ERROR PROTECTION
- o VOLUME: 1000 cm^3 ; POWER: 0.4W; CMOS TECHNOLOGY

*"ON-BOARD IMAGE COMPRESSION FOR THE RAE LUNAR MISSION," W. H. MILLER,
T. J. LYNCH, IEEE TRANS. ON AEROSPACE AND ELECTRONIC SYS., VOL. AES-12,
NO. 3, MAY 1976, PP 327-335

ENTROPY

INFORMATION IS DEFINED IN TERMS OF THE LOGARITHM OF THE PROBABILITY OF A GIVEN OUTPUT FROM A DATA SOURCE.

FOR A MEMORYLESS SOURCE (ALL OUTPUTS ARE INDEPENDENT):

$$I_i = -\log_2 P_i$$

WHERE I_i IS THE INFORMATION OF THE i^{TH} OUTPUT, P_i IS THE PROBABILITY OF THE i^{TH} OUTPUT

ENTROPY IS THE AVERAGE INFORMATION

FOR A MEMORYLESS SOURCE:

$$H_I = -\sum_{i=1}^M P_i \log_2 P_i$$

WHERE H_I IS THE ENTROPY OF THE SOURCE, M IS THE NUMBER OF POSSIBLE OUTPUTS

FOR A SOURCE WITH MEMORY, ASSUMING A FIRST ORDER MARKOV MODEL:

$$H_{(Y/X)} = - \sum_{i=1}^M \sum_{j=1}^M P(i,j) \log_2 P(j/i)$$

WHERE $P(i,j) = P(i) P(j/i)$

MAXIMUM COMPRESSION RATIO

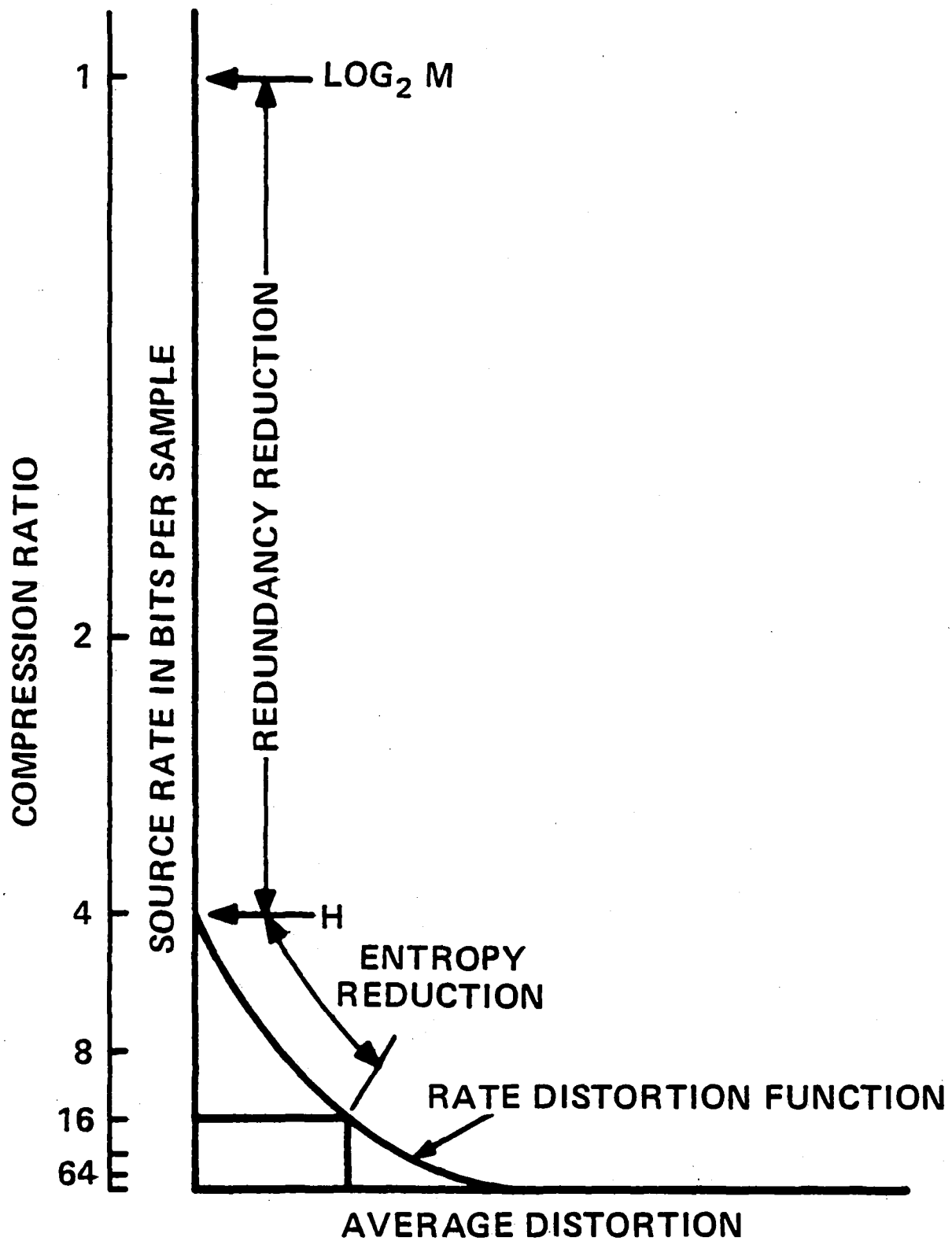
$$\text{ACTUAL BIT COMPRESSION RATIO} = \frac{\text{NUMBER OF UNCOMPRESSED BITS IN A BLOCK}}{\text{NUMBER OF COMPRESSED BITS IN SAME BLOCK}}$$

$$\text{MAXIMUM COMPRESSION RATIO} = \frac{\text{NUMBER OF UNCOMPRESSED BITS/SAMPLE}}{\text{MINIMUM NUMBER OF BITS/SAMPLE}}$$

$$\text{Max CR} = \frac{\log_2 M}{H}$$

WHERE M IS THE NUMBER OF LEVELS

H IS THE ENTROPY



RECENT MEASUREMENTS OF ENTROPY

ENTROPY MEASUREMENTS MADE FOR 2 IMAGES ORIGINALLY
AT 3 METER RESOLUTION*

NATURAL (GEOLOGICAL) IMAGE
CULTURAL (URBAN) IMAGE

		3M	9M	30M
GEOLOGIC	H_I	5.078	5.059	4.888
	H_M	2.506	3.051	2.853
URBAN	H_I	5.336	5.312	5.128
	H_M	2.725	3.283	2.834

*ENTROPY MEASUREMENTS AND MAXIMUM COMPRESSION RATIO WITH NO DISTORTION,
W. H. MILLER, T. J. LYNCH, C. R. KILGORE, GSFC MAY 1982

TRADE-OFF ISSUES

- o COMPRESSION RATIO vs DISTORTION
- o COMPRESSION RATIO vs COMPLEXITY
- o COMPRESSION SCHEME vs TECHNOLOGY SPEED LIMITATION

COMPRESSION vs DISTORTION

- o EFFECT ON SPATIAL RESOLUTION
E.G. EDGE BLUR
- o EFFECT ON RADIOMETRIC RESOLUTION/ACCURACY
E.G. AMPLITUDE OFFSET DUE TO:
UNCORRECTED CHANNEL ERRORS
- o POSSIBLE ARTIFACTS IN RECONSTRUCTED IMAGE DUE
TO ATMOSPHERIC EFFECTS

COMPRESSION vs COMPLEXITY

- o ADAPTIVE vs NON-ADAPTIVE
- o NUMBER OF OPERATIONS PER PIXEL
- o BUFFER STORAGE
- o ERROR CONTROL

Modular Data Transport System (MDTS)

COMPARISON GaAs/Si MULTIPLIER (8 x 8)

	Si(TTL)	Si(ECL)	GaAs
MULTIPLY TIME (TWO 8 BIT NO.)	45ns	19ns	6ns
POWER	0.9w	4.4w	0.3w
MANUFACTURER	MMI	MOTOROLA	ROCKWELL



USGS REMOTE IMAGE PROCESSING SYSTEM (RIPS)

- o RIPS PROCESSORS BASED ON CROMEMCO Z80 MICROCOMPUTERS WILL PROVIDE IMAGE ANALYSIS CAPABILITIES AT USGS CENTERS
- o RIPS PROCESSORS COMMUNICATE WITH ONE ANOTHER AND THE HP3000 BASED IDIMS SYSTEM AT EROS DATA CENTER VIA A PROTOCOL THAT HAS PROVISIONS FOR DATA COMPRESSION AND ERROR CORRECTION
- o EROS DATA CENTER WILL PROVIDE PORTIONS OF LANDSAT SCENES (256x240x4 BANDS) ON 8" FLOPPY DISKS

- o DISPLAY RESOLUTION

96x140x6 - 512x512x16,000,000

- o MICROPROCESSORS

6502 1Mz - 68000 8Mz

- o MEMORY SIZE

64K - 2000 K

- o SOFTWARE

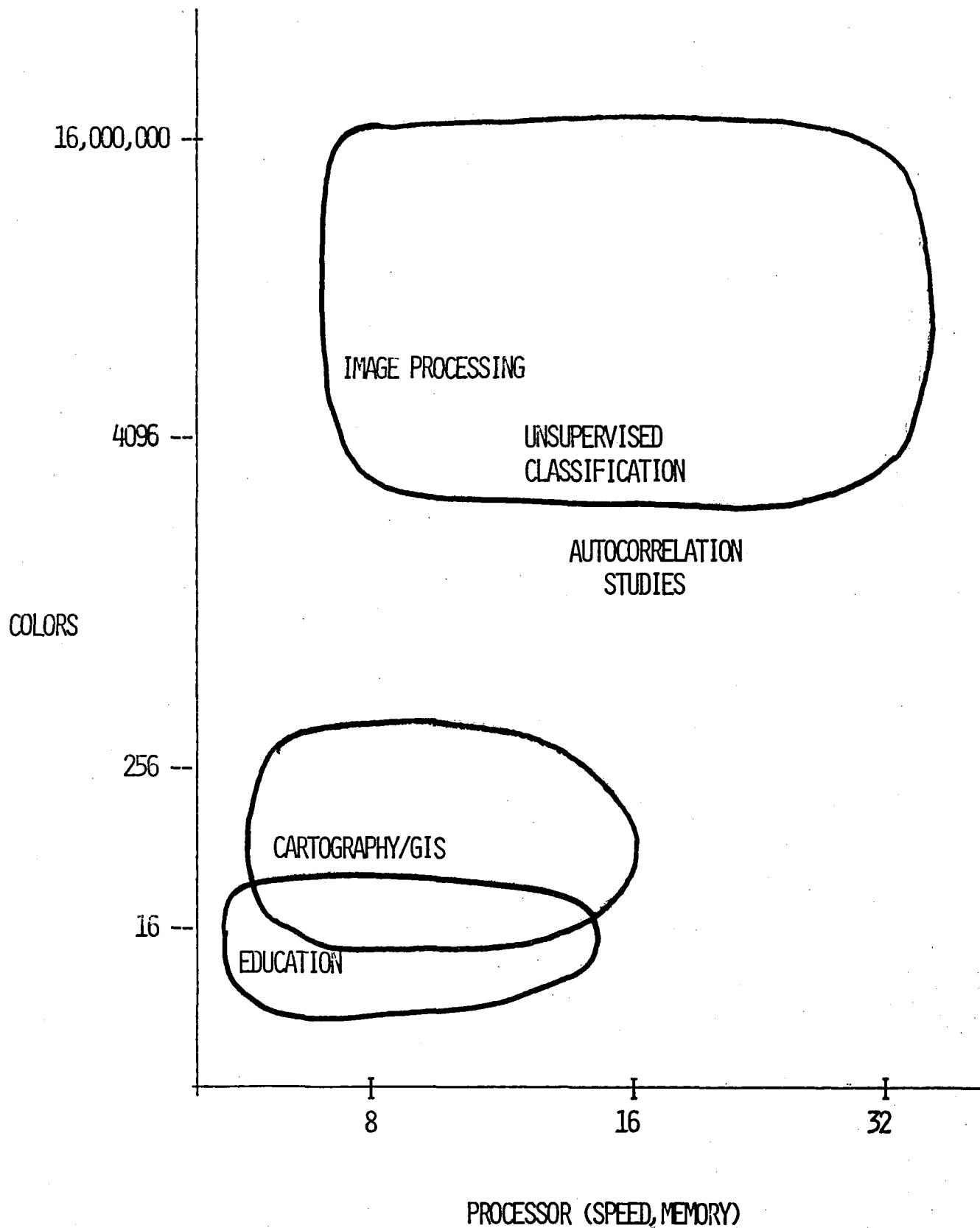
IMAGE ANALYSIS- GEOGRAPHIC INFORMATION SYSTEMS
ASSEMBLY LANGUAGE - FORTRAN

- o PERIPHERALS

9 TRACK TAPE DRIVE
HARD DISK 5-300 MBYTES
FLOPPY DISK 80-1M BYTE

- o COST

\$4000-\$45,000



<u>SYSTEM</u>	<u>APPLEIPS</u>	<u>AIPE</u>	<u>MIPS</u>	<u>IMPAC</u>
DISPLAY RESOLUTION	96x140 PIXELX x 6 COLORS	40x40x16	80x160x16	128x120x16
IMAGE SIZE	192x280 PIXELS x 4 BANDS	40x40x4	80x160x4	128x128x16
COMPUTER	APPLE II	APPLE II	ATARI 800	VECTOR MZ
MEMORY	64 K	64 K	64 K	64 K
DISK STORAGE	124 K	124 K	80 K	630 K
LANGUAGE	BASIC, ASSEMBLY	BASIC	BASIC, ASSEMBLY	FORTRAN
SOURCE CODE	BASIC ONLY	BASIC	BASIC, ASSEMBLY	NOT AVAILABLE
COST (HARDWARE, SOFTWARE)	\$3,650	\$3,150	\$2,600 .	\$13,000
CONTACT	TELESYS GROUP	FRED GUNTHER	E.J. MASUOKA	EGBERT SCIENTIFIC SOFTWARE

	<u>APPLEIPS</u>	<u>MIPS</u>	<u>IMPAC</u>
DENSITY SLICE	1	1	1
IMAGE ALGEBRA	1	1	1
HISTOGRAM	1	1	
FILTERING	2		
HARDCOPY GRAPHICS	2	1	1
COMMUNICATIONS ROUTINES	1	1	2
CLASSIFIERS:			
PARALLELPIPED	1	1	1
MINIMUM DISTANCE	2		
MAXIMUM LIKELIHOOD	2		2
UNSUPERVISED CLUTTERING	2		2
PRINICPAL COMPONENTS			2

1 = STANDARD SYSTEM

2 = OPTIONAL AND/OR UNDER-DEVELOPMENT

<u>SYSTEM</u>	<u>ERIM</u>	<u>RIPS</u>	<u>ERDAS</u>
DISPLAY RESOLUTION	240x256 PIXELS 256 COLORS	256x242x4096	256x240x32,000 w/1 GRAPHICS PLANE 512x480x16
IMAGE SIZE	LIMITED BY DISK STORAGE	256x240x4 BANDS	LIMITED BY DISK STORAGE
COMPUTER	CROMEMCO Z80	CROMEMCO Z80	CROMEMCO Z80
MEMORY	64 K	64 K	64 K
FLOPPY DISK STORAGE	780 K	780 K	780 K
HARD DISK STORAGE	10 M	--	16 M, 80 M
9 TRACK TAPE DRIVE	YES	--	YES
FLOATING POINT	--	--	YES
PROCESSOR			
LANGUAGES	FORTRAN, ASSEMBLY	FORTRAN, ASSEMBLY	FORTRAN, ASSEMBLY
SOURCE CODE	NOT AVAILABLE	YES	APPLICATIONS PROGRAM ONLY
COST	\$25,000	\$21,000	\$45,000-\$65,000
CONTACT	ERIM	EROS DATA CENTER	ERDAS

	<u>RIPS</u>	<u>ERIM</u>	<u>ERDAS</u>
FALSE COLOR DISPLAY	X	X	X
COLOR SLICED DISPLAY	X	X	X
GRAY LEVEL MAPS	X	X	X
HISTOGRAMS	X	X	X
RATIOS	X	X	X
CONTRAST ENHANCEMENT	X	X	X
FILTERING	X		X
SMOOTHING	X		X
IMAGE RECTIFICATION			X
CLASSIFICATION:			
MAXIMUM LIKELIHOOD		X	X
MINIMUM DISTANCE			X
SUITS WAGNER ALGORITHM	X		
UNSUPERVISED CLUSTERING			X
G.I.S. FUNCTIONS	NONE	UNDER DEVELOPMENT	IMGRID

<u>SYSTEM</u>	<u>GAS</u>	<u>MIDAS</u>
DISPLAY RESOLUTION	256x242x4096	512x512x16,000,000
MICROPROCESSORS	8086/8087,Z80	68000/8087
MEMORY	2.5 MBYTES	2 MBYTES
FLOPPY DISK	1 M	
HARD DISK	160 M	160 M
TAPE DRIVE	9 TRACK 25 IPS	
LANGUAGE	FORTRAN	FORTRAN
USERS	3	1
COST	\$31,000	\$36,600
CONTACT	E.J. MASUOKA/GSFC	WALT DONOVAN, INFORMATICS, INC. LARRY HOFFMAN, NASA/AMES

IMAGE PROCESSING VIA VLSI

A Concept Paper

Robert Nathan, Ph.D.

19 January 1981

Image Processing via VLSI

Abstract

The general purpose digital computer is not able to handle the data rates and subsequent throughput requirements of data systems in the mid-80's and early 90's. In particular vast quantities of image data will have to be calibrated, geometrically projected, mosaicked and otherwise manipulated and merged at rates that far exceed the capacities of present systems. Even the "super" computers, some of which have been designed explicitly for image processing, promise insufficient throughput capacity. Implementing specific image processing algorithms via Very Large Scale Integrated systems offers a potent solution to this perplexing problem. Two algorithms stand out as being particularly critical -- geometric map transformation and filtering or correlation. These two functions form the basis for data calibration, registration and mosaicking. VLSI presents itself as an inexpensive ancillary function to be added to almost any general purpose computer and if the geometry and filter algorithms are implemented in VLSI, the processing rate bottleneck would be significantly relieved. This work develops the set of image processing functions that limit present systems to deal with future throughput needs, translates these functions to algorithms, implements via VLSI technology and interfaces the hardware to a general purpose digital computer.

Objectives

- * Design and fabricate special purpose VLSI chips to perform specific image processing algorithms.
- * Integrate such chips into interface systems which are under the control of a central general purpose processor assigned to image processing.

- * In particular, design and test filter system and a cubic spline geometric reprojection system.
- * Examine and develop VLSI design concepts for other image processing requirements.

Motivation

Bracken (1) has spelled out the need for improving the processing speed of image data collected from an ever increasing array of satellites each with a larger information bandwidth than its predecessor. The processing problem has several dimensions.

- * In order to enable the end user to use new information, the data must be restructured to match a previous information base. A common requirement is to reproject and register images taken from an oblique satellite view to a normal projection on the surface. This reprojection along with the need to correct for any systematic camera distortions requires that images be stretched like a "rubber sheet" to fit the desired reprojection. This shift which entails many rotations and magnifications within each image requires relocation of interpolated data to locations which may be far distant from some original position.
- * In order to determine the precise shift which will bring two images into registration, match points must be determined. Modified cross correlation calculations can be used to maximize the best fit of these match points. Correlation and filtering have similar mathematical structure and both can be implemented with a special purpose VLSI system. The filtering operation is also used to smooth noisy data or enhance fine image detail. Image enhancement has been applied rather infrequently in spite of image improvement because

it is an expensive process. VLSI operation can reduce the cost and time of processing. Filtering also enables certain feature detection and extraction algorithms.

- * Another dimension of image processing relates to where in the data stream the processing is to be performed. Our present technology thus far requires transmission of unprocessed images. As high speed compact processing technology evolves, processing can be moved on to the satellite and transmission bandwidth reduced by several orders of magnitude.
- * Pipeline processing implies placing simultaneous hardwired algorithms in tandem. Other image processing functions such as sorting maximum values, change detection, developing time dimensions on accumulated data bases become accessible in near real time when thinking in terms of modular hardware.

Background

Digital image processing became a working reality in the early 1960's with the advent of JPL's Ranger, Surveyor and Mariner series. We (Nathan-2) had effectively established the requirements for various processing algorithms from pragmatic pressures. Filtering was performed to remove systematic noises from the camera and geometric corrections also were required to correct camera distortion. Filtering further evolved to enhance fine image detail without stretching low frequency data to cause image saturation. In those early missions it was generally possible to keep up with the data load with the processing power of computers available at the time. No real attempt was made to do more than refine those algorithms using commercially available machines. Since that time the situation has dramatically changed in terms of volume while the algorithms have remained relatively static.

Several attempts at creating special parallel processors have proven expensive and unwieldy. A comparison of several "super" computers was performed by Mitre Corporation (3). They were given several classes of very limited tests against which to measure processing effectiveness. Some of the computers compared were the Cray I, the DAP (English), the PEPE (Army), the Illiac IV, the Cyber 203, the AP-120B, the CLIP 3 and the MPP (Goddard-Goodyear). All but the AP-120B are extremely expensive (several millions of dollars each) whereas the AP-120B is very much slower. Mitre judged the MPP to be the best as determined from the given conditions. But the filter and geometric test problem was much too constrained and just fit the 128x128 area of parallel memory in MPP. Only a kernel of 20x20 can be filtered against a 128x128 image. Only a shift of 8 pixels using linear interpolation is allowed for geometric remapping. These restrictions have been hardwired and only slow software can overcome them. The heart of the MPP is a general purpose VLSI processing unit. The direction of the concept is still in terms of multiple function performance by a particular hardware unit.

VLSI is a general tool which can be viewed as an extension of software in the sense of the next generation of computing power. These concepts have been under development at Caltech under Mead (4). JPL has a very close relationship with the campus. We have recently been working with Mead to aid in the rapid evolution of the software techniques for designing VLSI circuitry and have, in addition, been developing filtering hardware concepts following a data flow algorithm from Cohen (5) which allows successive multiplier-accumulators to be pipelined. A modification in memory handling allows an extension to two dimensions and is being breadboarded to fit the VLSI design. As a seed effort we have started to

design a VLSI chip which will allow us to create a 31x31 element kernel that will compete favorably timewise and dollarwise against the MPP.

Approach

VLSI design is still a rapidly evolving field. Computer languages are under development which will eventually allow high level statements to be made which establish functional criteria and these statements would be converted to n-channel metal oxide semiconductor (n-MOS) or complementary c-MOS wire lists. These lists are in turn converted by computer to drawings of different overlays of metal and metal oxides. The drawings are then photo-reduced and photo-etched onto silicon or sapphire wafers which are then cut and wired to form individual chips.

The amount of logic that can be placed on a single chip is also evolving rapidly. Today many tens of thousands of transistors can be stored on a surface 7x7 mm sq. Within three to five years that number is expected to increase by 2 to 3 orders of magnitude. At JPL we are experimenting with ways to develop languages which will allow variation of parameters, number of multipliers, number of bits/multipliers, serial or parallel additions/multiply and other parameters which will allow us to tailor fit to customer need without massive redesign effort.

As we contemplate the marriage of VLSI technology with image processing requirements, not all the pieces are yet in place. Some of the designing effort is still initiated by manual drawings to meet VLSI design rule requirements. The logic for multiplication is still not finalized as competition for area (on the chip) and speed (minimum clock cycles per multiply) is under study. Conceptual design for the geometry operation is under rapid restructuring as various experts are consulted (Billingsley-6). Projects like these are studied by Caltech students in

Prof. Mead's classes and valuable interchange is derived from those discussions. The whole idea is to be able to upgrade design concepts and create new VLSI chips as though debugging computer software.

In parallel with the actual chip development hardware is being developed to interface the VLSI to existing computer structures. A not too surprising result emerges as this effort progresses. VLSI allows an improvement in throughput over a serial general purpose computer by a factor of 2 to 3 orders of magnitude. We very quickly become I/O bound in terms of magnetic tape or disk. Consideration must be given to grabbing the data once from mass (serial) storage, and performing all processes at once (pipeline serial) before sending the restructured data or extracted information back on to tape or out to the customer.

We have spent some time with the initial development of a VLSI chip which presently has four multipliers each of which stores 20 bits and multiplies an 8-bit pixel by a 12-bit weight. The chip has been submitted for fabrication external to JPL. Turnaround is about two months. JPL's role is not to compete with the commercial fabrication process, but we are more interested in developing more versatile VLSI design tools.

Some effort has gone into the concept of a pipelined geometry remapping chip. An initial concept designed by us (Nathan) was tried successfully by Northrup for the Air Force. But that was only a nearest neighbor design. We have developed many software algorithms over the years, and recently thought is being given to a four point modified cubic spline which should not degrade the image as does nearest neighbor or linear interpolation. The concept is to perform two orthogonal stretches (or contractions) along each axis as serial operations (pipelined in two VLSI functions) while have direct access to several megabytes of random

access memory from the computer main frame. The proposed speed of transformation is many times that presently available.

Expected Results

Two sets of hardwired algorithms are to be produced. One algorithm will perform two dimensional filtering or correlation on an arbitrarily large image using a 31x31 kernel (at present design -- a modifiable parameter). The other algorithm is a pair of one dimensional cubic spline geometry remapping functions which under software control will "rubber sheet" one image to another according to pre-established pass points. It is expected that these systems will be installed for use in JPL's Image Processing Laboratory (IPL) and be used in their image processing production mode.

Progress is anticipated in the development of software which utilizes the filter hardware to establish "pass points" and these in turn will generate the correction grid for the geometry hardware.

Also investigation into class extraction using the filter hardware will be started. Studies of this sort exist as software only. It is desired to explore increased dimension of class search once a fast hardware filter becomes available.

Another product which can be expected is the ability to reproduce other VLSI configurations with minor changes in design parameters. This ability gives us the power to update new hardware without major mechanical redesign as customer needs change.

As concepts develop regarding the utility of other imaging operations, these too shall be pursued.

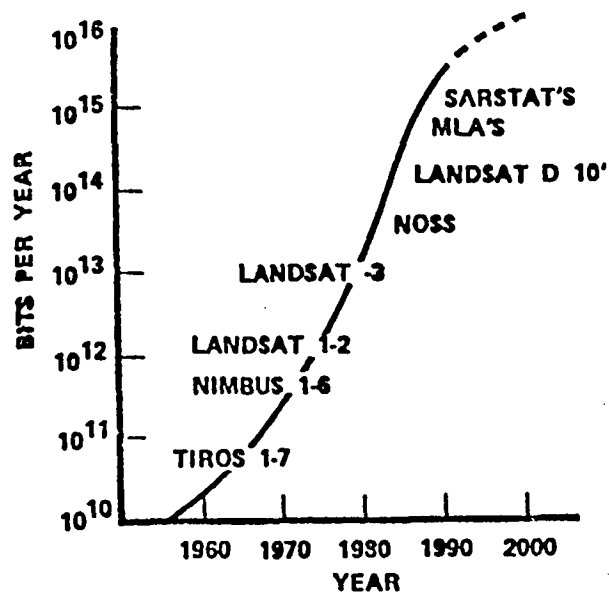
References

1. Bracken, P.A. (1980) - "Earth Resource Observations Data Systems in the 1980's" in 1980 Annual Meeting of American Astronautical Society and AIAA Paper 80-240.
2. Nathan, R. (1966) - "Digital Video Data-Handling," Technical Report JPL 32-877.
3. MITRE Corp. (1979) - "Parallel Processor Technology Trade-off Study for the NASA End-to-End Data System (NEEDS) ."
4. Mead, C.A. and Conway, L.A. (1980) - "Introduction to VLSI Systems," Addison-Wesley pub.
5. Cohen, D. (1978) - "Mathematical Approaches to Computational Networks," 151/RR-78-73 Information Sciences Institute/USC.
6. Billingsley, F.C. (1981) - "Modelling Misregistration and Related Effects on Multispectral Classification," JPL report in press.

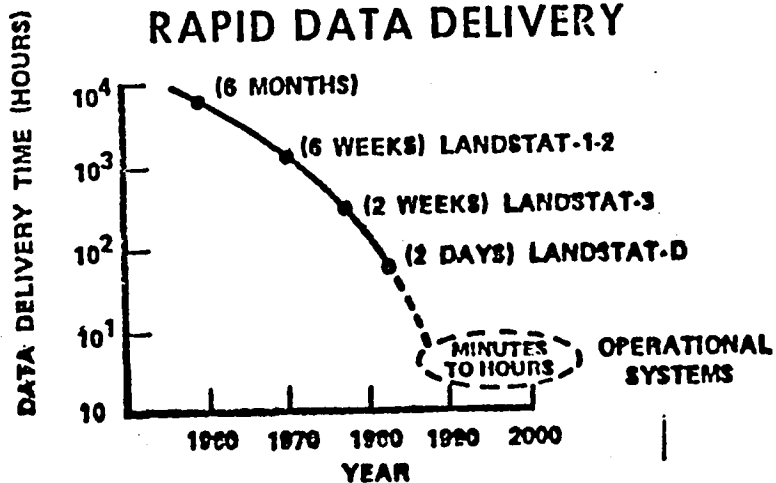


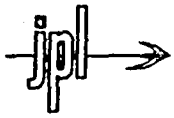
DATA SYSTEM DRIVER

DATA VOLUME

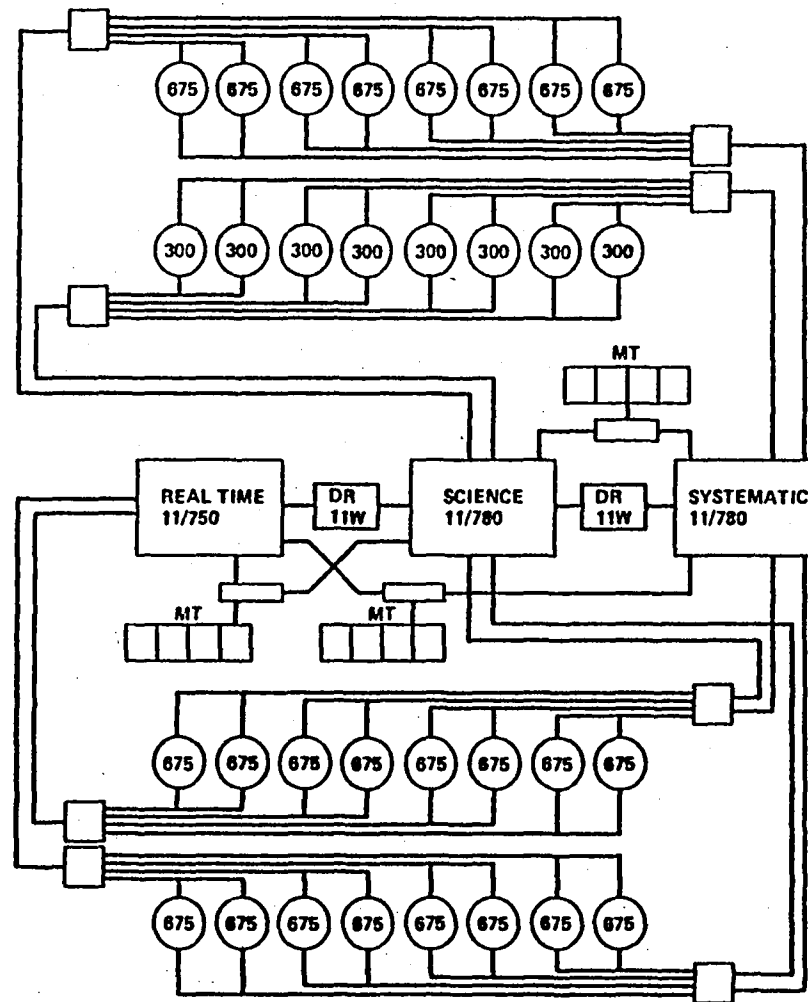


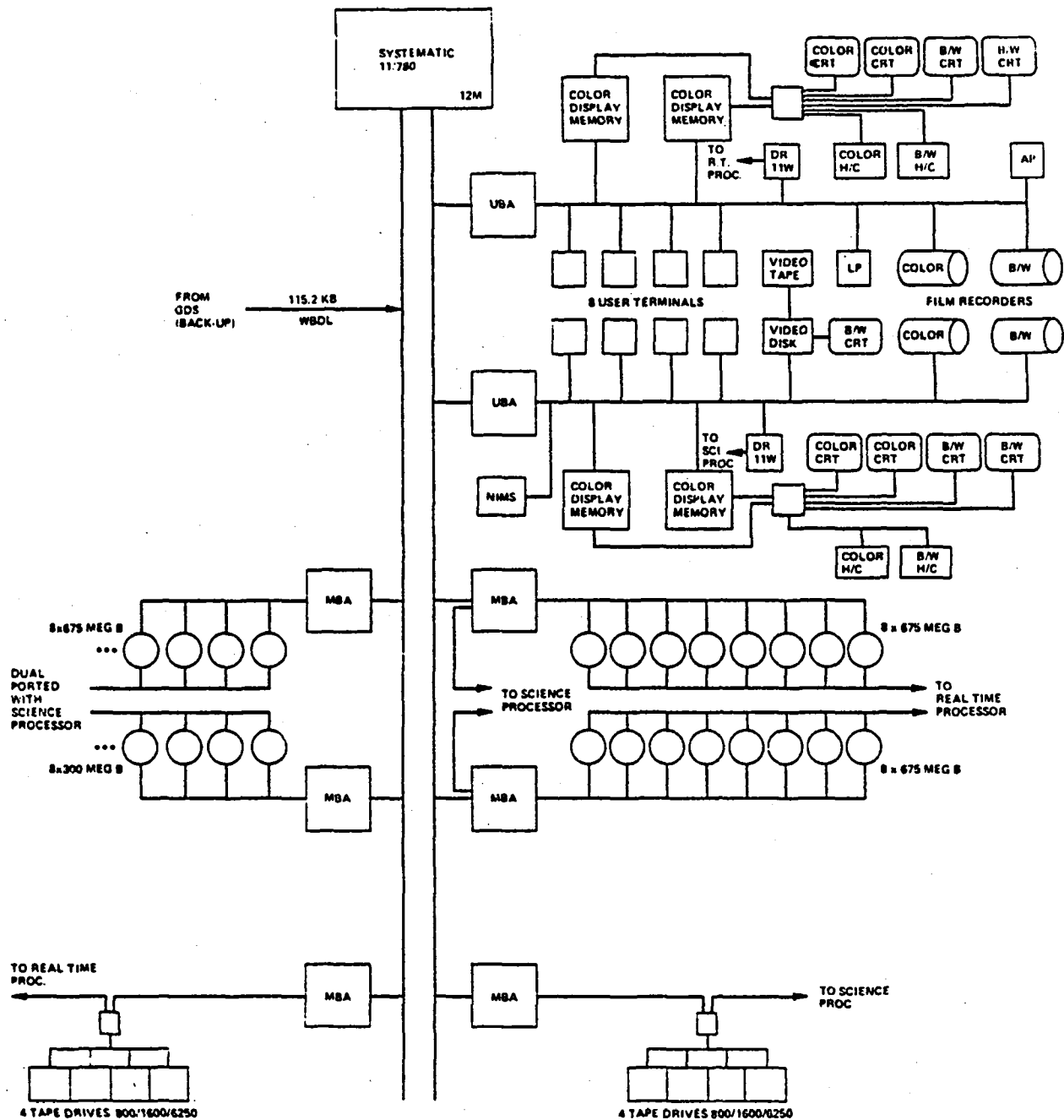
RAPID DATA DELIVERY



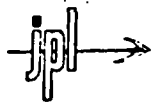


MIPL VAX CONFIGURATION

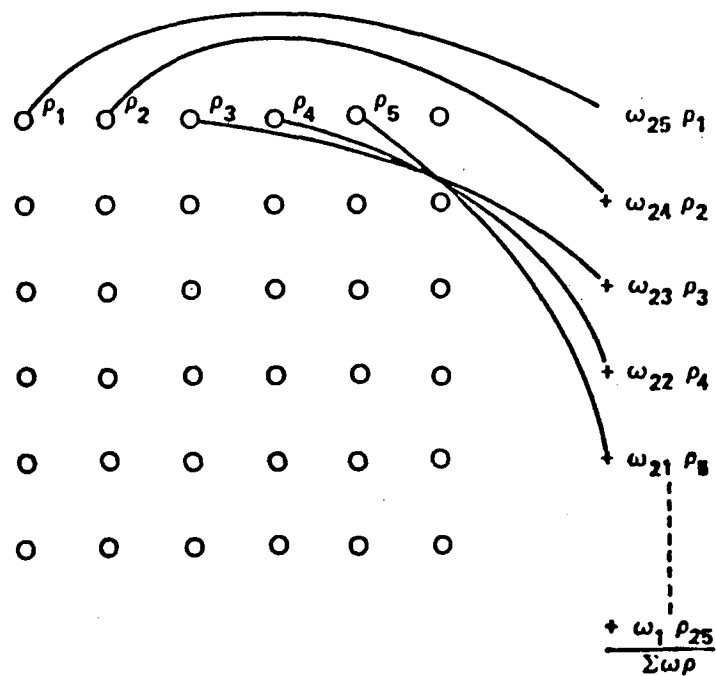




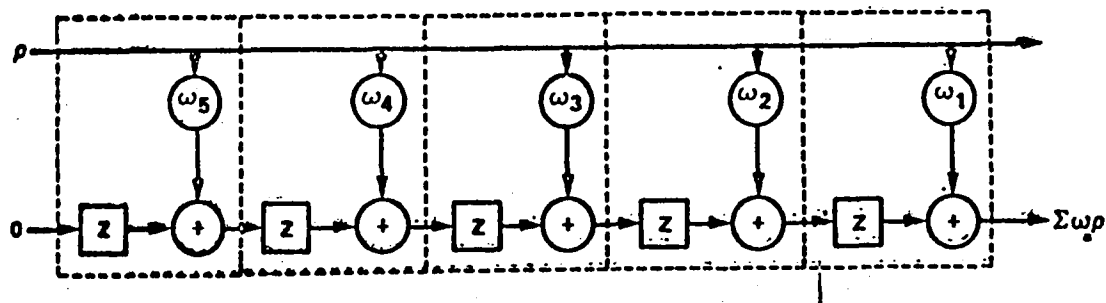
Model	KCPS	Model	KCPS	Model	KCPS
NCR V-8560	281	121 Honeywell 63/17*	700	101 NAs AS/5-3 MP	1.53*
Univac 70/61 (RCA)	287	122 IBM 360/78	700	102 Honeywell 66 40 (2X)	1.6
Univac 70/7 (RCA)	287	123 Honeywell DPS 8/44	710	103 Univac 1100/62	1.76
Univac 2000E	295	124 Burroughs 4340	718	104 Univac 1100/81	1.800
IBM 370/145	308	125 DEC 1077 (2X)	748	105 CDC 173	1.870
Univac 70/60 (RCA)	300	126 IBM 4341	708	106 IBM 370/155	1.900
Univac 70/3 (RCA)	300	127 Univac 1108	700	107 Univac 1100/42	1.918
DEC 1055 (2X)	307	128 Burroughs 6310	705	108 Univac 1110 (2X2)	1.943
CDC Omega 400-I	321	129 Burroughs 6811	705	109 Burroughs 7770	1.960
Magnuson M303	321	130 Burroughs 6812	705	110 Honeywell DPS 8/70	1.937
Univac 60/70	328	131 NCR V-8535M	778	111 Burroughs 7811	2.108
Burroughs 4708	340	132 Univac 90/80-3	800	112 IBM 300/85	2.100
Burroughs 6030	340	133 Univac 90/80	825	113 Univac 1100/62 H1	2.244
Burroughs 6207	340	134 DEC 1000 KL	828	114 Honeywell 66/60	2.278
Univac 3700	344	135 DEC 1000	828	115 IBM 370/168	2.300
Honeywell 63/10	350	136 DEC 2050	829	116 Honeywell 66/80 (2X)	2.340
Nanodata CMX 6303	360	137 IBM 370/158	829	117 Burroughs 7765	2.350
Burroughs 6203	362	138 NAS AS/5-1	829	118 Amdahl	2.437
NCR V-8570	383	139 DEC VAX-11/760	831	119 CDC 74	2.500
Univac 1100/11	392	140 Magnuson M30/42	834	120 CDC 6600	2.500
Univac 1103	400	141 Burroughs 7003	845	121 IBM 370/168-3	2.500
Univac 413-III	400	142 Burroughs 7750	845	122 IBM 3032	2.500
Honeywell 22/05 (2X)	405	143 Nanodata CMX 6343	880	123 Burroughs 7780	2.535
NCR V-8535M	424	144 NCR V-8575 MP	884	124 NCR V-8650	2.650
Burroughs 8700	425	145 Burroughs 7805	900	125 Univac 1100/43	2.753
IBM 370/148	425	146 Honeywell 68/40	900	126 Univac 1100/62	2.000
Magnuson M30/31	430	147 IBM 370/158-3	900	127 CDC 174	2.005
Burroughs 8008	450	148 NAS AS/5-3	900	128 Amdahl 470 V-5-II	2.850
Burroughs 6005	459	149 CDC Omega 480-III	950	129 Burroughs 7775	3.000
DEC 2040	462	150 Magnuson M30/43	985	130 NAS AS/6	3.00*
Honeywell DPS 3/20	473	151 CDC 72	1,000	131 CDC 76	3.12*
DEC 1000	486	152 NAS AS/4 MP	1,000	132 Univac 1110 (4X4)	3.303
DEC 1070 KI	497	153 Honeywell 66/20 (2X)	1,008	133 Univac 1100/82	3.350
DEC POP 11/60	510	154 Univac 1100/12	1,044	134 Amdahl 470 V6	3.450
CDC 171	520	155 IBM 3031	1,045	135 Honeywell DPS 8/70	3.576
Honeywell 63/10 (2X)	525	156 Univac 1100/41	1,052	136 Univac 1100/44	3.615
Magnuson M30/4	531	157 Univac 90 50-4	1,100	137 CDC 6700	3.700
Magnuson M30/22	531	158 Honeywell 68/27*	1,120	138 Amdahl 470 V-6-II	3.750
NCR V-8555 MP	531	159 Univac 1100/61 H1	1,120	139 Amdahl 470 V-7B	3.825
Honeywell 63/07*	540	160 Univac 1110 (1X1)	1,143	140 Burroughs 7785	3.900
Burroughs 6207	544	161 Burroughs 6817	1,147	141 Burroughs 7821	4,000
Univac 110/70 C1	544	162 Burroughs 6818	1,150	142 IBM 3033N	4,000
Burroughs 6003	545	163 Univac 1100/60 H1	1,153	143 Amdahl 470 V-7A	4,250
IBM 370/155	550	164 DEC 1099 (2X)	1,160	144 NCR V-8670	4,293
Nanodata CMX 6303	550	165 DEC 1038 (2X)	1,180	145 IBM 370/195	4,750
CDC Omega 480-II	553	166 Honeywell DPS 8/52	1,200	146 Honeywell DPS 8/70 (3X)	5,007
Honeywell 65/20	560	167 CDC 172	1,220	147 Univac 1100/83	5,040
Univac 1100/61 C1	560	168 Burroughs 6821	1,260	148 CDC 175	5,060
IBM 300/68	568	169 Burroughs 6822	1,260	149 IBM 3033U	5,900
Univac 1108-II	571	170 Honeywell 66 60	1,286	150 Amdahl 470 V-7	5,950
NCR V-8575	576	171 Univac 1108 MP	1,290	151 Amdahl 470 V-8	6,375
NAS AS/4	595	172 Burroughs 7755	1,300	152 Univac 1100/84	6,400
DEC POP 11/70	600	173 CDC 73	1,300	153 Honeywell DPS 8/70 (4X)	6,510
DEC 1066 (2X)	608	174 Honeywell 66 60	1,309	154 CDC 176	9,360
Univac 9000-2	609	175 NCR V-8535 MP	1,340	155 CDC 7670	10,000
Univac 1108/11 (overlog)	614	176 Univac 1100/61 H2	1,344	156 CDC Cyber 205	—
Univac 498	650	177 NAS AS/5-1 MP	1,407	(vector)	— 900 000
NCR V-8565	658	178 Univac 1100/60 H2	1,496	157 Cray 1 Sivection	— 900 00*
Univac 1100/61 C2	672	179 Univac 1100/62 E1	1,496		
Univac 1100/60 C2	690	180 Burroughs 7750	1,528		



SERIAL FILTER



PIPELINE FILTER





VLSI

VERY LARGE SCALE INTEGRATED SYSTEMS

PARALLEL/PIPELINE PROCESSING

CONCURRENT VS. SERIAL

MANY (>10,000 TRANSISTORS) ON A SINGLE CHIP

INEXPENSIVE WHEN COMPARED TO DISCRETE LOGIC

NEXT EVOLUTIONARY STEP BEYOND SOFTWARE

COMPUTERS GENERATING COMPUTERS

HIGH LEVEL LANGUAGE USED TO CONVERT

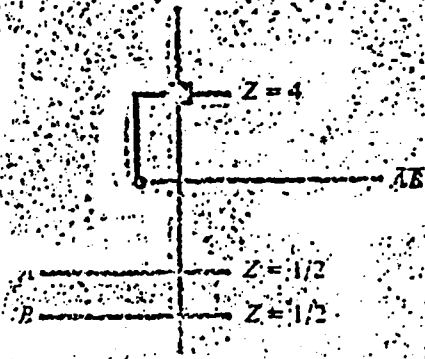
ALGORITHMS INTO HARDWARE

COST EFFECTIVE COMPARED TO SERIAL PROCESSORS

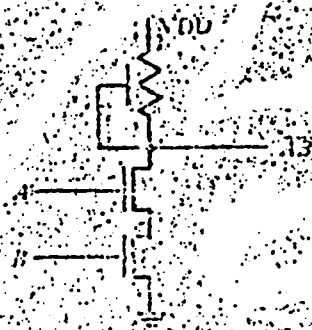
Scale in λ
 0 1 2 3 4 5 6



(a) NAND gate layout geometry.



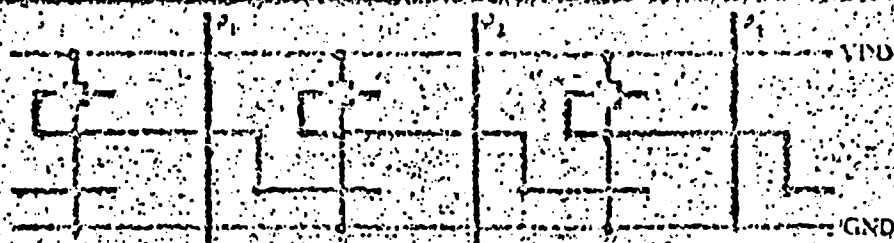
(b) NAND gate topology (stick diagram).



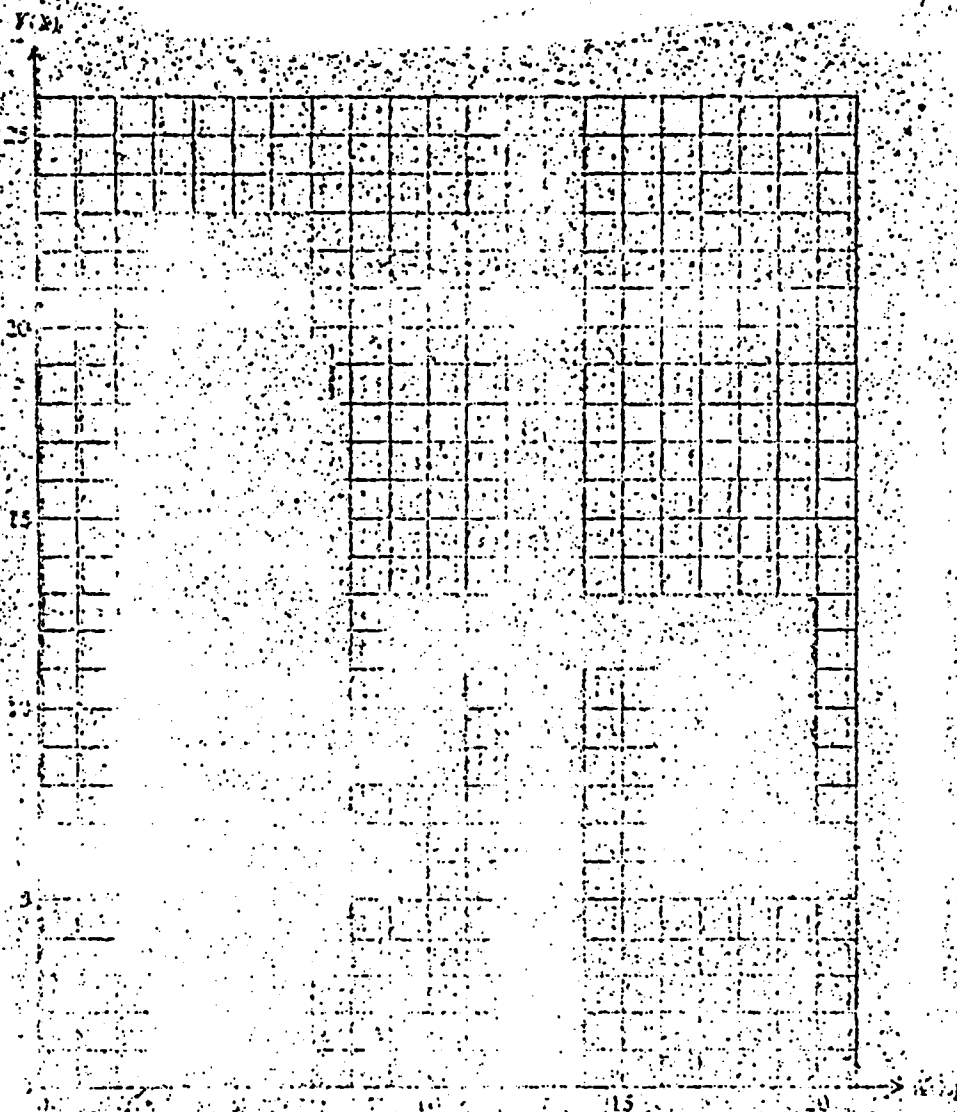
(c) NAND gate circuit diagram.



(d) NAND gate logic symbol.



(a) Stick diagram of one row of a shift register array.

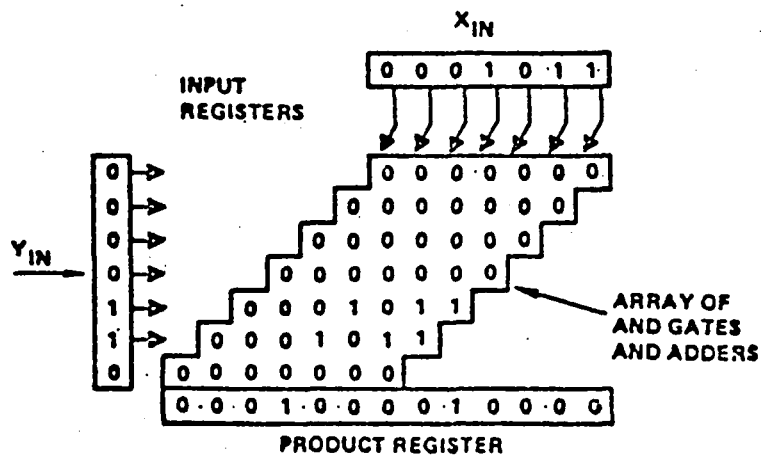


(b) Layout of one row of the shift register array.

FIG. 1. (a) Stick diagram of one row of a shift register array.

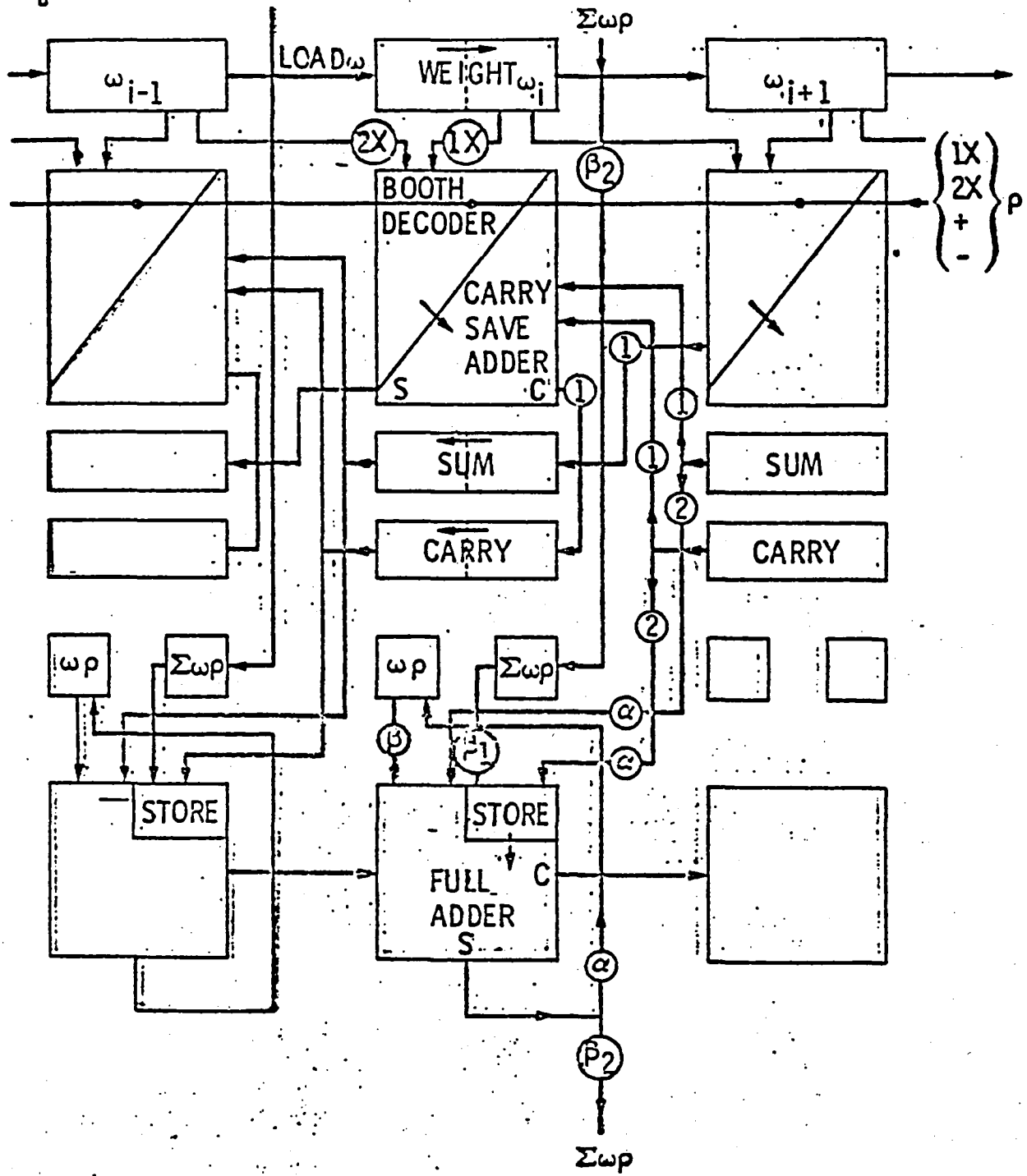
DIGITAL MULTIPLIER

- TYPICAL IC MULTIPLIERS CONTAIN REGISTERS FOR MULTIPLIER AND MULTIPLICAND OPERANDS.
- AN ADDITIONAL REGISTER IS PROVIDED FOR THE PRODUCT.
- MODERN LSI MULTIPLIERS PERFORM ADDITIONS IN A RIPPLE FASHION. THAT IS, EACH SUM IS PASSED ON FROM ONE ADDER TO THE NEXT WITHOUT THE USE OF CLOCKED SEQUENTIAL CIRCUITS. THEREFORE, THE MULTIPLIER IS COMPRISED OF AN ARRAY OF GATES AND ADDERS.

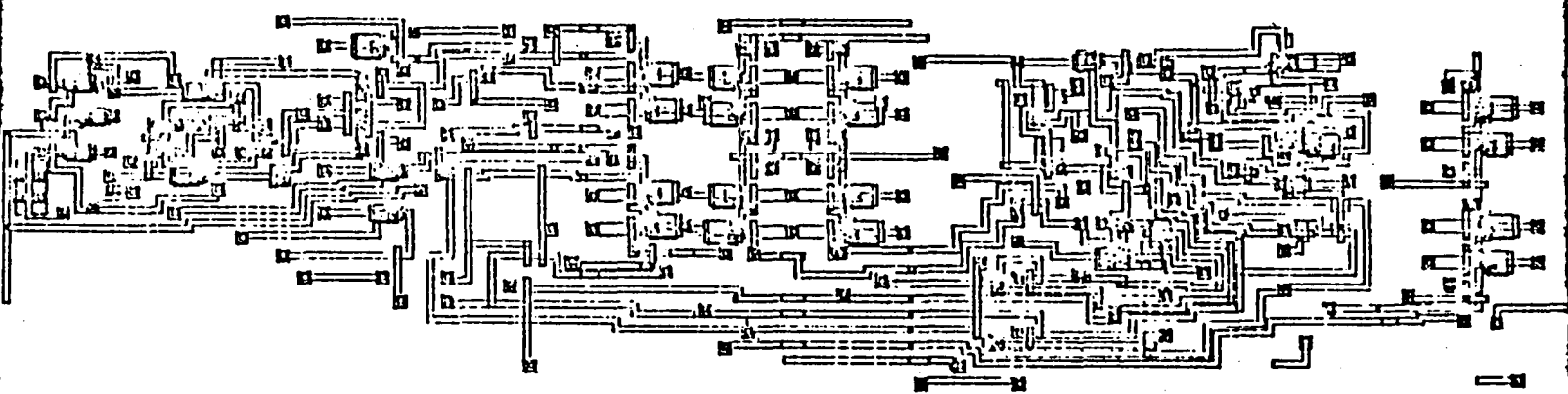


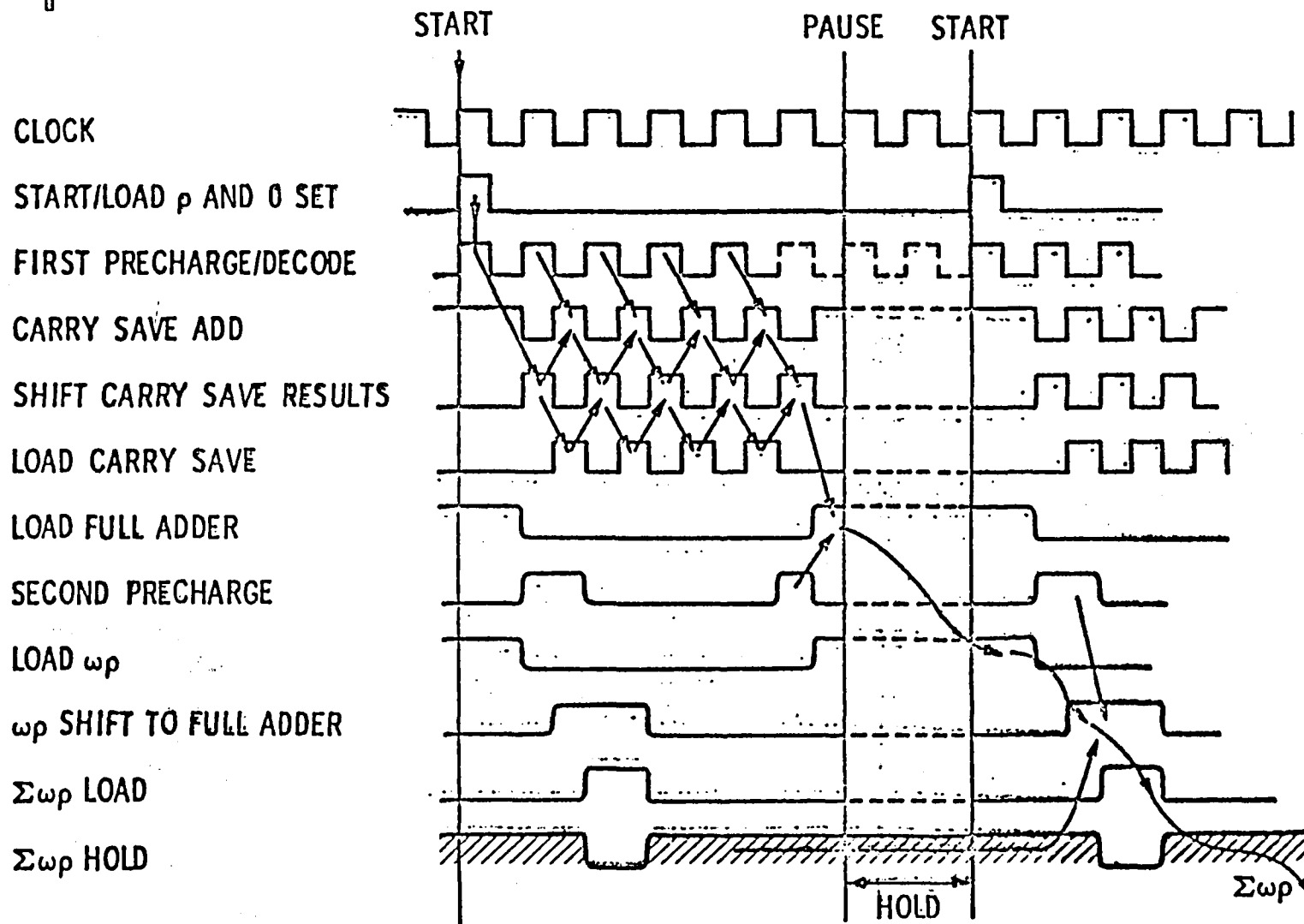
jpl →

MULTIPLY UNIT



R. NATHAN
4/24/51

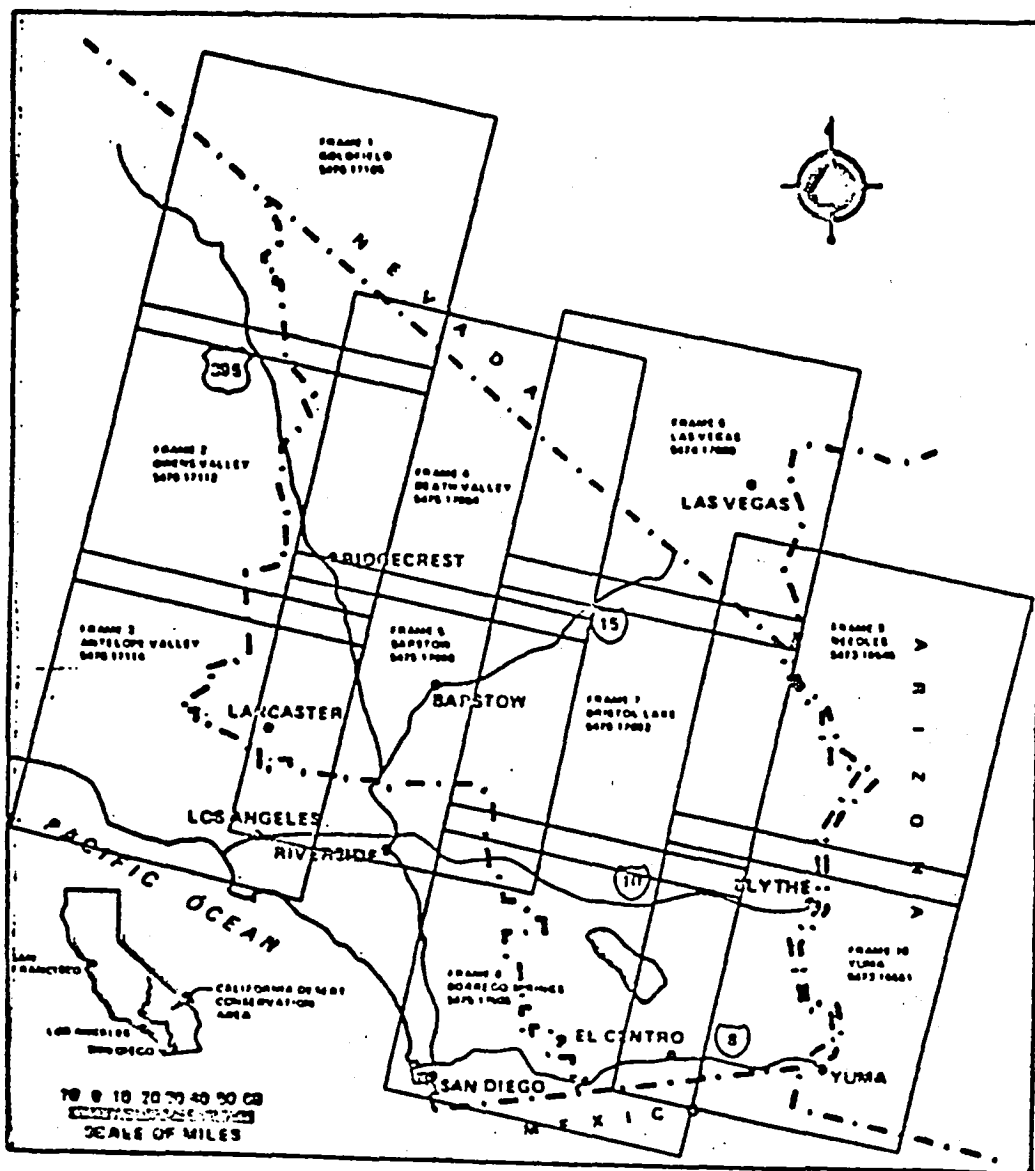




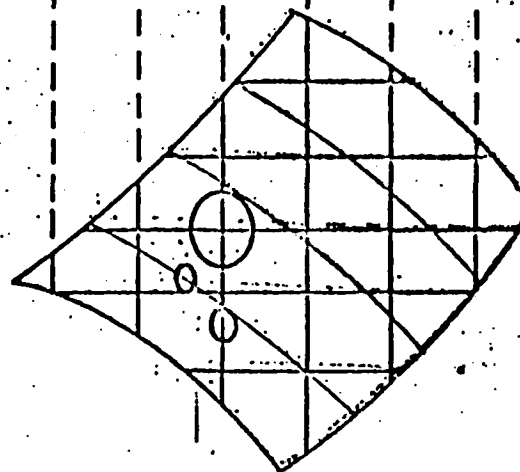
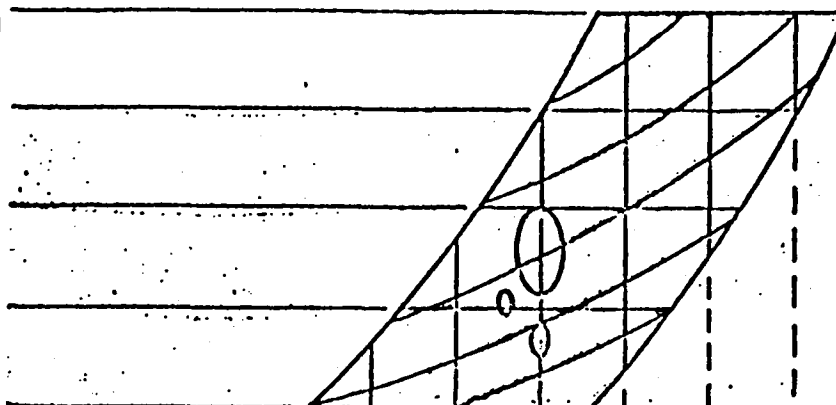
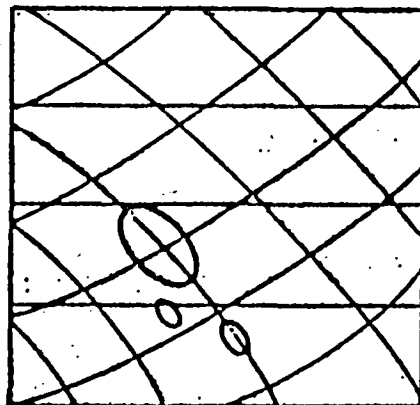


BUREAU OF LAND MANAGEMENT CALIFORNIA DESERT CONSERVATION AREA LOCATION OF LANDSAT SCENES

BLM



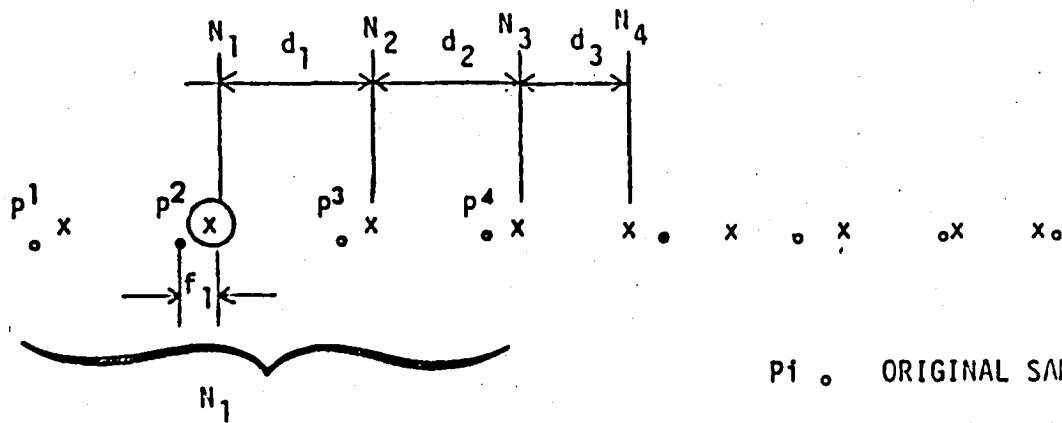
jpl →



•	•	•	•	•	•
•	X	X	X	X	•
•	X	⊗	⊗	X	•
•	X	⊗ ⁺	⊗	X	•
•	X	X	X	X	•
•	•	•	•	•	•

GEOMETRIC REPROJECTION

RESAMPLING



p^i . ORIGINAL SAMPLES

N_i x NEW SAMPLES

f FRACTIONAL
DISTANCE
BETWEEN POINTS

$$N = p_1 \cdot w_1 + p_2 \cdot w_2 + p_3 \cdot w_3 + p_4 \cdot w_4$$

FOR LINEAR INTERPOLATION OF NEW SAMPLE VALUES

$$w_1 = w_4 = 0$$

$$w_2 = 1 - f$$

$$w_3 = f$$

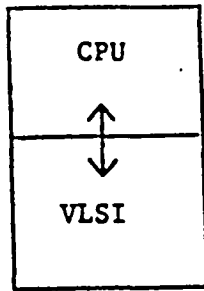
THEREFORE $N_1 = p_2 (1 - f_1) + p_3 f_1$

FOR CUBIC INTERPOLATION ALL FOUR w_i ARE A TABLE LOOK UP
FUNCTION OF f_i .

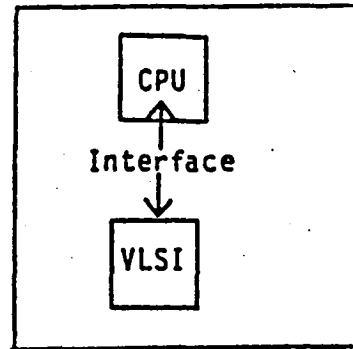
THE NEW INTERSAMPLE DISTANCE (d) CAN ALSO BE NONLINEAR.
ALLOWANCE IS MADE FOR CUBIC SPLINE ADJUSTMENT FOR NON-LINEAR SAMPLING.

RNATHAN
MARCH 1982

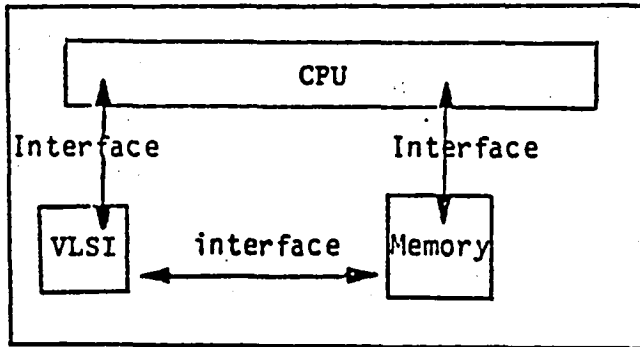
①



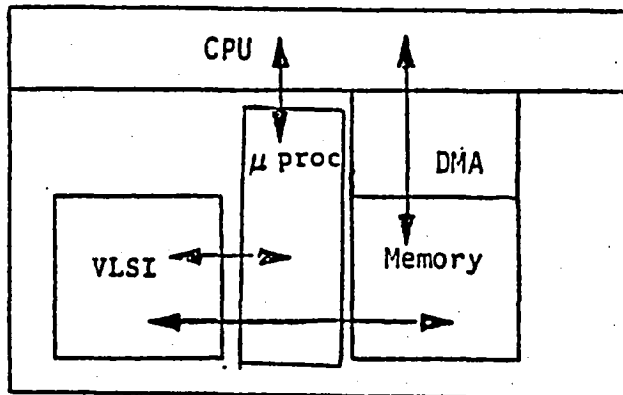
②



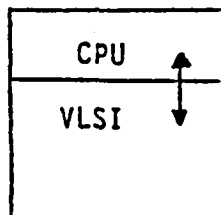
③



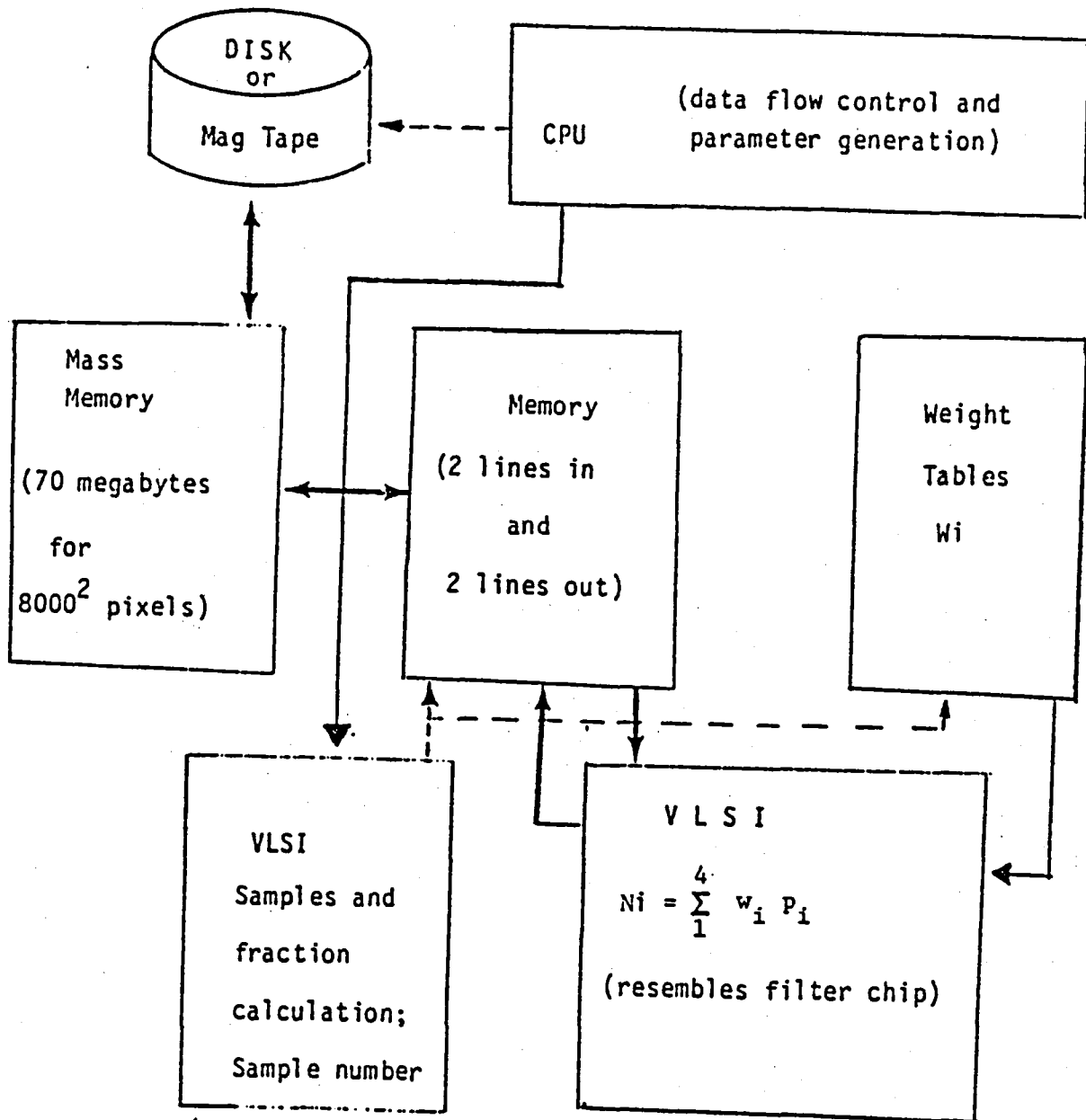
④



⑤

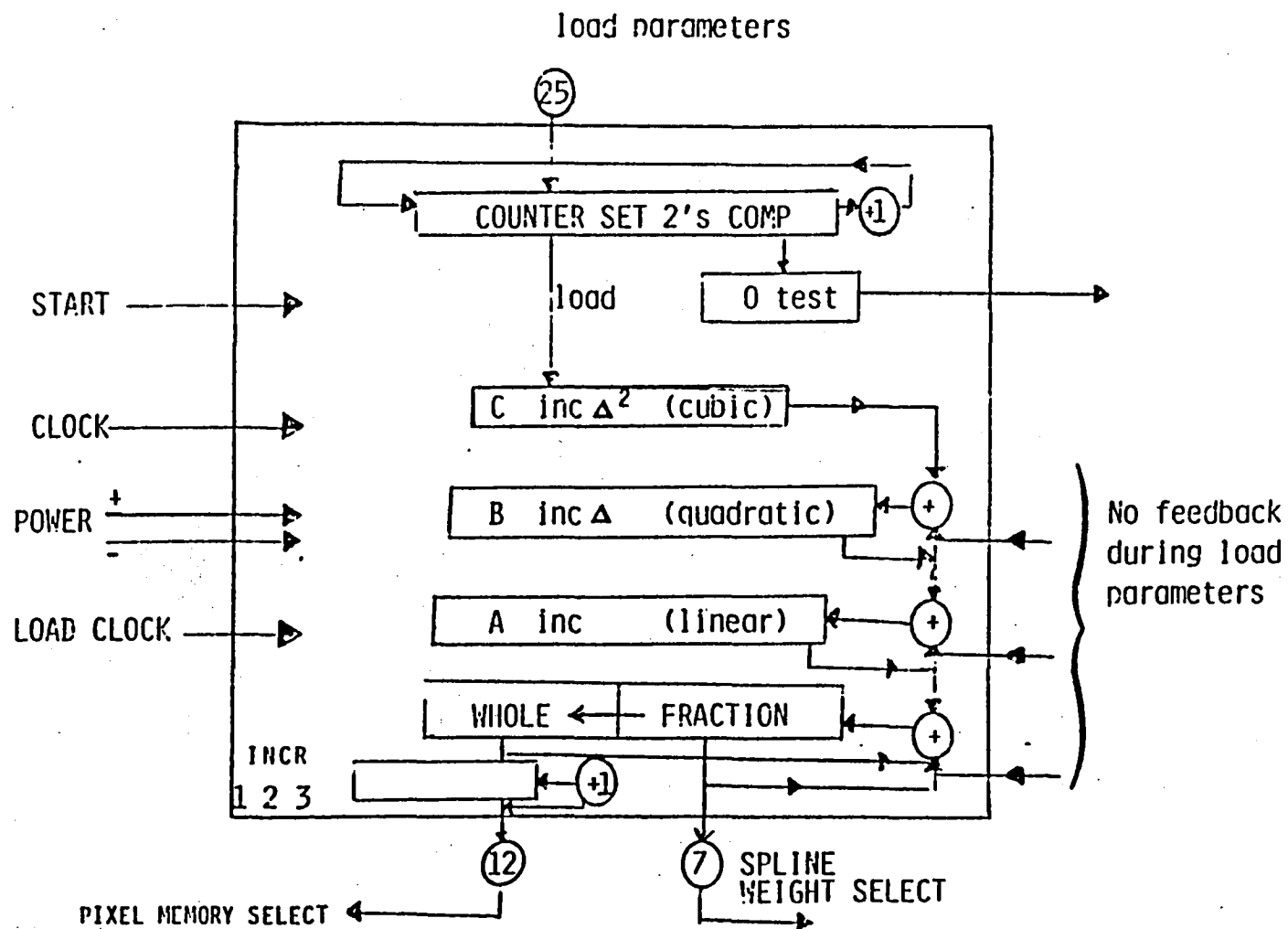


GEOMETRIC REPROJECTION

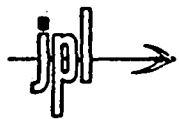


R. NATHAN
3/82

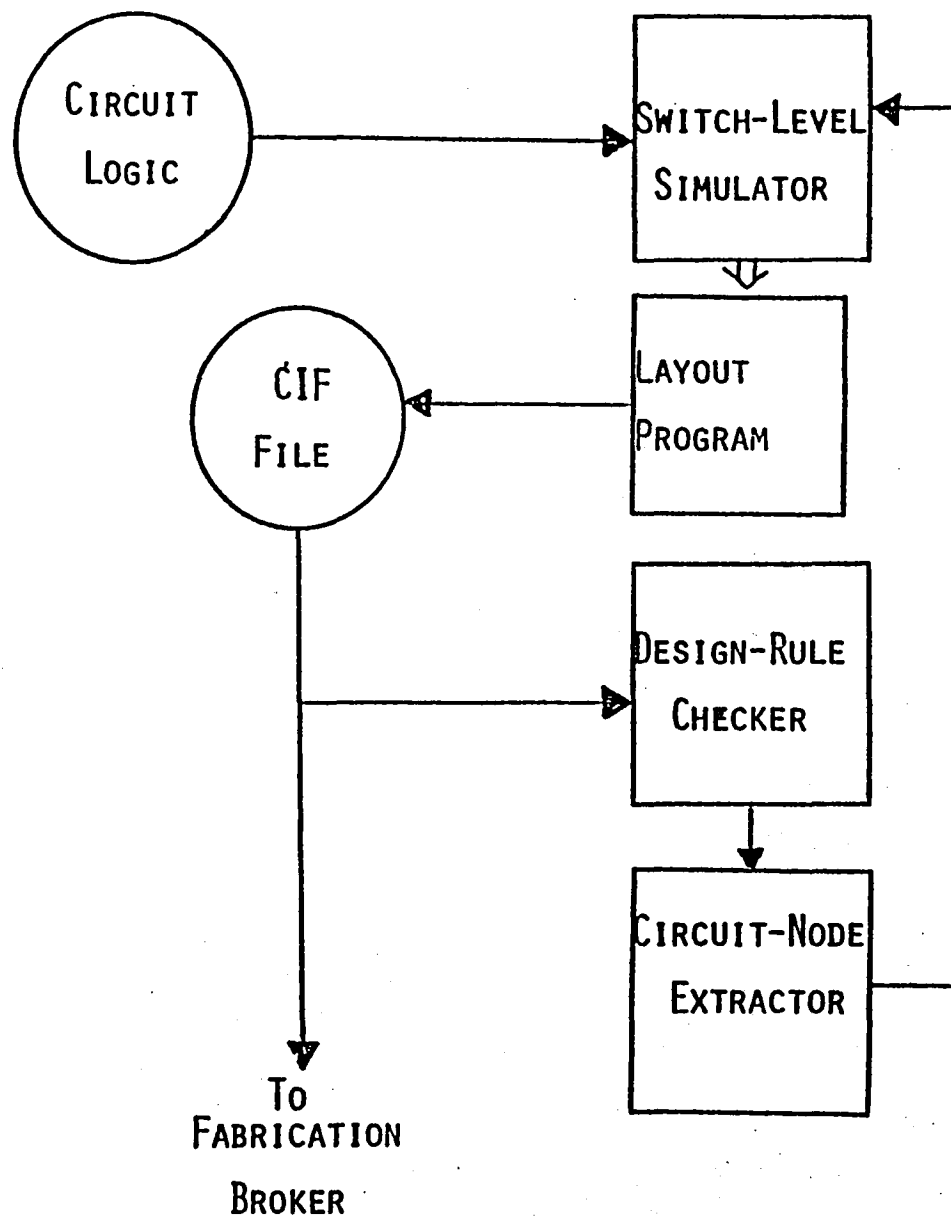
load parameters



RNATHAN.
MARCH 1982



FUNCTIONAL ELEMENTS OF CAMPUS DESIGN SYSTEM



NOTES:

1. AT JPL, SYSTEM WILL RUN USING MAINSAIL COMPILER ON VAX 11/780 WITH VMS OPERATING SYSTEM
2. SWITCH-LEVEL SIMULATOR IS BASED ON MIT WORK OF BRYANT AND TEMANS.



FUTURE

INDUSTRY DOES NOT WISH TO DEVELOP CUSTOM CHIPS

INTERESTED IN MASS MARKET

JPL AND OTHER USER INSTITUTIONS NEEDED TO

DEVELOP HIGH LEVEL SOFTWARE TO CONVERT

ALGORITHMS TO PARALLEL HARDWARE

POTENTIAL APPLICATION AREAS

PATTERN EXTRACTION

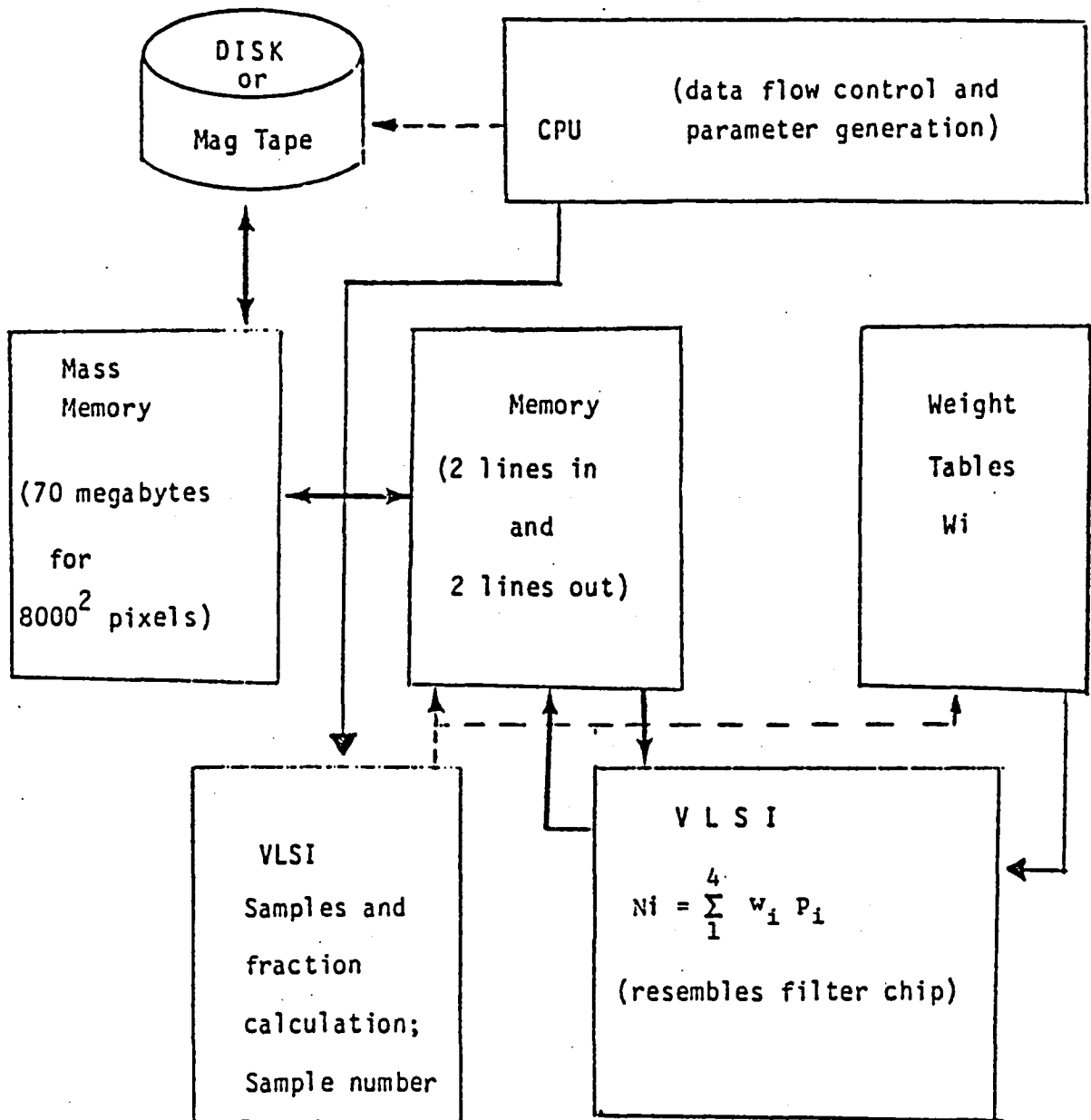
SAR

I/O PARALLEL DATA FLOW

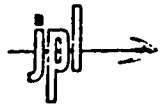
OTHER DATA BOTTLENECKS

|

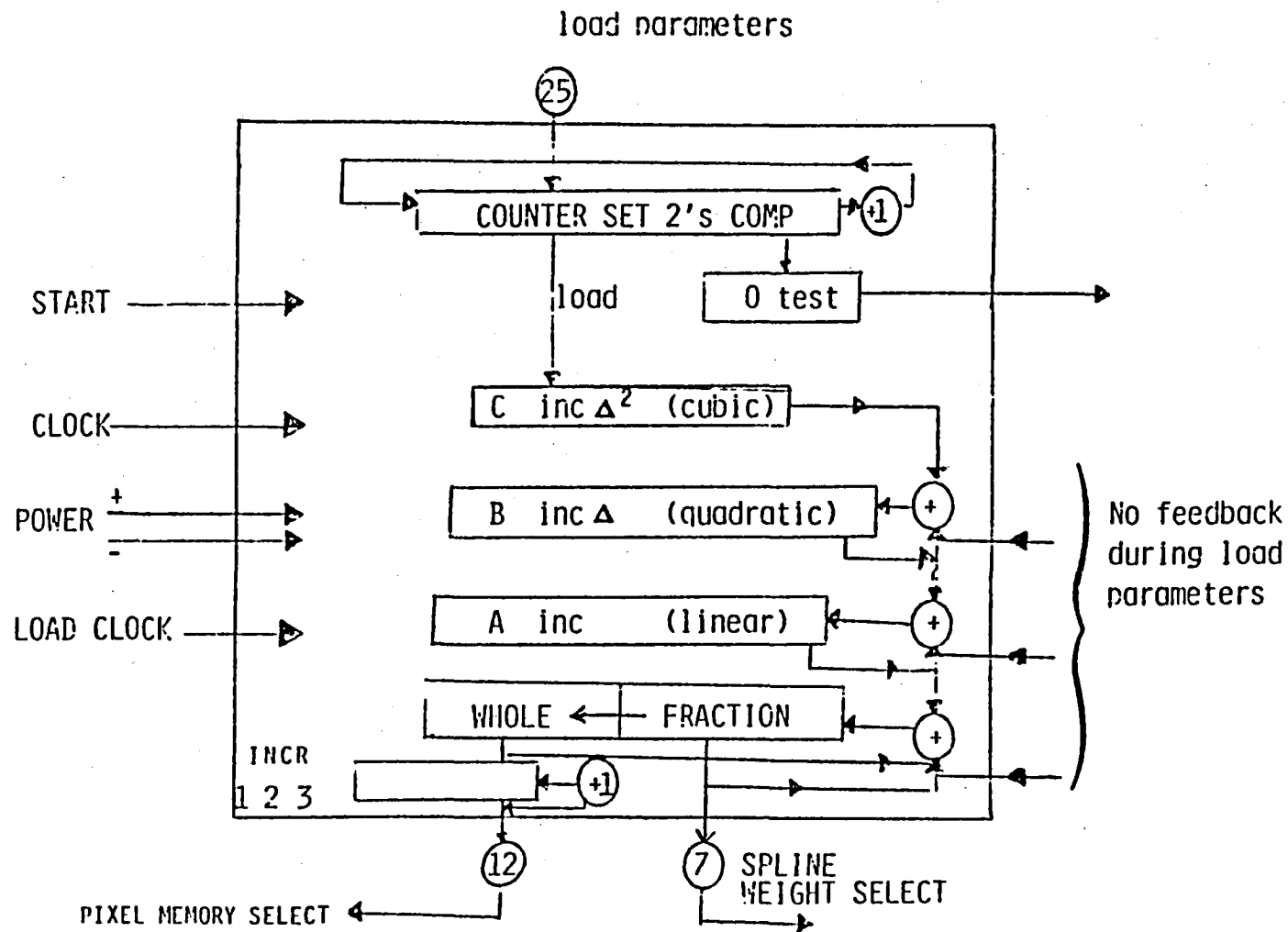
GEOMETRIC REPROJECTION

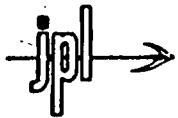


R.NATHAN
3/82

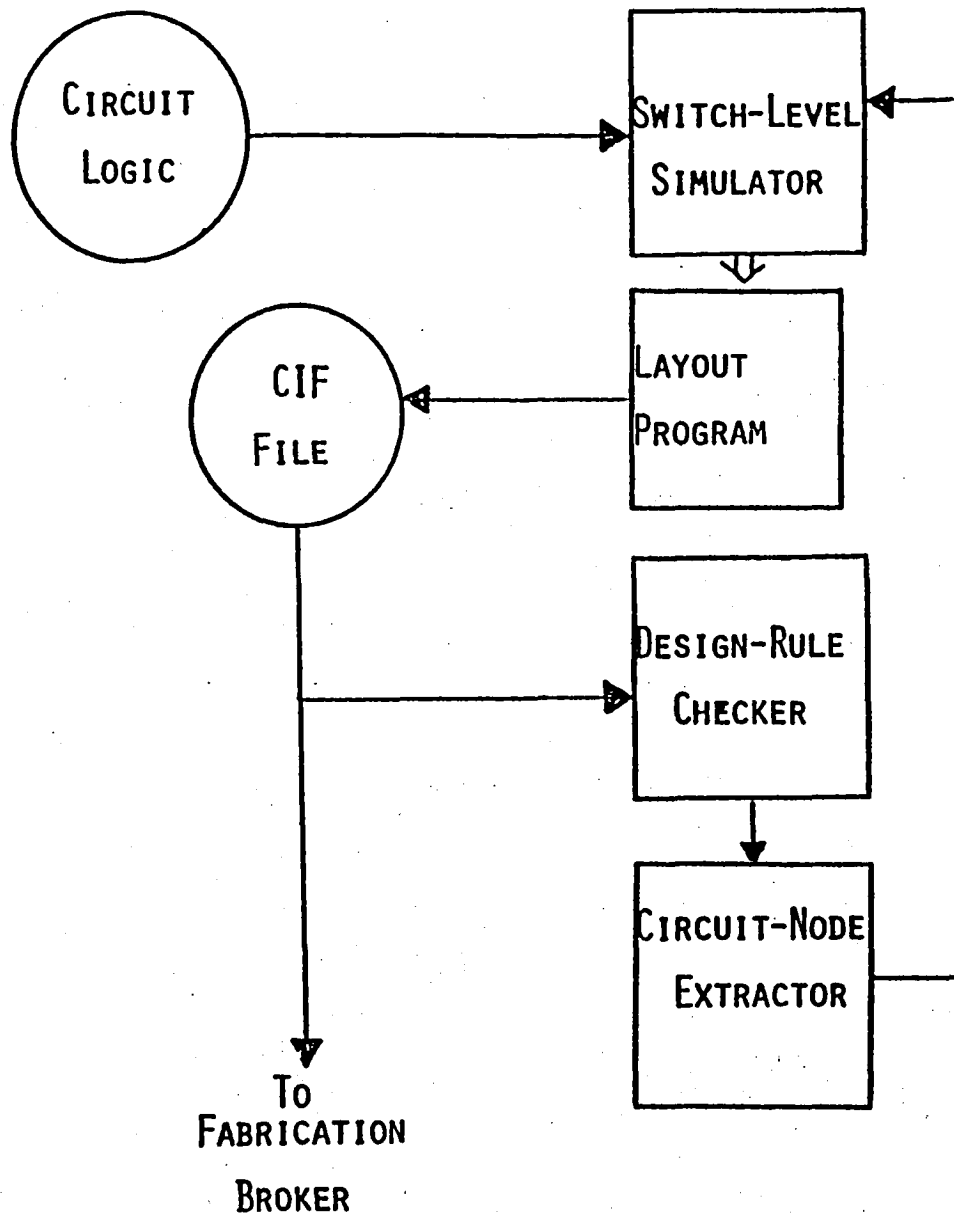


SELECT & COUNT





FUNCTIONAL ELEMENTS OF CAMPUS DESIGN SYSTEM



NOTES:

1. AT JPL, SYSTEM WILL RUN USING MAINSAIL COMPILER ON VAX 11/780 WITH VMS OPERATING SYSTEM
2. SWITCH-LEVEL SIMULATOR IS BASED ON MIT WORK OF BRYANT AND TEMANS.



FUTURE

INDUSTRY DOES NOT WISH TO DEVELOP CUSTOM CHIPS

INTERESTED IN MASS MARKET

JPL AND OTHER USER INSTITUTIONS NEEDED TO

DEVELOP HIGH LEVEL SOFTWARE TO CONVERT

ALGORITHMS TO PARALLEL HARDWARE

POTENTIAL APPLICATION AREAS

PATTERN EXTRACTION

SAR

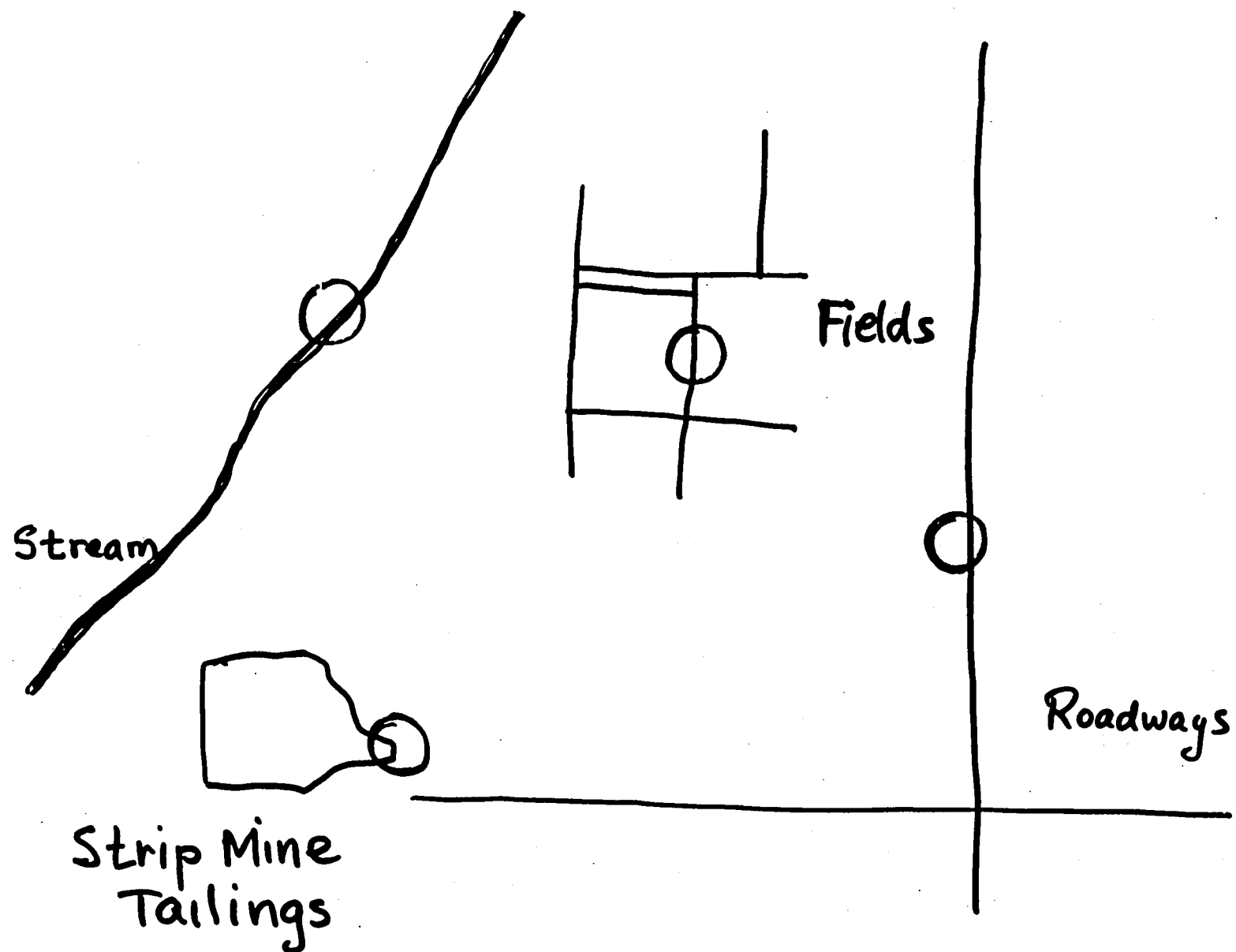
I/O PARALLEL DATA FLOW

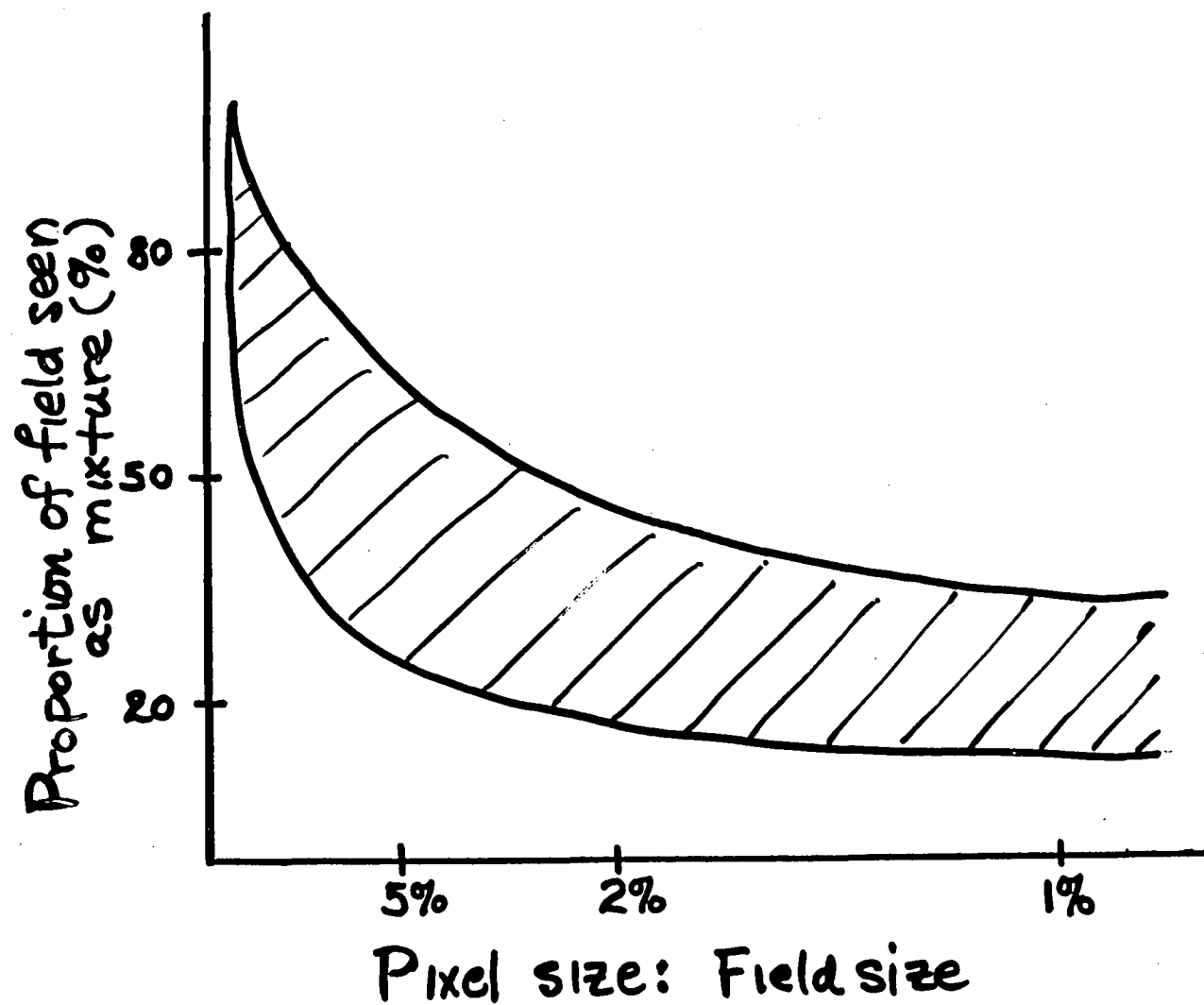
OTHER DATA BOTTLENECKS

MIXTURE PIXELS

P. SWAIN

- I. HISTORICAL PERSPECTIVE
- II. ORIGINS OF THE PROBLEM
- III. INDUCED PROBLEMS
- IV. APPROACHES TO SOLVING THE PROBLEM AND "STATE OF THE ART"
- V. DISCUSSION: RELEVANCE IN THE PRESENT CONTEXT





Adapted from Nalepka & Hyde
(ERIM)

PROBLEMS

1. CLASSIFICATION
2. TRAINING
3. LOCATION OF SMALL OBJECTS, BOUNDARIES
4. REGISTRATION, RECTIFICATION
5. AREA ESTIMATION

APPROACHES

1. RESOLVE MIXED PIXELS INTO COMPONENTS
2. RESOLVE AREAS INTO COMPONENTS
3. INCORPORATE SPATIAL CLUES
 - NEIGHBORHOODS
 - STRUCTURES
4. INCORPORATE TEMPORAL CLUES
5. THE ULTIMATE SOLUTION

m CLASSES, n SPECTRAL CHANNELS

CLASSES $\sim N(A_i, M_i)$, $i = 1, 2, \dots, m$

PROPORTION VECTOR $\lambda = (\lambda_1, \lambda_2, \dots, \lambda_m)^t$

MIXTURE DISTRIBUTION $\sim N(A_\lambda, M_\lambda)$

$$A_\lambda = \sum \lambda^i A_i = A\lambda = [A_1 \ A_2 \dots A_m]\lambda$$

$$M_\lambda = \sum \lambda^i M_i$$

MAX. LIKELIHOOD SOLUTION:

$$\underset{\lambda}{\text{minimize}} F(\lambda) = n|M_\lambda| + (y-A_\lambda)^t M_\lambda^{-1} (y-A_\lambda)$$

SUBJECT TO $\lambda^i \geq 0$

$$\sum \lambda_i = 1$$

MIXED PIXELS: A BIBLIOGRAPHY

1. R. F. Nalepka and P. D. Hyde, "Classifying Unresolved Objects from Simulated Space Data," Proc. 8th Int'l. Symp., on Remote Sensing of Environment, ERIM, 1972, pp. 935-949.
2. H. M. Horwitz, P.D. Hyde and W. Richardson, "Improvements in Estimating Proportions of Objects from Multispectral Data," Rept. No. NASA CR-ERIM 190100-25-T, ERIM, April 1974.
3. H. M. Horwitz, J. T. Lewis and A. P. Pentland, "Estimating Proportions of Objects from Multispectral Scanner Data," Rept. No. NASA CR-ERIM 109600-13-R, ERIM May 1975.
4. W. A. Malila, J. M. Gleason and R. C. Cicone, "Investigation of Spatial Misregistration Effects in Multispectral Scanner Data," Rept. No. NASA CR-ERIM 109600-68-F, ERIM, May 1976.
5. F. Sadowski and J. Sarno, "Forest Classification Accuracy as Influenced by Multispectral Scanner Spatial Resolution," Rept. No. NASA CR-ERIM 109600-71-F, ERIM, May 1976.
6. C. B. Chittineni, "Estimation of Proportions in Mixed Pixels Through Their Region Characterization," Proc. 1981 Machine Processing of Remotely Sensed Data Symp., Purdue University (LARS), June 1981, pp. 292-303.
7. Teicher, H., "Identifiability of Mixtures," Ann. Math. Stat. 34., 1265 (1963).
8. S. Yakowitz and J. Spragins, "On the Identifiability of Finite Mixtures," Ann. Math. Stat., 39, 209 (1968).
9. Three papers from The LACIE Symposium: Proc. Technical Sessions (Vol. II), October 1978:
 - A. H. Feiveson, "Estimating Crop Proportions From Remotely Sensed Data," pp. 633-646.
 - J. D. Bryant, "On the Clustering of Multidimensional Pictorial Data," pp. 646-660.
 - R. K. Lenington and M. E. Rassback, "CLASSY-An Adaptive Maximum Likelihood Clustering Algorithm," pp. 671-690.
10. T. B. Dennis, "Investigation of Boundary Handling Procedures," Rept. No. SR-LO-04013 JSC-16838 (AgRISTARS), Johnson Space Center, Dec. 1980.

BIBLIOGRAPHIC DATA SHEET

1. Report No. CP-2260	2. Government Accession No.	3. Recipient's Catalog No.	
4. Title and Subtitle The Multispectral Imaging Science Working Groups: Final Report		5. Report Date September 1, 1982	
		6. Performing Organization Code 902.1	
7. Author(s) Scott C. Cox, editor		8. Performing Organization Report No.	
9. Performing Organization Name and Address Goddard Space Flight Center Greenbelt, Maryland 20771		10. Work Unit No.	
		11. Contract or Grant No.	
12. Sponsoring Agency Name and Address National Aeronautics and Space Administration Washington, D.C.		13. Type of Report and Period Covered Conference Publication	
		14. Sponsoring Agency Code	
15. Supplementary Notes			
16. Abstract Proceedings of the Multispectral Imaging Science Working Group Meetings held in Pasadena, CA, San Antonio, TX, and Silver Spring, MD, 1982.			
17. Key Words (Selected by Author(s)) Remote Sensing		18. Distribution Statement Star Category 43	
19. Security Classif. (of this report) Unclassified	20. Security Classif. (of this page) Unclassified	21. No. of Pages 35 292	22. Price*

National Aeronautics and
Space Administration

Washington, D.C.
20546

Official Business

Penalty for Private Use, \$300

SPECIAL FOURTH CLASS MAIL
BOOK

Postage and Fees Paid
National Aeronautics and
Space Administration
NASA-451



NASA

POSTMASTER: If Undeliverable (Section 158
Postal Manual) Do Not Return
